Sensur av hovedoppgaver

Høgskolen i Sørøst-Norge
Fakultet for teknologi og maritime fag

Prosjektnummer: **2016-06**
For studieåret: **2015/2016**
Emnekode: **SFHO3201**

Prosjektnavn
Små Satellittmekanismer
Small Satellite Mechanisms

Utført i samarbeid med: Kongsberg Space

Ekstern veileder: Karl Patrik Mandelin, Jostein H. R. Ekre

Sammendrag: De siste årene har det vært et økt fokus på mindre og billigere satellitter som sendes opp av private aktører. Dette skaper etterspørsel for mindre og billigere tilleggsutstyr, blant annet en lavkostnad pekemekanisme for antenner. Etter over 6 måneder med planlegging, design og implementering, har vi utviklet en tidlig prototype av en slik mekanisme i aluminium og rustfritt stål. I tillegg har vi utviklet et kontrollsystem for å styre mekanismen.

Stikkord:
- Romfart
- Antennepekemekanisme
- Lav kostnad

Tilgjengelig: Ja

Prosjekt deltagere og karakter:

Navn	Karakter
Gisle Hovland Stenseth	
Magnus Dybendal	
Torstein Sundnes	
Elise Løken	
Stian Laugerud	
Vebjørn Orre Aarud	

Dato: 9. Juni 2016

_____
Sigmund Gudvangen
Intern Veileder

_____
Karoline Moholth
Intern Sensor

_____
Karl Patrik Mandelin
Ekstern Sensor

Antenna Pointing Mechanism Assembly

Bachelor thesis 2016

Group 6

Project: Small Satellite Mechanisms

Employer: Kongsberg Space

Doc ID: SSM-1010

i. Abstract

This is the bachelor thesis performed by Small Satellite Mechanisms in cooperation with Kongsberg Defence & Aerospace, division Space. The document contains an introduction, which gives a description of the project assignment, and summarizes the research and development process. The next sections are the "Project planning and description," "System design," "Test & verification" and "User manuals", where the project is described in detail. The document ends with the conclusion and status of the project and the group members' experiences throughout the project period.

ii. Contents

iii. Document history

Table 1: Document history

Rev.	Date	Author	Approved	Description
0.1	03.05.16	EL		Document created Added chapter 2-5. Written chapter 1 – Introduction
1.0	20.05.16	All	All	Reviewed and published

iv. Abbreviations

2D	Two-dimensional
3D	Three-dimensional
AA	Azimuth actuator
ADC	Analog-to-Digital Converter
AIT	Assembly, Integration and Test
APM	Antenna Pointing Mechanism
APMA	Antenna Pointing Mechanism Assembly
ATOX	Atomic oxygen
BLDC	Brushless Direct Current
Bw	Bandwidth
C	Compliant
C1	Construction 1
C2	Construction 2
C3	Construction 3
CAN	Controller Area Network
CCW	Counterclockwise
CM	Commanding microcontroller
CMC	Ceramic matrix composite
CNR	Carrier to noise ratio
CoG	Center of Gravity
COTS	Commercial off-the-shelf
CW	Clockwise
DAC	Digital-to-Analog Converter
dB	Decibel
dBi	Decibel(isotropic)
DC	Direct current
DI	Digital Input
DIO	Digital Input Output
DO	Digital Output
DSC	Digital Signal Controller

E1	Elaboration 1
E2	Elaboration 2
EA	Elevation actuator
ECSS	European Cooperation for Space Standardizations
EIRP	Equivalent isotropic radiated power
EL	Elise Løken
EMI	Electro Magnetic Interference
ESA	European Space Agency
FDTD	Finite-difference time-domain
FOC	Field Orientated Control
FPGA	Field Programmable Array
GHS	Gisle Hovland Stenseth
HDRM	Hold Down and Release Mechanisms
HPB	Half power beamwidth
HR	Human resources
HSE	Health safety and environment
Hz	Hertz
I1	Inception 1
IC	Integrated circuit
IDE	Integrated development environment
IF	Interface
IR	Insulation Resistance
KDA	Kongsberg Defence and Aerospace
KIFI	Kongsberg Institute of Engineering
LCA	Low-Cost Actuator
LEO	Low Earth Orbit
MCU	Microcontroller unit
MD	Magnus Dybendal
MIG	Metal inert gas
MMC	Metal matrix composite
NA	Not applicable

SSM
SMALL SATELLITE MECHANISMS

NC	Not compliant
NVIC	Nested Vector Interrupt Controller
OP-AMP	Operational Amplifier
PCB	Printed Circuit Board
PFPAE	Perflouropolyalkylether
PLL	Phase Locked Loop
PMC	Polymer matrix composites
PMSM	Permanent Magnet Synchronous Machine
PSU	Power Supply Unit
PTFE	Polyetraflurethylene
PWM	Pulse Width Modulation
R&D	Resource and development
RF	Radio Frequency
RF	Radio Frequency
RFN	Radio Frequency Feed network
RFS	Radio Frequency System
RJ	Rotary Joint
RX	Receive
SC	Spacecraft
SCC	Stress corrosion cracking
SITRAP	Situation report
SL	Stian Laugerud
SMD	Surface-mount device
SoC	System on Chip
SNR	Signal to noise ratio
SRA	Small Rotary Actuator
SRAM	Static Random Access Memory
SSM	Small Satellite Mechanisms
SV	Space Vector
SVPWM	Space vector pulse width modulation
T1	Transition 1

TBC	To be confirmed
TBD	To be determined
TC	Twist capsule
TIG	Tungsten inert gas
TRR	Test readiness review
TS	Torstein Sundnes
TX	Transmit
UART	Universal asynchronous Receiver/Transmitter
USN	University Collage of Southeast Norway
VOA	Vebjørn Orre Aarud
Wrt	With respect to
ZOH	Zero-Order Hold
SoC	System on Chip

1. Introduction

The purpose of the chapter is to give a systematic overview of the SSM project and to introduce the different analysis and reports performed by the group throughout the project. This chapter also refers to other chapters in the document to give an overview of where the different information is found.

List of figures

1.1. Task description and project planning

Kongsberg Space has developed an antenna pointing mechanism (APM) for Downlink Satellites. Present APM costs are set to €1M per unit and the weight of the mechanism is approximately 8 kg.

Low cost satellites represent a new interesting development in the market. For the same price as an APM (€1M), one can buy 2-5 of these satellites. Due to the cost, the already existing APM is not an applicable pointing mechanism for these satellites. The obvious need for a low-cost pointing mechanism is the baseline for this bachelor project. KDA wants to develop a new low-cost antenna pointing mechanism assembly (APMA) for Inter Satellite Links. The given assignment for the SSM project was a research study dealing with alternative solutions and concepts of this new APMA.

The SSM project group has established the system requirements, conceptually developed the APMA and made a real-life prototype of the system. Analysis and tests of the prototype have been executed to verify the system's performance.

A detailed description of the SSM project and its stakeholder, the planning process, the project model, a cost budget and the goals of the project are available in the "Project plan", chapter 2.1.

The system requirements were established early in the project. These requirements are created in cooperation with the employer; they are prioritized and divided into different categories. The mechanism shall be operative in space. This makes the assignment even more complex. Due to this, the project has important environmental requirements, which are crucial for many aspects of the project. Chapter 2.2 contains the "requirement specification" for the APMA.

A "Test & verification specification", ref. chapter 2.3, which is closely related to the "requirement specification", is also developed. This specification includes a plan for the verification of the requirements. At the end of the project, the specification is updated with test results from the functional testing of the real-life prototype. The tests were executed at the laboratory at KDA.

Evaluation of the risks associated with a project is highly important. Therefore, the SSM project group did a comprehensive risk analysis. The risks were defined and mitigation actions and a mitigation responsible was selected. During the project period, the total risk is clearly reduced through the mitigations. Chapter 2.4 contains the detailed "Risk Management", and shows the gradual reduction of the risks through three mitigation phases.

The group chose the unified process inspired "Iterative Development" model as the model for the project, and the project period was divided into seven time-boxed iterations. Before entering a new iteration, the tasks, activities and goals for the next iteration were planned. At the end of each iteration, the group wrote a situation and status report of the project's progressivity, which also included the plan for the next iteration. These reports are available in chapter 2.5.

1.2. Concept selection and verification

The concept of the APMA system had to be chosen before the design process of the mechanism could begin. In the "Concept analysis" in chapter 3.1, the most favorable concept for the mechanism was chosen: the double mirror reflector antenna. Two other concepts were also evaluated: "the APM with inclined mirror and offset reflector antenna" and "the gimbal APM with reflector antenna", the concept of the already existing mechanism. The three concepts are compared with respect to important criteria through a Pugh's concept selection matrix. Due to the high cost of rotary joints, they had to be avoided if the cost requirement was to be achievable. The double mirror reflector antenna has no rotary joints, while the inclined mirror concept has one, and the gimbal has two. In addition to some

other favorable aspects with the "double mirror reflector antenna" concept, this was the crucial reason for the selection of the final concept. Figure 1.1 shows a schematic drawing of the concept.
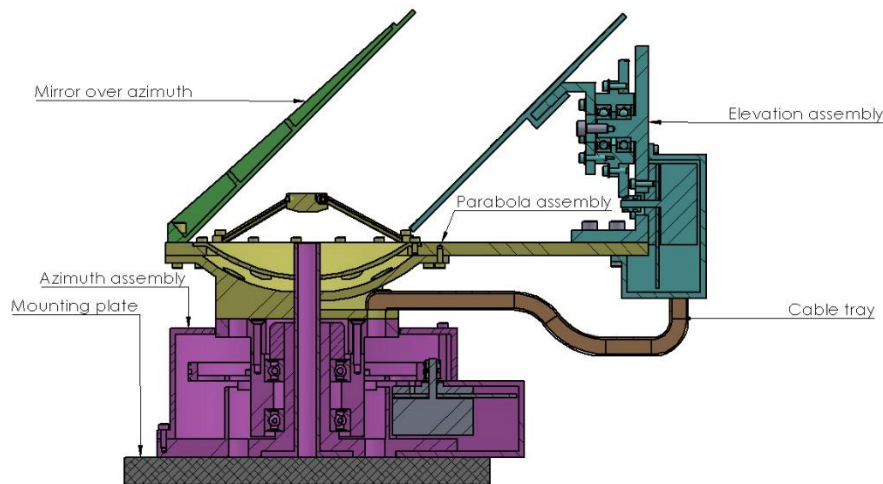

Figure 1. 1: Double mirror reflector antenna

A link analysis is a sum of all the gains and losses in a system, resulting in values for data transfer rates and signal to noise ratios. To check the feasibility of the concept, a link analysis was performed. The result of this analysis gave promising values for the data transfer parameters, and the SSM project was seen as feasible. The link analysis with corresponding reasoning, explanations and calculations is available in chapter 3.2.

The design process of the APMA started with top-level design of the mechanism and some technical budgets were created. When necessary, the budgets have been updated throughout the project. Chapter 3.3 contains mass budget, a power budget, a torque budget and a pointing budget. These budgets have been the baseline for the continued design of the mechanism, and some of the requirements are theoretically verified through them.

A research and development cost budget for the low-cost APMA is in chapter 3.4. This budget includes all the costs associated with the SSM project, the ordered parts and the hours spent on the project. The costs in the budget are divided into the three different disciplines (electrical, mechanical and software), and the total R&D cost of the project is also found; approximately 636 000 NOK.

1.3. Detailed system design

1.3.1. Electrical and software design

The detailed design of the APMA started with a "Component trade-off", where electrical components as motor, motor drive, microcontroller and antenna system was selected. The trade-off is available in chapter 3.5. Through the trade-off a STM32F415ZGT6 microcontroller, an EC 45 flat 70 W brushless direct current motor and the L6230 motor drive was chosen for the mechanism. The brushless DC motor was evaluated as the most favorable alternative with respect to the velocity, current and torque requirement for the project.

Through the trade-off, the concept for the antenna system was also chosen. After requests from the employer, the group performed a more detailed "Antenna trade-off", which compares the Cassegrain antenna system and the horn antenna system. Both alternatives are evaluated in detail and dimensioned in the trade-off. Due to the size of the antenna systems needed to reach the gain requirement, the Cassegrain antenna was chosen as the final antenna system for the APMA. The main reflector of the system has a diameter of 11 cm and a depth of 1.8 cm. The calculations and dimensions for both alternatives and the comparisons of them are fully covered in chapter 3.8. Figure 1.2 shows the dimensions of the antenna with the main- and sub-reflectors and the feed.
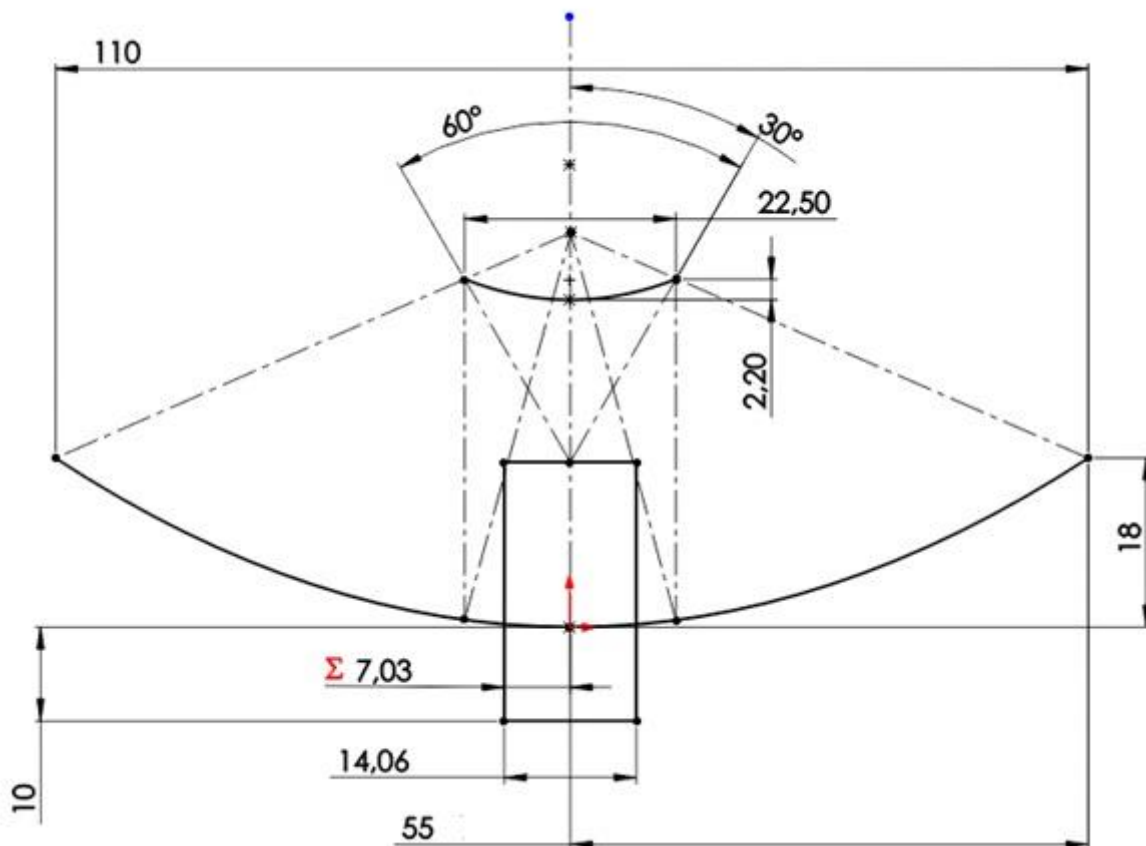
Figure 1. 2: Cassegrain antenna system design

The control system was the most comprehensive part of the electrical and software design in the project. The system controls the 3-phase brushless DC actuators driving both the azimuth and the elevation stages. Due to limited time, the group chose to focus on the azimuth stage.

The control system should be able to control the current, acceleration, velocity and position of the system. Due to this, the system is built as a cascade controller. The controller has three control loops; the inner current loop, the velocity loop and the outer position loop. Each loop contains PID controllers that controls the error of the feedback compared with the reference. Before the control system was implemented in software, a model of it was built, simulated, and tested in Simulink. Chapter 3.7 describes in detail the design and implementation of the control system. Figure 1.3 shows the top-level design of the control system.
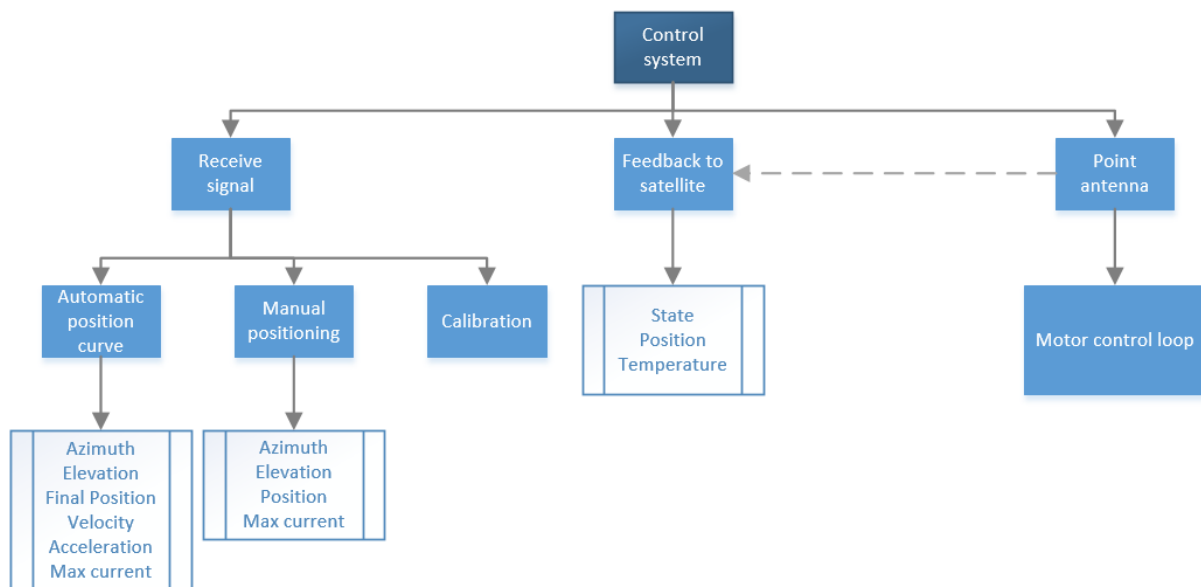
Figure 1. 3: Top-level control system design

Chapter 3.6. "Electrical design" describes the different circuits connecting the APM to the control system, including current measurement, voltage regulation circuits, motor drive circuits and microcontrollers. The chapter includes the final electrical design of the APMA and the design used for testing in the real-life prototype.

1.3.2. Mechanical design

In the mechanical part of the project, two comprehensive mechanical studies have been performed, and a DAK model of the system has been drawn.

The material and mechanical technology study, available in chapter 3.9, focuses on three different points: a study of different types of materials and how they behave in general and in space, a study of bearing behavior in space and in general, and a study of lubricant behavior in space.

The goal for this study has been to collect the right data, to enable selection of the correct materials for the bearings and lubricants for the project. The antenna and the structure will be made in aluminum AA1050. Two radial bearings are chosen for the APMA and stainless steel 440C as the material for use in the bearings. The lubrication selected through the study is grease. Braycote 601EF is recommended.

A bearing setup is also executed in the project and is included in chapter 3.10. This chapter shows estimations of the loads that can be observed in bearings during operation. Different setup and bearing types are discussed to optimize load distribution. Through the study, clamping, preload, friction, etc. are calculated and the chosen bearing for the azimuth stage of the APMA is the W6005 deep grove ball bearing. For the elevation stage, the W6000 deep grove ball bearing is chosen.

A detailed "Design description" of the DAK model is available in chapter 3.11. Here, the design of different assemblies of the APMA is described and the dimensions given. The chapter also includes 2D-drawings of all the parts of the mechanism. Devotek and Koberg manufactured some of these parts, and some were 3D-printed. The group assembled the real-life prototype. A report from the assembly of the mechanism and the adjustments that had to be done is given in chapter 3.12, "As built". Figure 1.4 shows a picture of the prototype.
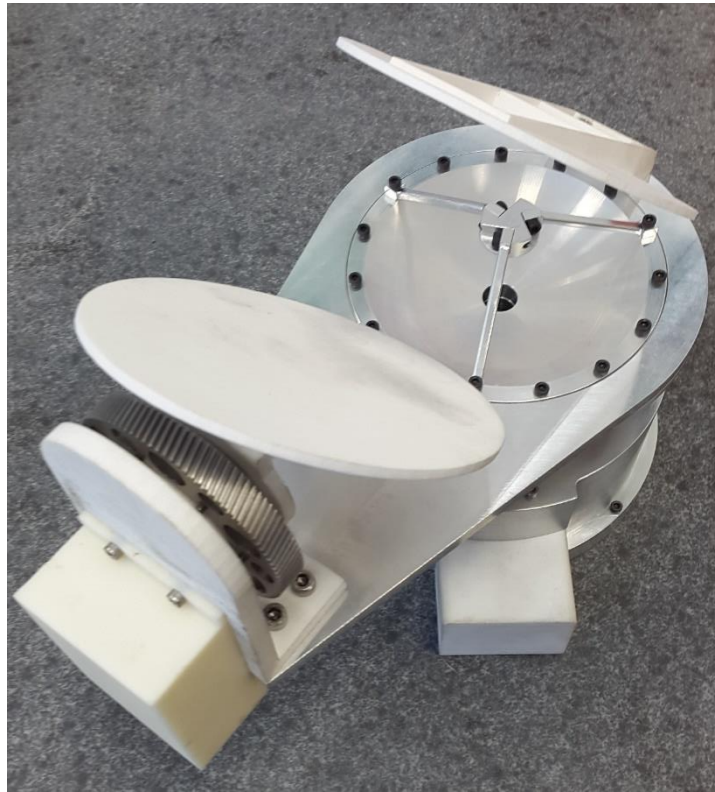
Figure 1. 4: Real-life prototype of the APMA.

1.3.3. System verification and validation

Some of the system requirements are verified through a functional test of the prototype. Through the test, torque, pointing accuracy and current was measured. These measurements are compared with the requirements and the calculated values for the APMA in the test report. Due to limited time, thermal vacuum test and life-test was not prioritized.

Chapter 4.1 contains the test procedure for the functional test that was executed. The test report and results are available in chapter 4.2.

In chapter 5.1 and 5.2, user manuals for the assembly of the mechanism and of how to send commands and communicate with the APMA are included.

2.   Project planning and description

2.1. Project plan

i.   Abstract

The purpose of this chapter is to present how the group will work throughout the project to ensure completion of the final goals. It visualizes the plan for the project period and lays the baseline for the continuation of the project.

ii. Contents

SSM
SMALL SATELLITE MECHANISMS

v. Document history

Table 2. 1. 1: Document history

Rev.	Date	Author	Approved	Description
0.1	27.01.16	TS, EL	-	Document created
0.2	28.01.16	TS, EL	GHS, SL	Corrected language Changed title 5 from abstract to scope Introduction deleted (7) Goals (7.6) deleted Figure 5 updated
1.0	29.01.16	TS, EL	GHS	Updated assignment description (7) Updated responsibilities (6.3) Updated primary stakeholder (7.2.1) Updated Gantt-chart(fig. 6 and 7) Updated dates in activity list(table 3) and milestones(table 4) due to new Gantt Updated table 3, activity list, with new activities Updated figure 8 Updated construction phases to three Updated risk analysis(11)
1.1	08.02.16	TS, EL	SL	Updated activity list(table 3) Changed test specification to test & verification specification
1.2	23.02.16	EL		Changed document layout Updated with link to the webpage Updated activity list Updated figure 4 Updated figure 5
2.0	02.03.16	EL	MD	Created and reviewed rev. 2.0
2.1	03.05.16	EL		Updated activity list Updated cost budget Changed layout into the final report layout.
3.0	18.05.2016	TS, EL	TS	Reviewed and published

2.1.1. Introduction

The purpose of this project plan is to present the project group and the given assignment. The chapter also contains the choice of project model and a long-term plan for the project. This includes an activity list where time consumption is estimated.

This section contains a presentation of the members of this project, a description of the given responsibilities, an overview of the supervisors and examiners, and the group's objectives.

The group consists of two mechanical engineering students, three electrical engineering students and one software engineering student. This interdisciplinary project contains the following members and responsibilities:

2.1.1.1. *Group members*
Table 2. 1. 2: Group members

Gisle Hovland Stenseth
Electrical engineering
Mail: Gislur@gmail.com
Phone: +47 47409066

Main responsibilities:
Group leader
Interface

Magnus Dybendal
Mechanical engineering
Mail: magnus.dybendal@gmail.com
Phone: +47 45506470

Main responsibilities:
Construction

Torstein Sundnes
Software engineering
Mail: torsun@hotmail.com
Phone: +47 47759989

Main responsibilities:
Documentation

Elise Løken
Electrical engineering
Mail: elise.loeken@gmail.com
Phone: +47 41845614

Main responsibilities:
Documentation

Stian Laugerud
Electrical engineering
Mail: Stian_laugerud@hotmail.com
Phone: +47 47238500

Main responsibilities:
Test & verification

Vebjørn Orre Aarud
Mechanical engineering
Mail: vebjrn_aarud@live.no
Phone: +47 93286539

Main responsibilities:
Test & verification

2.1.1.2. *Supervisors and examiners*

Internal supervisor:
Name: Sigmund Gudvangen
Phone: +47 31008905
Mail: sigmund.gudvangen@hbv.no

Internal examiner:
Name: Karoline Moholth Mcclenaghan
Phone: +47 31008898
Mail: Karoline.moholth@hbv.no

External examiner and supervisor:
Name: Karl Patrik Mandelin
Phone: +47 41477668
Mail: karl.patrik.mandelin@kongsberg.com

External supervisor:
Name: Jostein Ekre
Phone: +47 95885549
Mail: Jostein.Ekre@kongsberg.com

2.1.1.3. *Responsibilities*

Responsibilities in this project have been chosen according to the specified task description.

Project leader
The group's project leader has been selected primarily for his connection to KDA. Thus, he has the main responsibility of communication with the employer.

The project leader is responsible for:

- Assigning duties and general supervision of the project.
- Making sure the group is on schedule according to the short- and long-term plans.
- Verifying all executive decisions.
- Ensuring good communication within the group.
- Ensuring the inclusion of group members.
- Dialogue with stakeholders.

Interface
The interface responsible is tasked with:

- Managing disciplinary interfaces
- Ensuring dialogue internally in the project.
- Coordinating documentation of operating instructions.
- Coordinating documentation of disciplinary interfaces.

Construction
The construction responsible is tasked with:

- Managing the projects design and construction.
- Coordinating the documentation concerning design.

Test & verification

The test and verification responsible is tasked with:

- Ensuring the testing and verification of the overall system.
- Supervising testing.
- Creating testing plans and documentation.

Documentation manager

The documentation managers are responsible for:

- Writing, controlling and mailing the summaries of:
  - Meetings.
  - Follow-up documents.
- The correct usage and creation of:
  - Mandatory documents.
  - Document standard.
  - Layouts.

2.1.1.4. *Objectives*

This section describes the objectives and the motivation for the SSM project group to complete this project with the highest determination.

The group members are all motivated to put in enough effort and time in the project to get the best result and grade as possible. An estimate of planned time consumption in this project is documented in the main plan (section 2.1.5)

The group will deliver a high quality product, conceptually and physically, that satisfies the employer. A good result requires dynamic and progressive work during the whole project period. The group contract, which is a part of the documentation, contains the main rules and goals for the group.

During the project, the group will attain experience and learn more about working as systems engineers in a professional market with professional facilities. The project lifecycle will also result in more knowledge about how crucial the different phases in a development process are, to achieve a successful project.

2.1.2. Assignment

This assignment is written in cooperation with Kongsberg Defence and Aerospace, division Space. Since October 2015, the group has established the framework for this bachelor thesis together with an external examiner and supervisor.

Kongsberg Space has developed an antenna pointing mechanism (APM) for Downlink Satellites. Present APM costs are set to €1M per unit.

The low cost satellites are a new interesting development on the market. For the same cost as an APM (€1M), you can get 2-5 of these satellites. Due to this, KDA wants to develop a new antenna pointing mechanism assembly (APMA) for Inter Satellite Links, yet low cost. The given assignment is a research study dealing with alternative solutions and concepts for this new APMA.

This pointing mechanism will have two-way communication simultaneously, in contrast to the original one, functioning only simplex. This may result in one additional antenna to the construction. The

requirements will also be notably reduced as the system will be (relatively) low-cost, low mass and an increased amount of units will be produced.

The group is going to establish a system requirement baseline and conceptually develop an APMA (including drive electronics) for use in the small low cost satellites, and further develop and prototype critical areas. Through tests of prototypes and/or analysis, the performance of the low cost APMA will be verified.

2.1.2.1. *Kongsberg Defence & Aerospace*

Kongsberg Defence and Aerospace is Norway's premier supplier of defence and aerospace-related systems. A large company with several divisions and subdivisions. KDA delivers products and systems for command and control, weapons guidance and surveillance, communications solutions and missiles, and advanced composites and engineering products for the aircraft and helicopter market.

This assignment is made in collaboration with Kongsberg Space, one of five operational units in the Space and Surveillance division. The other units of this division are Kongsberg Norspace AS, Kongsberg Norcontrol IT AS, Kongsberg Spacetec AS and Satellite Services.

Space and Surveillance delivers a broad spectrum of equipment, system and services related to space and maritime surveillance customers in more than 40 countries. This includes components for the European heavy-lift launcher Ariane 5, different satellites (communication and earth observation) and scientific space probes. The division is a world-leading supplier of satellite ground stations for downloading and processing satellite data, and of satellite services from ground stations.

Kongsberg Space is Norway's largest supplier of equipment and services to the European Space Agency (ESA). [5]

2.1.2.2. *Stakeholders*

Stakeholders are those who have interest in a project or organization. They are often categorized as primary- or secondary stakeholders. Primary stakeholders are those directly affected by the project, while secondary stakeholders are those who have indirect relations to it.

2.1.2.2.1. Primary stakeholders

Primary stakeholders for the SSM project are:

- University College of Southeast Norway (USN): This project is the final bachelor thesis of our engineering education at USN. Because of this, USN is one of the main stakeholders. They have their own requirements (documentation, time planner, presentations) to the project, and the internal supervisor and examiner is given by them.
- Kongsberg Defence and Aerospace (KDA): This project is a research study dealing with alternative solutions and concepts to an already existing mechanism developed by KDA. They are the employer in this project and a main stakeholder.
- Small Satellite Mechanisms (SSM): The project group, which is going to develop the concept of the new APMA, is a stakeholder in this project.
- Examiners and supervisors: Examiners and supervisors (internal and external) have direct influence on the project itself and the project process.

2.1.2.2.2.   Secondary stakeholders

Secondary stakeholders for the SSM project are:

- The customers and users, who are buying the APMA of Kongsberg Defence and Aerospace.
- Suppliers of the different parts of the APMA.
- Maintainers of the APMA during its lifecycle

2.1.2.3. *Life Cycle assessment*

In the SSM project, the design of the new Antenna Pointing Mechanism Assembly is developed with life cycle requirements. This means that the whole lifeline of the product, from conception to disposal, will be considered when designing the APMA. There are some lifecycle requirements for the mechanism from KDA, which must also be satisfied. These are specified in the Requirements Specification.

2.1.2.4. *Prerequisites*

All formal documentation will be written in English. This is a Kongsberg standard set in place due to the company dealing with international customers and employees. The project presentations will be documented in English, but the presentations themselves will be Norwegian.

Kongsberg Space is expected to pay for any parts or services needed in direct connection with the product/process. Any costs related to supplies for working space and other non-essential equipment will be provided by the group itself, with some exceptions.

Documents describing the standard requirements and functionality of previous systems will be available from Kongsberg Space. This includes standards and handbooks for requirements.

Significant changes in the requirements given by KDA will not be accepted after 23.03.2016.

2.1.2.5. *Boundaries*

The system-of-interest will be taken apart and the group will decide which parts to focus on. This includes physical parts, but also requirements and tests that are deemed too complex for a bachelor project lasting one semester.

The given assignment is to create an antenna pointing mechanism. The main focus will be the construction of the pointing mechanism, including material choices, and the control system of this mechanism. Additionally, considering gain margins and possible multiplexing of the antenna link. Specifics may be added at a later date, but for the moment these are the main sections currently looked to improve. The start phase will be to see the project as a whole, and eventually take a closer look at the individual critical parts of the system.

Another important factor is the time/cost/quality aspect of the project. If there are a lot of requirements to increase the quality of the product, the cost and time may increase. If we do not put in enough work hours, the quality will be decreased and the cost may increase later in the development if there are grave errors. This is constantly kept in mind while coming up with new concepts and ideas for the project.

2.1.3. Project model

The choice of our working model is explained in this section. The choice represents the group's work-methods and the project setup. The selected model will determine the scheduling, iteration, layout and revision of all group activities and project content.

2.1.3.1. *Spiral model*

When costs and risks are important drives and the systems contains complex requirements, the spiral model is an efficient project process. It is a dependable and secure way of ensuring a well-documented and revised system, but also ensures an iterative way of ensuring the quality of the system. The solid documentation control makes the administrative processes move fluently forward, ensuring a well-documented and thorough system.
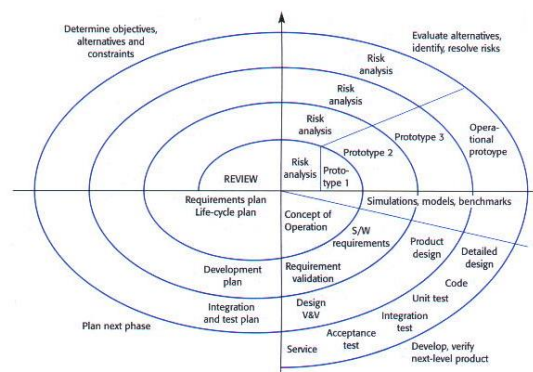

Figure 2. 1. 1: Spiral model [7], p. 113

This systems design relates to a complex system with many aspects. In the start-up of the project, there are only the top-level requirements, which rely on a good model for iteration. It is important to ensure that the model chosen will give a good progression during the project.

We have chosen to discard the spiral model due to the risk of limited iterations during the course of the project. Choosing the spiral model possibly results in an incomplete and unfinished product, if deadlines for iterations are not specified in the model. Moreover, early internal work has been consistent with the unified process, making it intuitive to proceed with this model.

2.1.3.2. *Unified process*

The Unified Process is a process development model, common in the development of software. Advantages with this model are the ensuring of iteration and the increments, by use of time boxing in the different phases. The Unified Process is also risk focused, which is an important part of our project.

The process has four main phases, where each phase divides into one or more iterations. The main phases are inception, elaboration, construction and transition. In each phase, there are also six stages, which are differently weighted. Their stages are business modeling, requirements, analysis and design, implementation, test and deployment.
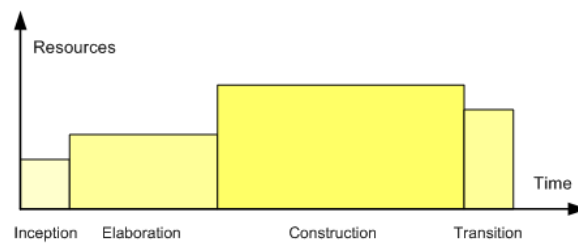
Figure 2. 1. 2: Typical relative size of the four phases of the Unified Process. [6]

2.1.3.2.1.   The inception phase

This is the start-up of the project and it should be quite short. The goal with this phase is to establish the frame of the project. This includes the establishing of the project scope and boundaries, a preliminary project schedule and an estimation of the cost of the project. Outlines of top-level requirements and architecture that will drive the design of our system, a feasibility evaluation and a risk analysis should also be included. Main stages are business modelling and requirements. The first presentation will be the final milestone in this phase.

2.1.3.2.2.   Elaboration Phase

Elaboration is the second phase in the Unified Process. It is separated into two time box iterations (E1 and E2). This phase includes definitions of the majority of system requirements, establishing and validation of system architecture and addressing of risk factors. The important stages are business modelling, analysis and design, and early implementation. Use cases and conceptual diagrams are often created in this phase. It is assumed that the second presentation will be a part of this phase.

At the end of the Elaboration phase the architecture shall satisfy the main system requirements for functionality, performance and cost.

2.1.3.2.3.   Construction phase

This phase is the most comprehensive, and is separated in four time boxed iterations. Detailed design, implementations, early testing and deployment are the main stages. By doing this in three iterations, the quality of the system is ensured. The time needed for testing in the last iteration should be less than the others, since most of the errors have already been improved in earlier iterations. This is visualized in the long-term project plan.

2.1.3.2.4.   Transition Phase

This is the final phase of the process, which includes the completion of the design, construction, implementation and testing. At the end of this iteration, the system shall satisfy its requirements and have the desired operational functionality. The system shall be deployed to the target users, and the phase also includes conversion and user training.

In this phase, the project needs to be completed. This includes the hand-in of the final report and documentations, and lastly the third and final presentation.
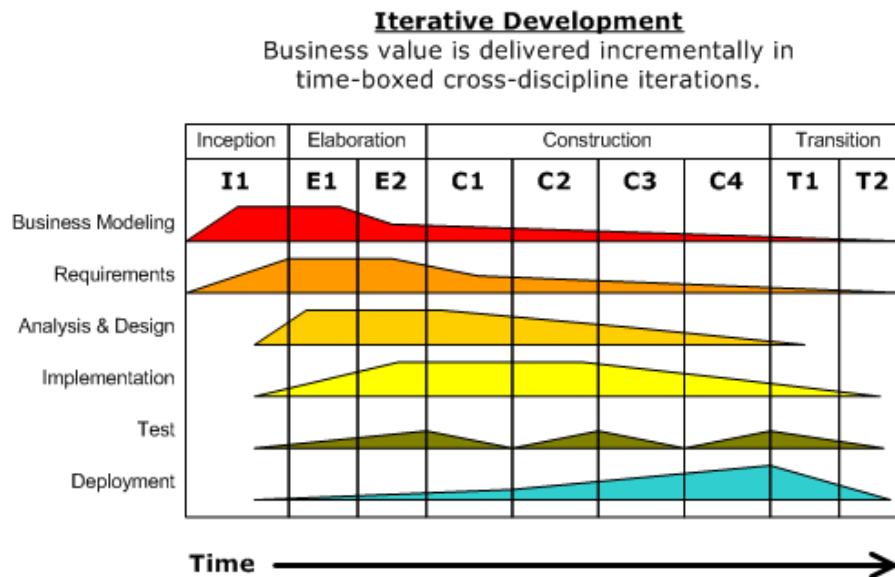

Figure 2. 1. 3: Unified Process Iterative Development [6]

2.1.3.2.5.   Project phases and deadlines

For this project we have decided not to use "use cases", and then the project model becomes only an iterative model. Listed below is a table, which shows the time boxed iterations the project is planning to carry out during the project. Clear goals will also be defined for each time box in the iterations reports. These reports will be written at the end of each iteration, and is a situation report and a plan for the next iteration [2]. Each iteration has a deadline, and at these deadlines, there is going to be a situation report (SITRAP). This report will contain a description of the work progression, if we accomplished our goals or not, and what to do next.

Table 2. 1. 3: Model phases for the project

Phase	Description	Start	Finish
I:1	Inception 1	11.01.2016	02.02.2016
E:1	Elaboration 1	10.02.2016	03.03.2016
E:2	Elaboration 2	14.03.2016	25.03.2016
C:1	Construction 1	07.04.2016	17.04.2016
C:2	Construction 2	18.04.2016	24.04.2016
C:3	Construction 3	25.04.2016	08.05.2016
T:1	Transition 1	09.05.2016	15.05.2016

2.1.4. Activities

In this section the different activities used during the project will be explained, to ensure progress and quality. The main groups of activities are administrative and curricular. At the end of this section, an activity list is included.

2.1.4.1. *Administrative activities*

The administrative activities are general procedures and routines for the project. They will be used periodically as an important part of the project framework.

2.1.4.1.1.   Meetings

This project has many stakeholders and a good communication process is crucial for success. Good procedures and periodically communication is considered an important part of the project. To achieve this, different meeting forms will be used:

2.1.4.1.1.1.   Internal group meetings

Several times a week. It is a short internal meeting, where only the group members are present. The agenda for these meetings is typically a situation report and short-term planning. If important group decisions are necessary, this is the meeting, which shall be performed. The group will not write minutes of meetings, but will ensure that important decisions are well documented.

2.1.4.1.1.2.   Internal group meetings with supervisor

Every Monday morning at 9.00, a weekly group meeting is set with the internal supervisor. The meeting will be a status report of how the project is going. The follow-up document, which includes information about the work done the preceding week, and plans for the following week, is discussed with the supervisor. There will also be time for guidance and important questions and issues, and internal supervisor has the opportunity to give constructive feedback. Minutes of meetings will be written and sent to all participants within twenty-four hours after the meeting.

2.1.4.1.1.3.   External group meeting with supervisor

Every second week there should be a meeting with the external and/or internal supervisor. This will be a status meeting where the employer will be updated on the progress in the project, and further work. Relevant issues and feedback will be given in bidirectional communication. Minutes of meetings will be written and sent to all participants within twenty-four hours after the meeting.

2.1.4.1.2.   Follow-up document

At the end of every week, there will be created and sent a follow-up document to internal and external supervisor. The document contains a summary of the work done the preceding week and a short-term plan for the following week. It also provides information about the general status of the project, critical areas and schedule. The tasks focus areas and activities for every group member will be specified individually, and the timesheets enclosed.

The document will be a part of the agenda for the Monday meetings with internal supervisor.

2.1.4.1.3. Presentations

Three presentations are set up during the project period. Examiners (internal and external), supervisors (internal and external) and the group members have to be present.

The frame of the first and second presentation is the same, but the content will differ. The presentations are divided into two parts:

- Public presentation(maximum 20 minutes)
- Oral examination/questioning(includes all related topics within the project)

2.1.4.1.3.1. The first presentation

In the first presentation, there will be an introduction to what is to be done in the project, and how this is to be executed. The process of the project is significant and important in this presentation. The first presentation is a final evaluation of the draft for the following documents:

- Project plan
- Requirements specifications
- Test & verification specifications

2.1.4.1.3.2. The second presentation

This presentation shall be more technical than the first one. It contains a walkthrough, status and the remaining activities of the project. The choice of concept and system tests will be explained.

2.1.4.1.3.3. The third presentation

The third presentation is the final presentation of the project. The final report and documents have to be completed, and after the presentation, there will be an oral examination if necessary. This presentation is divided into three parts:

- Sale of the product(20 minutes)
- Technical presentation(20 minutes)
- Questioning of the whole group (20 minutes)

All group members are required to perform during the first two presentations.

2.1.4.1.4. Webpage

A mandatory part of the project is to develop and design a webpage for the project. The webpage will be a simple, yet descriptive information sheet with information regarding the project, group members and presentations. It gives the reader an overview of the SSM project group and the assignment given by KDA.

The webpage is available at: home.hbv.no/web-gr6-2016

2.1.4.2. *Disciplinary activities*

Disciplinary activities are the other main part of the project activities. They includes all activities that have direct disciplinary connection with the APMA development. For the long-term plan, the disciplinary activities are not, but will be, specified progressively throughout the project. So far, the disciplinary activities are divided into the following sub activities:

- Mechanical:
  - Mechanical design
  - Modelling and numerical mathematics
  - Final element analysis
- Electrical/software:
  - Control systems
  - Antenna system design (amplification, size)
  - "CANbus" interface

2.1.4.3. *Activity list*

Table 2.1.4 gives an overview of already planned activities for this project. Each activity is specified with a unique number, a time estimate and a deadline (for the iteration). The table also shows who has the main responsibility for the activities.

Table 2. 1. 4: Activity list with time estimation from the long-term plan in Microsoft Project.

Activity nr.	Activity description	Who	Time estimate (hrs)	Deadline
900	Concept draft	All	80	15.02.2016
1000	Administrative tasks (revisions/iterations)	All	200	
1001	Project plan	TS, EL	100	02.02.2016
1002	Iteration reports	All	20	13.05.2016
1003	Presentations	All	25	
1010	Final documentation	All	100	23.05.2016
1100	Meetings	All	50	
1200	Risk document	All		13.05.2016
1300	R&D cost budget	VOA		13.05.2016
2000	Requirements specification	GHS, MD	100	02.02.2016
3000	Test& verification specification	VOA, SL	100	02.02.2016
3001	Testing	All		13.05.2016
3002	Test procedure	SL, GHS		01.05.2016
4000	Webpage	TS, EL	25	21.01.2016
5000	Simulation/testing	All	330	
5100	Design (prototype 1)	All		25.03.2016

5110	Electric design (prototype 1)	SL, EL, GHS	340	25.03.2016
5111	Technology document - electrical	GHS, EL, SL		
5112	Link analysis	GHS		
5113	Motor drive	GHS, EL, SL		
5114	Control system - electrical	GHS, EL, SL		
5120	Mechanical design (prototype 1)	VOA, MD	270	25.03.2016
5121	DAK	VOA, MD		
5122	FEM	VOA, MD		
5123	Mechanical documentation	VOA, MD		
5130	Software design (prototype 1)	TS	200	25.03.2016
5131	Software design document	TS		
5132	Control system - software	TS		
5200	Design functional (prototype 2)	All		17.04.2016
5210	Electric design (prototype 2)	SL, EL, GHS	300	17.04.2016
5211	Antenna Trade-off	EL, GHS		
5220	Mechanical design (prototype 2)	VOA, MD	230	17.04.2016
5221	DAK E2	MD		
5222	FEM	VOA, MD		
5223	Bearing report	VOA, MD		
5230	Software design (prototype 2)	TS	180	17.04.2016
5231	Control system design	TS, GHS, EL, SL		
5300	Design functional and acceptable (prototype 3)	All		24.04.2016
5310	Electric design (prototype 3)	SL, EL, GHS	180	24.04.2016
5320	Mechanical design (prototype 3)	VOA, MD	150	24.04.2016
5321	DAK C1	MD		
5330	Software design(prototype 3)	TS	110	24.04.2016

5400	Design functional and acceptable (prototype 4)	All		18.04.2016
5410	Electric design (prototype 4)	SL, EL, GHS	160	08.05.2016
5420	Mechanical design (prototype 4)	VOA, MD	130	08.05.2016
5430	Software design (prototype 4)	TS	100	08.05.2016
5443	Design Description			
5500	Assembly and test setup	All	300	
5900	Material analysis	VOA, MD		
5901	Technical budgets	VOA, MD, EL		
6000	Assembly	VOA, MD		
10 000	Part verification			
Total time estimation				**3780**

2.1.4.4. *Milestones*

Table 2.1.5 shows the milestones for the project, also visualized in the long-term plan from Microsoft Project.

Table 2. 1. 5: Milestones of the project

Date:	Milestone:
02.02.2016	Completion of inception phase (I:1) - Revision 1.0 of requirement specification completed - Revision 1.0 of test & verification specification completed - Revision 1.0 of project plan completed SITRAP
05.02.2016	*First presentation*
03.03.2016	Completion of elaboration phase 2.1 - Evaluation of concepts, select final concept - Draft of concept design(prototype1) completed - Testing of prototype 1 - SITRAP Revision updates of documents
09.03.2016	*Second presentation*
25.03.2016	Completion of elaboration phase 2.2 - Functional design(prototype2) completed - Testing of prototype 2 - SITRAP Revision updates of documents
17.04.2016	Completion of construction phase 3.1 - Functional design updates (prototype 3) completed - Testing of prototype 3 - SITRAP Revision updates of documents
25.04.2016	Completion of construction phase 3.2

	- Functional and acceptable design(prototype 4) completed - Testing of prototype 4 - SITRAP Revision updates of documents
08.05.2016	Completion of construction phase 3.3 - Physically development of the APMA - System testing with test reports - SITRAP Revision updates of documents
15.05.2016	Completion of transition phase 4.1 - Deployment and sale - SITRAP Revision updates of documents
23.05.2016	*Deliver the final report*
08.06.2016	*Final presentation*

2.1.5. Main plan

This section describes and gives examples of different plans used in the SSM project. The group is using a long-term plan, short-term plans and timesheets to plan and document what will be done and what is completed. Explanations and examples of the different plans are given below.

An estimate of a cost budget is also introduced in this section.

2.1.5.1. *Short-time planner*

This plan describes the weekly planning and progression of the work in details. At the end of each week, a short time plan is made for the next seven days. The plan visualizes the activities prioritized the next week, and contains a distribution of the group resources. The purpose of this plan is for a group member to know exactly which activity/activities to work with at any time. Figure 2.1.4 shows an example of a short-term plan:

Who:	Activity number:	Description:
Gisle	5110 5130	Electrical design Design of motor drive Control system Design Control system Software
Magnus	5100 5120 5901	Prototype 1 model (simulation) Mechanical design Mass- and torque budget
Torstein	5110 5130	Electrical design Software Design Control system Software Control system Design
Elise	5110	Electrical design Design of motor drive Control system Design
Stian	5110	Electrical design Design of motor drive Control system design
Vebjørn	5100 5120 5901	Prototype 1 model (simulation) Mechanical design Mass-and torque budget

Figure 2. 1. 4: Short-time plan

2.1.5.2. Timesheets

To documet what each group member is doing, individual timesheets will be written. The timesheets are updated daily, and lasts for a week. They show which activity is being worked with that specific day and how much time is spent on it. An example of a timesheet is given below.

Timesheet week 5

Activity	Activity description	Gisle H. Stenseth							Torstein Sundnes							Elise Løken							Total hours per activities:
		Mo	Tu	We	Th	Fr	Sa	Su	Mo	Tu	We	Th	Fr	Sa	Su	Mo	Tu	We	Th	Fr	Sa	Su	
0900	Concept			2	2	1					2	2	1					2	2	1			30
1000	Project general activities	2							2	2						2	1						24
1001	Project plan	2,5	9													2	2	2					42,5
1002	Iteration report																						4
1003	Presentation			3	3	2										0,5	4	1	3	2			28,5
2000	Requirement specification								2	3	3	3	2										13
3000	Test specification																						0
3001	Testing																						0
4000	Webpage																						0
5111	Electrical technology doc																						0
5110	Prototype Electrical																						0
5130	Software design																						0
5120	Prototype Mechanical																						0
5900	Material study																						0
Total hours per day:		4,5	9	5	5	3	0	0	4	5	5	5	3	0	0	4,5	7	5	5	3	0	0	**Total hours this week:**
Total hours per week:		26,5							22							24,5							142

Figure 2. 1. 5: Time sheet

2.1.5.3. *Long-term plan*

The long-term plan is a timeline and a Gantt-chart, which visualize overarching activities, milestones and deadlines for the whole project period. The plan clearly defines the different phases and iterations planned for the project, due to the chosen project model.

The long-term plan will continue to be specified and updated throughout the project period. Figure 2.1.6 and 2.1.7 show an early draft of the long-term plan for the SSM project.
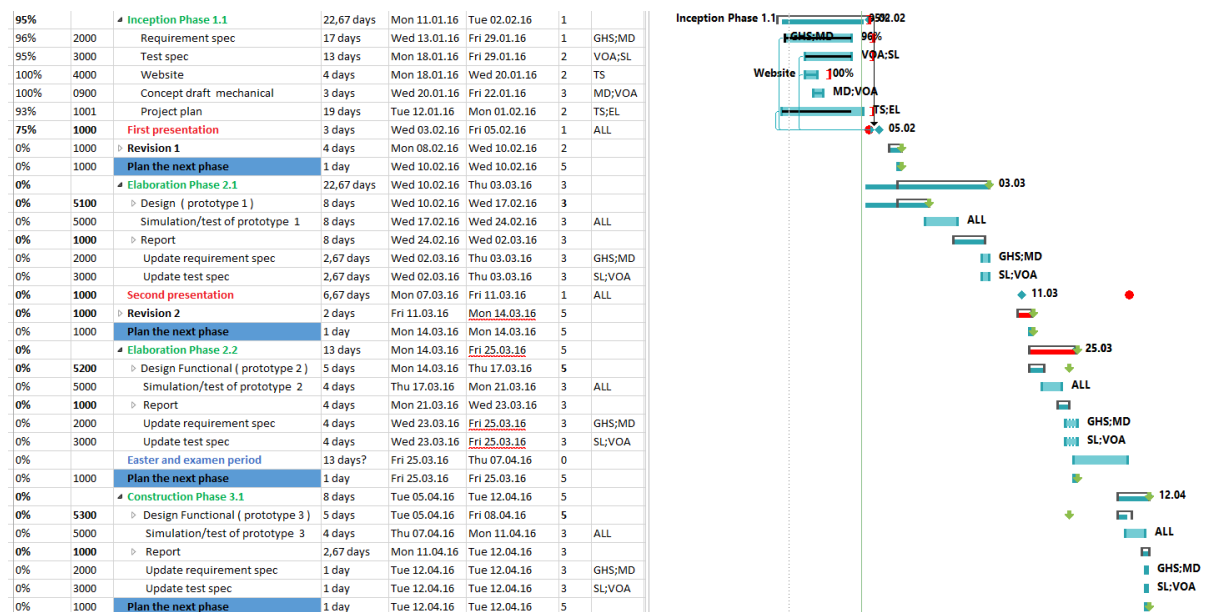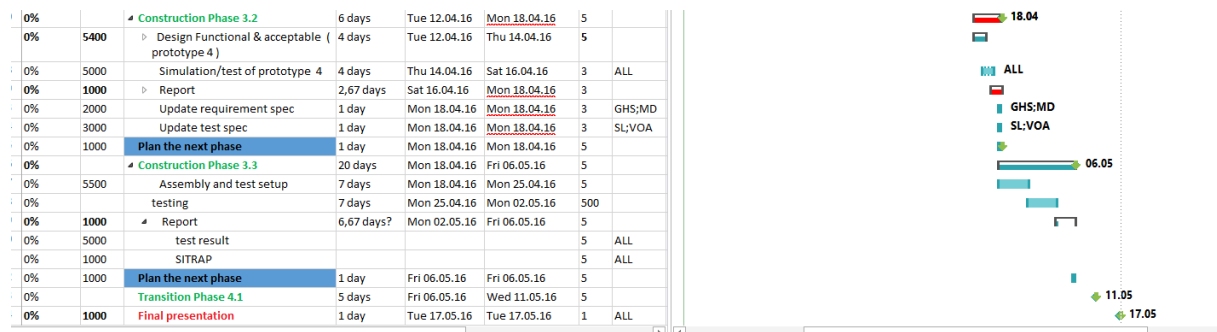

Figure 2. 1. 6: Gantt-chart, part 1

0%		◢ Construction Phase 3.2	6 days	Tue 12.04.16	Mon 18.04.16	5		
0%	5400	▷ Design Functional & acceptable (prototype 4)	4 days	Tue 12.04.16	Thu 14.04.16	5		
0%	5000	Simulation/test of prototype 4	4 days	Thu 14.04.16	Sat 16.04.16	3	ALL	
0%	1000	▷ Report	2,67 days	Sat 16.04.16	Mon 18.04.16	3		
0%	2000	Update requirement spec	1 day	Mon 18.04.16	Mon 18.04.16	3	GHS;MD	
0%	3000	Update test spec	1 day	Mon 18.04.16	Mon 18.04.16	3	SL;VOA	
0%	1000	Plan the next phase	1 day	Mon 18.04.16	Mon 18.04.16	5		
0%		◢ Construction Phase 3.3	20 days	Mon 18.04.16	Fri 06.05.16	5		
0%	5500	Assembly and test setup	7 days	Mon 18.04.16	Mon 25.04.16	5		
0%		testing	7 days	Mon 25.04.16	Mon 02.05.16	500		
0%	1000	◢ Report	6,67 days?	Mon 02.05.16	Fri 06.05.16	5		
0%	5000	test result				5	ALL	
0%	1000	SITRAP				5	ALL	
0%	1000	Plan the next phase	1 day	Fri 06.05.16	Fri 06.05.16	5		
0%		Transition Phase 4.1	5 days	Fri 06.05.16	Wed 11.05.16	5		
0%	1000	Final presentation	1 day	Tue 17.05.16	Tue 17.05.16	1	ALL	

Figure 2. 1. 7: Gantt-chart, part 2

Figure 2.1.8 below gives an estimated overview of the time consumption (in working days) for the phases in this project. It also specifies the time of the different activities in each phase.
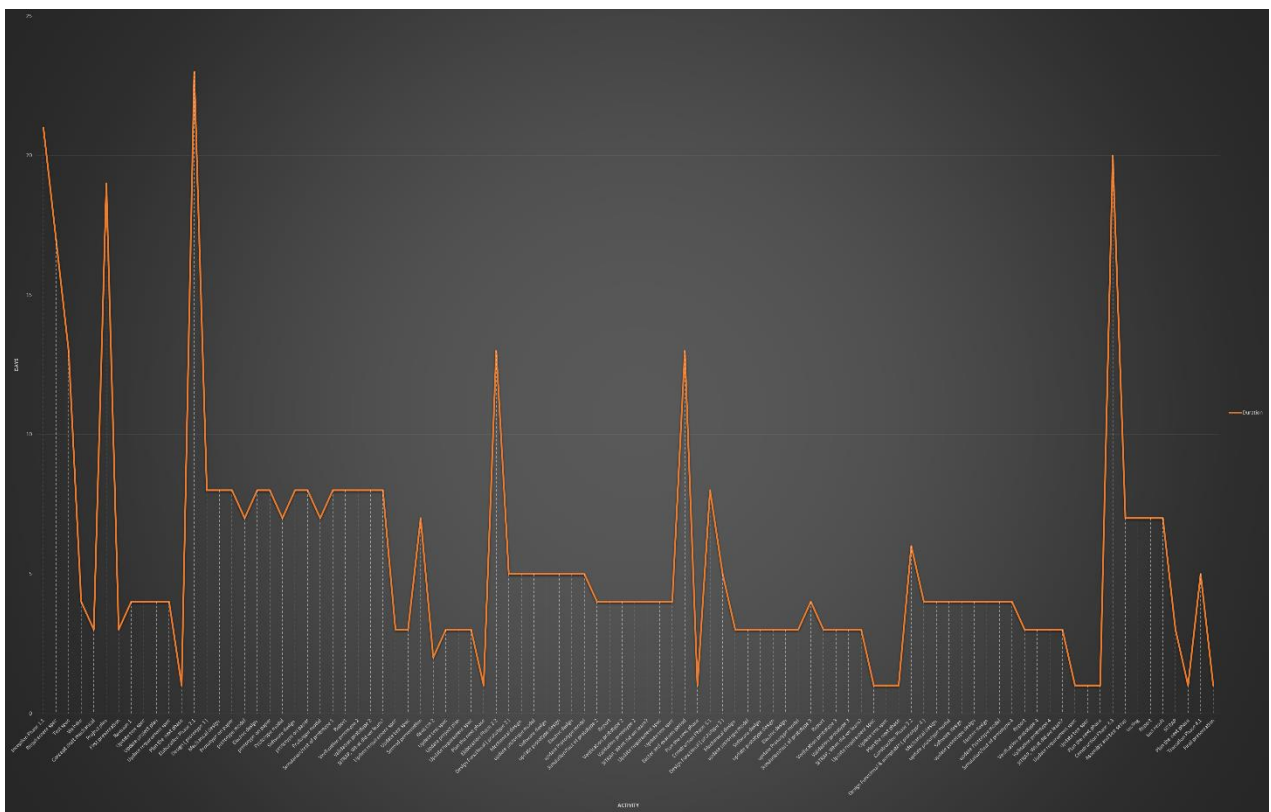
Figure 2. 1. 8: Time estimation (in days) at the different phases in the project

2.1.5.4. Cost budget

This section contains an estimation of a cost budget. The budget is divided in two parts, a budget for the SSM project and a budget for the APMA, based on 1000 produced units. KDA has a requirement to the reel cost of the mechanism itself, maximum €10k.

Table 2. 1. 6: Project budget

Project budget

Description	Price (€)	Amount	Total price (€)
Motor with encoder	300	4	1200
Circuit board (evaluation kit)	300	2	600
Waveguide	300	1	300
Cables	50	1	50
Antenna	1000	1	1000
Bearings	150	2	300
Construction	5000	1	5000
Total			**8450**
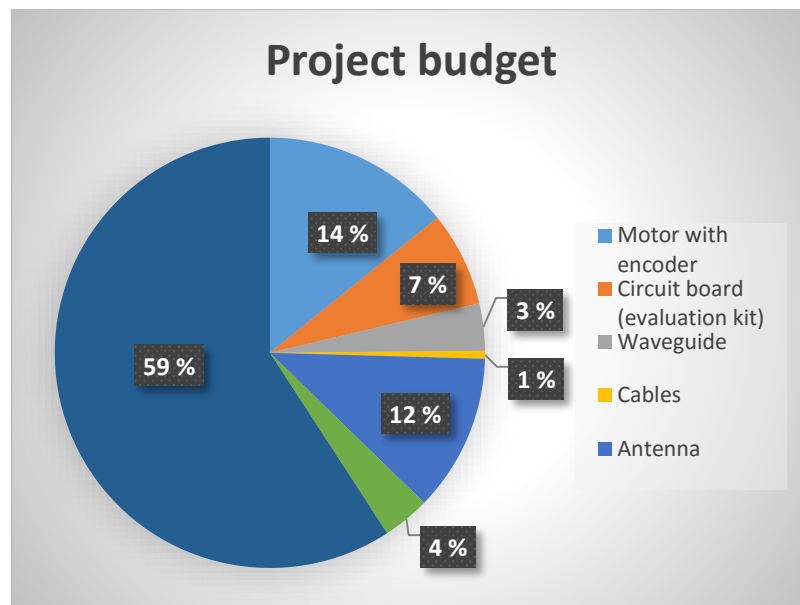
Figure 2. 1. 9: Project budget - sector diagram

Table 2. 1. 7: Cost budget - 1000 units

Budget - 1000 units

Description	Price (€)	Amount	Total price (€)
Motor with encoder	200	2	400
Circuit board	200	1	200
Waveguide	200	1	200
Cables	50	1	50
Antenna	700	1	700
Bearings	100	2	200
Construction	3500	1	3500
Testing	2000	1	2000
Assembly	1000	1	1000
Total			**8250**
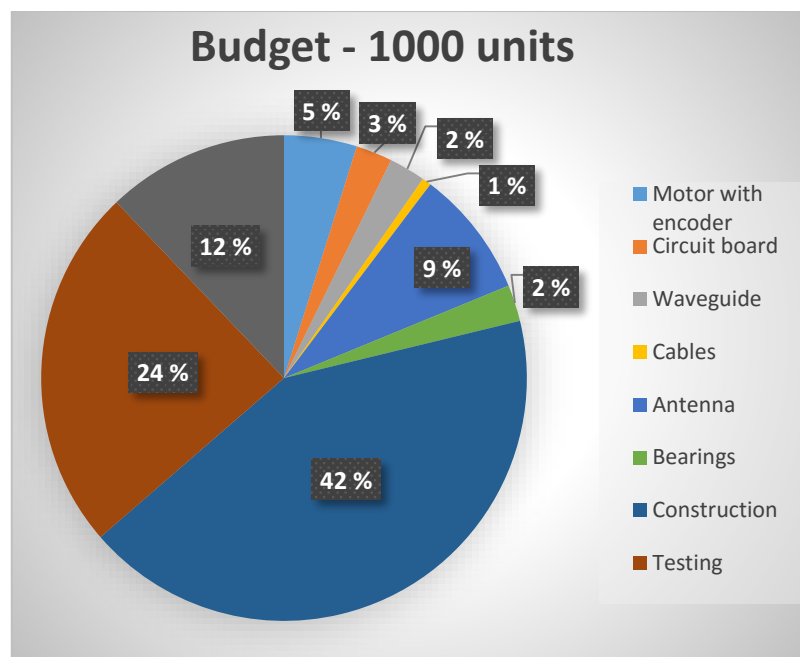
Figure 2. 1. 10: Cost budget - 1000 units, sector diagram

2.1.6. RISK analysis

As a part of the project, the group has done a research of risks associated with the given assignment. The purpose of the risk analysis is to obtain a mitigation plan for what to do when the risks occurs.

A top-level part of the qualitative risk analysis the group performed is shown below. A more detailed qualitative risk analysis is available in SSM-1200, Risk Document [3]. This document includes a mitigation plan that specifies a mitigation action.

The different risks have got a unique score due to impact and likelihood of risk. Explanations of the different levels of likelihood and impacts are given in the tables below. The scores are defined as risk levels, and have their colors from the risk matrix.

Table 2. 1. 8: Risk Matrix

Impact

	1	2	3	4	5
1	1	2	3	4	5
2	2	4	6	8	10
3	3	6	9	12	15
4	4	8	12	16	20
5	5	10	15	20	25

Likelihood

Table 2. 1. 9: Risk level explanations

Risk level	Explanation
20-25	Unacceptable. Measures shall be taken to eliminate the risk
15-16	Unacceptable. Measures shall be taken to eliminate the risk
10-12	Unacceptable. Measures should be taken to eliminate the risk
8-9	Acceptable. Measures should still be taken to eliminate the risk
4-6	Acceptable. Measures can be taken to eliminate the risk
1-3	Acceptable. No countermeasures needed

SSM

SMALL SATELLITE MECHANISMS

Table 2. 1. 10: Mitigation strategy explanations

Mitigation strategy	Explanation
Acceptance	No action is taken to reduce the risk
Contingency	The risk is accepted, but an action is planned should it happen
Reduction	Measures are taken to reduce the probability of the risk happening or at least to limit the consequences should it happen
Transference	The risk is transferred to another phase/entity of the project
Prevention	Measures are taken to eliminate the probability of the risk happening, and the consequences of the risk

Table 2. 1. 11: Impact explanations

Impact	Explanation
5	Can severely halt the project/render the system unusable
4	Can cause large delays
3	Can cause small delays
2	Needs to be fixed if the risk should occur
1	Minor bump. No real impact on the project

Table 2. 1. 12: Probability explanations

Probability	Explanation
5	>90%
4	>80
3	>50
2	>20%
1	<20%

Table 2. 1. 13: Top-level risk

#	Risk	Likelihood	Impact	Total Risk
1	Space Environment	3.5	4.1	**14.4**
2	Operational Risks	2.7	4.5	**12.0**
3	Cost risks	2.3	3.0	**7.0**
4	Schedule risks	2.8	4.0	**11.0**
5	Safety Risks	1.3	3.8	**5.1**
6	Development risk	3.4	3.1	**10.3**
7	Human resources risk	2.0	3.2	**6.4**

2.1.7. References

[1] S. Laugerud, V. O Aarud, "Test & Verification Specification", Small Satellite Mechanisms, Kongsberg SSM-3000, rev.1.1, 18.02.16.

[2] S. Laugerud, E. Løken, "Iteration Reports", Small Satellite Mechanisms, Kongsberg, SSM-1002, rev 1.0, 02.02.2016.

[3] G.H.Stenseth, M. Dybendal, "Risk document", Small Satellite Mechanisms, SSM-1200, rev.1.1, 18.02.2016.

[4] Spacecraft Mechanical loads analysis handbook, ECSS-HB-32-26A, 19.02.2013.

[5] Kongsberg Gruppen. (19.01.2016). Space & Surveillance. Available: http://kongsberg.com/en/kds/products/spacetechnologyandsystems/.

[6] Wikipedia. (21.01.2016). Unified Process. Available: https://en.wikipedia.org/wiki/Unified_Process.

[7] A. Solo, *System Engineering, Theory and Practice*, Madrid, Spain: UNE, 2014.

[8] O.H. Graven, "Prosjekthåndbok 2016", USN, Kongsberg, Norway, 2016.

2.2. Requirement specification

i. Abstract

The chapter is an overview of requirements the APMA has to meet in order to be operational. These requirements give clarity in how the system has to be designed, and are developed through collaboration with the customer.

The SSM project as a whole is more closely referenced in the project plan [1].

ii. Contents

iii. List of tables

SSM

SMALL SATELLITE MECHANISMS

iv. Document history

Table 2. 2. 1: Document history

Rev.	Date:	Author:	Approved:	Description
0.1	19.01.16	GHS, MD	-	Document created
0.2	26.01.16	MD, GHS	-	REQ-1.1.1.1, REQ-1.3.2, REQ-2.3.1 REQ-2.3.2
				- Removed
				REQ-1.2.1, REQ-1.2.2, REQ-1.5.1 REQ-2.1.1, REQ-2.2.1, REQ-2.6.2 REQ-2.7.2
				- Changed
				REQ-2.3.3, REQ-2.5.3, REQ-2.6.8 REQ-3.1.1
				- Added
				6.2 Standard – [6] added Corrected typo Added T,A,R specification to all requirements
1.0	28.01.16	GHS, MD	TS	Corrected typos Added table for abbreviations
1.1	08.02.16	GHS, TS	GHS	REQ-1.3.3, REQ-2.4.2, REQ-2.4.3 REQ-2.4.4, REQ-2.4.5, REQ-2.6.2 REQ-2.8.2, REQ-3.3.1, REQ-2.5.1
				- Changed
				Corrected typo Added half duplex REQ-2.4.6, REQ-2.5.3, REQ-2.5.5, REQ-2.5.6, REQ-2.5.7, REQ-2.5.8, REQ-2.7.3, REQ-2.7.4, REQ-2.7.5, REQ-2.7.6, REQ-2.7.7, REQ-2.7.8
				- Added
				Document structure changed Changed document layout
1.2	01.03.16	VOA	GHS	REQ-1.1.1, REQ-1.1.2, REQ-1.1.3, REQ-1.1.4, REQ-1.2.1, REQ-1.2.2 REQ-2.2.1, REQ-2.4.2, REQ-2.4.3 REQ-2.4.4, REQ-2.4.5, REQ-2.4.6 REQ-2.5.1 – Verification Method changed
2.0	03.02.16	GHS	MD	REQ-2.1.1.1, REQ-2.1.1.2, REQ-2.2.1.1, REQ-2.2.1.2, REQ-2.9.5
				- Added
				2.2.9 changed to "Electrical characteristics"
2.1	09.05.16	VOA		Changed with Verified post and updated.
2.2	10.05.16	VOA	EL	Updated after test. REQ-2.9.4, deleted due to system wiring, the motor windings are connected Wye.

					REQ-2.2.1 changed to failed.
2.2	13.05.16	GHS			Added column for compliance status Changed compliance status for all requirements Added Verification criteria to Evaluated-column.
3.0	14.05.16	GHS, MD	EL		Reviewed and published

2.2.1. Introduction

The requirements in this chapter are divided into three categories:

Table 2. 2. 2: Requirement categories

A	These requirements have to be met in order for the system to be functional
B	These requirements should be met
C	These requirements are optional

The requirements have a link to the test in which they are to be verified [2] and the originator of the requirement. In each category of requirements, an explanation of the category is given.

Below the requirement's number, a verification criterion is given:

Table 2. 2. 3: Verification criteria's

T	Verification by test
A	Verification by analysis
R	Verification by review of design

A column showing where the requirements are evaluated is added next to the verification column. An additional column stating the compliance status is added to show if the requirement is met. Compliant means the requirement is met. The compliance status is set to "Not applicable" if the requirement has not been evaluated. The status is also set to "Compliant" if the requirement is verified through only one of the verification criteria. E.g. if a requirement is set as "T,A,R," but is only verified through review. The status is set to "Not compliant" if the requirement is specifically not met, i.e. a failed test. Requirements met by test are automatically considered compliant, even if they were supposed to be verified by analysis or review.

2.2.2. Requirements

2.2.2.1. *Environmental Requirements*

2.2.2.1.1.   Physical properties

During launch and journey to space, vibrations are caused by the rocket. This means there are some specific requirements regarding physical properties.

Table 2. 2. 4: Physical properties

Nr:	Requirement	Class	Originator	Verification	Evaluated	Compliance status
REQ-1.1.1 T, A	The system shall withstand a static stress of TBC without degradation.	B	SSM	TST-1.1.0	Not evaluated	NA
REQ-1.1.2 T, A	The system shall withstand the sinusoidal vibration defined in [3] Figure 8-2.	A	KDA	TST-1.1.2	Not evaluated	NA
REQ-1.1.3 T, A	The system shall withstand a random vibration at the levels seen in table 2.2.5.	A	KDA	TST-1.1.3	Not evaluated	NA
REQ-1.1.4 T, A	The system shall have an eigenfrequency of > 140 Hz. Ref: [7], §8.4 [3]	A	KDA	TST-1.1.4	Not evaluated	NA

Table 2. 2. 5: Vibration

Axis	Frequency (Hz)	Qualification Level
All (3 axes)	20 – 100	+ 12 dB/oct
	100 – 300	$1.5g^2/Hz$
	300 – 650	-15 dB/oct
	650 – 850	$0.03\ g^2/Hz$
	850 – 2000	-6 dB/oct
	g rms	21.4

SSM

SMALL SATELLITE MECHANISMS

2.2.2.1.2. Thermal Requirements

The interface temperatures of the spacecraft are regulated internally. This limits the temperature related requirements for the APMA.

Table 2. 2. 6: Thermal Requirements

Nr:	Requirement	Class	Originator	Verification	Evaluated in:	Compliance status
REQ-1.2.1 T, A	The system shall be able to operate at interface temperatures between [-25, +65] ℃.	A	KDA	TST-1.2.0	R: 5111 – Components trade-off R: 5900 – M&M study	NA
REQ-1.2.2 T, A	The system shall tolerate temperatures between [-25, +65] ℃ while not operating.	A	KDA	TST-1.2.0	R: 5111 – Components trade-off R: 5900 – M&M study	NA

2.2.2.1.3. Vacuum Environment

In space there is no atmosphere. This has an impact on the materials that can be used for the system.

Table 2. 2. 7: Vacuum environment

Nr:	Requirement	Class	Originator	Verification	Evaluated in:	Compliance status
REQ-1.3.1 A	The system shall have a maximum outgassing of TBC [Molecules/Volume].	A	SSM	TST-1.3.0	Not evaluated	NA
REQ-1.3.3 T	The electronics of the system shall be able to operate in a pressure of less than TBC hPa.	A	KDA	TST-1.3.0	Not evaluated	NA

2.2.2.1.4. Radiation Environment

LEO (Low earth orbit) and space in general contains a huge amount of radiation. This means the APMA needs to withstand this to survive the environment.

Table 2. 2. 8: Radiation environment

Nr:	Requirement	Class	Originator	Verification	Evaluated in:	Compliance status
REQ-1.4.1 R	The system shall withstand the radiation levels in LEO without degradation.	A	KDA/SSM	TST-1.4.0	R: 5900 - M&M study R: 5111 - Component trade-off	C

SSM

SMALL SATELLITE MECHANISMS

2.2.2.1.5. Earth Environment

The satellite will travel through the earth's atmosphere during launch. Therefore the APMA needs to withstand the given levels of humidity in the earth's atmosphere.

Table 2. 2. 9: Earth Environment

Nr:	Requirement	Class	Originator	Verification	Evaluated in:	Compliance status
REQ-1.5.1 A	The system shall withstand humidity levels of TBC.	B	SSM	TST-1.5.0	Not evaluated	NA

2.2.2.2. *Technical Requirements*

The technical requirements control the technical solutions not directly associated with the environment.

2.2.2.2.1. Power

A small satellite (<500kg) does not have a large power supply. This means the APMA has to be very energy efficient.

Table 2. 2. 10: Power

Nr:	Requirement	Class	Originator	Verification	Evaluated in:	Compliance status
REQ-2.1.1 T,R	The system shall have a power consumption of $\leq$ 15 W, including electronics and actuators.	A	KDA	TST-2.1.0	T: 3003 - Test report R: 5901- Technical budgets	C
REQ-2.1.1.1 T, R	The motors shall have a maximum power consumption of 12 W [9].	A	SSM	TST-2.1.0	T: 3003 - Test report R: 5901 – Technical budgets	C
REQ-2.1.1.2 T, R	The control system shall have a maximum power consumption of 3 W [9].	A	SSM	TST-2.1.0	T: 3003 - Test report R: 5901 – Technical budgets	C

2.2.2.2.2. Mass

Table 2. 2. 11: Mass

Nr:	Requirement	Class	Originator	Verification	Evaluated in:	Compliance status
REQ-2.2.1 T, R	The mass of the system shall be maximum 4 kg, including electronics.	A	KDA	TST-2.2.0	R: 5901 – Technical budgets	NC
REQ-2.2.1.1 T, A, R	The mass of the mechanism shall be maximum 3 kg [9].	B	SSM	TST-2.2.0	R: 5901 – Technical budgets	NC
REQ-2.2.1.2 T,A	The mass of the electronics shall be maximum 1 kg [9].	B	SSM	TST-2.2.0	Not evaluated	NA

2.2.2.2.3. Torque

Table 2. 2. 12: Torque

Nr:	Requirement	Class	Originator	Verification	Evaluated in:	Compliance status
REQ-2.3.3 T,A,R	Motorization according to ECSS-E-ST-33-01C shall be satisfied.	B	SSM	TST-2.3.2	T: 3003 - Test report R: 5901 - Technical budgets	C
REQ-2.3.3.1 T, A	The motor for the azimuth stage shall produce a torque of minimum 0.114 Nm [9]	B	SSM	TST-2.3.2	T: 3003 - Test report R: 5901 – Technical budgets, [10]	C
REQ-2.3.3.2 T, A	The motor for the elevation stage shall produce a torque of minimum 0.108Nm [9]	B	SSM		R: 5901- Technical budgets, [10]	NA

2.2.2.2.4. Pointing

The system shall allow for communication between two satellites in low earth orbit. This makes requirements related to pointing strict. At some time the satellites will be moving in opposite directions of each other, therefore requirements related to speed and acceleration were added.

Table 2. 2. 13: Pointing

Nr:	Requirement	Class	Originator	Verification	Evaluated in:	Compliance status
REQ-2.4.1 T,R	The system shall have a pointing error of < 0.5 deg, half cone, 3 sigma.	A	KDA	TST-2.4.0	T: 3003 - Test report R: 5901 - Technical budgets	NC
REQ-2.4.2 T, R	The elevation stage shall be able to move minimum ± 90 deg.	A	KDA	TST-2.4.0	R: 5120 - Design description R: 5131 – Design description	NA
REQ-2.4.3 T, R	The azimuth stage shall be able to move minimum ± 180 deg.	A	KDA	TST-2.4.0	T: 3003 - Test report R: 5120 - Design description R: 5131 – Control system design	C
REQ-2.4.4 T, A,R	The system shall be able to move with a velocity of ≥ 60 deg/s.	A	KDA	TST-2.4.1	T: 3003 - Test report R: 5131 – Control system design	C
REQ-2.4.5 T, A,R	The system shall be able to accelerate at a rate of ≥ 40 deg/s^2.	A	KDA	TST-2.4.1	T: 3003 - Test report R: 5131 – Control system design	C
REQ-2.4.6 T,R	The system shall be able to move along both axes simultaneously.	A	SSM		Not tested. R: 5120 - Design description	NA

2.2.2.2.5. Communication with the spacecraft

The mechanism's electrical subsystem will receive position commands from the spacecraft.

Table 2. 2. 14: Communication with the spacecraft

Nr:	Requirement	Class	Originator	Verification	Evaluated in:	Compliance status
REQ-2.5.1 T,R	The system shall receive absolute position commands from the spacecraft.	A	KDA	TST-2.5.0	T: 3003 - Functional Test Report R: 5131 - Control system design	C
REQ-2.5.2 T,R	The system shall send position updates to the spacecraft.	A	KDA	TST-2.5.0	T: 3003 - Functional Test Report R: 5131 - Control system design,	C
REQ-2.5.3 T, R	The system shall send temperature updates to the spacecraft.	C	KDA	TST-2.5.0	T: 3003 - Functional Test Report R: 5131 – Control system design	C
REQ-2.5.4 T	The system shall communicate between the spacecraft using the CANbus protocol.	A	KDA	TST-2.5.0	R: 5131 – Control system design	NA
REQ-2.5.5 T	The system shall be able to receive commands from the spacecraft at a frequency of 100 hertz.	B	KDA SSM	TST-2.5.1	T: 3003 - Functional Test Report	C
REQ-2.5.6 T	The system shall allow the spacecraft to adjust the antenna position at any given time.	A	SSM	TST-2.5.1	T: 3003 - Functional Test Report	C
REQ-2.5.7 T	The system shall send feedback when it is moving.	A	KDA	TST-2.5.1	T: 3003 - Functional Test Report	C

Nr:	Requirement	Class	Originator	Verification	Evaluated	Compliance status
					R: 5131 – Control system design	
REQ-2.5.8 T	The system shall send feedback when it is not moving.	A	KDA	TST-2.5.1	T: 3003 - Functional Test Report R: 5131 – Control system design	C

2.2.2.2.6.   Radio communication

A part of the project is to make an antenna sub system for full duplex communication.

Table 2. 2. 15: Radio Communication

Nr:	Requirement	Class	Originator	Verification	Evaluated	Compliance status
REQ-2.6.1 T,R	The system shall be able to communicate full duplex.	A	KDA	TST-2.6.0	R: 5211 - Antenna trade-off	NA
REQ-2.6.2 T, A,R	The overall gain of the system shall be ≥ 23 dBi.	A	KDA	TST-2.6.1	R: 5211 - Antenna trade-off	NA
REQ-2.6.3 T, A,R	The system shall be able to communicate at a carrier frequency of 23 GHz.	A	KDA	TST-2.6.2	R: 5211 - Antenna trade-off	NA
REQ-2.6.4 T	The system shall tolerate a transmit power of 5 W.	A	KDA	TST-2.6.3	Not evaluated	NA
REQ-2.6.5 T	The system shall not impose a group time delay variation of more than 0.1 ns on the received signal at ± 200 MHz of the carrier frequency.	A	KDA	TST-2.6.4	Not evaluated	NA
REQ-2.6.6 R	The system shall contain a transmit sub-system.	A	KDA	TST-2.6.5	R: 5211 - Antenna trade-off	C

Nr:	Requirement	Class	Origin	Verification	Evaluated	Compliance status
REQ-2.6.7 R	The system shall contain a receive sub-system.	A	KDA	TST-2.6.5	R: 5211 - Antenna trade-off	C
REQ-2.6.8 T, A,R	The gain variation shall be maximum ± 1 dBi.	A	KDA	TST-2.6.6	A: 5112 - Link analysis	NA

2.2.2.2.7.   Control system

The space industry has strict requirements regarding the stability of control systems.

Table 2. 2. 16: Control system

Nr:	Requirement	Class	Origin	Verification	Evaluated	Compliance status
REQ-2.7.1 R	The system shall contain a motor control system.	A	SSM	TST-2.7.0	R: 5131 - Control system design	C
REQ-2.7.2 A,R	The control system shall comply with [6].	A	KDA	TST-2.7.0	Not evaluated	NA
REQ-2.7.3 T, R	The control system shall be able to control the velocity of the system	A	KDA	TST-2.7.1	R: 5131 - Control system design T: 3003 - Functional Test Report	C
REQ-2.7.4 T, R	The control system shall be able to control the acceleration of the system	A	KDA	TST-2.7.1	R: 5131 - Control system design T: 3003 - Functional Test Report	C
REQ-2.7.5 T, R	The control system shall be able to control the motor current.	A	KDA	TST-2.7.1	5131 - Control system design 3003 - Test Report	C

REQ-2.7.6 T,R	All pointing variables shall be set for each configuration call.	B	SSM	TST-2.7.2	R: 5131 - Control system design	C
REQ-2.7.7 T,R	The control system shall be able to calibrate the zero position.	A	KDA	TST-2.7.2	5131 - Control system design T: 3003 - Functional Test Report	C
REQ-2.7.8 T,R	The system shall not move until a position command is received.	A	KDA	TST-2.7.2	R: 5131 - Control system design T: 3003 – Functional Test Report	C
REQ-2.7.9 T,R	The control system shall be able to control the position of the system.	A	KDA	TST-2.7.1	R: 5131 - Control system design T: 3003 - Functional Test Report	C

2.2.2.2.8. Life

Table 2. 2. 17: Life

Nr:	Requirement	Class	Origin	Verification	Evaluated	Compliance status
REQ-2.8.1 T,A	The system shall be able to complete 500 000 cycles where each cycle is a sweep $\pm$ 180 deg.	A	KDA	TST-2.8.0	Not evaluated	NA
REQ-2.8.2 A,R	The system shall be able to operate in LEO for $\geq$5 years.	A	KDA	TST-2.8.1	Not evaluated	NA

2.2.2.2.9. Electrical characteristics

Table 2. 2. 18: Electrical insulation

Nr:	Requirement	Class	Origin	Verification	Evaluated in:	Compliance status
REQ - 2.9.1 T	Electrical wires shall be insulated from the structure by > 50 MΩ with a DC voltage of 500V applied [4].	A	SSM	TST-2.9.0	Not evaluated	NA
REQ - 2.9.2 T	Electrical wires shall be insulated from each other by > 50 MΩ with a DC voltage of 500 V applied [4].	A	SSM	TST-2.9.0	Not evaluated	NA
REQ - 2.9.3 T	Electric motor windings shall be insulated from the structure by > 100 MΩ with a DC voltage of 500 V applied [4].	A	SSM	TST-2.9.0	T: 3003 - Functional Test report	C
REQ - 2.9.5 T,R	They system shall tolerate a supply voltage of 28V	A	SSM	TST-2.9.1	T: 3003 - Functional Test report R: 5415 - Electrical design document R: 5111 - Components trade-off	C

2.2.2.3. Cost

2.2.2.3.1. System cost

Table 2. 2. 19: System cost

Nr:	Requirement	Class	Origin	Verification	Evaluated in:	Compliance status
REQ- 3.3.1 R	The system shall have a cost of maximum €10.000 per unit. Assuming a batch size of 1000 units.	A	KDA	N/A	R: 1300 – R&D Cost budget R: 0900 – Concept analysis	C

2.2.3. References

[1] E. Løken and T. Sundnes, "Project Plan", SSM-1001, rev.1.1, 18.02.2016.

[2] V.O. Aarud and S. Laugerud, "Test & Verification Specification", SSM-3000, rev.1.1, 18.02.16.

[3] Space Engineering - Spacecraft Mechanical loads analysis handbook, ECSS-HB-32-26A, 19.02.2013.

[4] Space Engineering - Mechanisms, ECSS-E-ST-33-01C, 06.03.2009.

[5] Space Engineering - Technical Requirements Spesification, ECSS-E-ST_10-06C, 06.03.2009.

[6] Space Engineering - Control Performance, ECSS-E-ST-60-10C, 15.11.2008.

[7] C. Heigerer, "KARMA 7, MSA Trade-off Report and Baseline definition (TN01.01) - Background IPR", KDA, Kongsberg, Norway, 26.09.2013.

[9] E. Løken et al, "Technical Budgets", SSM-5901, rev 0.1, 18.02.2016

[10] Maxon motor, http://www.maxonmotor.com/medias/sys_master/root/8816806920222/15-263-EN.pdf, 9.5.16

2.3. Test & verification specification

i.   Abstract

The test & verification specification chapter gives an overview of the tests that will be performed during this project. This to ensure that the specified requirements are met and to verify that the system is built correctly.

ii. Contents

iii. List of tables

iv. Document history

Table 2. 3. 1: Document history

Rev.	Date	Author	Approved	Description
0.1	19.01.16	SL, VOA		Document created
0.2	29.01.16	SL	EL	TST-1.1.0, changed TST-1.1.2, changed TST-1.1.1, removed TST-1.2.0, changed REQ-1.3.2 removed from TST-1.3.0 TST-1.3.1, added TST-2.1.0, changed TST-2.2.0, changed TST-2.3.0, removed TST-2.3.1, removed TST-2.3.2, added REQ-2.5.3 added to TST-2.5.0 TST- 2.6.6, added 5.2.8 Life, added 5.2.9 Electrical insulation, added Verification criteria, added Title "Introduction" changed to "Scope" "Test Overview" added
1.0	02.02.16	SL, VOA	GHS,TS	Reviewed and published
1.1	10.02.16	SL	EL	TST-1.3.3, changed TST-2.4.0, changed TST-2.4.1, changed TST-2.6.2, changed TST-2.8.2, changed Document name changed
1.2	23.02.16	SL	EL	Document layout changed
1.3	01.03.16	SL	EL	Updated accordingly to E:1 TST-2.2.0 verified (A) TST-2.4.1 verified (A) Test result overview updated 8.1.5 changed to "Earth Environment" and 8.2.9 changed to "Electrical characteristics" TST-2.1.0, TST-2.2.0, TST-2.3.2, TST-2.4.0, TST-2.4.1, TST-2.5.0, TST-2.6.1, TST-2.6.2, TST-2.6.6, - Changed TST-2.5.1, TST-2.7.1, TST-2.7.2, TST-2.9.1 - Added Test results (verification) added Updated "Test results overview"
2.0	04.03.16	VOA, SL	EL	Reviewed and published
2.1	18.04.16	SL	EL	TST-2.3.2, changed
2.2	12.05.16	VOA, SL		Updated after testing and corrected errors and requirements
3.0	14.05.16	SL	EL	Reviewed and published

2.3.1. Introduction

The test & verification specification will ensure that the system, at the end of the project, meets the specified requirements through testing, analysis or review of design. The different tests are divided into environmental and technical tests, and each test is linked to at least one requirement. The tests have a pass criteria and an execution description, and will be verified based on the criteria in table 2.3.2.

Example: TST-0.0.0-TAR

Table 2. 3. 2: Verification criteria's

T	Verification by test
A	Verification by analysis
R	Verification by review of design

2.3.2. Test & Verification overview

Phase	
Elaboration Phase 2.1	• Prototype 1
Simulation	• Correct materials and coding for critical parts (17.-24. feb. 2016)
Verification and validation	• Report (24. feb - 2. mars 2016)
Elaboration Phase 2.2	• Prototype 2
Functional simulation, individuality	• Correctly assembled system model with correct materials and codes. (17.-21. mars 2016)
Verification and validation	• Report (21.-23. mars 2016)
Construction Phase 3.1	• Prototype 3
Functional simulation individuality	• Correctly assembled system with correct materials and codes. Updated from prototype 2. • Startup problems shall be fixed (7.-11. april 2016)
Verification and Validation	• Report (11.-12. april 2016)
Construction Phase 3.2	• Prototype 4
Final Functional simulation individuality	• Correctly assembled system with correct materials and codes. Updated from prototype 3. • Result should be acceptable (14.-16. april 2016)
Verification and Validation	• Report (16.-18. april 2016)
Construction Phase 3.3	• Functionality test with the full functional system (9. -11.may 2016)
Conclution	• Report (9.- 11.may 2016)

2.3.3. Test and resources

2.3.3.1. *Environmental*

2.3.3.1.1. Physical properties

Table 2. 3. 3: TST-1.1.0

TST-1.1.0-TA Physical properties	REQ-1.1.1			
Date				
Pass criteria	The system shall withstand a static stress of TBC without degradation.			
Execution	Conduct a test where the system is affected by static stress and is checked for degradation.			
Result	Not tested			
Comment				

Table 2. 3. 4: TST-1.1.2

TST-1.1.2-TA Physical properties	REQ-1.1.2			
Date				
Pass criteria	Conduct a sinusoidal vibration test with parameters defined in [5] table 6-9.			
Execution	The system shall go through a sinusoidal vibration test.			
Result	Not tested			
Comment				

Table 2. 3. 5: TST-1.1.3

TST-1.1.3-TA Physical properties	REQ-1.1.3			
Date				
Pass criteria	The system shall go through a random vibration test with parameters defined in table 2.3.7.			
Execution	Mount the mechanism on a platform for random vibration testing. Make sure that the system is well placed and not in danger of loosening.			
Result	Not tested			
Comment				

Table 2. 3. 6: TST-1.1.4

TST-1.1.4-TA Physical properties	REQ-1.1.4			
Date				
Pass criteria	Eigenfrequency > 140 Hz			
Execution	Measure the eigenfrequency of the system.			
Result	Not tested			
Comment				

Table 2. 3. 7: Vibration

Axis	Frequency (Hz)	Qualification Level
All (3 axes)	20 – 100	+ 12 dB/oct
	100 – 300	$1.5g^2$/Hz
	300 – 650	-15 dB/oct
	650 – 850	$0.03\ g^2$/Hz
	850 – 2000	-6 dB/oct
	g rms	21.4

2.3.3.1.2. Thermal

Table 2. 3. 8: TST-1.2.0

TST-1.2.0-TR Thermal	REQ-1.2.1	REQ-1.2.2		
Date				
Pass criteria	The system shows no weaknesses and is still fully operational after the test is done.			
Execution	The mechanism shall be tested fully operational and while not operating within the temperature range of -25 ℃ to +65 ℃ in a vacuum chamber.			
Result	Not tested			
Comment				

2.3.3.1.3. Vacuum

Table 2. 3. 9: TST-1.3.0

TST-1.3.0-A Vacuum	REQ-1.3.1			
Date				
Pass criteria	The system shall have a maximum of TBD outgassing particles.			
Execution	There will be sensors measuring outgassing particles from the system at a pressure of TBC hPa. The system will be operating. This test will take place in a vacuum chamber with normal operating temperature.			
Result	Not tested			
Comment				

Table 2. 3. 10: TST-1.3.1

TST-1.3.1-T Vacuum	REQ-1.3.3			
Date				
Pass criteria	The electronics shall be able to operate in a pressure of less than TBC hPa.			
Execution	The system shall be placed in a vacuum chamber at a specific pressure while operating.			
Result	Not tested			
Comment				

2.3.3.1.4. Radiation

Table 2. 3. 11: TST-1.4.0

TST-1.4.0-R Radiation	REQ-1.4.1			
Date	10.05.16 (R)			
Pass criteria	The system shall withstand the radiation levels in LEO without degradation.			
Execution	The verification will happen through review of the design			
Result	Verified (R)			
Comment	See M&M study [9] and Components Trade-off [10] reports for comments.			

2.3.3.1.5. Earth environment

Table 2. 3. 12: TST-1.5.0

TST-1.5.0-A Earth environment	REQ-1.5.1			
Date				
Pass criteria	The system shall withstand humidity levels of TBD.			
Execution	TBD			
Result	Not tested			
Comment				

2.3.3.2. *Technical*

2.3.3.2.1. Power

Table 2. 3. 13: TST-2.1.0

TST-2.1.0-TR Power	REQ-2.1.1	REQ-2.1.1.1	REQ-2.1.1.2	
Date	10.05.16 (T)(R)	10.05.16 (T)(R)	10.05.16 (T)(R)	
Pass criteria	Maximum system power consumption of 15 W, including electronics and actuators. (Maximum 12 W for motors, 3 W for the control system.)			
Execution	The system shall operate with all electronics and actuators connected to simulate normal operation. The power consumption shall be measured.			
Result	Verified (T)(R)			
Comment	See Functional Test Report [11] for verification comments and Technical budgets [7] for information.			

2.3.3.2.2. Mass

Table 2. 3. 14: TST-2.2.0

TST-2.2.0-TAR Mass	REQ-2.2.1	REQ-2.2.1.1	REQ-2.2.1.2	
Date	29.02.2016 (A)			
Pass criteria	Mass $\leq$ 4 kg (maximum weight for the mechanism = 3 kg, electronics = 1 kg).			
Execution	The object shall be in fully mounted in operation stance. The object will be connected to a base plate on a scale and the mass will be measured.			
Result	Failed(A)			
Comment	Verified through Technical budgets [7].			

2.3.3.2.3. Torque

Table 2. 3. 15: TST-2.3.2

TST-2.3.2-TAR Torque	REQ-2.3.3	REQ-2.3.3.1	REQ-2.3.3.2	
Date	10.05.16 (T)(R)	10.05.16 (T)(R)		
Pass criteria	Motorization according to [6] shall be satisfied and the motor shall produce a minimum torque of 0.114 Nm in the azimuth stage and 0.108 Nm in the elevation stage.			
Execution	Verify			
Result	Verified (R), Partly verified (T)			
Comment	See functional test report [11] and Technical budgets [7] for more information. Only the azimuth stage was tested due to unfinished implementation of the elevation stage.			

2.3.3.2.4. Pointing

Table 2. 3. 16: TST-2.4.0

TST-2.4.0-TR Pointing	REQ-2.4.1	REQ-2.4.2	REQ-2.4.3	
Date	29.02.16 (R) 10.05.16 (T)	29.02.16 (R)	29.02.16 (R) 10.05.16 (T)	
Pass criteria	Pointing accuracy < 0.5º, half cone, 3 sigma. Elevation stage $\geq \pm 90$ º. Azimuth stage $\geq \pm 180$º.			
Execution	Conduct a functional test where accuracy, elevation stage and azimuth stage is verified.			
Result	Verified (R), partly verified (T)			
Comment	See Technical budgets [7] and Test report [11]. The test was only performed for azimuth due to unfinished implementation of elevation.			

Table 2. 3. 17: TST-2.4.1

TST-2.4.1-TA Pointing	REQ-2.4.4	REQ-2.4.5	REQ-2.4.6	
Date	10.05.16 (T)	10.05.16 (T)	10.05.16 (R)	
Pass criteria	Movement speed ≥ 60 º/s, acceleration ≥ 40 º /s^2 for both axes simultaneously.			
Execution	Measure the velocity and acceleration of the APMA and verify that the system is moving along both axes simultaneously.			
Result	Verified (R), Partly verified (T)			
Comment	Verified through Technical budgets [7] and Test report [11]. Elevation is not implemented and cannot be tested.			

2.3.3.2.5. Communication with the spacecraft

Table 2. 3. 18: TST-2.5.0

TST-2.5.0-TR Communication with the spacecraft	REQ- 2.5.1	REQ-2.5.2	REQ-2.5.3	REQ-2.5.4
Date	10.05.16 (T)(R)	10.05.16 (T)(R)		

Pass criteria	Two way communication between the APMA and the spacecraft (position and temperature) using CANbus protocol.
Execution	Verify that the system sends and receives position updates and temperature through CANbus protocol.
Result	Partly verified (R)(T).
Comment	See Control System Design [12] and Functional Test Report [11] for further information. UART protocol has been implemented instead of CANbus.

Table 2. 3. 19: TST-2.5.1

TST-2.5.1-T Communication with the spacecraft	REQ- 2.5.5	REQ-2.5.6	REQ-2.5.7	REQ-2.5.8
Date	10.05.16 (T)	10.05.16 (T)	10.05.16 (T)	10.05.16 (T)
Pass criteria	The system shall be able to receive commands from the spacecraft at a frequency of 100 Hz, be able to adjust position at any given time, send feedback while/while not running.			
Execution	Through software, verify that the system can handle the frequency and is able to adjust position and send feedback while/while not running.			
Result	Verified (T)			
Comment	See Test Report [11] for more information.			

2.3.3.2.6. Radio communication
Table 2. 3. 20: TST-2.6.0

TST-2.6.0-TR Radio communication	REQ-2.6.1			
Date	10.05.16 (R)			
Pass criteria	The system shall be able to communicate full duplex.			
Execution	TBD			
Result	Partly verified (R)			
Comment	See Antenna Trade-off [13] for more information.			

Table 2. 3. 21: TST-2.6.1

TST-2.6.1-TA Radio communication	REQ-2.6.2			
Date	02.03.2016 (A)			
Pass criteria	Overall system gain, $\geq$ 23 dBi.			
Execution	Test the overall system gain by sending a signal towards the APMA and measuring the gain output.			
Result	Verified (A)			
Comment	Verified through Link Analysis [8] and Antenna Trade-off [13].			

Table 2. 3. 22: TST-2.6.2

TST-2.6.2-TA Radio communication	REQ-2.6.3			
Date	02.03.2016 (A)			
Pass criteria	Communication at a carrier frequency of 23 GHz			
Execution	Test and verify that the system handles a carrier frequency of 23 GHz.			
Result	Verified (A)			
Comment	Verified through Link Analysis [8] and Antenna Trade-off [13].			

Table 2. 3. 23: TST-2.6.3

TST-2.6.3-T Radio communication	REQ-2.6.4			
Date				
Pass criteria	Transmit power = 5 W.			
Execution	Verify that the system can handle a transmit power of 5 W.			
Result	Not tested			
Comment				

Table 2. 3. 24: TST-2.6.4

TST-2.6.4-T Radio communication	REQ-2.6.5			
Date				
Pass criteria	Group time delay variation < 0.1 ns on the received signal at the carrier frequency of ± 200 MHz of the carrier frequency.			
Execution	TBD			
Result	Not tested			
Comment				

Table 2. 3. 25: TST-2.6.5

TST-2.6.5-R Radio communication	REQ-2.6.6	REQ-2.6.7		
Date	10.05.16 (R)	10.05.16 (R)		
Pass criteria	Contain transmit and receive subsystem.			
Execution	Verify			
Result	Partly verified (R)			
Comment	Partly verified through Antenna Trade-off [13].			

Table 2. 3. 26: TST-2.6.6

TST-2.6.6-TA Radio communication	REQ-2.6.8			
Date	02.03.2016 (A)			
Pass criteria	The gain variation shall be maximum ± 1 dBi.			
Execution	Test respective to the calculations done in the design.			
Result	Verified (A)			
Comment	Verified through Link Analysis [8].			

2.3.3.2.7. Control system

Table 2. 3. 27: TST-2.7.0

TST-2.7.0-AR Control system	REQ-2.7.1	REQ-2.7.2		
Date	10.05.16 (R)			
Pass criteria	The system shall contain a motor control system complying with Space Engineering: Control performance [4].			
Execution	Make an analysis and verify the design.			
Result	Partly verified (R)			
Comment	See Control System Design [12] for comments.			

Table 2. 3. 28: TST-2.7.1

TST-2.7.1-TR Control system	REQ-2.7.3	REQ-2.7.4	REQ-2.7.5	REQ-2.7.9
Date	10.05.16 (T)(R)	10.05.16 (T)(R)	10.05.16 (T)(R)	10.05.16 (T)(R)
Pass criteria	The system shall be able to control position, velocity, acceleration and current.			
Execution	The system shall be operating, and by sending specific position commands, it is able to verify these requirements.			
Result	Verified (R)(T)			
Comment	See Control system design [12] and Functional Test report [11].			

Table 2. 3. 29: TST-2.7.2

TST-2.7.2-TR Control system	REQ-2.7.6	REQ-2.7.7	REQ-2.7.8	
Date	10.05.16 (R)(T)	10.05.16 (R)(T)	10.05.16 (R)(T)	
Pass criteria	All pointing variables shall be set for each configuration call. The control system shall be able to calibrate zero position and the system shall not move until a position command is received.			
Execution	Verify through a control system test and review.			
Result	Verified (R)(T)			
Comment	See Control system design [12] and Functional Test report [11].			

2.3.3.2.8.　　Life

Table 2. 3. 30: TST-2.8.0

TST-2.8.0-TA Life	**REQ-2.8.1**			
Date				
Pass criteria	The system shall be able to complete 500 000 cycles where each cycle is a sweep of ±180º.			
Execution	TBD			
Result	Not tested			
Comment				

Table 2. 3. 31: TST-2.8.1

TST-2.8.1-AR Life	**REQ-2.8.2**			
Date				
Pass criteria	The system shall be able to operate in LEO for ≥ 5 years.			
Execution	Tentative			
Result	Not tested			
Comment				

2.3.3.2.9.　　Electrical characteristics

Table 2. 3. 32: TST-2.9.0

TST-2.9.0-T Electrical characteristics	**REQ-2.9.1**	**REQ-2.9.2**	**REQ-2.9.3**	
Date			10.05.16 (T)	
Pass criteria	Resistance > 100 MΩ for electric motor windings to the structure, resistance > 50 MΩ for electrical wires at 500 VDC.			
Execution				
Result	Partly verified (T)			
Comment	See Functional Test report [11] for comments. Due to no final electrical design, wires were not prioritized during functional testing.			

Table 2. 3. 33: TST-2.9.1

TST-2.9.1-TR Electrical characteristics	**REQ-2.9.5**			
Date	10.05.16 (T)(R)			
Pass criteria	The system shall tolerate a supply voltage of 28 V.			
Execution	Through design and test, verify that the system handles a supply voltage of 28 V.			
Result	Verified (T)(R)			
Comment	See Functional Test Report [11], Electrical design document [14] and Component Trade-off [10] for information.			

2.3.4. Test results overview

Table 2. 3. 34: Test results overview

Test ID	Test status	Date	Responsible
TST-1.1.0-TA	Not tested		
TST-1.1.2-TA	Not tested		
TST-1.1.3-TA	Not tested		
TST-1.1.4-TA	Not tested		
TST-1.2.0-TR	Not tested		
TST-1.3.0-A	Not tested		
TST-1.3.1-T	Not tested		
TST-1.4.0-R	Verified (R)	10.05.16	VOA, SL
TST-1.5.0-A	Not tested		
TST-2.1.0-TR	Verified (T)(R)	10.05.16	GHS
TST-2.2.0-TAR	Failed (A)	29.02.16	MD
TST-2.3.2-TAR	Verified (R), partly verified(T)	10.05.16	EL, GHS
TST-2.4.0-TR	Verified (R), partly verified (T)	29.02.16	MD, EL
TST-2.4.1-TA	Verified (R), Partly verified (T)	29.02.16	GHS, EL
TST-2.5.0-TR	Partly verified (T)(R)	10.05.16	GHS, TS
TST-2.5.1-T	Verified (T)	10.05.16	GHS
TST-2.6.0-TR	Partly verified (R)	10.05.16	GHS, EL
TST-2.6.1-TA	Verified (A)	02.03.16	GHS, EL
TST-2.6.2-TA	Verified (A)	02.03.16	GHS, EL
TST-2.6.3-T	Not tested		
TST-2.6.4-T	Not tested		
TST-2.6.5-R	Partly verified (R)	10.05.16	GHS, EL
TST-2.6.6-TA	Verified (A)	02.03.16	GHS, EL
TST-2.7.0-AR	Partly verified (R)	02.03.16	EL, TS
TST-2.7.1-TR	Verified (T)(R)	02.03.16	EL, TS, GHS
TST-2.7.2-TR	Verified (T)(R)	10.05.16	EL, TS, GHS
TST-2.8.0-TA	Not tested		
TST-2.8.1-AR	Not tested		
TST-2.9.0-T	Partly verified (T)	10.05.16	GHS
TST-2.9.1-TR	Verified (T)(R)	10.05.16	GHS, SL

2.3.5. References

[1]　E. Løken and T. Sundnes, "Project plan", SSM-1001, rev. 1.1, 18.02.2016.

[2]　G. H. Stenseth and M. Dybendal, "Requirement specification", SSM-2000, rev. 1.1, 18.02.2016.

[3]　Space Engineering: Testing, ECSS-E-ST-10-03C, 12.06.2012.

[4]　Space Engineering: Control performance, ECSS-E-ST-60-10C, 15.11.2008.

[5]　Space Engineering: Spacecraft mechanical loads analysis handbook, ECSS-E-HB-32-26A, 19.02.2013.

[6]　Space Engineering: Mechanisms, ECSS-E-ST-33-01C, 06.03.2009.

[7]　E. Løken et al, "Technical budgets", SSM-5901, rev. 0.2, 29.02.2016.

[8]　G. H. Stenseth, "Link Analysis", SSM-5112, rev 1.0.

[9]　V. O. Vebjørn and M. Dybendal, "Material and mechanical technology study", SSM-5900, rev. 1.0, 03.03.2016.

[10]　G. H. Stenseth and S. Laugerud, "Component Trade-off", SSM-5111, rev. 1.0, 04.03.2016.

[11]　G. H. Stenseth, "Functional Test Report", SSM-3003, rev. 1.0, 15.05.2016

[12]　E. Løken and T. Sundnes, "Control System Design", SSM-5131, rev. 1.2, 13.05.2016

[13]　E. Løken and G. H. Stenseth, "Antenna Trade-off", SSM-5211, rev. 1.1, 05.04.2016

[14]　G. H. Stenseth and S. Laugerud, "Electrical Design Document", SSM-5415, rev. 0.1, 13.05.2016

2.4. Risk management

i.　　Abstract

This chapter contains a qualitative risk analysis for the SSM project, where top-level and sub-level risks are described. The chapter includes a mitigation plan, which will be updated during the project.

iii. List of tables

Table 2. 4. 1: Document history

Rev.	Date	Author	Approved	Description
1.0	03.02.16	GHS, VOA, MD	SL, TS, EL	Document created
1.1	18.02.16	GHS, VOA, MD		Changed test specification to test & verification specification. Changed document structure.
1.2	23.02.16	EL		Changed document layout
2.0	02.03.16	VOA, GHS	TS	Created rev 2.0 Table 6: Space environment risks, updated Table 7: Operational risks, updated Table 8: Cost risks, updated Table 9: Schedule risks, updated Table 10: Safety risks, updated Table 11: Development risks, updated Table 12: Human Resources Risks, updated Changed document layout and added introduction Added conclusion
2.1	21.03.2016	SL, GHS, EL		Document layout updated Table 7: operational risks, point 2.2.1 mitigation date updated Table 16 added
2.2	03.05.2016	VOA		Rev 2.2 created
2.3	12.05.2016	MD, EL		Created rev 2.3 Updated document, mitigation 3. Table 6: Space environment risks, updated Table 7: Operational risks, updated Table 8: Cost risks, updated Table 9: Schedule risks, updated Table 10: Safety risks, updated Table 11: Development risks, updated Table 12: Human Resources Risks, updated Changed document title to "Risk Management"
3.0	13.05.2016	MD	TS	Reviewed and published

2.4.1. Introduction

Risk management is an important part of systems engineering. The goal is to reduce/eliminate the likelihood of a risk occurring and the impact it has on the project if it should occur.

For the SSM project, this is done by following these steps:

- Do a qualitative risk analysis to discover the risks and evaluate their likelihood and impact.
- Create specific actions to reduce the risk. These actions have a due date and a responsible person to make sure they are done.
- Update the risk document throughout the project to see of risks have been reduced/eliminated, or if new risks have to be added.

2.4.2. Qualitative Risk Analysis Explanations

2.4.2.1. Risk Matrix

Table 2. 4. 2: Risk Matrix

		Impact				
		1	2	3	4	5
Likelihood	1	1	2	3	4	5
	2	2	4	6	8	10
	3	3	6	9	12	15
	4	4	8	12	16	20
	5	5	10	15	20	25

2.4.2.2. Risk Level

Table 2. 4. 3: Risk level explanations

Risk level	Explanation
19-25	Unacceptable. Measures shall be taken to eliminate the risk
14-18	Unacceptable. Measures shall be taken to eliminate the risk
10-13	Unacceptable. Measures should be taken to eliminate the risk
8-9	Acceptable. Measures should still be taken to eliminate the risk
4-6	Acceptable. Measures can be taken to eliminate the risk
1-3	Acceptable. No countermeasures needed

2.4.2.3. *Likelihood*
Table 2. 4. 4: Probability explanations

Probability	Explanation
5	>90%
4	>80
3	>50
2	>20%
1	<20%

2.4.2.4. *Impact*
Table 2. 4. 5: Impact explanations

Impact	Explanation
5	Can severely halt the project/render the system unusable
4	Can cause large delays
3	Can cause small delays
2	Needs to be fixed if the risk should occur
1	Minor bump. No real impact on the project

2.4.3. Space Environment Risks

Table 2. 4. 6: Space environment risks

#	RISK	Before mitigation					Mitigation 1			After mitigation 1			Mitigation 2			After mitigation 2			Mitigation 3			After mitigation 3		
		Likelihood	Impact	Total risk	Explanation Likelihood	Explanation Impact	Mitigation action	Mitigation responsible	Mitigation date	Likelihood	Impact	Total risk	Mitigation action	Mitigation responsible	Mitigation date	Likelihood	Impact	Total risk	Mitigation action	Mitigation responsible	Mitigation date	Likelihood	Impact	Total risk
1	**Space Environment**	3,5	4,1	14,4						3,5	3,2	11,2				3,3	3,2	10,4				3,0	2,8	8,4
1.1	Wrong materials	2,0	4,0	8,0						2,0	4,0	8,0				1,5	4,0	6,0				1,0	3,5	3,5
1.1.1	Not defining the right safety factor for components	2,0	4,0	8,0	These safety factors should be clearly defined by the environmental requirements	Wrong safety factors can lead to system failure and delays	SSM-5900 Materials and mechanical technology study	Vebjørn Orre Aarud Magnus Dybendal	E1	2,0	4,0	8,0		-		1,0	4,0	4,0	Follow ECSS standards		-	1,0	3,0	3,0
1.1.2	Communication errors	2,0	4,0	8,0	Close quarters-low likelihood	Can cause errors in material selection	Control agreement within documents	Vebjørn Orre Aarud Magnus Dybendal	E1	2,0	4,0	8,0	-	-		2,0	4,0	8,0	Control agreement within documents	Vebjørn Orre Aarud Magnus Dybendal	C3	1,0	4,0	4,0
1.2	Known hazards	5,0	4,3	21,5						5,0	2,4	11,9				5,0	2,4	11,9				5,0	2,1	10,6
1.2.1	Collision	5,0	5,0	25,0	The likelihood of collision with micro meteorites in space is high	A collision can cause holes in materials and break electronics	SSM-5900 Materials and mechanical technology study	Vebjørn Orre Aarud Magnus Dybendal	E1	5,0	3,5	17,5	-	-		5,0	3,5	17,5	-		C3	5,0	3,5	17,5
1.2.2	Radiation	5,0	4,0	20,0	The satellite will be hit by radiation	Radiation causes electronics to degrade	SSM-5111 Technical document-Electrical SSM-5900 Materials and mechanical technology study	Stian Laugerud Vebjørn Orre Aarud Magnus Dybendal	E1	5,0	2,0	10,0	-	-		5,0	2,0	10,0	-		C3	5,0	2,0	10,0
1.2.3	Thermal	5,0	3,0	15,0	The satellite will be exposed to a harsh thermal environment	While the thermal environment is harsh, the satellite will regulate the temperature	SSM-5111 Technical document-Electrical	Vebjørn Orre Aarud Magnus Dybendal Elise Løken	E1	5,0	2,0	10,0	-	-		5,0	2,0	10,0	SSM-5423 Bearing report	Vebjørn Orre Aarud Magnus Dybendal	C2	5,0	1,5	7,5
1.2.4	Pressure	5,0	5,0	25,0	The satellite will operate in vacuum	Vacuum can cause outgassing of electronic components	SSM-5111 Technical document-Electrical SSM-5900 Materials and mechanical technology study	Elise Løken Vebjørn Orre Aarud Magnus Dybendal	E1	5,0	2,0	10,0	-	-		5,0	2,0	10,0	SSM-5423 Bearing report, SSM-5900 Materials and mechanical technology study	Vebjørn Orre Aarud Magnus Dybendal	C3	5,0	1,5	7,5

2.4.4. Operational Risks

Table 2. 4. 7: Operational risks

ID	Name	P	C	R	Cause	Effect	Ref	Resp	Cat	P	C	R	Ref	Resp	Cat	P	C	R	Ref	Resp	Cat	P	C	R
2	**Operational Risks**	2,7	4,5	12,0						2,3	4,5	10,1				2,3	3,8	8,6				1,6	3,8	6,1
2.1	Performance degradation	2,3	4,0	9,3						1,5	4,0	6,0				1,5	3,7	5,5				1,2	3,7	4,3
2.1.1	Increased pointing errors	2,0	4,0	8,0	Electronic and mechanical failures/degradation can lead to increased pointing errors	The main task of the system is to point accurately. Increased pointing errors will cause requirements to not be met	SSM-x000 Pointing budget	Elise Løken Magnus Dybendal Torstein Sundnes	E2	2,0	4,0	8,0	SSM-x000 Pointing budget	Elise Løken Magnus Dybendal Torstein Sundnes	E2	2,0	4,0	8,0	SSM-5901 Technical Budgets	Elise Løken	C3	1,0	4,0	4,0
2.1.2	Increased power consumption	2,0	4,0	8,0	Risk 2.1.3 and degradation in the electronics can lead to this risk	This risk can cause the system to not meet requirements	SSM-5901 Technical budget	Stian Laugerud	E1	1,0	4,0	4,0	Motor selection SSM-5111 Technical document electrical. Bearing calculations	Stian Laugerud Vebjørn Orre Aarud Magnus Dybendal	E2	1,0	3,0	3,0	SSM-5901 Technical Budgets, Calculations with safety factors	Vebjørn Orre Aarud		1,0	3,0	3,0
2.1.3	Consumable articles failure	3,0	4,0	12,0	Selection of the wrong lubricant etc. can lead to this risk	This risk can cause increased friction/wear leading to risk 2.1.2 and 2.1.1	SSM-5900 Materials and mechanical technology study	Vebjørn Orre Aarud Magnus Dybendal	E1	1,5	4,0	6,0	-	-	-	1,5	4,0	6,0	Accept			1,5	4,0	6,0
2.2	Reliability	3,0	5,0	15,0						3,0	5,0	15,0				3,0	4,0	12,0				2,0	4,0	8,0
2.2.1	Unstable architecture	3,0	5,0	15,0	Limited time for testing/verification can lead to unstable systems	An unstable control system can lead to the system spinning out of control. Mechanically this can cause parts to fail.	SSM-x000 Functional test procedure SSM-x000 Life test procedure	Stian Laugerud Vebjørn Orre Aarud	C1	3,0	5,0	15,0	SSM-x000 Functional test procedure SSM-x000 Life test procedure	Stian Laugerud Vebjørn Orre Aarud Gisle H. Stenseth	C1	3,0	4,0	12,0	SSM-3002 Functional test procedure SSM-3003 Functional test report	Stian Laugerud Gisle H. Stenseth	C3	2,0	4,0	8,0

2.4.5. Cost Risks

Table 2. 4. 8: Cost risks

ID	Name	P	C	R	Cause	Effect	Ref	Resp	Cat	P	C	R	Ref	Resp	Cat	P	C	R	Ref	Resp	Cat	P	C	R
3	**Cost risks**	2,8	3,0	9,0						2,3	3,0	7,0				2,2	2,5	5,4				1,2	2,3	2,7
3.1	Going over budget	2,8	3,0	9,0						2,3	3,0	7,0				2,2	2,5	5,4				1,2	2,3	2,7
3.1.1	Technical budgets	3,5	4,0	14,0	The technical budget is given by the employee and the likelihood to exceed may appear.	The technical budgets are made using the customers requirements. Exceeding the technical budgets may lead to failing requirements	Technical analysis for each iteration	Torstein Sundnes Elise Løken	E1	2,5	4,0	10,0	Techinical analysis for each iteration	Torstein Sundnes Elise Løken	Each iteration	2,5	3,0	7,5	Update technical budgets wrt torque and pointing accuracy.	Torstein Sundnes Elise Løken	C1	1,0	3,0	3,0
3.1.2	Economical budgets	3,0	3,0	9,0	The cost reduction for this system compared to existing systems is extremely high	The system will be made for the commercial market. Cost is an important factor	Make a cost budget. SSM-1001 Project plan	All	E1	2,5	3,0	7,5	Make a cost budget. SSM-1001 Project plan rev. 2.1	All	E2	2,5	2,5	6,3	SSM-1300 R&D cost budget	Stian Laugerud	C1	1,5	2,0	3,0
3.1.3	Internal Project budget	2,0	2,0	4,0	Since only part of the system will be manufactured, the risk of exceeding the internal project budget is low	Should be avoided, but accepted	Make a cost budget. SSM-1001 Project plan	All	E1	2,0	2,0	4,0	Make a cost budget. SSM-1001 Project plan rev. 2.1	All	E2	1,5	2,0	3,0	Update cost budgets. SSM-1300 R&D cost budget	Vebjørn Orre Aarud	C3	1,0	2,0	2,0

SSM
SMALL SATELLITE MECHANISMS

2.4.6. Schedule Risks

Table 2. 4. 9: Schedule risks

4	Schedule risks	2,8	4,0	11,0						2,0	4,0	8,0				1,5	4,0	6,0				1,2	4,0	4,8
4.1	Wrong model	2,0	3,0	6,0	The group has discussed different models and chosen the most fitting one	Following the wrong model can cause project delays and increase cost	SSM-1001 Project plan.	Torstein Sundnes Elise Løken	02.02.16				Accept	-	-				Accept	-	-			
										1,0	3,0	3,0				1,0	3,0	3,0				1,0	3,0	3,0
4.2	Failure to follow Engineering model	3,0	4,0	12,0	This is the first time the group has followed the chosen model	Following the wrong model can cause project delays and increase cost	Iteration Reports SSM-1002	Stian Laugerud Elise Løken	23.02.16	2,0	4,0	8,0	Iteration Reports SSM-1002	Elise Løken	Each Iteration	1,0	4,0	4,0	Iteration Reports SSM-1002	Elise Løken	Each Iteration	1,0	3,0	3,0
4.3	Time slips	4,0	4,0	16,0	While the model does not allow for time slips, some of these cannot be controlled	Project delay	SSM-1001 Project Plan SSM-1002 Iteration Reports	Torstein Sundnes Elise Løken Stian Laugerud	23.02.16	3,0	4,0	12,0	SSM-1001 Project Plan SSM-1002 Iteration Reports	Torstein Sundnes Elise Løken Stian Laugerud	Each iteration	3,0	4,0	12,0	SSM-1001 Project Plan SSM-1002 Iteration Reports	Torstein Sundnes Elise Løken Stian Laugerud	Each iteration	1,0	4,0	4,0
4.4	Late changes in requirements	2,0	5,0	10,0	The likelihood of late changes in requirements is moderate/low but may appear	If fundamental requirements are changed late in the project, this may cause delays/project failure	Do not accept determinental changes to requirement specification after 2. presentation Specify in project plan SSM-1001	Torstein Sundnes Elise Løken	02.02.16	2,0	5,0	10,0	Do not accept determinental changes to requirement specification after 2. presentation Specify in project plan SSM-1001	Torstein Sundnes Elise Løken	E2	1,0	5,0	5,0	Accept			1,0	5,0	5,0
4.5	Document setup changes	4,0	5,0	20,0	The likelihood of changes in document setup is moderate	Delay	Meeting with supervisor	All	E1	4,0	5,0	20,0	Meeting with supervisor	All	Every Monday	3,0	5,0	15,0	Meeting with supervisor	All	Every Monday	2,0	5,0	10,0

2.4.7. Safety Risks

Table 2. 4. 10: Safety risks

5	Safety Risks	1,3	3,8	5,1						1,3	3,8	5,1				1,3	3,8	5,1				1,3	3,7	4,9
5.1	Workplace injury	1,0	4,0	4,0	Norway has strong regulations for school environment including HSE.	If a student or supervisor/examinator is affected by an injury, the project can in a worst case scenario be delayed or even put on hold.	HSE regulation gets an update to prevent future injuries and the student/supervisor/examinator shall be taken into healthcare. Norwegian authority/school is informed.	Torstein Sundnes/USN	Immediately after the injury is known.	1,0	4,0	4,0	HSE regulation gets an update to prevent future injuries and the student/supervisor/examinator shall be taken into healthcare. Norwegian authority/school is informed.	Torstein Sundnes/USN	Immediately after the injury is known.	1,0	4,0	4,0	HSE regulation gets an update to prevent future injuries and the student/supervisor/examinator shall be taken into healthcare. Norwegian authority/school is informed.	Torstein Sundnes/USN	Immediately after the injury is known.	1,0	4,0	4,0
5.2	Work overload	2,0	3,5	7,0	The project plan and the project is mainly designed by students duing their first bachelor thesis.	If a student or supervisor/examinator is affected by overload in work, the cause can be motivation loss or sickness that may delay the project.	A situation report is executed around the problem to reschedule the work load.	Gisle Hovland Stenseth	Immediately after the problem is identified.	2,0	3,5	7,0	A situation report is executed around the problem to reschedule the work load.	Gisle Hovland Stenseth	Immediately after the problem is identified.	2,0	3,5	7,0	A situation report is executed around the problem to reschedule the work load.	Gisle Hovland Stenseth	Immediately after the problem is identified.	2,0	3,0	6,0
5.3	Unanticipated safety situations	1,0	4,0	4,0		If a student or supervisor/examinator is affected by an unanticipated safety situation such as acute sickness, bone fracture, car crash or even death the project can be in worst case be cancelled or delayed.	Accept. Divide extra workload	Gisle Hovland Stenseth	Immediately after the problem is identified.	1,0	4,0	4,0	Accept. Divide extra workload	Gisle Hovland Stenseth	Immediately after the problem is identified.	1,0	4,0	4,0	Accept. Divide extra workload	Gisle Hovland Stenseth	Immediately after the problem is identified.	1,0	4,0	4,0

2.4.8. Development Risks

Table 2. 4. 11: Development risks

6	Development risk	3,4	3,1	10,3						3,4	3,1	10,3				3,3	3,1	10,1				1,7	2,9	4,9
6.1	Software bugs	5,0	2,0	10,0	Errors in software development are expected.	Known to happen, small project delay	Accept. Functional test procedure SSM-3002	Gisle Hovland Stenseth / Torstein Sundnes	C1	5,0	2,0	10,0	Functional test procedure SSM-3002	Gisle Hovland Stenseth / Torstein Sundnes	C1	5,0	2,0	10,0	SSM-5131 Control system design, SSM-3003 Functional test report	Stian Laugerud Torstein Sundnes	C3	3,0	2,0	6,0
6.2	Test risk	3,3	3,3	11,1						3,3	3,3	11,1				3,3	3,3	11,1				1,8	3,3	6,1
6.2.1	Not vaild test	4,0	3,0	12,0	The project members have not preformed such tests before. Some errors will be a part of the development.	Known to happen, medium project delay	Create test procedures	Vebjørn Orre Aarud/ Stian Laugerud	C1	4,0	3,0	12,0	Create test procedures	Vebjørn Orre Aarud/ Stian Laugerud	C1	4,0	3,0	12,0	SSM-3002 Functional test procedure	Stian Laugerud Gisle Hovland Stenseth	C3	2,0	3,0	6,0
6.2.2	Wrong test	3,0	3,0	9,0	The project members do not have the knowledge to always perform the right test. This is a part of the development phase.	Known to happen, medium project delay	Create test procedures	Vebjørn Orre Aarud/ Stian Laugerud	C1	3,0	3,0	9,0	Create test procedures	Vebjørn Orre Aarud/ Stian Laugerud	C1	3,0	3,0	9,0	SSM-3002 Functional test procedure	Stian Laugerud Gisle Hovland Stenseth	C3	1,5	3,0	4,5
6.2.3	Fail during test	3,0	4,0	12,0	The project members do not have the knowledge at this point to design correctly from start, and errors are a part of the development process.	Known to happen, TBC project delay	Accept. Verificaton analysis	Vebjørn Orre Aarud/ Stian Laugerud	C1	3,0	4,0	12,0	SSM-3002 Funtional test report	Vebjørn Orre Aarud/ Stian Laugerud	C1	3,0	4,0	12,0	SSM-3003 Funtional test report	Vebjørn Orre Aarud/ Stian Laugerud	T1	2,0	4,0	8,0
6.3	Mechanical/electrical	3,0	3,3	9,8						3,0	3,3	9,8				2,8	3,3	9,2				2,0	3,3	6,5
6.3.1	Design errors	3,0	3,0	9,0	The project members may be in a rush or tired, design errors are common during development.	Known to happen, small project delay	TRR	Vebjørn Orre Aarud/ Stian Laugerud	C3	3,0	3,0	9,0	TRR	Vebjørn Orre Aarud/ Stian Laugerud	C3	2,5	3,0	7,5	TRR	Vebjørn Orre Aarud/ Stian Laugerud	C3	2,0	3,0	6,0
6.3.2	Manufacturing errors	3,0	3,0	9,0	Manufacturing errors is a factor of more than one thing, see 6.3.1, 6.3.3, 6.3.4	Known to happen, medium project delay	Manufacturing readiness review	Vebjørn Orre Aarud/ Elise Løken	C2	3,0	3,0	9,0	Manufacturing readiness review	Vebjørn Orre Aarud/ Elise Løken	C2	2,8	3,0	8,5	Manufacturing readiness review	Vebjørn Orre Aarud/ Elise Løken	16.04.2016	2,0	3,0	6,0
6.3.3	Drawing erros	3,0	3,0	9,0	See 6.3.1	Known to happen, small project delay	Manufacturing readiness review	Vebjørn Orre Aarud/ Elise Løken	TBD	3,0	3,0	9,0	Manufacturing readiness review	Vebjørn Orre Aarud/ Elise Løken	TBD	3,0	3,0	9,0	Manufacturing readiness review	Vebjørn Orre Aarud/ Elise Løken	16.04.2016	2,0	3,0	6,0
6.3.4	Communication errors	3,0	4,0	12,0	Common during a project.	Known to happen, medium/high project delay	Meetings act. num #1000	Elise Løken	Immediately after the problem is identified.	3,0	4,0	12,0	Meetings act. num #1000	Elise Løken	Immediately after the problem is identified.	3,0	4,0	12,0	Meetings act. num #1000	Elise Løken	Immediately after the problem is identified.	2,0	4,0	8,0

2.4.9. Human Resources Risks

Table 2. 4. 12: Human resources risks

7	**Human resources risk**	2,0	3,2	6,4						2,0	3,2	6,4						2,0	3,2	6,4				1,7	2,2	3,7
7.1	Human relations	2,0	3,0	6,0						2,0	3,0	6,0						2,0	3,0	6,0				1,3	3,0	4,0
7.1.1	Leaving group	1,0	3,0	3,0	The motivation for the group members seem high.	Delay in project, work overload	Situation report, reschedule project / meeting with KDA and USN	Gisle Hovland Stenseth	Immediately after the problem is identified.	1,0	3,0	3,0	Situation report, reschedule project / meeting with KDA and USN	Gisle Hovland Stenseth	Immediately after the problem is identified.	1,0	3,0	3,0	Situation report, reschedule project / meeting with KDA and USN	Gisle Hovland Stenseth	Immediately after the problem is identified.	1,0	3,0	3,0
7.1.2	Long time leave	2,0	3,0	6,0	The motivation for the group members seem high.	Delay in project, work overload	Situation report, reschedule project internal or with KDA and USN	Gisle Hovland Stenseth	Immediately after the problem is identified.	2,0	3,0	6,0	Situation report, reschedule project internal or with KDA and USN	Gisle Hovland Stenseth	Immediately after the problem is identified.	2,0	3,0	6,0	Situation report, reschedule project internal or with KDA and USN	Gisle Hovland Stenseth	Immediately after the problem is identified.	1,0	3,0	3,0
7.1.3	Work enviorment	3,0	3,0	9,0	The work facilities can be discussed. (air) Group members seem to work fine.	Sickness and demotivation/communication loss	Situation report/ meeting with KDA and USN	Gisle Hovland Stenseth	Immediately after the problem is identified.	3,0	3,0	9,0	Situation report/ meeting with KDA and USN	Gisle Hovland Stenseth	Immediately after the problem is identified.	3,0	3,0	9,0	Situation report/ meeting with KDA and USN	Gisle Hovland Stenseth	Immediately after the problem is identified.	2,0	3,0	6,0
7.2	Supervisors leaving	1,0	4,0	4,0	Employed with contract to USN and KDA with resignation time.	Delay/stop in project	Situation report/ meeting with KDA and USN	Gisle Hovland Stenseth	Immediately after the problem is identified.	1,0	4,0	4,0	Situation report/ meeting with KDA and USN	Gisle Hovland Stenseth	Immediately after the problem is identified.	1,0	4,0	4,0	Situation report/ meeting with KDA and USN	Gisle Hovland Stenseth	Immediately after the problem is identified.	1,0	3,0	3,0
7.3	Sickness	2,0	3,0	6,0	Normal health assumed	Delay in project, work overload	Internal meeting with situation report	Gisle Hovland Stenseth	Immediately after the problem is identified.	2,0	3,0	6,0	Internal meeting with situation report	Gisle Hovland Stenseth	Immediately after the problem is identified.	2,0	3,0	6,0	Internal meeting with situation report	Gisle Hovland Stenseth	Immediately after the problem is identified.	2,0	2,0	4,0
7.4	Not utilizing project members	2,0	3,0	6,0	Motivation is good, planning can be an issue	Delay in project, work overload for individual students	Divide work during meetings	Gisle Hovland Stenseth	Every meeting	2,0	3,0	6,0	Divide work during meetings	Gisle Hovland Stenseth	Every meeting	2,0	3,0	6,0	Divide work during meetings	Gisle Hovland Stenseth	Every meeting	2,0	3,0	6,0
7.5	Communication	3,0	3,0	9,0	Communication problems will occur	Delay in project, work overload	Frequent meetings	Gisle Hovland Stenseth	Immediately after the problem is identified.	3,0	3,0	9,0	Frequent meetings	Gisle Hovland Stenseth	Immediately after the problem is identified.	3,0	3,0	9,0	Frequent meetings	Gisle Hovland Stenseth	Immediately after the problem is identified.	2,0	3,0	6,0

2.4.10. Conclusion

Table 2. 4. 13: Risk summary before mitigation

#	Risk	Likelihood	Impact	Total Risk
1	Space Environment	3.5	4.1	**14.4**
2	Operational Risks	2.7	4.5	**12.0**
3	Cost risks	2.3	3.0	**7.0**
4	Schedule risks	2.8	4.0	**11.0**
5	Safety Risks	1.3	3.8	**5.1**
6	Development risk	3.4	3.1	**10.3**
7	Human resources risk	2.0	3.2	**6.4**

Table 2.4.13 shows the summary of the main risk categories. Environmental, operational, scheduling and development risks are unacceptable, and measures shall be taken to eliminate the risks.

Table 2. 4. 14: Risk summary after mitigation 1

#	Risk	Likelihood	Impact	Total Risk
1	Space Environment	3.5	3.2	**11.2**
2	Operational Risks	2.3	4.5	**10.4**
3	Cost risks	2.3	3.0	**6.9**
4	Schedule risks	2.0	4.0	**8.0**
5	Safety Risks	1.3	3.8	**5.1**
6	Development risk	3.4	3.1	**10.3**
7	Human resources risk	2.0	3.2	**6.4**

Table 2. 4. 15: Risk reduction

Risk	Reduction %
Space Environment	22.22
Operational Risks	13.33
Cost risks	1.42
Schedule risks	27.27
Safety Risks	0
Development risk	0
Human resources risk	0

The risk analysis after mitigation 1 shows a clear reduction in environmental, operational and schedule risks. This is due to mitigation actions being performed. A complete cost budget has not been created, leading to only a small change in cost risk. No reduction is seen in development risks due to the action dates being in the construction phase. Safety and human resources risks are not reduced as these do not have specific mitigation action dates.

Table 2. 4. 16: Risk summary after mitigation 2

		After mitigation 2		
#	**Risk**	**Likelihood**	**Impact**	**Total Risk**
1	Space Environment	3.3	3.2	**10.6**
2	Operational Risks	2.3	3.8	**8.7**
3	Cost risks	2.2	2.5	**5.5**
4	Schedule risks	1.5	4.0	**6.0**
5	Safety Risks	1.3	3.8	**4.9**
6	Development risk	3.3	3.1	**10.2**
7	Human resources risk	2.0	3.2	**6.4**

Table 2. 4. 17: Risk reduction after mitigation 2

Risk	**Reduction %**
Space Environment	5.36
Operational Risks	16.35
Cost risks	20.29
Schedule risks	25.00
Safety Risks	3.92
Development risk	0.97
Human resources risk	0

After mitigation 2, there are not significant changes and reductions in the risks. From table 2.4.17, the reduction in the cost risk is a result of the cost budget which has been derived in E2. The pointing budget should have been derived in E2 to reduce the operational risks, but due to changed focus in the project, this task slipped in this iteration.

Table 2. 4. 18: Risk summary after mitigation 3

		After mitigation 3		
#	**Risk**	**Likelihood**	**Impact**	**Total Risk**
1	Space Environment	3	2.8	**8.4**
2	Operational Risks	1.6	3.8	**6.1**
3	Cost risks	1.2	2.3	**2.8**
4	Schedule risks	1.4	4	**5.6**
5	Safety Risks	1.3	3.7	**4.8**
6	Development risk	1.7	2.9	**4.9**
7	Human resources risk	1.7	2.2	**3.7**

Table 2. 4. 19: Risk reduction after mitigation 3

Risk	Reduction %
Space Environment	20.75
Operational Risks	29.89
Cost risks	49.10
Schedule risks	6.67
Safety Risks	2.04
Development risk	51.96
Human resources risk	42.19

After mitigation 3 we can see a clear reduction in space environment, operational, cost, development and human resources risk. Table 2.4.19 shows that the risk of development has been reduced with 52 % since mitigation 2 due to the design being finished in C2, parts were manufactured and the software has been completed. As shown in table 2.4.18 all the risks are acceptable, but measures can be taken to eliminate some of the risks, except for the environmental, which should be eliminated further in the next phase of the project. This is since under the project, changes were made and almost everything concerning environmental was eliminated due to time schedule.

2.4.10.1. *Before mitigation vs. after mitigation 3*
Table 2. 4. 20: Before mitigation vs. after mitigation 3

#	Risk	Before mitigation			After mitigation 3		
		Likelihood	Impact	Total Risk	Likelihood	Impact	Total Risk
1	Space Environment	3.5	4.1	**14.4**	3	2.8	**8.4**
2	Operational Risks	2.7	4.5	**12.0**	1.6	3.8	**6.1**
3	Cost risks	2.8	3.0	**8.4**	1.2	2.3	**2.8**
4	Schedule risks	2.8	4.0	**11.0**	1.2	4	**4.8**
5	Safety Risks	1.3	3.8	**5.1**	1.3	3.7	**4.8**
6	Development risk	3.4	3.1	**10.3**	1.7	2.9	**4.9**
7	Human resources risk	2.0	3.2	**6.4**	1.7	2.2	**3.7**

Table 2. 4. 21: Risk reduction before mitigation vs after mitigation 3

Risk	Reduction %
Space Environment	**41.82**
Operational Risks	**49.33**
Cost risks	**67.14**
Schedule risks	**56.36**
Safety Risks	**5.89**
Development risk	**52.08**
Human resources risk	**41.56**

During the project one of the milestones was to reduce the risks as much as possible. As shown in table 2.4.21, the reductions has been clearly remarkable in most of the top level risks. Throughout this project one of our main requirements were to reduce the cost as much as possible, therefore the cost risk is one of the main risks we have been focusing on.

2.4.10.2. *Purpose of risk management during APMA project*

During the development of this project, it is important to show risk reduction in the top level risks to keep the interest of the stakeholders, due to the financial foundation of the project funded by the stakeholders.

As shown in table 2.4.21 most of the top level risks have been reduced about 40%. This shows that the project has had significant progress during the different segments, which makes the project more interesting to potential stakeholders. This has a huge influence on research and development, and will contribute to a more detailed second prototype considering the economical starting point, available research sources and opportunities.

Some of the risk reductions may be wrong since certain factors are excluded or are approximated. However, estimations are still important, to ensure progress in the project. This leads to further optimizations, ensuring a high quality final result according to stakeholder requirements.

The technical aspect of risk reduction is in line with the economics. This is an important factor with respect to the progress of the project according to the technical requirements. Mainly, it's the financial part that is important since it contributes to better resources to perform more analysis, tests and reports.

2.4.11. References

[1] V. O. Aarud and S. Laugerud, "Test & Verification Specification", SSM-3000, Rev.1.1, 18.02.16.

[2] T. Sundnes and E. Løken, "Project Plan", SSM-1001, Rev.1.1, 18.02.2016.

[3] E. Løken and S. Laugerud, "Iteration Reports", SSM-1002, Rev 1.0, 02.02.2016.

[4] Spacecraft Mechanical loads analysis handbook, ECSS-HB-32-26A, 19.02.2013.

[5] Space project management: Risk management, ECSS-M-ST-80C, 31.07.2008.

2.5. Iteration reports

i.   Abstract

This chapter contains iteration reports written in the end of each iteration in the project, as a result of the Unified Process Iterative Development model. The reports will be written throughout the project and give an overview of the project status.

ii. Contents

v. Document history

Table 2. 5. 1: Document history

Rev	Date	Author	Approved	Description
0.1	31.01.16	EL, SL	-	Document created Report from iteration 1 is added
1.0	02.02.16	EL, SL	TS	Reviewed and published
1.1	09.02.16	EL, SL	TS	Added activities 1000, 5111 and 5121 under title 4.4. Changed name to iteration report. Corrected typos
1.2	23.02.16	EL, SL	MD	Changed document layout Added iteration report from E.1.
2.0	07.03.16	EL	TS	Reviewed and published
2.1	22.03.16	EL		Added iteration report from E.2.
3.0	23.03.16	EL	TS	Reviewed and published
4.0	15.04.16	EL	TS	Added iteration report from C.1
5.0	24.04.16	EL	TS	Added iteration report from C.2
6.0	06.05.16	EL		Added iteration report from C.3
7.0	13.05.16	EL	GHS	Added iteration report from T.1 Reviewed and published

2.5.1. Introduction

An iteration report is a summary of an iteration or phase. It contains a description of the purpose of the iteration, the status of the project in the end of the phase, and a detailed plan for the next phase.

This chapter will be updated with new iteration reports summarizing the project status through the whole project period. By the end of the project, this chapter will be complete, containing a report from all the planned iterations and a conclusion of how the iterations have affected the project.

2.5.2. First iteration: Inception 1 (11.01.16 – 02.02.16)

The purpose of the first iteration, inception 1 (I: 1), is to establish the frame of the project and to understand what to do, how to do it and why. The customer is the target of this phase and the project will be planned with a focus on risks.

2.5.2.1. *Project Status*

The goals for this phase is to understand the given assignment, choose a project model, give the group members different responsibilities and sign contracts. During this phase, the following documents are created: Project plan, requirements specification and test & verification specification. These documents shall be the main content of the first presentation (05.02.2016), which is the milestone of this iteration. In addition to the documents above, a website has been designed, a concept draft has been made, and the concept has been 3D printed.

The project is almost on schedule. The only delayed element is the risk analysis, which is a part of the project plan. A late meeting with the external supervisor caused this delay and the risk analysis will be completed by 02.02.2016.

The group has also started the concept analysis for the APMA, and looked into some concepts. Two of these concepts have been extended to virtual models, resulting in a 3D-print, which will be presented at the first presentation.

2.5.2.2.   *Highlights*

Breakthroughs, accomplishments, major decisions or changes in the project plan:

- The project model is been set to Unified process.
- Group leader and other responsibilities are set.
- After discussion with employer/costumer, the APMA will be designed with only one antenna. (The APMA shall transmit and receive signals simultaneously).
- The main requirements for the project are specified.

2.5.2.3.   *Tasks in progress or completed:*

List of the tasks that each member of the project worked on in inception 1:

Table 2. 5. 2: Task list for inception 1

Activity nr.	Activity name	Description	Who	% complete
900	Concept	Early concept analysis started (mechanical)	VOA, MD, GHS, TS, SL, EL	100%
1001	Project plan	Creation of document, revision 1.0	EL, TS, GHS, VOA	100%
2000	Requirement specification	Creation of document, revision 1.0	GHS, MD	100%
3000	Test & Verification Specification	Creation of document, revision 1.0	SL, VOA	100%
4000	Webpage	Creation of webpage, design, domain	TS, EL	90%

2.5.2.4.   *Tasks for the next iteration:*

The list below gives an overview of the activities the project group is planning to work with during the next iteration, elaboration 1. This iteration will have a great focus on the design and analysis, as well as tests and simulations. In addition to this, all the previous documents will be updated based on the experience from I1.

Table 2. 5. 3: Task list for the next iteration, E1

Activity nr.	Activity name	Description	Who
900	Concept	Detailed concept analysis Choose concept	VOA, MD, GHS, TS, SL, EL
1000	SITRAP	Report containing experiences from E1	VOA, MD, GHS, TS, SL, EL
1001	Project plan	Update to revision 2.0	EL, TS
2000	Requirement specification	Update to revision 2.0	GHS, MD
3000	Test & Verification Specification	Update to revision 2.0	SL, VOA
4000	Webpage	Get a domain for the website	TS
5000	Test and simulation	Simulation of the first prototype/parts, verification and validation	VOA, MD, GHS, TS, SL, EL
5100	Design	Give a draft of all the designs (mechanical, electrical and software)	VOA, MD, GHS, TS, SL, EL
5111	Technology document - Electronics	Document including motor, antenna and material analysis	EL, SL, GHS, TS
5120	Technology document -Mechanical	Document including material analysis	VOA, MD

2.5.3. Second iteration: Elaboration 1 (10.02.16 – 03.03.16)

The purpose of the second iteration, elaboration 1 (E.1), is to capture the majority of requirements to ensure a stable system architecture, which continues in E.2. At the end of elaboration phase 2, the system will have a stable architecture.

2.5.3.1. *Project status*

Elaboration 1 started with a detailed concept analysis [4], where 3 different concepts were evaluated and compared. Due to the given cost requirements, rotary joints had to be avoided in this project, and the chosen concept for the low-cost APMA is the double mirror reflector antenna.

To ensure the feasibility of this concept, a link analysis [5] was done. This is an analysis of the radio frequency signal strength in the communication between two antennae. The analysis gave a signal strength that is within required limits, and the concept is feasible.

Further, the top-level design of the chosen concept was started. A 3D-model of prototype 1 [6] was sketched; mechanical materials, lubrication and fastening was chosen in a material study [7], and some technical budgets (mass, power and torque) were created, [8]. An electrical technical document [9] has also been written. This document includes the selection of antenna, controller, motor and motor driver. A short description of electrical materials and components that are to be avoided in space is also included.

The group has started working with the design of the control system. The control system software design has started [10], and part of the software has already been developed. A part of the already existing mechanism KDA has developed is physically available for the project, and the early testing of the space vector pulse-width modulation (SVPWM) software is tested on this mechanism. The testing and further development of the software will continue in the next phase, elaboration 2.

At the end of elaboration 1, the group had a situation report where documents were updated. This included the project plan [3], requirement specification [2], test & verification specification [1] and the risk document [11]. The design of prototype 1 complies with the requirements given in table 2.5.4, and the risks in table 2.5.5 are reduced:

Table 2. 5. 4: Requirements met by the design of prototype 1

Requirement number	Requirement criteria
REQ- 2.1.1	The system shall have a power consumption of ≤15Watt, including electronics and actuators.
REQ-2.1.1.1	The motors shall have a maximum power consumption of 12 W.
REQ-2.1.1.2	The control system shall have a maximum power consumption of 3 W.
REQ-2.2.1	The mass of the system shall be maximum 4 kg, including electronics.
REQ-2.2.1.1	The mass of the mechanism shall be maximum 3 kg.
REQ-2.2.1.2	The mass of the electronics shall be maximum 1 kg.
REQ- 2.3.3	Motorization according to ECSS-E-ST-33-01C shall be satisfied.
REQ-2.3.3.1	The motor for the azimuth stage shall produce a torque of minimum 0.127 Nm.
REQ-2.3.3.2	The motor for the elevation stage shall produce a torque of minimum 0.107Nm.
REQ-2.4.2	The elevation stage shall be able to move minimum ± 90 deg.
REQ-2.4.3	The azimuth stage shall be able to move minimum ± 180 deg.
REQ-2.4.4	The system shall be able to move with a velocity of ≥ 60 deg/s.
REQ-2.4.5	The system shall be able to accelerate at a rate of ≥ 40 deg/s^2.
REQ-2.5.4	The system shall communicate between the spacecraft using the CANbus protocol.
REQ-2.6.2	The overall gain of the system shall be ≥ 23 dBi.

REQ-2.6.3	The system shall be able to communicate at a carrier frequency of 23 GHz.
REQ-2.6.6	The system shall contain a transmit sub-system.
REQ-2.6.7	The system shall contain a receive sub-system.
REQ-2.6.8	The gain variation shall be maximum± 1 dBi.
REQ-2.7.1	The system shall contain a motor control system.

Table 2. 5. 5: Risk evaluation, before vs. after mitigation [11]

		Before mitigation			After Mitigation 1		
#	Risk	Likelihood	Impact	Total Risk	Likelihood	Impact	Total Risk
1	Space Environment	3,5	4,1	14,4	3,5	3,2	11,2
2	Operational Risks	2,7	4,5	12,0	2,3	4,5	10,4
3	Cost risks	2,3	3,0	7,0	2,3	3,0	6,9
4	Schedule risks	2,8	4,0	11,0	2,0	4,0	8,0
5	Safety Risks	1,3	3,8	5,1	1,3	3,8	5,1
6	Development risk	3,4	3,1	10,3	3,4	3,1	10,3
7	Human resources risk	2,0	3,2	6,4	2,0	3,2	6,4

Some of the most important features will be presented in our second presentation (09.03.16), which is a milestone for this iteration.

The project is on schedule according to the project plan, even though some additional and unforeseen tasks have appeared. This includes updates of document layout after feedback from internal supervisor and some aspects of the design which has to be reevaluated before taking finally decisions (antenna- and controller selection).

2.5.3.2. *Highlights*

Breakthroughs, accomplishments, major decisions or changes in the project plan:

- Concept selection: Double mirror reflector antenna
- Concept feasibility checked through a link analysis
- Technical budgets is derived: mass, power and torque
- Mechanical materials, lubrication and fastening is chosen
- Prototype 1 of the 3D-model is designed
- Motor control has reached a nearly completed design.
- Motor selection: Brushless DC-motor, EC45 flat 70W
- Controller selection: ST microelectronics STEVAL-IHM039V1 with a STM32F414ZGT6 ARM Cortex-4M processor
- Motor driver selection: L6230
- Antenna selection: Cassegrain antenna
- Second Presentation

2.5.3.3. *Tasks in progress or completed*

Table 2. 5. 6: Tasks in progress or completed, E1

Activity nr.	Activity name	Description	Who	% complete
0900	Concept analysis	Finished	EL,VOA,MD	100 %
1001	Project plan	Updated	EL, TS, GHS, VOA	100 %
1002	Iteration report, E1	Finished	EL, VOA	100 %
1003	2. presentation	Started	All	50 %
1200	Risk	Updated	VOA,GHS,MD	100 %
2000	Requirement specification	Updated	GHS, MD	100 %
3000	Test & Verification Specification	Updated	SL, VOA	100 %
4000	Webpage	Got domain	TS	100 %
5111	Technical document-electro	Almost finished	GHS,TS,SL,EL	80 %
5112	Link analysis	Finished	GHS	100 %
5113	Motor drive design	Started	GHS	50 %
5121	CAD model prototype 1	Finished	MD	100 %
5123	Mechanical description	Finished	MD	100 %
5221	CAD model prototype 2	Started	MD	5 %
5131	Control system design	Started	TS, GHS	50 %
5132	Control system software	Started	TS	25 %
5900	Material study	Finished	VOA	100 %
5901	Technical budgets	Finished	EL,VOA,MD	100 %

2.5.3.4. *Tasks for the next iteration*

In the next iteration, elaboration 2, the design of the APMA will continue to give the system a stable architecture. The design of the motor control system will be in focus for the electrical- and software engineers, while simulation and testing of the 3D – model will be in focus for the mechanical engineers.

Planned task that will be continued or started in the next phase is given in table 2.5.7:

Table 2. 5. 7: Tasks for the next iteration, E2

Activity nr.	Activity name	Description	Who
1000	SITRAP	Report containing experiences from E2	All
1001	Project plan	Update to revision 3.0	EL, TS
2000	Requirement specification	Update to revision 3.0	GHS, MD
3000	Test & Verification Specification	Update to revision 3.0	SL, VOA
5000	Test and simulation	Simulation of the second prototype/parts, verification and validation	VOA, MD, GHS, TS, SL, EL
5111	Technical document-electro	Finishing the antenna and controller selection	GHS,TS,SL,EL
5113	Motor drive design	Finish the design, start testing	GHS, SL, EL
5114	Control system design	Finish the design, start testing	GHS, TS, EL, SL
5221	CAD model prototype 2	Update	MD,VOA
5130	Software design	Make the software design stable, continue testing	TS, GHS
XXXX	Technology document (mechanical)	Make sure req is met for stable architecture.	MD,VOA
XXXX	Technology document (electro)	Make sure req is met for stable architecture.	EL,GHS,EL
XXXX	Technology document (software)	Make sure req is met for stable architecture.	TS
XXXX	Cost budget	Make a cost budget for the APMA	TS, SL
XXXX	Pointing budget	Make a pointing budget for the APMA	MD, TS, EL
XXXX	Functional test procedure	Make a functional test procedure	SL, VOA
XXXX	Life test procedure	Make a life test procedure	SL, VOA

2.5.4.　Third iteration: Elaboration 2 (07.03.16 – 23.03.16)

The purpose of the third iteration, elaboration 2 (E.2), is to capture the majority of requirements to ensure a stable system architecture.

A stable architecture means that top-level concepts and solutions for the system is chosen, and the detailed design and improvement of these solutions will continue in the construction phase.

2.5.4.1. *Project status*

The elaboration 2 iteration started with the second presentation of the project, which was in focus in the first days of this iteration. The feedback the group got from sensors and supervisors after the presentation was to continue the work with the same progressivity.

The main goals for this phase were to focus on the motor control system, simulations and tests of the 3D-model. This focus changed after feedback from external supervisors, and the control system electrical was not prioritized that much in this phase. The main focus areas have been the antenna trade- off, bearing calculations and control system design.

In the antenna trade-off, two different antenna system concepts were dexplaind in detail (Cassegrain reflector antenna and horn antenna) and evaluated. This included dimensioning of the system, calculations of total gain in the system including different losses, simulations of radiation patterns and mass estimations. The antenna system concept chosen for the APMA is the Cassegrain reflector antenna design. This is more complex than the horn antenna, but with respect to size, mass and performance this concept has been deemed the most favorable.

In software design, a function that allows us to more precisely determine a velocity for the motors has been implemented. Acceleration and deceleration are added to the mechanism, both forward and backwards. The software also recognizes input (0-360 degrees), and the encoder is implemented, allowing us to set the position with an accuracy of 40 960 steps per 360 degrees. Timers have been set up to calculate the accelerations and velocities independent of the main code. The control system design document has been updated accordingly.

For the mechanical part, initially the main focus for elaboration 2 was to satisfy the last major requirements. After a meeting with KDA, the main focus for this phase was changed due to the importance of bearings. The bearing study will be divided into iterations, where the focus in the first iteration is to look at mechanical laws about bearings, such as calculation factors, miles equation and general bearing equations.

Additionally, an estimated cost budget (added in the project plan) is developed in this iteration. Electronics are also ordered. Due to the changed focus in this iteration, some of the planned tasks have slipped. This includes the design of the control system and the pointing budget, along with tests of the 3D model.

The work done with the antenna trade-off and the bearing design are detailed and specific, and had to be done at a later point anyways. Thus, the changed focus in this iteration does not mean that the project is delayed. Some tasks are delayed and some tasks planned to do in the next iterations are already done. Overall, the project is mainly on schedule.

Table 2.5.8 gives an overview of the requirements that are satisfied by the present design of prototype 2:

Table 2. 5. 8: Requirements met by the design of prototype 2

Requirement number	Requirement criteria	Satisfied
REQ- 2.1.1	The system shall have a power consumption of ≤15Watt, including electronics and actuators.	E1
REQ-2.1.1.1	The motors shall have a maximum power consumption of 12 W.	E1
REQ-2.1.1.2	The control system shall have a maximum power consumption of 3 W.	E1
REQ-2.2.1	The mass of the system shall be maximum 4 kg, including electronics.	E1
REQ-2.2.1.1	The mass of the mechanism shall be maximum 3 kg.	E1
REQ-2.2.1.2	The mass of the electronics shall be maximum 1 kg.	E1
REQ- 2.3.3	Motorization according to ECSS-E-ST-33-01C shall be satisfied.	E1
REQ-2.3.3.1	The motor for the azimuth stage shall produce a torque of minimum 0.127 Nm.	E1
REQ-2.3.3.2	The motor for the elevation stage shall produce a torque of minimum 0.107Nm.	E1
REQ-2.4.2	The elevation stage shall be able to move minimum ± 90 deg.	E1
REQ-2.4.3	The azimuth stage shall be able to move minimum ± 180 deg.	E1
REQ-2.4.4	The system shall be able to move with a velocity of ≥ 60 deg/s.	E1
REQ-2.4.5	The system shall be able to accelerate at a rate of ≥ 40 deg/s^2.	E1
REQ-2.5.4	The system shall communicate between the spacecraft using the CANbus protocol.	E1
REQ-2.5.7	The system shall send feedback when it is moving.	E2
REQ-2.5.8	The system shall send feedback when it is not moving.	E2
REQ-2.6.2	The overall gain of the system shall be ≥ 23 dBi.	E1
REQ-2.6.3	The system shall be able to communicate at a carrier frequency of 23 GHz.	E1
REQ-2.6.6	The system shall contain a transmit sub-system.	E1
REQ-2.6.7	The system shall contain a receive sub-system.	E1
REQ-2.6.8	The gain variation shall be maximum± 1 dBi.	E1
REQ-2.7.1	The system shall contain a motor control system.	E1
REQ-2.7.8	The system shall not move until a position command is received.	E2
REQ-2.7.9	The control system shall be able to control the position of the system	E2
REQ-3.3.1	The system shall have a cost of maximum €10.000 per unit. Assuming a batch size of 1000 units.	E2

Table 2.5.9 and figure 2.5.1 gives an overview of the risk reduction so far in the project:

Table 2. 5. 9: Risk evaluation, before vs. after mitigations [11]

#	Risk	Before mitigation			After mitigation 1			After mitigation 2		
		Likelihood	Impact	Total Risk	Likelihood	Impact	Total Risk	Likelihood	Impact	Total Risk
1	Space Environment	3,5	4,1	14,4	3,5	3,2	11,2	3,3	3,2	10,6
2	Operational Risks	2,7	4,5	12,0	2,3	4,5	10,4	2,3	3,8	8,7
3	Cost risks	2,8	3,0	8,4	2,3	3,0	6,9	2,2	2,5	5,5
4	Schedule risks	2,8	4,0	11,0	2,0	4,0	8,0	1,5	4,0	6,0
5	Safety Risks	1,3	3,8	5,1	1,3	3,8	5,1	1,3	3,8	4,9
6	Development risk	3,4	3,1	10,3	3,4	3,1	10,3	3,3	3,1	10,2
7	Human resources risk	2,0	3,2	6,4	2,0	3,2	6,4	2,0	3,2	6,4
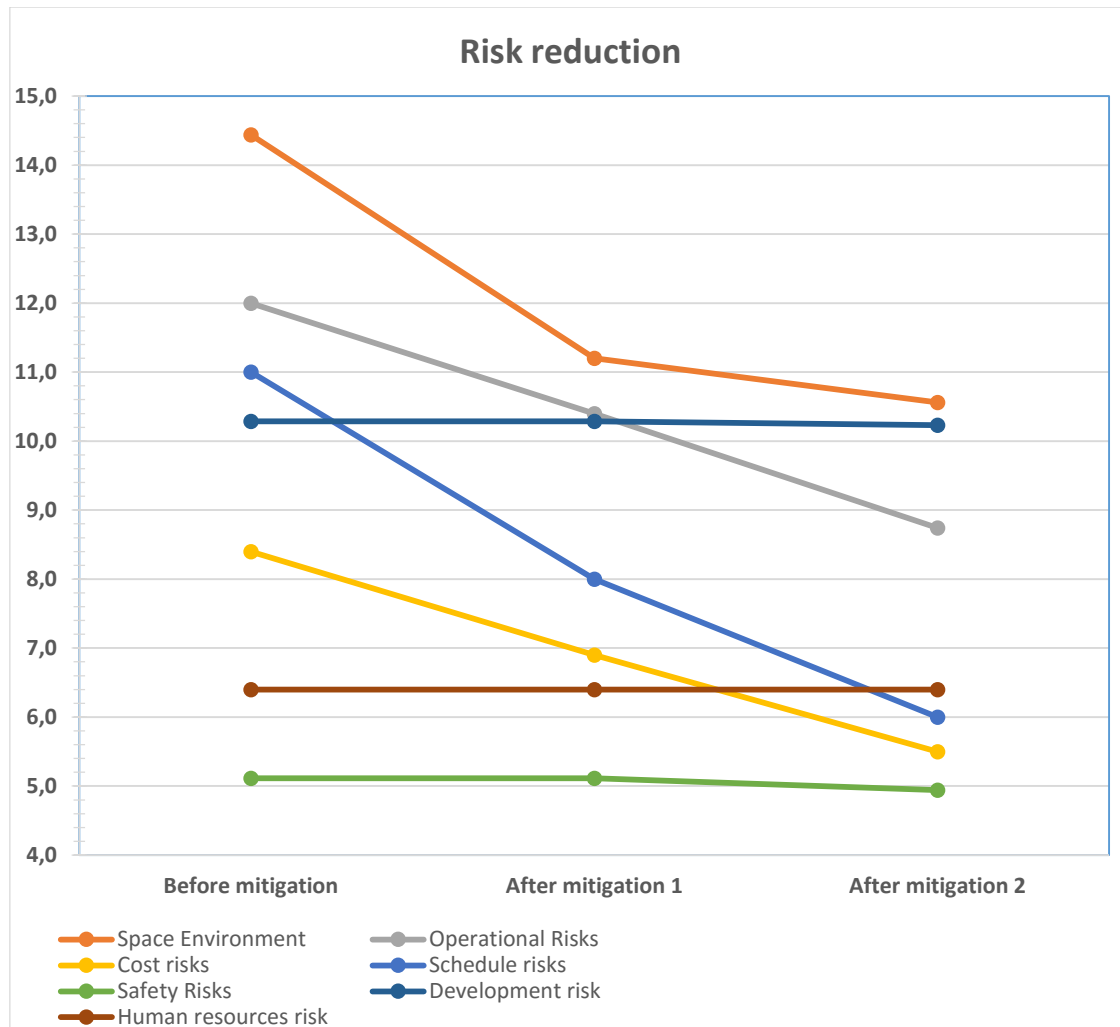
Figure 2. 5. 1: Risk reduction diagram

The following list gives an overview of the chosen solutions giving the APMA a stable architecture at the end of the Elaboration 2 phase:

- The APMA concept is chosen through the concept analysis: Double mirror reflector antenna.
- The concept feasibility is verified through the "Link Analysis".
- Brushless DC motor, motor drive and controller is selected through "technical document – electrical" and ordered.
- The Cassegrain antenna system is selected through the "Antenna Trade-off".
- Technical budgets are created (Torque, mass, power) in "Technical budgets".
- Mechanical materials are selected through the "Material Analysis"
- DAK-model of the concept is modelled in "Design description"
- Top-level software for the motor control system is developed, "Control system software".
- Space vector pulse width modulation is developed in the software.

2.5.4.2. *Highlights*

Breakthroughs, accomplishments, major decisions or changes in the project plan:

- Second presentation complete
- Design of the antenna system is selected through an antenna trade-off

- Electronics are ordered: motor, motor drive, etc.
- Estimated cost budget developed
- Bearing calculations and design started
- Acceleration formula developed for software
- Technical document control system changed to control system design
- Design of the motor control system and the pointing budget are delayed according to the project plan.

2.5.4.3. *Tasks in progress or completed*
Table 2. 5. 10: Tasks in progress or completed, E2

Activity nr.	Activity name	Description	Who	% complete
1001	Project plan, cost budget	Draft finished	SL	100 %
1002	Iteration report, E2	Finished	EL, VOA	100 %
1003	2. presentation	Finished	All	100 %
1200	Risk	Updated	VOA,GHS,MD	100 %
2000	Requirement specification	Updated	GHS, MD	100 %
3000	Test & Verification Specification	Updated	SL, VOA	100 %
5111	Technical document-electro	Almost finished	GHS,TS,SL,EL	100 %
5113	Motor drive design	Finished	GHS	100 %
5211	Antenna Trade-off	Draft finished	EL, GHS	90 %
5214	Control system, electrical	Started	SL, EL, GHS	20 %
5221	CAD model prototype 2	Started	MD	70 %
5223	Bearing report	Started	MD, VOA	25 %
5231	Control system design	Started	TS	40%
5232	Control system, software	Started	TS	45 %

2.5.4.4. *Tasks for the next iteration*
In the next iteration, the project is entering a new phase – the construction phase. This phase will be separated into three time boxed iterations. Detailed design, implementations, early testing and deployment are the main stages. By doing this in three iterations, the quality of the system is ensured, [3].

In the next iteration, construction 1, the design of the APMA already has a stable architecture. The design will continue, but now the project will go more into the depth and the design will be more detailed and specific. The design of the motor control system will be in focus for the electrical- and software engineers. Due to the unexpected work with the antenna trade-off in elaboration 2, the design of the control system slipped in E2. Further calculations and design of the bearings will be the focus area for the mechanical engineers, where the focus will be on hertzian stress, clamping and preload.

Planned tasks that will be continued or started in the next phase are given in table 2.5.11:

Table 2. 5. 11: Tasks for the next iteration, C1

Activity nr.	Activity name	Description	Who
1000	SITRAP	Report containing experiences from C1	All
5000	Test and simulation	Simulation of the second prototype/parts, verification and validation	VOA, MD, GHS, TS, SL, EL
5314	Control system design	Finish the design, start testing	GHS, TS, EL, SL
5321	CAD model prototype 3	Update	MD,VOA
5331	Control system design	Continue developing and testing	TS, GHS
1001	Cost budget	Update the cost budget with more details	SL, EL
XXXX	Pointing budget	Make a pointing budget for the APMA	MD, GHS, EL
XXXX	Functional test procedure	Make a functional test procedure	GHS
XXXX	Life test procedure	Make a life test procedure	SL, VOA
XXXX	Test procedure and verification analysis	Make test procedures and verification analysis	SL, VOA

2.5.5. Fourth iteration: Construction 1 (06.04.16 – 15.04.16)

The construction phase is the most comprehensive phase in the project. The purpose of this phase is to implement system features in a series of iterations. Analysis & design, implementation, testing and deployment should be the focus areas.

For this project, the construction phase will be divided into three iterations. The goal for construction 1 is to work with detailed design of the APMA, based on the stable architecture from elaboration 1.

2.5.5.1. *Project status*

The construction 1 iteration was a relative short iteration. The plan for this iteration was to continue the design of the motor control system and the design of the bearings (hertzian stress, clamping and preload).

This week the group also had a meeting with the external supervisor of the project. The time is running fast, and some boundaries and focus areas for the rest of the project had to be set. After discussing this with Kongsberg Space, the following areas will be prioritized during the last period of the project:

- Building the azimuth assembly (possibly 3D-print of the elevation assembly).
- The motor control system
- Gear, bearings etc.
- Test procedure, functional test
- Test and test report
- Updating the budgets
- Pointing budget

The following areas will not be prioritized:

- Worst-case scenario analysis (Monte Carlo)
- Thermal vacuum test
- Vibration test
- Implementing of CANbus (replaced by UART).

The design of the control system is chosen, and we have been working with modelling and simulations of it in Simulink. The control system is built as a Cascade controller. This means that it regulates in three steps: a current regulator, a velocity regulator and a position regulator. The reference for the system is an S-curve, which combines the references of position, speed and acceleration. When running the simulation, the model works as expected.

The next part in the design of the control system is the implementation of the Simulink model in software. This work is one of the main focus points, and different solutions will be evaluated and tested (implementation by writing the software code or direct interface between the microcontroller and Simulink). Currently, implementing the code to C has been successful so far.

The group has also worked with solutions to get the desired feedback from the physical system, which is needed in the regulator. This contains the position feedback from the encoder, filtering of the position feedback to get the velocity feedback and measurement of the 3-phase currents from the motor.

In this iteration we also got the microcontroller which is going to be used in the control system. The main focus has been testing it and learning how to program it, as this something completely different from the microcontrollers programmed earlier. We are now working with the implementation of the control system in this controller.

Mechanically, the final design of the azimuth assembly and the 2D drawings are completed. They will be sent to production on Monday and produced next week. Completing this design was difficult because of the relation between the design of the assembly and the dimensions of the bearings.

The bearing is chosen with respect to distance between the bearings and external forces. The preloads are decided and the calculations to find the final dynamics tensions in the bearings are in focus now. This is important to find the friction forces in the system.

The group has also started writing the test procedure for the functional test.

New limitations for the project goal is set, due to unexpected occurrences and changed focus areas. With respect to these new limitations, the group is on schedule according to the plan, but there is a lot to do to finish the project. Yet, the group is working with technically advanced tasks and problems, and it is difficult to estimate how much time they will consume.

Table 2.5.12 gives an overview of the requirements that are satisfied by the present design of prototype 3:

Table 2. 5. 12: Requirements met by the design of prototype 3.

Requirement number	Requirement criteria	Satisfied	Comment
REQ-1.2.1	The system shall be able to operate at interface temperatures between [-25, +65] ºC.	E2	By analysis, material and component selection
REQ-1.2.2	The system shall tolerate temperatures between [-25, +65] ºC while not operating.	E2	By analysis, material and component selection
REQ- 2.1.1	The system shall have a power consumption of ≤15Watt, including electronics and actuators.	E1	Power budget
REQ-2.1.1.1	The motors shall have a maximum power consumption of 12 W.	E1	Power budget
REQ-2.1.1.2	The control system shall have a maximum power consumption of 3 W.	E1	Power budget
REQ-2.2.1	The mass of the system shall be maximum 4 kg, including electronics.	E1	Mass budget, prototype 1 of the DAK model
REQ-2.2.1.1	The mass of the mechanism shall be maximum 3 kg.	E1	Mass budget, prototype 1 of the DAK model
REQ-2.2.1.2	The mass of the electronics shall be maximum 1 kg.	E1	Mass budget, prototype 1 of the DAK model
REQ- 2.3.3	Motorization according to ECSS-E-ST-33-01C shall be satisfied.	E1	Torque calculations, technical budgets
REQ-2.3.3.1	The motor for the azimuth stage shall produce a torque of minimum 0.127 Nm.	E1	Torque calculations, technical budgets

REQ-2.3.3.2	The motor for the elevation stage shall produce a torque of minimum 0.107Nm.	E1	Torque calculations, technical budgets
REQ-2.4.2	The elevation stage shall be able to move minimum ± 90 deg.	E1	Implemented in Arduino. TBC in the microcontroller.
REQ-2.4.3	The azimuth stage shall be able to move minimum ± 180 deg.	E1	Implemented in Arduino. TBC in the microcontroller.
REQ-2.4.4	The system shall be able to move with a velocity of ≥ 60 deg/s.	E1	Motor selection, electrical technology document.
REQ-2.4.5	The system shall be able to accelerate at a rate of ≥ 40 deg/s^2.	E1	Motor selection, electrical technology document.
REQ-2.5.4	The system shall communicate between the spacecraft using the CANbus protocol.	E1	Implemented in Arduino. Will not be prioritized in further software development.
REQ-2.5.7	The system shall send feedback when it is moving.	E2	Implemented in Arduino. TBC in the microcontroller.
REQ-2.5.8	The system shall send feedback when it is not moving.	E2	Implemented in Arduino. TBC in the microcontroller.
REQ-2.6.2	The overall gain of the system shall be ≥ 23 dBi.	E1, E2	Link Analysis, Antenna Trade-Off
REQ-2.6.3	The system shall be able to communicate at a carrier frequency of 23 GHz.	E1, E2	Link Analysis, Antenna Trade Off
REQ-2.6.6	The system shall contain a transmit sub-system.	E1	
REQ-2.6.7	The system shall contain a receive sub-system.	E1	
REQ-2.6.8	The gain variation shall be maximum± 1 dBi.	E2	Antenna Trade-Off
REQ-2.7.1	The system shall contain a motor control system.	E1	
REQ-2.7.8	The system shall not move until a position command is received.	E2	Implemented in Arduino. TBC in the microcontroller.
REQ-2.7.3	The control system shall be able to control the velocity of the system	C1	Implemented in Simulink, TBC in software.
REQ-2.7.4	The control system shall be able to control the acceleration of the system	C1	Implemented in Simulink, TBC in software.

REQ-2.7.5	The control system shall be able to control the motor current.	C1	Implemented in Simulink, TBC in software.
REQ-2.7.9	The control system shall be able to control the position of the system	E2	Implemented in Arduino. TBC in the microcontroller.
REQ-3.3.1	The system shall have a cost of maximum €10.000 per unit. Assuming a batch size of 1000 units.	E2	Cost budget, TBC

2.5.5.2. *Highlights*

Breakthroughs, accomplishments, major decisions or changes in the project plan:

- Prioritized and not prioritized tasks for the final part of the project.
- Almost completed Simulink model of the motor control system.
- Design and drawings of the azimuth assembly are completed and sent to production
- Received some of the ordered electronics
- Selected bearing
- Deriving the pointing budget is delayed according to the project plan and will be prioritized when the most important technical issues are completed.
- Successfully implemented a small section of the Simulink control system in the STM32F407 (microcontroller).

2.5.5.3. *Tasks in progress or completed*

Table 2. 5. 13: Tasks in progress or completed, C1

Activity nr.	Activity name	Description	Who	% complete
1002	Iteration report, C1	Finished	EL	100 %
2000	Requirement specification	Updated	GHS, MD	100 %
3000	Test & Verification Specification	Updated	SL, VOA	100 %
3002	Functional test procedure	Started	SL, GHS	80 %
5111	Technical document-electro	Finished	GHS,SL	100 %
5211	Antenna Trade-off	Finished	EL	100 %
5314	Control system, electrical	Started	SL, EL, GHS	60 %
5321	CAD model prototype 3, azimuth	Started	MD	100 %
5323	Bearing report	Started	MD, VOA	70 %
5331	Control system design	Started	TS, GHS, EL	75%
5332	Control system, software implementation	Started	TS	20 %

2.5.5.4. *Tasks for the next iteration*

Planned tasks that will be continued or started in the next phase are given in table 2.5.14:

Table 2. 5. 14: Tasks for the next iteration, C2

Activity nr.	Activity name	Description	Who
1001	Cost budget	Update the cost budget with more details	MD, VOA
1003	Iteration report	Report containing experiences from C2	EL
3002	Functional test procedure	Complete the functional test procedure	SL
5000	Test and simulation	Simulation of the second prototype/parts, verification and validation	VOA, MD, GHS, TS, SL, EL
5414	Control system, electrical	Complete and verify the design	GHS, TS, EL, SL
5421	CAD model prototype 4	Update according to the elevation (not prioritized)	MD
5423	Bearing report	Complete the report and include calculations.	MD, VOA
5431	Control system design	Continue development and verify the design	TS, GHS
5432	Control system, software implementation	Implement the software design into the STM32F4 microcontroller.	TS
5901	Technical budgets	Update	MD, VOA

2.5.6. Fifth iteration: Construction 2 (18.04.16 – 24.04.16)

The construction phase is the most comprehensive phase in the project. The purpose of this phase is to implement system features in a series of iterations. Analysis & design, implementation, testing and deployment should be the focus areas.

2.5.6.1. *Project status*

This iteration was also a short iteration. The goal of the group was to write a functional test analysis, finishing the bearing study, finishing the design of the control system and the documentation of this, and find new suppliers for the azimuth part of the APMA. The group has reached all these goals, and additionally the work with the implementation of the control system has continued. Almost the whole system is implemented, but there are still some unsolved problems. This will be one of the prioritized tasks in the next iteration.

The group has also worked with electrical circuits and design. For example, circuits limiting the voltage seen at the microcontroller's input pins have been designed. The electric design will be documented in a report.

Another goal for this iteration was to get the produced azimuth parts, but since the contract was broken by the supplier, this is a bit delayed. New suppliers have been found, and all the parts will be delivered during the next week if everything works out according to the plan.

This is the status of the project. We are working hard to reach our goals, but according to the plan this is fully achievable if we do not get any more delays.

Table 2.5.15 gives an overview of the requirements that are satisfied by the present design of prototype 4:

Table 2. 5. 15: Requirements met by the design of prototype 4.

Requirement number	Requirement criteria	Satisfied	Comment
REQ-1.2.1	The system shall be able to operate at interface temperatures between [-25, +65] ºC.	E2	By analysis, material and component selection
REQ-1.2.2	The system shall tolerate temperatures between [-25, +65] ºC while not operating.	E2	By analysis, material and component selection
REQ- 2.1.1	The system shall have a power consumption of ≤15Watt, including electronics and actuators.	E1	Power budget
REQ-2.1.1.1	The motors shall have a maximum power consumption of 12 W.	E1	Power budget
REQ-2.1.1.2	The control system shall have a maximum power consumption of 3 W.	E1	Power budget
REQ-2.2.1	The mass of the system shall be maximum 4 kg, including electronics.	E1	Mass budget, prototype 1 of the DAK model.
REQ-2.2.1.1	The mass of the mechanism shall be maximum 3 kg.	E1	Mass budget, prototype 1 of the DAK model.

REQ-2.2.1.2	The mass of the electronics shall be maximum 1 kg.	E1	Mass budget, prototype 1 of the DAK model.
		C2	Not compliant, prototype 4.
REQ- 2.3.3	Motorization according to ECSS-E-ST-33-01C shall be satisfied.	E1	Torque calculations, technical budgets
REQ-2.3.3.1	The motor for the azimuth stage shall produce a torque of minimum 0.127 Nm.	E1	Torque calculations, technical budgets
REQ-2.3.3.2	The motor for the elevation stage shall produce a torque of minimum 0.107Nm.	E1	Torque calculations, technical budgets
REQ-2.4.2	The elevation stage shall be able to move minimum ± 90 deg.	E1	Implemented in Arduino.
		C2	Not prioritized, azimuth-stage is prioritized.
REQ-2.4.3	The azimuth stage shall be able to move minimum ± 180 deg.	E1	Implemented in Arduino.
		C2	Implemented in the microcontroller.
REQ-2.4.4	The system shall be able to move with a velocity of ≥ 60 deg/s.	E1	Motor selection, electrical technology document.
		C2	Tested on the azimuth drive while implementing the control system.
REQ-2.4.5	The system shall be able to accelerate at a rate of ≥ 40 deg/s^2.	E1	Motor selection, electrical technology document.
		C2	Tested on the azimuth drive while implementing the control system.
REQ-2.5.7	The system shall send feedback when it is moving.	E2	Implemented in Arduino. TBC in the STM32 microcontroller.
REQ-2.5.8	The system shall send feedback when it is not moving.	E2	Implemented in Arduino. TBC in the STM32 microcontroller.
REQ-2.6.2	The overall gain of the system shall be ≥ 23 dBi.	E1 E2	Link Analysis, Antenna Trade-Off
REQ-2.6.3	The system shall be able to communicate at a carrier frequency of 23 GHz.	E1 E2	Link Analysis, Antenna Trade Off
REQ-2.6.6	The system shall contain a transmit sub-system.	E1	
REQ-2.6.7	The system shall contain a receive sub-system.	E1	

REQ-2.6.8	The gain variation shall be maximum± 1 dBi.	E2	Antenna Trade-Off
REQ-2.7.1	The system shall contain a motor control system.	E1	By design
REQ-2.7.8	The system shall not move until a position command is received.	E2 C2	Implemented in Arduino. Implemented in the microcontroller.
REQ-2.7.3	The control system shall be able to control the velocity of the system	C1	Implemented in Simulink.
REQ-2.7.4	The control system shall be able to control the acceleration of the system	C1	Implemented in Simulink.
REQ-2.7.5	The control system shall be able to control the motor current.	C1	Implemented in Simulink.
REQ-2.7.9	The control system shall be able to control the position of the system	E2	Implemented in Arduino.
REQ-3.3.1	The system shall have a cost of maximum €10.000 per unit. Assuming a batch size of 1000 units.	E2	Cost budget, TBC

2.5.6.2. *Highlights*

Breakthroughs, accomplishments, major decisions or changes in the project plan:

- Functional test procedure is written.
- Bearing report is finished.
- The design of the control system is finished.
- The parts for the azimuth drive are ordered.
- The control system is partly implemented in software.

2.5.6.3. *Tasks in progress or completed*

Table 2. 5. 16: Tasks in progress or completed, C2.

Activity nr.	Activity name	Description	Who	% complete
1002	Iteration report, C2	Finished	EL	100 %
3002	Functional test procedure	Draft finished	SL, GHS	95 %
5211	Antenna Trade-off	Finished	EL	100 %
5314	Control system, electrical	Draft finished	SL, EL, GHS	90 %
5321	CAD model prototype 4, azimuth	Finished	MD	100 %
5323	Bearing report	Draft finished	MD, VOA	90 %
5331	Control system design	Draft finished	TS, GHS, EL	95%
5332	Control system, software implementation	Started	TS	60 %

2.5.6.4. *Tasks for the next iteration*

Planned tasks that will be continued or started in the next phase are given in table 2.5.17:

Table 2. 5. 17: Tasks for the next iteration, C3

Activity nr.	Activity name	Description	Who
1003	Iteration report	Report containing experiences from C3	EL
3002	Functional test procedure	Approve the procedure	GHS, TS
5000	Test and simulation	Simulation of the second prototype/parts, verification and validation	VOA, MD, GHS, TS, SL, EL
5414	Control system, electrical	Complete and approve the documentation.	TS, EL
5421	CAD model prototype 4	Update according to the elevation (not prioritized)	MD
5423	Bearing report	Approve the document	MD, TS
5432	Control system, software implementation	Implement the software design into the STM32F4 microcontroller.	TS, GHS, SL, EL
5901	Technical budgets	Update and approve	MD, VOA
5415	Electrical design document	Design of measurement circuits, wiring, etc.	GHS
XXXX	Assembly of the azimuth parts		VOA, MD
XXXX	Pointing budget	Will not be prioritized,	EL, SL, GHS
XXXX	Final report	Start writing a final report	All

2.5.7. Sixth iteration: Construction 3 (25.04.16 – 06.05.16)

The construction phase is the most comprehensive phase in the project. The purpose of this phase is to implement system features in a series of iterations. Analysis & design, implementation, testing and deployment should be the focus areas.

2.5.7.1. *Project status*

This iteration was the last construction iteration and it had a duration of two weeks. The practical goals for this iteration were finishing the design of the APMA according to the project boundaries and limits, finishing the implementation of the control system in software and assembling the final prototype.

All these tasks are done in this iteration, and the project is still on schedule according to the plan. The electronics for the azimuth stage are implemented in the final prototype and the control system is running. The software is expected to be completed during the weekend.

Making a pointing budget, finishing the bearing report, the test procedure, the control system report and the electrical design document and start writing the final report were also planned to be done in this iteration. Some of these documents are done and some are not. Therefore, the project has some small delays. Due to this, the group had an internal meeting, where the two last weeks of the project were planned in detail. Final deadlines are set and have to be reached. These are fully achievable, and the project is currently under control.

Additionally, an "As built" report from the assembly is almost finished and an assembly user manual is completed. This is part of the deployment stage of the project. A fixture for the functional test is also designed and produced.

Table 2.5.18 gives an overview of the requirements that are satisfied by the present design of prototype the final prototype:

Table 2. 5. 18: Requirements met by the design of the final prototype.

Requirement number	Requirement criteria	Satisfied	Comment
REQ-1.2.1	The system shall be able to operate at interface temperatures between [-25, +65] ℃.	E2	By analysis, material and component selection
REQ-1.2.2	The system shall tolerate temperatures between [-25, +65] ℃ while not operating.	E2	By analysis, material and component selection
REQ-1.3.1	The system shall have a maximum outgassing of TBC [Molecules/Volume].	E2/C3	Taken into account by design and material selection. Not verified.
REQ-1.4.1	The system shall withstand the radiation levels in LEO without degradation.	E2/C1	Taken into account by design and material selection. Not verified.
REQ-1.5.1	The system shall withstand humidity levels of TBC.	E2/C1	Taken into account by design and material selection. Not verified.

REQ- 2.1.1	The system shall have a power consumption of ≤15Watt, including electronics and actuators.	E1	Power budget
REQ-2.1.1.1	The motors shall have a maximum power consumption of 12 W.	E1	Power budget
REQ-2.1.1.2	The control system shall have a maximum power consumption of 3 W.	E1	Power budget
REQ-2.2.1	The mass of the system shall be maximum 4 kg, including electronics.	E1 C3	Mass budget, prototype 1 of the DAK model. Not met by the final design of prototype 4.
REQ-2.2.1.1	The mass of the mechanism shall be maximum 3 kg.	E1 C3	Mass budget, prototype 1 of the DAK model. Not met by the final design of prototype 4.
REQ-2.2.1.2	The mass of the electronics shall be maximum 1 kg.	E1	Mass budget, prototype 1 of the DAK model.
REQ- 2.3.3	Motorization according to ECSS-E-ST-33-01C shall be satisfied.	E1	Torque calculations, technical budgets
REQ-2.3.3.1	The motor for the azimuth stage shall produce a torque of minimum 0.127 Nm.	E1	Torque calculations, technical budgets
REQ-2.3.3.2	The motor for the elevation stage shall produce a torque of minimum 0.107Nm.	E1	Torque calculations, technical budgets
REQ-2.4.1	The system shall have a pointing error of < 0.5 deg, half cone, 3 sigma.	C3	Pointing budget
REQ-2.4.2	The elevation stage shall be able to move minimum ± 90 deg.	E1 C2	Implemented in Arduino. Not prioritized, azimuth-stage is prioritized.
REQ-2.4.3	The azimuth stage shall be able to move minimum ± 180 deg.	E1 C2	Implemented in Arduino. Implemented in the microcontroller.
REQ-2.4.4	The system shall be able to move with a velocity of ≥ 60 deg/s.	E1 C2	Motor selection, electrical technology document. Tested on the azimuth drive while implementing the control system.
REQ-2.4.5	The system shall be able to accelerate at a rate of ≥ 40 deg/s^2.	E1	Motor selection, electrical technology document.

		C2	Tested on the azimuth drive while implementing the control system.
REQ- 2.5.1	The system shall receive absolute position commands from the spacecraft.	C3	Implemented in the microcontroller.
REQ-2.5.7	The system shall send feedback when it is moving.	E2 C3	Implemented in Arduino. Implemented in the STM32 microcontroller.
REQ-2.5.8	The system shall send feedback when it is not moving.	E2 C3	Implemented in Arduino. Implemented in the STM32 microcontroller.
REQ-2.6.2	The overall gain of the system shall be ≥ 23 dBi.	E1 E2	Link Analysis, Antenna Trade-Off
REQ-2.6.3	The system shall be able to communicate at a carrier frequency of 23 GHz.	E1 E2	Link Analysis, Antenna Trade Off
REQ-2.6.6	The system shall contain a transmit sub-system.	E1	
REQ-2.6.7	The system shall contain a receive sub-system.	E1	
REQ-2.6.8	The gain variation shall be maximum± 1 dBi.	E2	Antenna Trade-Off
REQ-2.7.1	The system shall contain a motor control system.	E1	By design
REQ-2.7.8	The system shall not move until a position command is received.	E2 C2	Implemented in Arduino. Implemented in the microcontroller.
REQ-2.7.3	The control system shall be able to control the velocity of the system	C1 C3	Implemented in Simulink. Implemented in the microcontroller.
REQ-2.7.4	The control system shall be able to control the acceleration of the system	C1 C3	Implemented in Simulink. Implemented in the microcontroller.
REQ-2.7.5	The control system shall be able to control the motor current.	C1 C3	Implemented in Simulink. Implemented in the microcontroller.
REQ-2.7.9	The control system shall be able to control the position of the system	E2 C3	Implemented in Arduino. Implemented in the microcontroller.
REQ-3.3.1	The system shall have a cost of maximum €10.000 per unit. Assuming a batch size of 1000 units.	E2 C3	Cost budget R&D cost budget

2.5.7.2. *Highlights*

Breakthroughs, accomplishments, major decisions or changes in the project plan:

- The pointing budget is created.
- The final prototype is assembled.
- Assembly user manual is made.
- The electronics of the azimuth stage is implemented.
- The control system is implemented and runs the azimuth stage of the prototype.
- The control system communicates both ways with a command station.

2.5.7.3. *Tasks in progress or completed*

Table 2. 5. 19: Tasks in progress or completed, C3.

Activity nr.	Activity name	Description	Who	% complete
1002	Iteration report, C3	Finished	EL	100 %
3002	Functional test procedure	Draft finished	SL, GHS	100 %
5000	Test and simulation	Started	All	20 %
5314	Control system, electrical	Finished	SL, EL, GHS	100 %
5323	Bearing report	Almost finished	MD, VOA	98 %
5531	Control system design	Almost finished	TS, GHS, EL	95%
5532	Control system, software implementation	Finished	TS	99 %
5415	Electrical design	Started	GHS, SL	60 %
5900	Technical budget – pointing budget	Almost finished	EL	95 %
10500	As built	Started	MD, VOA	60 %
10600	Assembly user manual	Finished	MD	100%
XXXX	Final report	Started	EL	10 %

2.5.7.4. *Tasks for the next iteration*

The deadlines set for the last iteration and the rest of the project are shown in table 2.5.20. The tasks have to be completed within the deadlines, and delays will not be accepted. The responsible for the task has to ensure this.

Table 2. 5. 20: Deadlines for the two last weeks of the project.

Deadline	Description	Responsible
09.05.2016	Meeting with external supervisor Test setup Verifying the test setup Documentation of the test setup	All GHS, MD, TS GHS, MD, TS MD
10.05.2016	Functional test according to the test procedure. Documentation of the test	GHS, MD, TS MD
11.05.2016	Functional test report Update the requirement specification Update the test & verification specification Approve the test report and the updates	GHS, MD, TS VOA SL EL
12.05.2016	Internal group – divide the final work with documentation and approving between the group members.	All
12.-18.05.2016	Completion of the research and development process and corresponding documentation. Complete the risk management and the iteration reports. Complete the final report.	All EL, VOA EL
18.-20.05.2016	Complete the project: Approving and printing the final report CD with documentation Make the poster (A3) Etc.	All

2.5.8. Seventh iteration: Transition 1 (06.05.16 – 13.05.16)

The transition phase is the final phase of the project, and includes the completion of the design, construction, implementation and testing. The goals are that the system shall satisfy its requirements and have the desired operational functionality at the end of this phase. The system shall be deployed to the target users, and the phase also includes conversion and user training.

In this phase, the project needs to be completed. This includes finishing the hand-in of the final report.

2.5.8.1. *Project status*

This iteration was the last iteration of the project, and it lasts for a week. The goals for this iteration were to execute the functional test of the APMA according to the test procedure, and write a test report where the results of the tests are discussed. The test was originally intended for C3, but due to delays in production it had to be rescheduled. The "Test & Verification specification" and the "Requirement Specification" should also be updated according to the test results. User manuals for the assembly process of the mechanism and for the control system are also written, so that the system is ready to be deployed to the target user. This is an important part of the transition phase.

Additionally, the focus in this iteration should be on the final report and the collection of all the analysis and reports written throughout the project.

All the deadlines the group has set for this iteration has been kept, which means the goals for the iteration are also reached. The project is on schedule according to the plan, and the final goal will be reached. In the last few days of the project the group will work with the final report and the last presentation. Table 2.5.21 shows the deadlines for the last days of the project.

Table 2. 5. 21: Deadlines for the last days of the project.

Deadline	Description	Responsible
12.-18.05.2016	Completion of the research and development process and corresponding documentation.	All
	Complete the risk management and the iteration reports.	EL, VOA
	Complete the final report.	EL
18.-20.05.2016	Complete the project: Approving and printing the final report CD with documentation Make the poster (A3) Etc.	All
20.05.2016	Hand in the project	All

An overview of the requirements met by the real-life prototype are available in the requirement specification, [2], and the test results are available in the functional test report, [12]. The SSM project has focused on the risk management, and through three mitigation processes the total risk has been significantly reduced. The total risk reduction after the mitigations are available in the "Risk Management", [11].

2.5.8.2. *Highlights*

Breakthroughs, accomplishments, major decisions or changes in the project plan:

- - The functional test of the real-life prototype is executed.
- - A functional test report with the test results is written.
- - A user manual for the control system is written.

2.5.8.3. *Tasks in progress or completed*

Table 2. 5. 22: Tasks in progress or completed, T1

Activity nr.	Activity name	Description	Who	% complete
1002	Iteration report, T1	Finished	EL	100 %
3002	Functional test procedure	Finished	SL, GHS	100 %
5000	Test and simulation	Finished	All	100 %
5314	Control system, electrical	Finished	SL, EL, GHS	100 %
5323	Bearing report	Finished	MD, VOA	100 %
5531	Control system design	Finished	TS, GHS, EL	100 %
5532	Control system, software implementation	Finished	TS	100 %
5415	Electrical design	Almost finished	GHS, SL	80 %
5900	Technical budget – pointing budget	Finished	EL	100 %
10500	As built	Finished	MD, VOA	100 %
10600	Assembly user manual	Finished	MD	100%
1010	Final report	Started	EL	60 %

2.5.9. Conclusion

The SSM group chose the Unified Process inspired "Iterative Development Model" as the project model in the start-up phase of the project. This has turned out to be a good choice. The four main phases and the seven iterations the project has been through have been really helpful and necessary to ensure that the project is always on schedule according to the long term plan.

The model has, due to the time-boxed iterations, continuously throughout the project period driven the SSM project towards the final goal. The model has been an important part of the planning process, and the iteration reports have been useful to get an overview of the status of the project. The detailed plans for the iterations, where clear deadlines had to be set, have been crucial to reach goals in the project without substantial time slips. There have been some small time-slips during the project period, and in cooperation with the employer some parts of the assignment have not been prioritized. The final goal of the project was to conceptually develop the APMA, real-life prototype, some parts of the mechanism and get the real-life prototype to rotate. The concept of the low-cost APMA is developed, a real-life prototype of the mechanism is built and the control system runs the azimuth stage of the mechanism.

We are satisfied with the result of the project, and that we reached our goals. Throughout the semester, each member has learned a lot from all three engineering fields, with a high level of motivation during the entire project.

2.5.10. References

[1]   S. Laugerud, V.Orre Aarud, "Test & Verification Specification", SSM-3000, Small Satellite Mechanisms, USN, Kongsberg, Rev.1.1, 18.02.16.

[2]   G.H. Stenseth, M. Dybendal, "Requirement specification", SSM-2000, Small Satellite Mechanisms, USN, Kongsberg, Rev. 1.1, 18.02.2016.

[3]   E. Løken, T. Sundnes, "Project Plan", SSM-1001, Small Satellite Mechanisms, USN, Kongsberg, rev.1.1, 18.02.2016.

[4]   M. Dybendal et al, "Concept analysis", SSM-0900, Small Satellite Mechanisms, Kongsberg, rev.2.0, 03.03.13.

[5]   G.H. Stenseth, "Link analysis", SSM-5112, Small Satellite Mechanisms, Kongsberg, rev.1.0, 03.03.16.

[6]   M. Dybendal, "Design description", SSM-5420, Small Satellite Mechanisms, USN, Kongsberg, SSM-5123, rev.1.0, 01.03.2016.

[7]   V.O. Aarud, "Material and mechanical technology study", SSM-5900, Small Satellite Mechanisms, USN, Kongsberg, rev.1.0, 01.03.2016.

[8]   E. Løken et al, "Technical budgets", SSM-5901, Small Satellite Mechanisms, USN, Kongsberg, rev.1.0, 04.03.16.

[9]   G.H. Stenseth et al, "Components Trade-off", SSM-5111, Small Satellite Mechanisms, USN, Kongsberg, rev.1.0, 04.03.16.

[10] T. Sundnes, "Technical document – Control system", SSM-5131, Small Satellite Mechanisms, USN, Kongsberg, rev1.0, 04.03.16

[11] G.H. Stenseth et al, "Risk Management", SSM-1200, Small Satellite Mechanisms, USN, Kongsberg, rev.3.0, 13.05.16.

[12] G.H. Stenseth, "Functional test report", SSM-3003, Small Satellite Mechanisms, USN, Kongsberg, rev. 1.0, 13.05.16.

3.   System design

3.1. Concept analysis

i.   Abstract

This chapter is a concept analysis of different actual concepts for the new low cost antenna pointing mechanism assembly (APMA). The concept analysis is based on a trade-off report done by Kongsberg Space when they developed the present APM, [1]. The project group has selected three concepts from this trade-off that will be considered with respect to present requirements and stakeholders. Therefore, some of the weighting and aspects will be altered compared to the existing trade-off.

ii. Contents

iii. List of figures

iv. List of tables

v. Document history

Table 3. 1. 1: Document history

Rev.	Date	Author	Approved	Description
0.1	09.02.16	VOA, EL	TS	Document created
0.2	10.02.16	VOA, EL, MD	TS	Document updated with concept information
1.0	12.02.16	EL, MD	TS	Created rev. 1.0
1.1	23.03.16	EL	SL	Changed document layout and numbering of the sections Title "Scope" changed to "Abstract" Title "System overview" changed to "Introduction". Section "Functional tree" merged with "Introduction". Changed table 3. Added reference [3].
2.0	03.03.2016	VOA, EL, MD	EL	Reviewed and published
2.1	03.05.2016	EL		Changed layout into the final report layout.
3.0	19.05.2016	VOA, MD, EL	TS	Reviewed and published

3.1.1. Introduction

A concept for the new low-cost antenna pointing mechanism assembly has to be chosen. The concept has to comply with the given requirements [3]. This document is an evaluation and comparison of three different concepts based on the "KARMA 7, MSA Trade-off Report and Baseline definition (TN01.01) - Background IPR" made by Kongsberg Space[1].

3.1.1.1. *System overview*

Figure 3.1.1 shows a schematic system overview from one of the concepts. Note that the schematic is highly dependent on selection of the concept, which has not yet been formulated. Common for the different concepts are the rotation axes. The system shall point the antenna/reflectors in different positions to send or receive signals, leading to all the concepts having an azimuth and elevation rotational axis. The concepts have different numbers of reflectors, rotary joints, motors etc. and this is important for the choice of concept.
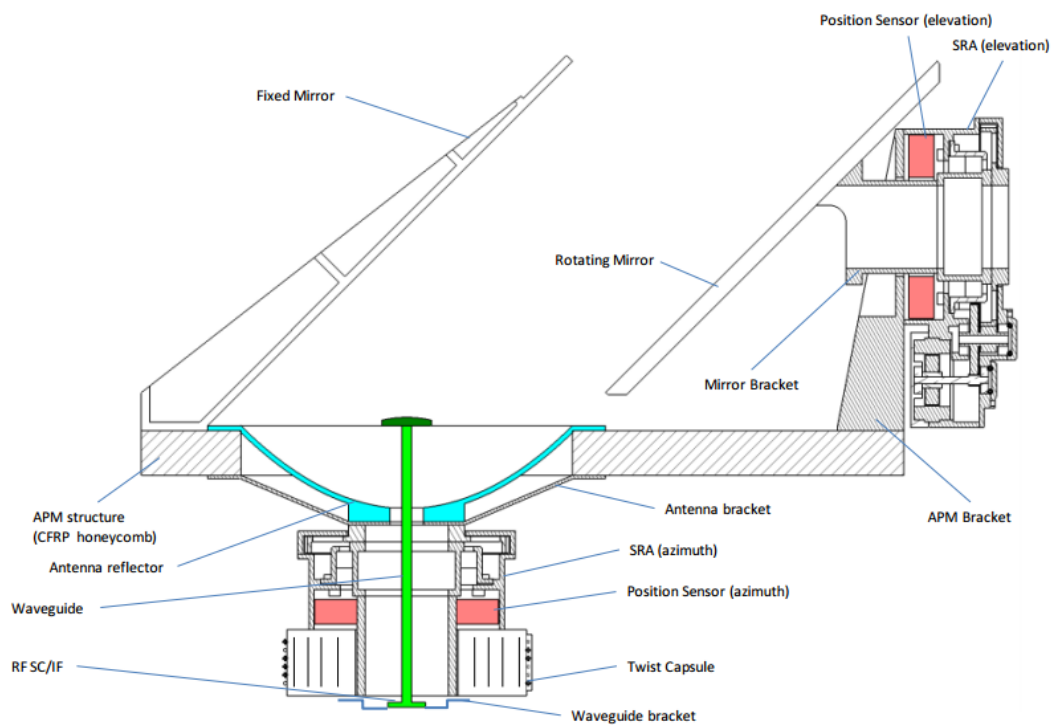
Figure 3. 1. 1: Double mirror reflector antenna, concept 3[1]

The top-level functionality of the system is to ensure two-way communication between satellites. Figure 3.1.7 at the end of this chapter gives an overview of the overall functionality of the Antenna Pointing Mechanism Assembly. The functional tree breaks this functionality down into more specific and concrete functions.

3.1.2. Concepts

In this section, chosen concepts will be explained detailed and evaluated according to advantages and disadvantages.

3.1.2.1. *Concept 1: Gimbal APM with reflector antenna*

3.1.2.1.1. Description

Concept 1, shown in figure 3.1.2, is a gimbal type, two axis pointing mechanism, with a top mounted reflector Antenna.

The APM consists of two drive actuators (SRA), arranged in elevation over azimuth configuration. Both actuators are supported by the APM structure. The SRA design can consist of identical components and parts, but the gear system, bearing and position sensor must remain the same. Because of the different interface needs in the individual stages, the SRA housings will probably be slightly different.

The reflector antenna is connected to the elevation stage via the antenna bracket, and then the bracket is connected to a rotary joint. Underneath the azimuth mechanism, a twist capsule that serves the signal transfer is located.
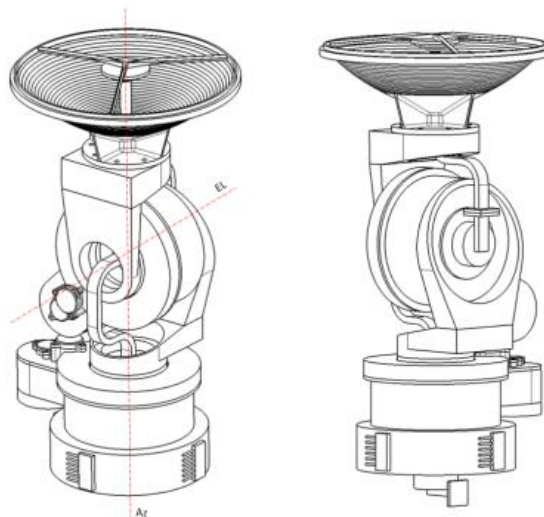
Figure 3. 1. 2: Gimbal APM with reflector antenna [1]

The baseline of the system consists of:

- Elevation over azimuth axis configuration for moving the antenna reflector.
- To transfer the signal, a twist capsule is placed over the azimuth drive mechanism.
- For each the azimuth and elevation axis two identical rotary joints are placed.
- Two identical SRA for elevation and azimuth: Hybrid stepper motor with spur gear drives.

In figure 3.1.3, a schematic assembly of the major components is shown.

- Gimbal two axis APM
- Reflector antenna
- 2x rotary joints (elevation + azimuth)
- Identical SRA for azimuth and elevation
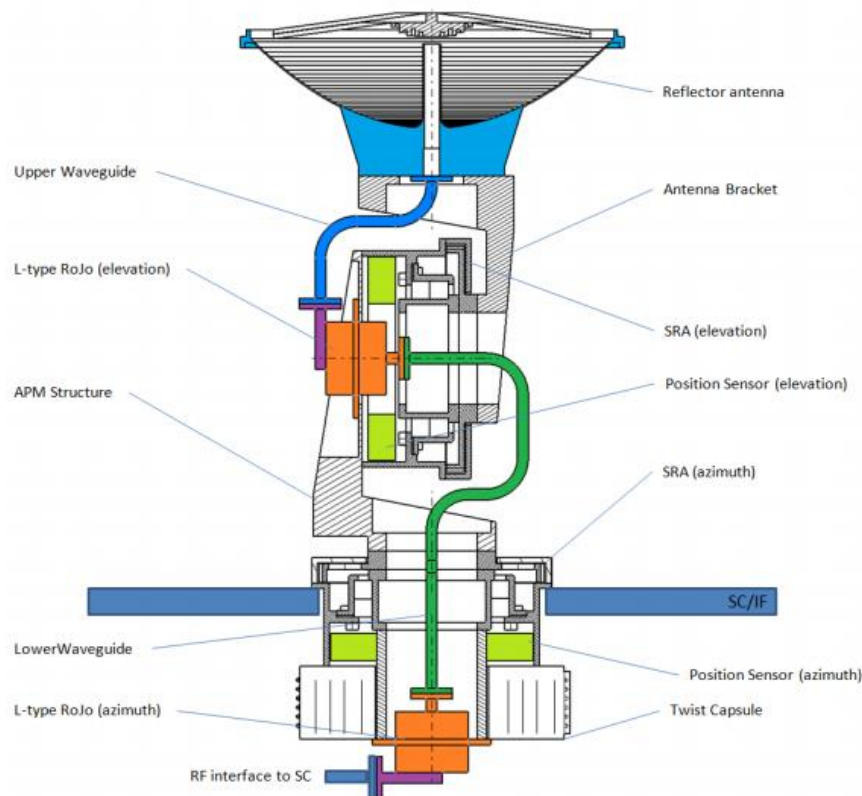
Figure 3. 1. 3: Gimbal APM with reflector antenna- schematics [1]

3.1.2.1.2.   Advantages and disadvantages

Concept 1 shows one of the most common ways of pointing an antenna and has been proven a success in several APMs. The main parts are simple and will not require complicated manufacturing and assembly processes. The reflector antenna is connected to the elevation stage via the antenna bracket. This makes it easy to change and install different types and sizes of antennae without changing the design or configuration of the APM.

One of the most notable disadvantages related to this project are the rotary joints (RJ). In the gimbal concept 1, two RJs are necessary to allow rotation around the elevation and azimuth axes. RJs have to be manufactured and the costs of these will have a huge impact on this low cost mechanism. Another disadvantage with the gimbal concept is that the configuration has the highest radio frequency (RF) loss. Reduction in RF feed network must be minimized in order to limit power dissipation and avoid severe temperature gradients over the SRA bearings. Due to the long feed lines/waveguides and the 2 rotary joints, concept 1 has the highest insertion loss, and the need for two RJs gives high complexity and risk of not meeting requirements such as life, torque and reliability.

3.1.2.2. *Concept 2: APM with inclined mirror and offset reflector antenna*

3.1.2.2.1.   Description

Figure 3.1.4 illustrates concept 2, APM with inclined mirror and offset antenna. The concept has a U-shaped APM structure, where the reflector antenna with integrated feed is attached. At the opposite part of the U-shape, there is a 45° inclined mirror. It rotates in the elevation axis, and is an important part of the pointing functionality, together with the azimuth mechanism. The U-shaped APM structure is mounted on the azimuth mechanism, which is the lower part of figure 3.1.4. This part rotates the U-

shaped structure in the azimuth axis.
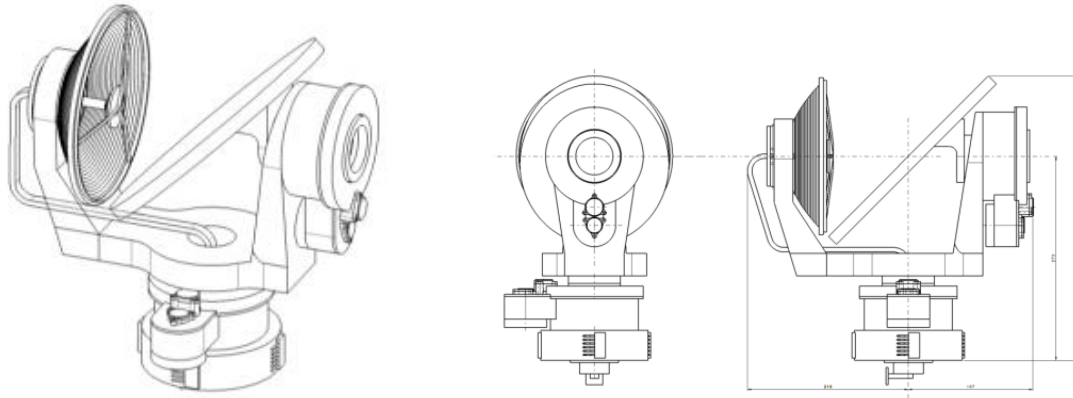
Figure 3. 1. 4: Concept 2 - APM with inclined mirror and offset reflector antenna [1]

3.1.2.2.2.   Advantages and disadvantages

In the Trade-off report developed by KDA [1], there are two variants of concept 2. In the other variant, the reflector antenna is mounted on the mirror, and takes part in the rotation of the elevation stage.

An advantage of separating the reflector antenna and the additional bracket where the reflector antenna is mounted, is that the horizontal center of gravity (CoG) can be aligned with the azimuth rotation axis. The inertia of the mirror (elevation axis) is less than the other variant of this concept, since the antenna is mounted on to the U-shape structure and does not take part in the elevation motion.

Another advantage is that the antenna has only one mechanical interface to the APM and one interface to the waveguide, which simplifies the design of the mechanism. One of the groups objectives is to simplify the design of the low cost APMA as much as possible, thus making it easier to meet the given requirements.

Thermally, the waveguide design in this concept is favorable, due to possibilities for proper thermal sinking onto the U-bracket.

A disadvantage of separating the antenna from the mirror (compared with the other variant of this concept) is the need of extending the structure of the APM. This adds mass to the mechanism and increases the sweeping radius around the azimuth rotational axis. Reducing the mass of the APMA is a main requirement given by KDA, leading this design to have a noticeable disadvantage compared to the similar concept.

Thermally, this concept also has some challenges and limitations. Due to the rotation of the mirror (elevation) and the U-shaped structure (azimuth), this part of the mechanism experiences unwanted, inhomogeneous orbital heat fluxes. Deformation of the mirror, which affects and reduces the pointing accuracy, is also a challenge for this concept.

Due to one rotary joint and a relative long waveguide, the heat dissipation in the system is moderate. KDA requires low power consumption of the overall system, and because of this, it is favorable to reduce the heat dissipation as much as possible. The rotary joint is also expensive, and constitutes an important cost-factor for the APMA. A main goal is to reduce the cost of the mechanism drastically,

and this is considered as one of the most notable disadvantages with this concept.

3.1.2.3. *Concept 3: Double mirror reflector antenna*

3.1.2.3.1.   Description

In concept 1 and 2 it is necessary to use at least one rotary joint. Because of these RJs, impact on the system in terms of mechanical complexity is high, and the cost increase and the RF performance is reduced. Figure 3.1.5 shows a double mirror solution, where there is no need for rotary joints.

The mechanism is based on two parallel and inclined mirrors that point the RF beam from the antenna reflector. Both the mirrors and antenna reflectors are connected to the APM structure, which sits on the SRA for azimuth motion. For the elevation motion, one of the mirrors are rotating, where the fixed mirror is rigidly attached to the APM structure. The RF feed in this concept is one straight waveguide through the antenna reflector. This will make this concept the most favorable in relation to the low cost budget.
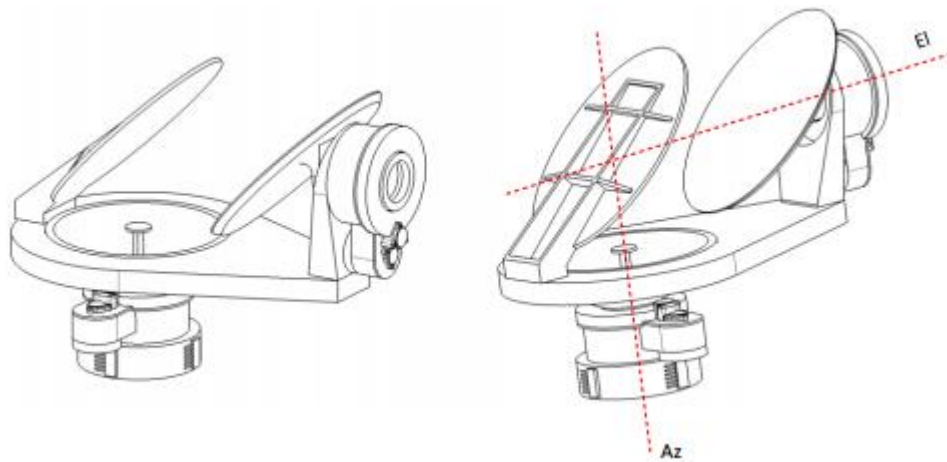
Figure 3. 1. 5: Double mirror reflector antenna [1]

A schematic assembly of the major components is shown in figure 3.1.6.

- 2x mirror
- Double mirror two axis APM
- Reflector antenna
- SRA Elevation + Azimuth
- Identical SRA for azimuth and elevation
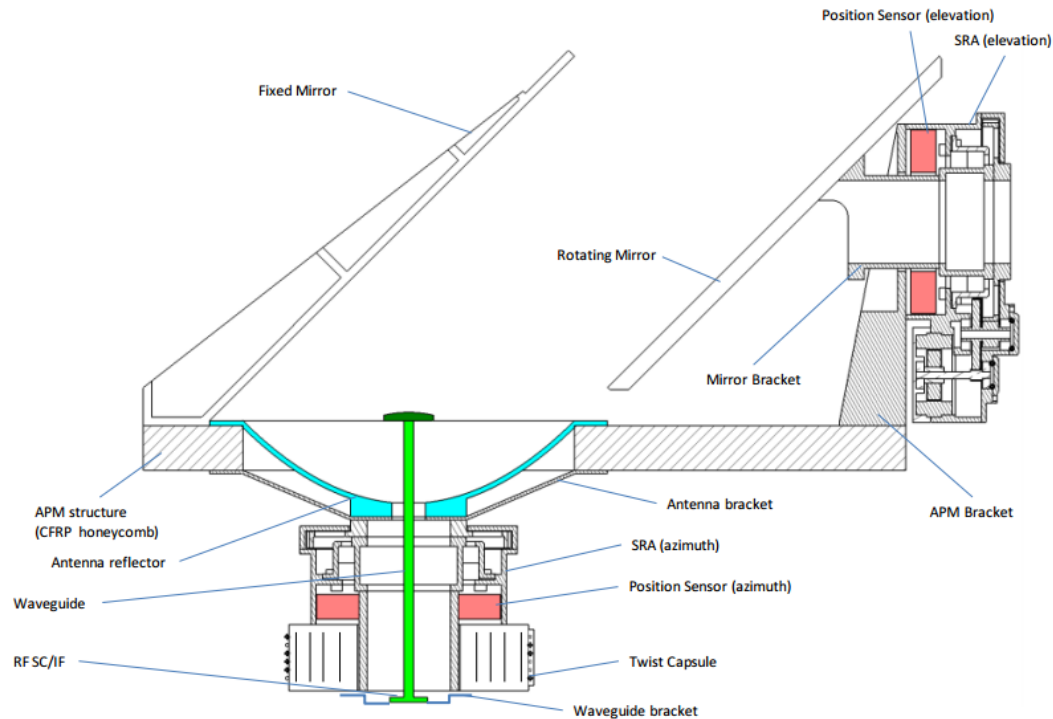
Figure 3. 1. 6: Double mirror reflector antenna – schematics [1]

3.1.2.3.2.   Advantages and disadvantages

One of the most remarkable disadvantages with concept 3 is the unwanted orbital heat fluxes, which results in complex shading patterns on the mirrors, and on the antenna. Another unfavorable aspect of concept 3 is the elevation motion. The loads from the bracket concentrate a load path. This concept has the biggest sweeping radius, and the mass is moderate. Because of the complexity in design, this system can only be tested in the full system.

Compared to the low cost project, the fact that this concept has no rotary joints will present a huge advantage related to cost and mass, and concept 3 also has the lowest insertion loss among all the presented concepts. Another advantage with no RJ is a lower risk of failing the life requirements.

3.1.3. Trade-off analysis

In this section the concepts are evaluated against to each other. The evaluation criteria and the weightings are explained in table 3.1.2 and 3.1.3.

3.1.3.1. *Criteria explanation*

Table 3. 1. 2: Criteria explanations

Criteria	Unit	Explanations
Mass	kg	What is the total mass of the concept?
Sweep radius	mm	How much space does the APMA require during operation? Since the available space on the satellite will be limited, a low sweep radius is beneficial
Loads	N, Nm	The 30g quasi–static accelerations generate axial and radial forces and moments on the main bearing. The bearing loads define the bearing size and are a measure for the need of a HDRM.
Inertia	kgm^2	Inertia is a dimensioning parameter for the SRA sizing. Additionally, high inertia and mass imbalances generate undesired reaction loads on the APMA to spacecraft/interface.
Thermal performance	-	Is the design inherently stable/ unstable with respect to thermo-elastic effects? Is pointing performance sensitive to thermo-elastic effects? Are there problematic joints with respect to thermo-elastic effects? The heat dissipation due to RF losses will be taken into account. High heat dissipation means a more complex thermal design.
RF Performance	-	Compliance with the RFS specification
Insertion loss	dB]	Insertion loss of the complete RF system.
Interface Complexity	-	Possible restrictions related to mounting of the APM on a satellite. How many interfaces to the spacecraft.
Verification Effort	-	How simple is the verification by test? Possibility to verify sub systems individually. What is needed in terms of instruments, facilities and ground support equipment?
Risk	-	What is the risk of not meeting requirements, budgets and schedule? How complex is the APMA architecture. How many suppliers and interfaces? Are there new processes or technologies required? Concept heritage
Rotary Joint	-	Rotation connection that can rotate around its own axis
Supplier costs	€	Cost of purchased and manufactured parts from external suppliers

AIT costs	€	How complex is the assembly of the APMA. Can parts be assembled in subassemblies? How is the tolerance stack up with respect to pointing performance?

3.1.3.2. *Weighting explanations*

Table 3. 1. 3: Weighting explanations

Criterial			Explanation
Mass	kg	15 %	Highly weighted. Weight is one of the key requirement and is very important for our project.
Sweep radius	mm	5 %	Lowly weighted. Sweep radius is important for a compact system. This requirement has a low priority for our system.
Loads	N, Nm	2 %	Lowly weighted. Load is important for every system. This requirement has a low priority for our system.
Inertia	kgm^2	5 %	Lowly weighted. Moment of inertia is important for every system. This requirement has a low priority for our system.
Thermal performance	-	7 %	Medium weighted. Thermal performance is important for every space system. This requirement has a medium priority for our system.
RF Performance	-	5 %	Lowly weighted. RF performance is important for the system, but very well known and not a focus point in this project.
Insertion loss	dB	5 %	Lowly weighted.
Interface Complexity	-	5 %	Lowly weighted. The mechanism in our project is designed simple to maintain low cost. The overall complexity shall be low.
Verification Effort	-	5 %	Lowly weighted. Verification is important for every project and especially for our project since it shall operate in a tough environment. Normally this shall be weighed high, but this is not a focus area for this project.
Risk	-	6 %	Medium weighted. Risk is an important factor for space mechanisms and needs to be taken into consideration due to the development of a new concept.
Rotary Joint	-	10 %	Medium weighted. Rotary joint is a complex part, which is heavy and expensive, and is an important factor in this project.
Supplier costs	€	16 %	Highly weighted. Cost is an A- requirement in this project, and is an important factor.
AIT costs	€	14 %	Highly weighted. Cost is an A- requirement in this project, and is an important factor.

3.1.3.3. *Evaluation*

3.1.3.3.1.   Evaluation of concept 1

In table 3.1.4, table 3.1.5 and table 3.1.6 the different concepts are compared and evaluated with the different criteria's. At each criteria the concept gets a score from 1 to 3, where 3 is the best.

Table 3. 1. 4: Evaluation of concept 1

Criteria	Evaluation	Advantages/disadvantages
Mechanical Performance		
Mass	3/3	The lowest mass of the 3 compared concepts.
Sweep radius	3/3	The smallest sweeping radius of the 3 compared concepts.
Load	Axial bearing load: 3/3 Radial bearing load: 3/3 Bending moment: 3/3	
Inertia	3/3	Low inertia (+).
Thermal performance	3/3	High thermal performance (+). Orbital fluxes spatially homogeneous on antenna (+). Antenna concept compact (+). Heat dissipation from azimuth waveguide + 2 RJ (-). System thermal design strongly dependent on RJ thermal design (-).
RF Performance		
RF Performance (overall)	3/3	
Insertion loss	1/3	High insertion loss (-). Due to the long feed line and the two RJs concept 1 has the highest insertion loss.
Interface complexity	3/3	Only one mechanical and RF interface (+). Flexible mounting (+). No additional HDRM (+).
Verification Effort	3/3	Low effort (+). APM and antenna can be designed and verified separately (+).
Risk	2/3	two RJs gives high complexity and risk of not meeting requirements (-). This type of mechanisms has been used in several space programs before (+).
Supplier costs	1/3	The need of two RJs increases the cost (-).
AIT cost	3/3	Simple design (+). Low number of parts (+).

3.1.3.3.2.   Evaluation of concept 2

Table 3. 1. 5: Evaluation of concept 2

Criteria	Evaluation	Advantages/disadvantages
Mechanical Performance		
Mass	2/3	
Sweep radius	2/3	
Loads	Axial bearing load: 1/3 Radial bearing load: 1/3 Bending moment: 2/3	
Inertia	2/3	
Thermal performance	2/3	Inhomogeneous orbital heat fluxes/shading patterns (-). Relatively long waveguide (-). Generally more favorable than concept 2 (+). Mirror thermal control (flatness)(-).
RF Performance		
RF Performance (overall)	2/3	
Insertion loss	2/3	One rotary joint (-). Loss due to antenna (-).
Interface Complexity	2/3	Highly integrated into the APM system, many dependencies (-).
Verification Effort	2/3	Antenna can be manufactured and tested separately from the APM (+).
Risk	3/3	Only one rotary joint => the risk of failing life and torque req. – lower than concept 1(+). Thermo-elastic effects of the mirror deemed to be problematic with respect to pointing accuracy (-). The number of pointing error sources is high (-).
Supplier costs	2/3	Lower costs than concept 1, due to rotary joints (+). Complex U-shaped antenna structure => increased costs for machined parts (-).
AIT-cost	2/3	Due to mirror alignment, a log tolerance chain has to be controlled and requires added assembly effort (-).

3.1.3.3.3. Evaluation of concept 3

Table 3. 1. 6: Evaluation of concept 3

Criteria	Evaluation	Advantages/disadvantages
Mechanical Performance		
Mass	1/3	Highest mass of the 3 compared concepts (-).
Sweep radius	1/3	Biggest sweeping radius of the 3 compared concepts (-).
Loads	Axial bearing load: 2/3 Radial bearing load: 2/3 Bending moment: 1/3	
Inertia	1/3	
Thermal performance	1/3	Displacement of mirror –> pointing errors (-). No waveguide, no RJ = no heat load (++). L-bracket unavailable for heat rejection, azimuth SAR radiator needed (-). No mirror dish bracket (+). Thermo-elastics –> L-bracket (-).
RF Performance		
RF Performance (overall)	2/3	
Insertion loss	3/3	
Interface Complexity	1/3	
Verification Effort	2/3	Cannot be sub tested (-). External HDRM require mechanical ground support equipment (-).
Risk	2/3	Low risk on failing the life and torque requirements (++). New design (-).
Supplier costs	3/3	No need for RJ (+++).
AIT costs	1/3	High tolerances (-)

3.1.3.3.4. Pugh's Concept Selection Matrix

Pugh concept selection matrix is a quantitative technique used to rank the multi-dimensional options of an option set. A basic decision matrix consists of establishing a set of criteria options. The concepts get a weighted score at each criteria, and the total score implies which is the best concept. [2]

3.1.3.3.5. Pugh's concept selection matrix

In table 3.1.7, the three concepts are compared with weighted criteria and with respect to the given requirements and their priority. The given score is from 1 to 5, where 5 is the best. The concept with the highest total score will be the chosen concept in this project.

Table 3. 1. 7: Pugh's concept selection matrix

Pugh's Concepts Selection Matrix					
Criteria	**Unit**	**Weight**	**Concept alternatives**		
			Concept 1	**Concept 2**	**Concept 3**
Mass	kg	15 %	4	3	2
Sweep radius	mm	5 %	4	3,5	3
Loads	N, Nm	2 %	3	2	3
Inertia	kgm^2	5 %	5	3	2
Thermal performance	-	7 %	4	3	3
RF Performance	-	5 %	3	3	3
Insertion loss	dB	5 %	1	3	5
Interface Complexity	-	5 %	4	4	3
Verification Effort	-	5 %	3	4	3
Risk	-	6 %	3	3	3
Rotary Joint	-	10 %	1	2	4
Supplier costs	€	16 %	1	3	5
AIT costs	€	14 %	4	4	4
Sum		**100 %**	40	40,5	43
Weighted sum			2.835	2.93	3.035

3.1.4. Conclusion

The complexity and manufacturing of rotary joints is expensive. Due to two of the higher priority requirements (A) of the project, reducing mass and cost, SSM decided that rotary joints should be avoided. This makes concept 1 and 2 unfavorable.

Concept 1 won the trade-off analysis done by KDA, due to a high overall score with respect to their project requirements. The requirements for SSM are different, and the criteria are weighted differently. If rotary joints were not that expensive and complex, concept 1 would be noticeably more promising.

In the results from the Pugh's matrix, the concept scores are similar and nearly non-separable due to tolerances given in weighting at a later point. Tolerances are excluded in this trade-off, due to the knowledge about the system being too low at this point.

The concept chosen by SSM from this analysis is concept 3. This concept has a lot of new problems related to cost and technical performance, which will need to be compensated for. SSM has to find out if the concept can be adapted to meet the system requirements, and gain knowledge about "honey cone"-structure to manipulate weight and cost. This concept gives more room for new thinking since it contains no rotary joint.

3.1.5. References

[1] C. Heigerer, "KARMA 7, MSA Trade-off Report and Baseline definition (TN01.01) - Background IPR", KDA, Kongsberg, Norway, 26.09.2013.

[2] Wikipedia. (09.02.2016). Decision-matrix method. Available: https://en.wikipedia.org/wiki/Decision-matrix_method.

[3] G.H. Stenseth, M. Dybendal, "Requirement specification", Small Satellite Mechanisms, SSM-2000, rev2.0, 03.03.16.
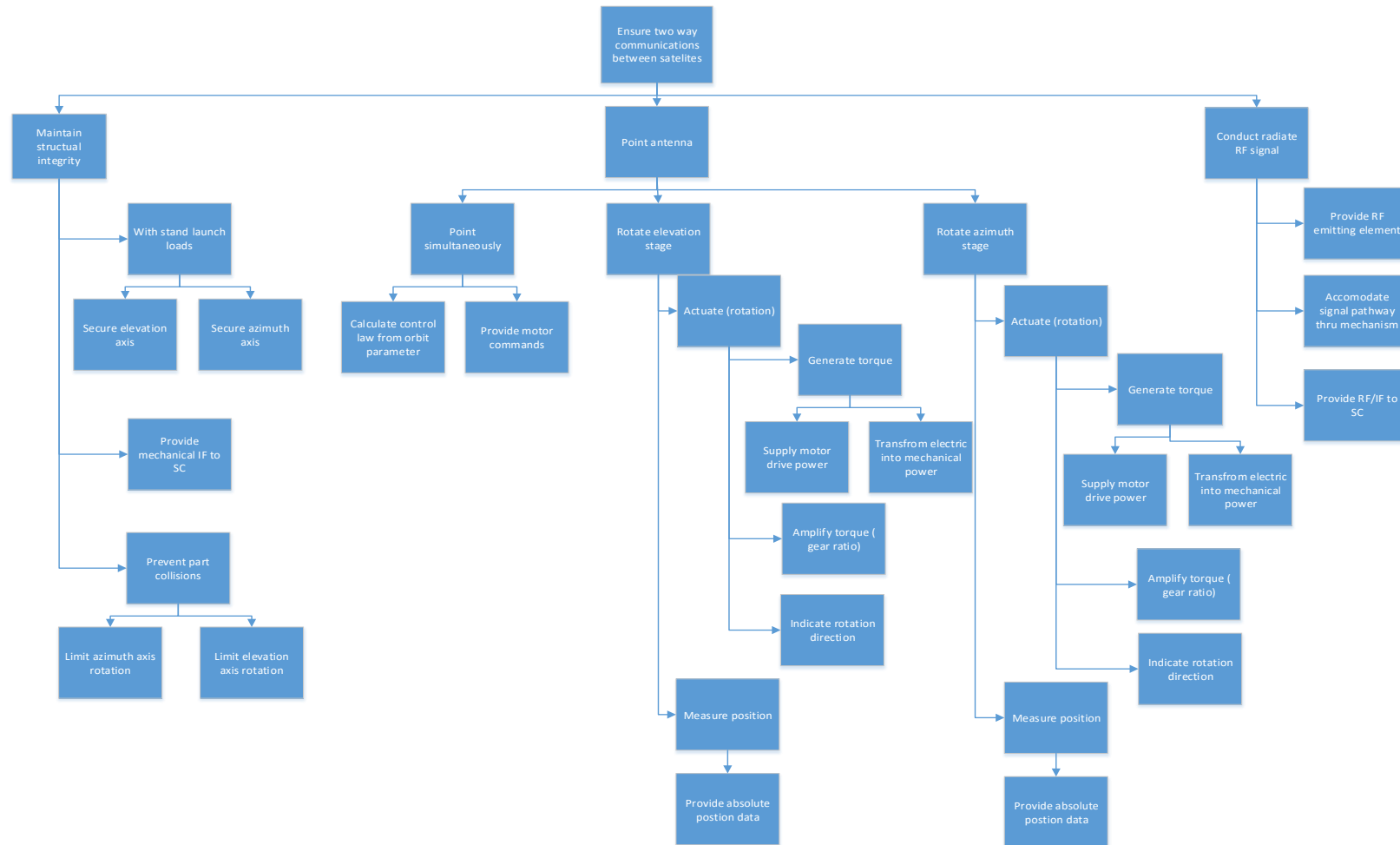
Figure 3. 1. 7: Functional tree [1]

3.2. Link analysis

i.   Abstract

This chapter contains a link analysis for the SSM project. A link analysis is a sum of all the gains and losses in a system, resulting in values for data transfer rates and signal to noise ratios (SNR). This link analysis is done to check the feasibility of the SSM project, and to calculate antenna dimensions.

iii. List of figures

iv. List of tables

v.   Document history

Table 3. 2. 1: Document history

Rev.	Date	Author	Approved	Description
0.1	18.02.16	GHS	-	Created
1.0	03.03.16	GHS	TS	Updated document setup Corrected typo in matlab script Updated all figure axis labels Updated references Added Introduction
1.1	03.05.16	EL		Changed layout into the final report layout.
2.0	19.05.16	GHS	MD	Reviewed and published

3.2.1. Introduction

The SSM project involves the design of an APMA for small satellites. This includes the design of an antenna based communication system. To explore the feasibility of the project, a link analysis is performed.

A link analysis is a calculation of the relationship of the transmitted signal's power compared to the power of the noise. This is done to calculate the possible data transfer rates of the system. In order to do this, all the different losses and gains in the system have to be evaluated.

The link in the SSM project is a transmission between two small satellites in low earth orbit. The main challenge in terms of signal to noise ratio is the small size and the high temperature of the antennae giving low gain and strong noise. The worst case distance between the satellites can be estimated using the height of the orbit and the number of satellites. This distance has a major impact on transmission rates as the loss, due to free space, increases quadratically with the distance.

3.2.2. Calculating antenna dimensions

The carrier frequency f is 23GHz and the minimum gain G is 23dBi [1], 2.2.6. In [2], the Cassegrain antenna design is chosen. The efficiency η of these antennae is ~65-70% [3]. Therefore, a conservative efficiency of 55% was chosen for the calculations below to allow some headroom.

3.2.2.1. *Antenna diameter*

The antenna diameter is found by plotting Eq. (3.2.1) [4].

Gain equation:

$$G = 10log_{10}\left(\frac{\pi D}{\lambda}\right)^{2} \eta \qquad (3.2.1)$$

Where G is the gain of the antenna, D is the diameter, λ is the wavelength of the signal and η is the efficiency of the antenna.
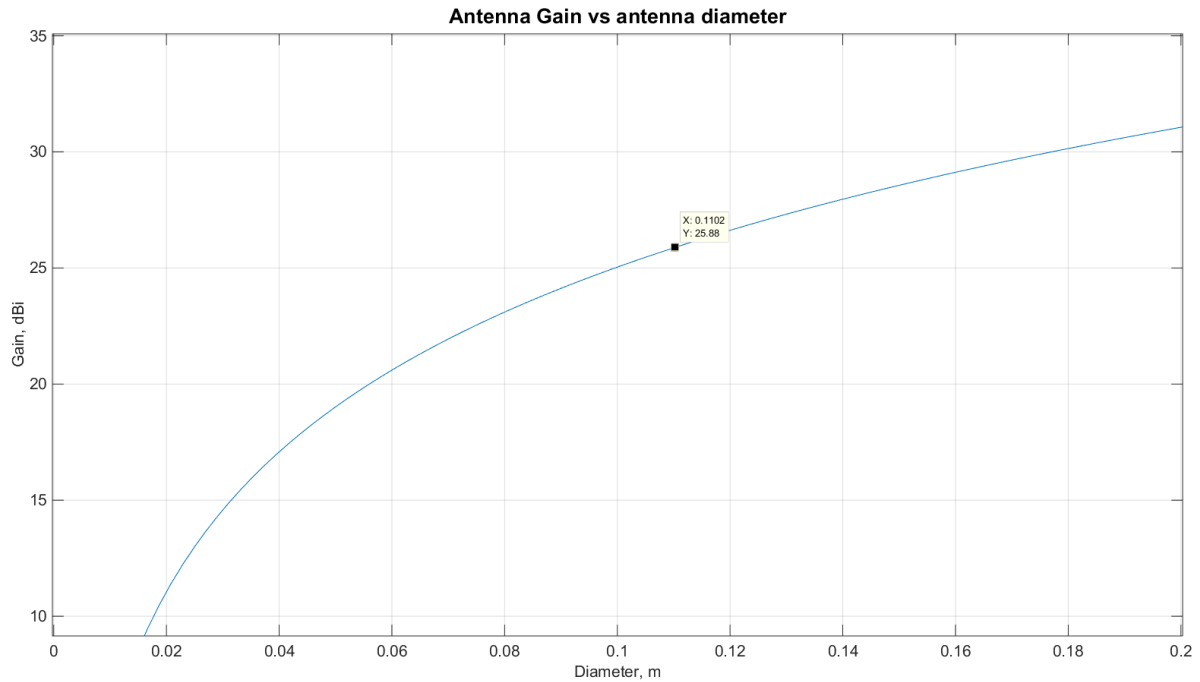
Figure 3. 2. 1: Antenna gain versus antenna diameter

The gain of 23 dBi defined in [1], is the gain of the system from the satellite to the antenna. To account for insertion losses etc. a gain of ~26 dBi was chosen, making the antenna diameter ~11 cm.

3.2.2.2. *Focal point and parabola depth*

Using solidworks [5] the dish depth was found to be ~2 cm, giving a calculated focal point at ~3.5 cm. Due to the cassegrain antenna design, the sub reflector will lie closer to the parabola.

3.2.2.3. *Pointing error impact*

In [1] the maximum pointing error is defined as 0.5 deg. To calculate the impact of this on antenna gain, the half power beamwidth (HPB) has to be found. HPB is defined as the angle where the signal power is halved (-3 dB) [4]. This angle is given by:

$$\theta_{3dB} = 70 \left(\frac{\lambda}{D} \right) = 8.3°$$

(3.2.2)

The gain at the angle α is given by [4]:

$$G(\alpha) = G - 12 \left(\frac{\alpha}{\theta_{3dB}} \right)$$

(3.2.3)

Using equation 3.2.3, the loss due to pointing error is:

$$Lp = -12 \left(\frac{0.5°}{8.3°} \right) = -0.0435$$

The gain loss due to pointing error is negligible.
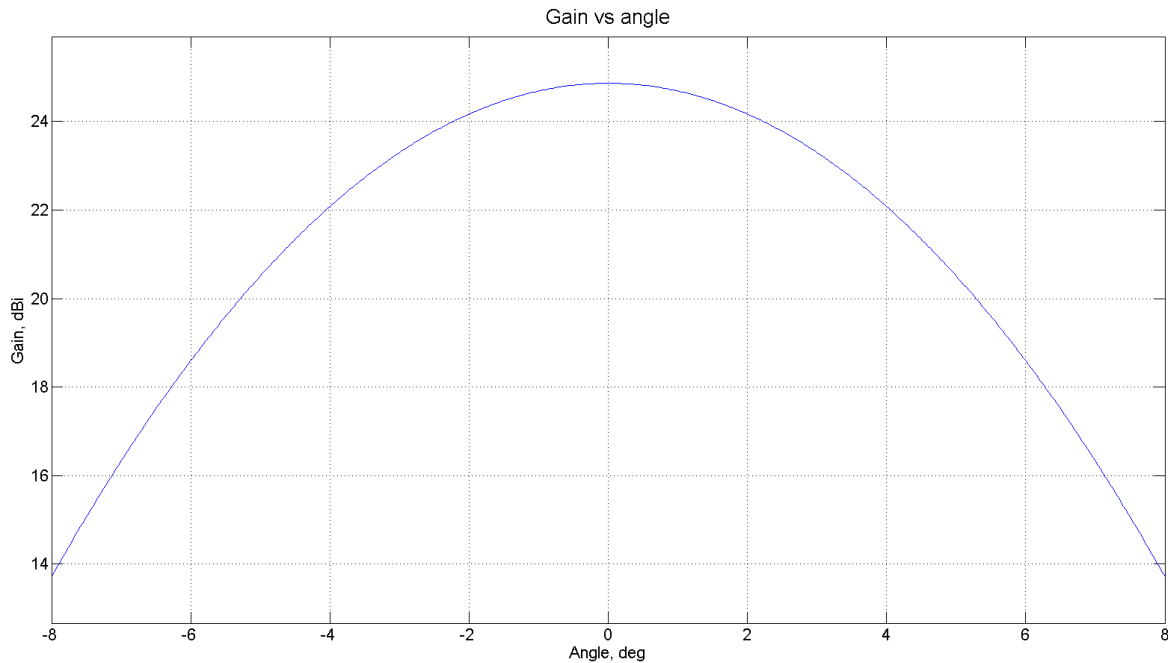
Figure 3. 2. 2: Antenna gain versus pointing accuracy (3)

Figure 3.2.2 shows the gain plotted versus the depointing angle. According to the graph, the mechanism has to point the antenna ~3 degrees before the gain drops below the requirement in [1].

3.2.3. Link analysis

In this link analysis, the most important factors will be considered. The main factors influencing the SSM project are:

- Antenna gain (G): The amplification a signal sees in an antenna system.
- Transmit power (P): The power of the signal sent to the antenna.
- Free space loss (Ls): Attenuation caused by the signal spreading while travelling through a free space.
- Noise temperature (T): Heat causes vibrations in the antenna material. This is seen as noise in the transmitted signal.
- Losses due to the bandwidth (Bw) of the data transmission: Increased bandwidth causes power to be spread over different frequencies in the transmitted signal.
- Additional losses (La): Attenuation caused by fading, polarization, bit error rate etc.

3.2.3.1. *Calculating the distance between satellites*

The AMPA is to be incorporated into a system of ~1000 satellites travelling in LEO. Taking this into consideration, the worst case distance between two satellites can be calculated.
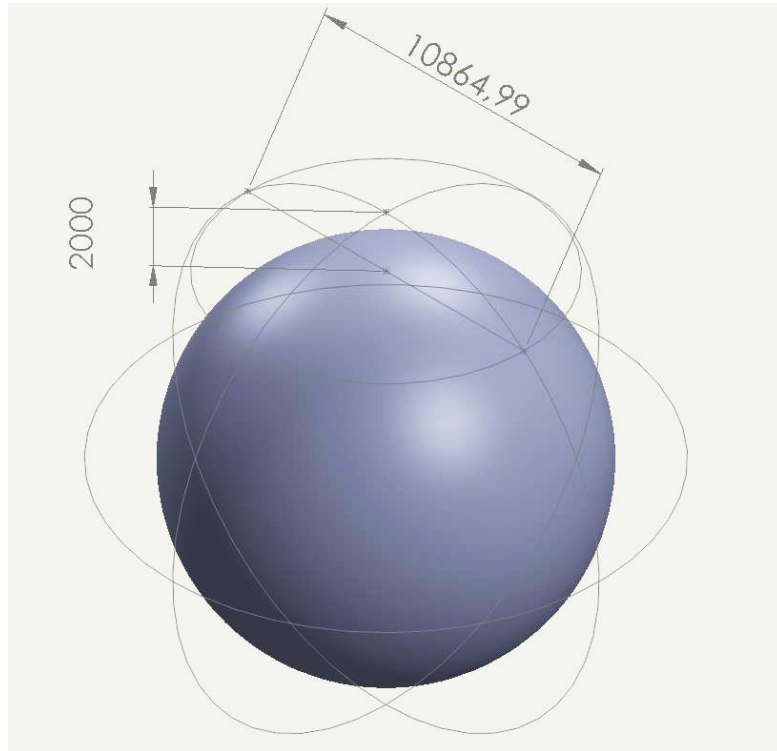
Figure 3. 2. 3: LEO

Figure 3.2.3 shows the worst case distance between two satellites calculated by taking into consideration the diameter of the earth and a distance of 2000 km (the largest distance for LEO) to the earth's surface. The calculated distance between the two satellites is approximately 10000 km. Taking into consideration the amount of satellites in the system, this distance is greatly reduced. The distance R used in the link analysis is limited to 200 km.

3.2.3.2. *Equivalent Isotropic Radiated Power (EIRP)*

EIRP is a measurement of the radiated power compared to an isotropic source [6]. In [1], the transmit power is specified at 5 W. As mentioned earlier, the gain of the antenna is increased (25.88 dBi) to account for insertion losses. For the analysis, the insertion loss is set to 1 dBi, which gives a total gain of 24.88 dBi. This gives:

$$EIRP = 10 \log(P) + G = 31.86 \text{ dBW} \tag{3.2.4}$$

3.2.3.3. *Free space loss (Ls)*

For the APMA system, the free space loss is calculated to [6]:

$$Ls = 20 \log \left(\frac{4\pi R}{\lambda}\right)^2 = 165.7 \text{ dB} \tag{3.2.5}$$

3.2.3.4. *Figure of merit for the receiver*

The figure of merit for the receiver is calculated by dividing the receiver antenna gain by the noise temperature of the receiving system [4]:

$$F = 10 \log \frac{G}{T}$$

$$(3.2.6)$$

The noise temperature for the receiver is set to 1500 K considering the small size of the antenna [4], 2.4.2.3. The receiving system is using the same antenna as the transmitting system, which means both systems have the same antenna gain.

3.2.3.5. *Received power*

The power received by the receiver can be expressed [4]:

$$Pr = \frac{G^2 P}{\left(\frac{4\pi}{\lambda}\right)^2} = 1.27 \cdot 10^{-11} \, W$$

$$(3.2.7)$$
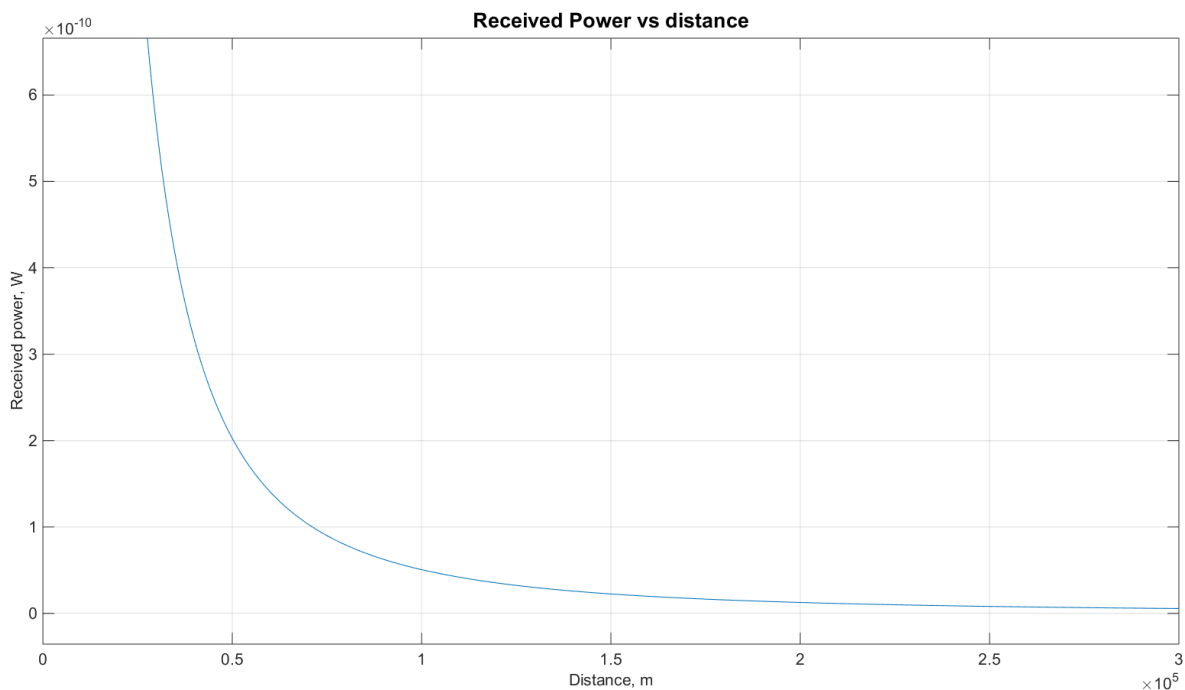
Figure 3. 2. 4: Recieved power versus distance satellites

Figure 3.2.4 shows that the signal strength decreases exponentially as the distance increases. While a signal received at 200 km is strong, signals at a closer distance are exponentially stronger.

3.2.3.6. *Carrier to noise ratio (CNR)*

CNR is defined as the strength of the carrier signal divided by the strength of the noise. To calculate the CNR, the total loss of the system is needed. In addition to the losses calculated above, the losses due to bandwidth need to be calculated. An approximation for the bandwidth was found by plotting the total CNR of the system versus the bandwidth using [4]:

$$CNR = EIRP - Ls + F - La - 10\log\frac{1}{kBw}.$$

(3.2.8)

La =40 dB is introduced as additional losses. $k = 1.38 \cdot 10^{-23}$ is the Boltzmann constant.
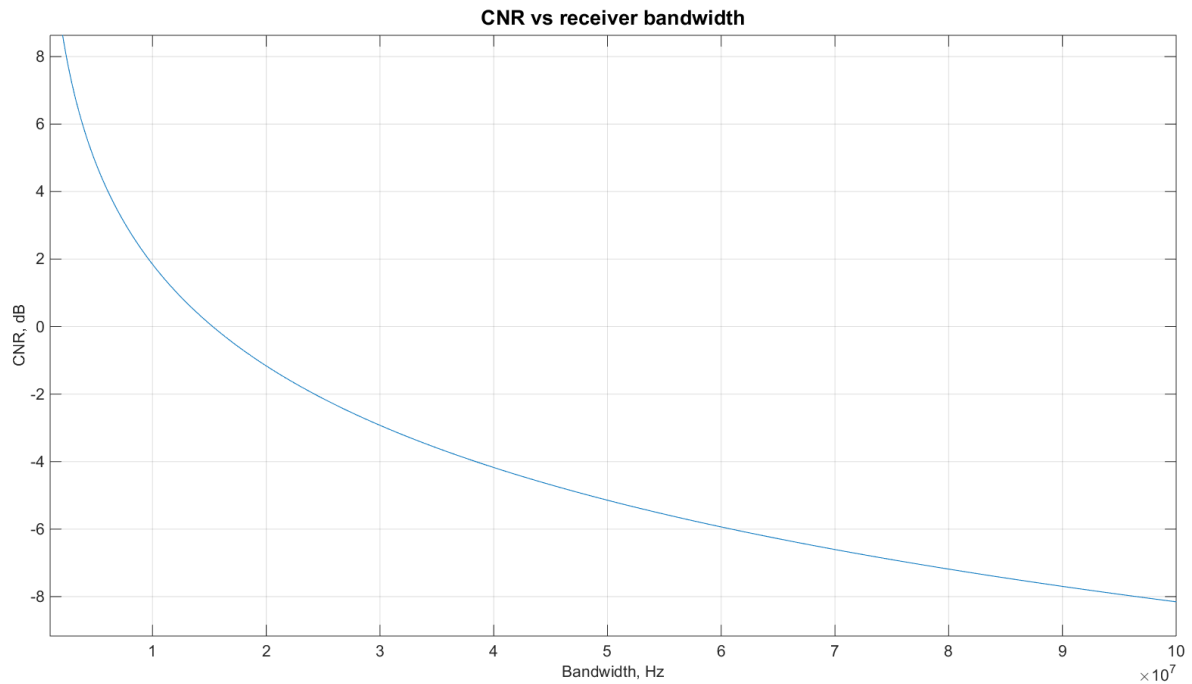
Figure 3. 2. 5: CNR versus bandwidth

In addition to plotting the CNR based on bandwidth, the bitrate C was also plotted using the Shannon-Hartley theorem [7]:

$$C = Bwlog_2(1 + CNR)$$

(3.2.9)
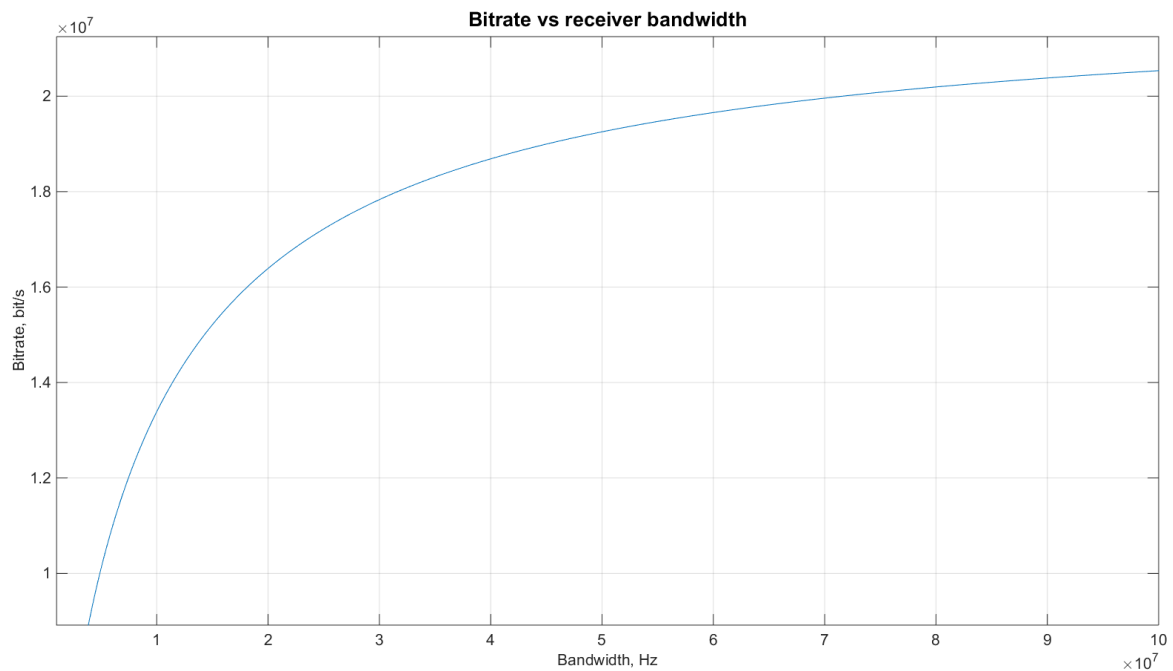
Figure 3. 2. 6: Bitrate versus bandwidth

A bitrate of approximately 13 Mbps is achievable at a bandwidth of 10 MHz. At this bandwidth, the CNR is ~2 dB. A CNR of 2 dB is a quite realistic goal for this system considering the size of the antennae and the distances between satellites.

3.2.4. Conclusion

Using cassegrain antennae at 11 cm with an estimated gain of 25.88 dBi the system shows promising CNR. The 13 Mbps bit rate calculated was using the Shannon-Hartley theorem. This theorem takes into consideration an ideal setting, and is only a rough estimate of the maximum possible data rate.

Figures 3.2.10 and 3.2.11 show that the noise temperature of the receiver has a large impact on CNR. This value was roughly estimated, using the data from a parabolic antenna with a diameter of 2 m. If the value is halved, the bit rate is increased by ~10 Mbps.

Decreasing the bandwidth would increase the CNR, but decrease the bit rate. This is a trade-off a potential customer has to consider depending on the modulation used.

From this analysis, the SSM project is seen as feasible.

3.2.5. References

[1] G. H. Stenseth and M. Dybendal, "Requirement Specification", SSM-2000, rev.1.1, 08.02.16,.

[2] T. Sundnes et al. "Technical document-electrical", SSM-5111, rev 0.2, 22.02.16,.

[3] Wikipedia , 24.11.15., Parabolic antenna. Available:
    https://en.wikipedia.org/wiki/Parabolic_antenna.

[4] G. Maral and M. Bousqet, *Satellite Communications Systems*. New York: Wiley, 1987.

[5] M. Dybendal, "Mechanical Design Description, SSM-5123,rev 0.1, 01.03.16,.

[6] NAROM, 11.11.13, Strekningsdemping. Available: http://ndla.no/nb/node/58964?fag=2600.

[7] S. Haykin*, Communication Systems, 4th ed.* New York: Wiley, 2001.

[8] Down East Microwave Inc, Calculating a Parabolic Dish's Focal Point. Available:
    http://01895fa.netsolhost.com/PDF/dishfp.PDF [28.02.16].

3.2.6. Appendices

3.2.6.1. *Appendix 1: Other graphs related to the link analysis*
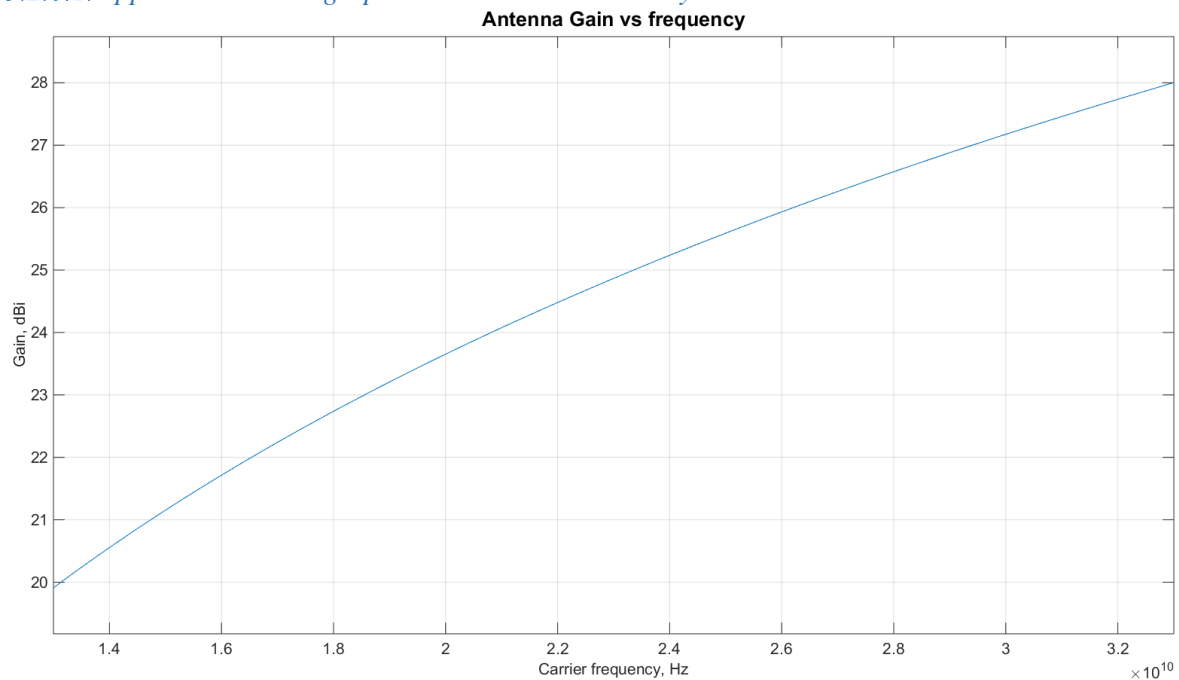
Figure 3. 2. 7: Antenna gain versus frequency

The graph in figure 3.2.7 shows the gain of the antenna versus the carrier frequency, and was plotted to check if the antenna would limit the bandwidth. The gain is calculated using the physical properties of the SSM antenna. The conclusion drawn from this graph was that the bandwidth of the system is not limited by the antenna.
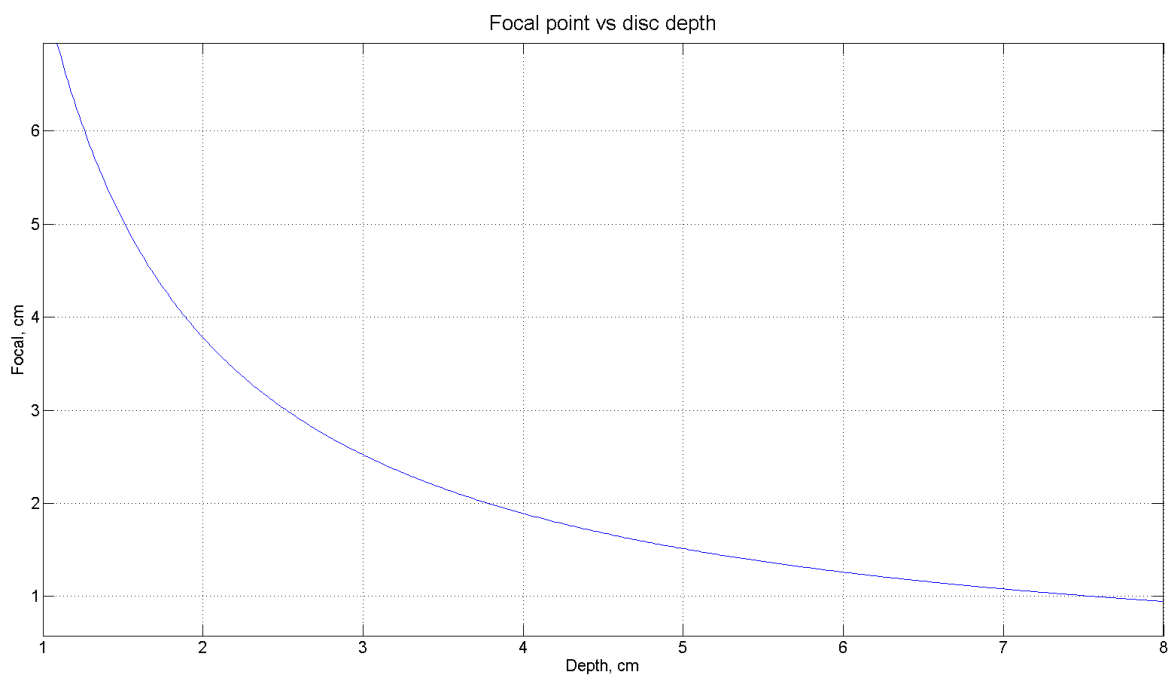
Figure 3. 2. 8: Focal point distance versus disc depth

Figure 3.2.8 shows the focal point of the SSM antenna at different parabola depths.
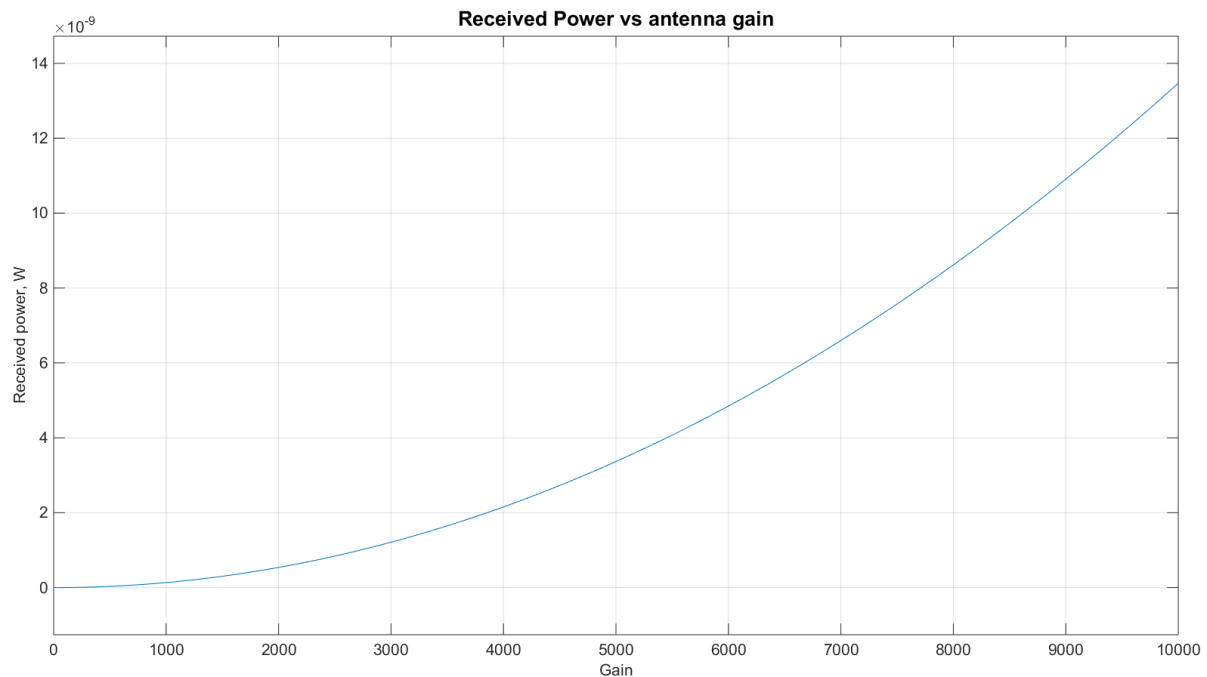
Figure 3. 2. 9: Received power versus antenna gain.

The graph in figure 3.2.9 was made using the distance defined in §3.2.3.1. It was made to show the impact of antenna gain on the received signal's power.
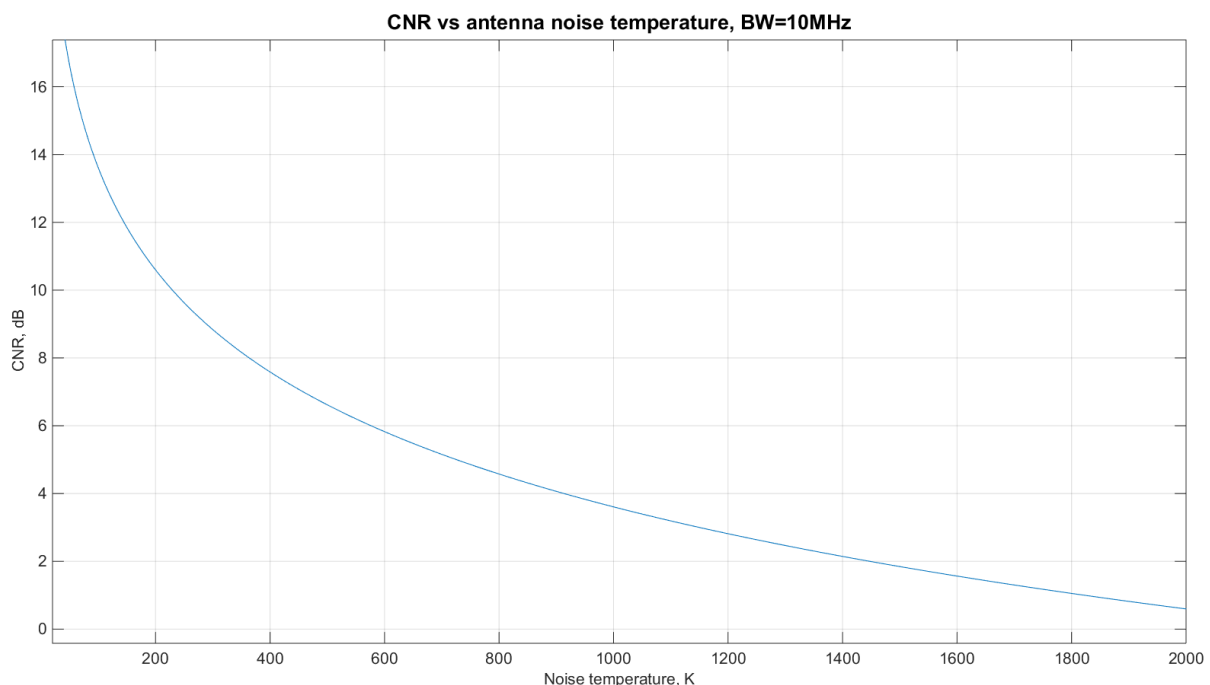
Figure 3. 2. 10: CNR versus receiver noise temperature.

The graph in figure 3.2.10 was made using a bandwidth of 10 MHz and shows how the receiving antenna's noise temperature impacts CNR.
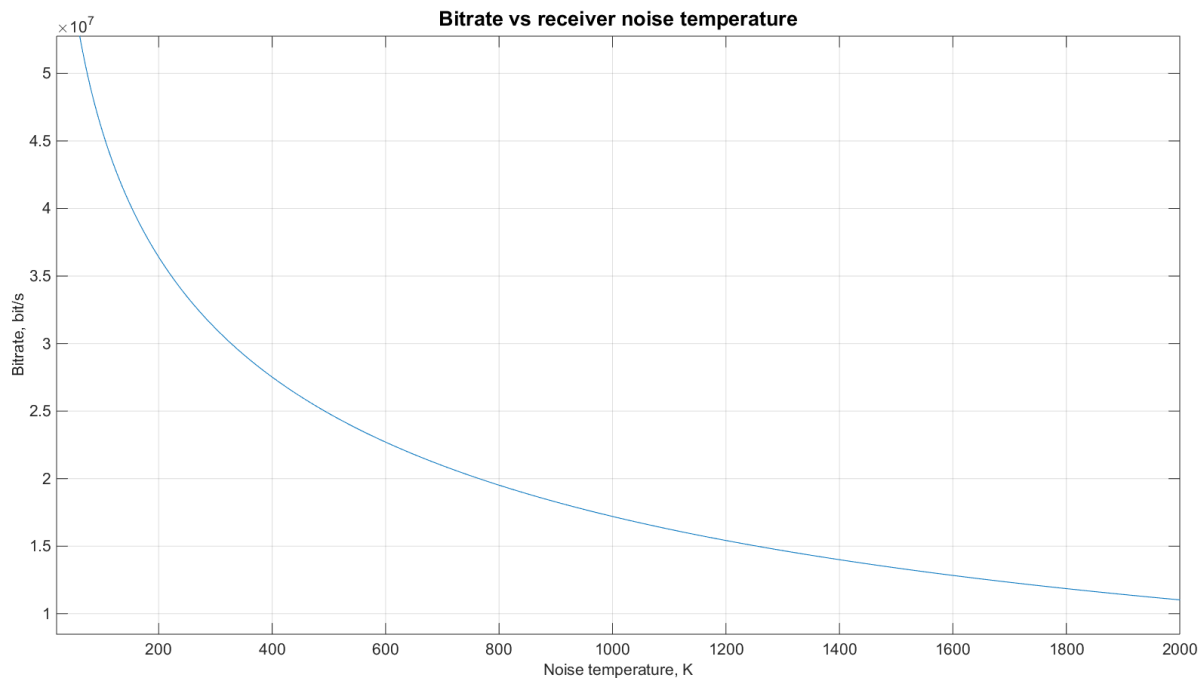
Figure 3. 2. 11: Link bitrate versus receiver noise temperature

The graph in figure 3.2.11 was made using a bandwidth of 10 MHz and shows the impact of the receiving antenna's noise temperature on the data transmission rate.

3.2.6.2. *Appendix 2: Matlab code*

The matlab script below was made to do the calculations for the link analysis. Running this script will give all the values and graphs noted in this document.

```matlab
%% Link analysis SSM

clc
clear all
close all
%% Parabolic antenna calculations
% Diameter
D = 0.11 %m
% Depth
d = 0.01973 %m
% Frequency
f = 23e9 %Hz
% Speed of light
c = 3e8 %m/s
% Efficiency
n = 0.55
% Antenna Gain
G = 10*log10(((pi*D/(c/f))^2)*n) %dBi
% Account for insertion loss (1dBi)
G = G-1
% Focal point
F = (D^2)/(16*d) %m
% Boltzmans constant
k = 1.38e-23 %dB/WHz
%% Link calculations
```

```matlab
% Satellite to satellite communications considering antenna gain,
transmit
% power and free space loss

% Distance between satellites in meters
R = 200e3 %m

% Gain (not in dB)
Gx= 10^(G/10)
% Transmit power
P = 5 %W

%%
% Equivalent Isotropically radiated power
EIRP = 10*log10(P)+G %dBW

%%
% Rx power (Power after the receiving antenna)
% Rx power in W
Pr = (Gx^2*P)/(((4*pi*R)/(c/f))^2) %W
% Rx power in dBW
Prdb = 10*log10(Pr)

%% Free space loss
%
L = 20*log10((4*pi*R)/(c/f))
%% Add LNA (20dB)

% Power after LNA (approximation)
% lna = Prdb +20 %dBw
% LNA = 10^(lna/10) %W

%% Plots
syms x
syms y
%%
% Gain
figure;
ezplot(10*log10(((pi*x/(c/f))^2)*n),[0,0.9])
grid on;
title('Antenna Gain vs antenna diameter','FontSize',20);
ylabel('Gain, dBi','FontSize',16);
xlabel('Diameter, m','FontSize',16);
set(gca,'fontsize',16)

%%
% Antenna gain vs frequency
figure;
ezplot(10*log10(((pi*D/(c/x))^2)*n)-1,[13e9,33e9])
grid on;
title('Antenna Gain vs frequency','FontSize',20);
ylabel('Gain, dBi','FontSize',16);
xlabel('Carrier frequency, Hz','FontSize',16);
set(gca,'fontsize',16)
%%
% Received power
figure;
ezplot((x^2*P)/(((4*pi*R)/(c/f))^2),[0,10000])
grid on;
title('Received Power vs antenna gain','FontSize',20);
```

```matlab
ylabel('Received power, W','FontSize',16);
xlabel('Gain','FontSize',16);
set(gca,'fontsize',16)
%%
% Received power
figure;
ezplot((Gx^2*P)/(((4*pi*x)/(c/f))^2),[10e3,300e3])
grid on;
title('Received Power vs distance','FontSize',20);
ylabel('Received Power, W','FontSize',16);
xlabel('Distance, m','FontSize',16);
set(gca,'fontsize',16)
%%
% Received power 0-200km
figure;
ezplot((Gx^2*P)/(((4*pi*x)/(c/f))^2),[0,300e3])
grid on;
title('Received Power vs distance','FontSize',20);
ylabel('Received power, W','FontSize',16);
xlabel('Distance, m','FontSize',16);
set(gca,'fontsize',16)
%%
% Focal point
figure;
ezplot(((D*100)^2)/(16*x),[1, 8])
grid on;
title('Focal point vs disc depth','FontSize',20);
ylabel('Focal, cm','FontSize',16);
xlabel('Depth, cm','FontSize',16);
set(gca,'fontsize',16)
%% Pointing error impact
% The impact of our maximum pointing error on antenna gain
% Half power beamwidth:
alpha3db= 70*((c/f)/D)

%%
% pointing error
alpha = 0.5

%%
% Gain with pointing error
Gpointing = Gx-12*(alpha/alpha3db)^2

%%
% Gain loss based on pointing error
Gpointing_loss=-12*(alpha/alpha3db)^2

%%
% Plot of total Gain including pointing error
figure;
ezplot(G-12*(x/alpha3db)^2,[-8, 8])
grid on;
title('Gain vs angle','FontSize',20);
ylabel('Gain, dBi','FontSize',16);
xlabel('Angle, deg','FontSize',16);
set(gca,'fontsize',16)
%% Carrier to noise ratio at receiver input
%
% SNR =  pr/(x*k*y)
% Additional losses:
```

```matlab
La = 40
%%
% CNR calc (EIRP-Free space loss + Figure of merit receiver - additional
% losses - boltzman constant - bandwidth). x replaces T as the noise
% temperature. Approximate temperature for receivers on satellites is
% in the order of ~1000K [SCS]Considering that the SSM's antenna is
small,
% the Antenna temperature is set to ~500K (worst case, pointing at the
% sun)

B = 10e6 %1MHz BW
CNR = EIRP - L + 10*log10(Gx/x) - 10*log10(La) - 10*log10(k)-10*log10(B);
figure;
ezplot(CNR,[20,2000])
grid on;
title('CNR vs antenna noise temperature, BW=10MHz','FontSize',20);
xlabel('Noise temperature, K','FontSize',16)
ylabel('CNR, dB','FontSize',16)
set(gca,'fontsize',16)
%%
% Calculating achieveable bitrate using CNR, BW and Shannon's theorem

%C = B*log2(CNR+1)
C = B*log2(10^(CNR/10)+1)
figure
ezplot(C,[20,2000])
grid on;
title('Bitrate vs receiver noise temperature','FontSize',20)
ylabel('Bitrate, bit/s','FontSize',16);
xlabel('Noise temperature, K','FontSize',16);
set(gca,'fontsize',16)
%%
% Calculating bitrate with respect to bandwidth. T set to 2000
T = 1500;

CNR = EIRP - L + 10*log10(Gx/T) - 10*log10(La) - 10*log10(k)-10*log10(x);
figure;
ezplot(CNR,[1e6,100e6])
grid on;
title('CNR vs receiver bandwidth','FontSize',20);
xlabel('Bandwidth, Hz','FontSize',16)
ylabel('CNR, dB','FontSize',16)
set(gca,'fontsize',16)
C = x*log2(10^(CNR/10)+1)
figure
ezplot(C,[1e6,100e6])
grid on;
title('Bitrate vs receiver bandwidth','FontSize',20)
ylabel('Bitrate, bit/s','FontSize',16);
xlabel('Bandwidth, Hz','FontSize',16)
set(gca,'fontsize',16)
```

3.3. Technical budgets

i. Abstract

This chapter contains different technical budgets of the low cost APMA. The budgets will ensure compliance with given requirements for the mechanism, and in the total budgets the worst-case scenarios are factored with a risk factor.

Technical budgets included in this document:

- Power budget
- Mass budget
- Torque budget
- Pointing budget

ii. Contents

iii. List of figures

iv. List of tables

Table 3. 3. 1: Document history

Rev.	Date	Author	Approved	Description
0.1	18.02.16	EL, VOA, MD		Document created.
0.2	29.02.16	MD, VOA	EL	Document layout updated and corrected typos. Updated torque budget Added section 4.3
1.0	04.03.16	EL, VOA, MD	EL	Rev. 1.0 created and reviewed
1.1	07.03.16	VOA		Torque adjusted to 1:15
1.1	18.4.16	VOA		Torque adjusted to 1:17.5
1.2	22.04.16	VOA		Friction adjusted Torque updated
1.3	25.04.2016	MD, VOA	TS, VOA	Updated mass budget + inserted new pictures
2.0	25.04.2016	EL	TS, VOA	Added pointing budget
2.1	28.04.16	MD		Added gear specification
2.2	05.05.16	VOA, EL		Updated torque and friction Updated pointing budget
3.0	12.05.16	EL, VOA, MD	TS	Reviewed and published

SSM

SMALL SATELLITE MECHANISMS

3.3.1. Introduction

Technical budgets are a break-down structure or bottom-up calculation of technical features of a system, and are useful for ensuring requirements are met. This project has important requirements regarding mass, power, torque and pointing, and due to this, these budgets are included in this chapter.

3.3.2. Power budget

The power budget in this section shows a breakdown structure of the power consumption in the different parts of the low-cost APMA. A small satellite (<500 kg) does not have a large power supply, generating the need to limit the power consumption in the system.

SSM has a power requirement given by KDA, which has to be met:

"The low cost APMA shall have a power consumption of ≤ 15 W, including electronics and actuators." [1]

The most critical power demands in the operating system are the BLDC-motors of the azimuth and elevation stage. The maximum operation of the motors has to be limited to 12 W (2 · 6 W) consumption. The power consumption due to the control system and the sensors are low compared to the motors.

3.3.2.1. *Breakdown structure*

Figure 3.3.1 is a breakdown structure, which shows the assumed power consumption in the different parts of the APMA.
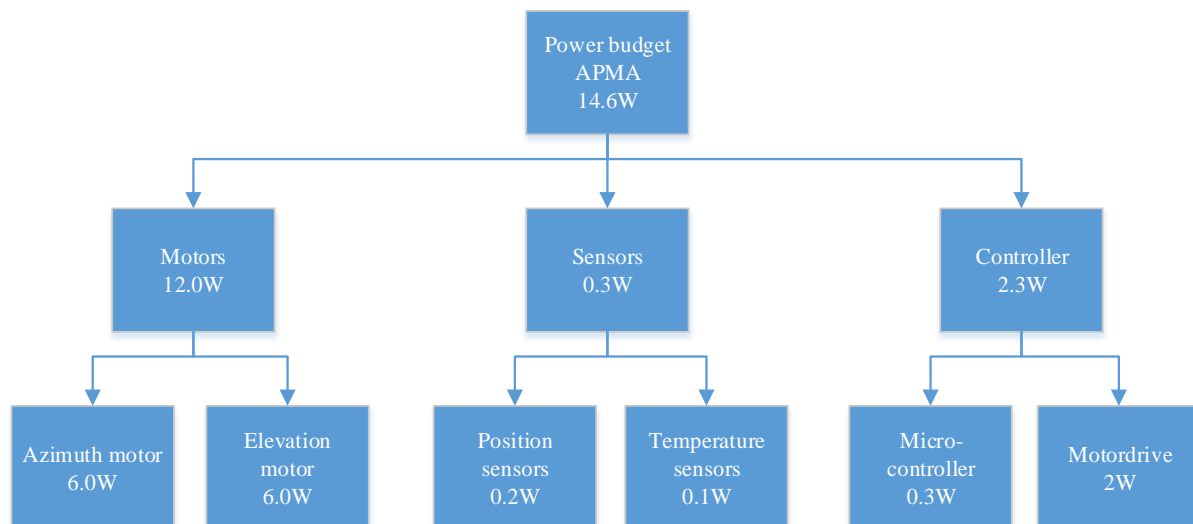
Figure 3. 3. 1: Breakdown structure - power consumption

3.3.2.2. *Total factored power budget*

Table 3.3.2 shows the total factored power budget for the low cost Antenna Pointing Mechanism assembly. The assumed worst-case power consumptions are factored with a risk factor of 1.1 (except motors).

Table 3. 3. 2: Total factored power budget

System	Worst case power consumption [W]	Risk factor	Worst case power consumption factored [W]	Explanation
Motors	12.00	1.00	12.00	2 motors, azimuth and elevation
Position sensors	0.20	1.10	0.22	2 encoders, controlling motor position
Temperature sensors	0.10	1.10	0.11	
Motor drive	2.00	1.10	2.20	
Microcontroller	0.30	1.10	0.33	
Total power consumption	**14.60**		**14.86**	

The total factored power budget for the mechanism is 14.86 W. Note that the assumed worst-case power consumption of the motors are for high performance of both. The actual consumed power in the motors are expected to be significantly lower.

SSM

SMALL SATELLITE MECHANISMS

3.3.3. Mass budget

With respect to chosen materials and sizes from the 3D-model in SolidWorks, the mass of the different assemblies of the APMA are calculated in this section. At the end, the masses are summarized and an assumed total mass (without electronics) are presented.

Figure 3.3.2 shows a schematic view of the APMA:
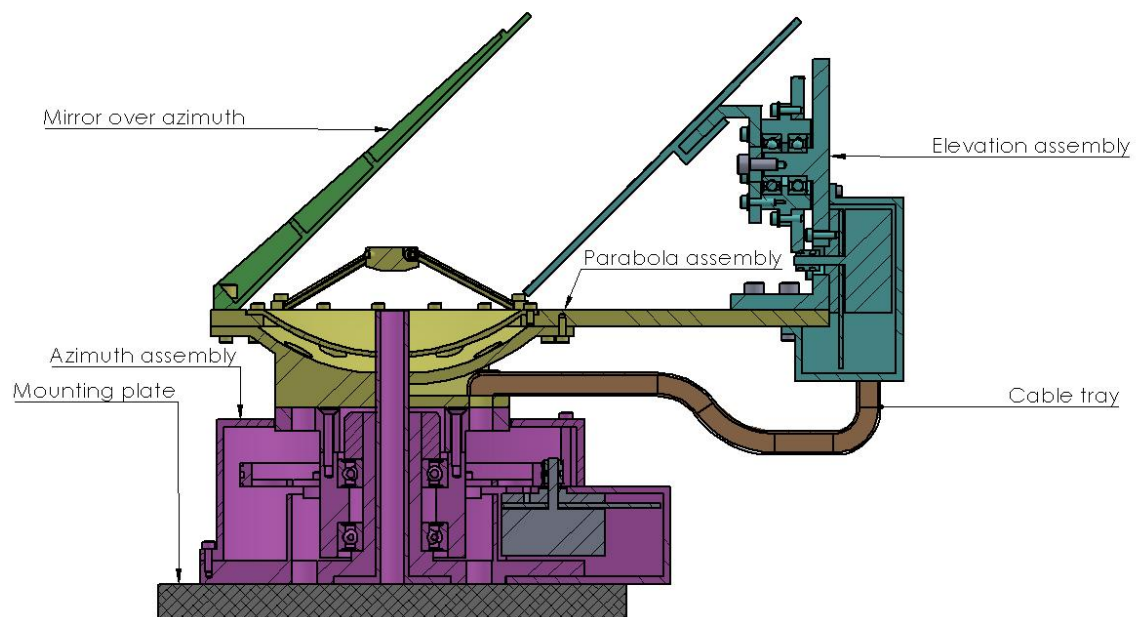
Figure 3. 3. 2: Schematic view of the APMA

3.3.3.1. *Breakdown structure*

Table 3. 3. 3: Elevation connection assembly

Mass budget elevation assembly		
Part name	**Part number**	**Mass (gram)**
Elevation bracket	10 201	179.20
Gear elevation	10 202	70.00
Motor	10 203	160.00
Connector elevation	10 204	49.05
Contact mirror connector	10 205	44.54
Mirror elevation	10 206	139.44
Motor house elevation	10 207	117.94
2 x W6000	10 208	35.20
Screws	-	4.52
TOTAL		**799.89**

Table 3. 3. 4: Mass over elevation

Mass over elevation	**Mass (gram)**
233.03	
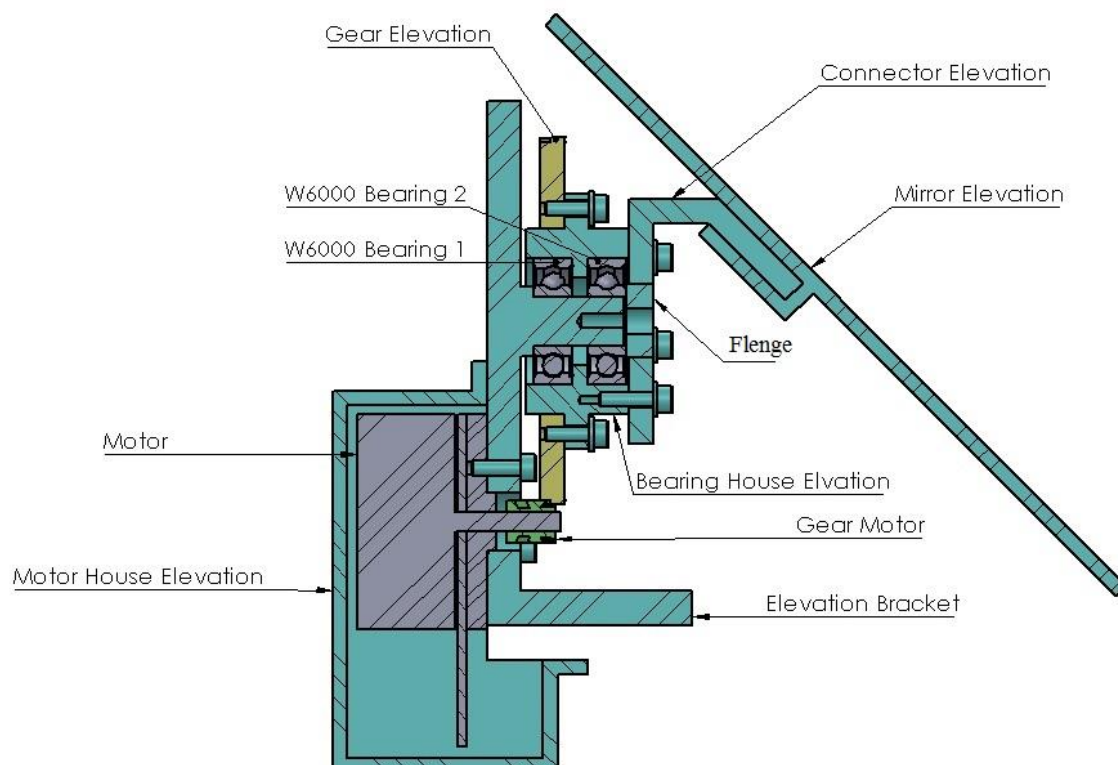
Figure 3. 3. 3: Elevation assembly

Table 3. 3. 5: Azimuth assembly

Mass Budget Azimuth		
Part name	**Part number**	**Mass (gram)**
Main contact plate	10 001	632.80
Waveguide	10 002	38.02
Motor	10 003	160.00
Motor housing azimuth	10 004	111.67
Cap azimuth	10 005	342.26
Bearing house azimuth	10 006	202.37
2 x W6005	10 007	146.2
Gear azimuth	10 008	253.35
Connector	10 009	190.32
KMT 5 NUT	10 010	130.00
Screws	-	4.83
TOTAL		**2211.82**

Table 3. 3. 6: Mass over azimuth

Mass over azimuth	Mass (gram)
2123.07	
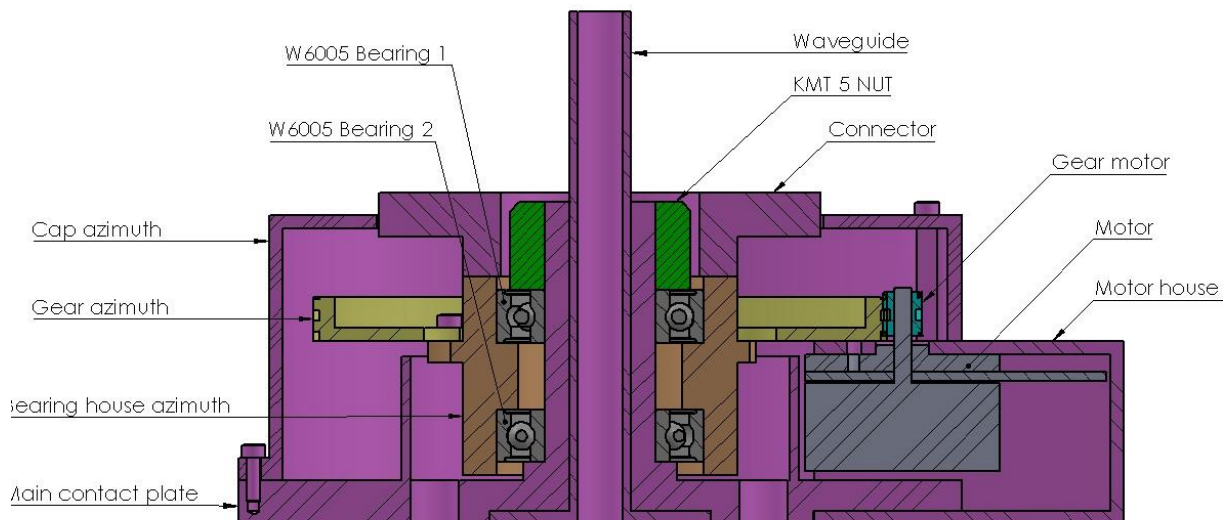
Figure 3. 3. 4: Azimuth assembly

Table 3. 3. 7: Parabola assembly

Mass budget parabola assembly		
Part name	Part number	Mass (gram)
Parabola holder	10101	341.20
Azimuth fishplate	10102	384.96
Parabola	10103	72.09
Subreflector	10104	6.28
3 x Struts	10105	6.96
Screws	-	3.80
TOTAL		**815.29**
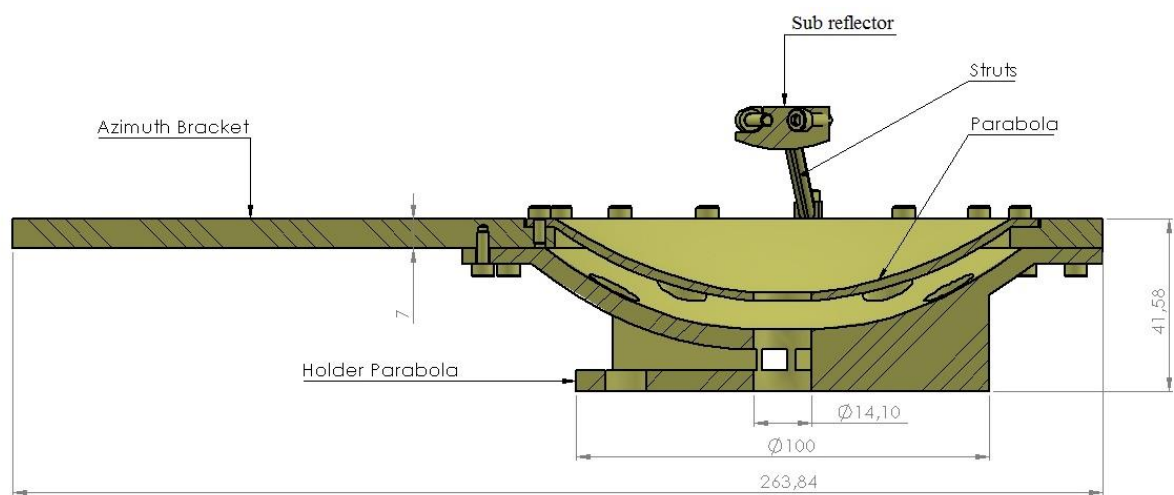
Figure 3. 3. 5: Parabola assembly

Table 3. 3. 8: Other parts

Other parts		
Part name	Part number	Mass (gram)
Mirror over azimuth	10 301	139.22
Cable tray	10 302	29.21
Screws	-	19.14
TOTAL		**187.57**
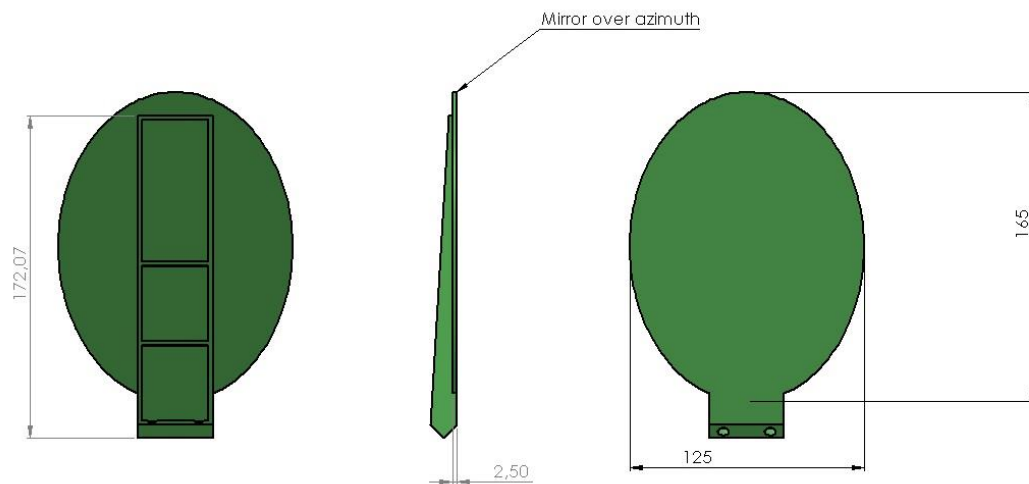
Figure 3. 3. 6: Mirror over azimuth
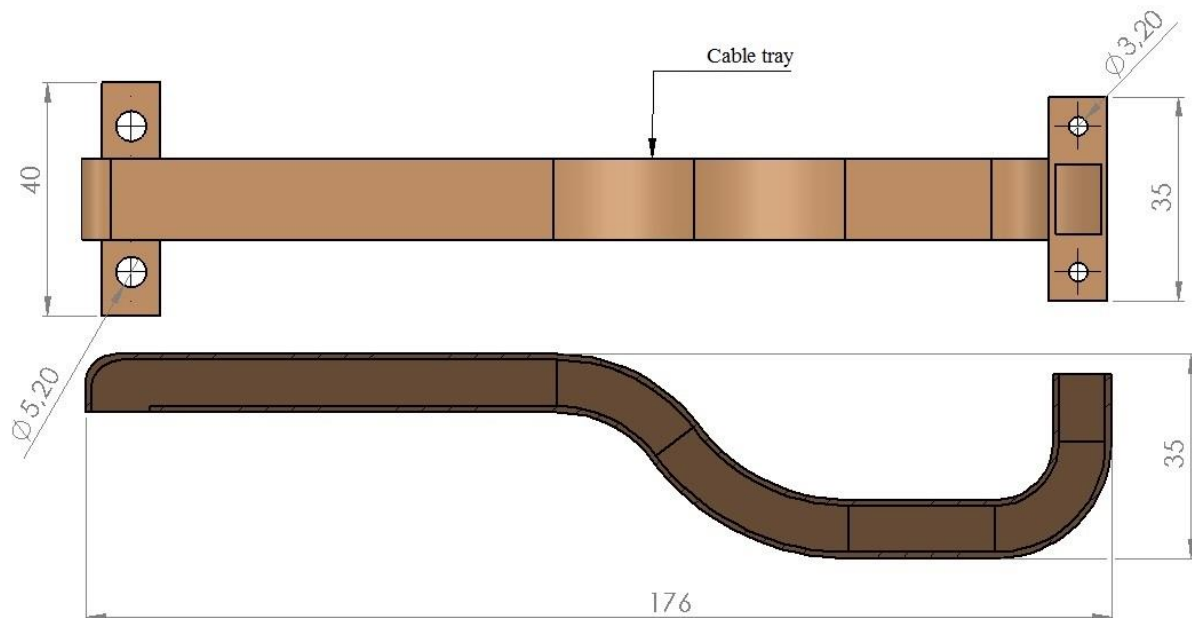
Figure 3. 3. 7: Cable tray

3.3.3.2. *Total mass budget*

In table 3.3.9 the assumed total mass of the low-cost APMA is calculated.
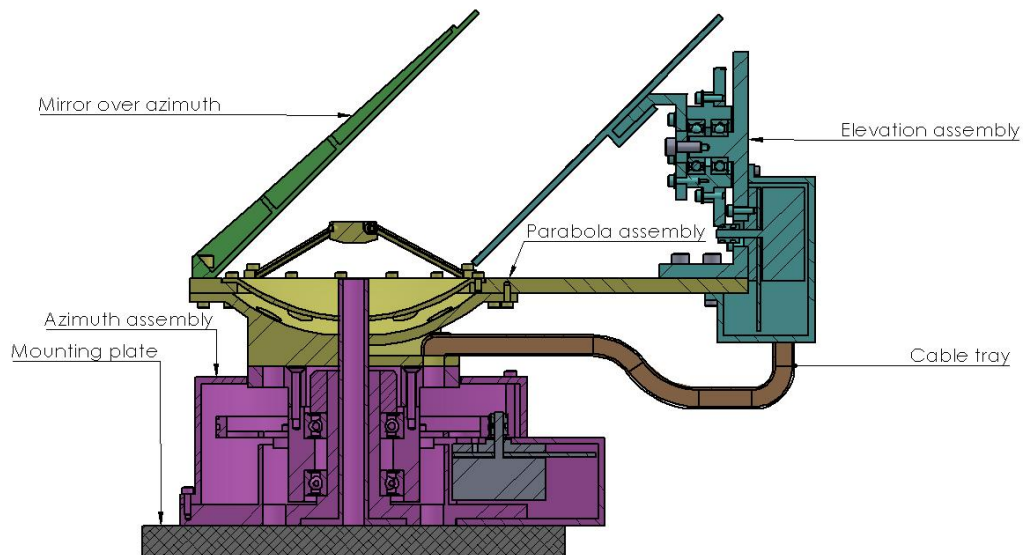
Figure 3. 3. 8: Schematic view of the APMA

Table 3. 3. 9: Total mass budget

Assemblies /parts	Mass (gram)
Azimuth assembly	2206.99
Elevation assembly	795.37
Parabola assembly	811.49
Cable tray	29.21
Mirror over azimuth	139.22
Screws	32.29
TOTAL	**4014.57**

At this point the APMA has a total mass of 4014,57 g which do not satisfy the given requirement related to mass. The total mass changed due to design changes during the project. The APM design is based on the bearing setup.

3.3.4. Torque budget

The motors driving the azimuth and elevation stage requires a certain amount of torque to drive the system. A COTS motor does not produce a high enough amount of torque, and in this system a set of gears are needed to reach the required speed to drive the mechanism.

3.3.4.1. *Breakdown structure*

For a gear structure, odd numbers of gears will keep the rotation the same way, while even numbers will give the opposite rotation from the input rotation. Using a small input gear and a large output gear will reduce output velocity and rise torque, while large input gear and a small output gear provides high output velocity, but low torque. Figure 3.3.9 shows the relationship between gear ratio and torque.
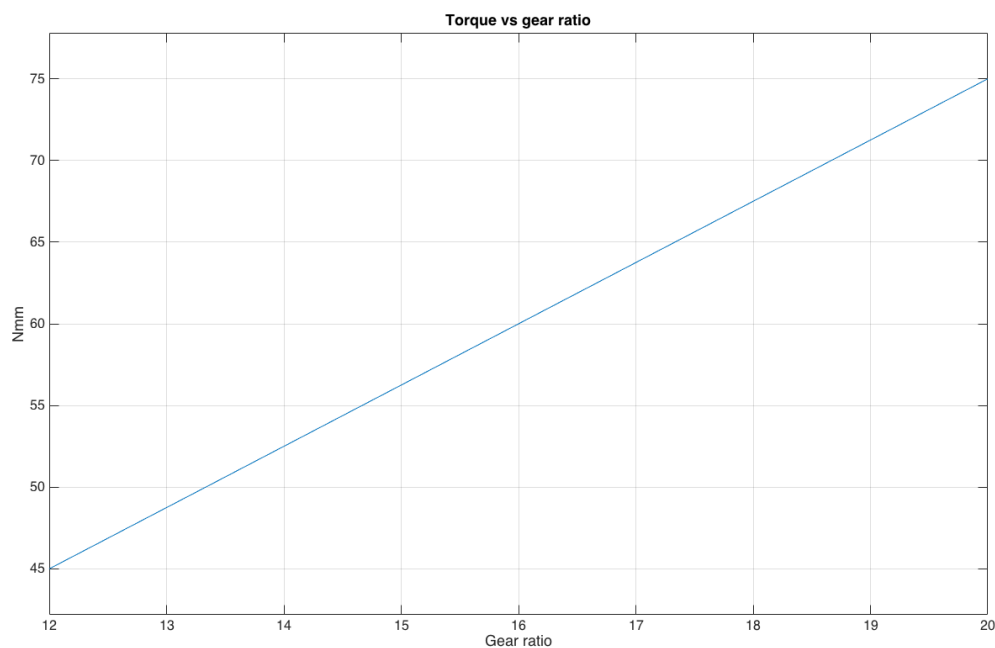
Figure 3. 3. 9: Torque vs gear ratio

3.3.4.2. *Total torque budget*

"The rotational analog of Newton's second law says that the net torque acting on a body equals the product of the body's moment of inertia and its angular acceleration".[1]

$$\sum \tau_z = I\alpha_z$$

(3.3.1)

where I is moment of inertia and α is angular acceleration [3].

3.3.4.2.1. Hand calculations

To check if the simulation results generated by SolidWorks are accurate, a test is performed: A hollow strut with a mass of 163 g with radius $R_1 = 114$ mm and $R_2 = 155$ mm shall be able to accelerate to 0.7 rad/s^2 in 1 second.

Moment of inertia for a hollow strut I:

$$I = \frac{1}{2}M(R_1^2 + R_2^2) \tag{3.3.2}$$

Where M is the mass, R_1 is the inner radius and R_2 is the outer radius. [4, table 9.2]

$$I = \frac{1}{2} \times 163g\left(\left(\frac{114mm}{2}\right)^2 + \left(\frac{155mm}{2}\right)^2\right) \tag{3.3.2.1}$$

$$\underline{I = 754303 \text{ gmm}^2} \\ \approx 7.5430 \times 10^{-4} \text{kgm}^2 \tag{3.3.2.2}$$

Torque needed for the hollow strut:

$$\sum \tau_z = I\alpha_z \tag{3.3.1}$$

$$\tau = 7.5430 \times 10^{-4} \text{kgm}^2 \times 0.7 \frac{\text{rad}}{\text{s}^2} \tag{3.3.1.1}$$

$$\underline{\tau = 0.000528 \text{ Nm}} \tag{3.3.1.2}$$

We need 0,000528 Nm to accelerate the strut to 0.7 rad/s^2 in 1 second.

3.3.4.2.1.1. Simulation result with the same parameters:
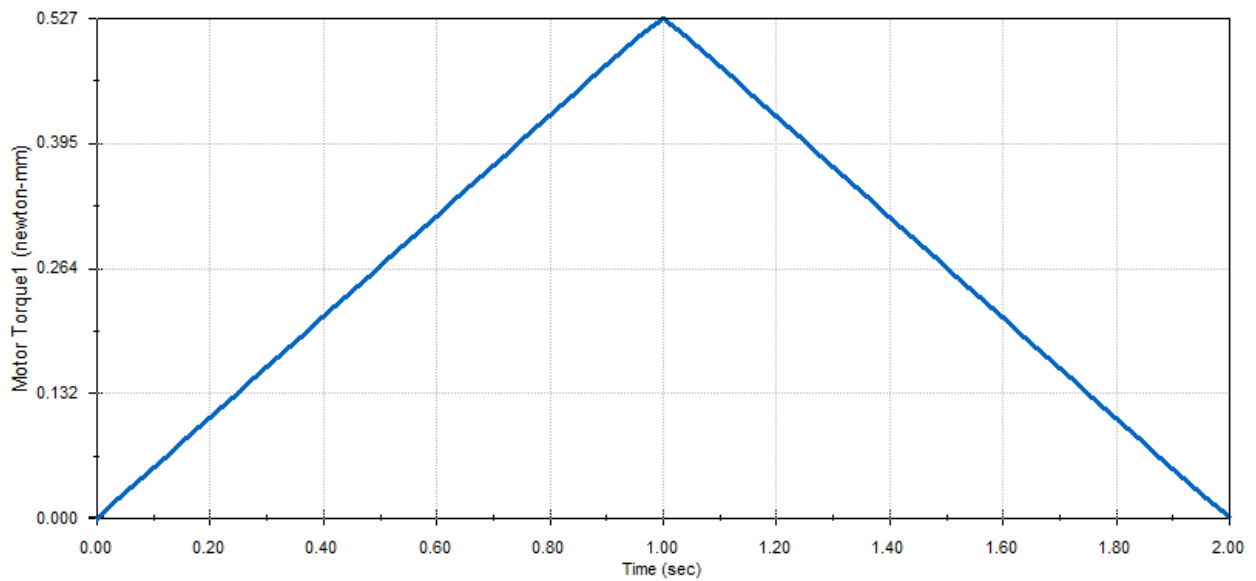
Figure 3. 3. 10: Output data from example simulation

From figure 3.3.10, 0.527 Nmm is required to accelerate the strut to $0,7 \text{ rad/s}^2$ in 1 second.

The conclusion is that we have 99,8 % accuracy when comparing the results from the hand calculations and the simulations. Following this example, the required torque for the system will be derived from simulation in SolidWorks.

3.3.4.2.2.   Gear specifications

Figure 3.3.11 shows an overview of the gear specifications chosen for the system.
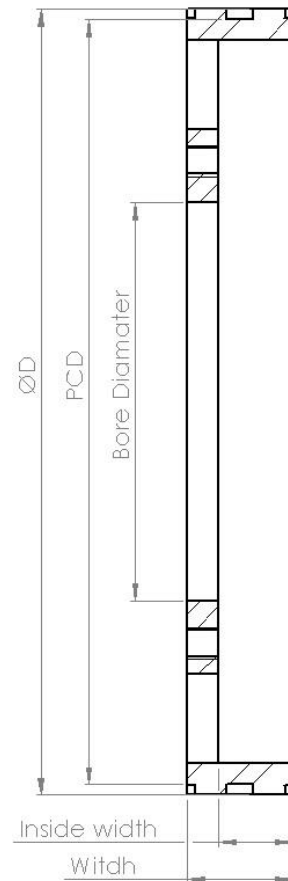
Figure 3. 3. 11: Gear

Table 3.3.10 and 3.3.11 shows the different parameters of each gear with respect to azimuth and elevation stage.

Table 3. 3. 10: Gear spesifications, azimuth

Gear azimuth			
Parameter	Unit	Pinion	Crown-wheel
Number of teeth	[-]	10	175
PCD	mm	7.35	128.63
ØD	mm	8.75	130.03
Bore diameter	mm	4	64
Width	mm	[-]	10
Inside width	mm	[-]	7
Weight	gram	4	[-]
Teeth angle	[°]	17	17

Table 3. 3. 11: Gear specifications, elevation

Gear elevation			
Parameter	Unit	Pinion	Crown-wheel
Number of teeth	[-]	10	100
PCD	mm	7.35	73.5
ØD	mm	8.75	74.9
Bore diameter	mm	4	38
Width	mm	[-]	10
Inside width	mm	[-]	7
Weight	gram	4	[-]
Teeth angle	[°]	17	17

3.3.4.2.3. APMA system: Azimuth dynamics
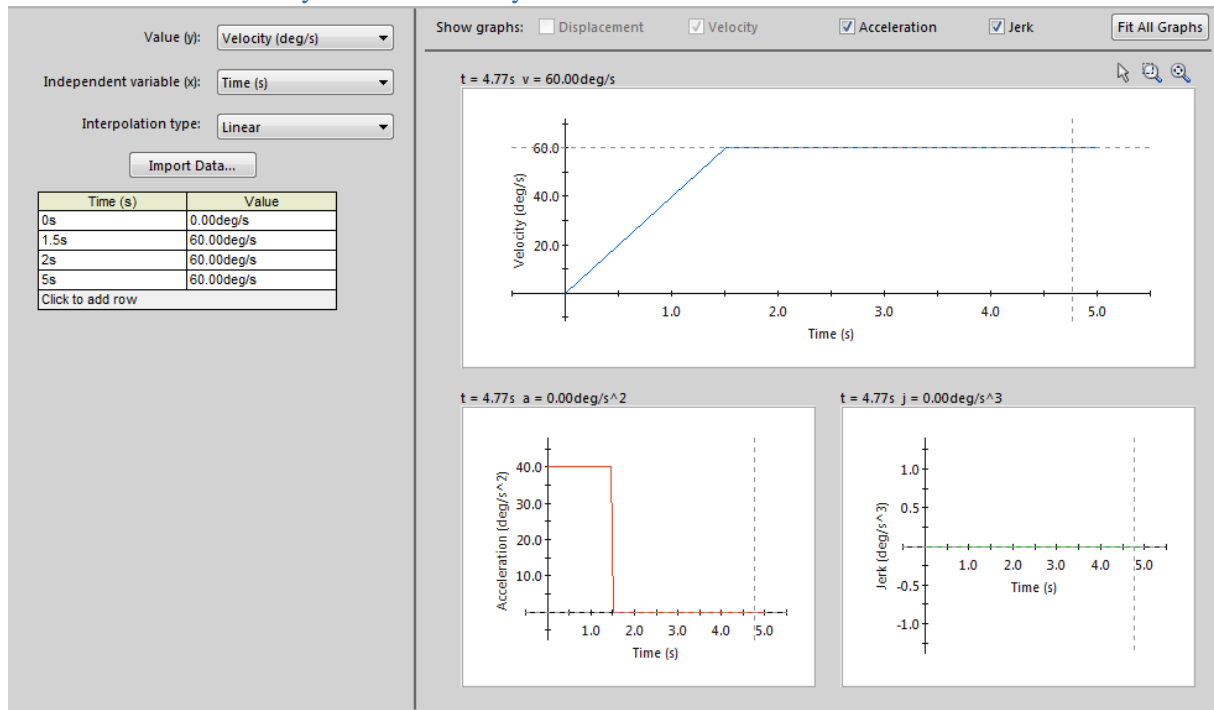
Figure 3. 3. 12: Input data for simulation

Figure 3.3.12 shows the azimuth system performance. The system has a gear ratio of 1:17.5 and shall obtain an acceleration of 40 deg/s^2 [1] and a maximum velocity of 60 deg/s[1]. A friction force estimated to 94.6 Nmm in bearing setup [12] is applied in these simulations. [5]
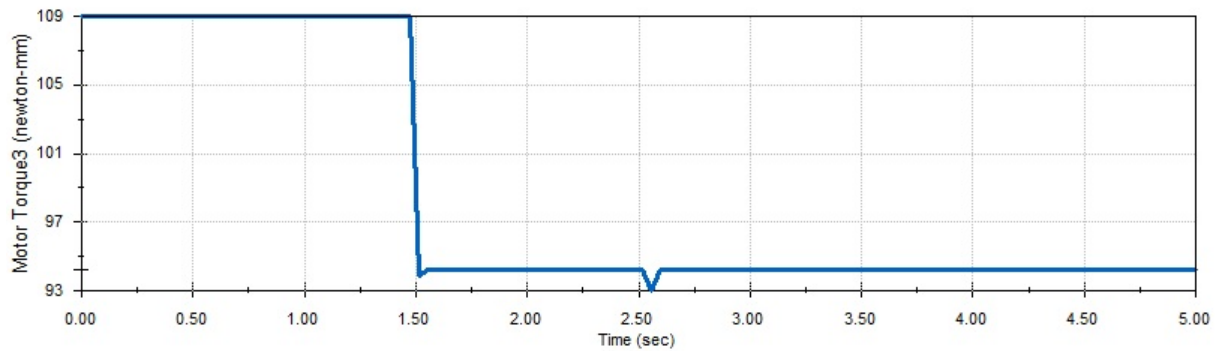
Figure 3. 3. 13: Simulation data, torque vs. time

Initially, the system starts from 0 deg/s, see figure 3.3.12. The torque needed to accelerate the system to 40 deg/s in 1 second is 109 Nmm, see figure 3.3.13. The torque needed to maintain maximum velocity is 95 Nmm. The spike shown in the graph is noise. Torque needed without friction is estimated to 13 Nmm.

To verify that the system meets the given requirements, [1] , a virtual sensor is placed on the system. The sensor measures velocity and acceleration at a specific point.
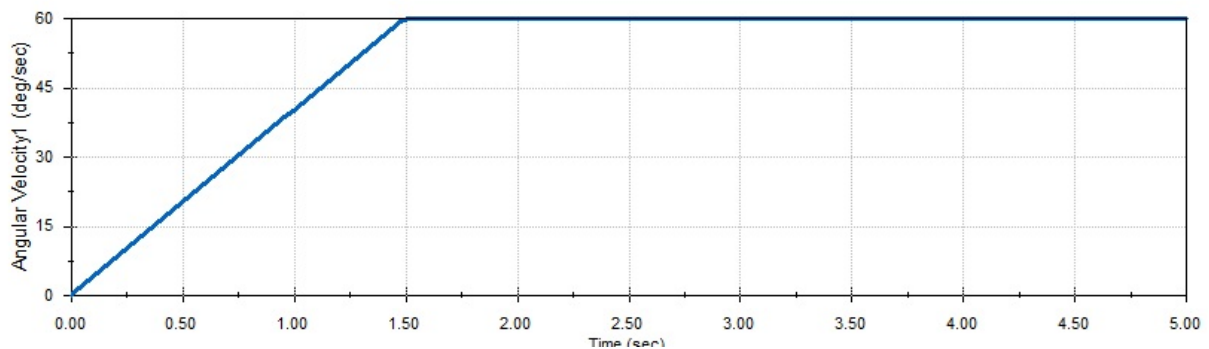
Figure 3. 3. 14: Velocity vs time

Figure 3.3.14 shows that after approximately 1 second the system has achieved 40 deg/s, and maximum velocity is achieved after approximately 2 seconds.

Dividing the torque needed to drive the system in the azimuth axis (0.109 Nm) to the gear ratio (1:17.5), the motor needs to produce a torque of 0.0623 Nm / 0,000742 Nm (without friction).

The motor also has to comply with an ECSS standard [6]:

Table 3. 3. 12: ECSS uncertainty factors

Component of resistance	Symbol	Value	Resource	Theoretical Factor	Measured Factor
Inertia	I	$\dfrac{0{,}000742 \ \text{Nm}}{0{,}97}$		1,1	1,1
Spring	S	Not relevant		1,2	1,2
Motor mag. losses	H_M	0.015 Nm	KDA	1,5	1,2
Friction	F_R	$\dfrac{0.1892 \ \text{Nm}/0{,}97}{17.5}$	In rev 1, a friction was estimated to 0.2 with respect to temperature, lubrication and preload. After calculations we did manage to get 94.6 Nmm for each bearing which gives us a total friction of 189.2 Nmm = 0.1892 Nm with the same parameters.	3	1,5
Hysteresis	H_Y	-		3	1,5
Others (Harness)	H_A	-		3	1,5
Adhesion	H_D	-		3	3

The equation for torque, 3.3.3, [6]:

$$T_{min} = 2(1{,}1I + 1{,}2S + 1{,}5H_M + 3F_R + 3H_Y + 3H_A + 3H_D) + 1{,}25T_D + T_L \qquad (3.3.3)$$

$$T_{min} = 2 \times (1{,}1 \times \frac{0{,}000742 \ \text{Nm}}{0{,}97} + 1{,}5 \times 0{,}015 + 3 \times \frac{0{,}1892 \ \text{Nm}/0{,}97}{17.5}) \qquad (3.3.3.1)$$

$$T_{min} = 0.114 \ Nm \qquad (3.3.3.2)$$

3.3.4.2.4.   APMA system: Elevation dynamics
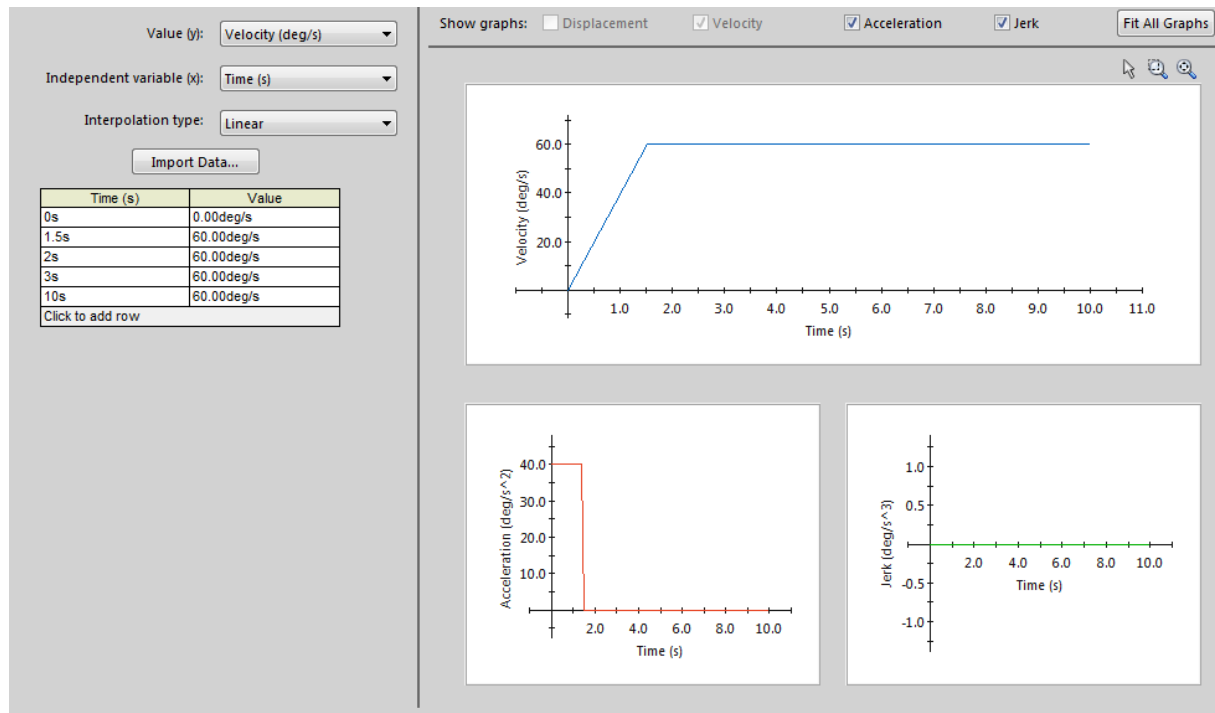
Figure 3. 3. 15: Input data for simulation

Figure 3.3.15 defines the elevation system performance. The system has a gear ratio of 1:10 and shall obtain an acceleration of 40 deg/s² [1] and a max speed of 60 deg/s [1]. A friction force estimated to 28 Nmm is applied in these simulations [5].
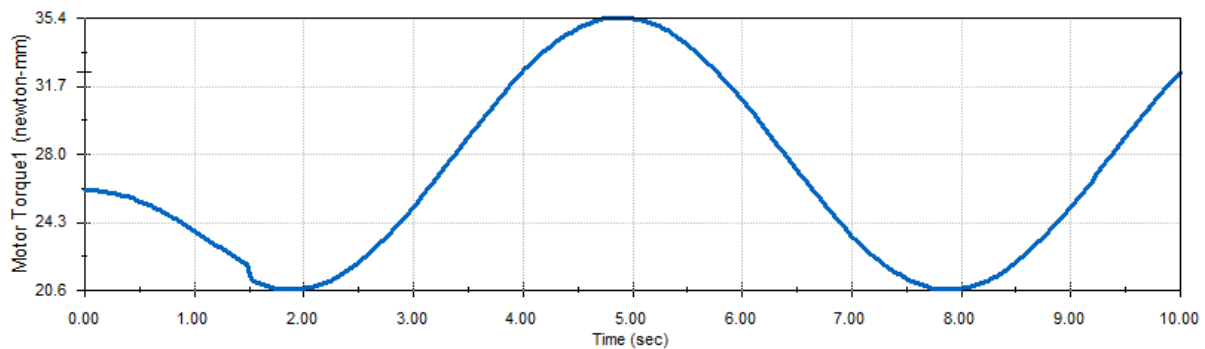
Figure 3. 3. 16: Simulation torque vs time

Initially, the system starts from 0 deg/s, see figure 3.3.17. As derived from figure 3.3.16, the torque needed to accelerate the system to 40 deg/s in 1 second, is 35,4 Nmm / 7,4 Nmm (without friction) The torque varies due to gravitation and geometry of the rotating model.

To verify that the system meets the given requirements, [1], a virtual sensor is placed on the system. The sensor measures velocity and acceleration at a specific point.
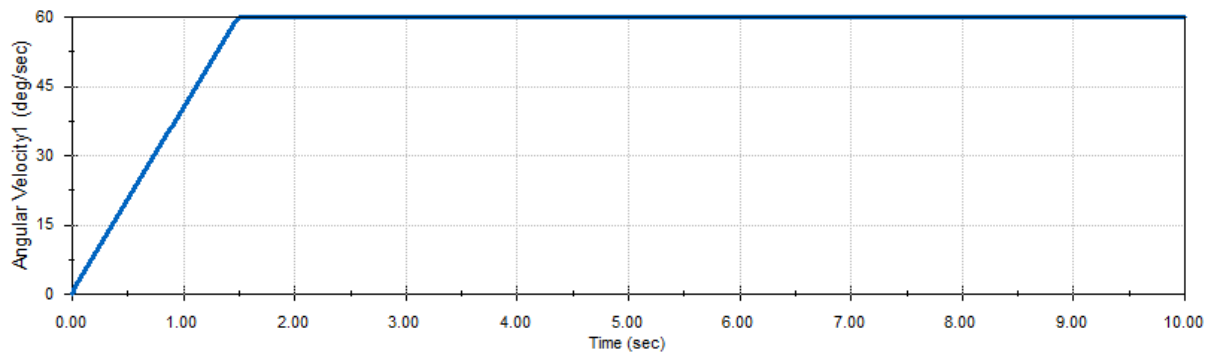
Figure 3. 3. 17: Velocity vs time

Figure 3.3.17 shows that the system has achieved 40 deg/s after 1 second. After 1.5 seconds the maximum velocity is achieved.

Dividing the torque needed to drive the system in the elevation axis (0.0354 Nm) to the gear ratio (1:10), the motor needs to produce a torque of 0.00354 Nm / 0.00074 Nm (without friction)

The motor also has to comply with an ECSS standard [6]:

Table 3. 3. 13: ECSS uncertainty factors

Component of resistance	Symbol	Value	Resource	Theoretical Factor	Measured Factor
Inertia	I	0.00074 Nm/0.97		1.1	1.1
Spring	S	Not relevant		1.2	1.2
Motor mag. losses	H_M	0.015	KDA	1.5	1.2
Friction	F_R	$\dfrac{0.1 \text{ Nm}/0.97}{10}$	KDA	3	1.5
Hysteresis	H_Y	-		3	1.5
Others (Harness)	H_A	-		3	1.5
Adhesion	H_D	-		3	3

The equation for torque, 3.3.3, [6]:

$$T_{min} = 2(1.1I + 1.2S + 1.5H_M + 3F_R + 3H_Y + 3H_A + 3H_D) + 1.25T_D + T_L \qquad (3.3.3)$$

$$T_{min} = 2 \times (1,1 \times \frac{0.00074 \text{ Nm}}{0.97} + 1.5 \times 0.015 + 3 \times \frac{0.1 \text{ Nm}/0.97}{10}) \qquad (3.3.3.1)$$

$$T_{min} = 0.108 \, Nm \qquad (3.3.3.2)$$

3.3.4.3. *Conclusion*

With a gear ratio of 1:17.5 in azimuth and 1:10 in elevation, the motor torque required for the azimuth movement is 0.0623 Nm and for the elevation movement is 0.00354 Nm.

From the simulations and calculations derived in this section, the motor torque required for the azimuth movement is 0.114 Nm and for the elevation movement is 0.108 Nm. With compliement to the given ECSS standard [6].

The friction is not estimated with calculations in elevation stage, only for azimuth. Experience from calculating the azimuth stage tell us that the torque needed for elevation should be reduced.

3.3.5. Pointing budget

This section contains a pointing budget for the APMA. The purpose of the budget is to derive the pointing accuracy of the mechanism and to verify the given requirement from KDA, [1], REQ-2.4.1:

"The system shall have a pointing error of < 0.5 deg, half cone, 3 sigma."

3.3.5.1. *Half cone error definition*

The half cone error is defined as the angle between the ideal boresight direction (the central axis of the cone) and the surface of the cone. Figure 3.3.18 illustrates this definition.
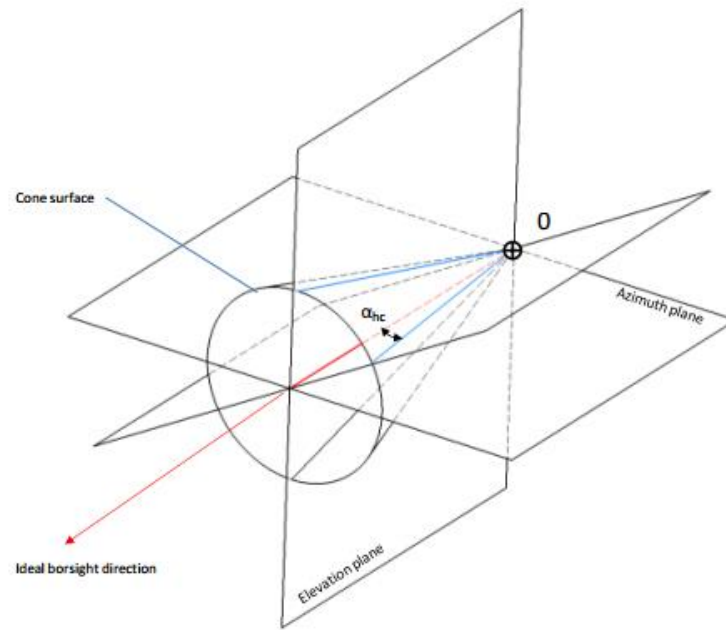
Figure 3. 3. 18: Half cone angle definition,[7]

To derive the pointing accuracy for the APMA, the pointing errors in the two rotational axes, azimuth and elevation, have to be taken into account. These errors are related to the half cone error by equation 3.3.4 and 3.3.5, [7]:

$$\cos(\alpha_{hc}) = \cos(\alpha_{hc}) \cos(\alpha_{el}) \tag{3.3.4}$$

$$\alpha_{az}(\alpha_{el}) = a\cos\left(\frac{\cos(\alpha_{hc})}{\cos(\alpha_{el})}\right) \tag{3.3.5}$$

where α_{hc} is the half-cone error, α_{el} is the elevation error and α_{az} is the azimuth error. For the given maximum half cone error at 0.5 degrees, the relationship between the azimuth and elevation angles are given in figure 3.3.19. When expecting that the pointing error in the azimuth and elevation axes equals each other, a maximum error angle of 0.35 degrees along each axis is accepted.
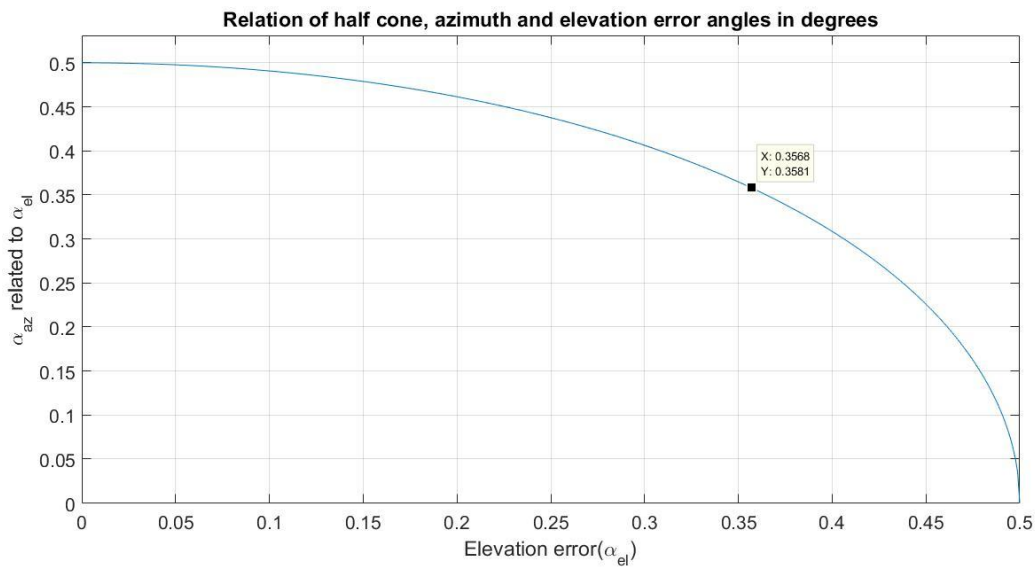
Figure 3. 3. 19: Relation of error angles.

3.3.5.2. *3-sigma definition*

The "3-sigma", specified in the pointing accuracy requirement is defined by equation 3.3.6, [8]:

$$\Pr(\mu - 3\sigma \leq x \leq \mu + 3\sigma) \approx 0.9973, \quad\quad (3.3.6)$$

where Pr is the probability, x is an observation from a normally distributed random variable, μ is the mean of the distribution and σ is the standard deviation.

For the APMA this means that a pointing error, which exceeds the limitations in equation 3.3.6, will be accepted in only 1 of 370 occasions.

Table 3.3.14 gives an overview of five different distribution methods with the correponsding uncertainty equations. To derive the half-cone 3 sigma error, the errors have to be calculated with a distribution method. The magnitude of the error (azimuth and elevation) multiplied with the normalized uncertainty factor gives the standard uncertainty. The combined standard uncertainty (u) can be calculated by the root sum of the squares of all the different uncertainties, [7]:
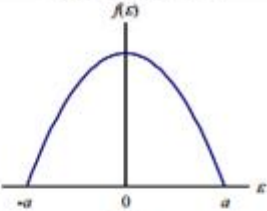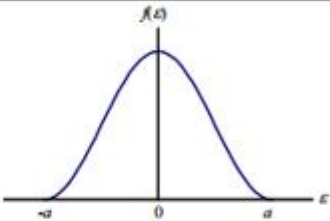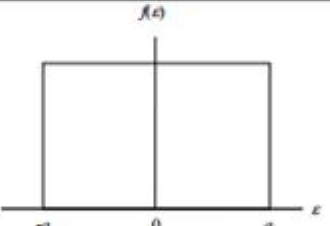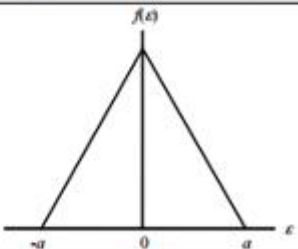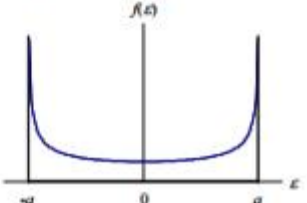
$$u = \sqrt{\sum_{i=1}^{n} u_i{}^2}, \quad\quad (3.3.7)$$

where u is the combined uncertainty, n is the number of errors and u_i is the standard uncertainty. To include the 3 sigma confidence, the combined standard uncertainty is expanded with a factor of 3 (coverage factor, k =3 for 3-sigma, 99.73% confidence). The expanded uncertainty, U, is given by equation 3.3.8, [7]:

$$U = k \cdot u \quad\quad (3.3.8)$$

where k is the coverage factor and u is the combined standard uncertainty.

Table 3. 3. 14: Distributions and uncertainty equations. [9]

Distribution	Distribution Plot	Uncertainty Equation
Quadratic		$u_\varepsilon = \dfrac{a}{\sqrt{5}}$ where $\pm a$ are the minimum bounding limits.
Cosine		$u_\varepsilon = \dfrac{a}{\sqrt{3}}\sqrt{1-\dfrac{6}{\pi^2}}$ where $\pm a$ are the minimum bounding limits.
Uniform (Rectangular)		$u_\varepsilon = \dfrac{a}{\sqrt{3}}$ where $\pm a$ are the minimum bounding limits.
Triangular		$u_\varepsilon = \dfrac{a}{\sqrt{6}}$ where $\pm a$ are the minimum bounding limits.
U-Shaped		$u_\varepsilon = \dfrac{a}{\sqrt{2}}$ where $\pm a$ are the minimum bounding limits.

From table 3.3.14, the normalization factors of the different distributions can be calculated. Table 3.3.15 shows these factors, which is used in the total pointing budget for the APMA, [7][9].

Table 3. 3. 15: Normalization factors

Distribution	Normalization factor
Normal	0.333
Quadratic	0.447
Cosine	0.362
Uniform	0.577
Triangular	0.408
U-shaped	0.707
Other	1.000

3.3.5.3. *Errors*

Many errors have to be taken into account when deriving the pointing accuracy of the APMA system. Errors are often categorized in two categories; systematic errors and random errors. The systematic errors are known within the operational environment, and due to that, they can be compensated for. Examples of systematic errors are offset errors in sensors and tuning and alignment errors. Random errors cannot be compensated for, and this includes for example errors due to backlash and dynamic motion.

3.3.5.4. *Pointing errors in the APMA system*

Errors in the APMA that affect the pointing accuracy errors are given in table 3.3.16:

Table 3. 3. 16: Errors in the APMA system

Error source	Description	Type	Comment
Errors due to electronics			
Position sensor error	Error due to encoder accuracy .	Random	Calculated
Control system errors	Error due to SVPWM accuracy. Errors due to calculations in the command for the APMA.	Random Systematic	Calculated Tested by running the software code.
Backlash	Error due to backlash.	Random	Calculated
Dynamic motion errors	Error due to deformation during acceleration and vibration	Random	Not evaluated in this budget. Vibration testing is not prioritized in this project.
Alignment errors			
Collimation error	Non orthogonality of the ideal antenna beam to the azimuth axis.	Systematic	Estimated in cooperation with KDA.
Axis skew and tilt	Non-orthogonality of the azimuth axis to the elevation axis and the azimuth axis from the true vertical (axis tilt).	Systematic	Estimated in cooperation with KDA.
Thermal errors	Error due to thermal distortion of the APMA in orbit. Errors due to reflector thermal expansion	Random Random	Estimated in cooperation with KDA. Thermal testing is not prioritized in this project.
Launch shift	Errors due to the launch phase of the SC.	Random	Not evaluated in this budget. Vibration and shock testing are not prioritized in this project.

3.3.5.4.1.   Position sensor error

The number of encoder steps gives the encoder error. The encoder in the APMA has 4096 step per revolution. The pointing error in the motor is then

$$\frac{360 \text{ degrees}}{4096} = 0.08789 \text{ degrees,}$$

which with respect to the gear ratio (1:17.5) gives a pointing error on the system of

$$\frac{0.08789 \text{ degrees}}{17{,}5} = 0.005022 \text{ degrees.}$$

3.3.5.4.2.   Control system errors

The error in the control system comes from SVPWM resolution and software calculations.
The error due to the SVPWM resolution is given by the number of steps in the motor, converted to degrees. The resolution of the SVPWM is 2000 steps per pole pair (8 pairs), which gives a pointing error on the motor of

$$\frac{360 \text{ degrees}}{8 \cdot 2000 \text{ steps}} = 0.0225 \text{ degrees.}$$

With respect to the gear ratio (1:17.5) the pointing error of the APMA is

$$\frac{0.0225 \text{ degrees}}{17.5} = 0.001286 \text{ degrees}$$

The error due to calculations varies with the velocity of the APMA, and is difficult to calculate. After tests and observations when running the code on the mechanism, this error was estimated to 0.05 degrees in both axis.

3.3.5.4.3.   Backlash error

The backlash in the gears will also cause a pointing error in the system. Due to different gear ratios in the azimuth and elevation stage, the errors do not equal each other. The backlash is calculated by the HPC approach explained in [10].

3.3.5.4.3.1.   Azimuth

The gears that will be used in the azimuth stage are SH0.7-10 (Gear1) and SH0.7-175 (Gear2). The gear spesifications are given in [11].

1) The diameters of the gears are given:
   $d_1 = 7.35$ mm
   $d_2 = 128.63$ mm

2) When the diameter and the normal modul (0.7) is known, the upper tooth thickness allowance, $A_{sne,}$ and the tooth thickness tolerance, $T_{sn,}$ can be found from the "e25 DIN 58405" table in [10]:

$A_{sne1} = 0.04$ and $T_{sn1} = 0.016$
$A_{sne2} = 0.063$ and $T_{sn2} = 0.024$

3) Calculating the lower tooth thickness allowance, $A_{sni,}$ for the gears given by equation 3.3.9, [10]:

$$A_{sni} = -A_{sne} - T_{sn},\qquad(3.3.9)$$

gives the following parameters:
$A_{sni1} = -0.056$
$A_{sni2} = -0.087$

4) The center distance tolerance for helical gears(A_s) is 0.009, ref. table "Tooth thickness tolerance" [10].

5) The change in the backlash due to center distance is calculated by equation 3.3.10, [10]:

$$\Delta j_a = 2A_s\frac{\tan(\alpha)}{\cos(\beta)} = 0.006851,\qquad(3.3.10)$$

where α is the normal pressure angle (α = 20 degrees for helical gears), β is the helix angle of the gears (β = 17 degrees, section 3.3.4.2.2, [11]) and A_s is the center distance tolerance.

6) The maximum circumferential backlash, j_t, can then be calculated by equation 3.3.11, [10]:

$$j_t = \frac{A_{sni1} + A_{sni2}}{\cos(\beta)} + \Delta j_a = 0.1564\ mm,\qquad(3.3.11)$$

where A_{sni} is the lower tooth thickness allowance, β is the helix angle of the gears and Δj_a is the change in backlash due to center distance.

7) The angular backlash is then calculated using equation 3.3.12, [10]:

$$j_\theta = \frac{360 j_t}{\pi d_2} = 0.1393\ \text{degrees},\qquad(3.3.12)$$

where j_t is the circumferential backlash and d_2 is the diameter of gear 2.

8) The angular backlash of 0.1393 degrees describes the total backlash. The pointing error of the APMA is then defined as:

$$\frac{0.1393\ \text{degrees}}{2} = \pm\ 0.06965\ \text{degrees}.\qquad(3.3.13)$$

3.3.5.4.3.2. Elevation
The gears that will be used in the elevation stage are SH0.7-10 (Gear1) and SH0.7-100 (Gear2). The gear specifications are given in section 3.3.4.2.2, [11].

1) The diameters of the gears are given by:
$d_1 = 7.35$ mm
$d_2 = 73.5$ mm

2) When the diameter and the normal module (0.7) is known, the upper tooth thickness allowance, $A_{sne,}$ and the tooth thickness tolerance, $T_{sn,}$ can be found from the "e25 DIN 58405" table in [10]:
$A_{sne1} = 0.04$ and $T_{sn1} = 0.016$
$A_{sne2} = 0.055$ and $T_{sn2} = 0.020$

3) Calculating the lower tooth thickness allowance, $A_{sni,}$ for the gears given by equation 3.3.9, [10]:

$$A_{sni} = -A_{sne} - T_{sn},$$ (3.3.9)

gives the following parameters:
$A_{sni1} = -0.056$
$A_{sni2} = -0.075$

4) The center distance tolerance for helical gears (A_s) is 0.009, ref. table "Tooth thickness tolerance" [10].

5) The change in the backlash due to center distance is calculated by equation 3.3.10, [10]:

$$\Delta j_a = 2A_s \frac{\tan(\alpha)}{\cos(\beta)} = 0.00685,$$ (3.3.10)

where α is the normal pressure angle (α = 20 degrees for helical gears), β is the helix angle of the gears (β = 17 degrees, section 3.3.4.2.2, [11]) and A_s is the center distance tolerance.

6) The maximum circumferential backlash, $j_t,$ can then be calculated by equation 3.3.11, [10]:

$$j_t = \frac{A_{sni1} + A_{sni2}}{\cos(\beta)} + \Delta j_a = 0.1438 \text{ mm},$$ (3.3.11)

where A_{sni} is the lower tooth thickness allowance, β is the helix angle of the gears and Δj_a is the change in backlash due to center distance.

7) The angular backlash is then calculated using equation 3.3.12, [10]:

$$j_\theta = \frac{360 j_t}{\pi d_2} = 0.2243 \text{ degrees},$$ (3.3.12)

where j_t is the circumferential backlash and d_2 is the diameter of gear2.

8) The angular backlash of 0.1393 degrees describes the total backlash. The pointing error of the APMA is then defined as:

$$\frac{0.2243 \text{ degrees}}{2} = \pm 0.11215 \text{ degrees}.$$ (3.3.14)

3.3.5.4.4. Alignment errors

The errors due to alignment (collimation, axis skew and tilt) are difficult to derive and calculate. These errors are therefore estimated in cooperation with KDA to 0.03 degrees in both axes.

SSM
SMALL SATELLITE MECHANISMS

3.3.5.4.5. Thermal errors

The errors due to thermal distortion and thermal expansion are also estimated in cooperation with KDA. The thermal testing of the prototype was not prioritized in this project, and the error could not be derived. The total thermal error was estimated to 0.02 degrees in both axes.

3.3.5.5. *Total pointing budget*

Table 3.3.17 gives an overview of the total pointing error in the APMA system.

Table 3. 3. 17: Pointing budget for the APMA

Error source	Error azimuth [deg]	Error elevation [deg]	Containment limits	Distribution	Normalization factor	Standard uncertianty, u_i	$u_i{}^2$
Encoder accuracy	0.0050	0.0050	0.0071	Uniform	0.577	0.00409	0.001
SVPWM accuracy	0.0013	0.0013	0.0018	Normal	0.333	0.00061	0.001
Calculations	0.0500	0.0500	0.0707	Normal	0.333	0.02355	0.001
Backlash	0.0697	0.1122	0.1320	Uniform	0.577	0.07617	0.006
Thermal errors	0.0200	0.0200	0.0283	Uniform	0.577	0.01632	0.001
Allignment errors	0.0300	0.0300	0.0424	Uniform	0.577	0.02448	0.001
				Combined standard uncertianty, u			*0.104*
				Coverage factor, k			3.000
				Expanded uncertainty, U=ku			***0.312***

3.3.5.6. *Conclusion*

The total pointing error is 0.312 degrees half cone – 3 sigma, which verifies the given requirement for the pointing accuracy. Not all errors are taken into account in this budget, but there are still approximately 0.2 degrees left. Some of the errors can also be compensated for in the design- and assembly process of the mechanism (for example the alignment errors and the calculation errors).

3.3.6. References

[1] G.H. Stenseth, M. Dybendal, "Requirement specification", Small Satellite Mechanisms, Kongsberg, SSM-2000, rev. 1.1, 26.02.2016.

[2] C. Heigerer, "KARMA 7, MSA Trade-off Report and Baseline definition (TN01.01) - Background IPR", KDA, Kongsberg, Norway, 26.09.2013.

[3] Young and Freedman, "Dynamics of rotational motion", University Physics, 13th edition, San Francisco, USA.

[4] Young and Freedman, "Rotation of rigid bodies", University Physics, 13th edition, San Francisco, USA

[5] SKF. SKF Bearing Calculator. Available: http://webtools3.skf.com/BearingCalc/selectProduct.action. [26.02.2016]

[6] Space engineering, Mechanism, ECSS-E-ST-33-01C, 03.03.2016

[7] C. Fjæreide, KARMA 7 GSTP MSDDA, KBA EQM Detail Design and Analysis(TN05.01), KDA, Kongsberg, Norway, 06.04.2015.

[8] Wikipedia, 68-95-99.7 rule, Available: https://en.wikipedia.org/wiki/68%E2%80%9395%E2%80%9399.7_rule. [27.04.2016]

[9] NASA, Measurement Uncertainty Analysis Principles and Methods,13.07.2010. Available: http://www.hq.nasa.gov/office/codeq/doctree/NHBK873919-3.pdf

[10] HPC, "Precision gears – Technical information, Spur and helical gears". Available: http://www.hpceurope.com/docFichesTechniques/PrecisionGears.pdf [26.04.2016]

[11] HPC, "Helical gears", Available: http://hpcgears.com/pdf_c33/24.8-24.11.pdf [26.04.2016]

[12] V.O. Aarud, M. Dybendal, "Bearing setup", Small Satellite Mechanisms, Kongsberg, SSM-5423, rev. 1.0, 12.05.2016

3.4. R&D cost budget

i. Abstract

This chapter shows how the cost of the SSM project is related to the R&D processes. Cost points are shown.

i. Contents

ii. List of tables

iii.   Document history

Table 3. 4. 1: Document history

Rev.	Date	Author	Approved	Description
0.1	26.04.16	VOA		Document created
0.2	10.05.16	VOA, EL		Updated Changed layout into final report layout.
1.0	16.05.16	VOA, EL	TS	Reviewed and published

3.4.1. Introduction

The purpose of this chapter is to show in details the cost of each activity through the research and development process, including the ordered parts.

3.4.2. Electrical R&D cost

Table 3.4.2 shows the cost related to the electrical segment of R&D of the SSM project. The total cost of the parts is 15 513.08 NOK and 106 800.00 NOK is the total cost of the labor. The overall total cost for the electrical R&D is 122 313.08 NOK

Table 3. 4. 2: Electrical cost

Part Number/id	Description	Development type	Cost (NOK)	Comment
469303	Motor with encoder and hall sensor	External part	10 692.00	
402687		External part		
462004		External part		
511-STEVAL-IHM039V1	Microchip	External part	4 289.44	
511-L6230PD	Motor drive	External part	417.84	
2128431	Sockets , wiring	External part	34.70	
9733175		External part	79.10	
5110	Prototype electrical	Labor	25 500.00	1hr =200 NOK
5111	Components trade-off	Labor	10 800.00	1hr =200 NOK
5112	Link analysis	Labor	4 700.00	1hr =200 NOK
5113	Motor drive	Labor	3 900.00	1hr =200 NOK
5114	Control system	Labor	61 900.00	1hr =200 NOK

		Total Cost R&D Electrical.	**122 313.08**	**NOK**

3.4.3. Mechanical R&D Cost

Table 3.4.3 shows the cost related to the mechanical segment of R&D. The total cost of the parts is 32 073.55 NOK and 103300.00 NOK is the total cost of the labor. The overall total cost for mechanical R&D is 135373.55 NOK.

Table 3. 4. 3: Mechanical cost

Part Number/id	Description	Development type	Cost (NOK)	Comment
10101	Parabola holder	3D-Printed		
10301	Mirror over azimuth	3D-Printed		
10004	Motor housing azimuth	3D-Printed		
10205	Contact mirror connector	3D-Printed	1 996.65	
10204	Connector elevation	3D-Printed		
10201	Elevation bracket	3D-Printed		
10206	Mirror elevation	3D-Printed		
10006	Bearing house azimuth	Manufactured	7 850.00	
10005	Cap azimuth	Manufactured		
10009	Connector	Manufactured		
10001	Main contact plate	Manufactured		
10103	Parabola	Manufactured		
10105	Struts	Manufactured	20 000.00	
10104	Sub reflector	Manufactured		
10002	Waveguide	Manufactured		
10102	Azimuth fish plate	Manufactured		
10007	Bearing azimuth	External part	1 279.20	
10208	Bearing elevation	External part	507.00	
10010	SKF lock nut	External part	440.70	
5120	Prototype mechanical	Labor	13 500.00	1hr =200 NOK
5121	DAK	Labor	900.00	1hr =200 NOK
5123	Mechanical Reports	Labor	4 800.00	1hr =200 NOK
5221	DAK (E:2)	Labor	500.00	1hr =200 NOK
5223	Bearing Report	Labor	33 700.00	1hr =200 NOK
5443	Design description	Labor	5 000.00	1hr =200 NOK
5321	DAK (C:1)	Labor	7 100.00	1hr =200 NOK
5901	Technical Budget, mechanical	Labor	15 000.00	1hr =200 NOK
5900	Material study	Labor	17 600.00	1hr =200 NOK
7000	Manufacture	Labor	5 200.00	1hr =200 NOK

	Total R&D Cost Mechanical.	**135 373.55**	**NOK**

3.4.4. Software R&D Cost

Table 3.4.4 shows the cost related to the software segment of R&D. The total cost of the labor is 102 400.00 NOK in labor, which gives a total cost for software R&D to 102 400.00 NOK.

Table 3. 4. 4: Software cost

Part Number/id	Description	Development type	Cost (NOK)	Comment
5130	Software design	Labor	10 400.00	1hr =200 NOK
5131	Technical document, software	Labor	18 000.00	1hr =200 NOK
5132	Control system, software	Labor	74 000.00	1hr =200 NOK

	Total R&D Cost Software.		102 400.00	NOK

3.4.5. Miscellaneous R&D cost

Table 3.4.5 shows the cost related to the miscellaneous segment of R&D. This segment includes the project planning, meetings, etc. The total cost of labor in this segment is 275 750.00 NOK in labor, which gives a total cost for miscellaneous R&D to 275 750.00 NOK.

Table 3. 4. 5: Miscellaneous cost

Part Number/id	Description	Development type	Cost (NOK)	Comment
900	Concept study	Labor	17 350.00	1hr =200 NOK
1000	General project activities	Labor	120 000.00	1hr =200 NOK
1001	Project plan	Labor	31 000.00	1hr =200 NOK
1002	Iteration reports	Labor	7 000.00	1hr =200 NOK
1003	Presentation	Labor	20 000.00	1hr =200 NOK
1100	Meetings	Labor	26 000.00	1hr =200 NOK
1200	Risk document	Labor	4 000.00	1hr =200 NOK
2000	Requirement spec	Labor	20 000.00	1hr =200 NOK
3000	Test spec	Labor	10 000.00	1hr =200 NOK
3001	Testing	Labor	1 400.00	1hr =200 NOK
3002	Test procedure	Labor	17 000.00	1hr =200 NOK
4000	Webpage	Labor	2 000.00	1hr =200 NOK

	Total R&D Cost Miscellaneous.		275 750.00	NOK

3.4.6. Conclusion

Table 3.4.6 shows the total R&D cost for the Small Satellite Mechanisms project. The total labor cost is 588 250.00 NOK, while the total cost of the parts is 47 586.63 NOK. This gives a total R&D cost of 635 836.00 NOK for the project.

Table 3. 4. 6: Total cost

Total cost	Cost (NOK)
Labor	588 250.00
Parts	47 586.63

Total R&D Cost.	635 836.63	NOK

3.4.7. References

[1] Small Satellite Mechanisms, «SSM-Timesheet,» SSM, USN, Kongsberg, 2016.

[2] Small Satellite Mechanisms, SSM-10500 Part list, Kongsberg: SSM, USN, 2016.

3.5. Components trade-off

i. Abstract

This chapter identifies electrical components for the creation of an APMA. Evaluation and performance summary is performed to select desired components to be implemented in the final design. The baseline for this analysis is the need of low-cost materials and parts for assembly of the APMA. The chapter contains analysis and selections of antenna, motor, controller, motor drive and electrical materials.

i.   Contents

ii.   List of figures

iii.   List of tables

iv. Document history

Table 3. 5. 1: Document history

Rev.	Date	Author	Approved	Description
0.1	17.02.16	SL, EL, GHS	TS	Document created
0.2	18.02.16	SL	TS	Added 6. Controller Selection Changed document structure
0.3	24.02.16	GHS		Edited References
1.0	01.03.16	GHS, SL	TS	Added references Added Motor driver selection Changed document layout Added comments to figures 6 and 7 Corrected typos Title 3.6 changed Added STEVAL evaluation board to controller selection
1.1	04.05.16	EL		Changed layout into the final report layout.
2.0	19.05.16	SL, GHS, TS	MD	Reviewed and published

3.5.1. Introduction

3.5.1.1. *System overview*

The main system consists of:

- Electrical constituents:
  - Control system
  - **Low-cost actuators(LCA)**
  - **Position Sensor**
  - Hold Down and Release mechanism(HDRM)
  - RF System(RFS)
    - **Radiating Element(Antenna)**
    - RF feed network(RFN)
- Mechanical constituents:
  - APM Structure
  - Thermal Hardware
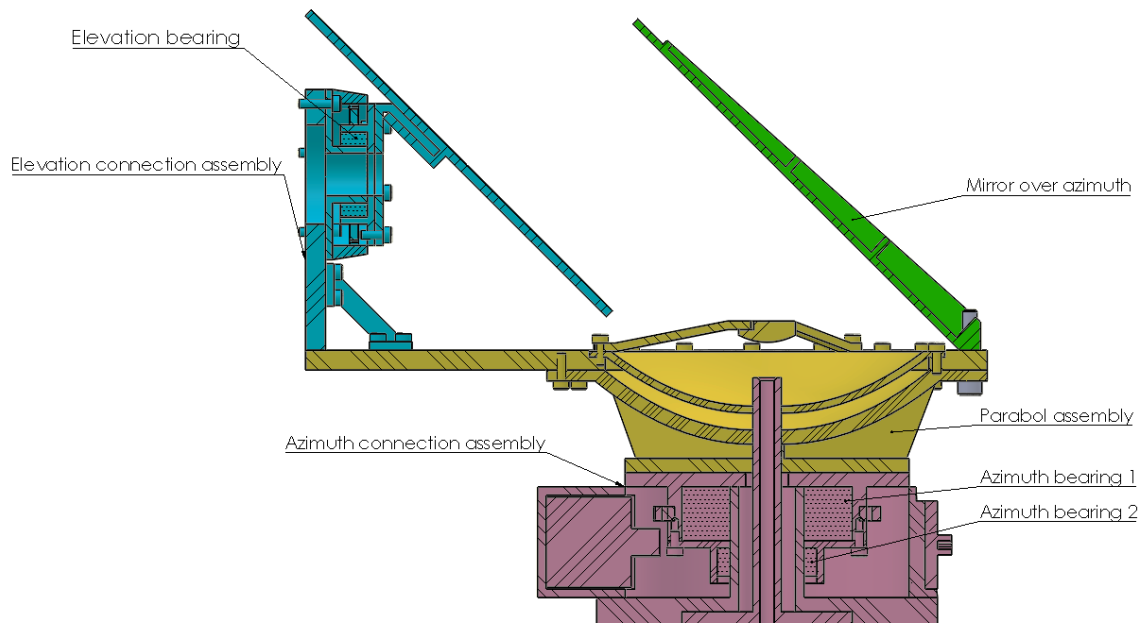
Figure 3. 5. 1: System overview

3.5.2. Controller selection

A control system is required in order to maintain the right speed and position. Motors are operated from the control system, by means of encoders and other sensors. To simplify the development process, evaluation boards will be used. These are circuit boards where all necessary components like voltage regulators, communication ports for programming etc. are present.

The evaluation boards considered for the APMA are:

- ST microelectronics STEVAL-IHM039V1 with a STM32F415ZGT6 ARM Cortex-4M processor [26].
- Arduino Due with an AT91SAM3X8E ARM Cortex-3M processor [5].
- Microchip DM330011 with a dsPIC33FJ256GP06 DSC [6].

For a final design, the boards will be redesigned to remove unnecessary parts and allow for operation in vacuum.

Table 3.5.2 shows a simple comparison of the two ARM-core based processors and the DSC these boards are built around. All the controllers have Harvard memory architecture meaning they can send two instructions to the ALU in one cycle. Only the ARM Cortex-4M based controller has the ability to perform the double mathematical operation of multiply and accumulate in one clock cycle.

Table 3. 5. 2: Comparison of controllers

Controller	AT91SAM3X8E ARM Cortex-3M	dsPIC33FJ256GP06 Digital Signal Controller	STM32F415ZGT6 ARM Cortex-4M
Flash	512 kB	256 kB	1024 kB
Max operating freq.	84 MHz	40 MIPS	168 MHz
CAN	Yes	Yes	Yes
ADC Resolution (bits)	12	12	12
ADC Speed (ksps)	1000	500	2000
DAC	2 x 12 bits	-	2 x 12 bits
SRAM	96 kB	30 kB	192kB
Temp. range deg C	-40 to +85	-40 to +85	-40 to +105
Operating voltage (Vcc)	1.62 to 3.6	1.62 to 3.6	1.8 to 3.6
Cost per unit (NOK),(farnell.com)	105	100	125

The APMA requires an encoder to function as intended. Being able to handle the incremental encoders, the system will need DIO-ports. For DI the controller is able to detect logic states and process the data, while the DO enables the possibility for the controller to send logic states.

The BLDC motors will be running on PWM signals. As a result, the controller is in need of handling them. PWM creates a simulated analog signal using square waves (switching between 5 V and 0 V). One of the main reasons for using PWM is the simple way of converting the signal into an analog result.

Sensors are often analog and for a digital system to handle the data from these, an ADC is required. An ADC converts analog signals into digital signals for the controller to process the data. For this project, analog temperature sensors measure the interface temperature of the mechanism.

Traditionally, CAN-bus was introduced to the automotive industry to eliminate the complex wiring with a two-wire bus. Introducing CAN-bus to this system makes the APMA easier for the customer to implement and use.

The ability to process data at high speed is important for this project and has been a crucial factor for choosing a controller for the system. A cluster network of satellites will communicate in LEO. Due to the high velocity, the controller needs to process the data it sends and receives rapidly.

From table 3.5.2 it is clear that STM32F415ZGT6 is the obvious choice in terms of processing power and operating temperature.

3.5.3. Motor selection

The torque, current, voltage, power, no-load and rotational velocity defines the performance of an actuator in the system. The variables are analyzed and compared in a final summary to pinpoint the favorable design in relation to the APMA system.

3.5.3.1. *Alternative 1 – Brush motor*

3.5.3.1.1. Motor definition

A brushed motor generally needs two wires to operate. The output voltage driven through the wires determines the speed of the motor. This simplifies the usage of brushed motors and allows for an easy setup and control system. This mechanism requires a controller to obtain the correct velocity and position.

The brush motor is also relatively cheap to manufacture. The simple design makes this alternative very valuable in low-cost projects.

3.5.3.1.2. Challenges

When the plane of the coil is parallel to the magnetic field, the torque equal zero. Once started, the moment ensures the motors continual rotation, but it is not possible to start the motor in this position. Another issue is short-circuit caused by the zero-torque position. However unlikely, it presents a possible risk for the system.

The brushes' continued physical contact with the coil causes stress to the structure of the motor. With enough of this strain, the brushes wear out and needs replacing. As this mechanism is going into space, such maintenance will be costly and highly unfavorable for this project.

Using a brush motor may cause arcing in certain situations. This in turn causes unwanted EMI via induction coupling. Figure 3.5.2 shows a model of the brush DC motor.
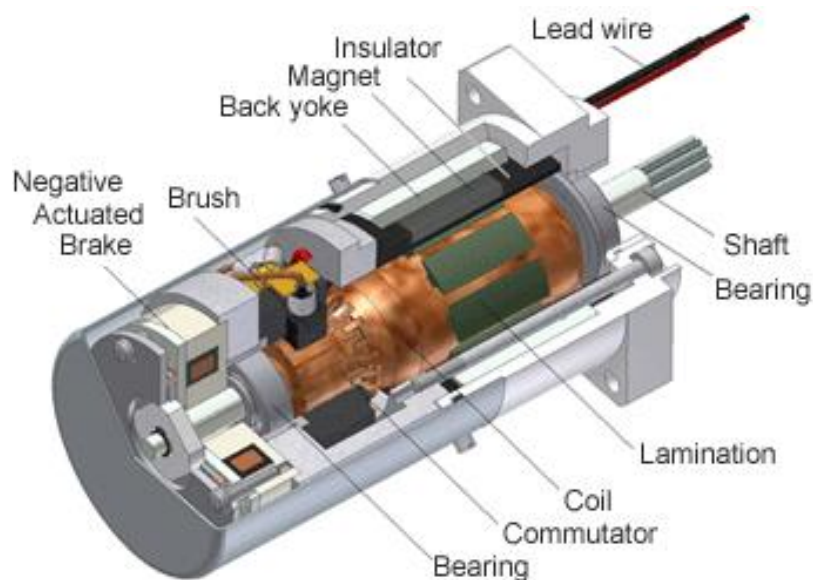
Figure 3. 5. 2: Brush DC motor [16]

3.5.3.2. *Alternative 2 – Brushless dc motor*
3.5.3.2.1.   Motor definition
Brushless dc motors are the most adaptive electric motors on the marked. They are the most cost-effective solution to high-accuracy positioning and tracking applications. Due to the motor containing no brushes, friction is reduced and higher speeds can be obtained. This is favorable in this project, due to the given speed and acceleration requirements. Depending on the amount of coils in the motor, the design ensures smooth mechanic motion.

For lightweight applications, this is the motor of choice. As well as for brush dc motors, brushless dc motors requires a control system to ensure the correct velocity and position. The angular velocity is controlled by measuring the current through the windings.

3.5.3.2.2.   Challenges
The main disadvantage with the brushless dc motor is the extra cost of a control system with complex electronics. This circuit requires the capability to control polarity switching. Figure 3.5.3 shows the principle of the brushless DC motor:
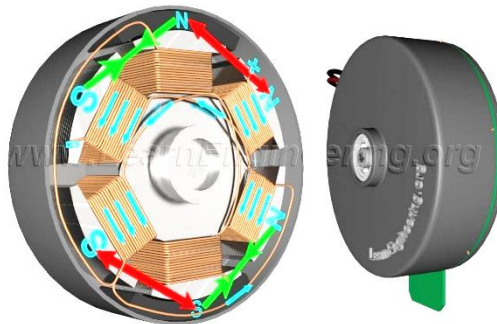
Figure 3. 5. 3: Brushless DC motor, [15]

3.5.3.3. *Alternative 3 – Stepper motor*
3.5.3.3.1.   Motor definition
A stepper motor operates in steps and is set in specific positions adjusted by the controller. Motion control is the key feature of this design, enabling the system to set a position, and then return to the exact previous location or step.

The stepper motor operates by keeping the winding currents high to hold the load at a specific step, thus increasing the power drain on the system. However, this creates a powerful holding torque, which makes the stepper motor exceptional for securing that the mechanism is in place. This feature also removes the need for a feedback mechanism in optimal conditions.

3.5.3.3.2.   Challenges
The stepper motor is designed for positioning, not for high-speed operations. This is unfavorable for this project, due to given speed- and acceleration requirements. Being designed for torque, stepper motors often have a large amount of windings, which increases the back EMF. The stepper motor requires power to remain position. Eventual mechanical failure in the design limits the accuracy of the stepper motor. Figure 3.5.4 shows a model of the principle of the stepper:
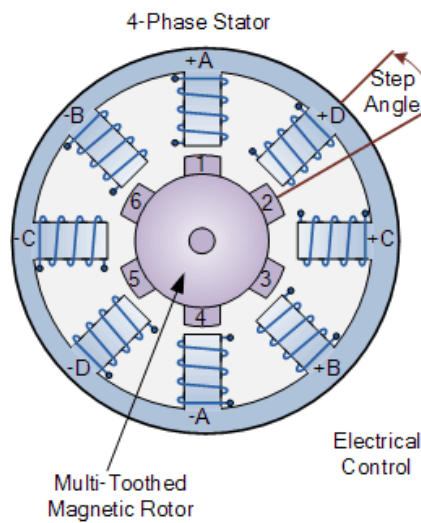
Figure 3. 5. 4: Stepper motor [11]

3.5.3.4. *Comparison of the alternatives:*

Table 3.5.3 is a comparison of the three different types of motors, based on criteria that is important for the project. The table is the baseline for the Pugh's Concept Selection Matrix in section 3.5.3.5.

Table 3. 5. 3: Comparison of the alternatives [9]

	Brushless DC Motor	**Brush DC Motor**	**Stepper Motor**
Controllability	Directly controls torque - closed loop to control position, velocity or acceleration - More controllable speed/torque than brushed.	Directly controls torque - closed loop to control position, velocity or acceleration	Directly controls position – open or closed loop to control velocity or acceleration
Power efficiency	$\approx 100\%$	$\approx 100\%$	0% at no load, $\approx 100\%$ at maximum load
Life	Limited by bearing	Mainly limited by brushes	Limited by bearings and gear assembly
Position resolution	Limited mainly by position transducer resolution	Limited mainly by position transducer resolution	Limited by motor step size
Speed capability (typically)	High speed	Moderate/high speed	Low speed, designed for positioning.
Power-off holding torque	None	None	Significant fraction of peak motor torque
Commutation technique	Position transducer or Hall effect device	Provided by brush assembly	None needed
Contamination sources	Electrical potting compounds and lubricants	Electrical potting compounds, brush debris, and lubricants	Electrical potting compounds and Lubricants

3.5.3.5. *Pugh's concept selection matrix*

Table 3.5.4 is a concept selection matrix where the different motors get a score from 1-5 at different weighted criteria. The motor with the highest total score will be the chosen one for the project.

Table 3. 5. 4: Pugh's Concept Selection Matrix

	Weight %	Brushless DC Motor	Brush DC Motor	Stepper Motor	Explanation
Controllability	15.0 %	4	4	4	The capability to control motor velocity and position
Power efficiency	25.0 %	5	3	3	Stepper needs power to hold a position, power loss due to brushes in brush DC motor.
Life	25.0 %	5	2	5	Brushes need to be replaced for brush DC motor.
Speed capability	20.0 %	5	4	3	Speed limitations for the stepper motor (high speed – low torque).
Motor controller complexity	15.0 %	3	3	5	Stepper does not need feedback control system.
Weighted sum	100.0 %	4.55	3.1	3.95	

3.5.3.6. *Conclusion*

Based on the analysis of the different types of motor above, the chosen motor for this project is a brushless direct current motor. Due to given requirements for the APMA, power efficiency, speed capability and life are highly-weighted criteria in the Pugh's Concept Selection Matrix. This makes the BLDC the most favorable motor.

The system will be designed with a BLDC-motor, but should also be suitable for a stepper, at employer's request.
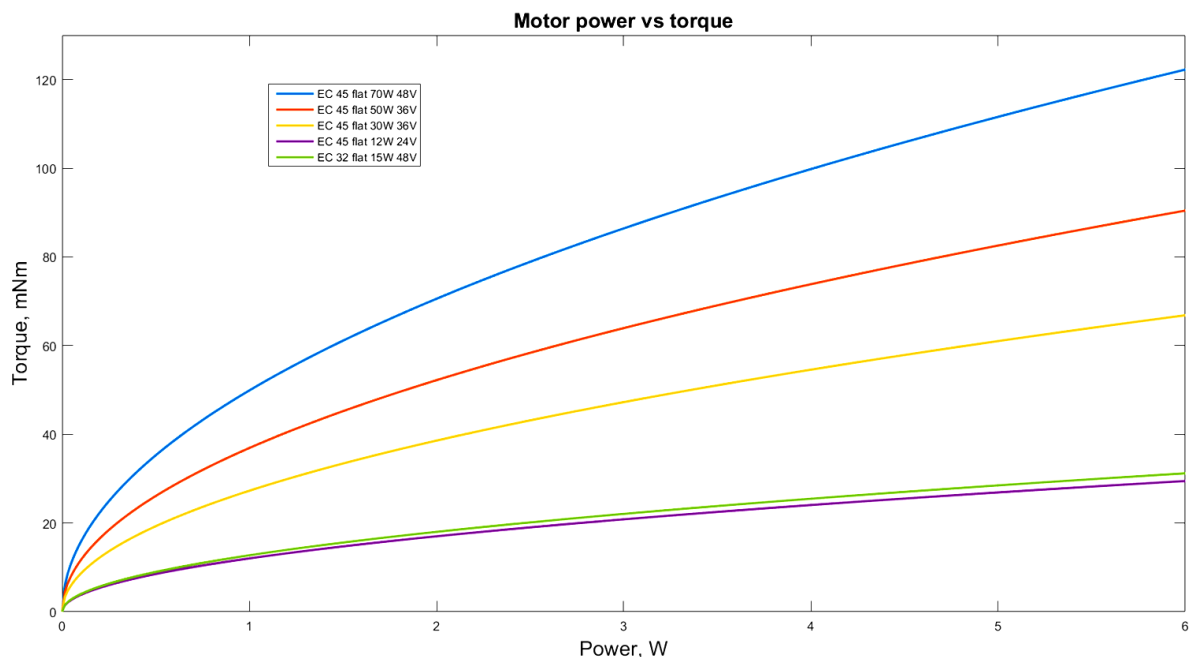
Figure 3. 5. 5: Power vs torque [17][24][25]

The specific motor chosen for the project is the EC 45 flat 70 W brushless motor from Maxon motor [17]. The reason for choosing a 70 W motor is the fact that the smaller motors are less efficient and therefore do not meet the torque requirement. Figure 3.5.5 shows the connection between power and torque from a variation of motors from Maxon motor [17][24][25]. The motor will run on a maximum power of 6 W and figure 3.5.5 is used to verify that the motor meets the projects requirement based on the torque and power budgets [18].

Figure 3.5.5 was plotted using the relation between the motor's torque constant k_t and the current I:

$$T = Ik_t$$
(3.5.1)

The current was found using the power P and the winding resistance R:

$$I = \sqrt{\frac{P}{R}}$$
(3.5.2)

3.5.3.7. *Required current for the EC45 flat 70W*
Using Eq (3.5.2) and data from [17], the required continuous motor phase to phase current is:

$$I = \sqrt{\frac{6W}{6.89\Omega}} = 0.933A$$

3.5.4. Motor driver selection
The motor driver is the final stage in the motor control system. It amplifies the PWM signal from the controller to drive the motor. For the SSM project, the driver needs to be power efficient, compliant with the thermal requirements and low cost. A few possible drivers have been evaluated.

3.5.4.1. *L293*
The L293 [19] is a low power, quadruple half-h motor driver from Texas Instruments. It has been tested by SSM, and can drive brushless motors using SVPWM. It meets the chosen motor's requirements regarding current and voltage levels, but the operating temperature of [0 to 70]°C makes it not suitable for space applications. The L293 is not made as an SMD, which means increased size and mass.

3.5.4.2. *SN75441*
The SN75441 [20] is the improved functional replacement for the L293. It has a higher operating temperature [-40 to +85] °C which makes it suitable for the SSM project's needs. However, the SN75441 is only partly compliant with the Arduino Due's 3.3V TTL levels. The SN75441 is not made as an SMD, which means increased size and mass.

3.5.4.3. *DRV8313*
The DRV8313 [21] is a triple half-h motor driver designed for three-phase brushless motors. It is compatible with the SSM project's current and voltage levels, and the operating temperature of [-40 to +125] °C makes it very desirable. The component can be bought as an SMD.

SSM

SMALL SATELLITE MECHANISMS

3.5.4.4. *L6230*

The L6230 [27] is a triple half-h motor driver designed for three-phase brushless motors. Like DRV8313, it is compatible with the SSM project's electrical characteristics. It does however have a higher operating temperature [-40 to +150] ℃.

3.5.4.5. *SSM design*

Self-design of a motor driver has been considered and an initial design layout has been created.
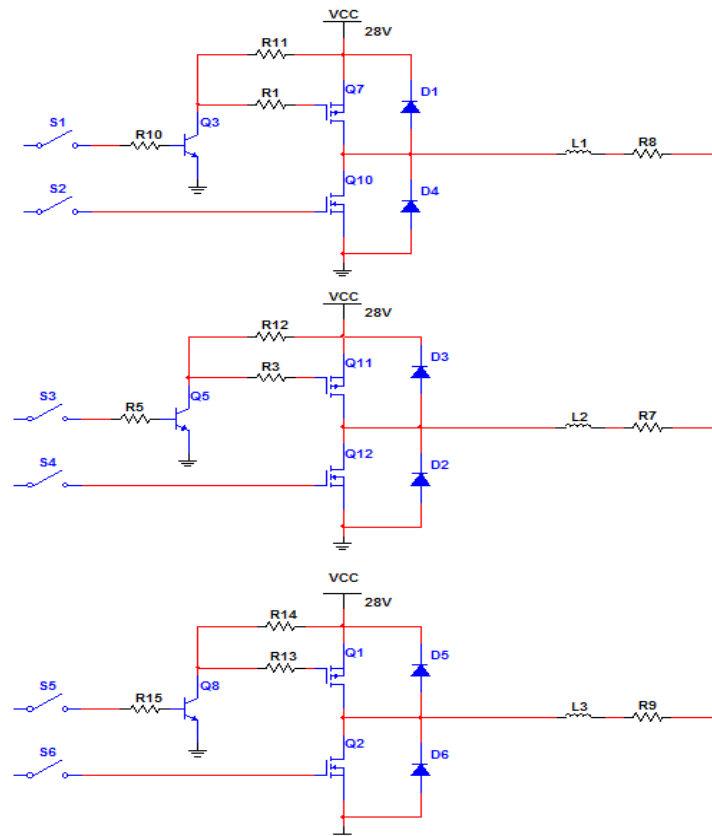
Figure 3. 5. 6: Initial motor driver design

Figure 3.5.6 shows the initial design for a motor driver inspired by [22]. The switches represent the inputs, and the coils represent the motor windings. In addition to this triple half-h, safety features would have to be implemented (circuitry preventing both half-bridge transistors being turned on at the same time, overcurrent protection, etc.). A self-design of the motor driver would allow complete control of the drive parameters, making it the best electrical solution for the SSM project. However; this would increase AIT and R&D costs to unacceptable levels as circuit boards would have to be developed and manufactured. The mass and physical size would also be larger.

3.5.4.6. *Driver comparison*

Table 3. 5. 5: Comparison of motor drivers

Criteria	Required	L293	SN75441	DRV8313	L6230	Self-design	Explanation
Operating temperature	-25 ℃ to +65 ℃ [1] REQ-1.2.1	0 ℃ to 70 ℃	-40 ℃ to 85 ℃	-40 ℃ to 125 ℃	-40 ℃ to 150 ℃	-40 ℃ to 85 ℃	Due to the thermal radiation in space, a large op. temp. span is desirable.
Output Current (continuous)	933mA	1000mA	1100mA	>1100mA	1400mA	~200mA	The maximum output current of the COTS IC's is well above what is needed for the SSM project. A self-design can be designed to meet the requirements exactly.
Output current (Peak)	933mA	2000mA	2000mA	2500mA	3550mA	~1000mA	
Supply Voltage	>28V	4.5V to 36V	4.5V to 36V	8V to 60V	8V to 52V	28V	All the drivers can operate at the voltage supplied by the SC.
Number of half bridges	3	4	4	3	3	3	Only three half-bridges are needed.
Current sensing	Desirable	No	No	Yes	Yes	Yes	Current sensing is desirable as it can be useful in the control system.
Individual control of transistors	Desirable	No	No	Yes	Yes	Yes	Individual control of transistors gives a higher flexibility in the design of the SVPWM generator and the

SSM

SMALL SATELLITE MECHANISMS

							control system
Physical Size/mass	Small size/mass is desirable [1] REQ-2.2.4	Small	Small	Very small	Very Small	Medium	The SSM project has strict mass requirements. A small size and mass is therefore desirable.
Parts cost	Low cost REQ-3.1.1	30NOK	20NOK	38NOK	75NOK	>38NOK	Cost is one of the main driving factors for the SSM project. Low cost especially in parts and AIT is desirable. Buying complete COTS drivers reduces the cost greatly.
R&D Cost	Low cost	Low	Low	Low	Low	High	
AIT costs	Low cost REQ-3.1.1	Low	Low	Low	Low	High	
Overcurrent Protection	Desirable	No	No	Yes	Yes	Yes	Overcurrent protection is desirable, as it can save the driver from being destroyed in case of short circuits etc.
Thermal protection	Desirable	No	Yes	Yes	Yes	Yes	Thermal protection is desirable, as it can save the driver from being destroyed due to overheating.
Digital input voltage levels	3.3V	5V. Partly compliant with 3.3V	5V. Partly compliant with 3.3V	3.3V or 5V	1.8V to 5V	3.3V	The STM3L DIO pins operate at 3V. A driver compatible with this voltage doesn't need

							extra conversion circuitry.

3.5.4.7. *Conclusion*

The conclusion drawn from the paragraphs above is that all the drivers except L293 are usable, but the DRV8313, L6230 and the self-designed driver are the best drivers, electrically, for the SSM project. Due to the small size and overall cost of DRV8313 and L6230 compared to the self-design, these are the best choices. Integrated circuits are also less susceptible to radiation than printed circuits as they cover a smaller area. The L6230 has the best operating temperature range of the two; therefore, the L6230 is chosen as the motor driver for the SSM project.

3.5.5. Antenna selection

Due to the nature of the SSM project, a highly directional and small antenna is required. While a parabolic antenna is the most obvious choice, recent developments in corrugated horn antennae have made these interesting [2].

3.5.5.1. *Parabolic reflector antenna*

The parabolic reflector antenna is the most common choice for highly directional applications. They produce the narrowest beam widths of any antenna type [10]. This means we can have a small antenna with high gain. The roughly calculated diameter of an antenna for the SSM project is 9-11 cm for 24-27 dBi depending on the insertion loss of the chosen concept. The depth of the parabolic dish can be adjusted, but given a diameter of 9-11 cm, should not exceed 3 cm.

The mass of a parabolic reflector antenna is dependent on the material chosen, and the total area of the antenna.

Due to the simple design of the parabola, the production costs are low, compared to other designs. Implementing a parabola into the system should be trivial.

The gain of a parabolic antenna is calculated using Eq. (3.5.3) [7] pp. 44,

$$G = 10log_{10}\left(\frac{\pi D}{\lambda}\right)^2 \eta,$$

(3.5.3)

where G is the gain of the antenna, D is the diameter, λ is the wavelength of the signal and η is the efficiency of the antenna.

The focal point of the antenna is calculated using Eq. (3.5.4) [12],

$$F = \frac{D^2}{16d},$$

(3.5.4)

where F is the distance from the origin of the parabola to the focal point, d is the depth of the parabolic dish and D is the diameter of the parabolic dish.
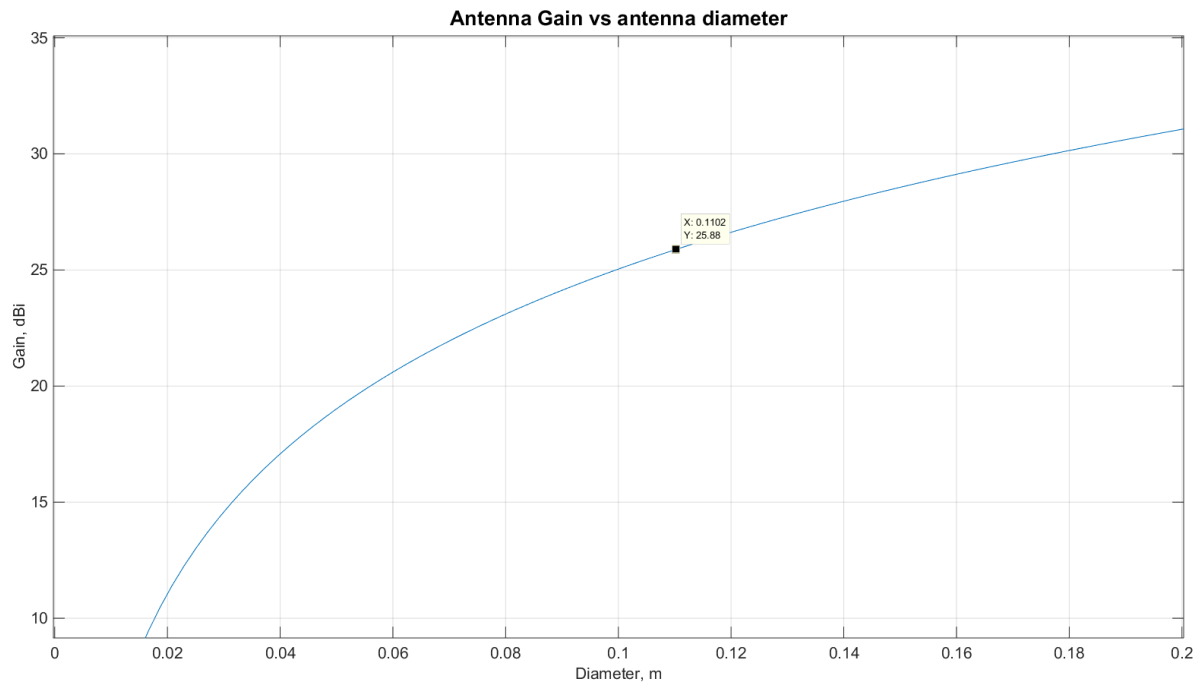
Figure 3. 5. 7: Graph showing antenna gain vs diameter. Eq. (3.5.1)

Figure 3.5.7 shows a plot of the antenna gain versus the antenna diameter using Eq. (3.5.3). A diameter of 11 cm gives an antenna gain of 25.88 dBi.
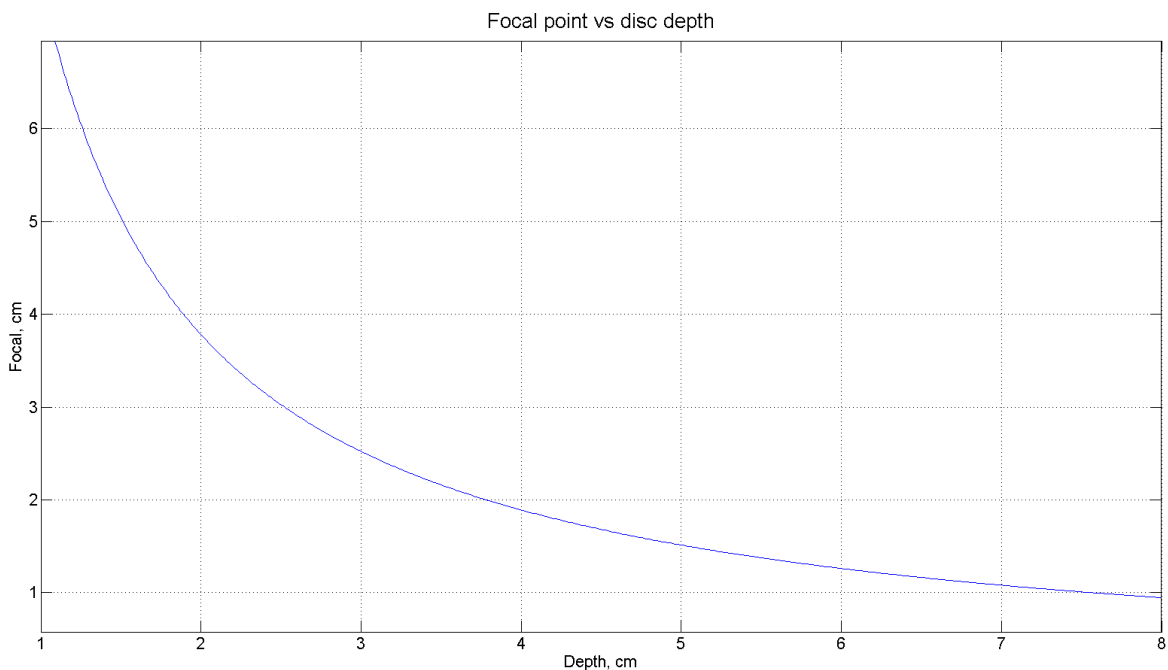
Figure 3. 5. 8: Graph showing Focal point vs dish depth. Eq. (3.5.2)

Figure 3.5.8 shows the focal point of a parabolic antenna with a diameter of 11 cm. The figure shows the tradeoff between the dish depth and the focal point distance.

3.5.5.1.1. Front feed

This is the simplest design for this type of antenna. The feed is placed directly in the focal point of the parabola dish. Placement of the feed in front of the reflector means waveguides and supports block parts of the signal. This leads to lower efficiency.
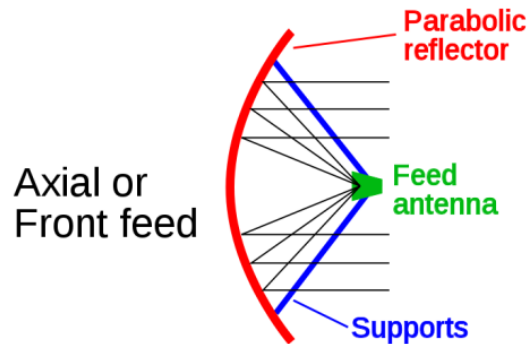
Figure 3. 5. 9: Front feed antenna [10]

3.5.5.1.2. Cassegrain
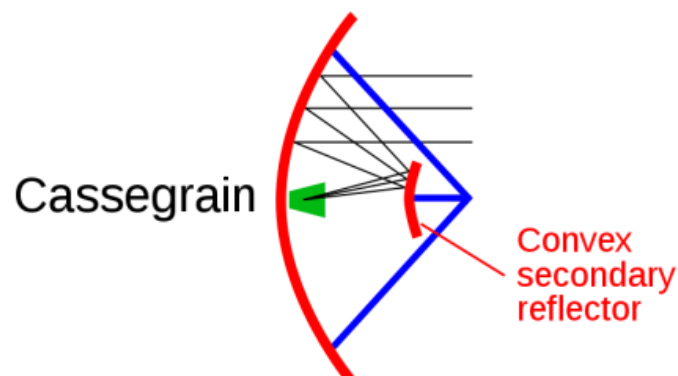
Figure 3. 5. 10: Cassegrain antenna [10]

In this design, the feed is placed in the center of the dish, and a hyperbolical sub-reflector is placed in front of the focal point [23]. The signal bounces off the hyperbolic reflector and into the feed. While this design blocks part of the signal with the sub-reflector and supports, it has a higher efficiency than the front feed antenna.

3.5.5.1.3. Gregorian

The Gregorian antenna works in the same way as the Cassegrain antenna except the sub-reflector is a parabola. Here the sub reflector is placed further from the main reflector (The focal point of the sub-reflector has to be coincident with the main reflector's focal point) [23]. This could cause design difficulties.
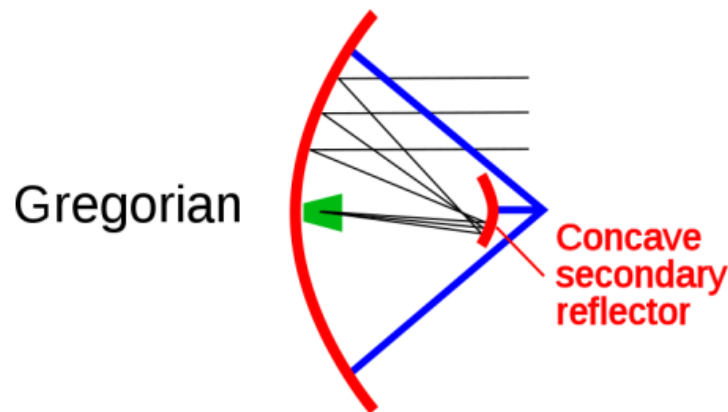
Figure 3. 5. 11: Gregorian antenna [10]

3.5.5.2. *Corrugated horn antenna*
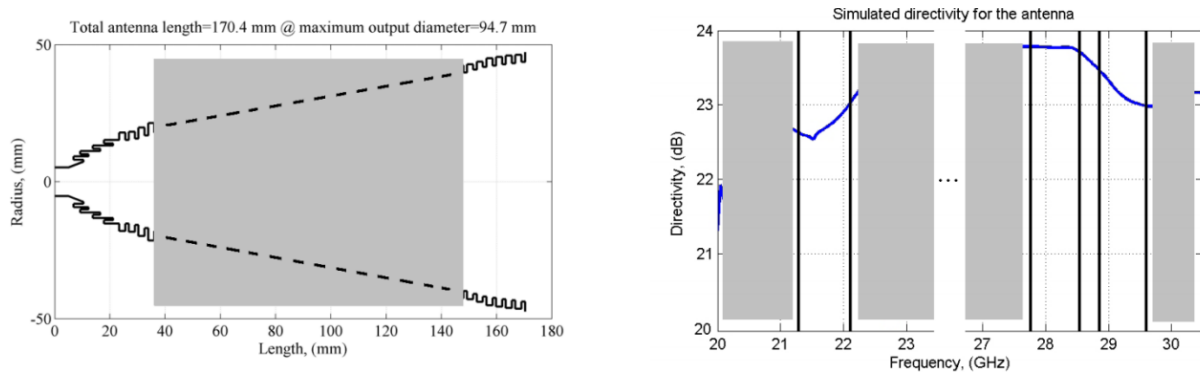
Figure 3. 5. 12: Vertically and horizontally corrugated horn antenna [2]

The size of a horn antenna can be reduced using both horizontal and vertical corrugations (Choked-Gaussian). The antenna discussed in [2] has promising directivity and a large bandwidth. The size is still too large for the mechanism. The antenna designed for Ka band frequencies has a length of ~17cm and a diameter of ~9.5cm. This is too large compared to the parabolic antenna.

The production cost is high due to the different corrugations, and the design is complex compared to the parabolic antenna.

The main advantage of this design is that it does not have a feed or sub-reflector assembly blocking the signal path.

3.5.5.3. *Conclusion*

From the discussion above, the parabolic reflector antenna is the obvious choice, due to the directionality, size and production cost. Because of the sub-reflector's distance on the Gregorian antenna and the low efficiency of the front feed antenna, the Cassegrain antenna is the selected design.

3.5.6. Materials- and component analysis

Due to the critical environment in space, materials need to be chosen carefully. In vacuum, materials behave differently and outgassing is an important factor to whether or not the material can be used. Other important factors in the process of choosing materials are moisture, temperature variations and radiation.

Electrical components need to withstand the space environment the same way as materials, but will also be more sensitive to vibration and shock during launch. Electrical parts require a high insulation resistance and voltage endurance for circuit insulation.

Due to the low cost aspect of this project, many of the electrical materials and components made for use in space are too expensive. After discussing this with employer, the decision has been made to avoid these materials and components.

Instead of doing a detailed electrical material- and components selection, components and materials not compatible for space use will be avoided.

3.5.6.1. *Not recommended materials and components:*

Materials and components that shall be avoided in this project are listed below [4]. The list will be the baseline for further decisions and choices due to electrical materials and components.

- Pure tin
- Hollow core resistors
- Non-metallurgical bonded diodes
- Semiconductor dice with unglassivated active area
- Tantalum capacitors
- Wire link fuses < 5 A
- TO5 relays without double welding of the mechanism to the header or with any type of integrated diodes inside
- Avoid components with gas and liquid

If possible and not too expensive, ceramic components are preferred. Chosen components will satisfy the given temperature requirement [1], automotive-standard components will be selected if possible.

3.5.7. References

[1] G. H. Stenseth and M. Dybendal, "Requirement Specification", SSM-2000, rev.1.1, 08.02.16.

[2] J. Teniente and C. del-Rio, "Astra 3B Horn Antenna Design", Grupo de Antenas, Universidad Pública de Navarra, Campus Arrosadía s/n, 31006 Spain, Available: http://antenas.unavarra.es/Publicaciones/Images/Pub347.pdf.

[3] Spacecraft Mechanical loads analysis handbook, ECSS-E-HB-32-26A, 19.02.13.

[4] Space product assurance, ECSS-Q-ST-60C, 21.10.13.

[5] Atmel, "SMART ARM-based MCU", SAM3X / SAM3A Series datasheet, 23.03.15.

[6] Microchip, "High-Performance 16-bit Digital Signal Controllers", dsPIC33FJXXXGPX06/X08/X10 Datasheet, 02.04.09.

[7] G. Maral and M. Bousqet, *Satellite Communications Systems*. New York: Wiley, 1987.

[8] M. Jouaneh. *Fundamentals of Mechatronics*, *SI ed.* Stamford: CT, 2013.

[9] P. L. Conley, *Space Vehicle Mechanisms, Elements of Successful Design*. New York: Wiley, 1998.

[10] Wikipedia. 24.11.15. Parabolic antenna. Available: https://en.wikipedia.org/wiki/Parabolic_antenna.

[11] ElectronicsTutorials. "DC Motors". Available: http://www.electronics-tutorials.ws/io/io_7.html [23.02.16].

[12] Down East Microwave Inc, Calculating a Parabolic Dish's Focal Point. Available: http://01895fa.netsolhost.com/PDF/dishfp.PDF [23.02.16].

[13] R.E. Wainerdi Ph.D et al. Analytical Chemistry in Space, Vol 35. Oxford, Great Britain: PP, 1970.

[14] C. Heigerer, "KARMA 7, MSA Trade-off Report and Baseline definition", KDA, Kongsberg, Norway, 26.09.16.

[15] Learn Engineering, 13.10.14, "Brushless DC Motor, How it works?" Available: http://www.learnengineering.org/2014/10/Brushless-DC-motor.html.

[16] Minebea, "DC Brush motor for Aircraft-use". Available: http://www.eminebea.com/en/engineering_info/rotary/brushmotor/brushmotor_aircraft/cat/001.shtml [23.02.16]

[17] Maxon motor. April 2015. "EC 45 flat 24 - 48 V". Available:

http://www.maxonmotor.com/medias/sys_master/root/8816806920222/15-263-EN.pdf

[18] Elise Løken et al. "Technical budgets". SSM-5901, rev 0.1. 18.02.16

[19]   Texas Instruments. "L293x Quadruple Half-H Drivers" Datasheet. January 2016

[20]   Texas Instruments. "SN754410 Quadruple Half-H Driver" Datasheet. January 2015

[21]   Texas instruments. "DRV8313 2.5A Triple 1/2-H bridge Driver" Datasheet. November 2015

[22]   Talking Electronics. 02.01.12. "The H-Bridge". Available:
       http://www.talkingelectronics.com/projects/H-Bridge/H-Bridge-1.html

[23]   TelescopeOptics. 14.07.06. "All-Reflecting Two-Mirror Telescopes". Available:
       http://www.telescope-optics.net/two-mirror.htm

[24]   Maxon motor. April 2015. "EC 32 flat". Available:

       http://www.maxonmotor.com/medias/sys_master/root/8816806592542/15-258-EN.pdf

[25]   Maxon motor. April 2015. "EC 45 flat 9 – 24 V". Available:

       http://www.maxonmotor.com/medias/sys_master/root/8816806723614/15-260-EN.pdf

[26]   ST Microelectronics. "STM32F415xx and STM32F417xx" Datasheet. October 2015

[27]   ST Microelectronics. "L6230 DMOS driver for three-phase brushless DC motor" Datasheet.
       June 2011

3.6. Electrical design

i.   Abstract

This chapter is a documentation of the different circuits of the APMA, including current measurement and connections for testing.

ii. Contents

iii. List of figures

iv. List of tables

v. Document history

Table 3. 6. 1: Document history

Rev.	Date	Author	Approved	Description
0.1	25.04.16	GHS, SL		Document created
1.0	16.05.16	GHS, SL	TS	Contents continually added since last rev. Reviewed and published

3.6.1. Introduction

Different electrical components are needed to control the APM. In this report, the different interface circuits and circuit diagrams for these are designed. In addition, the chapter contains a complete overview of the system. Due to time limitations, the system design had to be made in two different phases; one breadboard model used in testing, and one model to be used in the final design.

3.6.1.1. *Encoder output*

The encoder from Maxon motor [1] has a line driver which outputs two 90º phase shifted channels (A and B). In addition to these two channels, the driver outputs the 180° phase shifted signal of each channel.
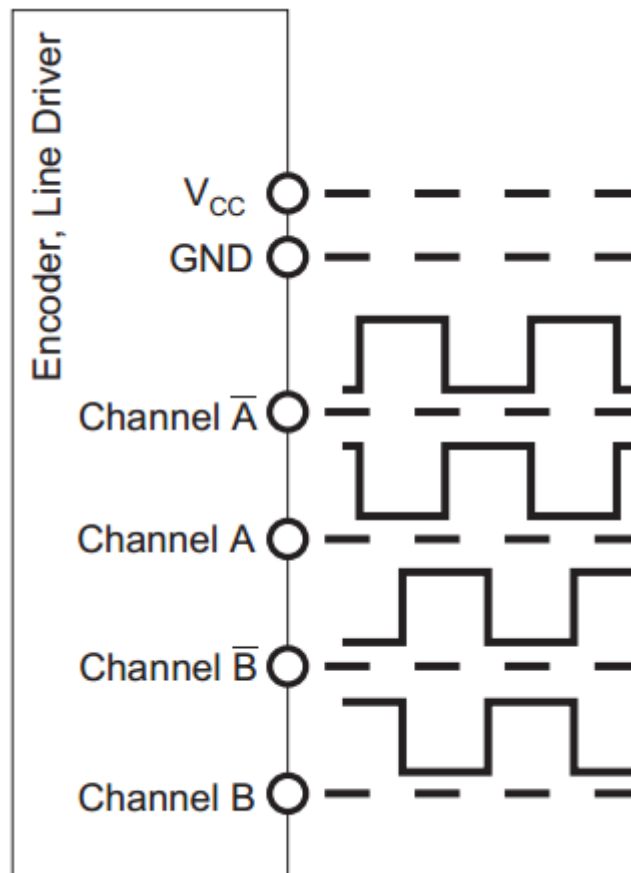
Figure 3. 6. 1: Encoder output [1]

This 180° phase shifted signal is added to account for potential errors in the transmission line between the encoder and the receiver. A line receiver that uses both the original and the 180° phase shifted signal is preferred. A possible circuit that utilizes this is discussed in 3.6.5.2.

The supply voltage and output voltage of the line driver is 5 V. This poses a problem, as the microcontroller's input pins only tolerate up to 3.6 V. The reduction of this voltage for the breadboard model is discussed in 3.6.5.1.

3.6.1.2. *Current measurement*

The control system described in [2] needs current feedback from all three motor windings as this is used in a regulation feedback loop. The easiest way of measuring the current in a winding is to set a low-ohm resistor in series with the winding and measure the voltage drop over the resistor. Another possible solution is to use a linear hall sensor.

From the Simulink model in [2], the peak phase currents are found to be ~0.94 A. The current measuring circuits should be made to measure currents above this peak current to account for possible inaccuracies and noise peaks in the winding. The current sensing circuits are discussed more closely in 0.

3.6.1.2.1.   Linear hall-effect sensor

The output voltage of a hall-effect sensor changes proportionally with the magnetic field surrounding it. In this case, the magnetic field is created by the current in the wire leading to the motor windings. Generally, these sensors are used to measure large currents where a resistor in series with the windings would be physically large.

3.6.1.2.2.   Series sensing resistor

Placing a resistor in series with the load changes the linearity of the system. The resistor's resistance therefore has to be as small as possible. The signal from small resistance needs higher amplification before being sent to the ADC. This introduces more noise in the signal. This noise will have to be filtered digitally in the microprocessor causing lower sampling rates.

Due to the availability of low-ohm resistors, this is the chosen solution for the breadboard model. For the final system, the current will be measured using hall sensors.

3.6.1.3. *Breadboard model system overview*

Due to time limitations, solutions including readily available components had to be made in order to get the system ready for testing. Figure 3.6.2 shows an overview of this system.
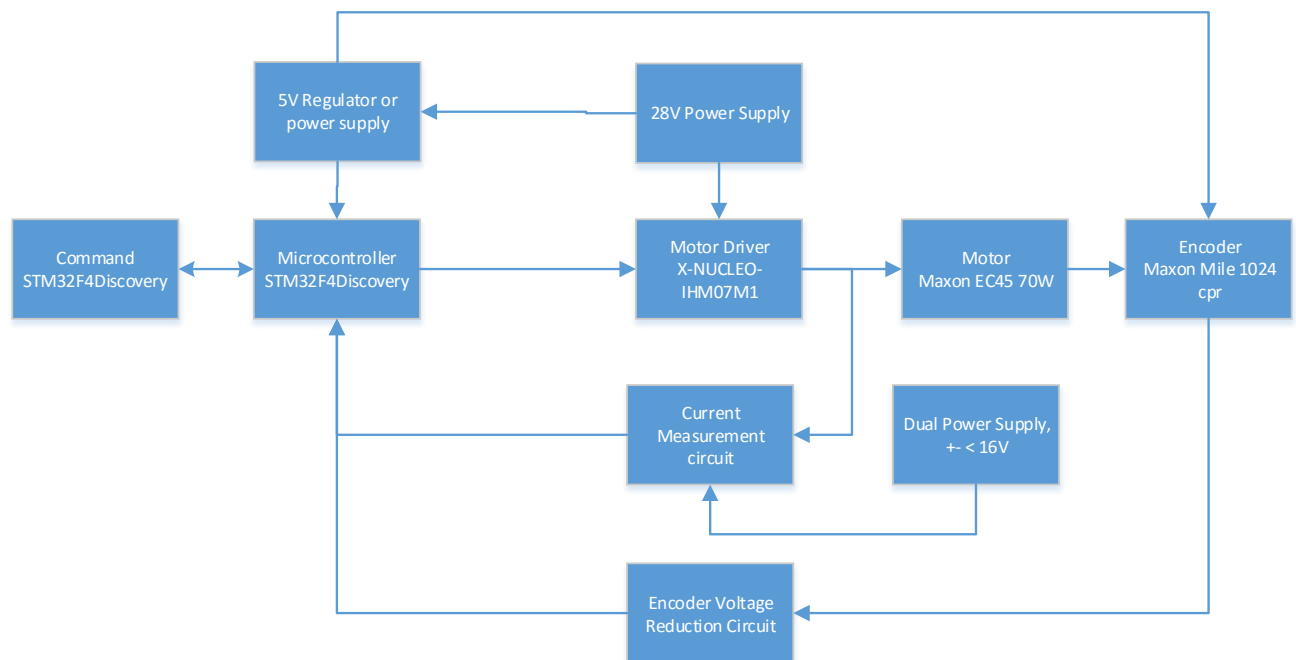
Figure 3. 6. 2: Breadboard overview of one axis

Main components such as the microcontroller, motor driver, motor and encoder are included in this design. The main differences lie in the different measurement circuits and voltage regulators.

3.6.1.4. *Final system overview*
Figure 3.6.3 shows an overview of the final design. All the important parts of the system are described throughout this document.
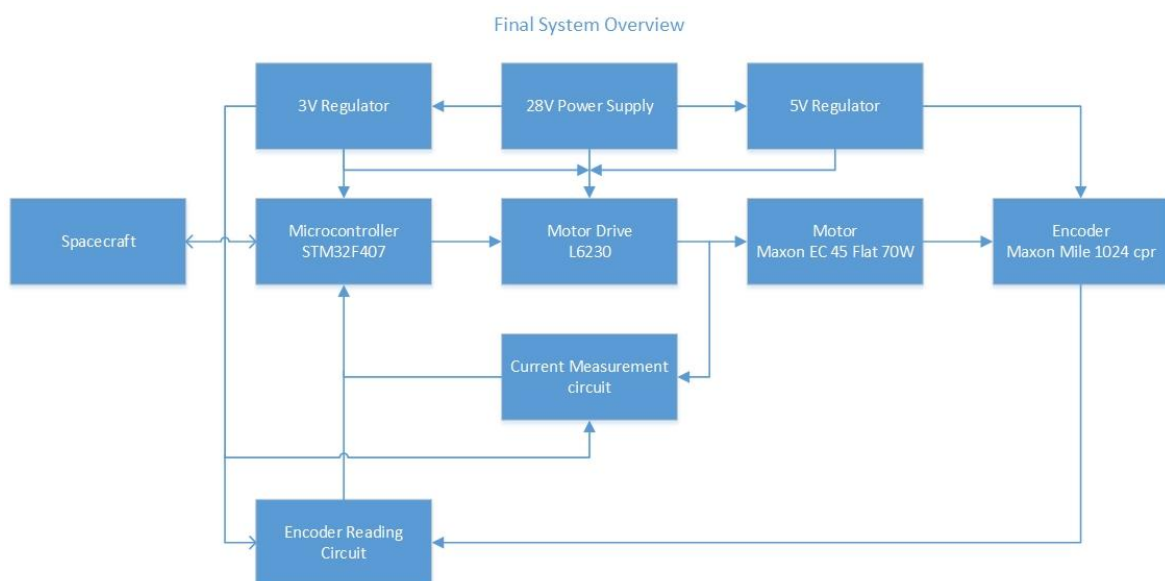
Figure 3. 6. 3: Final system overview

3.6.2. System schematic

3.6.2.1. *Breadboard model*

Figure 3.6.4 shows a simple overview of the preliminary system schematic. The MCU represents the STM32F407 discovery board that includes the chosen microcontroller, and the motor drive represents the X-NUCLEO-IHM07M1 board which includes the L6230 motor drive. The microcontroller and the motor drive are included in the final design.
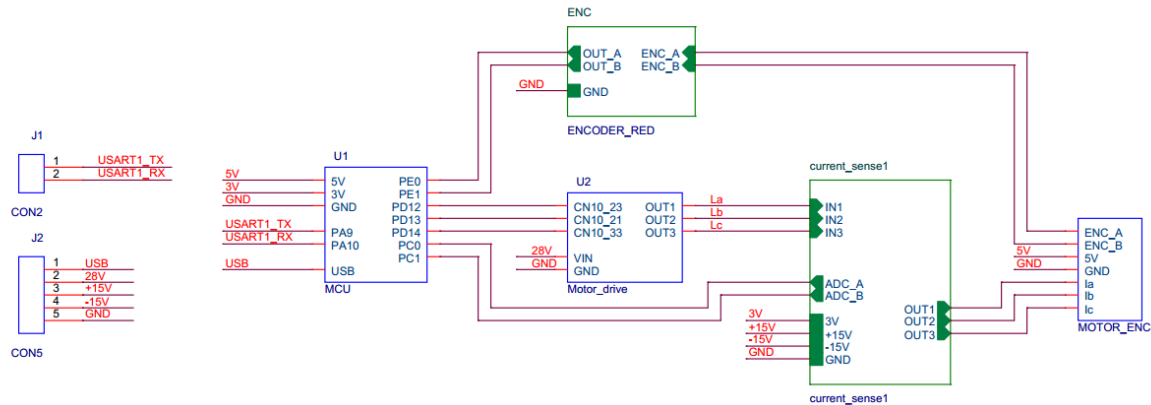
Figure 3. 6. 4: Breadboard model schematic

3.6.3. Voltage regulation circuits

The spacecraft will only provide ± 28 V. Voltage regulation circuits are therefore needed. These circuits will ensure correct power distribution to all the system components and keep the output voltage stable. Figure 3.6.5 shows the final schematic design.
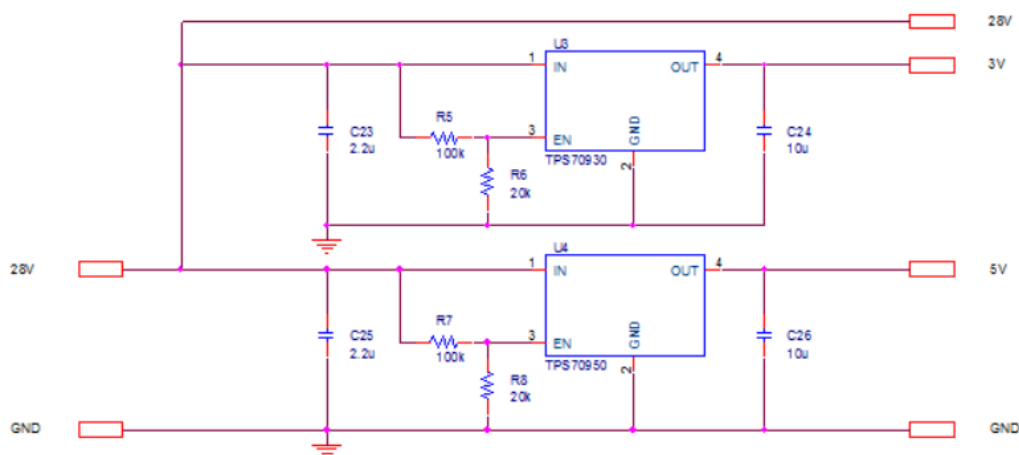
Figure 3. 6. 5: PDU schematic

3.6.3.1. *3 V Regulator*

The 3 V regulator is of the type TPS70930 from TI [3] and will provide the system with 3 V. The regulator handles an input voltage of up to 30 V, which will result in an output of 3 V. The enable pin requires a voltage of less than 6.5 V and a voltage divider is therefore used to provide the correct voltage. This regulator will supply the MCU and the motor drive, but will also supply the current measurement circuit and the encoder reading circuit.

3.6.3.2. *5 V Regulator*

Similar to the 3 V regulator, the 5 V regulator will provide power to specific system components. The regulator is a TPS70950 from TI [3] and is in the same family as the 3V regulator. Because of this, the approach of creating a stable regulator is exactly the same as for the 3 V regulator.

3.6.4. Motor driver circuit

3.6.4.1. *Motor driver*

The motor driver chosen for this project is the L6230 from STMicroelectronics and the schematic is based on the datasheet [4]. The L6230 consists of six power MOSFETs, which will transform the SVPWM signal into a three-phase output signal for the BLDC motor.

The upper transistors in the bridge require a gate drive voltage above the power supply range. Thus, a charge pump is designed. The VCP pin produces a square wave at 600 kHz with a 10 V amplitude, which will increase the input voltage of the VBOOT pin. Component values are chosen as recommended in the L6230 datasheet [4].

Figure 3. 6. 6: Motor Drive L6230PD

3.6.4.2. *Motor current measurement circuits*

3.6.4.2.1.   Breadboard model 1

In order to measure the current in the motor windings, a low ohm resistor is placed in series with the motor coils. The current in the winding is proportional to the voltage over the resistor. In order to measure this voltage, an analog-to-digital converter (ADC) is used. This ADC measures values between 0 V and 3 V, while the voltage over the resistor is

$$V_{Rs} = \pm Ix \cdot Rsense. \tag{3.6.1}$$

Rsense (R_5) in this case is less than 1 Ω (preferably ~1 mΩ. For the breadboard model, a 0.47 Ω resistor was used) and Ix less than 1.5A. In addition to the voltage being too small to get an accurate measurement, it is also biased around 0V.

To amplify the voltage, a differential amplifier is used. The voltage is amplified to be in the area of ± 1.5 V. This voltage is then fed into a new differential amplifier circuit, which raises the bias voltage to 1.5V. This way, the signal is varying between 0 V and 3 V.
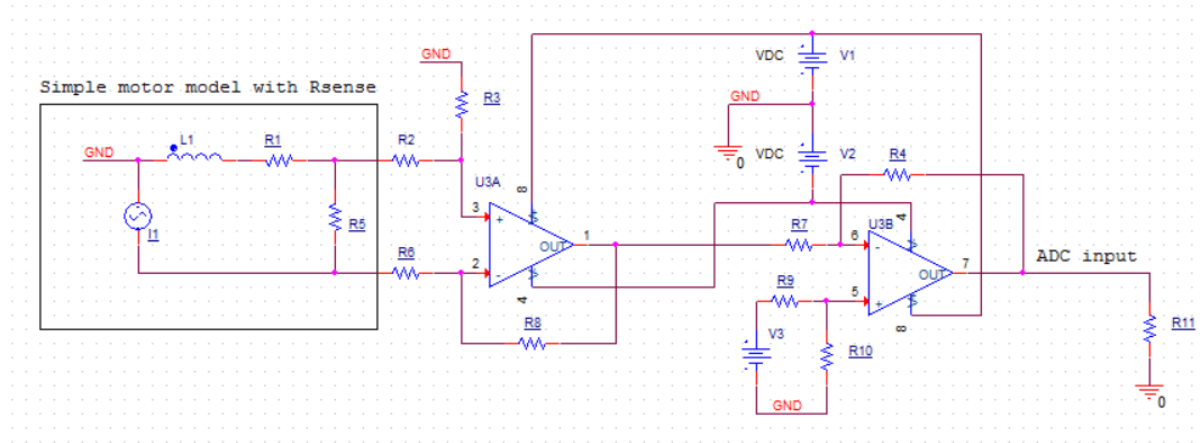
Figure 3. 6. 7: Current measurement circuit for one phase

Figure 3.6.7 shows breadboard model 1 of the current measurement circuit.

The output voltage of the first op-amp can be calculated, [5]:

$$V_{out} = -V_{in1}\left(\frac{R_8}{R_6}\right) + V_{in2}\left(\frac{R_3}{R_2 + R_3}\right)\left(\frac{R_6 + R_8}{R_6}\right), \tag{3.6.2}$$

where V_1 is the voltage from the left side of R_6 to ground, and V_2 is the voltage from the left side of R_2 and ground. This can be simplified, [5]:

$$V_{out} = \left(\frac{R_8}{R_6}\right)(V_{in2} - V_{in1}) \tag{3.6.3}$$

if $R_2 = R_6 \cap R_3 = R_8$.

To calculate the output bias of the last op-amp, the left side of R_7 is connected to ground. By doing this, and comparing the two inputs of the op-amp, the voltage at the negative input can be calculated

$$V_{-in} = V_3\left(\frac{R_{10}}{R_9 + R_{10}}\right). \tag{3.6.4}$$

If R_7 and R_4 are equal, the output bias voltage is

$$V_{out} = 2 \cdot V_{-in}. \tag{3.6.5}$$

This model was used to confirm that the control loop implemented in the microcontroller was functional. The design was updated in breadboard model 2.

3.6.4.2.2. Breadboard model 2

Breadboard model 1 was shown to have some issues concerning the high common mode voltage at the input pins of the first op-amp. This common mode voltage exceeded the supply voltage, causing the op-amp to saturate. To fix this problem, a solution using instrumentation amplifiers was proposed. Instrumentation amplifiers allow the user to reduce the input voltage by means of a simple voltage divider.

Due to the low availability of instrumentation amplifiers, these had to be made using standard op-amps.
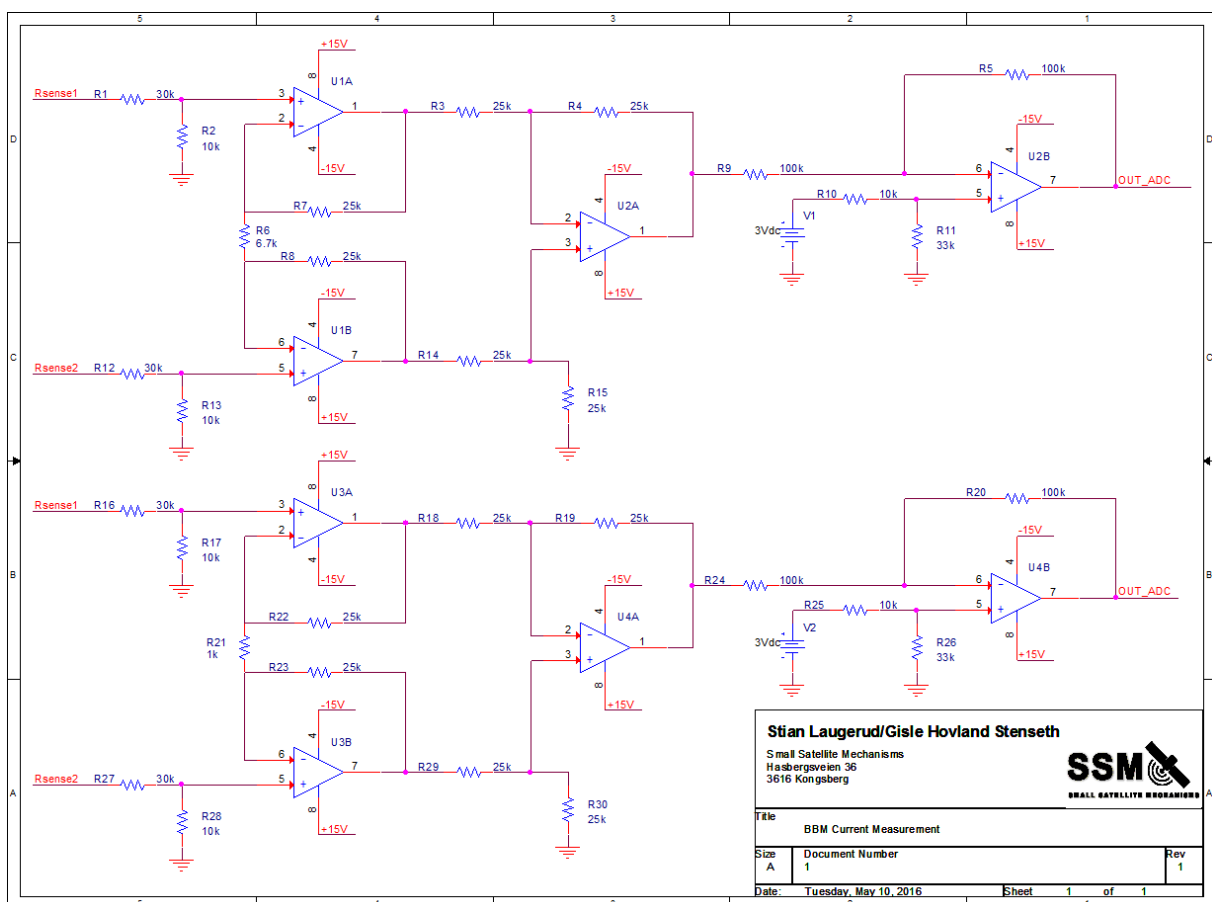
Figure 3. 6. 8: Current measurement circuit for two phases, breadboard model 2

Figure 3.6.8 shows the new breadboard model, which accepts higher common mode voltages. The input voltage is reduced to $\frac{1}{4}$th of the original voltage by means of voltage dividers (R1/R2, R12/R13, R16/R17, R27/R28). This means the gain has to be four times higher in order for the circuit to deliver

an output voltage of 0 V to 3 V. A higher gain gives a higher noise level in the signal, but in this case, due to the high resistance of the resistors used for testing (0.47 Ω), this is acceptable.

The circuit in figure 3.6.8 measures two phases. U1A, U1B and U2A are part of the first instrumentation amplifier. The resistors "inside" the instrumentation amplifier (R3, R4, R7, R8, R14, R15) are all set to R= 25 kΩ. Making these resistors equal, means the gain can be calculated easily [6]:

$$G = 1 + \frac{2R}{R5}.$$

(3.6.6)

The gain needed for the current measurement can be calculated:

$$G = \frac{1.5\ V}{\frac{V_{Rs}}{4}} \approx 8.51,$$

(3.6.7)

where $V_{Rs} = 0.705\ V$ using (3.6.1).

The output bias is set the same way as in breadboard model 1. Using a rail-to-rail op-amp for the output circuit to be able to limit the output voltage to 0 V - 3 V would be preferable, but these were not available.

3.6.4.2.3. Final

For the final design, a concept using linear hall sensors is chosen. This simplifies the overall design of the current sensing circuit since this creates a galvanic isolation between the sensing circuit and the motor drive circuit. The galvanic isolation allows a smaller supply voltage for the op-amps in the circuit, which simplifies the design greatly.

The chosen hall sensor is AH49F from Diodes [7] and its simple design makes it useful for this project. The hall sensor only needs a supply voltage of 5 V to operate and the sensor should be placed over the circuit that should be measured.

A rail-to-rail instrumentation amplifier called INA326 from TI is used to amplify the output signal from the hall sensor. The hall sensor's output signal is biased at 2.5 V and varies with the magnetic field of the wire at 2.1 mV/G. The magnetic field around the wire can be calculated

$$B = \frac{\mu_0 I}{2\pi r} \cdot 10^4,$$

(3.6.8)

where B is the magnetic field in Gauss, $\mu_0 = 4\pi 10^{-7} T \cdot m/A$ is the permeability of free space, r is the distance from the wire to the sensor in meters and I is the current flowing through the wire in amperes [8].

Using (3.6.8) with a current of 1.5 A, and a distance of 1 mm, the magnetic field is calculated to 3 G. This gives an output voltage peak at 6.3 mV.

The gain needed in the amplifier circuit is then

$$G = \frac{1.5\ V}{6.3\ mV} = 238.1.$$

(3.6.7a)

The final design uses an instrumentation amplifier from TI called INA326 [9]. Based on the current measurement circuit for phase A in figure 3.6.9, the gain can be calculated by taking

$$G = \frac{2(R14||R15)}{R12} = 237.5,$$

(3.6.9)

which will give an acceptable output voltage peak of 1.496 V. One also has to remember that the additional 1.5 V input on the reference input, will bias the output around 1.5 V which will result in an output voltage peak equal to 2.996 V.
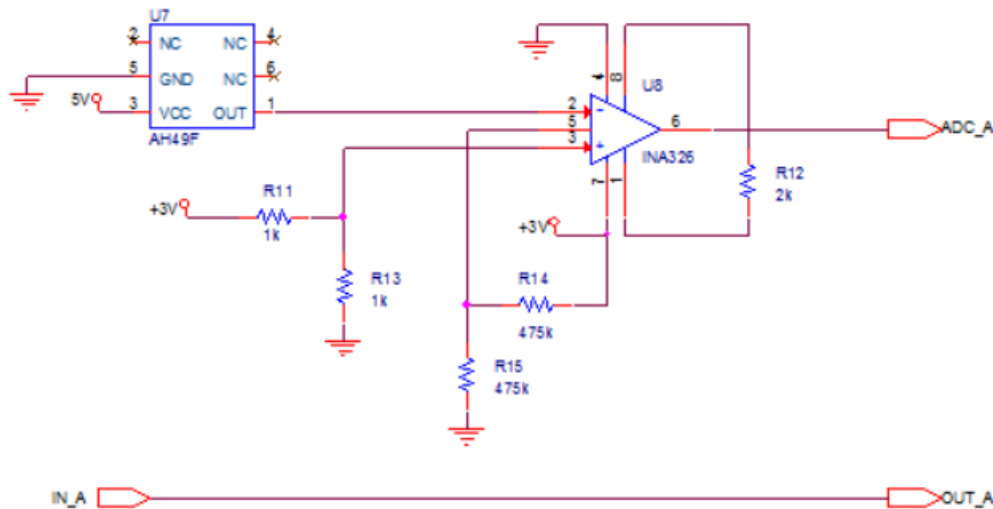
Figure 3. 6. 9: Final current measurement scheme

3.6.5. Encoder line receiver

3.6.5.1. *Breadboard model*

To simplify the test design, two diodes in series for encoder output A and B were implemented in the circuit to reduce the voltage from 5 V to 3.6 V as mentioned in section 3.6.1.1. Figure 3.6.10 shows the circuit used for testing, where ENC_A and ENC_B are the signals from the encoder at 5 V. OUT_A and OUT_B are the signals at 3.6 V connected to the MCU.
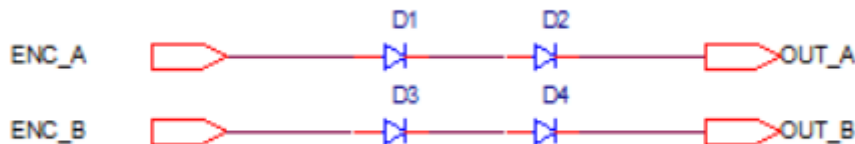
Figure 3. 6. 10: Encoder preliminary circuit

3.6.5.2. *Final*

The encoder sends two signals A and B and two related 180° phase shifted signals. Since the output of the line driver is 5 V and the microcontroller's I/O pins only handles 3.6 V, a line receiver with

voltage capping at 3 V is designed. Figure 3.6.11 shows a possible solution to this issue and will be used in the final design. This way of connecting an op-amp is called double-ended differential mode and uses two opposite-polarity signals as inputs [10]. The output is only high if the two input signals are 180 ° phase shifted, ensuring correct functionality even with long transmission lines.
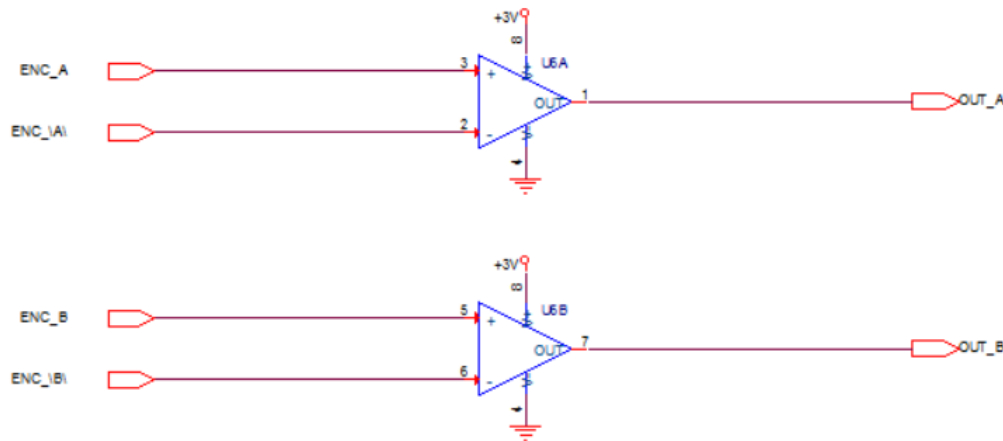
Figure 3. 6. 11: Encoder line receiver

3.6.6. Microcontroller

The MCU circuit in figure 3.6.12 is designed based on the recommendations from the datasheet of the STM32F407 [11] and capacitors and resistors are placed as specified.

The microcontroller has a 16 MHz internal RC oscillator, which is the default clock of the MCU. An external clock source of 8 MHz is added to the circuit (Y1). This clock source is more accurate than the internal oscillator, and is used to clock the processor. The system will automatically switch back to the internal clock if the external oscillator fails. The external clock is connected to a PLL, which makes it possible to multiply the frequency up to 168 MHz.

The VDD pins power the I/O pins and the internal regulator and should be within 1.8 V to 3.6 V. VDDA must be connected to VDD and VSSA to VSS (GND) in order to power the ADC, DAC, Reset blocks, RCs and PPL. The DAC uses VREF as voltage reference and is slightly lower than VDDA.

VBAT powers the RTC and backup registers when VDD is not present.

The NRST is internally connected to a pull-up resistor, which makes the MCU command an internal reset if connected to ground. This is normally done by implementing a push button into the design, but for the final design, this reset function is not preferred. If desired by the customer, this pin can be used as a reset line by the spacecraft.
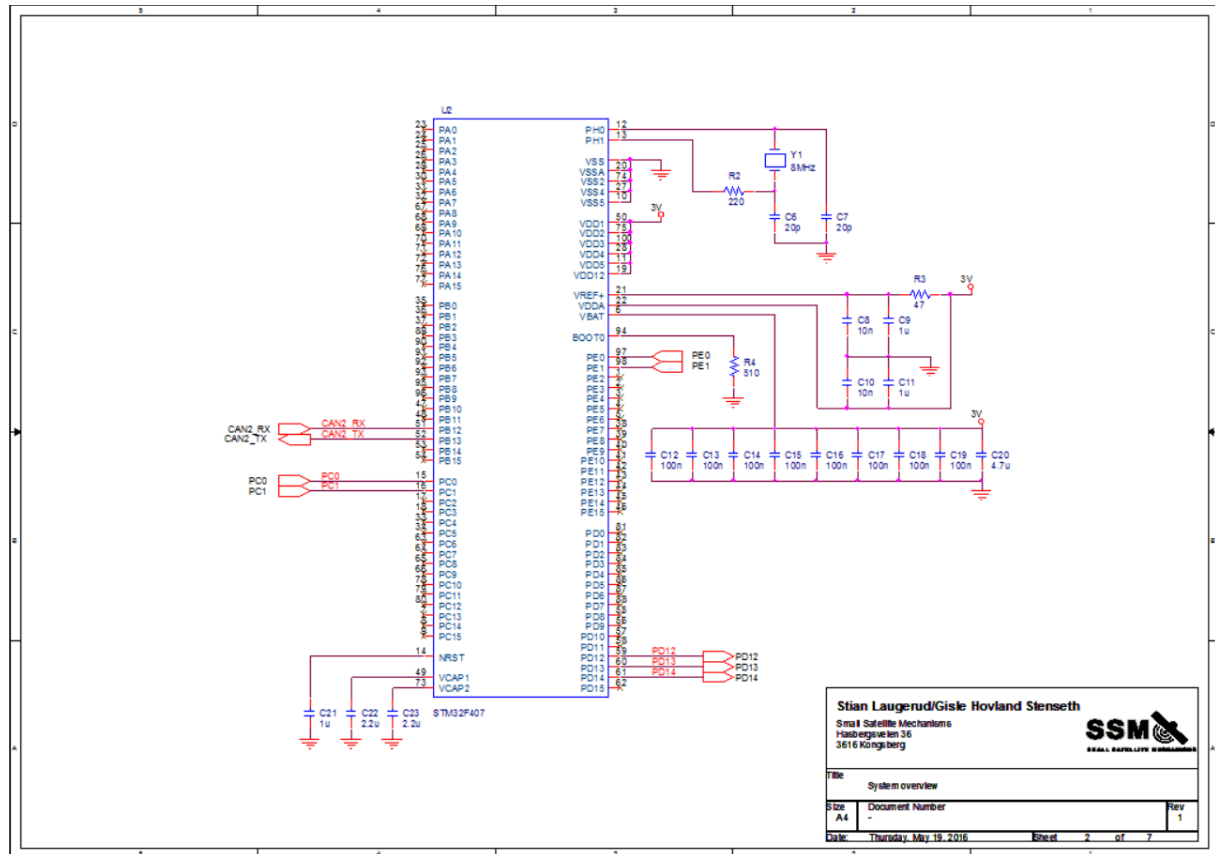
Figure 3. 6. 12: Microcontroller STM32F407

3.6.7. Branchline coupler

To be able to test the RF system, circular polarization is necessary. Instead of buying an expensive polarizer, the idea was to produce a branchline coupler to be able to verify the requirements connected to the RF system. Due to lack of design equipment and time limitations, the coupler was never implemented. On the other hand, the microstrip- and PCB characteristics were in place and are explained in the following sections.

A branchline coupler is a quadrature hybrid coupler with one input. The result of the coupler is two outputs which are 90º phase shifted of each other. For lower frequencies, these designs are easily designed and fabricated, but for higher frequencies, details are extremely important. As figure 3.6.13 shows [12], the branchline coupler is designed to be symmetrical. This means that one could choose any port to be the input, [13] [12].
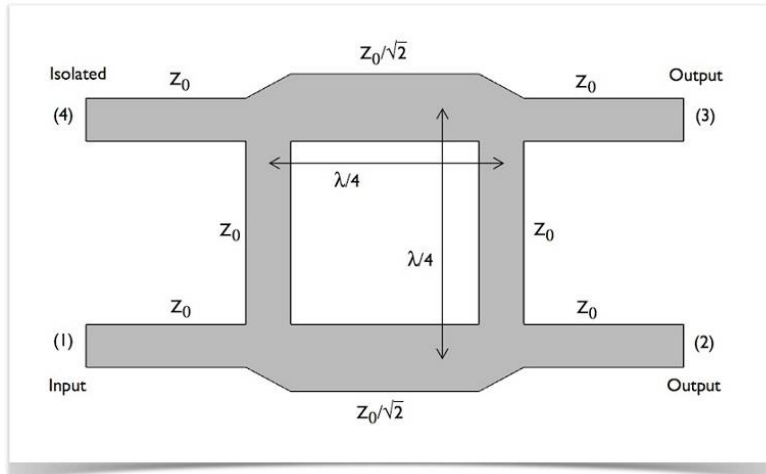
Figure 3. 6. 13: Branchline coupler

These outputs can easily be used to produce circular polarization by placing two RF feeds perpendicular on each other in a circular waveguide. Figure 3.6.14 shows a rectangular waveguide with the same setup. For the SSM project, the rectangular waveguide would be changed to a circular waveguide, while the RF feeds would be placed in the same way.
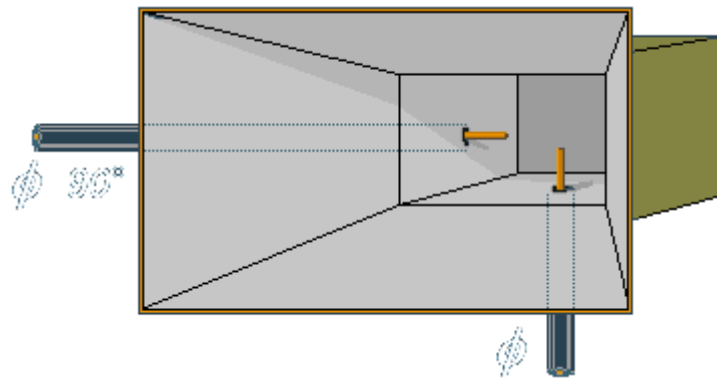
Figure 3. 6. 14: Circular polarization creation

3.6.7.1. *PCB characteristics*

When choosing a laminate to use for the microstrip board one needs to consider certain factors. The most important ones are the dielectric constant and the specified frequency to be used. These are closely related and one should choose a laminate that gives a natural microstrip length based on the design. For higher frequencies like 23 GHz, one should consider a Teflon based laminate (PTFE). This is because the dielectric losses are very low in these laminates. There is no blueprint to designing branchline couplers with microstrip, but one needs to consider certain factors when calculating the microstrip characteristics. The following points summarize the most important factors of the PCB design.

- AD300 PTFE laminate
- 0.5 mm thick board
- Double sided 1 oz. copper
- Dielectric constant of 3.0
- Dissipation factor of 0.003
- 23 GHz signal frequency

3.6.7.2. *Microstrip*

A microstrip transmission line is a simple and effective way of transferring microwave-frequency signals on printed circuit boards (PCB). The principle of the microstrip is a copper conductor separated from a ground plane by a dielectric material. When a signal is sent through the microstrip, some of the energy will dissipate through the air and some through the dielectric material. Depending on the structure of the microstrip, the effective dielectric constant for the waves will lie around 50-85% of the dielectric constant for the specific material [14].

3.6.7.2.1. Microstrip characteristics

The parameters found in table 3.6.2 are used to calculate the microstrip characteristics in this chapter. Due to the number of equations and the connection between them, the calculations are done with Matlab. For further information about the calculations, see [14].

Table 3. 6. 2: Parameters used in the calculations

ε_r	Dielectric constant	t	Conductor thickness
ε_{eff}	Effective dielectric constant	u_p	Phase velocity
ε_{eff_c}	Corrected effective dielectric constant	λ	Wavelength
W	Microstrip width	λ_e	Effective wavelength
W_e	Effective microstrip width	c	Speed of light
H	Board height	f	Frequency
Z_0	Microstrip impedance		

For this project, a frequency of 23 GHz is used and the wavelength can be calculated:

$$\lambda = \frac{c}{f} = \frac{3 \cdot 10^8}{23 \cdot 10^9} = 0.013 \ m. \tag{3.6.10}$$

For the PCB design, the distance in the branch line coupler is said to be $\lambda/4$, but because this will result in a very small and unreliable design a length of $5\lambda/4$ is chosen. One could also use a length of $3\lambda/4$, $7\lambda/4$ etc. depending on the design.

The phase velocity along the microstrip is given by:

$$u_p = \frac{c}{\sqrt{\varepsilon_{eff}}} = 1.9321 \cdot 10^8. \tag{3.6.11}$$

The effective dielectric constant will mainly be depending on the width of the microstrip. To achieve the maximum ε_{eff}, one needs a very wide microstrip. The wide microstrip will result in concentrated electric field lines more or less only between the microstrip and the ground plane, while a narrow microstrip will result in the electric field lines being about equally divided between the air and the printed circuit board. The following formulas presents the effective dielectric constant.

$$\frac{1}{2}(\varepsilon_r + 1) \leq \varepsilon_{eff} \leq \varepsilon_r, \tag{3.6.12}$$

where the effective dielectric constant is calculated by

$$\varepsilon_{eff} = \frac{\varepsilon_r + 1}{2} + \frac{\varepsilon_r - 1}{2}\left[\left(1 + 12\frac{h}{W}\right)^{-1/2}\right] = 2.4109, \qquad (3.6.13)$$

for $\frac{W}{h} \geq 1$. The microstrip impedance is given by:

$$Z_0 = \frac{60}{\sqrt{\varepsilon_{eff}}}\ln\left(8\frac{h}{W} + \frac{W}{4h}\right) \qquad (3.6.14)$$
$$= 50\ \Omega.$$

Due to the SMA connector impedance of 50 Ω [15], and that the maximum power transfer is found when input and output impedance are equal, the microstrip should have an impedance of 50 Ω.

3.6.7.2.1.1. Corrected microstrip characteristics and dispersion

The above equations do not consider the conductor thickness and therefore corrections are introduced. The effective microstrip width W_e will replace the width in the equations above and can be calculated by

$$W_e = W + \frac{t}{\pi}\left[1 + ln\left(\frac{2h}{t}\right)\right] = 1.2672\ mm, \qquad (3.6.15)$$

for $\frac{W_e}{h} \geq \frac{1}{2\pi}$. For these corrections to apply, the conditions $t \leq h$ and $t < \frac{W_e}{2}$ must be true. Usually, in practice, these are easily achieved. The effective dielectric constant can now be calculated by inserting the corrected width in the following equation:

$$\varepsilon_{eff\_c} = \frac{\varepsilon_r + 1}{2} + \frac{\varepsilon_r - 1}{2}\left[\left(1 + 12\frac{h}{W_e}\right)^{-1/2}\right] = 2.4176. \qquad (3.6.13a)$$

The impedance should be 50 Ω and the microstrip width is calculated based on that. Due to corrections it is natural that the microstrip impedance will change, and the corrected impedance is given by

$$Z_{0\_c} = \frac{120\Pi}{\sqrt{\varepsilon_{eff\_e}}\left(\frac{W_e}{h} + 1.393 + 0.667ln\left(\left(\frac{W_e}{h}\right) + 1.444\right)\right)} = 50\ \Omega, \qquad (3.6.16)$$

for $\frac{W_e}{h} \geq 1$. Due to the microstrip characteristics and the corrections done, the effective wavelength is

$$\lambda_e = \left(\frac{\left(\frac{c}{f}\right)}{\sqrt{\varepsilon_{eff\_c}}}\right) = 0.0084\ m. \qquad (3.6.17)$$

Dispersion is an important factor while working with microstrip because of its inhomogeneous characteristics. The effective dielectric constant increases non-linear as the frequency is increased and similar changes will occur to the impedance in the microstrip lines. Yamashita's formula for dispersion gives an accuracy of about 99 % and will give a good estimation for the dispersion [16]. The formulas apply if $2 < \varepsilon_r < 16$, $0.006 < W/h < 16$ and $0.1\ GHz < f < 100\ GHz$, which will satisfy the parameters of this system. Yamashita's formula for dispersion is given by

$$\varepsilon_r(f) = \varepsilon_{eff\_c} \left(\frac{1 + \frac{1}{4} k F^{1.5}}{1 + \frac{1}{4} F^{1.5}} \right)^2 = 3.0, \tag{3.6.18}$$

where

$$k = \sqrt{\frac{\varepsilon_r}{\varepsilon_{eff\_c}}} = 1.1140 \tag{3.6.19}$$

and

$$F = \frac{4h\sqrt{\varepsilon_r - 1}}{\lambda_e} \left(0.5 + \left(1 + 2log \left(1 + \frac{W}{h} \right) \right)^2 \right) = 2.7191 \cdot 10^3. \tag{3.6.20}$$

Table 3. 6. 3: Parameter overview

ε_r	Dielectric constant	3.0	t	Conductor thickness	1 oz.
ε_{eff}	Effective dielectric constant	2.4109	u_p	Phase velocity	1.9321e8 m/s
ε_{eff_c}	Corrected effective dielectric constant	2.4176	λ	Wavelength	0.013 m
W	Microstrip width	1.219 mm	λ_e	Effective wavelength	0.0084 m
W_e	Effective microstrip width	1.2672 mm	c	Speed of light	3e8 m/s
h	Board height	0.5 mm	f	Frequency	23 GHz
Z_0	Microstrip impedance	50 Ω			

Table 3.6.3 shows the final results of the calculations in this paragraph.

3.6.8. Conclusion

Of the circuits in this document, only the breadboard models have been tested [17]. These have shown the intended functionality. The circuits for the microcontroller and motor driver are designed based on the evaluation boards from STMicroelectronics [11]. Parts not needed for the final design have been removed. Considering the design is based on the evaluation boards and datasheets, these circuits should have the intended functionality. The final designs for the line receiver, voltage regulation and current measurement have not been tested, but have been partially proven through simulations.

The branch line coupler was not built due to the incredible accuracy needed in the production, and the costs involved. According to the calculations, it should work.

3.6.9. References

[1] Maxon Motor, "Encoder MILE 256–2048 CPT, 2 Channels, with Line Driver," 04 2015. [Online]. Available: http://www.maxonmotor.com/medias/sys_master/root/8816811180062/15-342-EN.pdf.

[2] E. Løken and T. Sundnes, "SSM-5131 Control System Design Rev. 1.4," Kongsberg, 2016.

[3] Texas Instruments, "TPS709," November 2015. [Online]. Available: http://www.ti.com/lit/ds/symlink/tps709.pdf.

[4] STMicroelectronics, "L6230 Motor drive," STMicroelectronics, June 2011. [Online]. Available: http://www2.st.com/content/ccc/resource/technical/document/datasheet/ca/5e/ea/cf/c5/c0/4f/ac/CD00287681.pdf/files/CD00287681.pdf/jcr:content/translations/en.CD00287681.pdf.

[5] "The Differential Amplifier," 22 08 2013. [Online]. Available: http://www.electronics-tutorials.ws/opamp/opamp_5.html. [Accessed 26 04 2016].

[6] T. R. Kuphaldt, "The Instrumentation Amplifier," [Online]. Available: http://www.allaboutcircuits.com/textbook/semiconductors/chpt-8/the-instrumentation-amplifier/. [Accessed 03 05 2016].

[7] Diodes, "AH49F," Diodes, June 2014. [Online]. Available: http://www.diodes.com/_files/datasheets/AH49F.pdf.

[8] C. R. Nave, 2012. [Online]. Available: http://hyperphysics.phy-astr.gsu.edu/hbase/magnetic/magcur.html#c3.

[9] Texas Instruments, "INA326," Texas Instruments, November 2004. [Online]. Available: http://www.ti.com/lit/ds/symlink/ina326.pdf.

[10] T. L. Floyd, Electronic Devices, Harlow: Pearson, 2014.

[11] STMicroelectronics, "STM32F407XX," STMicroelectronics, May 2012. [Online]. Available: http://udel.edu/~furkan/cpeg423/13summer/stm32f4/DM00037051.pdf.

[12] F. Littmarck, "Modeling a branch line coupler," 14 March 2014. [Online]. Available: https://www.comsol.com/blogs/modeling-branch-line-coupler/.

[13] Microwaves101, "Branchline couplers," [Online]. Available: http://www.microwaves101.com/encyclopedias/branchline-couplers. [Accessed 15 April 2016].

[14] California State University, Sacramento, "What is a microstrip transmission line and how do you design one?," [Online]. Available: http://athena.ecs.csus.edu/~oldenbuj/EEE244/Chapter2/MicrostripDesCompl.pdf. [Accessed 15 April 2016].

[15] Emerson, "SMA 26.5 GHz Connector Datasheet," Emerson, 13 September 2009. [Online]. Available: http://www.mouser.com/ds/2/643/dr-142-1701-821-739332.pdf.

[16] S. Jahn, "Single microstrip line," 30 Desember 2007. [Online]. Available: http://qucs.sourceforge.net/tech/node75.html.

[17] G. H. Stenseth, "SSM-3003, Functional Test Report Rev.1.0," Kongsberg, 2016.

[18] G. H. Stenseth and M. Dybendal, "SSM-2000, Requirement Specification," Kongsberg, 2016.

[19] Maxon Motor, "EC 45 fl at Ø42.8 mm, brushless, 70 Watt," April 2015. [Online]. Available: http://www.maxonmotor.com/medias/sys_master/root/8816806920222/15-263-EN.pdf.

[20] J. W. Nilsson and S. A. Reidel, Electric Circuits, 9th ed., Upper Saddle River: Perason Education, 2011.

[21] Microwaves101, "Microstrip," [Online]. Available: http://www.microwaves101.com/encyclopedias/microstrip. [Accessed 15 April 2016].

3.7. Control system design

i. Abstract

This technical report highlights the design of the control system in the APMA. Specifications of the control system are described in detail. The introduction section serves as an explanation of the system as implemented in chapter 2-4. A Simulink model of the system is explained and simulation results presented. Lastly, software implementation of the Simulink model, in addition to the full control system, is presented.

iii. List of figures

iv. List of tables

V. Document history

Table 3. 7. 1: Document history

Rev.	Date	Author	Approved	Description
0.1	17.02.16	TS	EL	Document created
0.2	01.03.16	TS		Added mechanism feedback Updated Control system overview Changed document structure Added velocity to output to satellite Changed introduction Added conclusion
1.0	03.03.16	TS	MD	Reviewed and published
1.1	04.03.16	TS		Added summary Added chapter 2 Added chapter 3
1.2	22.03.16	TS	GHS	Abstract changed Control system includes electrical components
1.3	14.03.16	EL		Added chapter 1.4, 1.5 and 1.6 Added chapter 4
1.4	22.04.16	EL		Moved chapter 1.2 and 1.3 to chapter 2 Swapped chapter 3 and 4
1.5	11.05.16	TS, GHS		Changed chapter 4 added chapter 4.1-4.10 Changed Figure 1 Removed general conclusion
2.0	16.05.16	TS, EL	GHS	Reviewed and published

SSM

SMALL SATELLITE MECHANISMS

3.7.1. Introduction

The control system is an integral part of the APMA. Performing necessary calculations, receiving inputs, sending outputs and overall system control are the main tasks of a control system.

The SSM project's focus is the implementation of low-cost parts and processes. In turn, this leads to a cheaper design than what is standard in current space projects. Included in a cheaper design is the microprocessor, motor, motor driver and motor encoder. This allows for lower requirements, but also limits our possibilities when it comes to power consumption, mass and cost of equipment. For these reasons, cheaper components have been selected to build this control system, as seen in [1].

This chapter contains a system overview, theory and explanations of elements that will be used in the motor control system for the APMA.

3.7.1.1. *System overview*

The main system consists of:

- Electrical constituents:
  - **Control system**
  - Low-cost actuators(LCA)
  - Position Sensor
  - RF System(RFS)
    - Radiating Element(Antenna)
    - RF feed network(RFN)
- Mechanical constituents:
  - APM Structure
  - Thermal Hardware
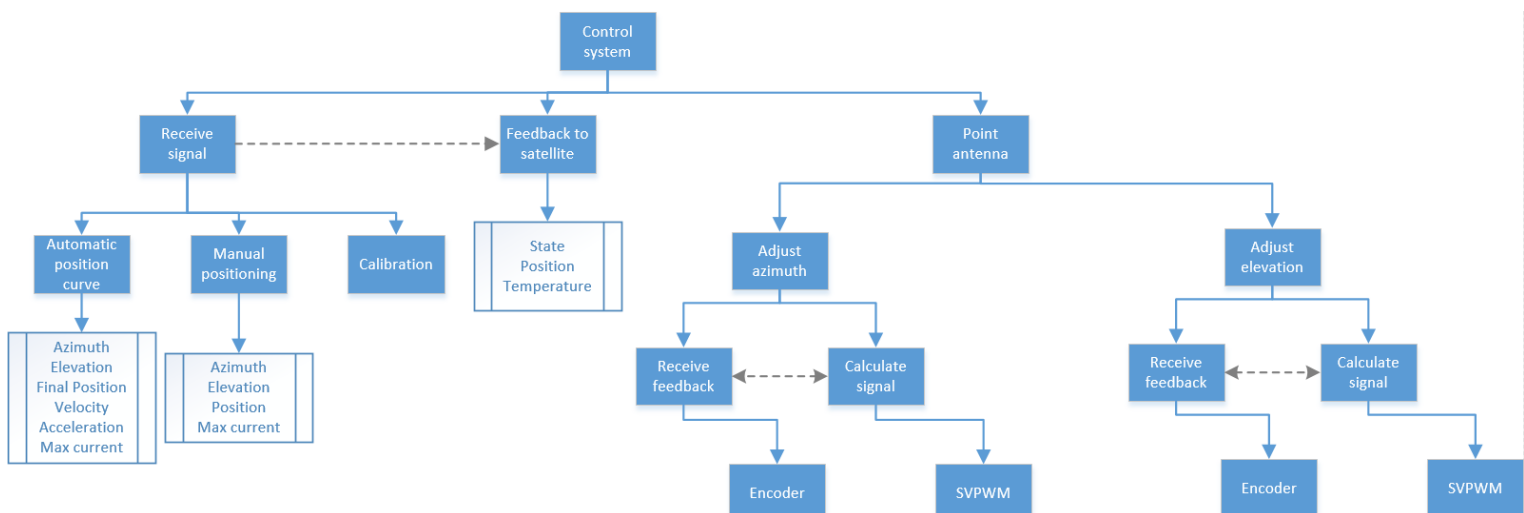
Figure 3. 7. 1: Control system object oriented overview

Figure 3.7.1 gives an overview of the control system's overall functionality and behavior. The control system in the APMA shall ensure the pointing position through the azimuth and elevation axes by controlling the actuator in both stages. The control system has to be accurate to point the antenna in

the desired position for sending/receiving data from another satellite.

3.7.1.2. PID-controller

A PID controller (proportional-integral-derivative controller) is an algorithm that controls the dynamic response of a system with respect to the feedback from the system. The controller uses an error value, which is the difference between a desired set point and the actual process value, and attempts to minimize this error over time. The controller consists of three terms; a proportional term, an integral term and a derivative term.

The output of a PID-controller is given by equation 3.7.1, [2]:

$$u(t) = K_p e(t) + K_i \int_0^t e(\tau)d\tau + K_d \frac{de(t)}{dt}, \tag{3.7.1}$$

where K_p, K_i, and K_d are the coefficients for the proportional, integral and the derivative terms (also called P, I and D) [2].

3.7.1.2.1. PID-term explanations

Sometimes not all the terms are used, then the controller is referred to as a PI, PD, P or I controller. Explanations of the different terms, [2]:

Proportional term: P accounts for present values of the error, and is a proportional gain for the error. The P-value influences the overshoot and the rapidity of the system response.

Integral term: I is the integral of the error over time and accounts for past values of the error. The accumulated error is multiplied by the integral gain, K_i. For example, if the current output is not strong enough, error will accumulate over time and the controller will respond by applying a stronger action. The main purpose of the integral term is to ensure that the system is reaching its target value (prevents a steady-state-error).

Derivative term: D accounts for possible future values of the error, based on the current rate of change. This term determines the slope of the error over time and multiplies this rate of change with the derivative gain, K_d. This term predicts the behavior of the system and improves the systems settling time and the stability. This term is often used in position/velocity control, but a problem is that it amplifies noise.

Figure 3.7.2 shows a block diagram of a PID-controller in the feedback loop of a system.
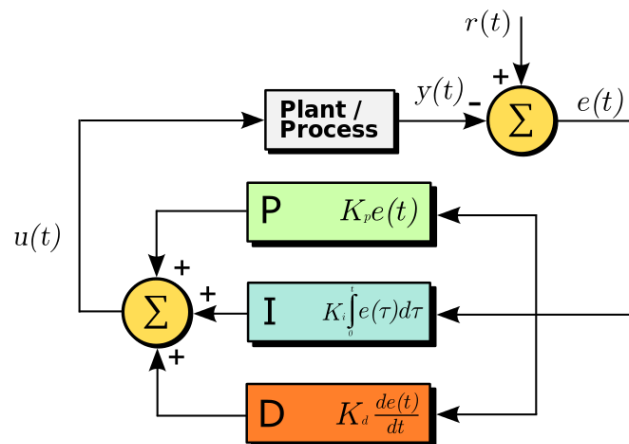
Figure 3. 7. 2: Block diagram of a PID-controller in the feedback loop. [2]

3.7.1.2.2.   Cascade controller

To get a better dynamic performance, two or more PID-controllers can be used together. This is called Cascade control. The purpose of the Cascade controller is that one PID controls the set-point of another. This control structure can be used if another control output than the one to be controlled may be measured. Then, the control system get an outer- and an inner loop controller, where the inner loop responds much more quickly. This structure recognizes deviations sooner than a single loop controller, starts the regulation earlier, and gives a more desired system response. This form of controlling a system will be used in the APMA.

Figure 3.7.3 shows the structure of a Cascade-controller with an inner- and an outer control loop.
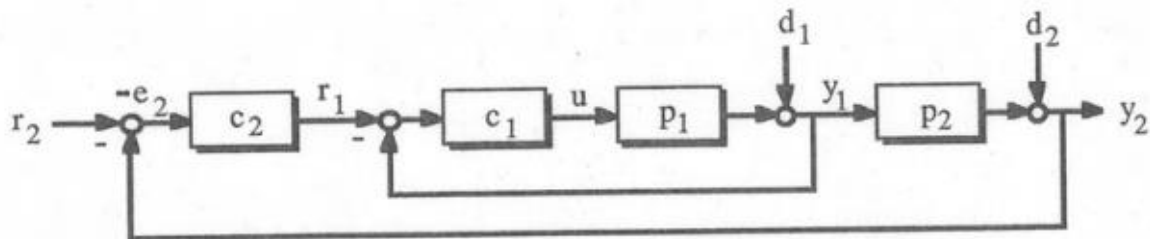
Figure 3. 7. 3: Cascade control structure. C1 and C2 are controllers and p1 and p2 are plants. [3]

3.7.1.2.3.   Ziegler-Nichols Tuning of the PID controller

Ziegler and Nichols have created two different methods for tuning the parameters of a PID controller. The most common method is called the ultimate sensitivity method, and is based on evaluating the amplitude and frequency of the oscillations of the system at the limit of stability.

The tuning starts with increasing the proportional gain until the system becomes marginally stable and continuous oscillations with amplitudes limited by the saturation of the actuator appear. This is the ultimate gain (K_u). The period of the oscillations is called the ultimate period, P_u. This period shall be measured when the amplitude of the oscillations is as small as possible. If describing the PID controller as $D_c(s) = k_p (1 + 1/T_I s + T_D s)$, the tuning parameters are selected as shown in table 3.7.2, [3]:

Table 3. 7. 2: Ultimate Sensitivity Method for tuning PID controllers. [4]

Type of controller:	Optimum gain:
P	$K_p = 0.5\ K_u$
PI	$K_p = 0.45\ K_u$ $T_I = P_u\ /\ 1.2$
PID	$K_p = 1.6\ K_u$ $T_I = 0.5\ P_u$ $T_D = 0.125\ P_u$

3.7.1.3. *Field orientated control*

The field orientated control (FOC) principle consists of controlling the angle and amplitude components of the stator field. Using Clarke and Park transformation changes the reference frame of the motor currents from balanced three-phase to a rotating reference frame, aligned with the rotor axis (q-quadrature, d-direct). The torque of a permanent magnet motor depends only on the quadrature current (q) component, also called the torque- component. To minimize the torque-current ratio and increase the efficiency of the motor, the most convenient control strategy is to set the direct-component of the current to zero. To control the current components, the present position of the rotor has to be known.

The Clarke and Park transformation required in field orientated control is described in detail in the next sections:

3.7.1.3.1.   Clarke and Park Transformations

A brushless DC-motor is a three-phase machine and is described by voltage and current differential equations. Due to time varying coefficients in the equations, the mathematical model of this system tends to be complex (flux linkages, induced voltages, continuously changing currents). For such systems, the mathematically transformations, including Clarke and Park, are used to referring all the variables to a common reference frame.

Figure 3.7.4 shows three different reference frames and their corresponding currents, which is a result of the Clarke and Park transformations:
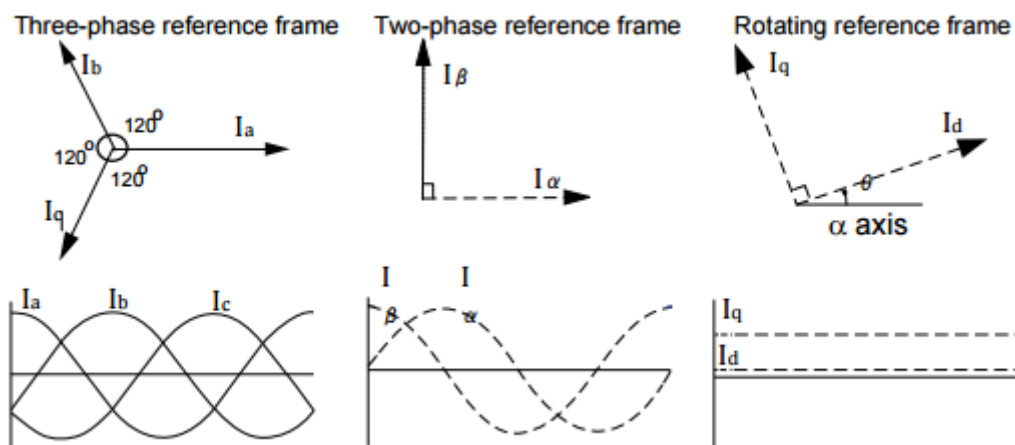
Figure 3. 7. 4: Three different reference frames. [5]

3.7.1.3.1.1.   Clarke transformation

Clarke transformation converts the balanced 3-phase system into the balanced 2-phase quadrature system, ref. figure 3.7.4. The reference frame changes from three-phase into two-axis orthogonal stationary frame. The transform is expressed by equation 3.7.2 and equation 3.7.3, [4]:

$$I_\propto = \frac{2}{3}I_a - \frac{1}{3}(I_b - I_c) \tag{3.7.2}$$

$$I_\beta = \frac{2}{\sqrt{3}}(I_b - I_c) \tag{3.7.3}$$

where I_α and I_β are the stationary orthogonal reference frame quantities and I_a, I_b and I_c are the three-phase quantities. Figure 3.7.5 shows a model of the Clarke transformation.
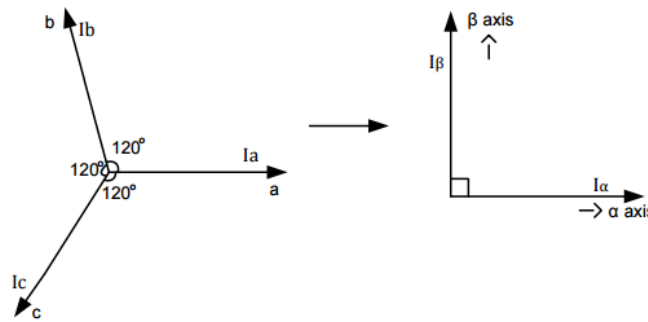
Figure 3. 7. 5: Clarke transformation. [5]

3.7.1.3.1.2.   Inverse Clarke transformation

The inverse Clarke transformation converts the quantities from the two-axial orthogonal stationary reference frame back to three-phase quantities by equation 3.7.4-3.7.6 [4]:

$$V_a = V_\propto \tag{3.7.4}$$

$$V_b = \frac{-V_\propto + \sqrt{3}V_\beta}{2} \tag{3.7.5}$$

$$V_c = \frac{-V_\propto - \sqrt{3}V_\beta}{2} \tag{3.7.6}$$

where V_α and V_β are the stationary orthogonal reference frame quantities, and V_a, V_b and V_c are the three-phase quantities. The transformation vectors and axes are shown in figure 3.7.6.
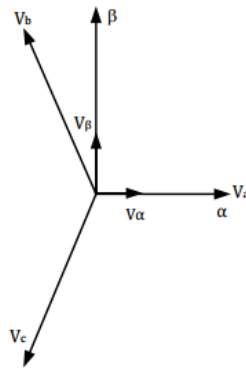
Figure 3. 7. 6: The inverse Clarke transformation. [5]

3.7.1.3.1.3.   Park transformation

The Park transformation converts the two-phase quantities from the orthogonal stationary reference frame into the rotating reference frame quantities, expressed by equation 3.7.7 and 3.7.8 [4]:

$$I_d = I_\propto \cos(\theta) + I_\beta \sin(\theta) \tag{3.7.7}$$

$$I_q = I_\beta \cos(\theta) - I_\alpha \sin(\theta) \tag{3.7.8}$$

where I_d and I_q are the rotating reference frame quantities, I_α and I_β are the stationary orthogonal reference frame quantities and θ is the rotation angle. Figure 3.7.7 shows the vectors, axes and angles used in the Park transformation.
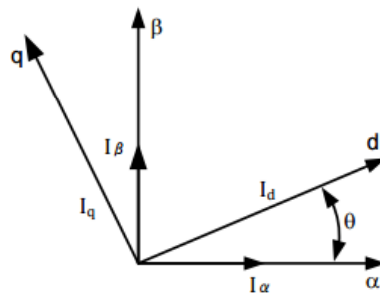
Figure 3. 7. 7: Park transformation. [5]

3.7.1.3.1.4.   Inverse Park transformation

The inverse Park transformation converts the rotating reference frame quantities back into stationary orthogonal reference frame quantities by equation 3.7.9 and 3.7.10 [4]:

$$V_\propto = V_d \cos(\theta) - V_q \sin(\theta) \tag{3.7.9}$$

$$V_\beta = V_q \cos(\theta) + V_d \sin(\theta) \tag{3.7.10}$$

where V_α and V_β are the orthogonal stationary reference frame quantities, V_d and V_q are the rotating reference frame quantities and θ is the rotation angle. Figure 3.7.8 shows the parameters in the Inverse Park transformation.
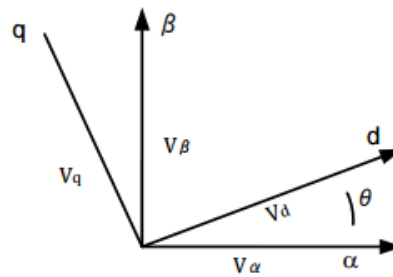
Figure 3. 7. 8: Inverse Park transformation. [5]

3.7.1.4. *Pulse Width Modulation*

Pulse width modulation can be explained as modulating the time on/time off relationship (duty cycle) of a square wave signal. Changing the duty cycle changes the average voltage of the signal.

Varying this duty cycle according to a sine wave amplitude creates an SPWM signal.

$$duty = \sin(\omega t) \tag{3.7.11}$$

3.7.1.5. *Space Vector Pulse Width Modulation*

Figure 3.7.9 shows a DC-power source three phase inverter. The inverter has six power switches (S1 to S6) which are controlled by the switching variables a, a', b, b', c and c'. The upper switches have corresponding lower switches. (S1 and S4, S3 and S6, S5 and S2). If the upper switch is turned on, then the corresponding lower switch is turned off, and vice versa. Due to this, the states of the upper transistors determine the output voltage.
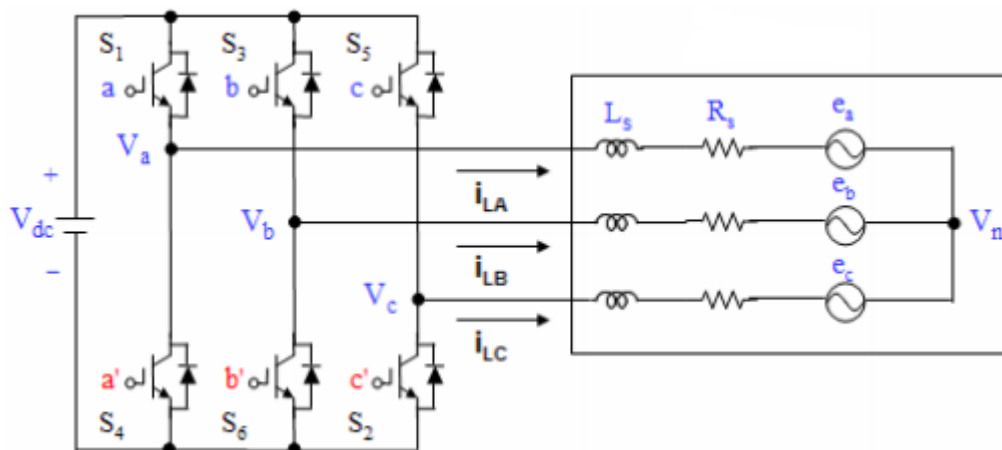
Figure 3. 7. 9: Three phase voltage source PWM inverter. [6]

There are eight different combinations of the state patterns to the three upper switches, which in the SVPWM conversion represents eight inverter voltage vectors (V_0 to V_7). The vectors and switching states are shown in figure 3.7.10:
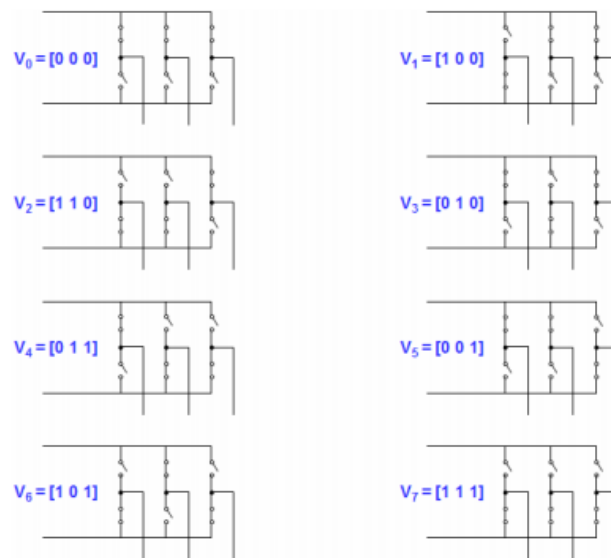
Figure 3. 7. 10: The eight inverter voltage vectors and switching states. [6]

The space vector PWM modulation represents a special switching sequence of the three upper switches of a three-phase inverter. The SVPWM generates less distortion on the output currents to the phases and has higher efficiency compared to sinusoidal modulation, [5]. The peak of the SVPWM signal equals $\frac{1}{\sqrt{3}}V_{dc}$, while the peak of the sine modulation equals $\frac{1}{2}V_{dc}$, ref. figure 11. This is why SVPWM is implemented in the APMA control system.
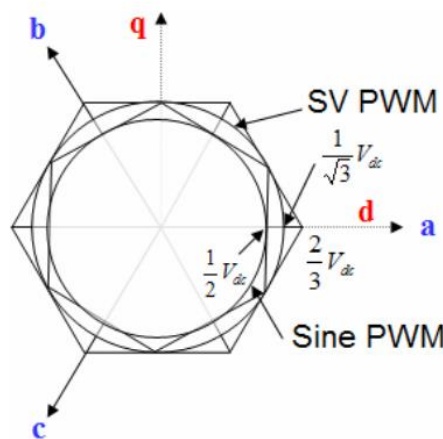
Figure 3. 7. 11: Sine PWM versus SVPWM. [6]

The implementation of space vector PWM requires the dq- reference frame, which is a result of the Clarke and Park transformation. Two of the space vectors, V_0 and V_7, are zero vectors, while the six non-zero vectors shape the axes of the hexagonal showed in figure 3.7.11 and 3.7.12. The angle between two of the vectors are 60 degrees, which divides the hexagonal into six sectors. These sectors are the six sectors of the SVPWM inverter. The purpose of the SVPWM technique is to approximate the reference voltage vector using the eight switching states.
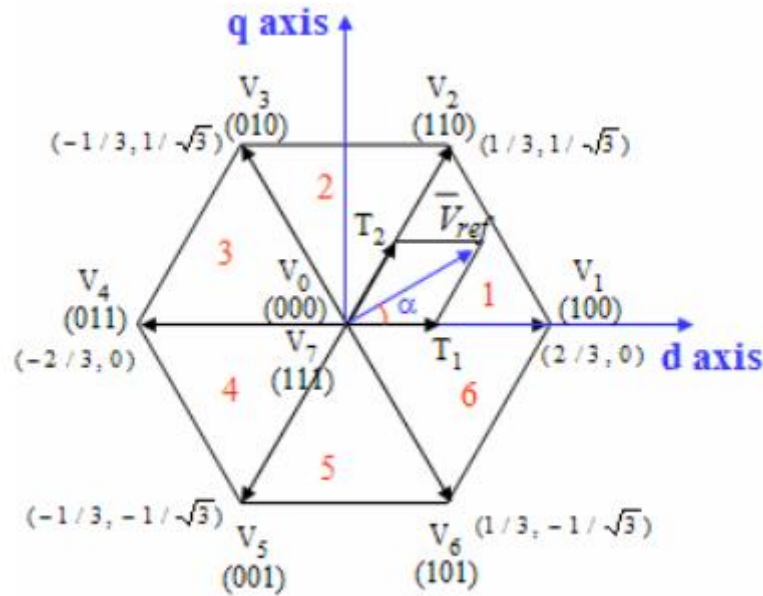
Figure 3. 7. 12: SVPWM switching vectors and sectors. [6]

3.7.1.5.1. Implementation of SVPWM

The SVPWM technique can be implemented by the three following steps, [5]:

Step 1: Determine V_d, V_q, V_{ref}, and the angle (α).
Step 2: Determine time duration, T_1, T_2 and T_0.
Step 3: Determine the switching time of the transistors (S1 to S6).

3.7.1.5.1.1. Step 1: Determine V_d, V_q, V_{ref}, and the angle (α)

The direct and quadrature components of the voltage reference (V_d and V_q) are found by changing the reference frame from the balanced 3-phase system into the rotary, orthogonal 2-phase reference frame (Clarke and Park transformation). Then, the magnitude of the voltage reference and the rotation angle is given by equation 3.7.12 and 3.7.13, [5]:

$$V_{ref} = \sqrt{V_d{}^2 + V_q{}^2},$$ (3.7.12)

where V_d and V_q are the direct and the quadrature component of the reference voltage.

$$\alpha = \tan^{-1}\left(\frac{V_q}{V_d}\right)$$ (3.7.13)

where V_d and V_q are the direct and the quadrature component of the reference voltage and α is the angle between the direct component and the voltage reference space vector, ref figure 3.7.13.
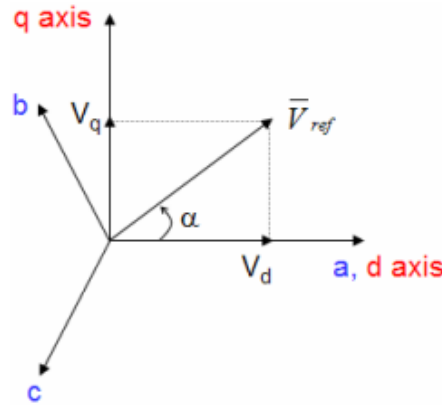
Figure 3. 7. 13: Voltage space vector and its components. [6]

3.7.1.5.1.2. Step 2: Determine time duration, T_1, T_2 and T_0.

The switching time durations at any sector of the hexagonal can be calculated by using equation 3.7.14-16, [5]:

$$T_1 = \sqrt{3}V_{ref}\sin\left(\frac{\pi}{3} - \alpha + \frac{n-1}{3}\pi\right), \tag{3.7.14}$$

$$T_2 = \sqrt{3}V_{ref}\sin\left(\alpha - \frac{n-1}{3}\pi\right), \tag{3.7.15}$$

$$T_0 = T_z - T_1 - T_2, \tag{3.7.16}$$

where V_{ref} is the voltage space vector, α is the angle shown in figure 3.7.13, n is the number of the sector and T_z is the period time. Figure 3.7.14 shows the relationship between the time duration and the vectors:
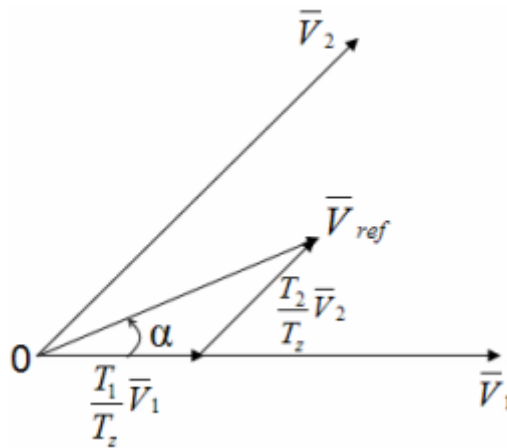
Figure 3. 7. 14: Voltage space vector versus time, [5]

SSM

SMALL SATELLITE MECHANISMS

3.7.1.5.1.3. Step 3: Determine the switching time of the transistors (S1 to S6).

Table 3.7.3 shows the required switching sequence of the six transistors in the different sectors, to get the desired SVPWM signal, [5]. The sequence can be derived from the space-vectors in figure 3.7.12.

Table 3. 7. 3: The SVPWM switching sequences. [6]

Sector	Upper Switches (S_1, S_3, S_5)	Lower Switches (S_4, S_6, S_2)
1	$S_1 = T_1 + T_2 + T_0 /2$ $S_3 = T_2 + T_0 /2$ $S_5 = T_0 /2$	$S_4 = T_0 /2$ $S_6 = T_1 + T_0 /2$ $S_2 = T_1 + T_2 + T_0 /2$
2	$S_1 = T_1 + T_0 /2$ $S_3 = T_1 + T_2 + T_0 /2$ $S_5 = T_0 /2$	$S_4 = T_2 + T_0 /2$ $S_6 = T_0 /2$ $S_2 = T_1 + T_2 + T_0 /2$
3	$S_1 = T_0 /2$ $S_3 = T_1 + T_2 + T_0 /2$ $S_5 = T_2 + T_0 /2$	$S_4 = T_1 + T_2 + T_0 /2$ $S_6 = T_0 /2$ $S_2 = T_1 + T_0 /2$
4	$S_1 = T_0 /2$ $S_3 = T_1 + T_0 /2$ $S_5 = T_1 + T_2 + T_0 /2$	$S_4 = T_1 + T_2 + T_0 /2$ $S_6 = T_2 + T_0 /2$ $S_2 = T_0 /2$
5	$S_1 = T_2 + T_0 /2$ $S_3 = T_0 /2$ $S_5 = T_1 + T_2 + T_0 /2$	$S_4 = T_1 + T_0 /2$ $S_6 = T_1 + T_2 + T_0 /2$ $S_2 = T_0 /2$
6	$S_1 = T_1 + T_2 + T_0 /2$ $S_3 = T_0 /2$ $S_5 = T_1 + T_0 /2$	$S_4 = T_0 /2$ $S_6 = T_1 + T_2 + T_0 /2$ $S_2 = T_2 + T_0 /2$

Figure 3.7.15 shows a picture of a general 3- phase space vector signal.
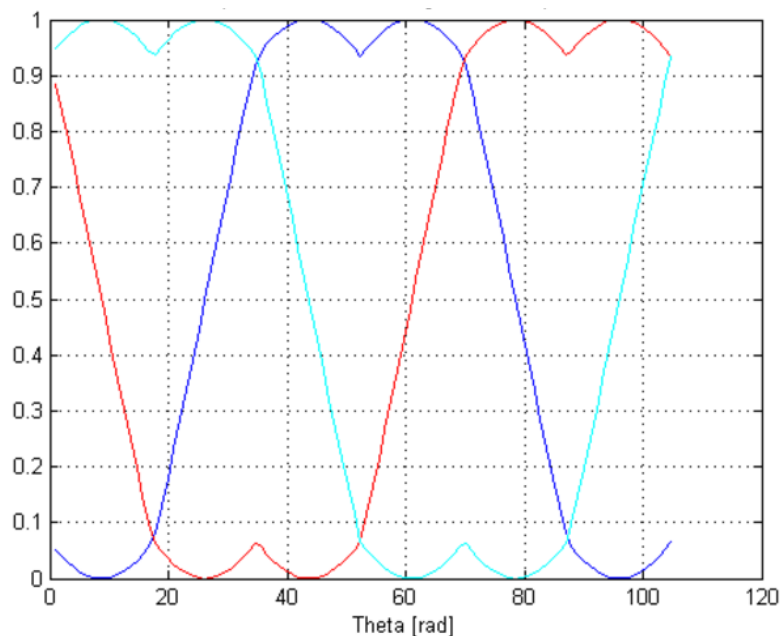
Figure 3. 7. 15: 3- phase space vector time. [7]

3.7.2. APMA control system description

The control system will ensure the steady operation of the mechanism. The spacecraft requests both frequent and infrequent position updates, calculated and performed in real-time by the controller. A calibration function keeps the mechanism running optimal during its entire lifecycle, and is performed by request from the spacecraft. Position, velocity and temperature will be transmitted back to the spacecraft, along with active or idle state.

3.7.2.1. *Internal spacecraft communication*

3.7.2.1.1. Input

The controller will receive position commands via CANbus [6], for adjusting the pointing of the mechanism. The satellite, on which the mechanism is connected, sends signal updates with an interval between 8 Hz and 100 Hz [6].

Pointing signals received from spacecraft:

- Position in the azimuth and elevation axes.
  - The spacecraft's control system shall do the necessary calculations for the relative positions, velocities and accelerations, and manually control the mechanism position based, together with current.
- Automatic S-curve generation in the azimuth and elevation axis.
  - The system will receive commands for position, velocity, acceleration and current, and create an S-curve for positioning.

When the satellite is moving at high speeds past other satellites, the velocity and accuracy is highly important. Rapid communication between the spacecraft and antenna ensures the pointing accuracy during the entire transmission to the other satellite.

Input variables for setting parameters are angular position, angular velocity, acceleration and maximum current.

When the controller receives a position command, the acceleration, maximum current and maximum velocity will also be altered. The system needs the configuration command to keep the system running smoothly, and within the satellite's desired parameters. For each position request, all variables have to be set [6], leading to less execution time and reliability compared to setting each value in order.

There will be an option to put the system in a calibration mode [6]. Ensuring accurate pointing requires the position encoders and the actual position of the mechanism to align, generating the need for a calibration function. After receiving the command, motors drive the mechanism to the -180° physical azimuth stop, and -90° physical elevation stop. The positions received from the encoders are adjusted to zero positions when the mechanism physically stops.

3.7.2.1.2. Output

Current temperature, velocity and position is transmitted back to the spacecraft [6]. The spacecraft needs to know the position of the antenna to keep it pointing in the right direction at given periods. The spacecraft also needs to know the velocity of the antenna to adjust the speed or keep the system going at given speeds through a desired timeframe. Temperature surveillance allows the satellite to protect the antenna from overexposure to temperature and radiation by rotating the mechanism away from the heat-source. Additionally, the mechanism will send feedback of whether or not it is in motion

[6].

3.7.2.2. *Motor control*

The mechanism will be able to point two actuators in specific angles simultaneously to provide a smooth mechanical movement along the antenna axes [6]. Accuracy is a key requirement. For every signal received from the internal spacecraft, the controller will compare the current position of the mechanism to the requested position, received from the spacecraft, and send the current position to the spacecraft.
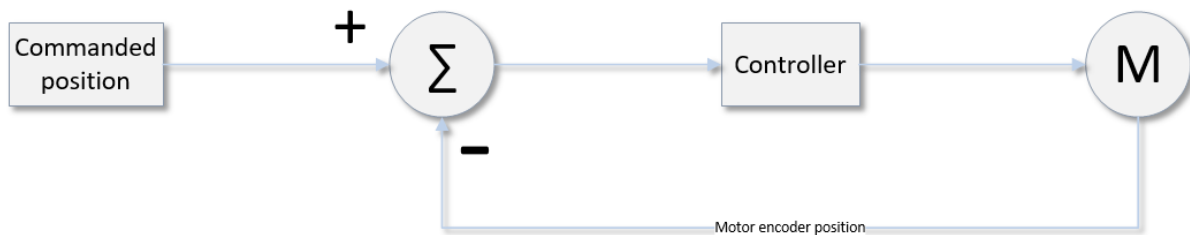
Figure 3. 7. 16: Control system position regulation example

As described in figure 3.7.16, the controller uses the acquired position and subtracts the current position from the encoder. This gives the difference in position as an output, and allows the controller to adjust the velocity accordingly. This is just one illustration, of many regulators that features in the final control system.

When the internal spacecraft has the need to change the requested position in the middle of a sequence [6], the mechanism will be able to decrease the velocity gradually. This is achieved by creating a positioning profile, which describes the change in velocity with respect to time, commonly known as acceleration. Figure 3.7.17 shows an example of this profiling.
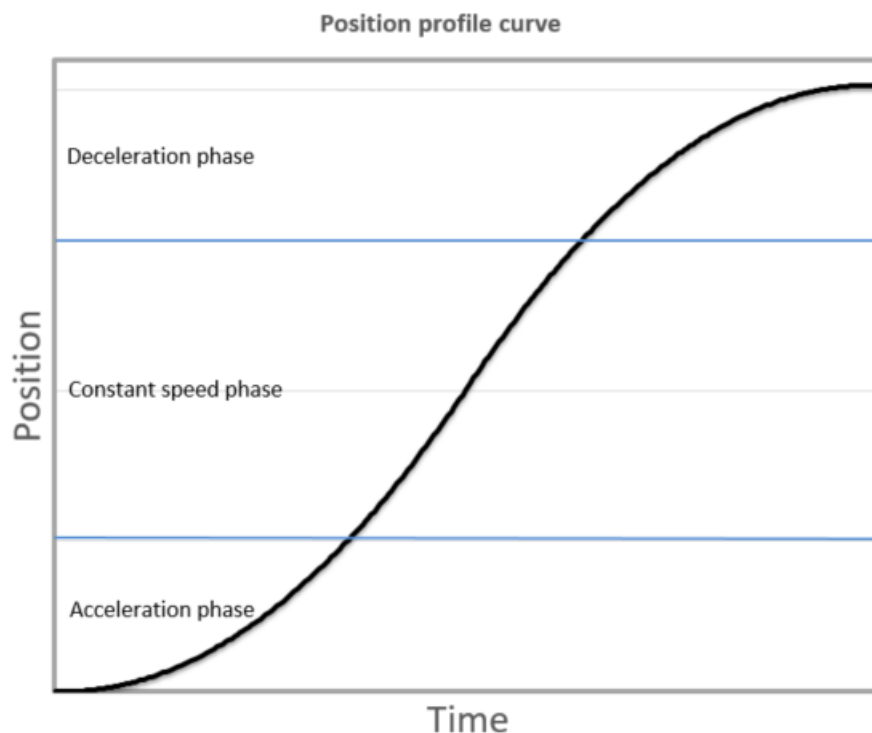
Figure 3. 7. 17: Positioning profile curve

The points marked on the figure represent the acceleration and deceleration phases of the mechanism. The phases vary for whenever the mechanism receives a new command for a final position. The requirement for this functionality comes from the risks associated with the mechanism accelerating too rapidly [6], possibly shifting the satellite out of course or rotational axis.

The input to the control system in the APMA will be a position profile curve if the position is not manually set.

3.7.3. Simulink model of the control system

This section contains a model of the control system of the APMA created in Simulink, an explanation of the model, simulations and simulation results.

Figure 3.7.18 shows a simplified model of the control system:
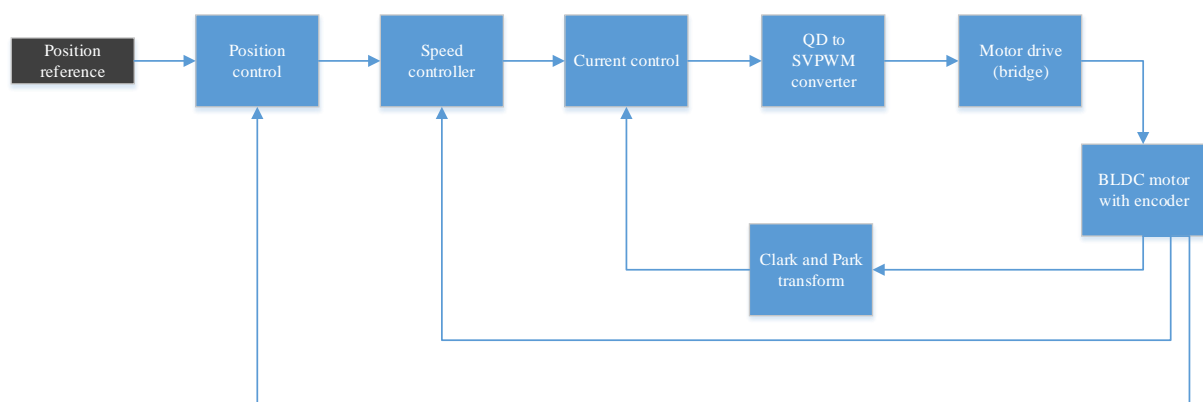
Figure 3. 7. 18: Control system overview

3.7.3.1. *Explanation of the control system model*

Figure 3.7.19 shows the top-level view of the control system model. The main blocks in the figure are the Cascade-controller, the universal bridge, the Permanent Magnet Synchronous Machine, PMSM, and the DC-voltage source.

The Cascade-controller block contains the control-loops and transformations (Clarke, Park, and QD to SVPWM) of the system, and has a position reference, a DC voltage and feedback from the motor as inputs. The position reference is a profile curve (ref. fig. 3.7.17), where the user has to set parameters for the acceleration, velocity and position.

The output of the Cascade-controller is a SVPWM signal that decides the switching of the transistors in the bridge. The motor driver in the physical model of the APMA will execute the switching action.

The PMSM is a model of the motor (EC 45 flat 70W) that will be used in the APMA, where some of the motor parameters are set in the motor block.
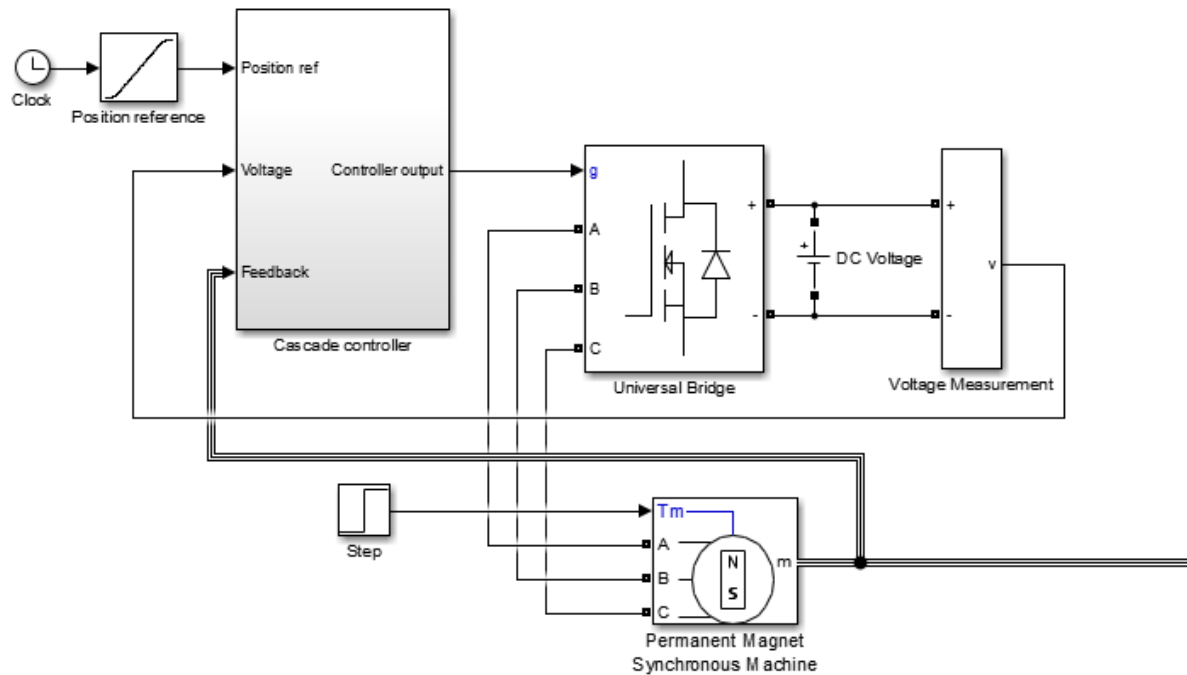
Figure 3. 7. 19: Top-level view of the Simulink Model

Figure 3.7.20 shows the control loops inside the Cascade controller block in figure 3.7.19. The system has a 3-step regulation. The control system has four PID-controllers (one for position, one for velocity and two for currents). The position control is the outer loop, the velocity controller is the middle loop and the current controllers are the inner loops of the system.

The inputs in the "Cascade controller" block are the profile curve, the voltage from the voltage source, the stator currents (Ia, Ib, Ic – 3-phase sinus signal, feedback from the motor), the velocity of the rotor (the filtered derivative signal of the position feedback) and the rotor position (feedback from the encoder).
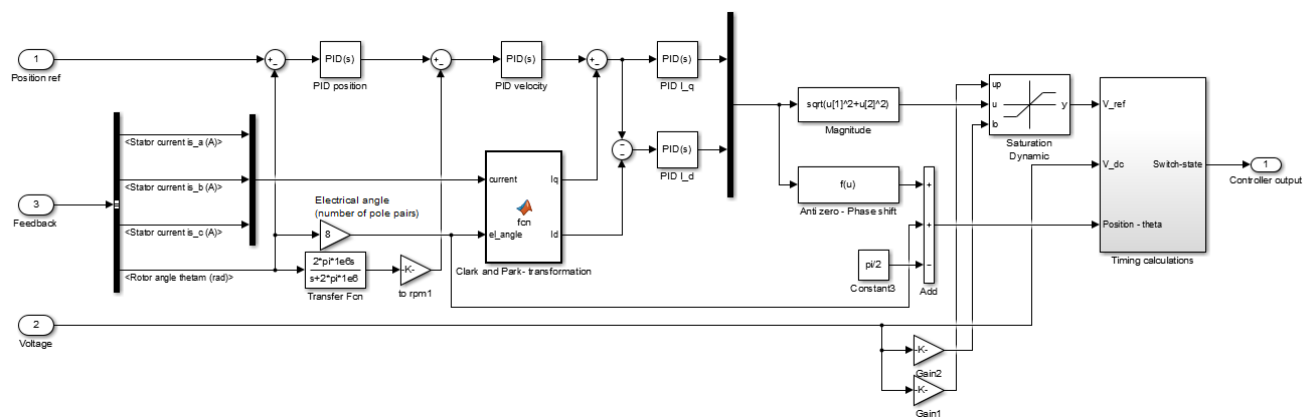
Figure 3. 7. 20: Cascade controller block, as featured in appendix 7.3.1.

3.7.3.1.1. The current controllers – inner control loop

The feedback in the current loop is the 3-phase current sine signal from the motor. Due to the complexity of controlling 3-phase signals in the control system, the Clarke and Park transformation (explained in section 3.7.1) is used. It transforms the balanced 3-phase currents (Ia, Ib, Ic) into orthogonal 2-phase rotating currents (Id and Iq) [4]. Controlling the components of these currents, which are DC values instead of the 3-phase signal, is called field orientated control and is used in the control system for the APMA.

3.7.3.1.1.1. Reference frames – Clarke and Park

Figure 3.7.21 shows the current and the angular position feedback from the motor. These signals are inputs to the "Clarke and Park transformation"-block. The angular position (mechanical) of the rotor is converted to electrical angular position by multiplying with the numbers of pole pairs in the motor.

The transformation changes the reference frame of the currents into a two-phase, orthogonal, rotary reference frame, and the outputs of this block is the direct (d) and the quadrature (q) components of the current. To maximize the efficiency of the motor, the purpose of the current-controllers is to regulate I_d to zero. The model has a PID for controlling I_q and another PID to control I_d, as seen in figure 3.7.21. The outputs of these controllers represent the actuation needed to control the currents.
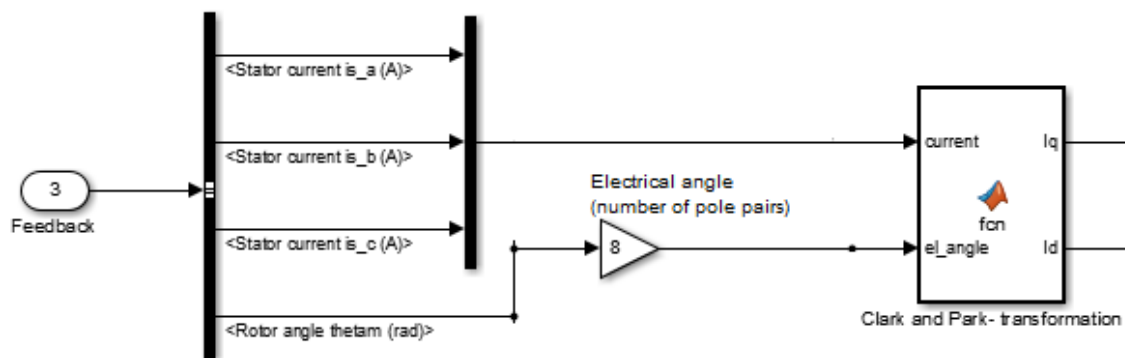
Figure 3. 7. 21: Current feedback, Clarke and Park transformation

3.7.3.1.1.2. QD-SVPWM converter

The next part of the control loop, from the output of the current-regulators to the motor inputs, is a conversion from the qd-frame to space vector pulse width modulation, which is the desired input for the motor. Figure 3.7.22 shows the QD to SVPWM converter of the control system.
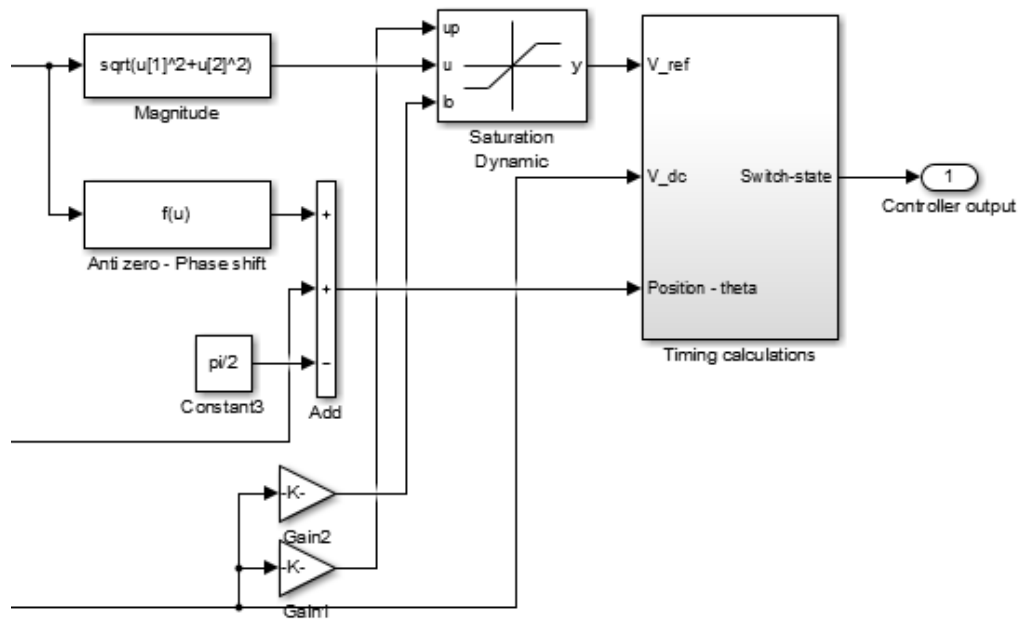
Figure 3. 7. 22: QD to SVPVM converter

The first signal to be calculated is the voltage reference. This is the magnitude of the required actuation voltage. This signal is fed into a saturation block, where the upper and lower limit is set by the maximum SVPWM peak (the DC voltage source divided by the square root of 3) [5]. This saturation-block is implemented as a max voltage value in the software implementation. This signal, the V_ref signal, is the input to the "timing calculations"-block, together with the DC-voltage from the voltage source and the angular position of the rotor.

The angular position of the rotor is calculated by the summation given in figure 3.7.23:
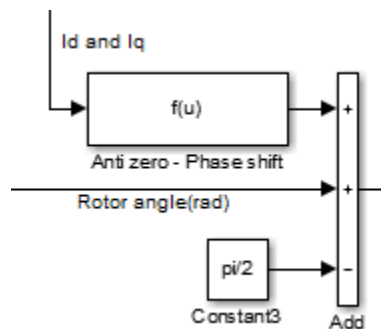
Figure 3. 7. 23: Calculation of the angular position of the current vector.

The anti-zero – phase shift function is given by Eq. 3.7.17 and 3.7.18:

$$If\ I_d \geq 0: \theta_2 = tan^{-1}(\frac{U_d}{U_q}),$$
(3.7.17)

$$If\ I_d < 0: \theta_2 = tan^{-1}(\frac{U_d}{U_q}) + \pi,$$
(3.7.18)

where U_d is the output signal from the PID-controller that controls I_d, and U_q is the output signal of the PID-controller that controls I_q. θ_2 is the angle between the direct component of the actuation signal and the actuation vector.
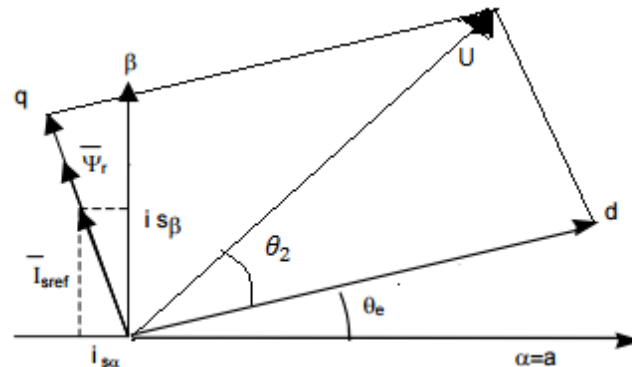
Figure 3. 7. 24: Figure 24: Actuation-vector, U.

The angular position of the rotor is equal to the direction of the direct component. In this model, the purpose is to control the direct component to 0. If θ_2 goes to $\pi/2$, the U-vector has the same direction as the q-component. Then the angular position of the rotor equals the angular position of the actuation vector, U, minus $\pi/2$ (due to the phase shift). The angular position of the actuation signal, U, is given by θ_2 plus θ_e (the angular position from the motor feedback). Then the angular position of the rotor is given by the summation in figure 3.7.23 (Angular position = feedback position + θ_2 - $\pi/2$).

3.7.3.1.1.2.1. *Timing calculations*

The next block in the Simulink model is the "timing calculations" block, whose inputs are already described; the voltage reference, the dc voltage and the angular position of the rotor. This block converts the voltage reference to a SVPWM signal. In the physical APMA, the SVPWM signal will be the input signals to the motor drive, which automatically switches the transistors in the bridge, and produces the input to the motor (balanced 3-phase signals).

The "timing calculations" block is shown in figure 3.7.25:
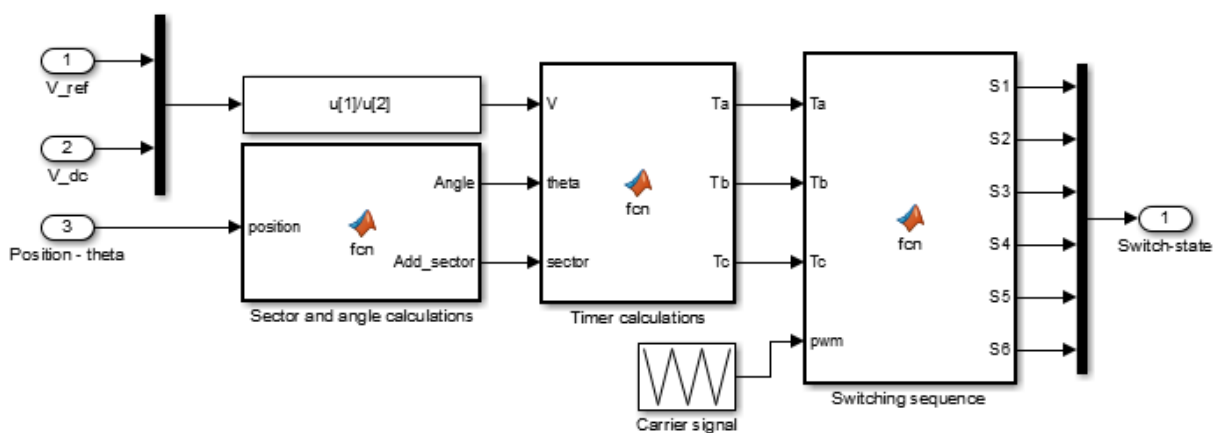
Figure 3. 7. 25: Timing calculations

The block contains three MATLAB-functions, a PWM carrier signal and the "u[1]/u[2]" – function (V_ref/V_dc).

The first MATLAB function, "Sector and angle calculations", calculates which SVPWM sector the voltage space vector is in, and returns this value and the angle of the voltage space vector, an angle that varies between 0 and $\pi/3$ radians. The input in the function is the angular position of the voltage space-vector.

The code inside the block is given by:

```
function [Angle, Add_sector] = fcn(position)
%#codegen


a = position/(2*pi);
b = floor(a);
c = position - 2*pi*b;


%Sector:
d = c/(pi/3);
e = floor(d);


Angle = c - e*pi/3;
Add_sector = e+1;
```

Figure 3. 7. 26: Sector and angles calculations

The next MATLAB-function block is the "Timer calculations". The inputs in this block are; the voltage reference, the angle that varies between 0 and $\pi/3$, and the number of the sector, in which the voltage space vector is found. Using the equations for calculating the time durations (equations 3.7.14-16 in section 3.7.1.5.1.2) and the switching sequence given in table 3.7.3, the block calculates the switching times for the three different phases.

The code for the calculations in the block is given by:

```
function [Ta, Tb, Tc] = fcn(V,theta,sector)
%#codegen

a = V*sqrt(3)*sin(pi/3-theta);
b = V*sqrt(3)*sin(theta);
c =(1-a-b)/2;

Ta =
(sector==1)*(a+b+c)+(sector==2)*(a+c)+(sector==3)*(c)+(sector==4)*(c)+(se
ctor==5)*(b+c)+(sector==6)*(a+b+c);

Tb =
(sector==1)*(b+c)+(sector==2)*(a+b+c)+(sector==3)*(a+b+c)+(sector==4)*(a+
c)+(sector==5)*(c)+(sector==6)*(c);

Tc =
(sector==1)*(c)+(sector==2)*(c)+(sector==3)*(b+c)+(sector==4)*(a+b+c)+(se
ctor==5)*(a+b+c)+(sector==6)*(a+c);
```

Figure 3. 7. 27: Timing calculations

The third and last MATLAB-function in this block is the "switching sequence". This block has the switching times and a PWM carrier signal as inputs. The block calculates the switching states of the

transistors in the bridge, which shapes the SVPWM input signal to the motor. The function compares the space-vector signal with the carrier signal, and sets the upper switch on if the space vector has a higher value than the carrier. If the space-vector signal has a lower value than the carrier, the upper switch is set low.

Figure 3.7.28 shows the principle of the modulation of a sine PWM (the principle is the same for space vector, then with the space vector signal instead of the sine).
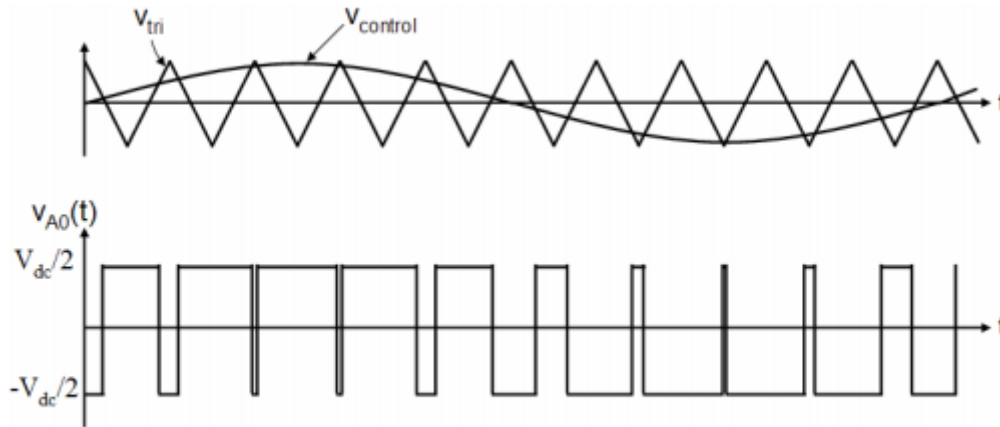
Figure 3. 7. 28: Pulse width modulation. [6]

The code for the calculations in the block is given by:

```
function [S1, S2, S3, S4, S5, S6] = fcn(Ta, Tb, Tc, pwm)
%#codegen
%Upper switches (S1, S3, S5), lower switches (S2, S4, S6)

if Ta > pwm
S1 = 1;
S2 = 0;
else
S1 = 0;
S2 = 1; end

if Tb > pwm
S3 = 1;
S4 = 0;
else
S3 = 0;
S4 = 1; end

if Tc > pwm
S5 = 1;
S6 = 0;
else
S5 = 0;
S6 = 1; end
```

Figure 3. 7. 29: Switching sequence

The output of this block is the output of the controller. This output enters the bridge and then the motor as shown in the top-level view of the control system, (Figure 3.7.19).

The loop explained in this section is the inner control loop of the system and represents the current controller.

3.7.3.1.2. The velocity controller

Figure 3.7.30 shows the controller with the current and the velocity loop. The velocity control loop is outside the current control loop.
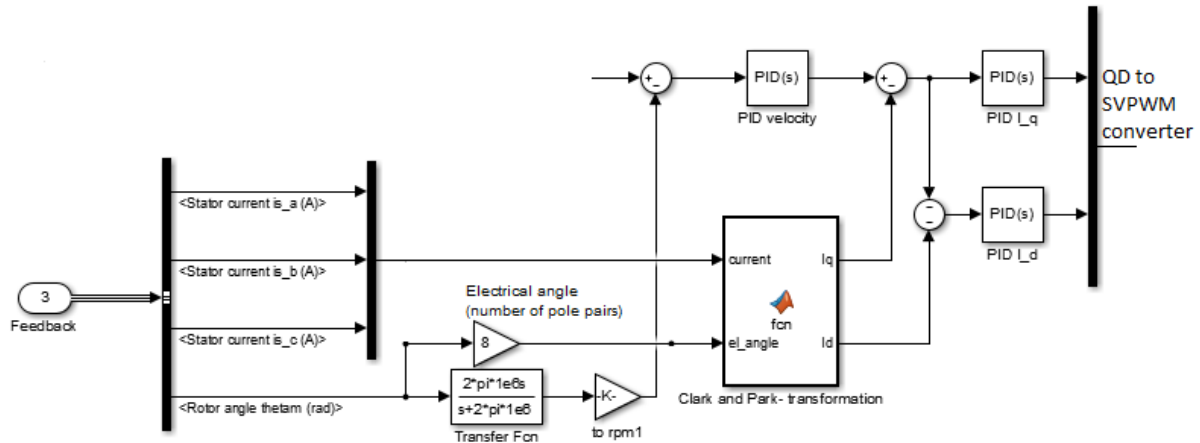
Figure 3. 7. 30: Controller with the current- and the velocity loop.

The feedback from the motor in the velocity control loop is the angular position of the motor. To get the velocity, the angular position signal is differentiated, and sent through a low-pass filter that filters away signal noise. The derivation and the filter is given by equation 3.7.19 (The step size in Simulink is $10^{-6.}$):

$$D_f(s) = \frac{\omega s}{s + \omega} = \frac{2\pi f s}{s + 2\pi f s} = \frac{2\pi \cdot 10^{-6} s}{s + 2\pi \cdot 10^{-6}} \tag{3.7.19}$$

Then, the error in velocity is calculated taking the velocity reference minus the velocity feedback. This error is fed into a PID-controller, and the output of this PID is the reference quadrature current.

3.7.3.1.3. The position controller – outer control loop

Figure 3.7.31 shows the control system with the three control loops; current, velocity and position. The position loop is the outer loop in the system. The position loop requires feedback from the motor, and in the Simulink simulation this feedback is available from the PMSM block. In the software implementation of control system, the position feedback comes from the encoder.

The position loop is the only one that has an external input reference. The position control loop calculates the error in position (desired position minus actual position), and this error is fed into a PID controller, that tries to minimize the error. Due to this being a Cascade- controller, the output of this PID is used as a reference for the velocity loop. The PID compares this output with the velocity feedback, and tries to make these two signals equal each other.
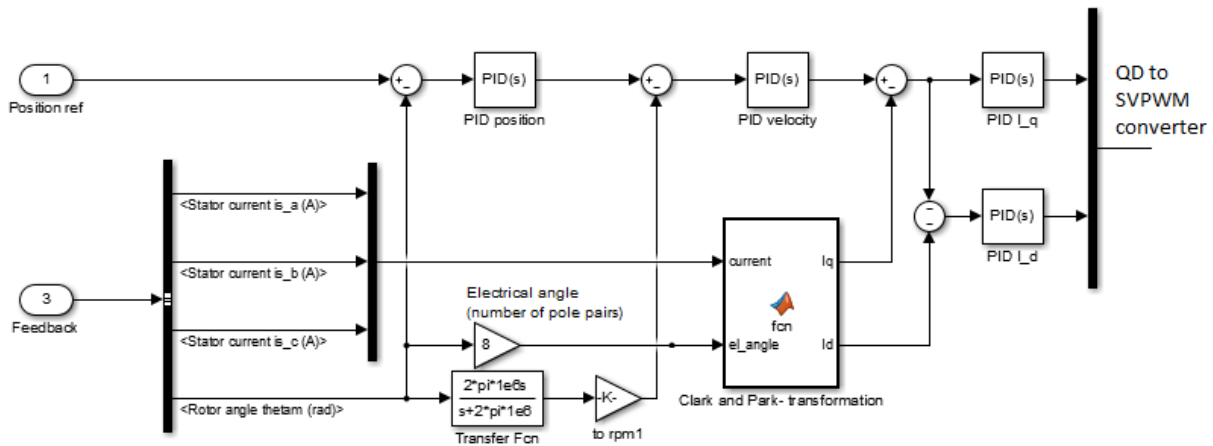
Figure 3. 7. 31: The Cascade controller with current-, velocity- and position loops.

3.7.3.2. *PID-regulator tuning*

The purpose of tuning a Cascade-controller, is to start tuning the inner loop, while the other loops are in "auto". The tuning parameters can be set by using the Ziegler-Nichols method. The next loop can be tuned when the inner loop is ok. In Simulink there is a function for auto tuning, but this system is so complex that Simulink cannot linearize the plant. Due to this, the PID – controllers were tuned by trying to follow Ziegler-Nichols method, and the parameter values are as follows. (The values differ from the real-life prototype):

3.7.3.2.1. Current controllers

The desired value for the direct current component is zero, and the controller has to regulate this. Both the controllers are P-controllers. With the following proportional gains, the currents produce a desired response:

- PID - Q: P = 60
- PID - D: P = 8

3.7.3.2.2. Velocity controller

This controller is a PI controller. The integral is included to remove the steady state error.

- P = 0.1
- I = 100

3.7.3.2.3. Position controller

This controller is a proportional controller, where the gain is tuned to the following value:

- P = 400

3.7.3.3. *Simulation and results*

This section includes some of the results and measurements from the simulation of the control system model in Simulink. In the simulation the values of the PID controllers are set to the tuned values described in section 3.7.3.2.

3.7.3.3.1.　　　　Simulation inputs

The frequency of the PWM carrier signal is set to 30 000 Hz, which gives a period time, Tz, of 0.0000333 s.

The solver properties which are set in the simulation:

- Solver: ode23tb(stiff/TR_BDF2)
- Max step size: 10^{-6}
- Relative tolerance: 10^{-4}
- Solver reset method: Robust

The motor parameters (from the datasheet of the EC 45 flat 70W motor, [7]) set in the PMSM block:

- Stator phase to phase resistance: 6.89 Ω
- Armature inductance, phase to phase: 5.85 mH
- Torque constant: 0.131 Nm/A_peak
- Inertia: 0.0000181 J
- Viscous damping: 7e-7 F
- Pole pairs: 8

The given requirement for the velocity of the APMA is that it should be able to move with a velocity of $\geq 60°/s$, [6]. With respect to the gear ratio of 1/17.5, the motor has to rotate with a velocity of $60°/s \cdot 17.5$, which equals to 1050°/s and 18.3 rad/s.

The APMA should also be able to accelerate at $40°/s^2$, [6], which equals to 12,2 rad/ s^2 with respect to the gear ratio.

In this simulation, the profile curve given in figure 3.7.32 is used as the position reference. The curve commands the motor to rotate to 18.3 radians in 1 s, which corresponds to the required velocity. The purpose of the simulation is to observe the behavior of the control system. It should be able to track the reference curve. The simulation time is 1.1 seconds.

Figure 3.7.33 shows the derivative of the profile curve, and represents the velocity reference for the motor. The two peaks and the "not constant acceleration areas" in the figure are results of some errors in the generation of the profile curve, but it does not have an impact on the simulations.
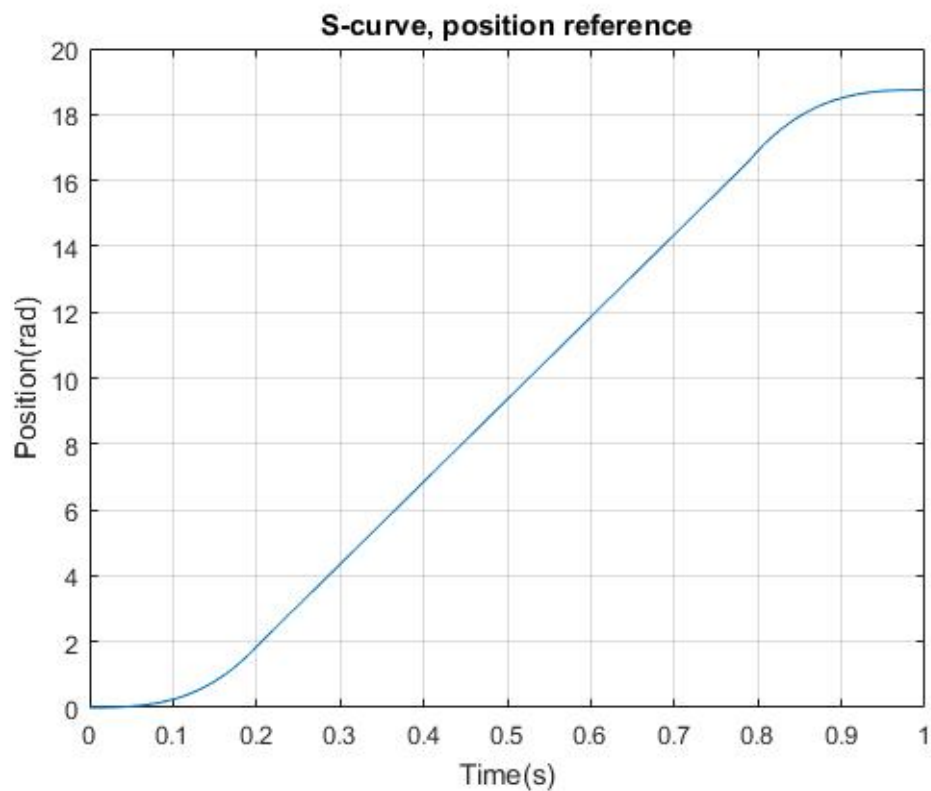
Figure 3. 7. 32: Position reference (S-curve) in the simulation.
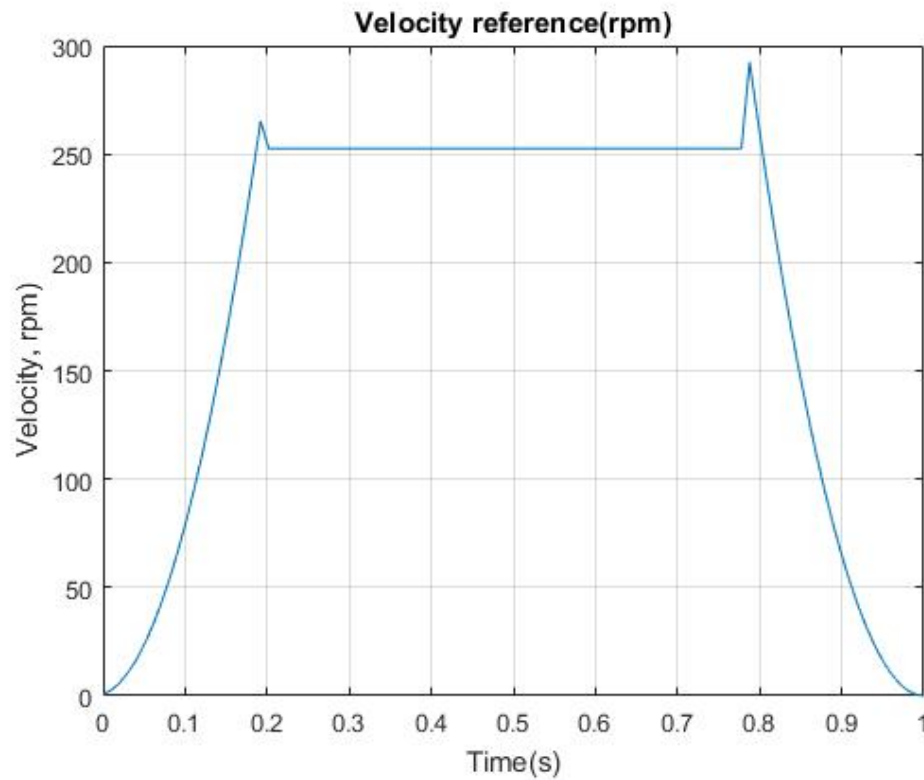
Figure 3. 7. 33: Velocity reference in the simulation

3.7.3.3.2.   Simulation results

Figure 3.7.34 shows the simulation results of the stator 3-phase currents, the direct- and quadrature current components and the rotor velocity in rpm (feedback from the motor).

- The 3-phase currents are smooth signals, that acts as desired. The amplitude varies between - 0.8 A and + 0.8 A.

- The quadratic and direct current components have some distortion in the signals. The controller sets the direct component (Id) to approximately zero, as expected and desired.

- The velocity in rad/s is almost equal to the reference curve for velocity. The maximum velocity reached in this simulation is approximately 24 rad/s, which equals to 82 degrees/sec for the APMA (with respect to gear ratio).
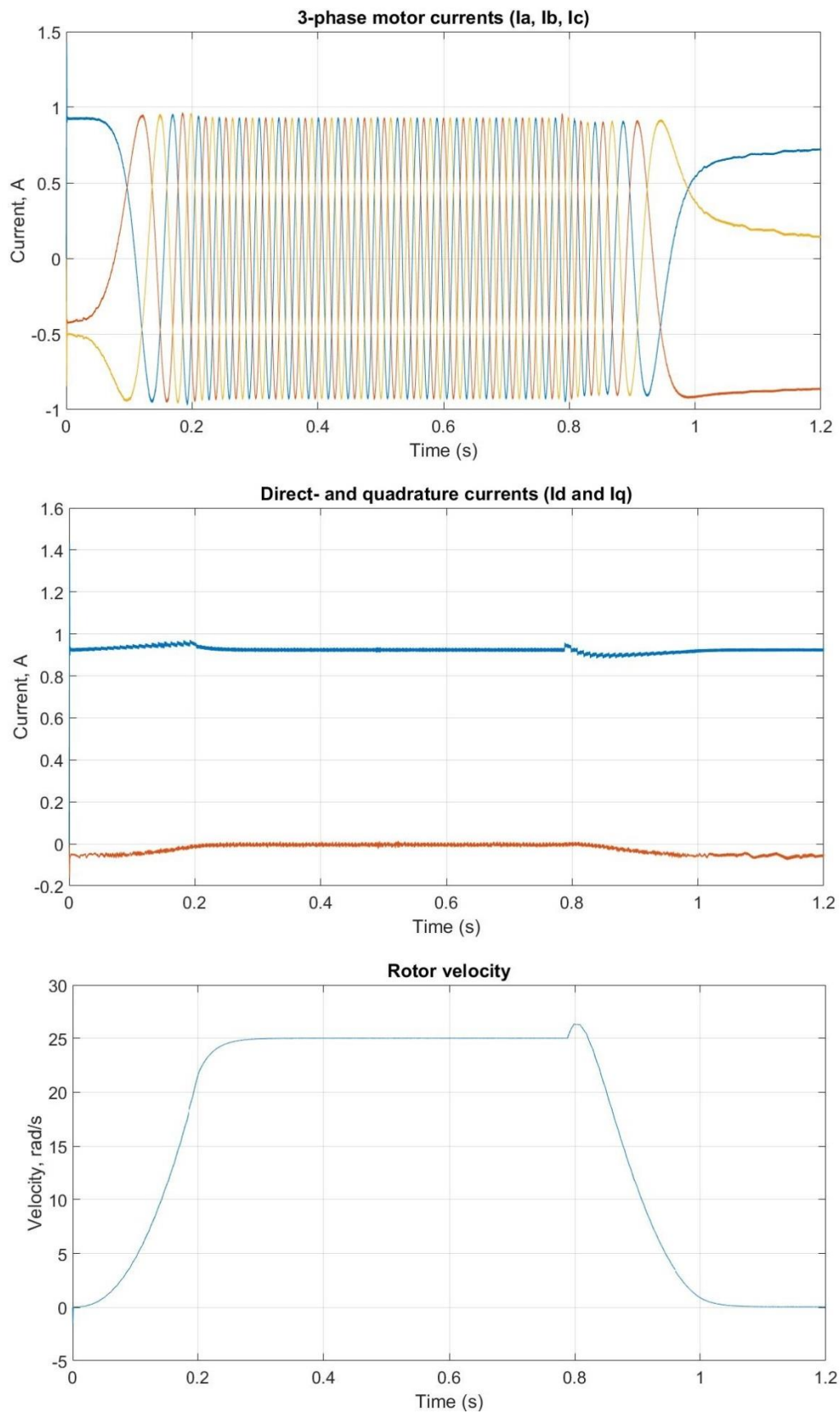
Figure 3. 7. 34: Simulation results: Stator currents (Ia, Ib,Ic), direct- and quadrature current components and rotor velocity(rad/s).

Figure 3.7.35 shows the simulation results for the rotor position and the electromagnetic torque:

- The position curve is almost equal to the profile curve, which means that the controller tracks the reference very well. The rotor reaches the desired position, 18.7 radians, in 1 second, without visible distortions.
- The torque signal also has some distortions, but it is stable and almost constant (not constant in the areas where the motor accelerates, as expected).
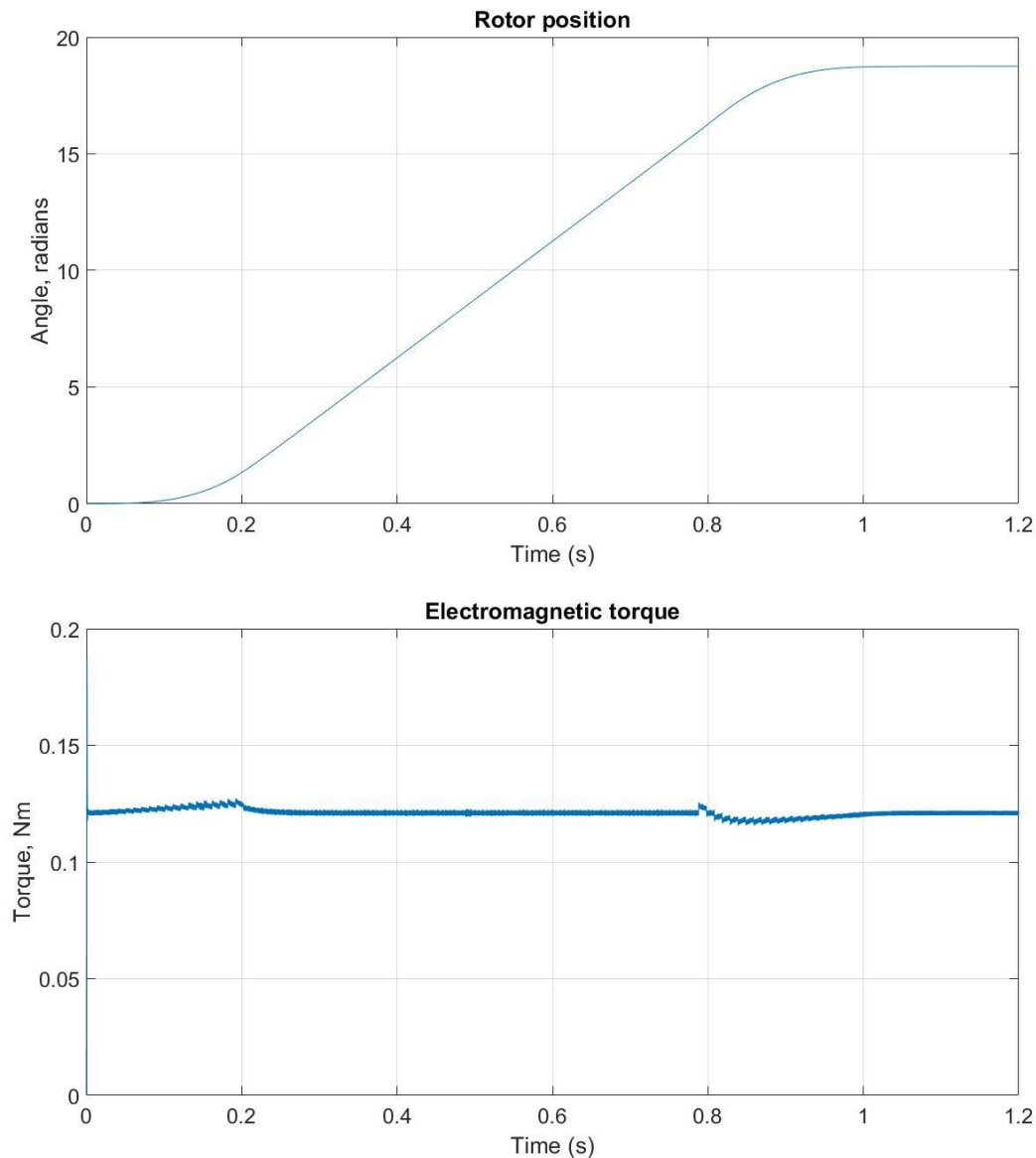
Figure 3. 7. 35: Simulation results: Rotor position (radians) and torque.

Figure 3.7.36 and 3.7.37 shows the timing space vectors, that compared with the PWM carrier signal creates the switching sequence of the transistors. The signals have the well-known space vector form,

and have 120 degrees phase shifts. The signals have some simulation distortions. Figure 3.7.37 shows all the 3 space vector signals in the same scope. It is easier to see the perfect 120 degrees phase-shift in this figure.
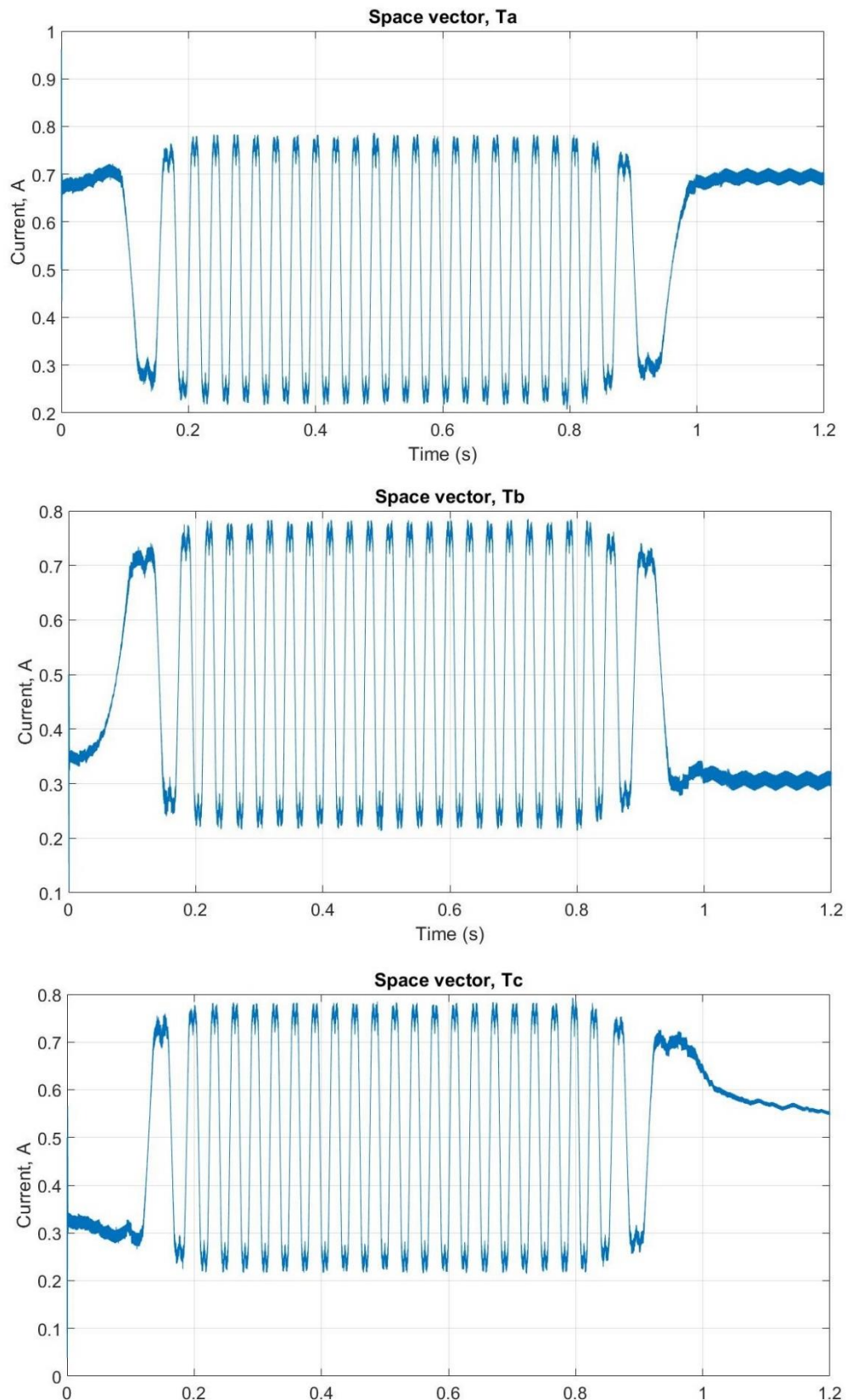
Figure 3. 7. 36: Simulation results: Space vectors, Ta, Tb and Tc.
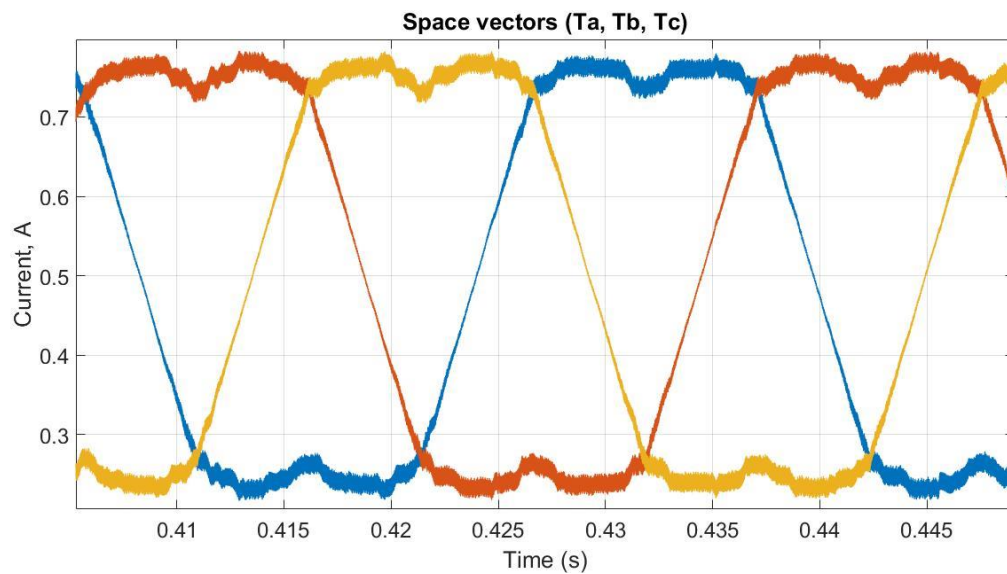
Figure 3. 7. 37: Simulation results: 3-phase space vectors (Ta, Tb, Tc).

Figure 3.7.38 shows the angle and sector calculations for the space vector signal. The angle varies from 0 to π/3 radians. Each time the angle reaches π/3 and starts from zero again, the sector number increases with 1. These results are as expected and confirms that the "sector and angle" calculations are correctly executed.
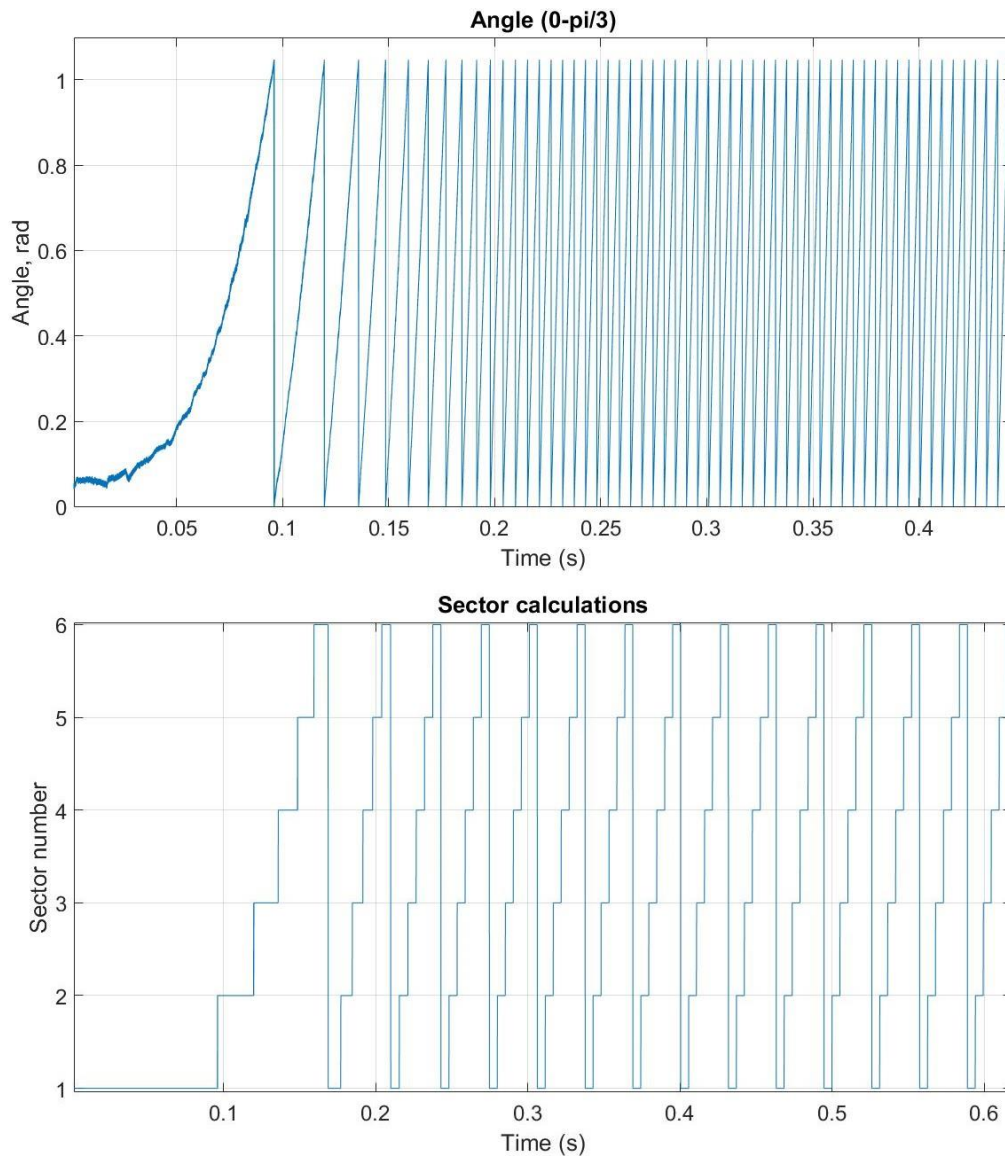
Figure 3. 7. 38: Simulation results: Space vector angle and sector selections.

3.7.3.3.3.   Simulation conclusion

The simulation of the motor control system in Simulink gives the desired results. The Cascade controller tracks the input position reference (the profile curve) accurately, without noise in the velocity and position curves. In some of the other signals (the direct- and quadrature currents, the torque and the space-vectors) there are some noise. This may come from tuning parameters, the feedback or simulation noise.

The peak values seen at the beginning of the simulations come from a "start-up torque". This torque represents the friction force the motor has to overcome before it starts rotating. In the simulation, the motor starts rotating the wrong way due to this applied force, and the controller starts regulating immediately. This will not happen in reality, and are only simulation errors.

The torque used in the simulation is constant through the whole simulation and equals to the start-up torque (including both inertia and friction). This is not correct, the torque should have been smaller later in the simulation (only equals to the friction torque). This may result in increased currents.

The simulations confirm the performance and the concept of the Cascade controller, and the control loops work as desired and expected. Due to these results, this model will be the final design of the control system for the APMA. The next section explains the implementation of the Simulink model in software to be used in the microcontroller, and in the real-life prototype of the mechanism.

3.7.4. Software implementation of the control system

Following sections describe the functions performed by the controller that has to be implemented in code. The motor control output contains all communication and signals residing between the controller and the motor drivers. This includes modulation, timing and algorithms related to the rotational operations.

The elevational stage is not included in the current prototype. The elevation stage has not been prioritized in the project due to time limits, and to ensure a thorough azimuth system.

In the software implementation, the PI regulators are named as PID regulators. This is just in case the further development of the control system contains derivatives in the regulators, which may be likely in a future continuation of the project.

3.7.4.1. *About the microcontroller*

The chip selected for the final design of the APMA is the STM32F415ZGT6 from ST microelectronics. The chip will be featured in the final circuit, and the STM32F4Discovery board is used only for testing and design purposes. More information about the choice of microcontroller and specifications can be found in the corresponding document, components trade-off [1]. For the first prototype, the STM32F407VGT6 is used for developing the software, as the originally intended chip is not available for ordering. However, these two microcontrollers have minimal differences, and the memory, speeds and resolutions are identical. During the prototyping, the chip is used with the STM32F4Discovery board.

Initial setup of the programming environment is done from the program STM32CubeMX [8], designed for developing software for ST's ARM cortex M4 chips. The interface sets up elements to be used in the code, allowing for further customization of these parts from several IDE's. When the code is generated, areas are marked as "USER CODE BEGIN" and "USER CODE END". Within these areas, custom code can be written, while all code outside these areas will be deleted if a setting is changed in the STM32CubeMX project, and overwritten in the project file. All code inside the user code sections is kept. Within the STM32CubeMX interface, settings like clock speeds and further configuration can be specified, although these can also be changed within the code with some knowledge of the library functions and hierarchy. The program creates three files; Main, _it and _hal_msp, which contain the generated configurations. If the STM32CubeMX will not be used for configurations in later revisions, these files can be edited.

The software used to program the microcontroller is the µVision from Keil [9].

The datasheet for the microcontroller can be found on the official site [10].

The libraries used in the software, HAL libraries, can be found on the official site [11].

3.7.4.2. *Internal spacecraft communication*

Communication in the final product is required to be implemented using the CAN protocol. The CAN protocol is a reliable way to organize interfaces via a master/slave hierarchy. CAN is a high level protocol, and can handle faults like error bits and ensures the correct systems receive the right commands, less complex than the MIL-STD-1553 standard already in use in space applications. The bits on the bus are user defined, and setting up UART is relatively quick, compared to a protocol system like CAN, containing several fail safes for steady bit transfer. Since the project scope is relatively large and only one person has software as the main focus, the first prototype will feature a UART interface. However, the interface is set up with the same design as the CAN system will be designed. Porting the system over to the CAN interface will only require implementation of the protocol, and no redesign of the source code.

3.7.4.2.1.   Signal reception from spacecraft

Both the CAN protocol and the UART interface sends data as bytes, from a high-level perspective. These bytes consist of several bits on the lower level, 8 bits per byte, which are sent via the serial bus. The APMA receives position commands, together with velocity and acceleration, which vary on a range from -180 degrees to 180 degrees. A byte only allows for values between -128 and 127, or between 0 and 255 unsigned, generating the need for an algorithm that adds up two bytes into a number with 16 bits and values between -32 768 and 32 767, or 0 and 65 000. The max values in a 16 bit integer may seem large, but the position transmission will be multiplied by 100 to allow for additional digits for pointing accuracy. An alternative solution consists of sending one digit for each byte, with the downside of wasting significant transmission rate.

```
/* Position. */
Position = 360;
buffer[2] = Position>>8;
buffer[3] = Position - (buffer[2]<<8);
```

Figure 3. 7. 39: Splitting up a 16 bit integer into two 8 bit integers

```
Request_Vars R;
int BYT_Start = 0x45;
if(HAL_UART_Receive_IT(&huart4, buffer, 8) == HAL_OK)
  {
  if(buffer[0] == BYT_Start)
  {
    R.state = buffer[1];
    R.Pos = (buffer[2]<<8) + buffer[3];
    R.Vel = (buffer[4]<<8) + buffer[5];
    R.Acc =  buffer[6];
    R.Vref = buffer[7];
```

Figure 3. 7. 40: Receiving a UART signal and merging two 8 bit integers into a 16 bit integer

Figure 3.7.39 shows the method for splitting up a 16 bit integer into two 8 bit integers, and figure 3.7.40 shows receiving and merging of two 8 bit integers into one 16 bit integer. The "<<" sign represents the shifting of the bits in the integer. In this case, for transmission, the bits are shifted by steps of eight. The first byte (buffer [2]) will represent the first eight bits of the 16 bit integer, while the second byte (buffer [3]) will represent the eight remaining bits by subtracting the first eight bits from the 16 bit integer. When converting from 16 to 8 bit integers, if the value is larger than 8 bits, it will become the maximum 8 bit value, 127. Figure 3.7.41 shows the different mode selection dependent on the state byte:

```
if(R.state == 1)
{
  CALIBRATION();
  return 0;
}
if(R.state == 2)
  Ref = R.Pos + 18000;

if(R.state == 3)
  POSITION_INIT(R);
```

Figure 3. 7. 41: State selection

The UART protocol bits are shown in figure 3.7.42:

| IDLE | Startbit (1'b0) | Bit [0] | Bit [1] | Bit [2] | Bit [3] | Bit [4] | Bit [5] | Bit [6] | Bit [7] | Stopbit (1'b1) | IDLE |
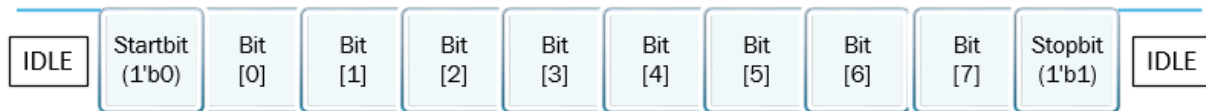
Figure 3. 7. 42: Visio: UART protocol

First off is the start bit in the UART protocol. This is to start the transmission. The bit is set low, and the receiving part recognizes this and starts loading the message onto the user-determined buffer. Next comes the eight bits culminating to one bit, which contains the data to be sent. Lastly, the stop bit ends the communication between the two nodes, and the process may repeat.

Figure 3.7.43 shows the packets being sent to the control system:

| Start byte | State | Position [0] | Position [1] | Velocity [0] | Velocity [1] | Acceleration | Voltage |
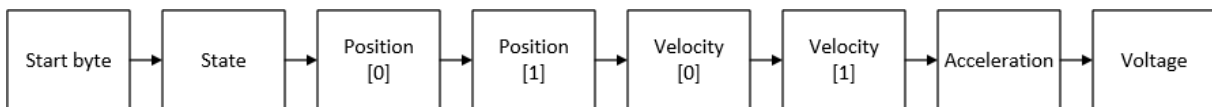
Figure 3. 7. 43: Visio: UART byte receive

The start byte is a predetermined value set on the receiver end, to ensure that the first received value is the first one that is sent, in case of timing errors between the two systems, or missed bytes. Values received are sent into S-curve generation or do manually assign pointing position, depending on the mode. Regardless of which mode is requested, all bytes need to be sent. When the manual positioning is selected, unnecessary bytes like velocity and acceleration are generally set to zero. Note that the control system receives voltage instead of current. This is because the only way to reduce current in the inner control system loop is to limit the max voltage from the magnitude function.

3.7.4.2.2. Signal transmission to spacecraft

The system shall send position, temperature and active state updates to the spacecraft [6]. Every 10th millisecond, an update will be sent from the mechanism to the spacecraft, containing the pointing position, temperature readings and whether or not it is moving. In addition, velocity will be transmitted to give a better indication of the state of the system. Figure 3.7.44 shows the signal transmission to the spacecraft, along with the S-curve position reference update and state updates. Bit shift is explained in 3.7.4.2.1.

SSM
SMALL SATELLITE MECHANISMS

```
INC_PosTimeStep++;
if(INC_PosTimeStep >= millis * 10)//each 10 ms.
{
  /* each second. */
  if(TXCount >= 100)
  {
  /* Prepare position and velocity. */
  txPos = Virtual_Encoder_Pos >= 0 ? (Virtual_Encoder_Pos*ConvertToRads*18000/PI):0;
  txVel = Velocity  >= 0 ? Velocity * 180/PI : abs(Velocity);
  /* Assign to buffer. */
  transmit_Buffer[0] = 0x45;
  transmit_Buffer[1] = 0x2;
  transmit_Buffer[2] = txPos>>8;
  transmit_Buffer[3] = txPos - (transmit_Buffer[2]<<8);
  transmit_Buffer[4] = txVel>>8;
  transmit_Buffer[5] = txVel - (transmit_Buffer[4]<<8);
  transmit_Buffer[6] = 0x0;
  transmit_Buffer[7] = 0x0;
  /* If the system is not moving, assign idle state. */
  if(txVel <= 0)
    transmit_Buffer[1] = 0x0;
  /* If the system runs on the auto-generated S-curve, assign state. */
  if(INC_Position < Array_Values)
  {
    INC_Position++;
    Ref = Reference_Pos[INC_Position] * 10;
    transmit_Buffer[1] = 0x3;
  }
  /* Transmit. */
  HAL_UART_Transmit_IT(&huart4, transmit_Buffer, 8);
  TXCount = 0;
  }
  INC_PosTimeStep = 0;
  TXCount++;
}
```

Figure 3. 7. 44: Transmission to spacecraft in main function.

Counters count up the time to update the buffer values and send the update to the spacecraft. The update is set to each second, and can be easily configured for shorter intervals. All values sent are unsigned integers, requiring the values to be positive, creating the need for always positive "txPos" and "txVel", which are the transmitted positions and velocities. If the mechanism has no velocity, it is idle, and will send the idle command, 0. If the system has generated an S-curve and has not yet completed, the S-curve state, 3, will be transmitted. If the mechanism is in movement, and no other states has been set, the system is in manual pointing mode. A similar code is implemented into the calibration function, transmitting the state value "1" to inform the spacecraft of the calibration mode.

The mechanism's temperatures in the low earth orbit, LEO, will often vary from -25ºC and +65ºC. Depending on the amount of time the mechanism spends in direct sunlight, certain parts may get damaged or electronics may be exposed for radiation or interference. Implementing a temperature sensor allows the spacecraft to detect when the temperature rises above the desired levels, following a possible repositioning of the mechanism. Temperature readings are listed as a low-priority requirement, and remains to be implemented.

3.7.4.3. *Encoder Interrupt*
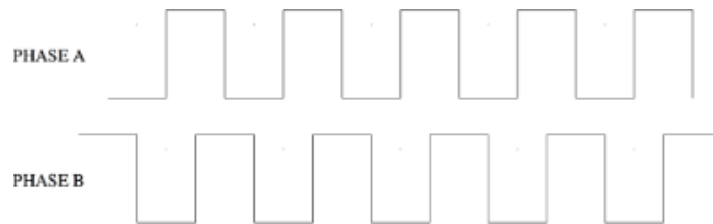
Figure 3. 7. 45: Encoder output

Encoders are fastened on both the motors for precision position readings. Each of the encoders have an accuracy of 4 096 positions per 360 degrees. Taking into account the gear ratio in relation to the actual mechanic rotation, this is multiplied by 17,5 giving 71 680 possible positions and an accuracy of 0.005 degrees. Reading the steps from the encoder is executed by connecting the phase A pin and the phase B pin to an interrupt pin on the microcontroller.

The microcontroller has 7 available software interrupt lines: 0, 1, 2, 3, 4, 5-9 and 10-15. The interrupt pins used are PE0 and PE1, with the corresponding interrupts in software, EXTI0 and EXTI1. Using pin PA0 for new interrupts will not create an independent interrupt, but distort the interrupt from PE0. The same applies to the 5 to 9 pins and 10 to 15 pins. Thus, 7 individual lines are available to use, with several external interrupt inputs on each line if desired.

```
/* Interrupt pin A. */
void EXTI0_IRQHandler(void)//A
{
  HAL_NVIC_ClearPendingIRQ(EXTI0_IRQn);
  HAL_GPIO_EXTI_IRQHandler(GPIO_PIN_1);
  {
  /*EXTI line interrupt detected */
  if(__HAL_GPIO_EXTI_GET_IT(GPIO_PIN_0) != RESET)
  {
    if(HAL_GPIO_ReadPin(GPIOE, GPIO_PIN_0))//IF A = HIGH
    {
      if(!HAL_GPIO_ReadPin(GPIOE, GPIO_PIN_1)){Encoder_Pos++; Virtual_Encoder_Pos++;}
      if(HAL_GPIO_ReadPin(GPIOE, GPIO_PIN_1)){Encoder_Pos--; Virtual_Encoder_Pos--;}
    }
    if(!HAL_GPIO_ReadPin(GPIOE, GPIO_PIN_0))//IF A = LOW
    {
      if(HAL_GPIO_ReadPin(GPIOE, GPIO_PIN_1)){Encoder_Pos++; Virtual_Encoder_Pos++;}
      if(!HAL_GPIO_ReadPin(GPIOE, GPIO_PIN_1)){Encoder_Pos--; Virtual_Encoder_Pos--;}
    }

    __HAL_GPIO_EXTI_CLEAR_IT(GPIO_PIN_0);
    HAL_GPIO_EXTI_Callback(GPIO_PIN_0);
  }
}
}
```

Figure 3. 7. 46: Interrupt handler for encoder position

Figure 3.7.46 shows the function updating the position of the mechanism. A Nested Vector Interrupt Controller, NVIC, is used to set the priority for every interrupt in the code. Both Encoder pin A and B have the same priority, while the UART, chapter 3.7.4.2.1, has a lower priority. Both the encoder position and the virtual encoder position are updated to get the pointing position, as explained in 3.7.4.5. Calibration. Each time the A interrupt is triggered, the program checks if the A pin is high. If this is the case, it means the encoder has just had a rising edge, and falling edge if it is low. Another check sees if the B trigger is high or low. Depending on the results, the positions get updated, and the

interrupt flag is cleared until the next interrupt trigger. The function for interrupt is an extension of the already defined library function for GPIO interrupt handling.

3.7.4.4. Current reading and moving average

The control system needs to read the amount of current in the motor phases to regulate the system. Current readings are used to adjust the voltage level output to the motor for regulating the amplitude of the SVPWM signal. The microcontroller reads input voltages via an analog to digital converter, ADC, from 0 to 3 volts. Since the voltage coming from the satellite will be 28 V, the op-amp circuit [12] is connected to the board's pin PC0 and PC1, which are set up as ADC inputs. The output from the op-amp is current.

```
float ADC_Poll_PhaseA(void)
{
  if (HAL_ADC_PollForConversion(&hadc1, 1) == HAL_OK)
        {
            return ((3.0f / 4096.0f) * HAL_ADC_GetValue(&hadc1)) - 1.5f;
        }
        return 0;
}
```

Figure 3. 7. 47: Polling the ADC input pin 0

To retrieve the values from the input, a poll function is executed as shown in figure 3.7.47. The input signal is a maximum of 4096 values, which is scaled down to between -1.5 and +1.5 to be within the required values for the regulator algorithms.

The values retrieved from the op-amp has regular spikes, giving faulty readings, and may impact the control system in a negative way. A moving average is calculated, retrieving the average value of 20 readings. Figure 3.7.48 shows how the array is filled up with one single value if this is the first time the function runs, and the last value is zero. Next, the ADC value is set into a place in the array, corresponding with the number of times the function has been running. All the new and old values in the array are added together, and in the end of the function, the average is returned to the regulators.

```c
float ADC_Average_PhaseA(void)
{
  float final_Val = 0;
  int n = 20;
  float current = ADC_Poll_PhaseA();

  //fill up on first run
  if(current_A[n-1] == 0)
      for(int z = 0; z < n; z++)
          current_A[z] = current;

  //assign variable to a place in the array
  current_A[A_inc] = current;

  //add all values together
  for(int y = 0; y< n; y++)
  final_Val += current_A[y];

  A_inc++;

  if(A_inc>=n)
    A_inc=0;

  //return total value divided by amount
  return final_Val/n;
}
```

Figure 3. 7. 48: Moving average of ADC polling for phase A

The polling function for the B phase is the same as the A phase, but the C phase is calculated as shown in figure 3.7.49:

```c
return (-ADC_Average_PhaseA() - ADC_Average_PhaseB());
```

Figure 3. 7. 49: Calculating Phase C current

3.7.4.5. Calibration

When the mechanism starts up, it has no way of knowing which position it is in. The mechanisms currently in space, designed by Kongsberg, are equipped with potentiometers, while some manufacturers use the encoders as a backup, allowing them to always know the pointing angles regardless of the encoders. Since this mechanism is totally dependent of incremental encoders for position readings, the position is reset each time the control system is switched off. To ensure correct pointing, the mechanism needs to be calibrated after each system reset.

```
/* Calibration of system. */
uint8_t CALIBRATION(void)
{
    TIM4->CCR1 = 1816;
    TIM4->CCR2 = 280;
    TIM4->CCR3 = 280;

    for(int i = 0; i<5000; i++)
    {
    Reference_Pos[i] = 0;
    }
Ref = 0;
    HAL_Delay(500);
    Encoder_Pos = 60;

int Cal_Count = 0;
int Encoder_Pos_2;
int Calibrated = 0;
```

Figure 3. 7. 50: Aligning the motor pole pairs and clearing position array

To allow the mechanism to be driven by the control loop, the motor pole pairs need to be aligned with the encoder. This means, the position that the controller thinks the motor pole pairs are in, needs to be the same as the encoder reading is in. If this is not the case, the motor will try to align with the encoder position, again changing the encoder position forward as the motor position changes forward. To counter this, in the beginning of the calibration function, the motor is forced into a set position, which is regarded by the control system as a 0-position. This is done by setting the start SVPWM values by forcing the motor in a certain position, then manually calibrating the encoder position in the code until the motor rotates at the same velocity in both directions when the control loop is executed. Effectively, on this motor, the encoder is placed 60 degrees on the pole pairs. This only needs to be done once, in the start of the calibration. Next, the array containing all the positions is reset, in case this calibration is not done after a system reset. A small delay gives the mechanism time to get to the given position, and the main calibration is ready to start:

```
while(!Calibrated)
{
  Encoder_Rads = (Encoder_Pos * ConvertToRads);
  el_Angle = Encoder_Rads * PolePairs * GearRatio;

  Theta_Position = ADD(-0.6, el_Angle, PI);

  Space_Vector = TIMING_CALC(4, Voltage, Theta_Position);

  TIM4->CCR1 = (Space_Vector.Ta+0.4f)*1137.8f;
  TIM4->CCR2 = (Space_Vector.Tb+0.4f)*1137.8f;
  TIM4->CCR3 = (Space_Vector.Tc+0.4f)*1137.8f;

  /* Transmit status and check if the mechanism has stopped. */
  Cal_Count++;
  if(Cal_Count >= millis * 100)//100 ms
    {
      /* Transmit. */
      if(txCount >= 10)// 1000 ms
      {
      Cal_Count = 0;
      if(Encoder_Pos == Encoder_Pos_2)
        {
          Calibrated = 1;
          Virtual_Encoder_Pos = 0;
        }
        else
          {
            Encoder_Pos_2 = Encoder_Pos;
          }
    }
}
  transmit_Buffer[1] = 0x0;
  HAL_UART_Transmit_IT(&huart4, transmit_Buffer, 8);
  return 0;
```

Figure 3. 7. 51: Calibration function while loop

The mechanism is driven with SVPWM all the way clockwise, until it arrives at the end-stop. When the controller sees that the encoder is not incrementing, but instead remains on the same position for about 100 milliseconds, it sets a new position called the virtual encoder position to 0. Finally, the controller sends a message declaring the calibration to be finished, and exits the while loop waiting for the calibration to complete. During the entirety of the calibration, position and calibration status is sent to the spacecraft.

The reason for setting a virtual position and not changing the encoder position variable, is that the motor's pole pairs are aligned with the encoder's position. The virtual encoder position is only used for the difference in position, not for generating the SVPWM signal sent to the motor, which is generated based on the motor/encoder position.

3.7.4.6. *Manual positioning*
The manual positioning is much like the automatic S-curve positioning, chapter 3.7.4.7, in that it is designed the same way as the spacecraft is expected to send its signals. The requested positions are received via UART, chapter 3.7.4.2.1, and are assigned to the reference position in the main function, chapter 3.7.4.8.

3.7.4.7. *Automatic S-Curve positioning*

A position initializing function is called to generate a velocity and acceleration based position curve. The satellite may want to point the satellite in a specific direction without sending an entire curve with acceleration and deceleration from their end. The reason for this might be the need for a quick adjustment of position to shield the mechanism from the sun, or simply to send it to a start position before a pass-by from another satellite. Either way, the function should be available for use, and will provide quick repositioning. The method for creating the S-curve will be similar to the way the spacecraft creates the S-curve for the manual positioning

3.7.4.7.1. Acceleration

Rotational acceleration is a fixed number, regulated by the internal spacecraft if necessary. The system accelerates when the mechanism is in the early stages of movement. The acceleration phase is calculated by incrementing the position value until the distance between each array value is higher than the maximum velocity set by the spacecraft. However, if the currently calculated position is halfway to the final position, the acceleration phase will also be over. The equation for the acceleration phase as calculated in the code is:

$$\theta_{+1} = \theta + 0.5\alpha t^2, \tag{3.7.20}$$

where θ is position in degrees, α is rotational acceleration and t is time. Figure 3.7.52 shows how this is implemented in the software.

```
while
  (fabsl(Reference_Pos[inc] - Reference_Pos[inc-1]) <= max_Vel * millis_Update &&
  ((pos_Req - start_Pos >= 0 && Reference_Pos[inc] <= (pos_Req - start_Pos)/2) ||
  (pos_Req - start_Pos <  0 && Reference_Pos[inc] >= (start_Pos - (start_Pos - pos_Req)/2))))
{
  Reference_Pos[inc+1] = pos_Req - start_Pos >= 0 ?
  Reference_Pos[inc]+0.5f*acc*((millis_Update*(inc+1))*(millis_Update *(inc+1))):
  Reference_Pos[inc]-0.5f*acc*((millis_Update*(inc+1))*(millis_Update *(inc+1)));
  inc++;
}

T2 = Reference_Pos[inc];
k = inc;
```

Figure 3. 7. 52: S-curve acceleration calculation

With the first four lines defining the parameters for when the acceleration will occur, and the next lines adding together the next position to be placed into the array.

When the acceleration phase is complete, the current position is saved as a value called T2. This value acts as a placeholder for the reference position where the acceleration loop has ended. The system will start its deceleration when the current position is larger than the requested position minus the position when the system decelerated, T2. When this occurs, the position steps are shortened with the use of the "k" value.
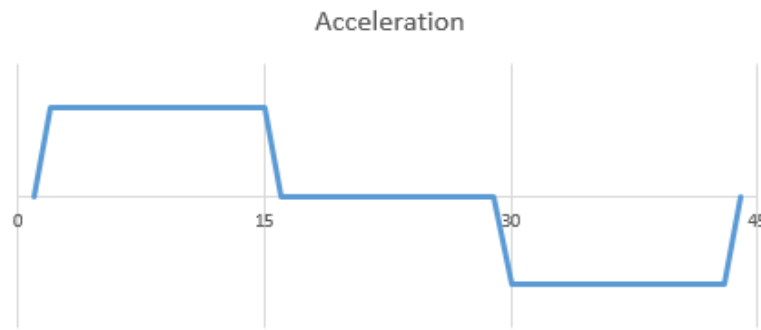
Figure 3. 7. 53: Trapezoidal acceleration profile

From figure 3.7.53, one can observe the four stages of the system:

- T1 – start of acceleration
- T2 – end of acceleration
- T3 – start of deceleration
- T4 – end of deceleration

If a position is requested that is lower than the current position the motor is stationed in, a "backward" statement is set true. This changes the values in the algorithm to compensate for negative difference in position, and keeps the deceleration start position (T2) the same, regardless of direction. Absolute values are also in place to ensure correct measurements. Absolute values are created using the "fabsl()" function, inputting a 64 bit floating point value and receiving a positive float, and the backward statements are the last statements in the while parameters. The multi-direction adjusted conditions are present in two of the while loops in the S-curve generation function; acceleration and velocity.

Deceleration happens at the end of the velocity phase, chapter 3.7.4.7.2, and the implementation in software is shown in figure 3.7.54. The velocity while loop is finished, and the deceleration while loop is entered. This loop runs until the "k"-variable reaches zero. Inside the loop is another positive/negative value condition, which slows down the position changes, applying deceleration. The formula is the same as in equation 3.7.20.

```
while(k > 0)
{
  Reference_Pos[inc+1] = pos_Req - start_Pos >= 0 ?
  Reference_Pos[inc] + 0.5f * acc * ((millis_Update * (k-1) ) * (millis_Update * (k-1) )):
  Reference_Pos[inc] - 0.5f * acc * ((millis_Update * (k-1) ) * (millis_Update * (k-1) ));
  inc++;
  k--;
}
```

Figure 3. 7. 54: S-curve deceleration calculation

3.7.4.7.2.   Velocity

After the acceleration calculations are over, the velocity loop is executed. The maximum velocity is determined by the spacecraft. If the current position is half way to the requested position, the velocity loop will be skipped. The equation for the velocity phase as calculated in the code is:

$$\theta_{i+1} = \theta_i + \omega t, \tag{3.7.21}$$

where ω is rotational velocity. Figure 3.7.55 shows the implementation in the software.

```
while
   ((pos_Req - start_Pos > 0 && Reference_Pos[inc] <= pos_Req - fabsl(T2) )||
   ( pos_Req - start_Pos < 0 && Reference_Pos[inc] - pos_Req >= start_Pos - fabsl(T2)))
{
   Reference_Pos[inc+1] = pos_Req - start_Pos >= 0 ?
   Reference_Pos[inc] + max_Vel * millis_Update:
   Reference_Pos[inc] - max_Vel * millis_Update;
   inc++;
}
```

Figure 3. 7. 55: S-curve Velocity calculation

Implementing the profile will give a velocity ramp as shown in figure 3.7.56, which is obtained from the acceleration in figure 3.7.53. The velocity is increased every clock cycle, based on the value obtained from the acceleration states.
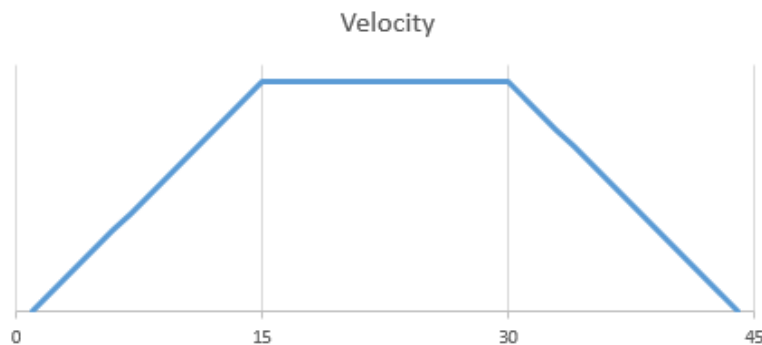
Figure 3. 7. 56: Trapezoidal velocity profile

The velocity while loop, like the acceleration while loop, has two conditions for two different scenarios. The first is only true when the requested direction is positive, or above zero. The other condition is when then request goes from a positive value to a negative. A similar check is executed in the loop itself, by the use of a simplified "if"-sentence, checking the direction of motion. The following addition, or subtraction, is decided by the condition. The conditions are true as long as the current position has not passed the requested value, minus the position when acceleration stopped.

3.7.4.8. *Position in the main function*

There are two ways of setting the position that the control system loop will use in the PI regulators. The first, and most common way, is the manual positioning command. When the spacecraft sends the requested position, the reference value in the PIDposition is changed from the "receive signal" function, as explained in 3.7.4.2.1. The reference variable is set into the position PI regulator. However, the automatic S-curve generation also accesses the reference variable. After the array of position values is filled up, a loop inn main is enabled. This loop controls the incremental speed of the given array, controlling the speed of the position shift, according to the delta time value in the position

initialize function. Each 10 milliseconds, the reference position is set equal to the current position, giving a smooth position curve.

```
if(INC_Position < Array_Values)
{
  INC_Position++;
  Ref = Reference_Pos[INC_Position] * 10;
  transmit_Buffer[1] = 0x3;
}
```

Figure 3. 7. 57: Set position from S-curve

The timing for the second count of the microcontroller is calculated by the frequency of the main method. Since the main loop is updated 61400 times per second, a function being called every 614 tick count will run every 10 millisecond. Likewise, a function being called every 6140 tick count will run every 100 millisecond. Figure 3.7.57 shows the time calculation for the assigning of position and transmission of status.

3.7.4.8.1. Velocity

To calculate the velocity of the actuator, the system position over time is found by subtracting the position by the previous position, calculated with 10 milliseconds in between, and multiplied by 100, to get the radians per second. The velocity is used in the PIDvelocity function, and also sent to the spacecraft as a status update together with position, 3.7.4.2.2. Figure 3.7.58 shows the implementation in software:

```
/* 2. Velocity. */
INC_Velocity++;
if(INC_Velocity >= millis * 10)
{
  Velocity =  (Encoder_Rads - Encoder_Rads_1) * 100;
  INC_Velocity = 0;
  Encoder_Rads_1 = Encoder_Rads;
}
```

Figure 3. 7. 58: Velocity calculation

3.7.4.9. *Inner control system loop*

The inner control system is the central part of the motor control. A model has been made as explained in chapter 3.7.1.1.3: Simulink model of the control system, which simulates the entire system regulating the motor. The inner control system loop's main task is to ensure the motor is driven with appropriate power, given the feedback from the rest of the system, together with the input from the spacecraft.

3.7.4.9.1. PI Position

The PI regulators are set up in the same manner in software as in the Simulink model. In the code, the functions have four variables: Error, Kp and Ki. The error is calculated in its own function, chapter 3.7.4.9.2, and the error value is returned and used in the PI regulators. The Kp and Ki values are adjusted with the Ziegler-Nichols tuning, 3.7.1.2.3, in addition to some compromises between accuracy and smooth motion. The resulting value is calculated as a discrete function. This function can be found by applying the ZOH method to a standard PI regulator [3]:

$$\frac{U(s)}{E(s)} = \left(K_p + \frac{K_i}{s}\right),$$ (3.7.22)

where U(s) is the output, E(s) is the error and s is the Laplace operator equal to $j\omega$.

Using the ZOH method to make a discrete equivalent:

$$\frac{U(z)}{E(z)} = K_p + \frac{TK_i z^{-1}}{1 - z^{-1}}$$ (3.7.23)

$$= \frac{U(z)}{E(z)} = \frac{K_p - K_p z^{-1} + TK_i z^{-1}}{1 - z^{-1}}$$ (3.7.23.1)

$$= U(z)(1 - z^{-1}) = E(z)\left(K_p - K_p z^{-1} + TK_i z^{-1}\right).$$ (3.7.23.2)

Where T is the sampling time and z is the z-operator equal to $re^{j\omega}$. Performing the inverse Z-transform, the difference equation or algorithm can be found as:

$$u(n) = u(n-1) + K_p e(n) + \left(K_i T - K_p\right)e(n-1).$$ (3.7.24)

Where n represents the current sample and $n-1$ represents the last sample. An example of the implementation is shown in figure 3.7.60.

The new PI output is returned from the function.

```
/* Error_pos-velocity(error), PID-regulator, (float, Kp, Ki). */
PID_Velocity = PID_Vel(Calc_Error(PID_Position, Velocity),1, 0);
```

Figure 3. 7. 59: Velocity regulator input in main function

```
/* PID regulator for Position and Velocity feedback. */
float PID_Vel(float Error, float Kp, float Ki)
{
  PID_Vel_u = PID_Vel_u + Kp * Error + (Ki * Clock_Time - Kp) * Vel_Error_1;
  Vel_Error_1 = Error;
  return PID_Vel_u;
}
```

Figure 3. 7. 60: Velocity regulator calculations

3.7.4.9.2. Error

The error function takes an input value and subtracts the second input value. The function has two float inputs, and returns the difference. The error function was created to get the difference between two values, for use in the PI regulators, in a way that maintained the Simulink circuit structure. A larger error results in a higher PI value.

```
/* Error calculations. */
float Calc_Error(float Reference, float Difference)
{
  return Reference - Difference;
}
```

Figure 3. 7. 61: Error calculation

3.7.4.9.3.   Clarke and Park transformation

The Clarke and Park transformation, from 3.7.1.3.1, contains the same formulas as the Simulink model. The input comes from the three current inputs; phase A, B and C, in addition to the electrical angle of the encoder. The function returns a structure containing two floats, which are the Id and Iq currents later used in PI regulators.

```c
/* Clark and park transform, (PhaseA, PhaseB, PhaseC, Angle). */
I = Clark_Park_Trans(ADC1_Val, ADC2_Val, ADC3_Val, el_Angle);
```

Figure 3. 7. 62: Clarke and Park transformation input

```c
/* Clark and Park transformation. */
current_struct Clark_Park_Trans(float Ia, float Ib, float Ic, float el_angle)
{
  current_struct output;

  float alpha = (2.0f/3.0f * (Ia - 0.5f * Ib - 0.5f * Ic));
  float beta = (2.0f/3.0f * sqrtf(3.0f)/2.0f * (Ib - Ic));

  output.Iq = cosf(el_Angle) * alpha + sinf(el_Angle) * beta;
  output.Id = sinf(el_angle) * alpha - cosf(el_angle) * beta;

  return output;

}
```

Figure 3. 7. 63: Clarke and Park transformation calculations

3.7.4.9.4.   Magnitude

The magnitude function limits the voltage reference input to the creating of the space vector values, chapter 3.7.4.9.6. The function receives the Id and Iq values as a structure, and uses them in the calculation. The function is set up with the spacecraft supply voltage as the top limit, in turn limiting the space vector values to coincide with the specified PWM spectrum, chapter 3.7.4.9.6.1.

```c
/* calculating current magnitude. */
float MAGNITUDE(current_struct current)
{
  if (sqrtf((current.Iq)*(current.Iq) + (current.Id)*(current.Id)) >= Voltage)
    return Voltage;
  else
    return sqrtf((current.Iq)*(current.Iq) + (current.Id)*(current.Id));
}
```

Figure 3. 7. 64: Voltage magnitude calculations

3.7.4.9.5.   Anti zero phase and ADD

The anti-zero phase function is the software implementation of chapter 3.7.3.1.1.2. To avoid division of zero, the function has a failsafe stating if Id equals to zero, the return value will default in pi/2. This is the approximate value of the calculation when the tangent function goes towards zero.

```c
/* calculating Anti zero-phase shift. */
float ANTI_ZERO_PHASE(current_struct current)
{
  if(current.Id > 0) return atanf(current.Iq / current.Id);
  else if(current.Id <0)  return PI + atanf(current.Iq / current.Id);
  else return PI/2;
}
```

Figure 3. 7. 65: Anti zero phase calculations

The anti-zero phase function returns a value that is used to calculate the theta position for space vector calculations. The anti-zero phase, electrical angle and pi are added together as shown in figure 3.7.66.

```c
/* Add anti zero-phase, electric angle and pi/2. */
float ADD(float PhaseShift, float angle, float pi)
{
  return PhaseShift + angle - pi/2;
}
```

Figure 3. 7. 66: The add function calculation

3.7.4.9.6. Timing calculation

The timing calculation function contains the same formula as shown in chapter 3.7.3.1.1.2.1. The input contains the voltage reference (chapter 3.7.4.9.4), total voltage and theta position (chapter 3.7.4.9.5). Figure 3.7.67 shows part of the function, defining sectors for the space vector values (chapter 3.7.1.5.1).

```c
/* Calculate the Space Vector values. */
spaceVector_struct TIMING_CALC(float V_Ref, float V_DC, float Pos_Theta)
{
  /* Theta position. */
  float a = Pos_Theta / (2.0f*PI);
  float b = floorf(a);
  float c = Pos_Theta - 2.0f * PI * b;
  float d = c / (PI / 3.0f);
  float e = floorf(d);

  /* Output. */
  float Angle = c - e * PI / 3.0f;
  int Sector = e + 1.0f;

  /* Velocity. */
  float V = V_Ref / V_DC;

  /* calc. */
  float A = V * sqrtf(3.0f) * sinf((PI / 3.0f) - Angle);
  float B = V * sqrtf(3.0f) * sinf(Angle);
  float C = (1 - A - B) / 2.0f;
```

Figure 3. 7. 67: Sector timing calculation

Figure 3.7.68 shows the software implementation of chapter 3.7.1.5.1.3. A structure containing the Ta, Tb and Tc-phase values is returned.

```
/* Assign sector values. */
spaceVector_struct SV;

if(Sector == 1){SV.Ta = A+B+C;  SV.Tb = B+C;    SV.Tc = C;}
if(Sector == 2){SV.Ta = A+C;    SV.Tb = A+B+C;  SV.Tc = C;}
if(Sector == 3){SV.Ta = C;      SV.Tb = A+B+C;  SV.Tc = B+C;}
if(Sector == 4){SV.Ta = C;      SV.Tb = A+C;    SV.Tc = A+B+C;}
if(Sector == 5){SV.Ta = B+C;    SV.Tb = C;      SV.Tc = A+B+C;}
if(Sector == 6){SV.Ta = A+B+C;  SV.Tb = C;      SV.Tc = A+C;}

return SV;
}
```

Figure 3. 7. 68: Determining switching times of the transistors

3.7.4.9.6.1. PWM switching and resolution values.

The timer set up for PWM contains three channels for PWM output. The three channels are assigned values based on the phase values retrieved from the timing calculation (chapter 3.7.4.9.6). These phase values are regulated according to the input voltage in the magnitude calculations (chapter 3.7.4.9.4), giving values between 0 and 1,4. The PWM resolution/period for the timer in use is set for 2048. The resolution is a result of dividing the system clock with the pre-scaler value, and again divide by the desired operational frequency for the PWM signal. Low frequencies will generate noticeable noise, resonating from the motor coil. With a system clock of 168 MHz, a pre-scaler of 1, and a desired frequency of around 82 kHz, the period is set to 2048. Therefore, to get a matching resolution, the space vector values are multiplied by 1463, giving a range of approximately 0 to 2048.

3.7.4.9.7. PI control

The PI regulator values were set up and tested before the functional test at KDA. The following values are currently set in the control loop:

Table 3. 7. 4: Regulator values

PI regulator	Kp	Ki
Position	150	0
Velocity	1	0
Current(Id)	1	0.8
Current(Iq)	1	0.8

3.7.4.10. *Control system conclusion*

The software is comprised of several modules, all working together to ensure the functionality of the system. The UART implementation allows the system to receive commands via the UART serial bus. The system also sends status updates back to the internal spacecraft, containing status, position and velocity. Additional feedback can easily be implemented.

The position of the system is regulated according to the encoder position, giving an actuator resolution of approximately 71680 steps for 360 degrees, with received commands having the resolution of 36 000 degrees. A calibration function is in place to ensure the mechanism is in the right position, and the pole pairs of the motor are aligned with the encoder steps.

The control loop, designed in Simulink, is implemented in a straightforward manner, keeping the block structure to ensure efficient tweaking and a simple overview.

3.7.5. References

[1] S. Laugerud, G. H. Stenseth and T. Sundnes, "Components trade-off," Small Satellite Mechanisms, Kongsberg, SSM-5111, Rev 1.0, 2016.

[2] Wikipedia, "Wikipedia," [Online]. Available: https://en.wikipedia.org/wiki/PID_controller#Cascade_control . [Accessed 18 04 2016].

[3] G. e. al, Feedback Contol of Dynamic Systems, Harlow, England: Pearson Education Limited, 2015.

[4] Microsemi, "Park, Inverse Park and Clarke, Inverse Clarke Transformations, MSS Software Implementation, User guide," Microsemi Corporation, Aliso Viejo, 2013.

[5] J. Jung, "Project #2 Space Vector PWM inverter," 20 02 2005. [Online]. Available: http://www2.ece.ohio-state.edu/ems/PowerConverter/SpaceVector_PWM_Inverter.pdf.

[6] G. H. Stenseth and M. Dybendal, "Requirement specifications," Small Satellite Mechanisms, Kongsberg, SSM-2000, Rev 2.0, 2016.

[7] Maxon Motor, "Datasheet: EC 45 flat, Ø42.8mm, brushless, 70 Watt," [Online]. Available: http://www.maxonmotor.com/medias/sys_master/root/8816806920222/15-263-EN.pdf. [Accessed 18 04 2016].

[8] STMicroelectronics, "STM32CubeF4," 2015. [Online]. Available: http://www2.st.com/resource/en/data_brief/stm32cubef4.pdf. [Accessed 16 05 2016].

[9] ARMKeil, "www.keil.com," ARMKeil, 2016. [Online]. Available: http://www2.keil.com/mdk5/uvision/. [Accessed 16 05 2016].

[10] STMicroelectronics, "www.st.com," 2016. [Online]. Available: http://www2.st.com/resource/en/datasheet/stm32f405rg.pdf. [Accessed 16 05 2016].

[11] STMicroelectronics, "UM1725 user manual," 2015. [Online]. Available: http://www.st.com/st-web-ui/static/active/jp/resource/technical/document/user_manual/DM00105879.pdf. [Accessed 16 05 2016].

[12] G. H. Stenseth and S. Laugerud, "SSM-5141, Electrical design document," USN, KIFI, SSM, Kongsberg, 2016.

[13] C. Lewin, "Mathematics of Motion Control Profiles," Performance Motion Devices, Lincoln, 2007.

[14] D. russell, Introduction to Embedded Systems, Lincoln: Morgan&Claypool publishers, 2010.

[15] E. Z. M.Morari, Robust process control, Englewood Cliffs: Prentice-Hall, 1991.

[16] StackExchange, " Robotics-beta," [Online]. Available: http://robotics.stackexchange.com/questions/261/what-do-the-commutation-waveforms-look-like-for-a-brushless-motor. [Accessed 20 04 2016].

[17] Texas Instruments, "Implementation of Vector Control for PMSM Using the TMS320F240 DSP," 12 1998. [Online]. Available: http://www.ti.com/lit/an/spra588/spra588.pdf. [Accessed 19 04 2016].

3.8. Antenna trade-off

i.   Abstract

This chapter is a trade-off analysis, where two different antenna designs for the Antenna Pointing Mechanisms Assembly are evaluated. The analysis includes calculations of size, mass, gain and losses for a Cassegrain- and a horn antenna design. The concepts are compared and the favorable concept for this project is chosen.

ii. Contents

iii. List of figures

iv. List of tables

v. Document history

Table 3. 8. 1: Document history

Rev.	Date	Author	Approved	Description
0.1	10.03.16	EL, GHS		Document created
1.0	22.03.16	EL, GHS	TS	Reviewed and published
1.1	15.04.16	EL		Changed layout into the final report layout.
2.0	19.05.16	EL, GHS	MD	Reviewed and published

3.8.1. Introduction

The antenna pointing mechanism assembly has an antenna subsystem for receiving and transmitting a radio signal. An antenna converts electric power into radio waves and vice versa. The APMA shall be able to communicate full duplex with a carrier frequency at 23 GHz and with an overall system gain at $\geq$ 23 dBi, [5].

In this trade-off, two different antenna concepts are evaluated: The horn antenna (conical and corrugated) and the Cassegrain antenna. The concepts are explained and evaluated in detail comparing dimensions, simulations and calculations. The purpose of this trade-off is ultimately to select the antenna system design for the APMA, which satisfies the given requirements for gain and carrier frequency.

3.8.2. Cassegrain antenna design

In [1], different types of reflector antennae were evaluated (Gregorian, Cassegrain and Front Feed). Because of the sub-reflector's distance on the Gregorian antenna and the low efficiency of the front feed antenna, the Gregorian design is discarded.

In this design, the feed is placed at the center of the dish, and a hyperbolical sub-reflector is placed in front of the focal point [2]. The signal is reflected off the hyperbolic reflector and into the feed.
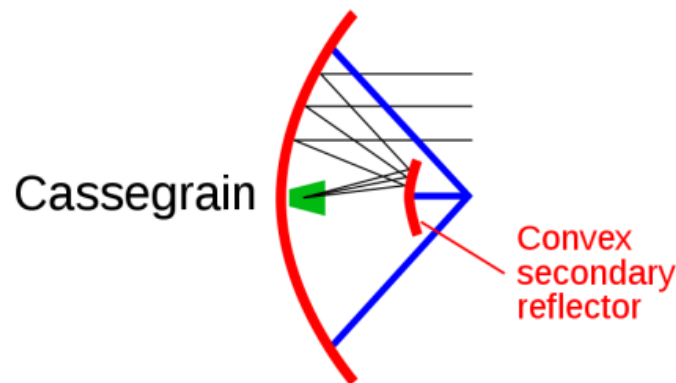
Figure 3. 8. 1: Cassegrain antenna design [7]

3.8.2.1. *Geometry of the Cassegrain antenna system*

Figures 3.8.2, 3.8.3 and 3.8.4 give an overview of the geometry of the Cassegrain antenna design. The calculations and dimensioning of the actual antenna system design for the APMA are mainly derived using the formulas and geometry from these figures:
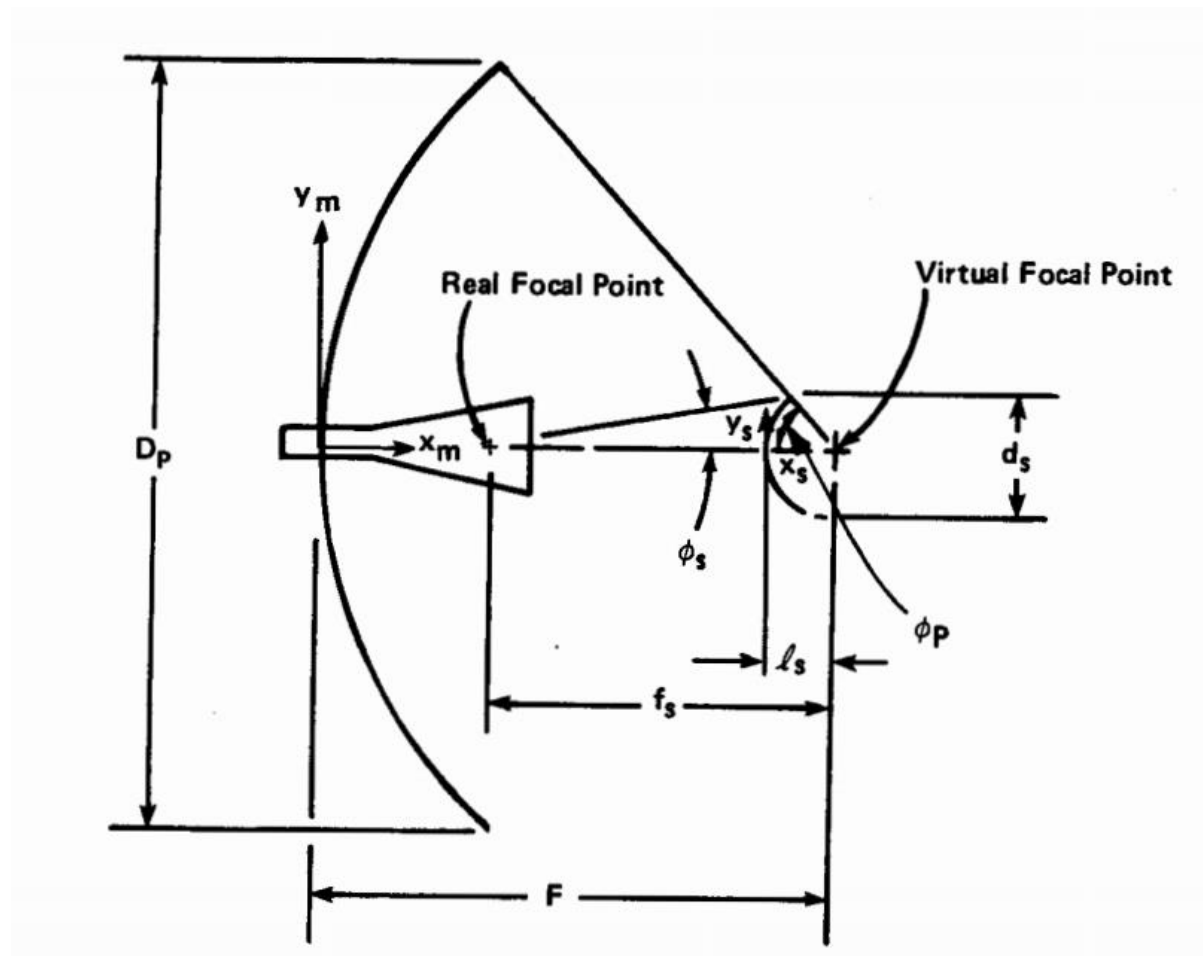
Figure 3. 8. 2: Geometry of the Cassegrain antenna design [3]
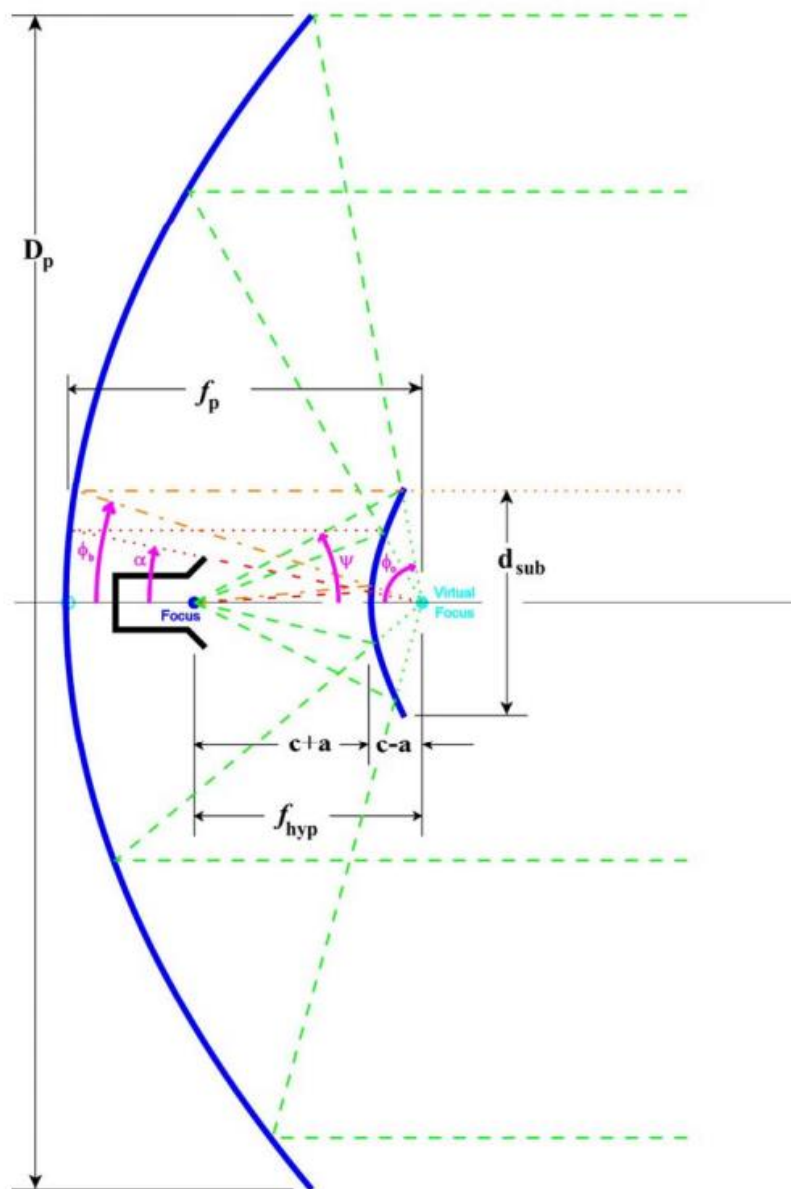
Figure 3. 8. 3: Geometry of the Cassegrain antenna design 2, [4]
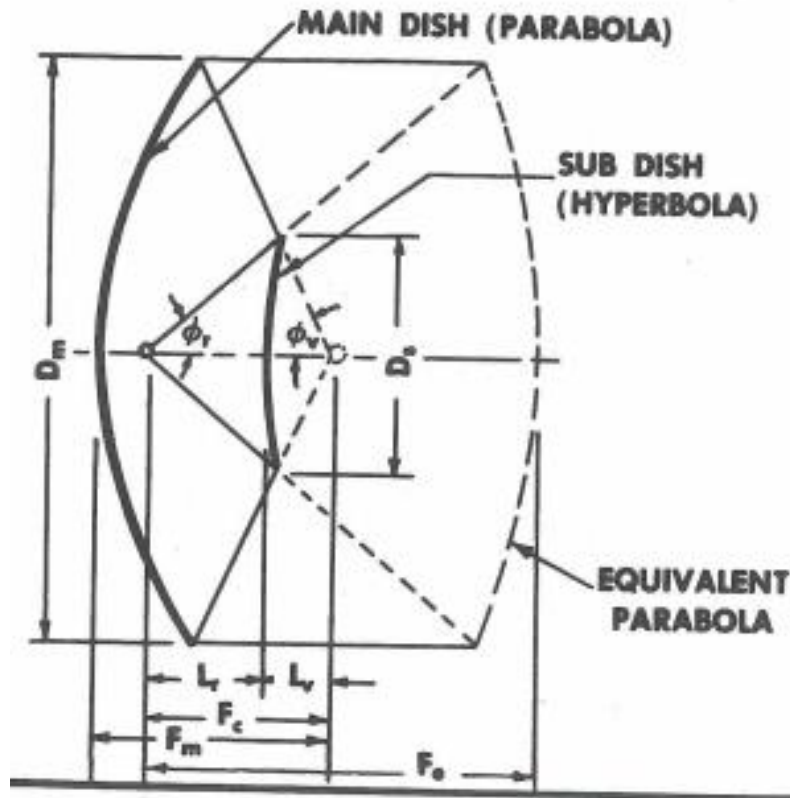
Figure 3. 8. 4: Geometry of the Cassegrain antenna design 3, [5]

Figure 3.8.2 and 3.8.3 have almost the same geometry and parameters. Figure 3.8.4 shows a different geometry, where some of the parameters are given by a fictional equivalent reflector placed to the right of the sub-reflector. This makes the formulas a bit different, but the ratios between the parameters should equal the other designs.

Figure 3.8.2, 3.8.3 and 3.8.4 uses different parameter names in their geometry. The calculations in this trade-off are based on all the three figures. Table 3.8.2 gives an overview of the parameters used in further calculations:

Table 3. 8. 2: Parameter overview

D_m	Diameter, main-reflector	D_w	Diameter, waveguide
d_m	Depth, main-reflector	f_s	Difference between real focal point and virtual focal point, ref. fig 3.8.2.
F_m	Focal length, main-reflector	F_e	Focal length, equivalent reflector, ref fig 4.
φ_m	Subtended angle, main-reflector	a	Difference, ref. fig. 3.8.3.
D_s	Diameter, sub reflector	c	Difference, ref. fig. 3.8.3.
d_s	Depth, sub-reflector	L_r	Difference, ref. fig 3.8.4.
φ_s	Subtended angle, sub-reflector	L_s	Difference, ref. fig. 3.8.4

3.8.2.2. *Design of the Cassegrain antenna system for the APMA*

3.8.2.2.1.   Main-reflector design

The wavelength of a signal is given by the general formula, Eq. 3.8.1:

$$\lambda = \frac{c}{f} = \frac{3 \cdot 10^8 m/s}{23 \cdot 10^9 Hz} = 0.01304 \text{ m},$$

(3.8.1)

where c is the speed of light ($3.0 \cdot 10^8$ m/s) and f is the signal frequency.
The gain of a parabolic antenna is calculated using Eq. (3.8.2) [3], p. 44,

$$G = 10 log_{10} \left(\left(\frac{\pi D}{\lambda} \right)^2 \eta \right),$$

(3.8.2)

where G is the gain in dBi, D is the diameter of the parabola, λ is the wavelength of the system and η is the efficiency constant. The efficiency η of the Cassegrain antenna is ~65-70% [4]. In these calculations the efficiency constant, η, is set to 0.55.

The given requirement for gain is that the overall system shall have a gain of ≥ 23 dBi [5]. This has to be taken into account when dimensioning the antenna system. Figure 3.8.5 shows the relationship between the diameter and the gain of the antenna at 23 GHz with $\eta = 0.55$.
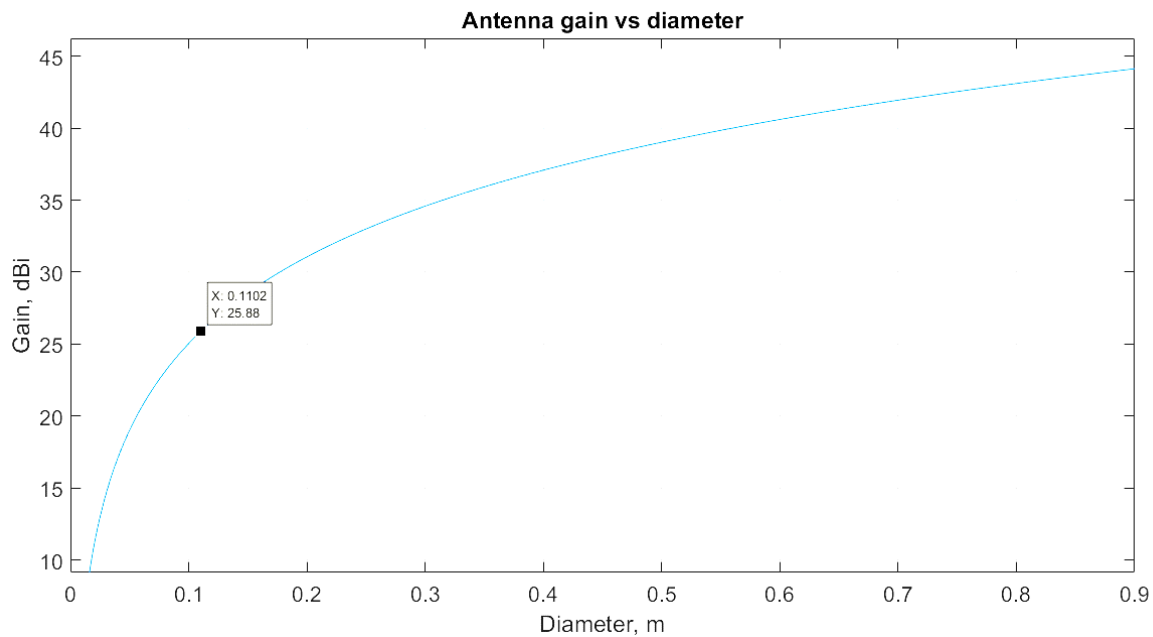
Figure 3. 8. 5: Antenna gain vs. diameter

The diameter of the main reflector for the APMA is chosen to be 11 cm. This gives a gain of 25.88 dBi, where the system has a "risk factor" of 0.55 for different losses. Typically, losses in the system are found in the waveguide, blockage and diffraction due to the sub-reflector, edge taper and electrical losses.

The depth of the reflector antenna, d_m, is estimated to be 1.8 cm.

Figure 3.8.6 shows the definition of the subtended angle, ψ_0 and the focal length, f, of a parabola.
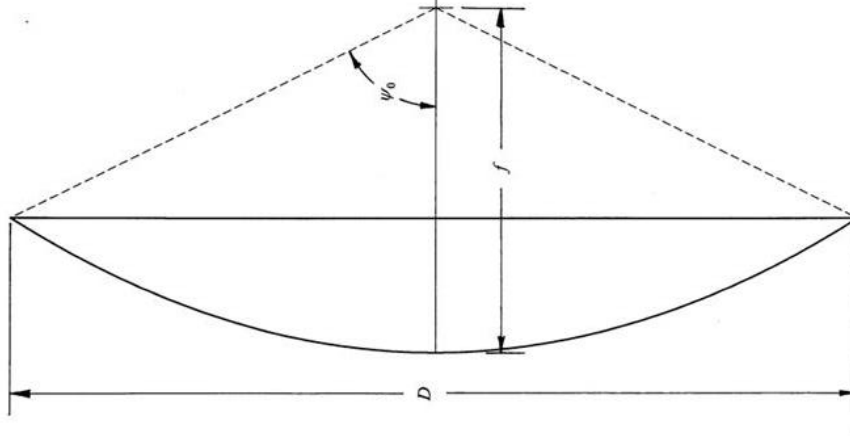
Figure 3. 8. 6: The subtended angle of a parabola. [9]

The focal length of the main reflector is given by Eq. 3.8.3, [6]:

$$F_m = \frac{D_m{}^2}{16\,d_m},$$

(3.8.3)

where D_m is the diameter and d_m is the depth of the main reflector.

$$F_m = \frac{0.11^2}{16 \cdot 0.018} = 0.0420\ m$$

(3.8.3a)

The subtended angle of the main reflector is given by Eq. 3.8.4, [7] sec. 36-4 :

$$\varphi_m = 2\,tan^{-1}\left(0.25\frac{D_m}{F_m}\right),$$

(3.8.4)

where D_m is the diameter and F_m is the focal length of the main reflector.

$$\varphi_m = 2\,tan^{-1}(0.25 \cdot \frac{0.11\ m}{0.0420\ m}) = 66.41°$$

(3.8.4a)

To verify the calculated parameters for the main reflector, the parameter relationship is checked using Eq. 3.8.5, [8], p. 18:

$$\frac{F_m}{D_m} = \frac{1}{4\tan(0.5\ \varphi_m)},$$

(3.8.5)

where F_m is the focal length and D_m is the diameter of the main reflector, φ_m is the subtended angle. The ratios are calculated below, and are equal each to other:

$$\frac{F_m}{D_m} = \frac{0.0420\ m}{0.11\ m} = 0.382$$

(3.8.5a)

$$\frac{1}{4\tan(0.5\ \varphi_m)} = \frac{1}{4\tan(0.5 \cdot 66.41)} = 0.382$$

(3.8.5b)

Eq. 3.8.5a and 3.8.5b are equal each other as expected, and then the ratio between the dimension of the focal length, F_m, the diameter of the main reflector, D_m and the subtended angle, φ_m are optimal.

A parabolic reflector reflects less energy at the edge of the dish than at the center, and the loss due to this is called the edge taper. The edge taper in dB, due to the main reflector, is given by Eq. 3.8.6, [9]:

$$edge\ taper = 20 \log \cos^2\left(\frac{\varphi_m}{2}\right),$$

(3.8.6)

where φ_m is the subtended angle of the main reflector.

$$edge\ taper = 20 \log \cos^2\left(\frac{66.413}{2}\right) = -3{,}0972\ dB$$

(3.8.6a)

3.8.2.2.2.　Design of the feed element

The diameter of the circular waveguide required for a carrier frequency of 23 GHz is 10.06 mm, [10] [11].

A feed horn, which has a larger diameter than the waveguide, results in a larger sub-reflector and higher blockage losses. Due to the required carrier frequency at 23 GHz in addition to the gain in the main reflector and the small size of the overall antenna design, this is unfavorable. The sub-reflector has to be as small as possible to minimize the blockage of the signal. Instead of using a feed horn, the antenna system for the APMA is designed with an open-ended circular waveguide as the feed element.

Figure 3.8.7 shows the far field pattern of the signal for the chosen open-ended waveguide. The optimum subtended angle related to the waveguide and the sub-reflector is the angle that gives a taper of 10 dB, [12], sec. 4. This results in an angle φ_s of approximately 30 degrees (ref. figure 3.8.7), which will be used in further calculations of the antenna design.
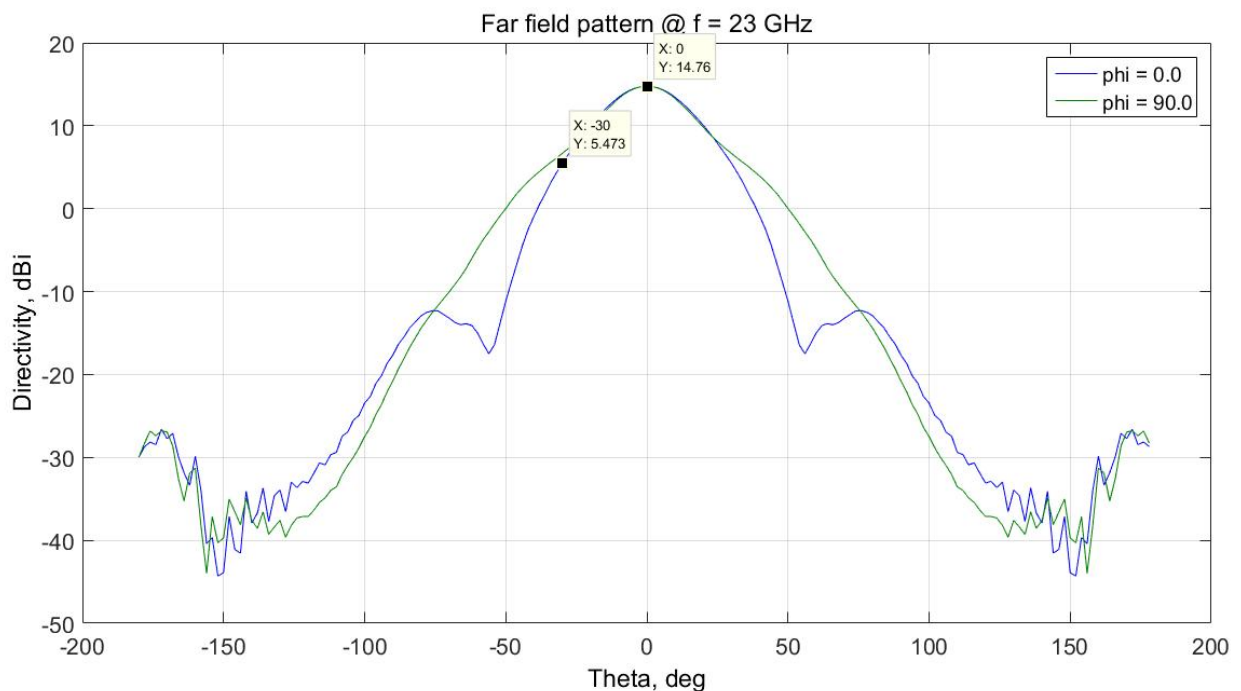
Figure 3. 8. 7: Far field pattern of the open-ended waveguide

3.8.2.2.3.   Reflector antenna equivalent

The subtended angle of the equivalent reflector (related to the feed and the sub-reflector) is derived from the radiation pattern of the signal from the waveguide, $\varphi_s = 30.0°$.

Focal length of the reflector antenna equivalent is given by Eq. 3.8.7 [8], p.18:

$$F_e = \frac{D_m}{4 \tan(0.5\varphi_s)} , \qquad (3.8.7)$$

where D_m is the diameter of the main reflector (The diameter of the equivalent reflector equals the main reflector). and φ_s is the subtended angle of the equivalent reflector.

$$F_e = \frac{0.11}{4 \tan(0.5 \cdot 30)} = 0.1026 \text{ m.} \qquad (3.8.7a)$$

To verify the relationships between the calculated parameters, Eq. 3.8.8, [8], sec 36-4, is used:

$$\frac{F_e}{F_m} = \frac{\tan(0.5 \, \varphi_m)}{\tan(0.5 \, \varphi_s)} , \qquad (3.8.8)$$

where F_e and F_m are the focal lengths of the equivalent and the main reflectors, and φ_s and φ_m are the related subtended angels. With inserted values, the formula is given by Eq. 3.8.8a and 3.8.8b:

$$\frac{F_e}{F_m} = \frac{0.1026 \, m}{0.0420 \, m} = 2.443 \qquad (3.8.8a)$$

$$\frac{\tan(0.5 \, \varphi_m)}{\tan(0.5 \, \varphi_s)} = \frac{\tan(0.5 \cdot 66.41)}{\tan(0.5 \cdot 30.0)} = 2.443. \qquad (3.8.8b)$$

3.8.2.2.4.   Sub-reflector design

The optimum diameter of the sub-reflector is given by Eq. 3.8.9, [12]:

$$D_{so} = \left| \frac{E\lambda \, (\cos(0.5\varphi_s))^4}{D_m 4\pi^2 \sin(\varphi_m)} \right|^{\frac{1}{5}} , \qquad (3.8.9)$$

where E is the edge taper as a ratio: $E = 10^{\left(\frac{taper \; in \; dB}{10}\right)}$ [12], λ is the wavelength, φ_s and φ_m are the subtended angles and D_m is the diameter of the main reflector. With inserted values, the edge taper is given by Eq. 3.8.10:

$$E = 10^{\left(\frac{-3.0972}{10}\right)} = 0.490, \qquad (3.8.10a)$$

and then the optimal diameter of the sub-reflector is given by Eq. 3.8.9a:

$$D_{so} = \left| \frac{0.049 \cdot 0.013\ m \cdot (\cos(0.5 \cdot 30))^4}{0.11m \cdot 4\pi^2 \sin(66.41)} \right|^{\frac{1}{5}} = 0.0295.$$

(3.8.9a)

Due to the overall small size of the antenna system, the sizes of the main reflector, waveguide and related angles, the diameter for the sub-reflector was estimated using SolidWorks to 0.02245 m. This value is used in further calculations.

Eq. 3.8.11, [7], sec 36-4, gives the relationship between the diameter of the sub-reflector and the distance between the two focal points (ref. figure 3.8.2):

$$f_s = D_s \frac{1}{2} (\cot(\varphi_m) + \cot(\varphi_s))$$

(3.8.11)

where f_s is the distance between the two focal points (main and equivalent reflector), φ_m and φ_s are the subtended angles.

$$f_s = 0.02245 \cdot \frac{1}{2} (\cot(66.41) + \cot(30)) = 0.0243$$

(3.8.11a)

To verify the relationships between the parameters in the sub-reflector design, Eq. 3.8.12, [8] sec. 36-4, is used to calculate and compare the following ratios:

$$\frac{\frac{D_s}{D_m}}{\frac{f_s}{F_m}} = \frac{\tan(\varphi_m)\tan(\varphi_s)}{2\tan(0.5\varphi_m)(tan(\varphi_m) + \tan(\varphi_s))},$$

(3.8.12)

where D_s and D_m are the diameter of the sub- and main reflector, f_s is the difference between the focal points and F_m is the focal length of the main reflector.

$$\frac{\frac{D_s}{D_m}}{\frac{f_s}{F_m}} = \frac{\frac{0.02245\ m}{0.11\ m}}{\frac{0.0243\ m}{0.042\ m}} = 0.3522$$

(3.8.12a)

$$\frac{\tan(\varphi_m)\tan(\varphi_s)}{2\tan(0.5\varphi_m)(tan(\varphi_m) + \tan(\varphi_s))} =$$

$$\frac{\tan(66.41) \cdot \tan(30)}{2 \cdot \tan(0.5 \cdot 66.41) \cdot (\tan(66.41) + \tan(30))} = 0.3522$$

(3.8.12b)

The distance between the center of the sub-reflector and the focal point of the main-reflector (ref. figure 3.8.2), is given by eq. 3.13, [8] p. 18:

$$l_s = 0.5 \left(1 - \frac{\sin(0.5(\varphi_m - \varphi_s))}{\sin(0.5(\varphi_m + \varphi_s))} \right) f_s,$$

(3.8.13)

where φ_m and φ_s are the subtended angles for the main- and sub-reflector and f_s is the distance between the two focal points.

$$l_s = 0.5 \left(1 - \frac{\sin(0.5(66.41-30))}{\sin(0.5(66.41+30))}\right) \cdot 0.0243 \, m = 0.00632 \text{m}$$

(3.8.13a)

The ratio between l_s and l_r (the distance from the center of the sub-reflector to the center of the main-reflector.) should equal the ratio $F_e/F_m = 2.443$, calculated in eq. 3.8.14 [8]:

$$\frac{L_r}{L_s} = \frac{f_s - L_s}{L_s} = \frac{0.0243 \, m - 0.0071 \, m}{0.0071 m} = 2.443$$

(3.8.14)

3.8.2.2.5. Blockage and diffraction losses due to the sub-reflector

The sub-reflector blocks some parts of the incoming signal due to its placement. This is an important factor for the efficiency of the antenna subsystem, and has to be taken into consideration in these calculations.

The size of the feed element, in this case the waveguide, has to be related to the sub-reflector. Then the angle shadowed by the feed element is smaller than the angle shadowed by the sub-reflector, and the feed element does not cause any loss. To ensure this, α has to be smaller than φ_b, ref. fig. 3.8.3. This has been taken into account in the design. The angles approximately equal each other, and the blockage by the feed is almost eliminated.

An approximated efficiency for the combination of blockage and diffraction losses by the sub-reflector is given by eq. 3.8.15, [13]:

$$\eta = \left[1 - C_b \left(1 + 4 \sqrt{1 - \frac{D_s}{D_m}}\right)\left(\frac{D_s}{D_m}\right)^2\right]^2,$$

(3.8.15)

where η is the efficiency, D_s is the sub-reflector diameter, D_m is the reflector diameter and C_b is given by [13]:

$$C_b = \frac{-\ln(\sqrt{E})}{1 - \sqrt{E}},$$

(3.8.16)

where E is the edge taper as a ratio [13]:

$$E = 10^{\left(\frac{egde \; taper \; in \; dB}{10}\right)}.$$

(3.8.10)

With inserted values for the parameters, the edge taper is given by Eq. 3.8.10a, C_b is given by eq. 3.8.16a and the efficiency, η, is given by Eq. 3.8.15a:

$$E = 10^{\left(\frac{-3.0972}{10}\right)} = 0.4901$$

(3.8.10a)

$$C_b = \frac{-\ln(\sqrt{0.4901})}{1 - \sqrt{0.4901}} = 1.1889$$

(3.8.16a)

$$\eta = \left[1 - 1.1889\left(1 + 4\sqrt{1 - \frac{0.0225\,m}{0.11\,m}}\right)\left(\frac{0.0225\,m}{0.11\,m}\right)^2\right]^2 = 0.5987$$

(3.8.15a)

Figure 3.8.8 shows the relationship between the diameter of the sub-reflector and the efficiency coefficient due to blockage- and diffraction losses:
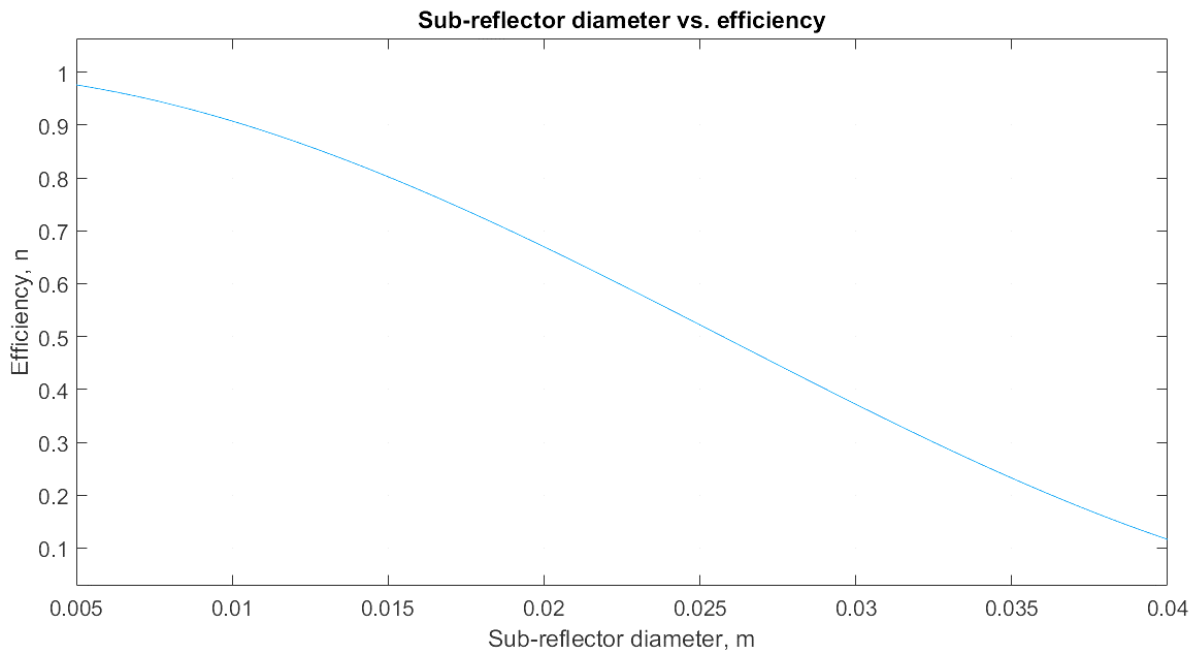
Figure 3. 8. 8: Diameter of the sub-reflector vs efficiency (blockage and diffraction).

The efficiency constant due to blockage and diffraction losses from the sub-reflector is 0.5987. The losses due to blockage and diffraction in dB can be calculated by eq. 3.8.17:

$$L = 10\log(\eta) = 10\log(0.5987) = \text{-2.23 dB}$$

(3.8.17)

Figure 3.8.9 shows the relationship between the diameter of the sub-reflector and the losses due to blockage and diffraction in dB:
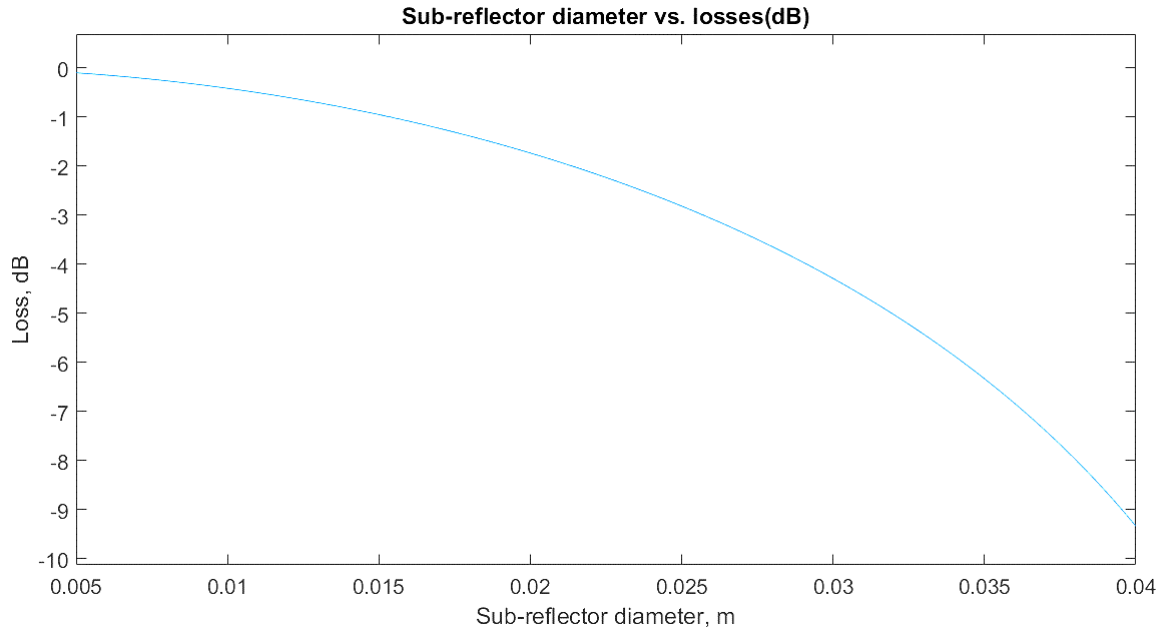
Figure 3. 8. 9: Diameter of the sub-reflector vs. loss in dB.

It is important that the sub-reflector must reshape the illumination from the effective feed f/d to F_m to D_m for the dish. This gives a magnification factor M in Eq. 3.8.18, [12] :

$$M = \frac{effective\ feed\left(\frac{f}{D}\right)}{\frac{F_m}{D_m}},$$

(3.8.18)

where the effective feed is given by f/d = 1/(4 tan(0.5 φ_s), [12], F_m and D_m are the focal length and the diameter of the main reflector.

$$M = \frac{\frac{1}{4\tan(0.5 \cdot 30)}}{\frac{0.042\ m}{0.11\ m}} = 2.4428$$

(3.8.18a)

This requires that the sub-reflector has an eccentricity e given in Eq. 3.8.19, [12]:

$$e = \frac{M + 1}{M - 1},$$

(3.8.19)

where M is the magnification factor. With inserted values for the parameters, the eccentricity, e, is given by Eq. 3.8.19a:

$$e = \frac{2.4428 + 1}{2.4428 - 1} = 2.3862.$$

(3.8.19a)

Then the sub-reflector parameters, a and c (ref. fig. 3.8.3), can be calculated in Eq. 3.8.20 and 3.8.21:

$$c = \frac{f_s}{2} = \frac{0.0243\ m}{2} = 0.0122\ m,$$

(3.8.20)

where f_s is the difference between the two focal points (main and equivalent reflector, ref. fig.3.8.2).

$$a = \frac{c}{e} = \frac{0.0122\ m}{2.3862} = 0.0052\ m,$$

(3.8.21)

where e is the eccentricity and c is the sub-reflector parameter calculated in Eq. 3.8.20.

(c-a) should equal L_s (ref. fig. 3.8.2 and fig. 3.8.3). L_s was calculated to 0.0071 m. (c-a) = 0.0122 m - 0.0051 m = 0.0071 m. The relationship between these parameters is verified.

Then the depth of the sub-reflector can be calculated using trigonometric relationships:

$$d_s = (c - a) - \frac{D_s/2}{\tan(\varphi_m)},$$

(3.8.22)

where c and a are the sub-reflector parameters given in figure 3.8.2, D_s is the diameter of the sub-reflector and φ_m is the subtended angle of the main reflector.

$$d_s = (0.0122\ m - 0.0051\ m) - \frac{0.0225\ m/2}{\tan(66.41)}$$
$$= 0.0022\ m$$

(3.8.22a)

3.8.2.2.6.   Far field

The last and final check in the design of the antenna system is to verify that the sub-reflector is placed in the far field of the feed element. Having the sub-reflector in the near field will cause significant disturbances (phase errors) and loss. Eq. 3.8.23, [12], gives the definition of the far field:

$$R = \frac{2D_w{}^2}{\lambda},$$

(3.8.23)

where D_w is the diameter of the waveguide and λ is the wavelength of the signal.

$$R = \frac{2 \cdot (0.01006\ m)^2}{0.01303\ m} = 0.0155\ m$$

(3.8.23a)

This means that the sub-reflector has to be placed minimum 1.55 cm away from the waveguide. The designed distance is given by c + a = 0.0122 m + 0.0051 m = 0.0173 m, which means that the sub-reflector is placed in the far field.

3.8.2.2.7.   Present Cassegrain antenna system design

Figure 3.8.10 shows the design of the Cassegrain antenna system as a result of the calcualtions and estimations derived in this section. In the figure, the waveguide has a diameter of 14.06 mm instead of 10.06 mm. This is because 14.06 mm is the outer radius of the waveguide.
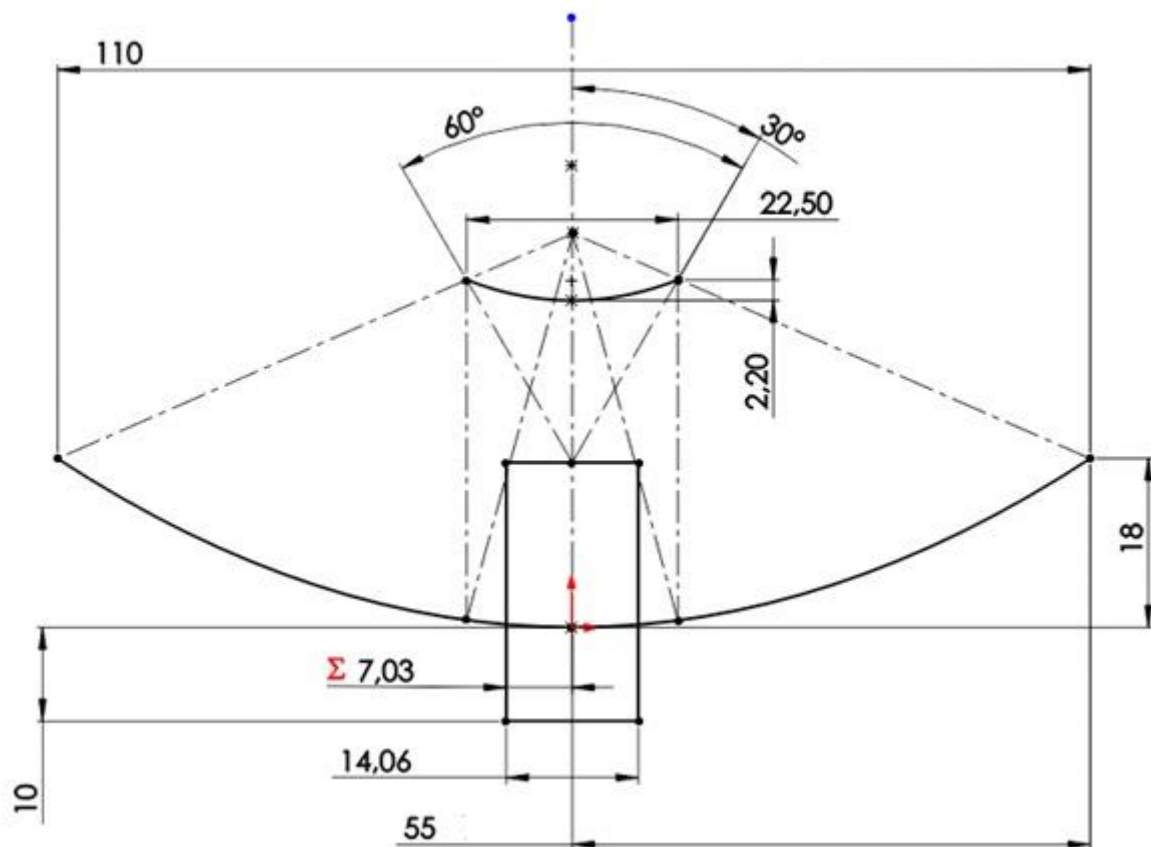
Figure 3. 8. 10: Present Cassegrain antenna design

3.8.2.2.8. Mass of the antenna assembly
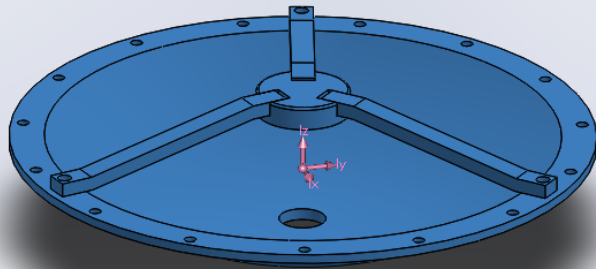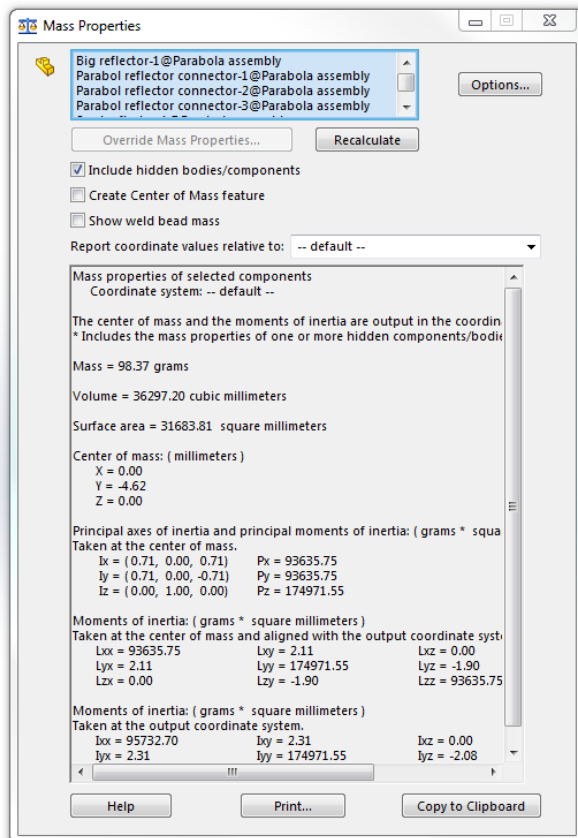
Figure 3. 8. 11: Cassegrain design mass

Figure 3.8.11 shows the mass of a Cassegrain design roughly identical to the design mentioned above. The mass is calculated to approximately 100 g.

3.8.3. Horn antenna design

Horn antennae are nothing more than flared-out waveguides. Flaring the open end of a waveguide improves the radiation pattern [14].
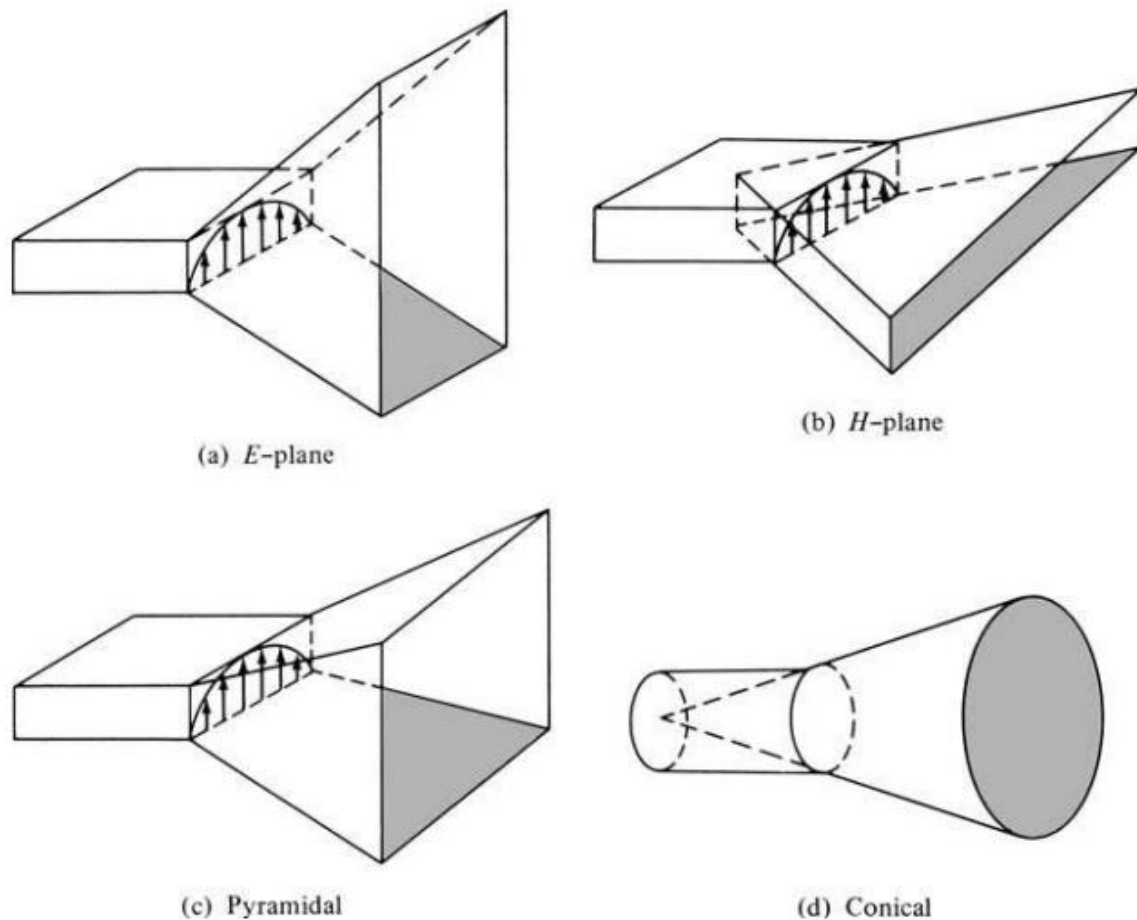
Figure 3. 8. 12: Different types of horn antennae [15]

Horn antennae can be designed in many forms to account for different polarizations of the input signal. The conical horn is chosen to account for a circular waveguide. The directivity of a horn antenna is a result of the aperture area and the flare angle [14].

3.8.3.1. *Optimum horn*
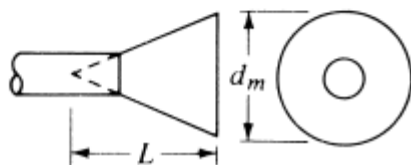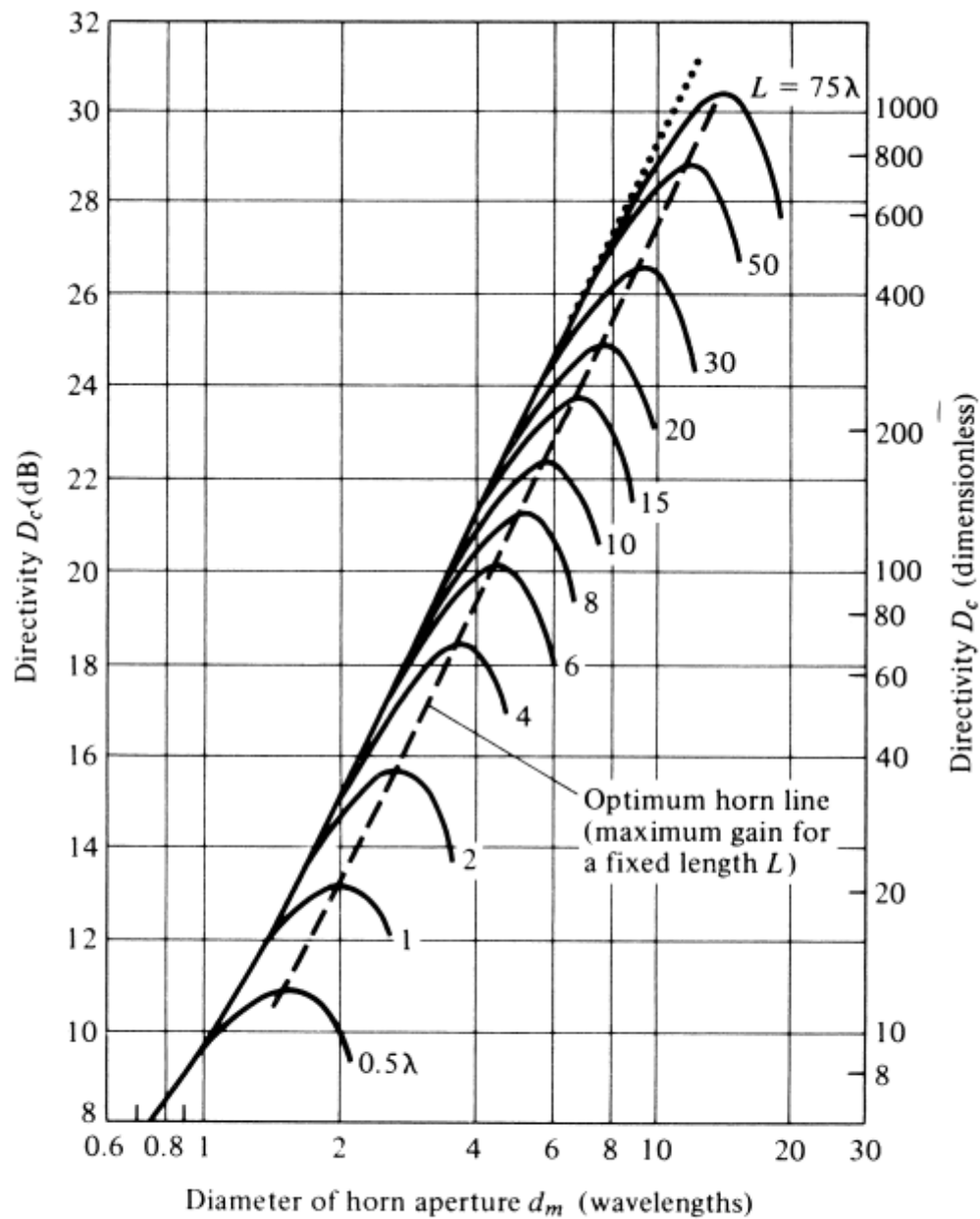
Figure 3. 8. 13: Directivity of a horn antenna with a fixed depth L, and a varying diameter dm. [15]

Figure 3.8.13 shows the directivity of a conical horn antenna with a fixed length. The directivity increases with the diameter until a certain point, where it starts to decrease. This point is the maximum directivity. This is used to calculate the optimum horn. The directivity of a horn antenna is maximum for a set diameter when the flare angle is zero: $\psi_c = 0 \ or \ L = \infty$.

3.8.3.2. *Calculating the directivity of an optimal horn*

The diameter d_m of an optimum horn can be calculated using the wavelength λ and the length l [14]:

$$d_m = \sqrt{3l\lambda}$$

(3.8.24)

The depth L can then be calculated using the Pythagorean theorem:

$$L = \sqrt{l^2 - d_m^2}$$

(3.8.25)

The circumference C can be calculated:

$$C = \pi d_m$$

(3.8.26)

The loss (in dB) due to aperture efficiency can be found using [14]:

$$L(s) \cong 0.8 - 1.71s + 26.25s^2 - 17.79s^3$$

(3.8.27)

Where s is the maximum phase deviation [14]:

$$s = \frac{d_m^2}{8\lambda l}$$

(3.8.28)

These calculations give a loss of about 2.9 dB, or an aperture efficiency of approximately 0.51.

Finally, the antenna directivity is found [14]:

$$Dc(dB) = 10\log_{10}\left(\frac{C}{\lambda}\right)^2 - L(s)$$

(3.8.29)

These formulas give:
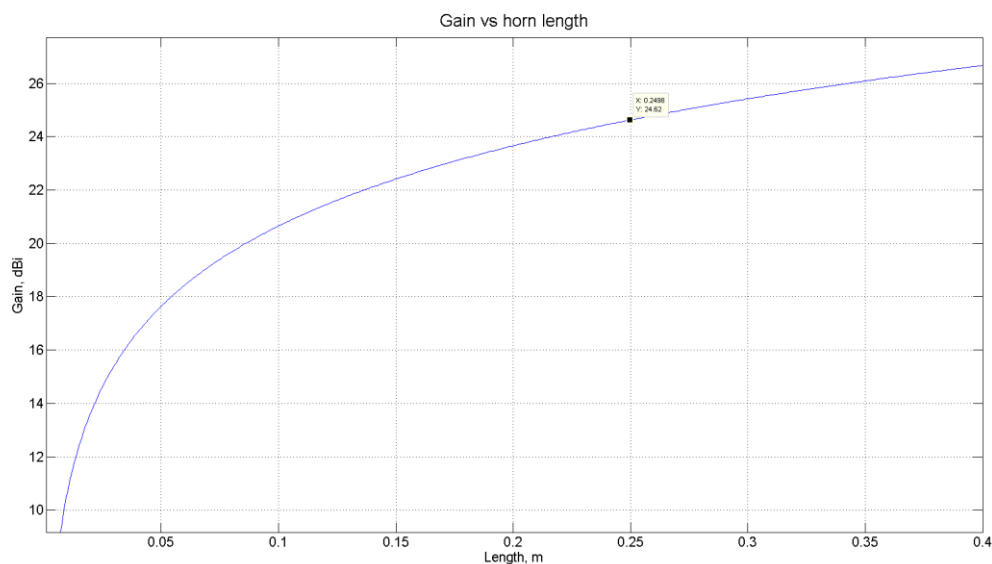
Figure 3. 8. 14: Directivity versus horn length
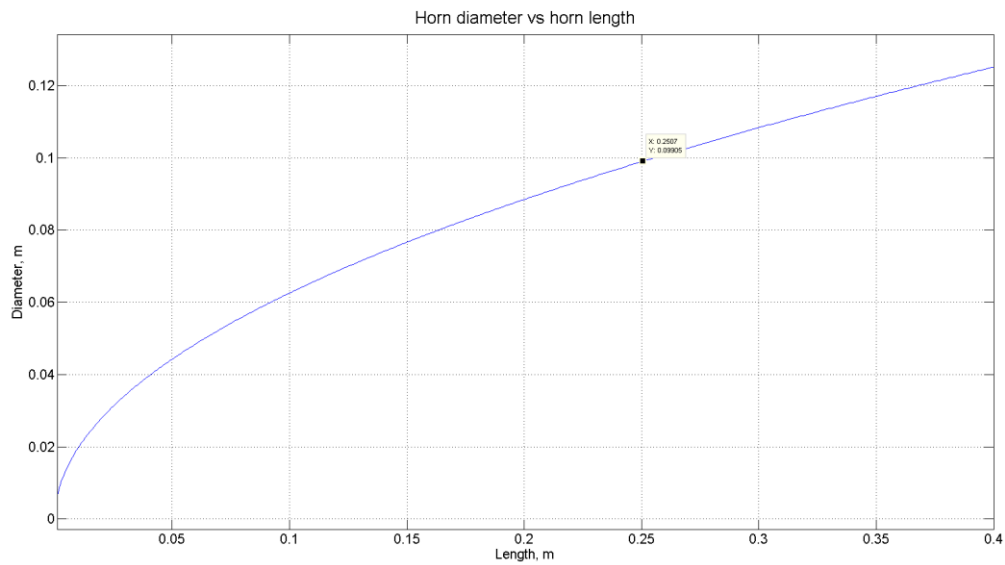
Figure 3. 8. 15: Horn diameter versus horn length
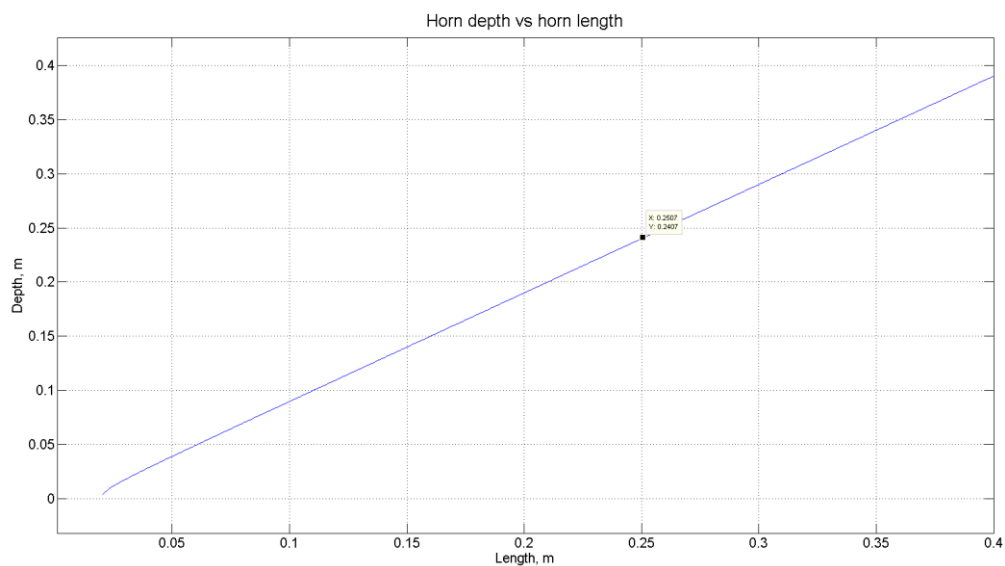
Figure 3. 8. 16: Horn depth versus horn length

To account for additional losses, a directivity of 24.6 dB was chosen; giving a length of approximately 25 cm. At this length, the diameter for the optimal horn is 10 cm and the depth is 24 cm.

3.8.3.2.1. Simulation of conical horn antennae

To confirm the results from the calculation, various horns were simulated using openEMS [15], a tool using FDTD to calculate antenna radiation patterns.
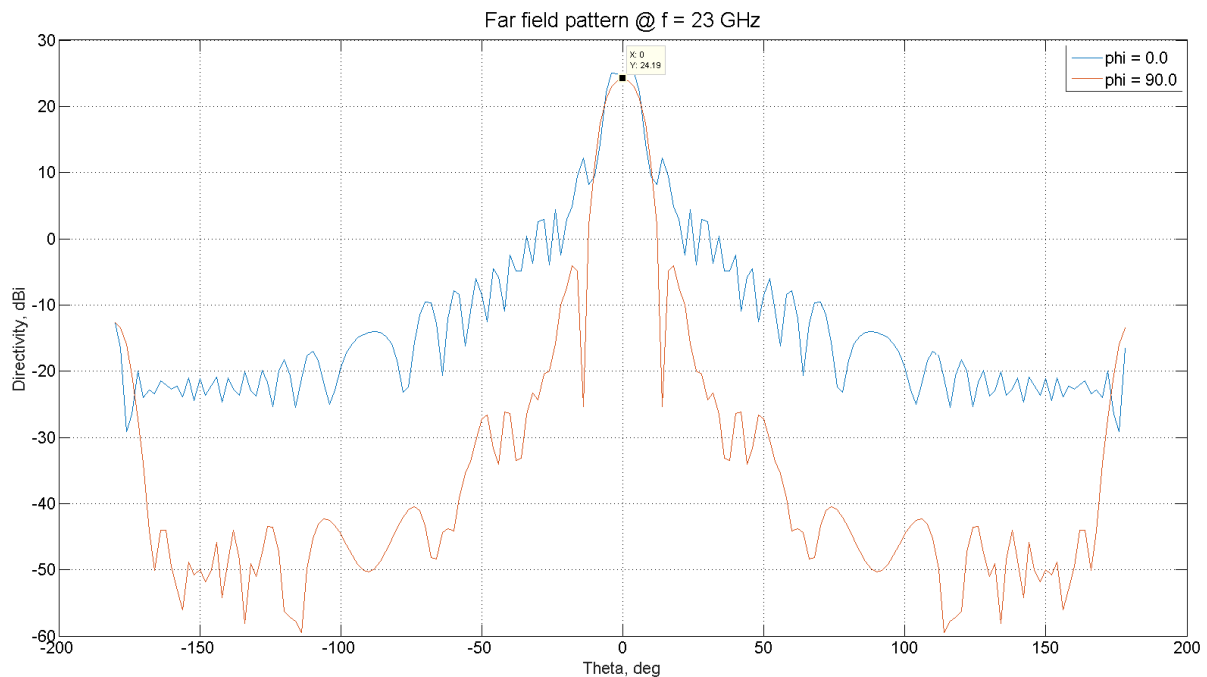
Figure 3. 8. 17: Far field pattern of a horn with L = 25 cm and d = 10 cm

The far field pattern in figure 3.8.17 shows that the approximate calculations for the optimum horn were correct. However, the plot also shows that the maximum directivity at $\phi = 90°$ is at $\theta = \pm 4°$. This is not optimal considering a pointing accuracy of 0.5°.
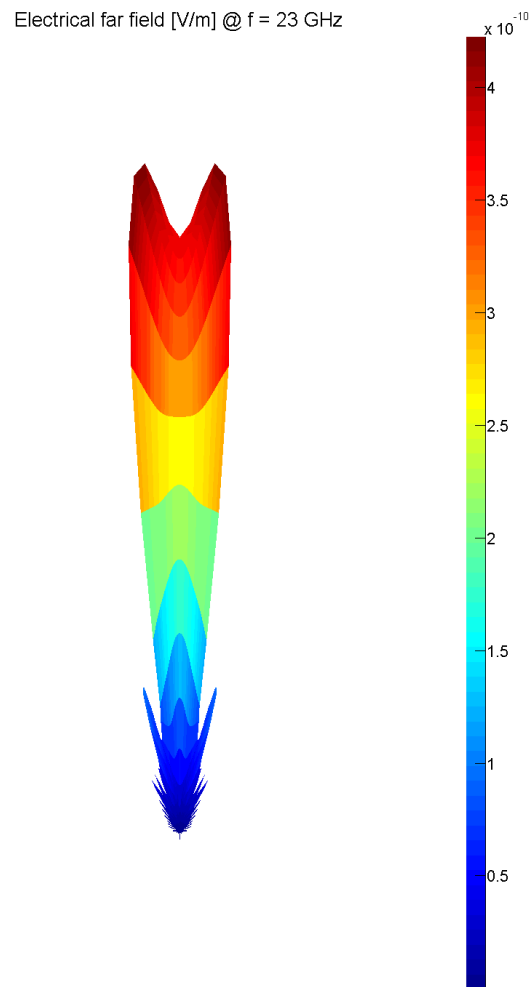
Figure 3. 8. 18: Electrical far field in [V/m]

Figure 3.8.18 shows the electrical far field at $\phi = 0$. It clearly shows the directivity problems at $\theta \in \pm 4°$. To overcome this, a horn with a larger diameter was simulated (12 cm).
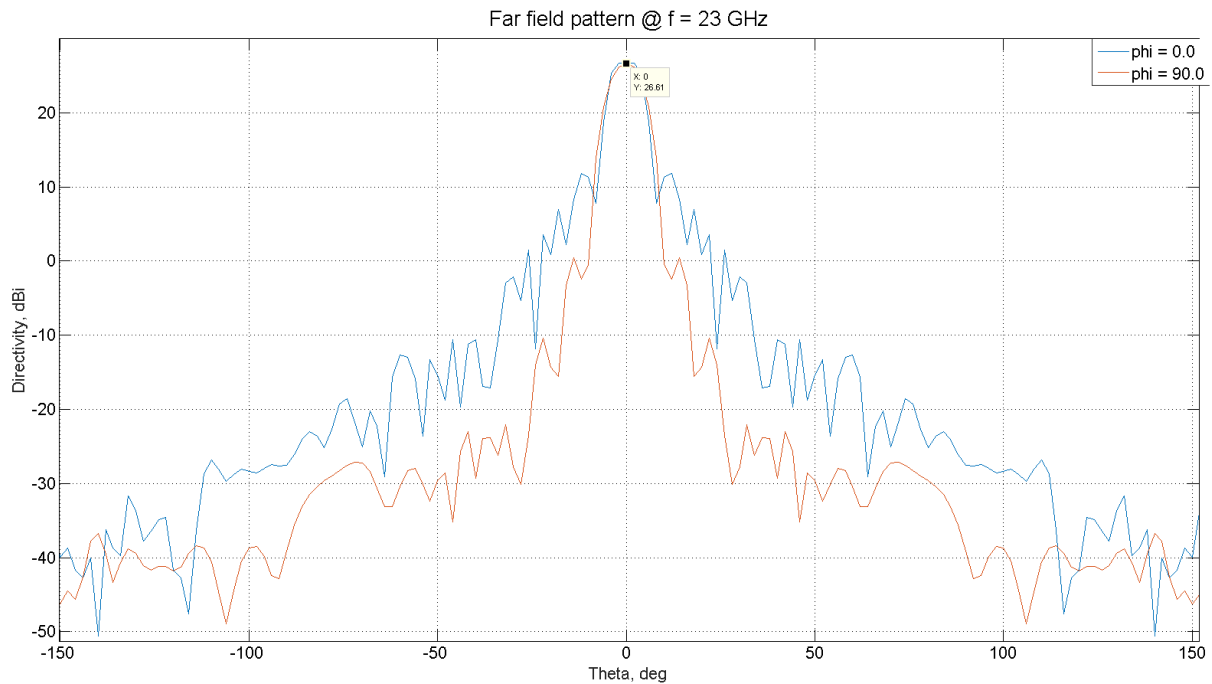
Figure 3. 8. 19: Far field pattern of a horn with L=25 cm and d=12 cm
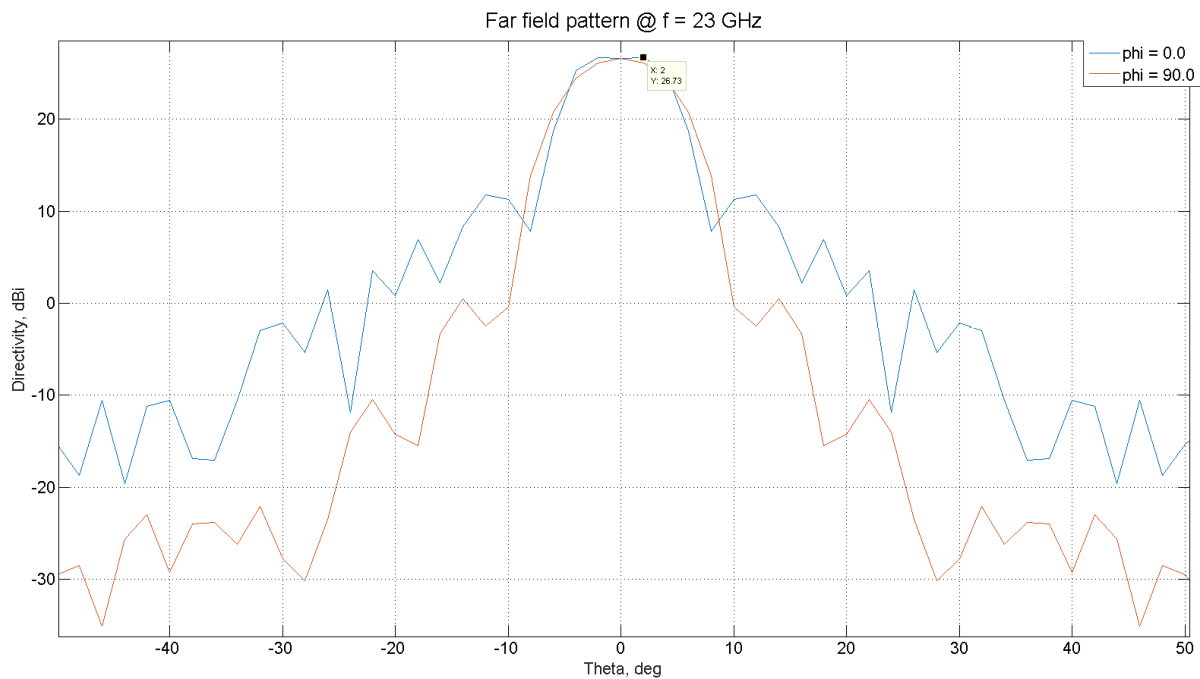
Figure 3. 8. 20: Far field pattern of a horn with L=25 cm and d=12 cm (zoomed in).
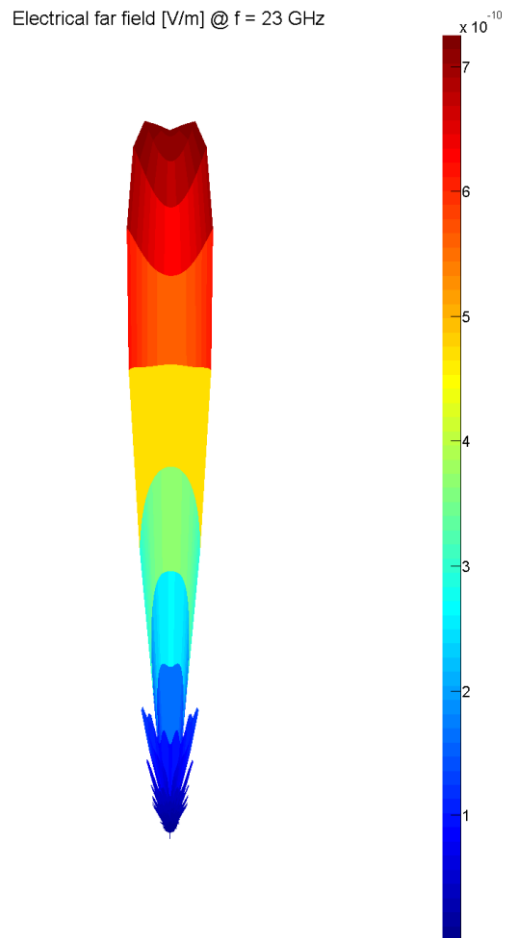
Figure 3. 8. 21: Electrical far field in [V/m]

Figures 3.8.19, 3.8.20 and 3.8.21 show the far field patterns of a horn with a 12 cm diameter. Peak directivity is seen at $\theta = \pm 2°$, however, the actual difference in directivity between $\theta = \pm 2°$ & $\theta = 0°$ is negligible.

3.8.3.2.2. Mass

The antennae were designed in Solidworks to find the mass
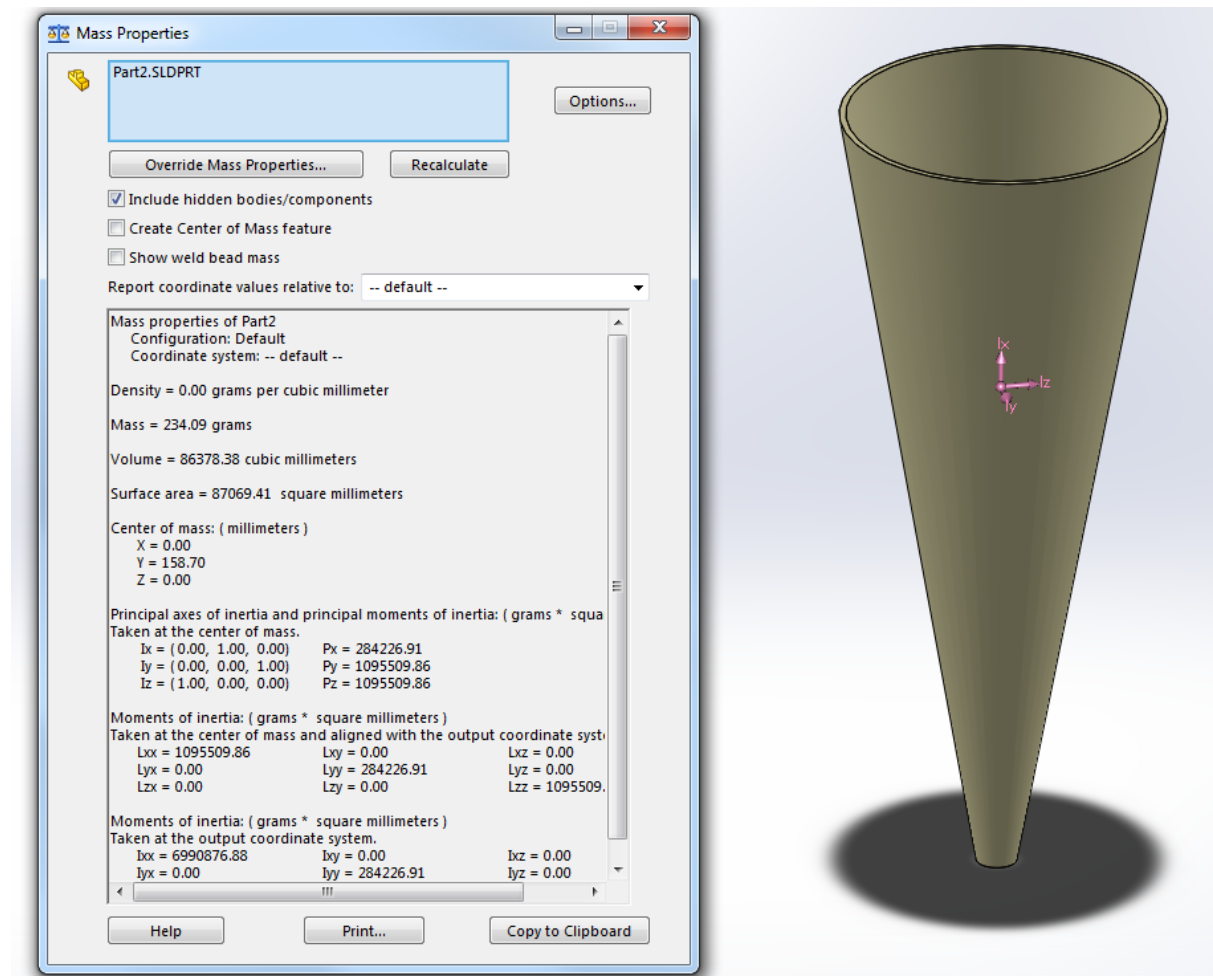
Figure 3. 8. 22: Mass properties of the horn with 10 cm diameter

Figure 3.8.22 shows the mass properties of the 10 cm-diameter conical horn. The mass is calculated to 234.09 g.
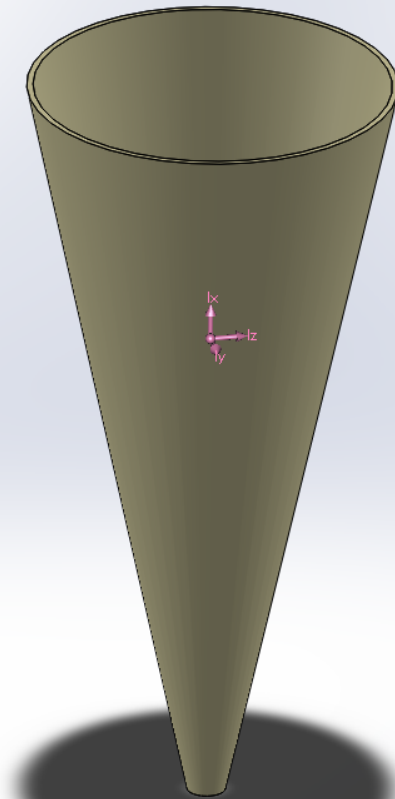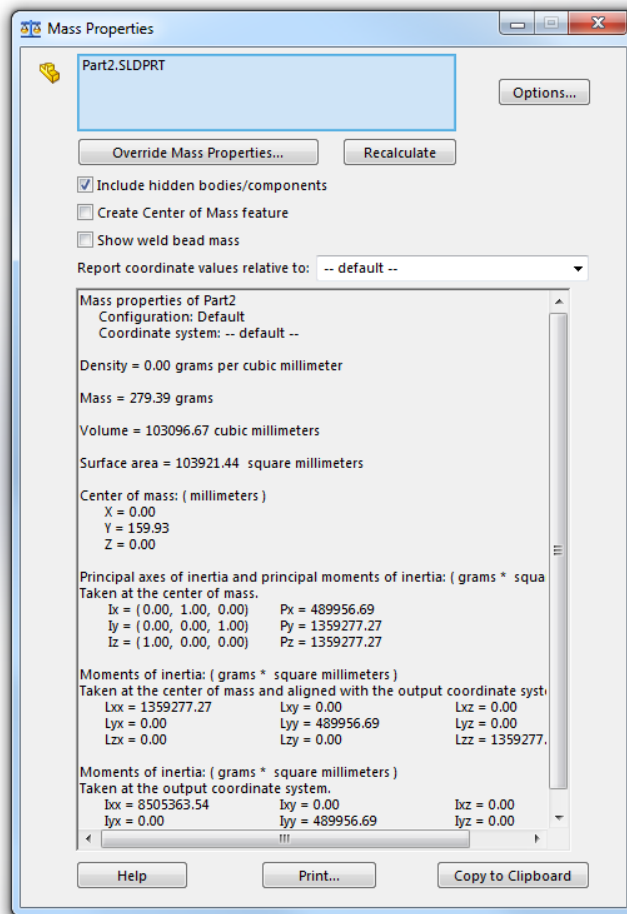
Figure 3. 8. 23: Mass properties of the horn with 12 cm diameter

Figure 3.8.23 shows the mass properties of the 12 cm-diameter conical horn. The mass is calculated to 279.39 g.

3.8.3.3. Corrugated horn

Adding corrugations to a horn antenna is a way to reduce losses due to spillover efficiency and cross-polarization. [16]
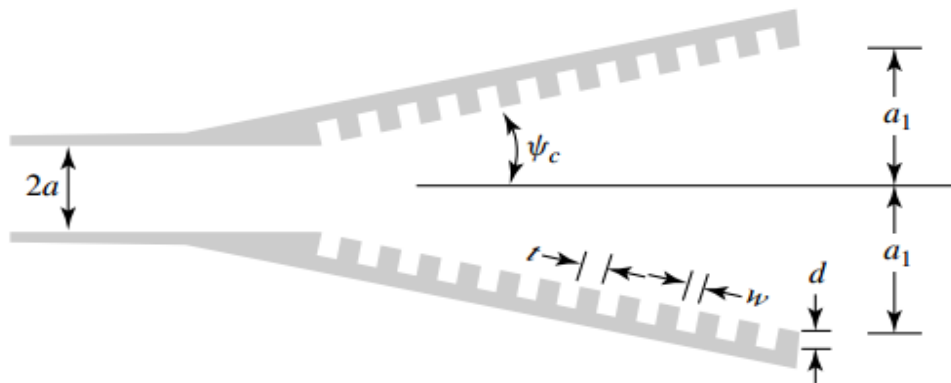
Figure 3. 8. 24: Horn corrugations [15]

Figure 3.8.24 shows how corrugations can be added to the horn. Figure 3.8.25 shows the impact of the corrugations on antenna directivity.
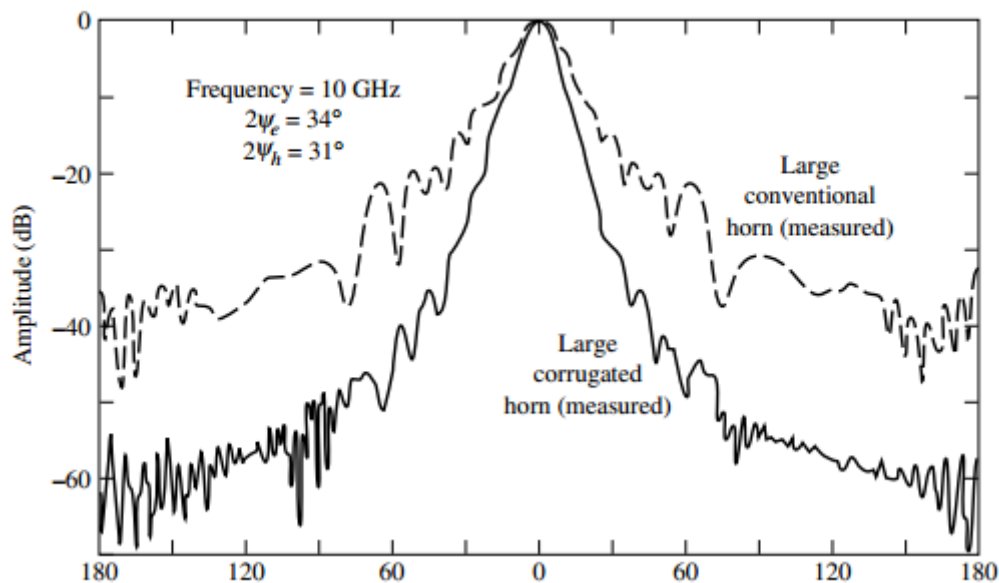
Figure 3. 8. 25: Impact of horn corrugations [15]

The maximum gain at $\theta = 0$ is the same for the corrugated horn and the conventional horn, but the side lobes are reduced. The size of the horn antenna remains the same. However, the mass is increased due to the corrugations. The corrugations themselves are placed $w = \frac{\lambda}{10}$ apart, and have a length of $d = \frac{\lambda}{2}$ to $d = \frac{\lambda}{4}$ [16]. The design of a corrugated horn antenna would ultimately end up being the same size as a standard antenna. Therefore, it is not directly evaluated in the trade-off.

3.8.4. Antenna design trade-off

Table 3.8.3 gives a summarized overview of the evaluated concepts and their performance at some criteria important for the APMA:

Table 3. 8. 3: Antenna design trade-off

Criteria	Cassegrain	Conical horn	Corrugated horn
Mass	100 g	>200 g	>200 g
Complexity	High	Low	High
Cost	Medium	Low	High
Performance	High	Low	Medium
Physical size	Small	Large	Medium
Calculation accuracy	Low	Low	Low

3.8.5. Conclusion

Mass, physical size, cost and gain are the crucial factors for the antenna system of the APMA, due to the given system requirements [5]. The Cassegrain antenna system, ref. table 3.8.3, is more complex than the corrugated- and conical horn, but it is also the most favorable with respect to size, mass and performance. The chosen antenna design for the low-cost APMA is the Cassegrain antenna system.

The overall gain of the chosen Cassegrain antenna system was calculated using Eq. 3.8.2 and figure 3.8.5 to 25,88 dBi (without losses). The losses due to the diffraction and the sub-reflector was calculated to 2.23 dBi in equation 3.8.17. This gives a total gain with respect to the calculated losses: 25.88 dBi – 2.23 dBi = 23.65 dBi. The losses due to the holders of the sub-reflector is difficult to calculate and are therefore not included in this trade-off. The given requirement for the overall gain of the system is 23 dBi, and then we still have a margin of 0.65 dBi.

The parameters and dimensions calculated in section 3.8.2 will be used in the further design of the APMA.

3.8.6. References

[1] Stian Laugerud, et al, "Components Trade-off," Small Satellite Mechanisms, HSN, Kongsberg, SSM-5111, Rev. 1.0, 2016.

[2] TelescopeOptics, "All-Reflecting Two-Mirror Telescopes," 14. 07. 2006. [Online]. Available: http://www.telescope-optics.net/two-mirror.htm.

[3] G. M. a. M. Bousqet, Satellite Communications Systems, New York: Wiley, 1987.

[4] Wikipedia, "Parabolic antenna," [Online]. Available: https://en.wikipedia.org/wiki/Parabolic_antenna. [Accessed 17. 03. 2016].

[5] G.H. Stenseth, M. Dybendal, "Requirement specification", SSM-2000, HSN, Rev. 1.1, 18.02.2016.

[6] D. E. M. Inc, "Calculating a Parabolic Dish's Focal Point," [Online]. Available: http://01895fa.netsolhost.com/PDF/dishfp.PDF. [Accessed 11. 03. 2016].

[7] R. C. Johnson, Antenna Engineering Handbook, 3. ed., New York: McGraw-Hill, Inc, 1993.

[8] T. S. Saad, Microwave Engineers' Handbook, 2. ed., Norwood: Artech House, Inc, 1971.

[9] T. A. Milligan, Modern Antenna Design, 2. ed., New Jersey: John Wiley & Sons, Inc, 2005.

[10] Militech, "Circular Waveguide Sizes," [Online]. Available: http://www.millitech.com/pdfs/circwave.pdf. [Accessed 16 03 2016].

[11] CERNEX, Inc, "Circular Waveguide Sizes," [Online]. Available: http://www.cernex.com/PRODUCTS_NEW/Tech_info/Circular%20Waveguide%20Sizes.pdf. [Accessed 16 03 2016].

[12] P. Wade, "Multiple Reflector Dish Antennas," 2004. [Online]. Available: http://www.w1ghz.org/antbook/conf/Multiple_reflector_antennas.pdf.

[13] M. Soe, "Performance Analysis and Design Consideration of Cassegrain for Satellite Communication," 2009. [Online]. Available: http://www.iaeng.org/publication/IMECS2009/IMECS2009_pp347-350.pdf.

[14] C. A. Balanis, Antenna Theory: Analysis and Design, 3rd ed., New Jersey: Wiley, 2005.

[15] T. Liebig, 2012. [Online]. Available: http://openems.de/index.php/Tutorial:_Conical_Horn_Antenna.

[16] J. D. Kraus, Antennas, 2nd ed., New York: McGraw-Hill, 1988.

[17] A. Rudge, K. Milne, A. Olver and P. Knight, The Handbook of Antenna Design, 1. ed., London: Peter Peregrinus Ltd., 1982.

[18] Antenna Designer, "Prime focus reflector," [Online]. Available: http://antennadesigner.org/prime_focus_reflector.html. [Accessed 17. 03. 2016].

[19] G. H. Stenseth, "Link Analysis," Small Satellite Mechanisms, HSN, Kongsberg, SSM-5112, rev.1.0, 2016.

3.9. Material and mechanical technology study

i.   Abstract

A material and mechanical technology study gives the designers and analysts an aspect of the material used for their product.

For the SSM project, three focus points of the study have been made: a study of different types of materials including how materials behave in general and in space, bearing behavior in space and in general, and lubricant behavior in space.

The goal for this study is to achieve the right data to select the correct materials, bearing and lubricants for the project.

ii. Contents

iii. List of figures

iv. List of tables

v. Document history

Table 3. 9. 1: Document history

Rev.	Date	Author	Approved	Description
0.1	10.2.16	MD,VOA		Document created
0.2	18.2.16	VOA	MD	Draft done Changed document layout
0.3	29.02.16	VOA		Document updated to new layout Added introduction
1.0	03.03.16	MD, VOA	TS	Reviewed and published
1.1	04.05.16	EL		Changed layout into the final report layout.
2.0	19.05.16	MD, VOA	TS	Reviewed and published

3.9.1. Introduction

Material technology is important in every design to validate that the final product meets its requirements with respect to stress, corrosion, vibration and more. The selection of materials for products is normally made in consultation with material engineers and designers. The general types of material used for general products are, [4]:

- Ferrous metals, such as carbon, alloys and stainless
- Nonferrous metals, such as aluminum, titanium and magnesium
- Polymers, such as thermoplastics, thermosets and elastomer
- Composite materials, such as PMC, MMC and CMC

The properties of materials can be divided into three categories: mechanical, physical and chemical. Mechanical properties include strength, ductility, hardness, toughness, elasticity, fatigue and shrinking resistance. Physical properties include density, specific heat, thermal expansion/conductivity, melting point and electrical/magnetic properties. Mass to strength ratio of materials is important for minimizing mass while maintaining the needed strength for the product. For many industries, especially aerospace, space and automotive, this feature is critical.

Chemical properties include oxidation, corrosion, degradation, toxicity and flammability. Chemical properties play a critical role under the hostile and normal environments this system will be exposed to.

The lifetime of a product is based on many factors, with the main aspects being: material choice, material use and environment. Improper choice of material can result in shortened lifetime of a product which can often be traced to the main factors, but also include wrong production method, wrong process control and poor maintenance.
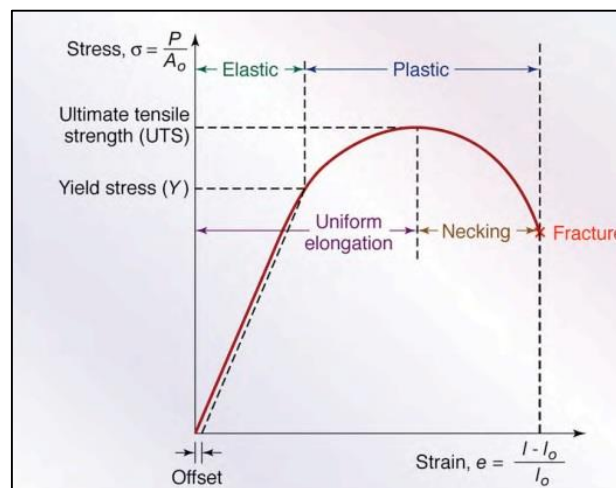
Figure 3. 9. 1: Stress-strain curve [6], ch. 2.

3.9.2. Material theory

3.9.2.1. *Stress-strain (metals)*

When exposing a specimen for a load less than the specimens yield stress, the specimen will elongate in proportion to the load, known as linear elastic behavior. When removing the load during this behavior, the specimen returns to its original shape and length. If the load is higher than the yield stress, also known as tensile strength, the specimen begins undergoing nonlinear elastic deformation. At this point, stress and strain are no longer proportional, the yield stress point is exceeded and permanent deformation will occur – the specimen will not return to original shape or length.

Permanent deformation, also known as plastic deformation, is when a load is so big atomic plans begin to glide and cause permanent changes in geometry. [4]

This means that when a load is applied to a specimen, less than the yield stress, the result is the same geometry when the load is removed. If exceeding the yield stress point, permanent deformation will take place and changes in geometry will occur. Permanent deformation will also strengthen the material, generating the need to apply more load to further deform the specimen. [4]

When the load reaches ultimate tensile strength, necking will occur, (Necking makes small fractures in the geometry, which will weaken the material) and less load is needed to further deform the specimen, potentially causing total fracture. Figure 3.9.1 shows a typical stress-strain curve.

3.9.2.2. *Rules (metals)*
The engineering strain is given by Eq. (3.9.1),

$$e = \frac{l - l_0}{l_0} \, , \qquad\qquad (3.9.1)$$

where e is the engineering nominal strain, I_o is the original length and l is the final length. [4]

The engineering stress is given by Eq. (3.9.2),

$$\sigma = \frac{P}{A_0} \, , \qquad\qquad (3.9.2)$$

where σ is nominal stress, P applied load and A_0 original cross-sectional area. [4]

In the elastic region the modulus of elasticity, E , or young's modulus is defined by Eq. (3.9.3):

$$E = \frac{\sigma}{e} \, , \qquad\qquad (3.9.3)$$

where σ is nominal stress, and e is the engineering nominal strain. This linear relationship is known as Hooke's law [4]

Engineering stress is based on the original cross selection area of the specimen, this means based on constant volume principle that the equation will not give true results but nominal results. To find the actual stress at a given point, true engineering stress needs to be calculated given by Eq. (3.9.4),

$$\sigma_t = \frac{P}{A} \, , \qquad\qquad (3.9.4)$$

where σ_t is true stress, P is applied load and A is actual cross-sectional area. [4]

For true strain, the rate of instantaneous increase in the instantaneous gauge length is taken in consideration. True engineering strain is given by Eq. (3.9.5)

$$\epsilon = \ln\left(\frac{l}{l_0}\right),$$

(3.9.5)

where ϵ is true strain, l is final length and l_0 is original length [4].
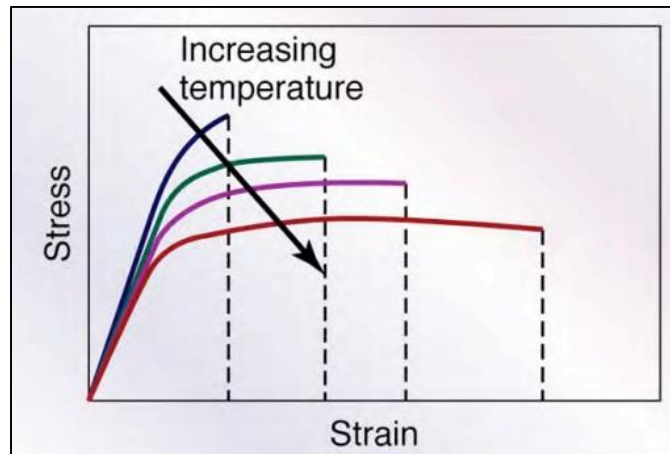
3.9.2.3. *Behavior (metals)*

Figure 3. 9. 2: Stress-strain curve related to temperature [6], ch. 2.

For most common materials such as aluminum and iron, such temperature differences can change some of the material properties. Increasing the temperature normally makes the material more ductile and tough, but yield stress and modulus of elasticity decreases. Generally, for most common materials expanding of the material can be seen, known as thermal expansion. Decreasing the temperature will make the material less ductile and tough and we can see some shrinking in the material. Figure 3.9.2 shows how the strain-stress curve changes with temperature. The temperature affect modulus of elasticity, yield stress, ultimate tensile strength and toughness can be seen in the figure. [4].

3.9.2.4. *Corrosion (metals)*
Corrosion is a natural process, which convert a refined metal to a more stable from, such as oxide. Over time corrosion will weaken the material and eventually destroy it. For ferrous metals such as iron (Fe) rust is a kind of corrosion that weakens/destroys the metal. Corrosion can also be good, for nonferrous metals such as aluminum (Al). When aluminum is produced and reacts with air, a thin oxide layer is created which prevent future corrosion, [7].

3.9.2.5. *Stress corrosion resistance*
Stress corrosion defines that a ductile material can fail where no tension is applied. Defects from corrosion can develop cracks over time or right after manufacturing that weakened the material. The susceptibility of metals to stress corrosion cracking depends mainly on the material stresses and environment. Figure 3.9.3 shows stress corrosion cracks on a rubber band, [5].
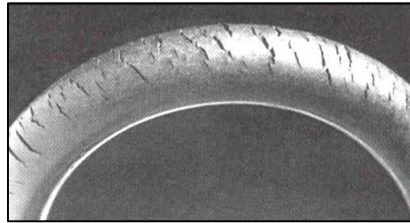
Figure 3. 9. 3: Stress corrosion cracks [8]

3.9.2.6. *Atomic oxygen*

In low Earth orbit (LEO) materials are exposed to a flux of atomic oxygen (ATOX). The oxygen on Earth is comprised of two atoms of oxygen while ATOX is only comprised of one atom. ATOX can react with the materials used on the APMA and cause damage in the form of oxidation, [9].

3.9.2.7. *Radiation*

ATOX is highly radioactive and can damage mechanisms in space. In general, radiation can manipulate the properties of a material such as yield strength, tensile strength, hardness, ductility and toughness. A metal that is exposed to high-energy radiation over time will increase yield strength, tensile strength and hardness but decrease ductility and toughness, [9].

3.9.2.8. *Vacuum outgassing*

Vacuum outgassing occurs whenever an absorbed gas in a material is released in vacuum. If a material has high outgassing it can cause issues with sensors, solar cells, etc. that needs a clean surface. If the antenna suffers from outgassing, wrong alignment of the reflected signal may occur, [2].

3.9.2.9. *Micrometeoroids and debris*

Collisions will occur in space due to micrometeoroids and debris. It is important that the system is collision stable, [2].

3.9.3. General about materials for space

For mechanisms in space, special factors need attention. Factors that will be dealt with in this study are mainly atomic oxygen, radiation, temperature, vacuum outgassing, stress corrosion resistance, micrometeoroids and debris.

3.9.3.1. *Antenna and structure*

Under vacuum conditions, materials have a tendency to cold weld. This phenomenon is enhanced by mechanical rubbing or any other process that removes oxide layers. From [1], aluminum will be used for the antenna. Aluminum alloys won't get affected by vacuum and the radiation levels in LEO. The same applies for the APMA structure, which will also be made out of aluminum, [2].

3.9.3.2. *Material for APMA*

It is important to choose the right aluminum alloy with respect to temperature, ATOX, SCC and overall specs. Based on [2], Aluminum ISO Al 99,5 – AA1050 is recommended for antenna and the structure.

Table 3. 9. 2: Aluminum AA1050

Aluminum: AA1050	
Properties relevant to space	**Typical Value**
Corrosion	Excellent resistance to atmospheric corrosion. For more severe environments, parts can be either: • Chromated • Chromated and painted Sulphuric anodized or chromic anodized
Stress corrosion	High resistance

Table 3. 9. 3: Aluminum AA1050, 2

Aluminum: AA1050		
General properties:	**Typical Value**	**Remarks**
Specific Gravity	2.71	At ambient temperature
Ultimate Tensile Strength	105 – 145 N/mm^2	At ambient temperature
True stress	55- 133 N/mm^2	At ambient temperature
Thermal Expansion Coefficient	24×10^{-6} /K	At ambient temperature
Thermal Conductivity	230 W/m.K	At ambient temperature
Electrical Resistivity	0.0282×10^{-6} Ω.m	At ambient temperature
Melting point	650°C	
Modulus of Elasticity	71000 N/mm^2	At ambient temperature

3.9.4. About bearings
3.9.4.1. *Types*
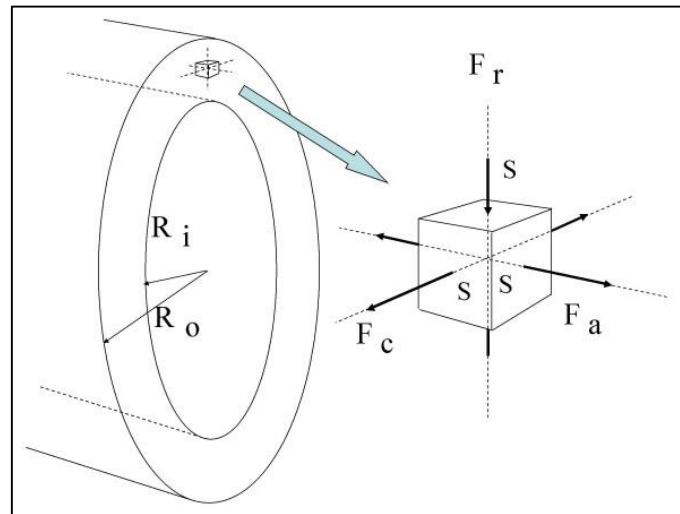
Figure 3. 9. 4: Radial and axial forces [11]

The most common bearing can be divided into two types; radial bearing and axial bearing, [10]:

An axial bearing is suitable to obtain forces in the radial direction. There are different kinds of axial bearings that can operate well in both directions. However, the axial bearing is favorable for radial loads.

Typical places to find axial bearings are where the force is acting in the radial direction for example in heavy drilling equipment for offshore plants.

A radial bearing is suitable to obtain forces in axial path. There are different kind of radial bearings that can operate well in both directions however, radial bearings are the most favorable for axial loads.

Radial bearings can be found in nearly every equipment around us. The bearing in the wheels of a bicycle is normally a radial bearing.

Figure 3.9.4 shows the represented forces, where F_r is radial and F_a is axial forces.

3.9.4.2. *Materials*
Bearings are made of various materials to maximize bearing performance and lifetime. Most bearings are made out of steel alloys such as chrome steel, stainless steel and carbon alloy steel, [3].

Chrome steel (SAE 52100) bearings are suitable for temperatures up to 120℃ and there are methods to make the alloy suitable for higher lifetime temperatures. [3] SEA52100 bearing steel has good hardness, wear-resistance and high lifetime. However, the corrosion resistance of chrome steel is low due to low content of chromium. To avoid this, every surface of the bearing must be protected.

Stainless steel bearings are suitable for temperatures up to 250℃. AISI 440C , Martensitic stainless steel bearings contain enough carbon for standard heat treatment to apply and can be hardened up to RC58, which is 20% lower than chrome steel bearings. The main advantage to stainless steel bearings is that the chromium reacts with oxygen and adds a passive film which protects the bearing against corrosion. There are different stainless steel alloys used for bearings. SV30 stainless steel alloys can be interesting because of the increased corrosion resistance, strength, hardness and lifetime, but the price is a disadvantage.

Carbon alloy steel can be divided in four categories: low content, medium content, high content and ultra-high content of carbon [14]. Bearings made out of low/medium carbon alloy steel are not suitable for precision work and are more dedicated to commercial use. They cannot carry heavy loads and need protection against corrosion. The main advantage for carbon alloy steel bearings is the price. Common carbon alloy steel used for bearings are AISI C1008 and C1010.

3.9.4.3. *Analysis of bearing*

For this project, cost is one of the most important stakeholder requirements and this need to be taken into account in the analysis. Carbon alloy steel and chrome steel bearing is not suitable for the project due to low corrosion resistance and precision. Stainless steel bearings were proposed by the main stakeholder in this project. There are two types of materials, SV30 and AISI 440C, which both fulfill the requirements for space-use, confirmed by our stakeholder.

Table 3. 9. 4: Stainless steel S30V [5]

Stainless steel: S30V		
General properties:	**Typical Value**	**Remarks**
Elastic Modulus	221000 n/mm^2	
Density	7,47g/cm^3	
Toughness	10.ft.lbs	Transvers charpy c-notch testing
Corrosion resistance	250 millivolts	
Thermal Expansion Coefficient:	293-473,15K	
Thermal Conductivity	17,31 W/m.K	

Table 3. 9. 5: Stainless steel AISI 440C [12]

Stainless steel: AISI 440C		
General properties:	**Typical Value**	**Remarks**
Elastic Modulus	210000 n/mm^2	
Density	7.8g/cm^3	
Toughness	2.5.ft.lbs	Transvers charpy c-notch testing
Corrosion resistance	75 millivolts	
Thermal Expansion Coefficient:	-	
Thermal Conductivity	24.2 W/m.K	

3.9.4.4. *Conclusion*

At this point the project group will look into both bearings. SV30 has a higher corrosion resistance, strength, hardness and lifetime, but costs more than the AISI440C with respect to table 3.9.4 and 3.9.5. To resolve this issue, the group was in contact with the company SKF, which concluded that SV30 is a special material they do not have in stock, and is very expensive to make. 440C is the material to use for bearings. At this point, SKF did not have axial bearings in this material, and proposed to use two radial bearings instead.

3.9.5. General about lubrication

[13] Lubrication can be divided into two groups: solid and liquid. There are four defined regimens of liquid lubrication: hydrodynamic, elastohydrodynamic, boundary and mixed. "These regimes are directly proportional to the oil viscosity and relative to velocity and inversely proportional to the load. Hydrodynamic lubrication is a regime known for complete separation of surfaces by a fluid film that is created by the flow of lubrication, which are going through the contact area. For non-conformal concentrated contacts, where loads are high enough to elastic deform the surfaces and speed/viscosity is not large enough to create the fluid film the second regimes comes in effect. This regime is known as elastohydrodynamic lubrication. Normally during hydrodynamic and elastohydrodynamic lubrication, wear takes no place since there are no contact between sliding surfaces. The thickness of the film created in each regime is different. For hydrodynamic lubrications the film is typically < $0.25\mu m$ thick and for elastohydrodynamic the film is typically $2.5\mu m$ to $0.025\mu m$ thick. When the thickness of the film is decreased under $0.0025\mu m$ the boundary lubrication regime comes in to play. In this regime asperity contact between the sliding surfaces takes place and the lubrication process becomes the shear of chemical compounds on the surface. This regime is dependent on lubrication additives within the oil that produce compounds on the surface which have the ability to shear and provide lubrication [13], pp. 5-6." Solid lubrication uses essentially the same as boundary lubrication except that there is no liquid reservoir to resupply lubrication. Instead a solid film is applied to the sliding surfaces before sliding commences. It is important that the film can withstand the lifetime of the component. An alternative is to use a solid lubricant material or a special coat, which wears a very small percentage for each cycle [13], pp. 6-7.

3.9.5.1. *Types*

For liquid state lubrication, many different lubrications have been used in space: silicones, mineral oils, PFPAE and more. Liquid lubrication needs a reservoir of liquid and a pumping system, for example aimed at gears. Meanwhile in bearing, the reservoirs are included in the housing and there is no need for an external reservoir and pumping system. For grease state lubrication, a mix of liquid lubricant and thickener, no advantage of a pumping system or reservoir are seen, since the thickener holds the lubrication together. Grease is commonly used for low speed to high-speed bearings and gears in space mechanisms.

For solid state lubrication one can find soft metal films such as gold, silver and lead, in addition to Polymers such as PTFE, polyimides and more. One can also find low share strength materials. A layer of solid state lubrication can be used on two surfaces, but is not suited for bearings and gears since the life time of a lubricant layer is reduced for every cycle. This may introduce dust that can damage the mechanism. The advantage for using a solid-state lubrication is that it can be applied without a reservoir and in situations where liquid is not suitable.

3.9.5.2. *Analysis of lubrication*

Table 3. 9. 6: Advantages and disadvantages of using liquid lubricates

Advantages and disadvantages of using liquid lubricates [13], pg. 20.	
Advantages	Disadvantages
- Long endurance lies if properly employed - Low mechanical noise in most lubrication regimes - Very low friction in elastohydrodynamic lubrication regime - No wear in hydrodynamic or elastohydro-dynamic regimes - No wear debris	- Finite vapor pressure (oil loss and contamination) - Lubrication temperature dependent (viscosity, creep and vapor pressure) - Friction (viscous) dependent on speed - Endurance life dependent on lubricant degradation or loss - Electrically insulation - Additives necessary for boundary lubrication regime - Long-term storage difficult - Accelerated testing difficult if not impossible

Table 3. 9. 7: Advantages and disadvantages of using solid lubricates

Advantages and disadvantages of using solid lubricates [13], pg. 21	
Advantages	Disadvantages
- Negative vapor pressure (no contamination) - Wide operating temperature range - No migration of lubricants - Good boundary lubrication and electrical conductivity - Minimal degradation - Accelerated testing possible - Good long-term storage - No viscosity effects - Corrosion protection	- Endurance life dependent on operating conditions - Finite life - Wear - Poor thermal characteristics - Reapplication difficult or impossible - Heavy transfer (can produce erratic torque at low speeds) - Inability to be evaluated in air for use in vacuum

3.9.5.3. *Conclusion*

Oil loss, temperature dependency and life time is important for a mechanism going into space over a long period of time without any maintenance. Therefore, selecting a lubrication that can survive the entire project is required. Grease should provide the essentials: no oil loss, long lifetime, no wear in hydrodynamic and elastohydrodynamic regimes and low friction in hydrodynamic and elastohydrodynamic regimes. In collaboration with our main stakeholder, Braycote 601EF is suitable for our mechanism.

3.9.6. Fastening

3.9.6.1. *Fundamental*

When joining two or more objects together with a mechanical feature such as a bolt or welding, there is a fastener. Forces from a bolt holds the surfaces together, in the same way as the mix of two materials from welding (melting process) also keeps it together.

3.9.6.2. *Types*

Fastener can be divided into two types: removable and non-removable. For removable fasteners the most common types are bolts, screws, pins and clips. Guideline can also be a removable fastener when used correctly. For non-removable fasteners the most common types are welding and crimping.

Bolts are amongst the most common of removable fasteners, and bring important features. Every bolt come in different classification and materials for each use. The classification gives the detailed strength of the bolt. The 8,8 bolt: The first number multiplied by 100 gives us the ultimate tensile strength of the bolt and the second number squared multiplied by 10 gives us the yield strength of the bolt. The 8.8 bolt has 800 N/mm^2 ultimate tensile strength and 640 N/mm^2 yield strength. Materials used for the bolts give it wear resistance. The most common materials used for bolts are carbon steel and stainless steel.

An advantage for bolts is that they are removable, which make them less complex to maintain and test. Calculation of strength is easy and can be changed by using different classifications. The downside of the bolt is that it adds time to the assembly due to montage and tightening with the right momentum. If the momentum is wrong, the bolt may loosen and compromise the rest of the system.

Welding is one most common method for non-removable fasteners. Welding can be divided into two groups, MIG and TIG. Usually, an electric arc melts the two pieces and join them. For MIG, the welding arc burns between the workpiece unshielded and continues to feed the thread melted by the electrode. The electrode arc and thread is shielded with a gas, normally argon or helium to prevent air into the weld that can weaken it. For TIG, a non-consumable electronic arc is used and the thread is fed externally while the whole process is shielded with argon gas. Both TIG and MIG are small melting processes for different use. Both are suited for aluminum but TIG grants the operator more control that allows the weld to be maximized for specific use.

The greatest advantage for welding is the versatility, that it can be used almost everywhere and the low cost and adaptable method of operation. The downside is that changes are permanent: once welded, the mechanism can't be disassembled.

3.9.7. Conclusion

Our mechanism will be stationed in space for 5 years. Thus, the right fastening, materials and lubrication with respect to its lifetime have to be chosen. Lifetime includes factors like stress, corrosion, etc.

From the sub-conclusions, the final conclusion is:

- Antenna and mirrors will be made out of aluminum AA1050
- Bearings will be made of AISI 440C – W standard at SKF
- Lubrication will be grease. Braycote 601EF

As fasteners, stainless steel bolts will be used, because of inspection and testing. Otherwise, if these are not feasible for complex parts, TIG welding is an option worth looking into.

3.9.8. References

[1]   C. Fjæreide, "KARMA 7 GSTP MSDDA, KBA EQM Detail Design and Analysis (TN05.01)", KDA, Kongsberg, Norway, Rev. A, 06.04.2015.

[2]   Space product assurance: Data for selection of space materials and processes, ECSS-Q-70-71A, 18.06.2004.

[3]   Technical Information, Bearing Materials, AST Bearings LLC, END-04-0553, 2010.

[4]   S. Kalpakjian, S.R. Schmid, *Manufacturing Engineering and technology,* 6. ed., Jurong, Singapore, Pearson Education, 2010.

[5]   Data Sheet Crucible CPM S30V, Crucible Industries LLC, Solvay, NY, 2007.

[6]   S. Kalpakjian, S. Schmid, *Manufacturing Engineering and Technology* 5. Ed., Upper Saddle River, NJ, Pearson Education, 2006.

[7]   Wikipedia. (23.01.2016) Corrosion. Available: https://en.wikipedia.org/wiki/Corrosion

[8]   Wikipedia. (2016) Ozone cracks in tube. Available: https://en.wikipedia.org/wiki/File:Ozone_cracks_in_tube1.jpg [13.02.2016].

[9]   T. Woods. (02.17.2011) Out of thin air. Available: http://www.nasa.gov/topics/technology/features/atomic_oxygen.html.

[10]   G. Dahlvig, S. Christensen, G. Strømsnes, *Konstruksjons-elementer*, 2.ed, Norway, Gyldendal Norsk Forlag AS, 2000.

[11]   ResearchGate. (2007). Definition of circum ferential, axial and radial wall stress. Available: https://www.researchgate.net/profile/Jacques_Noble/publication/6150309/ [15.02.2016].

[12]   MatWeb. (2015) Martensitic Stainless Steel 440C. Available: http://www.matweb.com/search/datasheet.aspx?matguid=850c5024f8d844af8ef95afab1a08792&ckck=1 [15.02.2016].

[13]   R.L. Fusaro, "Lubrication of Space Systems," NASA, Pittsburgh, Pennsylvania, 1994.

[14]   Wikipedia. (03.03.2016) Carbon steel. Available: https://en.wikipedia.org/wiki/Carbon_steel

3.10. Bearing setup

i. Abstract

This chapter shows estimations of the loads that can be observed in bearings, located in space. Different setup and bearing types are discussed to optimize load distribution. The bearings that will be used in the APMA are selected through this analysis.

ii. Contents

v. Document history

Rev.	Date	Author	Approved	Description
0.1	05.03.16 10.03.16	VOA MD	TS	Created document & introduction Created bearing calculations Approved until chapter 3
0.2	10.3.16	VOA		Rev 0.2 created Errors fixed. Preload/clamping – chapter created. Friction – chapter created. Preload method –chapter created. Updated to C1
0.3	17.4.16	VOA		Preload estimation added Updated to C2
0.3	21.4.16	VOA	EL	Updated calculation input in preload chapter Rewritten preload chapters Error fixed
1.0	12.05.16	VOA	TS	Reviewed and approved

3.10.1. Introduction

In space, gravity does not apply in the same way as on earth. In order to adjust this system for the space environment, some calculations are needed with respect to bearing setup, loads etc. This is done to ensure that the right bearing is selected in relation to stress, preload and clamping.

Forces that may occur in bearings are radial and axial forces, as shown in figure 3.10.1.

These forces are related to how the bearings are affected by the system. Factors like lifetime, stress and Hertzian stress [2] need to be estimated.
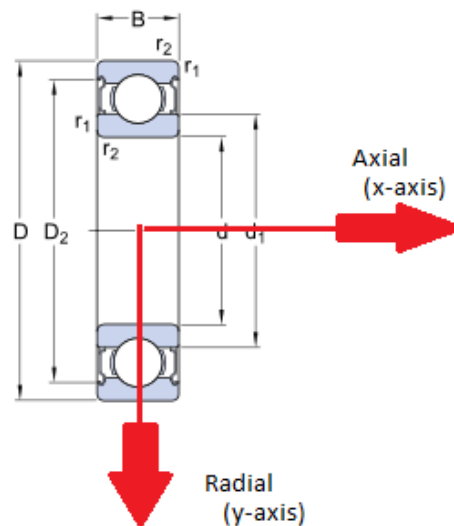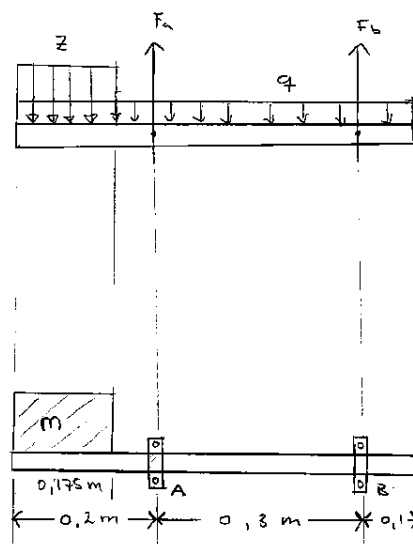

Figure 3. 10. 1: Force distribution, bearings

Figure 3. 10. 2: Forces in example 1

Example 1:

Figure 3.10.1 shows a schematic overview of a system with load and bearings. The mass equals to $M = 10$ kg and the rod (Q) has a mass of 7.5 kg. The system is on earth, so gravity acceleration equals to $g \approx 10 \ m/s^2$.

First, the force z generated by the mass M has to be found, [3];

$$z = Mg = 10 \text{ kg} \times 10 \ \frac{\text{m}}{\text{s}^2} = 100 \text{ N}, \tag{3.10.1}$$

where M is the mass and g is the acceleration.

Since the force applies over a length, Z equals to:

$$Z = \frac{z}{l} = \frac{100 \text{ N}}{0.175 \text{ m}} \approx 570 \frac{\text{N}}{\text{m}}, \tag{3.10.1.1}$$

where Z represents the box with a mass M, with respect to gravity and effective length, l.

Then the force Y generated by the mass Q of the rod is found:

$$Y = \frac{Qg}{l} = \frac{7.5 \text{ kg} \times 10 \ \text{m/s}^2}{0.6 \text{ m}} = 125 \ \frac{\text{N}}{\text{m}}. \tag{3.10.1.2}$$

F_a and F_b in figure 3.10.2 represent the radial forces in the bearings, and have to be calculated.

Taking the momentum around A, ref. figure 3.10.2, $F_a = 0$ and F_b will be the unknown, [4] chp. 3.3:

$$\sum \circlearrowright M_a = 0, \tag{3.10.2}$$

so

$$\frac{125 \frac{\text{N}}{\text{m}} \times (0.3+0.1) \text{ m}}{2} \times \frac{(0.3+0.1)\text{m}}{2} - F_b \times 0.3 \text{ m} - \frac{570 \frac{\text{N}}{\text{m}} \times 0.175 \text{ m}}{2} \times \left(\frac{0.2}{2} + \frac{0.175}{2}\right) \text{m} - \frac{(125 \times 0.2)\text{m}}{2} \times \frac{0.2 \text{ m}}{2} = 0. \tag{3.10.2.1}$$

Solving for F_b:

$$F_b \tag{3.10.2.2}$$

$$= \frac{\frac{125 \frac{\text{N}}{\text{m}} \times (0.3 + 0.1) \text{ m}}{2} \times \frac{(0.3 + 0.1) \text{ m}}{2} - \frac{570 \frac{\text{N}}{\text{m}} \times 0.175 \text{ m}}{2} \times \left(\frac{0.2}{2} + \frac{0.175}{2}\right) \text{ m} - \frac{125 \frac{\text{N}}{\text{m}} \times 0.2 \text{ m} \ 0}{2} \times \frac{0.2}{2} \text{ m}}{0.3}$$

$$\tag{3.10.2.3}$$

$$\approx -18.7 \text{ N}.$$

F_b is now known and we can take $\sum \uparrow F_y = 0$, since the only unknown force is F_a:

$$\sum \uparrow F_y = 0 \tag{3.10.3}$$

$$F_a + F_b - Q - Z = 0. \tag{3.10.3.1}$$

Solving for F_a in equation 3.10.3.2:

$$\tag{3.10.3.2}$$

$$F_a = -F_b + Q + Z \tag{3.10.3.3}$$

$$= -(-18,7)\ \text{N} + \frac{125\frac{\text{N}}{\text{m}} \times 0{,}6\ \text{m}}{2} + \frac{570\frac{\text{N}}{\text{m}} \times 0.175\ \text{m}}{2} \tag{3.10.3.4}$$

$$\approx 106\ \text{N}.$$

To make sure that the calculations are correct, equation 3.10.3 is used as a check.

$$\sum \uparrow \text{F}_y = 0 \tag{3.10.4}$$

$$F_a + F_b - Q - Z = 0 \tag{3.10.4.1}$$

$$106\ \text{N} + (-18,7)\ \text{N} - \frac{125\frac{\text{N}}{\text{m}} \times 0.6\ \text{m}}{2} - \frac{570\frac{\text{N}}{\text{m}} \times 0.175\ \text{m}}{2} \approx 0. \tag{3.10.4.2}$$

$$\tag{3.10.4.3}$$

The expected result shall be 0, accordingly to equation 4, which verifies the calculations.

Since mass is independent of gravity in space, (zero g-force) also known as weightlessness, it is normal to think that there are no forces applied to the system. This is not correct. The system has internal vibration, which causes acceleration. This acceleration is known as G_{RMS} (root mean square acceleration [5]), which tells us how fast a "particle" changes direction in relationship to vibration and frequency. G_{RMS} is given by equation 3.10.5 (Miles Equation), [5]:

$$G_{RMS} = \sqrt{\frac{\pi}{2} f_n Q [ASD_{input}]}, \tag{3.10.5}$$

where f_n is the natural frequency of the system, $Q = \frac{1}{2\zeta}$ is the transmissibility at the natural frequency, ζ is the critical damping ratio and ASD_{input} is input acceleration spectra density at the natural frequency $(\frac{g^2}{Hz})$. To use this acceleration we have to multiply it with three-sigma load with respect to design usage [5]. Now, the forces working on the system in space can be estimated.

Example 2:

Looking at the same situation as in example 1. With a load, two bearings and an estimated natural frequency of 100 Hz, what will the internal vibration be? Looking at the spectra given for our project, an ASD input of 1.5 $\frac{g^2}{Hz}$ is desirable. The critical damping ratio is estimated to 0.04.
G_{RMS} can then be calculated using equation 3.10.5, [5]:

$$G_{RMS} = \sqrt{\frac{\pi}{2} 100\ \text{Hz} \times \frac{1}{2 \times 0.04} \times 1{,}5 \frac{g^2}{Hz}} \tag{3.10.6}$$

$$= \sqrt{2945.3}\ m/s^2 \tag{3.10.6.1}$$

$$= 54.3\ m/s^2. \tag{3.10.6.2}$$

We do now have the acceleration working on the system and the force can be calculated [3]:

$$F = \text{Mass} \times \text{accelecation} \tag{3.10.7}$$

$$= (M + Q)\, 3\sigma G_{RMS} \tag{3.10.7.1}$$

$$= (3 + 7.5)\,\text{kg} \times 54.3\,\text{m/s}^2 \times 3\sigma \tag{3.10.7.2}$$

$$= 1710.45\,\text{N}. \tag{3.10.7.3}$$

This force F is working in both axial and radial direction and is equal along both axes. This force works through the center of gravity of the system. This has to be adjusted for, when calculating the radial and axial forces in the bearings.

The center of gravity for the system can be calculated by equation 3.10.8, [4] chp.10.2:

$$x_o = \sum \frac{(M \times x)}{M} \tag{3.10.8}$$

$$y_o = \sum \frac{(M \times y)}{M}, \tag{3.10.8.1}$$

where M (kg) is the mass and x is half the distance of the local CoG (m). x_o and y_0 represents the coordinates for θ, ref. figure 3.10.3.

$$x_0 = 0.178\,\text{m} \tag{3.10.9}$$

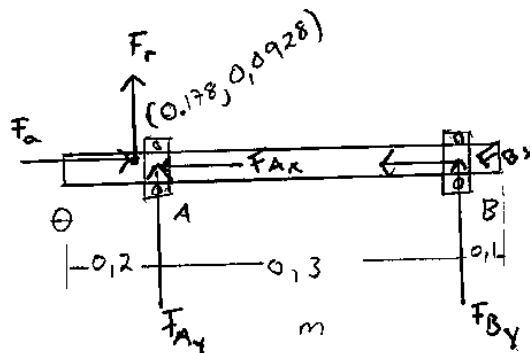$$y_0 = 0.0928\,\text{m}. \tag{3.10.9.1}$$

Figure 3. 10. 3: Updated system overview, with forces

Figure 3.10.3 shows an overview of the system with the applied forces. The forces (radial) can now be calculated with the same method as described in example 1.

$$F_{by} = 125{,}43\,N \tag{3.10.10}$$

$$F_{ay} = -1835{,}88\,N \tag{3.10.10.1}$$

To check that the calculation is correctly executed:

$$\sum \uparrow F_y = 0 \qquad (3.10.11)$$

$$F_{ay} + F_{by} + F_r = 0 \qquad (3.10.11.1)$$

$$125.43\ N + (-1835.88)N + 1710{,}45\ N \qquad (3.10.11.2)$$
$$= 0$$
$$\approx 0\ N. \qquad (3.10.11.3)$$

The calculations are correct according to equation 3.10.11.

There are axial forces in the system when hovering in space and the method to calculate these are similar to the calculations of the radial forces.

3.10.2. Calculations

3.10.2.1. *General calculations*

For this project, the eigenfrequency of the system is chosen to be 150 Hz, due to requirement REQ-1.1.4 [9], which says that the eigenfrequency shall be > 140 Hz. The damping factor, ζ, is chosen to be 0.02. This gives:

$$Q = \frac{1}{2\zeta} = 25 \qquad (3.10.12)$$

The value of the ASD_{input} is found in figure 3.10.4, for the given eigenfrequency of the system (150 Hz). The ASD_{input} is found to be 1.5 g^2/Hz.
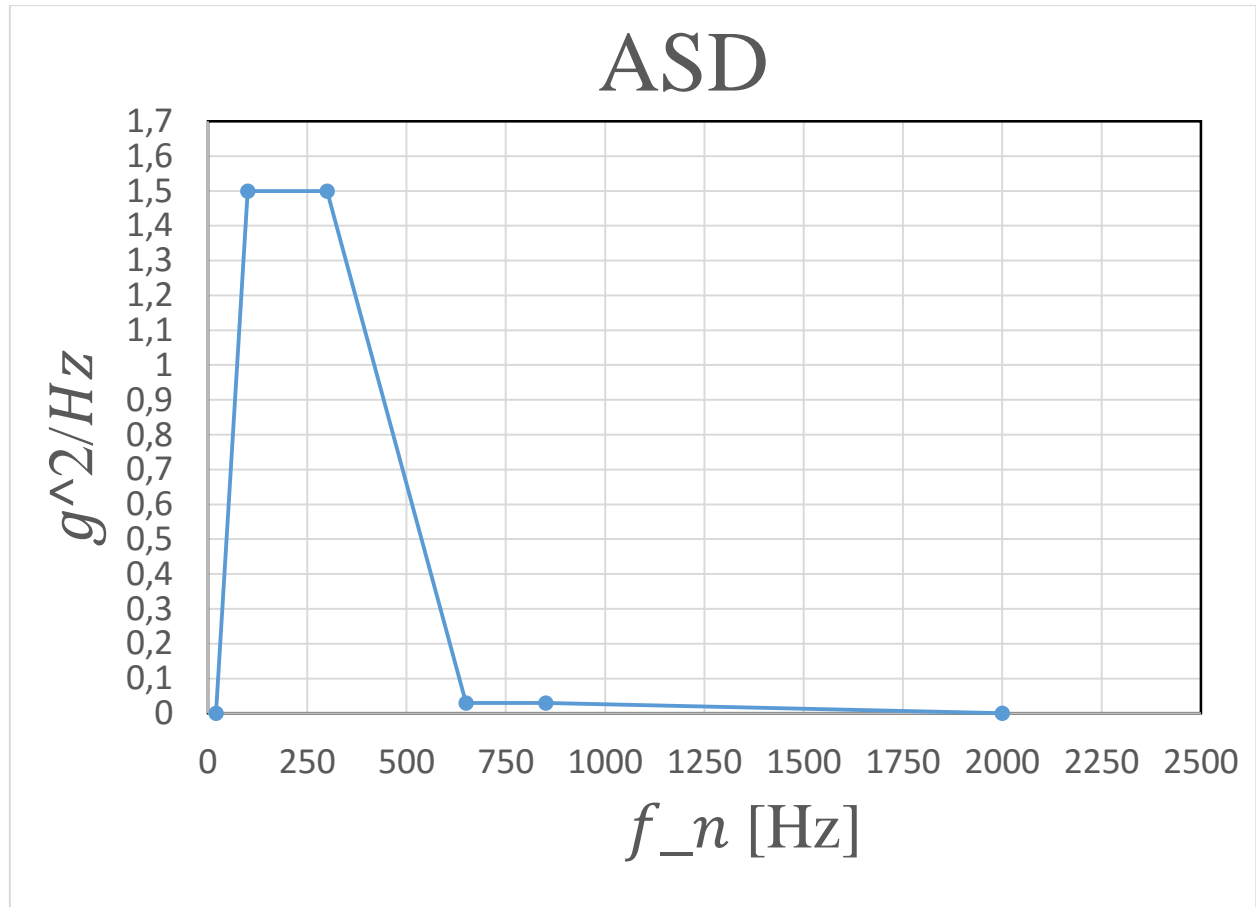
Figure 3. 10. 4: ADS values

The G_{RMS} for the system will be, [5]:

$$G_{RMS} = \sqrt{\frac{\pi}{2} f_n Q[ASD]} = \sqrt{\frac{\pi}{2} 150 \text{ Hz} \times 25 \times 1.5 \text{ g}^2/\text{Hz}} = 94 \text{ m/s}^2. \tag{3.10.12.1}$$

The total acceleration for the system, with respect to 3σ, is then given by:

$$a_{tot} = G_{RMS} 3\sigma = 282 \text{ m/s}^2. \tag{3.10.12.2}$$

Because of simultaneous eigenfrequency, the radial and axial forces will be equal each other. The radial and axial forces will be:

$$F_r = F_a, \tag{3.10.13}$$

where F_r is the radial force, and F_a is the axial force [3].

$$F_R = F_r \text{ and } F_{ax} = F_a \tag{3.10.13.1}$$

$$F_R = F_{ax} = ma_{tot} = 2.0 \text{ kg} \times 282 \frac{\text{m}}{\text{s}^2} = 564 \text{ N}. \tag{3.10.13.2}$$

3.10.2.2. *Azimuth*

The forces calculated from Miles Equations work through CoG. Therefore, the axial and radial forces that occur through the bearings have to be calculated. Figure 3.10.5 shows a simplified overview of the system, containing the azimuth stage. Point A and B represents the bearings, where the forces F_{AR} and F_{BR} representing the radial forces in the bearing, and F_{ax} represents the axial force.
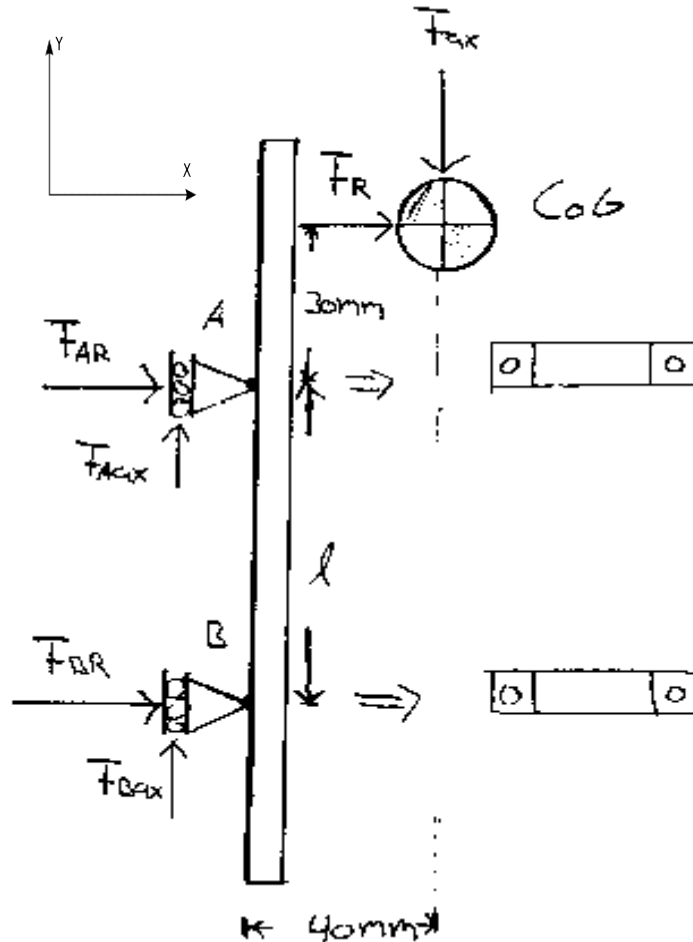

Figure 3. 10. 5: Forces for azimuth

The distance between the bearings vary with a length l. For azimuth, the values of $l = 20\text{ mm}, 30\text{ mm}, 40\text{ mm}$ and 50 mm.

Four different calculations are needed. The general equation for every calculation with respect to the length l will be [4]:

$$\sum \circlearrowleft M_A = 0; \tag{3.10.14}$$

$$F_{ax} \times 0.040\text{ m} + F_R \times 0.030\text{ m} - F_{BR} \times l = 0 \tag{3.10.14.1}$$

$$F_{BR} = \frac{F_{ax} \times 0.040\text{ m} + F_R \times 0.030\text{ m}}{l} \tag{3.10.14.2}$$

and

$$\sum_{\overrightarrow{F_x}} = 0; F_{AR} + F_{BR} + F_R = 0 \tag{3.10.15}$$

$$F_{AR} = -(F_{BR} + F_R). \tag{3.10.15.1}$$

To find the most suitable bearing for azimuth stage, different bearings based on size, inner and outer diameter, depth of the bearing, and type of bearing, has to be evaluated. In this project, two types of bearings have been looked into; angular contact ball bearing and deep groove ball bearing. For each calculation, some factors need to be added [6], [7].

For angular contact ball bearing, [6]:

$$e = 1.14, \tag{3.10.16}$$

where e is a calculation factor.

If

$$F_a/F_r \leq e, \tag{3.10.17}$$

$$P = F_r. \tag{3.10.17.1}$$

where F_a is the axial force and F_r is the radial force in angular contact ball bearing and P is the dynamic equivalent bearing load.

If

$$F_a/F_r > e, \tag{3.10.18}$$

$$P = 0.35F_r + 0.57F_a \tag{3.10.18.1}$$

The static load rating C_0 is given by equation 3.10.19:

$$C_0 > 2P. \tag{3.10.19}$$

The static load rating C_0 is set to be $> 2P$. This is because of the de-rating in the material. Due to the relationship between "ball" and "race", the Herzian stress varies with the cubic root of the load,

$$2^{\frac{1}{3}} \approx 1.2, \tag{3.10.19.1}$$

which gives us a de-rating of 20 %. Therefore, the C_0 is sat to be $> 2P$. This will eliminate the de-rating in the further calculations. The de-rating occur because materials loses strength and tension when the temperatures increasing or decreasing.

For deep groove ball bearing [7]:

If

$$F_a/F_r \leq e, \qquad (3.10.20)$$

Then

$$P = F_r. \qquad (3.10.20.1)$$

where F_a is the axial force and F_r is the radial force in the deep groove ball bearing, e is a calculation factor displayed in table 3.10.1 and P is the dynamic equivalent bearing load.

If

$$F_a/F_r > e, \qquad (3.10.21)$$

$$P = XF_r + YF_a, \qquad (3.10.22)$$

where X and Y are different weightings of the forces (calculation factors), given in table 3.10.1.

The static load rating C_0:

$$C_0 > 2P. \qquad (3.10.23)$$

Table 3. 10. 1: Calculation factors, [8]

$f_o\, F_a/C_0$	e	X	Y
0.172	0.19	0.56	2.3
0.345	0.22	0.56	1.99
0.689	0.22	0.56	1.71
1.03	0.28	0.56	1.55
1.38	0.30	0.56	1.45
2.07	0.34	0.56	1.31

From equation 3.10.2 with respect to the azimuth stage and a length of 20 mm between the bearings, F_{AR} and F_{BR} is calculated in equation 3.10.24 and 3.10.25:

$$\sum \circlearrowright M_A = 0 \; ; 564\,\text{N} \times 0.040\,\text{m} + 564\,\text{N} \times 0.030\text{m} - F_{BR} \times l = 0 \qquad (3.10.24)$$

$$F_{BR} = \frac{564\,\text{N} \times 0.040\,\text{m} + 564\,\text{N} \times 0.030\,\text{m}}{0.020\,\text{m}} = 1\,974\,\text{N} \qquad (3.10.24.1)$$

$$\sum_{\overrightarrow{F_x}} = 0; F_{AR} + F_{BR} + F_R = 0 \qquad (3.10.25)$$

$$F_{AR} = -F_{BR} - F_R = -1\,974\,\text{N} - 564\,\text{N} = -2\,538\,\text{N}. \qquad (3.10.25.1)$$

Figure 3.10.6 shows the relationship between the distance l, and the sum of the forces that occur in the bearings.
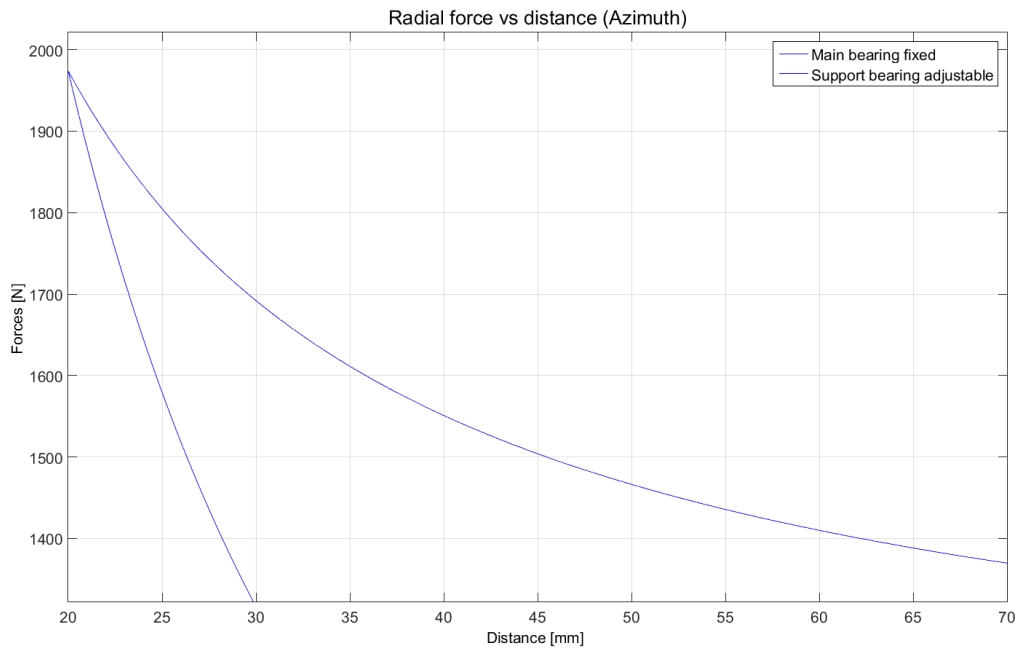

Figure 3. 10. 6: Radial force vs distance

For angular contact ball bearing [6]:

For angular contact ball bearing, the calculations factors are given by SKF [6].

In equation 3.10.13.2, F_a was calculated to 564 N and in equation 3.10.25.1 the highest radial force was found, $F_{AR} = 2538$ N. These forces are used as input in equation 3.10.17:

$$Fa = 564 \text{ N and } F_r = F_{AR} = 2538 \text{ N}$$

$$\frac{F_a}{F_r} = \frac{564 \text{ N}}{2538 \text{ N}} \tag{3.10.26}$$

$$= 0{,}22222 \leq \text{e.} \tag{3.10.27}$$

Since $\frac{F_a}{F_r} \leq e$ (equation 3.10.17), the dynamic equivalent bearing load, *P,* will be:

$$\tag{3.10.28}$$

$$P = F_r = 2538 \text{ N.}$$

$$C_0 > 2P \tag{3.10.29}$$
$$= 2 \times 2538 \text{ N} = 5076 \text{ N}$$

SSM

SMALL SATELLITE MECHANISMS

For deep groove ball bearing, [7]:

Table 3.10.1 shows calculation factors for deep grove ball bearings [4][7]:

$$\frac{F_a}{F_r} = \frac{564\ N}{2538\ N} \tag{3.10.30}$$

$$= 0{,}2222 > e. \tag{3.10.31}$$

Since $\frac{F_a}{F_r} < e$ from equation 3.10.21, the dynamic equivalent bearing load P is given by:

$$P = XF_r + YF_a \tag{3.10.32}$$

To get an exact answer for e we need interpolation [10]:

$$f(x) = f_1 + (f_2 - f_1)\frac{(x - x_1)}{(x_2 - x_1)} \tag{3.10.33}$$

$$e = 0.19 + (0.22 - 0.19) \times \frac{(0.2222 - 0.172)}{(0.345 - 0.172)} \tag{3.10.33.1}$$
$$= 0.1986.$$

This gives the values for X and Y:

$$X = 0.56 \tag{3.10.34}$$
$$Y = 2.20. \tag{3.10.34.1}$$

X and Y inserted in equation 3.10.28, gives us a bearing load, P:

$$P = 2538\ N \times 0.56 + 2.2 \times 564\ N \tag{3.10.35}$$
$$= 2662.1\ N$$

and static load rating $C_0 > 2P$:

$$C_0 > 2P = 2 \times 2662.1\ N = 5324.2\ N. \tag{3.10.36}$$

The same calculations are done with respect to the different lengths, l.

Table 3. 10. 2: Azimuth calculations

Azimuth	F_{BR} (N)	F_{AR} (N)	P (N) Anuglar contact ball bearing	$C_o > 2P$ (N) Anuglar contact ball bearing	P (N) Deep groove ball bearing	$C_o > 2P$ (N) Deep groove ball bearing
20 mm	1974	2538	2538	5076	2662.2	5324.2
30 mm	1316	1880	1880	3760	2293.6	4587.2
40 mm	987	1551	1551	3102	2109.4	4218.8
50 mm	789.6	1353.6	1353.6	2707.2	2000.5	4001

3.10.2.3.   *Elevation*

The same procedure for calculations is executed on the elevation stage. The distance between the bearings varies with a length, l. For elevation, the values of $l = 10$ mm, 15 mm, 20 mm. Therefore, three calculations were made. Figure 3.10.7 shows the relationship between the distance, l, and force with respect to the radial forces that occur in the bearings. Table 3.10.3 shows the results of the calculations.
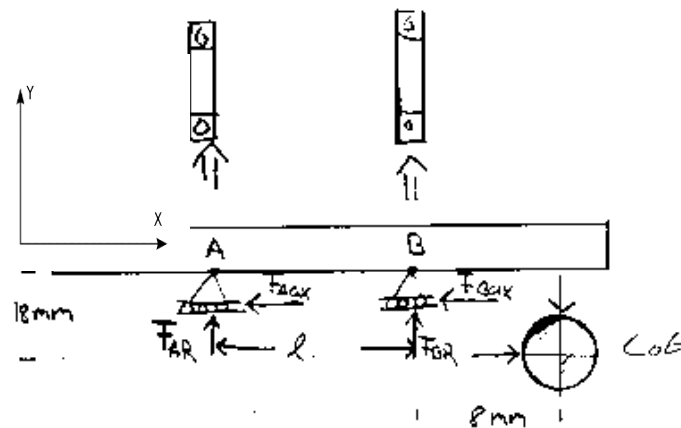

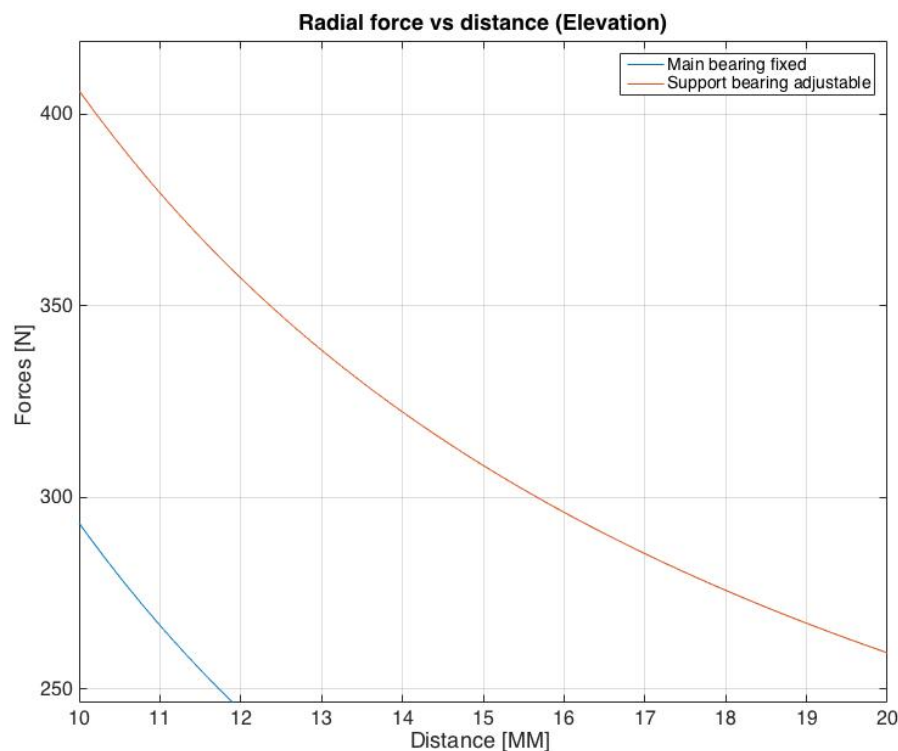*Figure 3. 10. 7: Force distribution, elevation*

Figure 3. 10. 8: Radial force vs distance, elevation

Table 3. 10. 3: Elevation calculations

Elevation	F_{BR} (N)	F_{AR} (N)	P (N) Anuglar contact ball bearing	$C_o > 2P$ (N) Anuglar contact ball bearing	P (N) Deep groove ball bearing	$C_o > 2P$ (N) Deep groove ball bearing
10	406.1	293.3	406.1	812.2	475.6	951.2
15	308.3	195.5	308.3	616.6	420.8	841.6
20	260	147.2	260	520	393.8	787.6

The results from azimuth and elevation calculations are presented in appendix. The tables also includes different bearing types [6], [7], [10],[11].

As mentioned earlier the two systems are simplified, this will not give us the exact answer to the dynamic equivalent bearing load but a bit higher than necessary. It will not affect our system that much, but the bearing dimensions perhaps could be a few millimeter smaller in diameter.

3.10.3. Clamping

3.10.3.1.   *Definition*

When receiving a ball bearing from a manufacturer, some clearance can be measured or felt. This clearance provides a smooth path for the balls and almost no friction can be felt, due to the layer of lubrication, discussed in SSM5900- M&M study. This is normal and it is carefully designed by the manufacturing company. Some systems are too sensitive to this "displacement" and the bearings need less or negative clearance. This is to provide accurate position and to withstand external loads, such as vibration or thermal changes [13]. When clamping a bearing, some of this clearance, or all of it, is removed. Figure 3.10.9 shows a deep grove ball bearing with a preload *(Fa)*. This kind of preload is used for the APMA system and will be discussed in more detail in chapter 3.10.5, Preloading method.
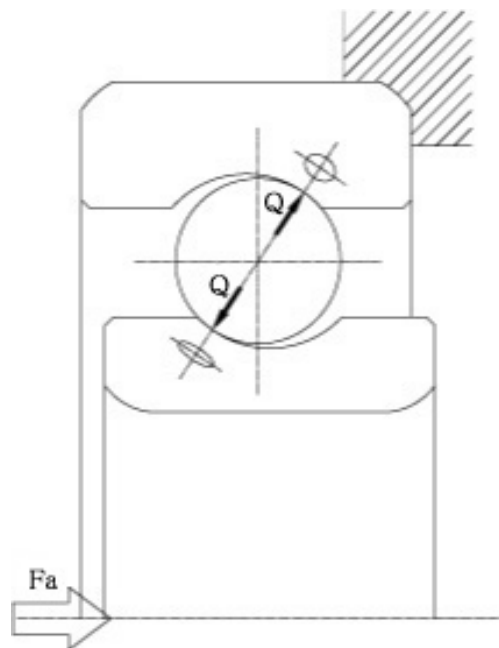

Figure 3. 10. 9: Preload illustration [13]

The three main purposes of preloading a bearing is to maintain the bearing in exact position, both radially and axially, to maintain accurate rotation and to withstand the external forces. There are some negative effects of preloading/clamping such as increased internal friction, reduced lifetime and oversized bearings due to hard preload, which results in increased mass.

3.10.3.1.1.   Vibration and Forces

When the system is hovering in space the only acceleration working on the system is G_{RMS}. This value was estimated to 282 m/s^2 in equation 3.10.12.2. This value inserted in equation 3.10.13 gives us a total force of 564 N. This means that the preload sizing has to be adjusted for this force to prevent displacement.

3.10.3.2.   *Calculations*

In collaboration with SKF we tried to figure out how small bearings that can be used to satisfy the loads applied. These loads include preload to the bearings with respect to lifetime and mass, and static/dynamic loads to maintain the given position for proper performance. The thermal and launch part is not included.

The following calculations are done with two W6005 bearings, with 30 mm spacing. The bearings will work with external loads, known from appendix 3.10.7.7.3. Due to this, analysis has to be done to check if they will work under preloading.

To estimate the preload, calculations of how the external forces, G_{RMS} changes the force distributions in the bearings have to be derived. The calculations are performed in collaboration with KDA.
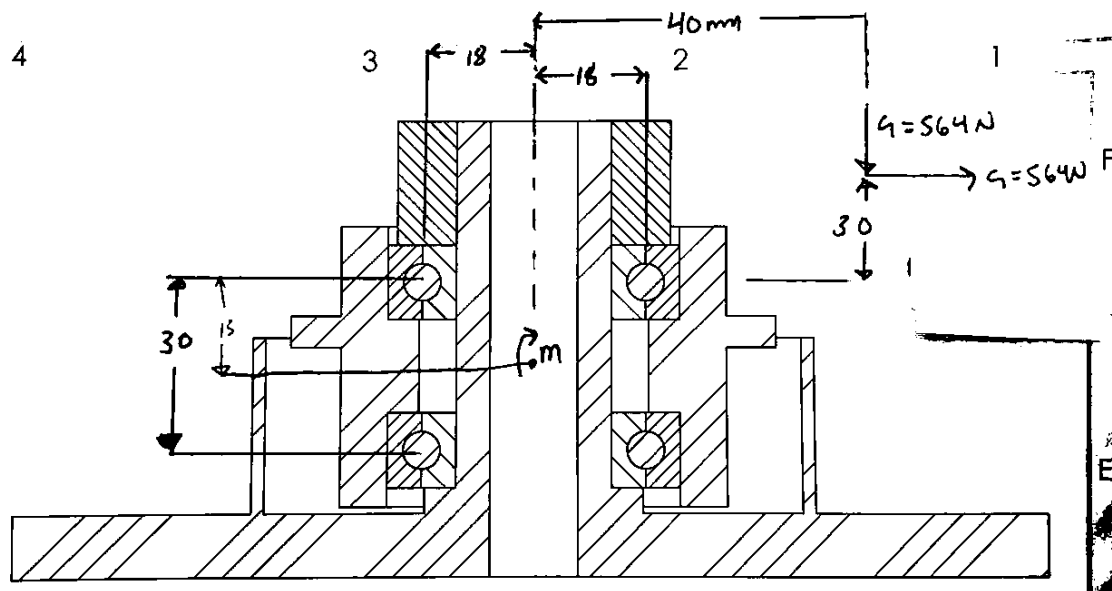

Figure 3. 10. 10: Force distribution, preload calculations

Total axial forces, inclusive preload, is equal to G_{RMS} = 564 N due to equilibrium of the two bearings caused by the bearing arrangement. G_{RMS} is also causing a momentum in the bearings, which leads to

axial and radial forces. The axial forces are much smaller than G_{RMS}, and due to this, no calculations are needed.

Taking the momentum *m,* around the center of arrangement to eliminate the X and Y direction of the forces of G_{RMS} for the radial forces, gives the following results:

$$M_a = \sum \circlearrowleft M_a$$

(3.10.37)

$$M_a = G_{RMS} \times 40mm + G_{RMS} \times 30mm$$

(3.10.37.1)

$$M_a = 39480Nmm = 39.5Nm$$

(3.10.37.2)

The total radial force working in the bearings will be:

$$F_{radial} = \sum \overrightarrow{F_x}$$

(3.10.38)

$$F_{radial} = \frac{M_a/2}{15mm} \pm G_{rms},$$

(3.10.38.1)

$\pm$ decides the direction of the force. When looking for the highest working force, the + sign has to be used. M_a is divided by two due to the two bearings:

$$F_{radial} = \frac{39.5Nm/2}{0.015m} + 564N$$

(3.10.38.2)

$$F_{radial} = 1846\ N$$

(3.10.38.3)

The input for the calculator [18] is therefore $F_{radial} = 1846\ N$ and $F_{axial} = 564\ N$, the highest force that can occur.

3.10.3.3.   *Results*
Table 3.10.4 shows the results of preloading the bearing and the highest external forces. Equivalent dynamic bearing load *P* is then 1850N.

Table 3. 10. 4: Input and result, bearing dynamics

Setup:		
	Value:	**Recourse:**
Bearing:	W6005	SKF [20]
Axial force	564 N	Ch. 3.10.3.2
Radial load	1846 N	Ch. 3.10.3.2
Distance between bearings	30mm	Calculated in 3.10.7.7.3
Speed (RPM)	10 RPM	REQ 2.4.4
Temperature	-20	Worst case estimated
Lubrication	Grease	5900_M&M_study_rev1.0
Result:		
Equivalent dynamic bearing load (P)	1.85 kN	SKF calculator [18]

To see if the bearings can survive the preload and the highest forces that occur, the following relationship is checked:

$$C_0 > 2P, \tag{3.10.39}$$

where C_0 still are 5800 N

$$C_0 > 2 \times 1846N \tag{3.10.39.1}$$
$$C_0 > 3692 \, N \tag{3.10.39.2}$$

The bearings are suitable and the preload reduces equivalent dynamic bearing load by $\approx 20\%$. Note that the safety factor also is increased to $\approx 36\%$.

Following engineering judgments and partially estimated calculations, the bearings will also have the life time needed for 5 years, 43800 hours (REQ2.8.2).

3.10.4. Friction

3.10.4.1. *Definition*
When the bearing is selected and the preloading set, the dynamic changes in the bearings have to be analyzed. As already mentioned, a negative factor is increased friction, which increases the torque and decreases the lifetime.

3.10.4.1.1. Hertzian stress (contact stress)
The applied load causes friction stress on the ball bearings, which is called contact stress, also known as Hertzian stress. The definition of Hertzian stress is deformation of solids that touch each other at one or more points. [13]

The force discussed in section 3.10.3.1.1, excluding preload/clamping, is related to the displacement of the ball in the ball bearing and is given by [13]. Preload/clamping must be included to find the maximum friction force working in the bearing [13]:

$$F = \frac{4}{3}E^*R^{\frac{1}{2}}d^{\frac{1}{2}}, \tag{3.10.40}$$

where R is the radius of the ball and d is depth of indention and E^* is:

$$\frac{1}{E^*} = \frac{1-v_1^2}{E_1} + \frac{1+v_2^2}{E_2}, \tag{3.10.41}$$

where E_1, E_2 are the elastic modulus and v_1, v_2 is poison's ratio of the ball and ball housing. The maximum Hertzian stress is given by P_0:

$$P_0 = \frac{3F}{2\pi a^2}, \tag{3.10.42}$$

where a is the radius of the indented circle given by :

$$a = \sqrt{Rd}, \tag{3.10.43}$$

where R is the radius of the ball and d is depth of indention.

To start the system from 0 deg/s , a minimum torque of 94,6 Nmm is needed, ref. table 3.10.5. 4.52 Nmm torque is needed to keep the "given" velocity, this with respect to friction only. The increased frictional moment changes the total torque slightly, described in SSM-5901 Technical budgets, [23].

Table 3. 10. 5: Input and results, bearing dynamics 2

Setup:		
	Value:	**Recourse:**
Bearing:	W6005	SKF [21]
Axial force	564 N	Chpt. 3.10.3.2
Radial load	1846 N	Chpt. 3.10.3.2
Distance between bearings	30 mm	Calculated in 3.10.7.7.3
Speed (RPM)	10 RPM	REQ 2.4.4
Temperature	-20	Worst case estimated
Lubrication	Grease	5900_M&M_study_rev1.0
		Results:
Displacement between IR and OR	0.100 mm	From SKF [17]
Total friction momentum in startup for the bearing	94.6 Nmm	From SKF calculator [18]
Rolling frictional moment	4.52 Nmm	From SKF calculator [18]

3.10.4.1.2. Press fit

In collaboration with Kongsberg Space & Surveillance, it has been decided that the press fit shall be light. This means that we can exclude this from the internal friction in the bearing, due to minimal dynamic changes. Light press also means that the bearing house has the same size as the outside diameter of the bearing.

Table 3.10.6 shows an example of a press fit for an inner ring (hub) and a shaft equal to the SSM system. The example has equal size and material. From the calculations in table 3.10.6, 459 N force is required to be pressed into the bearing, and the bearing holds on to the shaft with a force of $5.8 \, N/mm^2$.

Table 3. 10. 6: Press fit example, calculated from MEDAinfo [14]

Shaft		
Young's Modulus, *Ei* (Gpa)	69,0	
Poisson's Ratio, *vi*	0,330	
Shaft Internal Diameter, *di* (mm)	14,500	
Shaft Nominal Diameter, *d* (mm)	25,000	
Shaft Upper Tolerance (mm)	0,005	
Shaft Lower Tolerance (mm)	0,000	
Shaft Maximum Diameter (mm)	25,005	
Shaft Minimum Diameter (mm)	25,000	
Hub		
Young's Modulus, *Eo* (Gpa)	193,0	
Poisson's Ratio, *vo*	0,300	
Hub Outer Diameter, *do* (mm)	52,00	
Hole Nominal Diameter, *d* (mm)	25,000	
Hole Upper Tolerance (mm)	0,001	
Hole Lower Tolerance (mm)	0,000	
Hole Maximum Diameter (mm)	25,001	
Hole Minimum Diameter (mm)	25,000	
Pressure Generated between Shaft and Hub		
Maximum Radial Interference, δmax (mm)	0,0025	
Max Pressure Generated, pmax (N/mm^2)	<u>5,8</u>	
	=	
Force Required to Engage/Disengage Shaft and Hub		
Width of Hub, w (mm)	10,00	
Friction Between Shaft and Hub, μ	0,10	
Area of Contact, A (mm²)	785	
Force Required, F (N)	<u>459</u>	
A MEADinfo Product		

Based on experience from KDA, a very light press fit is enough to hold the bearings in position. Additionally, a nut is screwed on the top of the bearing arrangement (discussed in section 3.10.5).

3.10.5. Preloading method

Figure 3.10.11 shows the bearing arrangement in the APMA. A special nut (KMT M25x1.5) is screwed on the top of the first bearing and tightened corresponding to the preload force. The blue lines show the stress distribution through the bearing arrangement. This kind of stress distribution can absorb stress both axially and radially, which suits the stress scenario due to bending momentum and axial forces.
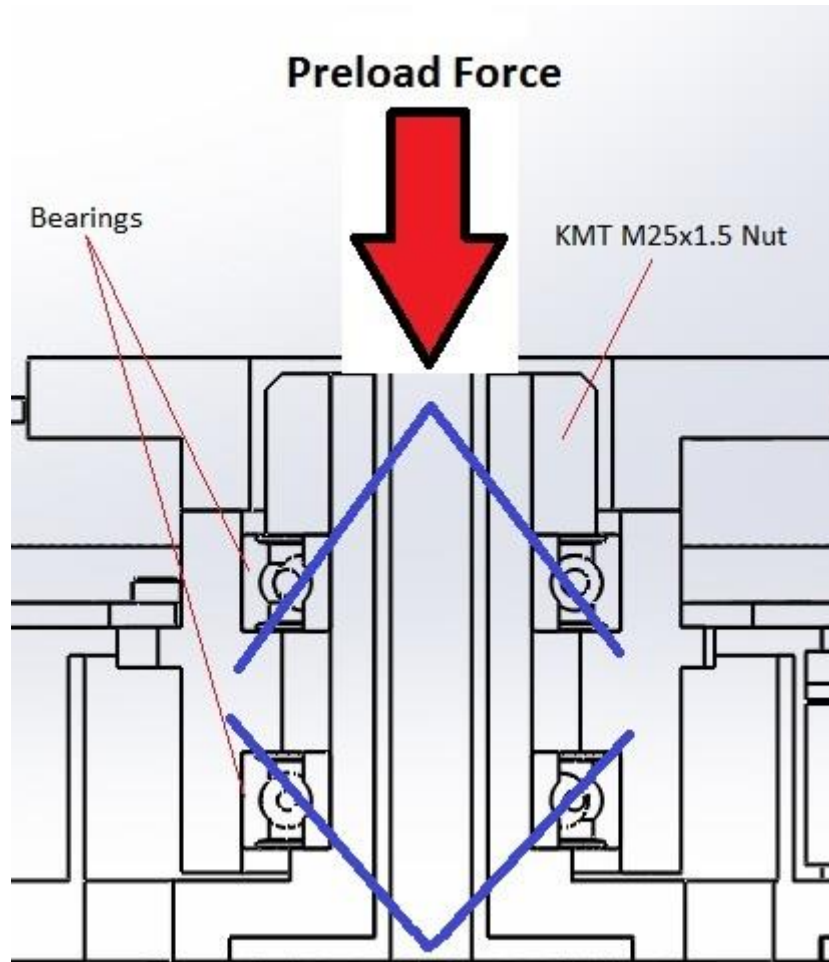

Figure 3. 10. 11: Force absorption, bearings

To estimate the momentum we need to tighten the nut. To obtain the given preload, some calculations have to be executed:

Total momentum is given by, [17]:

$$M = M_v + M_s, \tag{3.10.44}$$

where M_v is friction and pitch momentum in the threads during tightening and loosening. M_v is given by:

$$M_v = F \frac{d_m}{2} tan(\varepsilon \pm \phi), \tag{3.10.45}$$

where F is the preload, d_m is pitch diameter, ε is friction angle and ϕ is thread pitch angle. $\pm$ determine if we are loosening the bolt (-), or tightening the bolt (+).

M_s is the momentum between the bolt head and the surface. M_s is given by:

$$M_s = Fr_m\mu'. \tag{3.10.46}$$

In this case, we are using a special nut from SKF and table 3.10.7 shows parameters needed for the calculations.

Table 3. 10. 7: SKF lock nut

KMT M25x1,5, [16]

		Value:	Resource:
Pitch	P	1.5mm	Given SKF [16]
Preload	F	570N	Given in chapter 3.10.3.2
Thread angle	α	30°	Given for M threads. [19]
Friction thread/thread	μ	0.5	Estimated for aluminum/steel
Friction bolt-head/surface	μ'	0.5	Estimated for aluminum/steel
Pitch diameter	$d_m = 25 - \dfrac{P}{2}$	24.25mm	Estimated based on SKF [16]
Friction angle	$\varepsilon = tan^{-1}\left(\dfrac{\mu}{cos\alpha}\right)$	1.27	[19]
Thread pitch angle	$\phi = tan^{-1}\left(\dfrac{P}{\pi d_m}\right)$	0.02	[19]

In our case the estimated momentum needed is:

$$M = F \frac{d_m}{2} tan(\varepsilon \pm \phi) + Fr_m\mu'. \tag{3.10.47}$$

The parameters inserted in equation 3.10.44 based on table 3.10.7 gives:

$$M = 570N \frac{24.25mm}{2} tan^{-1}(1.27 + 0.02) + 570N \times 12.125mm \times 0.5 \tag{3.10.48}$$

$$= 27418.4 \, Nmm$$

$$= 27.4 \, Nm.$$

Figure 3.10.12 shows a sketch of the forces and elongations that applies in the bolt, where C to A represent the elongation of the screw (0.003 mm) and A to D the elongation of the nut (0.00085 mm). The total elongation is of 0.00385 mm under preload.
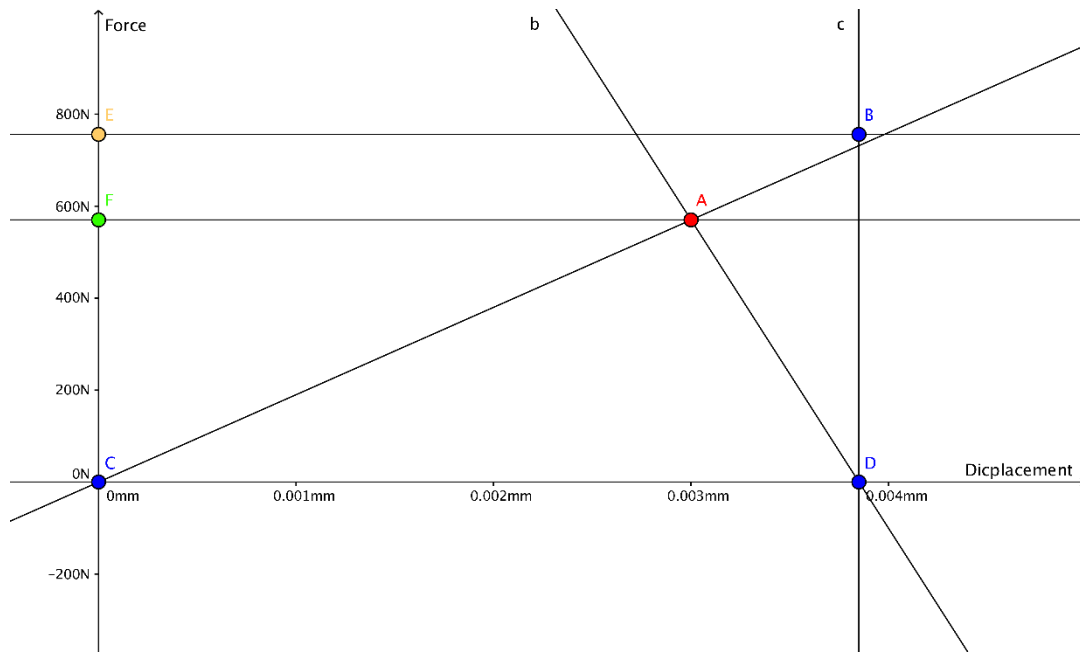
Figure 3. 10. 12: Screw diagram

This is highly estimated and should only give us an estimation. Preload and bolt etc. calculations are highly complex and almost impossible to get 100% accurate. KDA uses a tolerance of $\pm$ 200 N during preload, which is very high.

To eliminate the problem with elongation, a special hollow strut in a stiff material is used between the inner rings of the bearings. The length of the hollow strut is carefully calculated to give the needed preload. In this case the hollow strut should have a height of 0.1mm (Table 3.10.5) less than the distance between the bearings.

This also increases the stiffness of our system and will be discussed during assembly of the prototype.

3.10.6. Conclusion

The main goal with this report was to calculate estimations of the bearing and bearing dynamics for the azimuth assembly.

The W6005 ball bearing is the most suiting for this assembly, and will fulfill the requirement goals according to lifespan. Some minor errors appear in the appendices. The calculations are made individually for each bearing with respect to the loads and not as a pair of bearings. This leads to higher equivalent dynamic bearing load *p* than in reality, which means that the bearings may be oversized and increased, and unnecessary mass may have been added.

Due to limited time in this project, the error will not be fixed in this prototype. However, this gives valuable input for the next prototype/the final product.

The further plan is to execute a functional test with this setup, including plausible oversized bearing.

3.10.7. References

[1]   SKF, "Deep groove ball bearings, single row, stainless steel," SKF, [Online]. Available:
        http://www.skf.com/uk/products/bearings-units-housings/ball-bearings/deep-groove-ball-
        bearings/stainless-steel-deep-groove-ball-bearings/single-row-stainless-
        steel/index.html?designation=W%20630/2.5-2Z&unit=metricUnit. [Accessed 16 March 2016].

[2]   J. Etter, "Tutorial Report on Hertzian Contact Stress Theory," [Online]. Available:
        http://fp.optics.arizona.edu/optomech/student%20reports/tutorials/Tutorial_Etter,%20Jacob.pdf
        . [Accessed 17 March 2016].

[3]   NASA, "Newton's Second Law," [Online]. Available: https://www.grc.nasa.gov/www/k-
        12/airplane/newton2.html. [Accessed 17 March 2016].

[4]   Ø. Vollen, Statikk og fasthetslære, Bekkestua: NKI Forlaget AS, 2010.

[5]   R. Simmons, "Miles' Equation," May 2001. [Online]. Available:
        https://femci.gsfc.nasa.gov/random/MilesEqn.html.

[6]   SKF, "Vinkelkontaktkullager," in *SKF Rullningslager*, SKF, 2014, pp. 475-535.

[7]   SKF, "Spårkullager," in *SKF Rullingslager*, SKF, 2014, pp. 295-419.

[8]   G. H. Stenseth and M. Dybendal, "SSM-2000, Requirement Specification," Kongsberg, 2016.

[9]   M.K. Samarin, "Linear Interpolation," 15 July 2012. [Online]. Available:
        https://www.encyclopediaofmath.org/index.php/Linear_interpolation.

[10]   NSK, "SPACEA - Bearings, Ball Screws and NSK Linear Guides, for Special Environments,"
        June 2011. [Online]. Available:
        http://www.nskamericas.com/cps/rde/dtr/na_en/na_literature_bearing/E1258b_-_SPACEA.pdf.

[11]   SKF, "Suffixes A - B," [Online]. Available: http://www.skf.com/group/products/bearings-
        units-housings/ball-bearings/principles/bearing-basics/basic-bearing-designation-
        system/prefixes-and-suffixes/suffixes-a-b/index.html. [Accessed 2016 March].

[12]   NSK, "Rolling Bearings - Preload," [Online]. Available:
        http://www.nskamericas.com/cps/rde/xbcr/na_en/Preload.pdf. [Accessed January 2016].

[13]   Wikipedia, "Contact Mechanics," [Online]. Available:
        https://en.wikipedia.org/wiki/Contact_mechanics. [Accessed 12 April 2016].

[14]   MEADinfo, "Press Fitt Pressure Calculator," 21 October 2012. [Online]. Available:
        http://www.meadinfo.org/2009/07/press-fit-pressure-calculator-optimize.html.

[15]   "Bearing preload," [Online]. Available: http://www.bearingtips.com/wp-
        content/uploads/2016/03/AST-image_1_preload300dpi.jpg. [Accessed 14 April 2016].

[16]   SKF, "KMT precision lock nuts with locking pins - KMT 5," SKF, [Online]. Available:
        http://www.skf.com/group/products/bearings-units-housings/bearing-accessories/lock-

nuts/precision-locking-pin/kmt-precision-lock-nuts-with-locking-pins/index.html?designation=KMT%205&unit=metricUnit. [Accessed 17 April 2016].

[17] H. Tveit, SKF, Application Engineer, Industrial Market Norway. [Online]. [Accessed 18 April 2016].

[18] SKF, "SKF - Bearing Calculator," [Online]. Available: http://webtools3.skf.com/BearingCalc/selectProduct.action. [Accessed 18 April 2016].

[19] Høgskolen i Gjøvik, "Styrkeberegning: skrueforbindelser," [Online]. Available: http://www.ansatt.hig.no/henningj/materialteknologi/Skriftserien/SB_Skrueforbindelser_2012_nr.2_(endret_2014).pdf. [Accessed 17 April 2016].

[20] SKF, "SKF Bearing Calculator," [Online]. Available: http://www.skf.com/group/knowledge-centre/engineering-tools/skfbearingcalculator.html. [Accessed 18 April 2016].

[21] SKF, "Deep groove ball bearings, single row, stainless steel - W6005," SKF, [Online]. Available: http://www.skf.com/uk/products/bearings-units-housings/ball-bearings/deep-groove-ball-bearings/stainless-steel-deep-groove-ball-bearings/single-row-stainless-steel/index.html?designation=W%206005&unit=metricUnit. [Accessed 18 April 2016].

[22] E. Løken et. al, "SSM-5901, Technical budgets," Kongsberg, 2016.

3.10.8. Appendices

This appendix includes tables of different types of bearings that are suitable and not suitable for the APMA system. All the tables below describe the specifications of the bearings, where all calculations are added.

3.10.8.1.   *Suffixes*

Table 3. 10. 8: Suffixes [12]

SUFFIXES (SKF Bearings)	
BEP (B + E + P)	Single row angular contact ball bearing with a 40° contact angle and optimized internal design, with molded cage of glass fiber reinforced polyamide 66
BECBP	B + E + CB + P
BE-2RZP	B + E + -2RZ + P
BEGAP	B + E + G + A + P
BECBY	B + E + CB + Y
BECBJ	B + E + CB + J
A	Deviating or modified internal design with same boundary dimensions. As a rule the significance of the letter is bound to the particular bearing or bearing series.
B	Deviating or modified internal design with same boundary dimensions. As a rule the significance of the letter is bound to the particular bearing series. Taper roller bearing to ABMA standard with external flange on the outer ring.
CB	Single row angular contact ball bearing for universal matching. Two bearings arranged back-to-back or face-to-face will have a Normal axial internal clearance before mounting. Controlled axial clearance of a double row angular contact ball bearing-

E	Deviating or modified internal design with same boundary dimensions; as a rule the significance of the letter is bound to the particular bearing series; usually indicates reinforced rolling element complement
H	Pressed snap-type steel cage, hardened. Needle roller bearing without inner ring with reduced inside diameter (under rollers) tolerance; followed by tolerance limits in µ m, e.g. /H+20+27.
J	Pressed steel cage, rolling element centred, unhardened; different designs are identified by a figure, e.g. J1
P	Injection moulded cage of glass fibre reinforced polyamide 66, rolling element centred
Y	Presset holder av messingplate. Forskjellige utførelser og materialer angis ved påfølgende tall. F.eks Y1.
(-)2RZ	RZ low-friction seal on both sides of the bearing
RZ	Sheet steel reinforced low-friction seal of acrylonitrile-butadiene rubber (NBR)
2RS1	RS1 contact seal on both sides of the bearing

3.10.8.2. *Azimuth 20 mm, Elevation 10 mm*

3.10.8.2.1. NSK Standard bearings

Table 3. 10. 9: NSK Standard bearings, 20 mm Azimuth, 10 mm Elevation [10]

20 mm Azimuth	10 mm Elevation								
NSK standard bearings									
Bearing number	Bore diameter(mm)	Outside diameter(mm)	width of open/shielded type (mm)	C_0 (N)	Calculated P Azimuth	Calculated P Elevation	Mass (g)	Good/ Bad Azimuth	Good/ Bad Elevation
6800	10	19	5	1460	5324.2	951.2	?		

6900		22	6	2290			?	
6000		26	8	3900			?	
6200		30	9	4350			?	
6300		35	11	6900			?	
6802		24	5	1760			?	
6902		28	7	3700			?	
6002	15	32	9	4750	5324.2	951.2	?	
6202		35	11	6500			?	
6302		42	13	9700			?	
6804		32	7	3400			?	
6904		37	9	5400			?	
6004	20	42	12	7950	5324.2	951.2	?	
6204		47	14	10900			?	
6304		52	15	13500			?	
6805		37	7	3800			?	
6905		42	9	5950			?	
6005	25	47	12	8550	5324.2	951.2	?	
6205		52	15	11900			?	

3.10.8.3. *NSK Angular contact ball bearing*

Table 3. 10. 10: NSK Angular contact ball bearing, 20 mm Azimuth, 10 mm Elevation [10]

20 mm Azimuth	10 mm Elevation								
NSK Angular contact ball bearings									
Bearing number	Bore diameter (mm)	Outside diameter(mm)	width of open/shielded type (mm)	C_0 (N)	Calculated P Azimuth	Calculated P Elevation	Mass (g)	Good/ Bad Azimuth	Good/ Bad Elevation
706A	6	17	6	1730			?		
708A	8	22	7	2840			?		
7000A	10	26	8	4250			?		
7001A	12	28	8	4600			?		
7902A5		28	7	3850			?		
7002A	15	32	9	4900			?		
7202A		35	11	6900			?		
7003A	17	35	10	5200	5076	812.2	?		
7904A5		37	9	5600			?		
7004A	20	42	12	8750			?		
7204A		47	14	11600			?		
7005A	25	47	12	9150			?		
7205A	25	52	15	13100			?		
7905A5	30	47	9	6700			?		

3.10.8.3.1. SKF Deep groove ball bearing

Table 3. 10. 11: SKF Deep groove ball bearing, 20 mm Azimuth, 10 mm Elevation [7]

20 mm Azimuth	10 mm Elevation								
SKF Deep groove ball bearings									
Bearing number	Bore diameter(mm)	Outside diameter(mm)	width of open/shielded type (mm)	C_0 (N)	Calculated P Azimuth	Calculated P Elevation	Mass (g)	Good/ Bad Azimuth	Good/ Bad Elevation
W 6300		35	11	3400			50.5		
W 6200		30	9	2320			29.1		
W 6000	10	26	8	1960	5324.2	951.2	17.6		
W 6300-2RS1		19	5	3400			50.9		
W 63800-2RS1		19	7	830			7.1		
W 6202		35	11	3600			42.2		
W 6302		42	13	5400			78.6		
W 6002	15	32	9	2800	5324.2	951.2	27.3		
W 6002 2RS1		35	11	3600			28.8		
W 6202 2RS1		32	9	2800			44.2		
W 61904		37	9	3650			33,2		
W 6204-2Z		47	14	6550			106		
W 6204	20	47	14	6550	5324.2	951.2	102		
W 6304		52	15	7800			140		
W 6004		42	12	5000			62.1		
W 6205	25	52	15	7650	5324.2	951.2	124		

Bearing number		Outside diameter (mm)	width (mm)	C_0 (N)			Mass (g)	Good/Bad Azimuth	Good/Bad Elevation
W 6305		62	17	11200			228		
W 6305-2Z		62	17	11200			236		
W 6005		47	12	5850			73.1		
W 6005-2Z		47	12	5850			78.2		

3.10.8.3.2.   SKF Angular contact ball bearing

Table 3. 10. 12: SKF Angular contact ball bearing, 20 mm Azimuth, 10 mm Elevation [6]

20 mm Azimuth	10 mm Elevation								
SKF Angular contact ball bearings									
Bearing number	Bore diameter (mm)	Outside diameter (mm)	width of open/shielded type (mm)	C_0 (N)	Calculated P Azimuth	Calculated P Elevation	Mass (g)	Good/Bad Azimuth	Good/Bad Elevation
7200 BEP	10	30	9	3350	5076	812.2	30		
7200 BECBP		30	9	3350			30		
7302 BECBP	15	42	13	6700	5076	812.2	80		
7302 BE-2RZP		42	13	6700			82		
7202 BE-2RZP		35	11	4400			45		
7302 BEP		42	13	6700			80		
7202 BECBP		35	11	4650			45		
7202 BEP		35	11	4400			45		
7202 BEGBP		35	11	4650			45		
7202 BEGAP		35	11	4650			45		
7204 BECBY	20	47	14	7650	5076	812.2	110		
7204 BECBJ		47	14	7650			110		

7204 BEGBP		52	15	10000			140		
7205 BECBPH		52	15	15600			130		
7205 BEGBY		52	15	9300			130		
7205 BEP	25	52	15	9300	5076	812.2	130		
7205 BECBP		52	15	10000			130		
7305 BEP		62	17	14000			230		

3.10.8.4.   *Azimuth 30 mm, Elevation 15 mm*

3.10.8.4.1.   NSK Standard bearings

Table 3. 10. 13: SK Standard bearings, 30 mm Azimuth, 15 mm Elevation [10]

30 mm azimuth	15 mm elevation								
NSK standard bearings									
Bearing number	Bore diameter(mm)	Outside diameter(mm)	width of open/shielded type (mm)	C_0 (N)	Calculated P Azimuth	Calculated P Elevation	Mass (g)	Good/ Bad Azimuth	Good/ Bad Elevation
6800		19	5	1460			?		
6900		22	6	2290			?		
6000	10	26	8	3900	4587.2	841.6	?		
6200		30	9	4350			?		
6300		35	11	6900			?		
6802		24	5	1760			?		
6902		28	7	3700			?		
6002	15	32	9	4750	4587.2	841.6	?		
6202		35	11	6500			?		

6302		42	13	9700			?		
6804		32	7	3400			?		
6904		37	9	5400			?		
6004	20	42	12	7950	4587.2	841.6	?		
6204		47	14	10900			?		
6304		52	15	13500			?		
6805		37	7	3800			?		
6905		42	9	5950			?		
6005	25	47	12	8550	4587.2	841.6	?		
6205		52	15	11900			?		

3.10.8.4.2.   NSK Angular contact ball bearings

Table 3. 10. 14: NSK Angular contact ball bearings, 30 mm Azimuth, 15 mm Elevation [10]

30 mm azimuth	15 mm elevation								
NSK Angular contact ball bearings									
Bearing number	Bore diameter(mm)	Outside diameter(mm)	width of open/shielded type (mm)	C_0 (N)	Calculated P Azimuth	Calculated P Elevation	Mass (g)	Good/ Bad Azimuth	Good/ Bad Elevation
706A	6	17	6	1730			?		
708A	8	22	7	2840			?		
7000 A	10	26	8	4250			?		
7001 A	12	28	8	4600	3760	616.6	?		
7902 A5	15	28	7	3850			?		
7002 A		32	9	4900			?		

7202 A		35	11	6900			?		
7003 A	17	35	10	5200			?		
7904 A5		37	9	5600			?		
7004 A	20	42	12	8750			?		
7204 A		47	14	11600			?		
7005 A	25	47	12	9150			?		
7205 A	25	52	15	13100			?		
7905 A5	30	47	9	6700			?		

3.10.8.4.3. SKF Deep groove ball bearings

Table 3. 10. 15: SKF Deep groove ball bearings, 30 mm Azimuth, 15 mm Elevation [7]

30 mm azimuth	15 mm elevation								
SKF Deep groove ball bearings									
Bearing number	Bore diameter (mm)	Outside diameter (mm)	width of open/shielded type (mm)	C_0 (N)	Calculated P Azimuth	Calculated P Elevation	Mass (g)	Good/ Bad Azimuth	Good/ Bad Elevation
W 6300		35	11	3400			50.5		
W 6200		30	9	2320			29.1		
W 6000	10	26	8	1960	4587.2	841,6	17.6		
W 6300-2RS1		19	5	3400			50.9		
W 63800-2RS1		19	7	830			7.1		
W 6202		35	11	3600			42.2		
W 6302	15	42	13	5400	4587.2	841.6	78.6		
W 6002		32	9	2800			27.3		

Bearing number	Bore diameter (mm)	Outside diameter (mm)	width of open/shielded type (mm)	C_0 (N)	Calculated P Azimuth	Calculated P Elevation	Mass (g)	Good/Bad Azimuth	Good/Bad Elevation
W 6002 2RS1		35	11	3600			28.8	(pink)	(green)
W 6202 2RS1		32	9	2800			44.2	(pink)	(green)
W 61904	20	37	9	3650	4587.2	841.6	33.2	(pink)	(green)
W 6204-2Z		47	14	6550			106	(green)	(green)
W 6204		47	14	6550			102	(green)	(green)
W 6304		52	15	7800			140	(green)	(green)
W 6004		42	12	5000			62.1	(green)	(green)
W 6205	25	52	15	7650	4587.2	841.6	124	(green)	(green)
W 6305		62	17	11200			228	(green)	(green)
W 6305-2Z		62	17	11200			236	(green)	(green)
W 6005		47	12	5850			73.1	(green)	(green)
W 6005-2Z		47	12	5850			78.2	(green)	(green)

3.10.8.4.4. SKF Angular contact ball bearings

Table 3. 10. 16: SKF Angular contact ball bearings, 30 mm Azimuth, 15 mm Elevation [6]

30 mm azimuth	15 mm elevation	SKF Angular contact ball bearings							
Bearing number	Bore diameter (mm)	Outside diameter (mm)	width of open/shielded type (mm)	C_0 (N)	Calculated P Azimuth	Calculated P Elevation	Mass (g)	Good/Bad Azimuth	Good/Bad Elevation
7200 BEP	10	30	9	3350	3760	616.6	30	(pink)	(green)
7200 BECBP		30	9	3350			30	(pink)	(green)
7302 BECBP	15	42	13	6700	3760	616.6	80	(green)	(green)

Bearing number	Bore	Outside	Width	C_0	Calc P Az	Calc P El	Mass	Good/Bad Az	Good/Bad El
7302 BE-2RZP		42	13	6700			82	🟩	🟩
7202 BE-2RZP		35	11	4400			45	🟩	🟩
7302 BEP		42	13	6700			80	🟩	🟩
7202 BECBP		35	11	4650			45	🟩	🟩
7202 BEP		35	11	4400			45	🟩	🟩
7202 BEGBP		35	11	4650			45	🟩	🟩
7202 BEGAP		35	11	4650			45	🟩	🟩
7204 BECBY		47	14	7650			110	🟩	🟩
7204 BECBJ	20	47	14	7650	3760	616.6	110	🟩	🟩
7204 BEGBP		52	15	10000			140	🟩	🟩
7205 BECBPH		52	15	15600			130	🟩	🟩
7205 BEGBY		52	15	9300			130	🟩	🟩
7205 BEP	25	52	15	9300	3760	616.6	130	🟩	🟩
7205 BECBP		52	15	10000			130	🟩	🟩
7305 BEP		62	17	14000			230	🟩	🟩

3.10.8.5.   Azimuth 40 mm, Elevation 20 mm

3.10.8.5.1.   NSK Standard bearings

Table 3. 10. 17: NSK Standard bearings, 40 mm Azimuth, 20 mm Elevation [10]

40 mm Azimuth	20 mm Elevation								
NSK standard bearings									
Bearing number	Bore diameter (mm)	Outside diameter (mm)	Width of open/shielded type (mm)	C_0 (N)	Calculated P Azimuth	Calculated P Elevation	Mass (g)	Good/Bad Azimuth	Good/Bad Elevation
6800	10	19	5	1460	4218.8	787.6	?	🟥	🟩
6900		22	6	2290			?	🟥	🟩

6000		26	8	3900			?		
6200		30	9	4350			?		
6300		35	11	6900			?		
6802		24	5	1760			?		
6902		28	7	3700			?		
6002	15	32	9	4750	4218.8	787.6	?		
6202		35	11	6500			?		
6302		42	13	9700			?		
6804		32	7	3400			?		
6904		37	9	5400			?		
6004	20	42	12	7950	4218.8	787.6	?		
6204		47	14	10900			?		
6304		52	15	13500			?		
6805		37	7	3800			?		
6905		42	9	5950			?		
6005	25	47	12	8550	4218.8	787.6	?		
6205		52	15	11900			?		

3.10.8.5.2. NSK Angular contact ball bearings

Table 3. 10. 18: NSK Angular contact ball bearings, 40 mm Azimuth, 20 mm Elevation [10]

40 mm Azimuth	20 mm Elevation								
NSK Angular contact ball bearings									
Bearing number	Bore diameter(mm)	Outside diameter(mm)	width of open/shielded type (mm)	C_0 (N)	Calculated P Azimuth	Calculated P Elevation	Mass (g)	Good/Bad Azimuth	Good/Bad Elevation
706A	6	17	6	1730			?		
708A	8	22	7	2840			?		
7000A	10	26	8	4250			?		
7001A	12	28	8	4600			?		
7902A5		28	7	3850			?		
7002A	15	32	9	4900			?		
7202A		35	11	6900			?		
7003A	17	35	10	5200	3102	520	?		
7904A5		37	9	5600			?		
7004A	20	42	12	8750			?		
7204A		47	14	11600			?		
7005A	25	47	12	9150			?		
7205A	25	52	15	13100			?		
7905A5	30	47	9	6700			?		

3.10.8.5.3.　SKF Deep groove ball bearings

Table 3. 10. 19: SKF Deep groove ball bearings, 40 mm Azimuth, 20 mm Elevation [7]

40 mm Azimuth	20 mm Elevation								
SKF Deep groove ball bearings									
Bearing number	Bore diameter(mm)	Outside diameter(mm)	Width of open/shie lded type (mm)	C_0 (N)	Calcula ted P Azimut h	Calcula ted P Elevati on	Ma ss (g)	Good/ Bad Azimut h	Good/ Bad Elevati on
W 6300	10	35	11	3400	4218.8	78.,6	50.5		
W 6200		30	9	2320			29.1		
W 6000		26	8	1960			17.6		
W 6300-2RS1		19	5	3400			50.9		
W 63800-2RS1		19	7	830			7.1		
W 6202	15	35	11	3600	4218.8	787.6	42.2		
W 6302		42	13	5400			78.6		
W 6002		32	9	2800			27.3		
W 6002 2RS1		35	11	3600			28.8		
W 6202 2RS1		32	9	2800			44.2		
W 61904	20	37	9	3650	4218.8	787.6	33.2		
W 6204-2Z		47	14	6550			106		
W 6204		47	14	6550			102		
W 6304		52	15	7800			140		
W 6004		42	12	5000			62.1		
W 6205	25	52	15	7650	4218.8	787.6	124		

W 6305		62	17	11200			228			
W 6305-2Z		62	17	11200			236			
W 6005		47	12	5850			73.1			
W 6005-2Z		47	12	5850			78.2			

3.10.8.5.4.   SKF Angular contact ball bearings

Table 3. 10. 20: SKF Angular contact ball bearings, 40 mm Azimuth, 20 mm Elevation [6]

40 mm Azimuth	20 mm Elevation								
SKF Angular contact ball bearings									
Bearing number	Bore diameter(mm)	Outside diameter(mm)	width of open/shielded type (mm)	C_0 (N)	Calculated P Azimuth	Calculated P Elevation	Mass (g)	Good/ Bad Azimuth	Good/ Bad Elevation
7200 BEP	10	30	9	3350	3102	520	30		
7200 BECBP		30	9	3350			30		
7302 BECBP	15	42	13	6700	3102	520	80		
7302 BE-2RZP		42	13	6700			82		
7202 BE-2RZP		35	11	4400			45		
7302 BEP		42	13	6700			80		
7202 BECBP		35	11	4650			45		
7202 BEP		35	11	4400			45		
7202 BEGBP		35	11	4650			45		
7202 BEGAP		35	11	4650			45		
7204 BECBY	20	47	14	7650	3102	520	110		
7204 BECBJ		47	14	7650			110		

Bearing number	Bore	Outside	Width	C_0			Mass		
7204 BEGBP		52	15	10000			140		
7205 BECBPH		52	15	15600			130		
7205 BEGBY		52	15	9300			130		
7205 BEP	25	52	15	9300	3102	520	130		
7205 BECBP		52	15	10000			130		
7305 BEP		62	17	14000			230		

3.10.8.6. *Azimuth 50 mm*

3.10.8.6.1. NSK Standard bearings

Table 3. 10. 21: NSK Standard bearings, 50 mm Azimuth [10]

50 mm azimuth								
NSK standard bearings								
Bearing number	Bore diameter(mm)	Outside diameter(mm)	Width of open/shielded type (mm)	C_0 (N)	Calculated P Azimuth	Mass (g)	Good/Bad Azimuth
6800		19	5	1460		?	
6900		22	6	2290		?	
6000		26	8	3900		?	
6200	10	30	9	4350	4001	?	
6300		35	11	6900		?	
6802		24	5	1760		?	
6902		28	7	3700		?	
6002	15	32	9	4750	4001	?	
6202		35	11	6500		?	
6302		42	13	9700		?	
6804		32	7	3400		?	
6904		37	9	5400		?	
6004	20	42	12	7950	4001	?	
6204		47	14	10900		?	
6304		52	15	13500		?	

6805		37	7	3800		?	
6905	25	42	9	5950	4001	?	
6005		47	12	8550		?	
6205		52	15	11900		?	

3.10.8.6.2. NSK Angular contact ball bearings

Table 3. 10. 22: NSK Angular contact ball bearings, 50 mm Azimuth [10]

50 mm azimuth							
NSK Angular contact ball bearings							
Bearing number	Bore diameter(mm)	Outside diameter(mm)	width of open/shielded type (mm)	C_0 (N)	Calculated P Azimuth	Mass (g)	Good/Bad Azimuth
706A	6	17	6	1730		?	
708A	8	22	7	2840		?	
7000A	10	26	8	4250		?	
7001A	12	28	8	4600		?	
7902A5		28	7	3850		?	
7002A	15	32	9	4900		?	
7202A		35	11	6900		?	
7003A	17	35	10	5200	2707.2	?	
7904A5		37	9	5600		?	
7004A	20	42	12	8750		?	
7204A		47	14	11600		?	
7005A	25	47	12	9150		?	
7205A	25	52	15	13100		?	
7905A5	30	47	9	6700		?	

3.10.8.6.3. SKF Deep groove ball bearings

Table 3. 10. 23: SKF Deep groove ball bearings, 50 mm Azimuth [7]

50 mm azimuth							
SKF Deep groove ball bearings							
Bearing number	Bore diameter(mm)	Outside diameter(mm)	Width of open/shielded type (mm)	C_0 (N)	Calculated P Elevation	Mass (g)	Good/Bad Azimuth
W 6300	10	35	11	3400		50.5	
W 6200		30	9	2320		29.1	
W 6000		26	8	1960		17.6	
W 6300-2RS1		19	5	3400		50.9	
W 63800-2RS1		19	7	830		7.1	
W 6202	15	35	11	3600		42.2	
W 6302		42	13	5400		78.6	
W 6002		32	9	2800		27.3	
W 6002 2RS1		35	11	3600		28.8	
W 6202 2RS1		32	9	2800		44.2	
W 61904	20	37	9	3650		33.2	
W 6204-2Z		47	14	6550		106	
W 6204		47	14	6550		102	
W 6304		52	15	7800		140	
W 6004		42	12	5000		62.1	
W 6205	25	52	15	7650		124	
W 6305		62	17	11200		228	
W 6305-2Z		62	17	11200		236	
W 6005		47	12	5850		73.1	
W 6005-2Z		47	12	5850		78.2	

3.10.8.6.4.   SKF Angular contact ball bearings

Table 3. 10. 24:SKF Angular contact ball bearings, 50 mm Azimuth [6]

50 mm azimuth							
SKF Angular contact ball bearings							
Bearing number	Bore diameter(mm)	Outside diameter(mm)	width of open/shielded type (mm)	C_0 (N)	Calculated P Elevation	Mass (g)	Good/Bad Azimuth
7200 BEP	10	30	9	3350		30	
7200 BECBP		30	9	3350		30	
7302 BECBP	15	42	13	6700		80	
7302 BE-2RZP		42	13	6700		82	
7202 BE-2RZP		35	11	4400		45	
7302 BEP		42	13	6700		80	
7202 BECBP		35	11	4650		45	
7202 BEP		35	11	4400		45	
7202 BEGBP		35	11	4650		45	
7202 BEGAP		35	11	4650		45	
7204 BECBY	20	47	14	7650		110	
7204 BECBJ		47	14	7650		110	
7204 BEGBP		52	15	10000		140	
7205 BECBPH	25	52	15	15600		130	
7205 BEGBY		52	15	9300		130	
7205 BEP		52	15	9300		130	
7205 BECBP		52	15	10000		130	
7305 BEP		62	17	14000		230	

3.11. Design description

i.   Abstract

This chapter presents the mechanical design of the APMA concept, which was selected through the concept analysis performed by SSM (chapter 3.1), [1]. Figure 3. 11. 1 shows a schematic system overview of the major components and assemblies of the system. The main system constituents are described in this chapter.

ii.   Contents

iii. List of figures

iv. List of tables

v. Document history

Table 3. 11. 1: Document history

Rev.	Date	Author	Approved	Description
0.1	01.03.16	MD	VOA	Document created
1.0	03.03.16	MD, VOA	VOA	Corrected typos
1.1	21.04.16	MD		Document updated
1.2	26.04.16	EL		Corrected typos
2.0	19.05.16	MD	TS	Reviewed and published

3.11.1. Introduction

The main system constituents of the APM, which are described in this document:

- Elevation assembly
- Parabola assembly
- Azimuth assembly
- Mirror over azimuth
- Cable tray
- Mounting plate, representing spacecraft
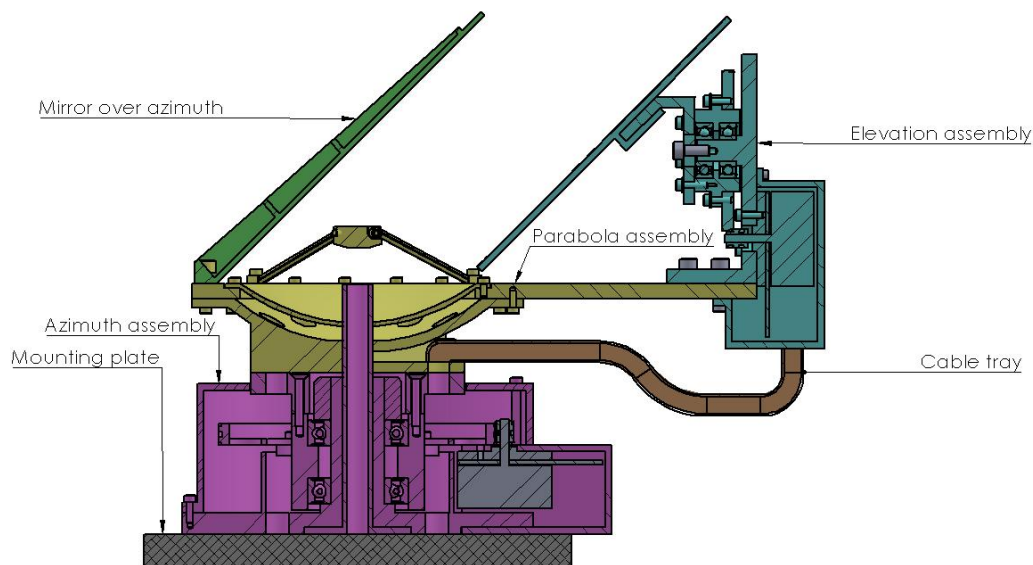
Figure 3. 11. 1: Double mirror reflector antenna - schematics

The APM consists of two drive actuators (SRA) arranged in the azimuth and the elevation stage. The actuators are identical due to cost, but they are placed on two different brackets.

The mirror reflectors are placed parallel to each other, with an angle of 45 degrees with respect to the azimuth bracket. The top-point of the "mirror over azimuth" is placed right over the bottom-point of the "elevation mirror", both with the same height, ref. Figure 3. 11. 1. In the azimuth assembly, a twist capsule is located and serves as the signal transfer.

All the dimensions in the figures such as diameters, lengths, heights etc. are engineering decisions taken during the development process due to the mass requirement, given in the requirement specification (chapter 2.2) , [2] REQ-2.2.1.

Figure 3. 11. 2 shows the APM in stowed position.
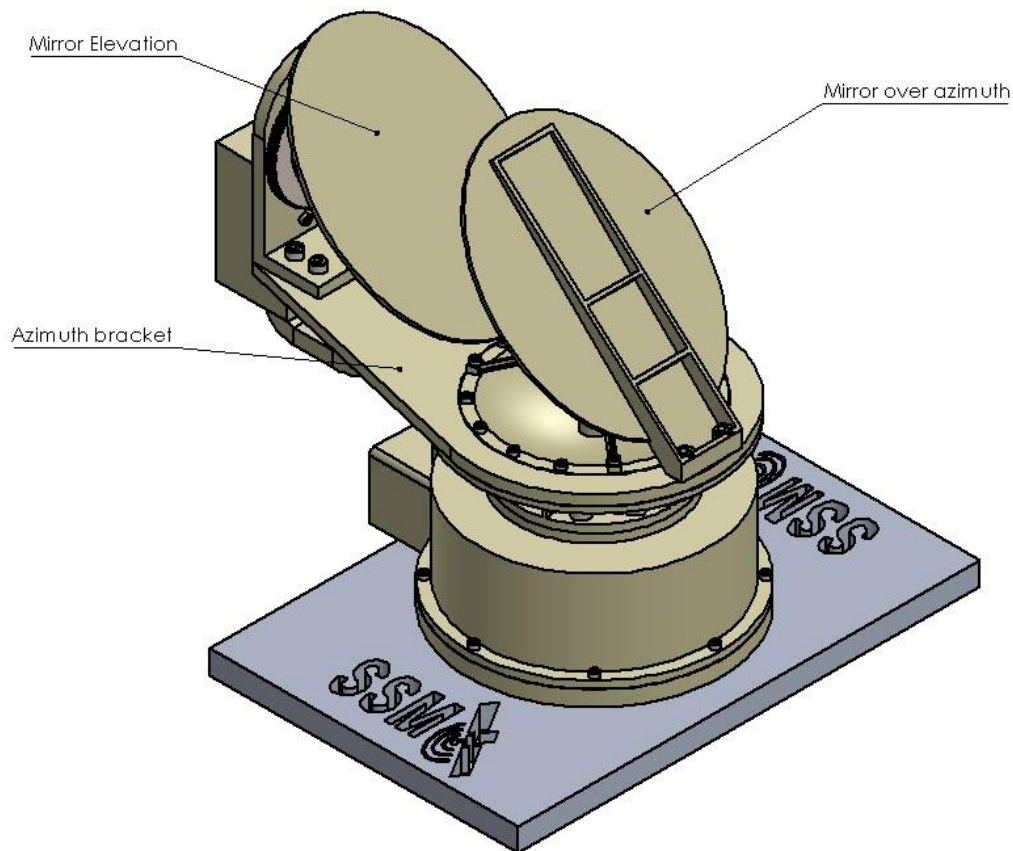
Figure 3. 11. 2: APM Assembly in stowed position

3.11.2. Design description

3.11.2.1.   *Azimuth*

Figure 3. 11. 3 shows a schematic overview of the azimuth assembly. The assembly consists of:

- 2x W6005 Bearings
- Waveguide
- 1x KMT 5 NUT
- Connector
- Gear motor
- Motor
- Motor House
- Main contact plate
- Bearing house, azimuth
- Gear azimuth
- Cap azimuth
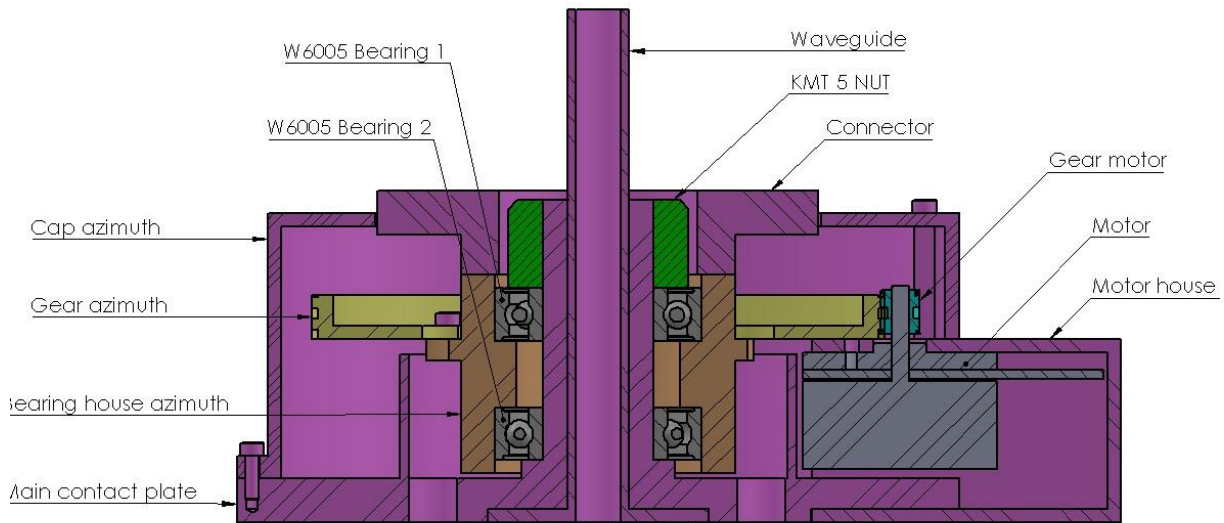
Figure 3. 11. 3: Azimuth stage

The concept is based on the bearing setup document performed by SSM (chapter 3.10), [5]. The preload is set with a KMT 5 NUT [5] from SKF, which is screwed on the rod from the main contact plate. The purpose of this is to preload the bearings so they get in the right position. The KMT 5 NUT is placed above W6005 Bearing 1. It connects the inner ring of the bearing, ref. Figure 3. 11. 3. This is done to ensure that the preload is added to the right place in the system [5].
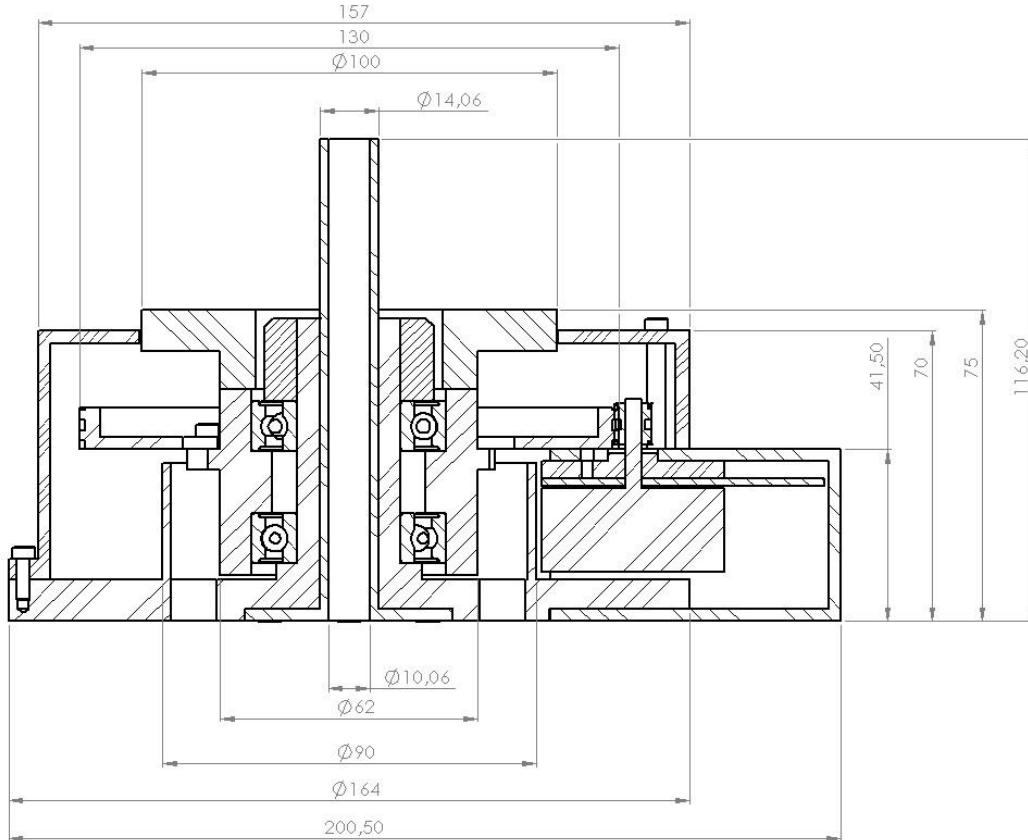
Figure 3. 11. 4: Dimension overview, azimuth

Figure 3. 11. 4 shows some of the dimensions in the azimuth stage (in mm). This, to give an overview of the size of the system. The "main contact plate" is the connector between the APM and the spacecraft. This part, including the cap azimuth and the waveguide, does not rotate. The need for two bearings [5] is due to the momentum, caused by CoG not being located over the azimuth stage, and because of the need for TC.

3.11.2.2. *Elevation*

Figure 3. 11. 5 shows a schematic overview of the elevation assembly. The assembly consist of:

- 2x W6000 Bearings
- Gear elevation
- Connector elevation
- Mirror elevation
- Flange
- Bearing house elevation
- Gear motor
- Elevation bracket
- Motor house elevation
- Motor
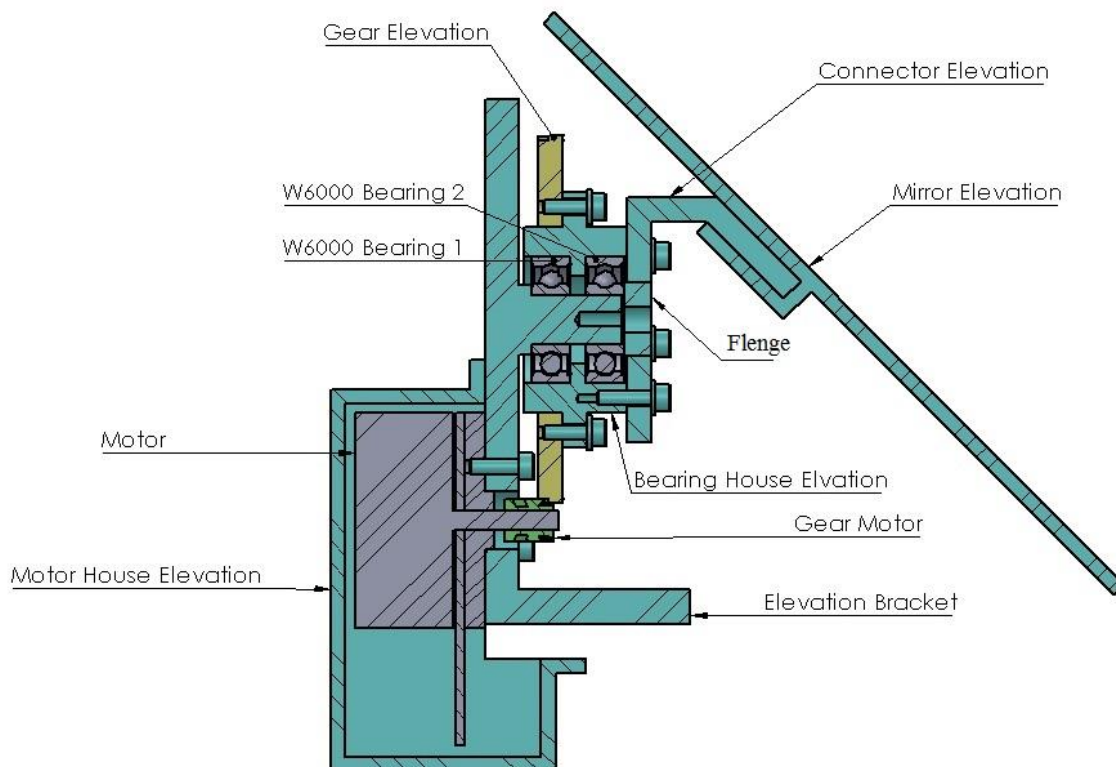
Figure 3. 11. 5: Elevation stage
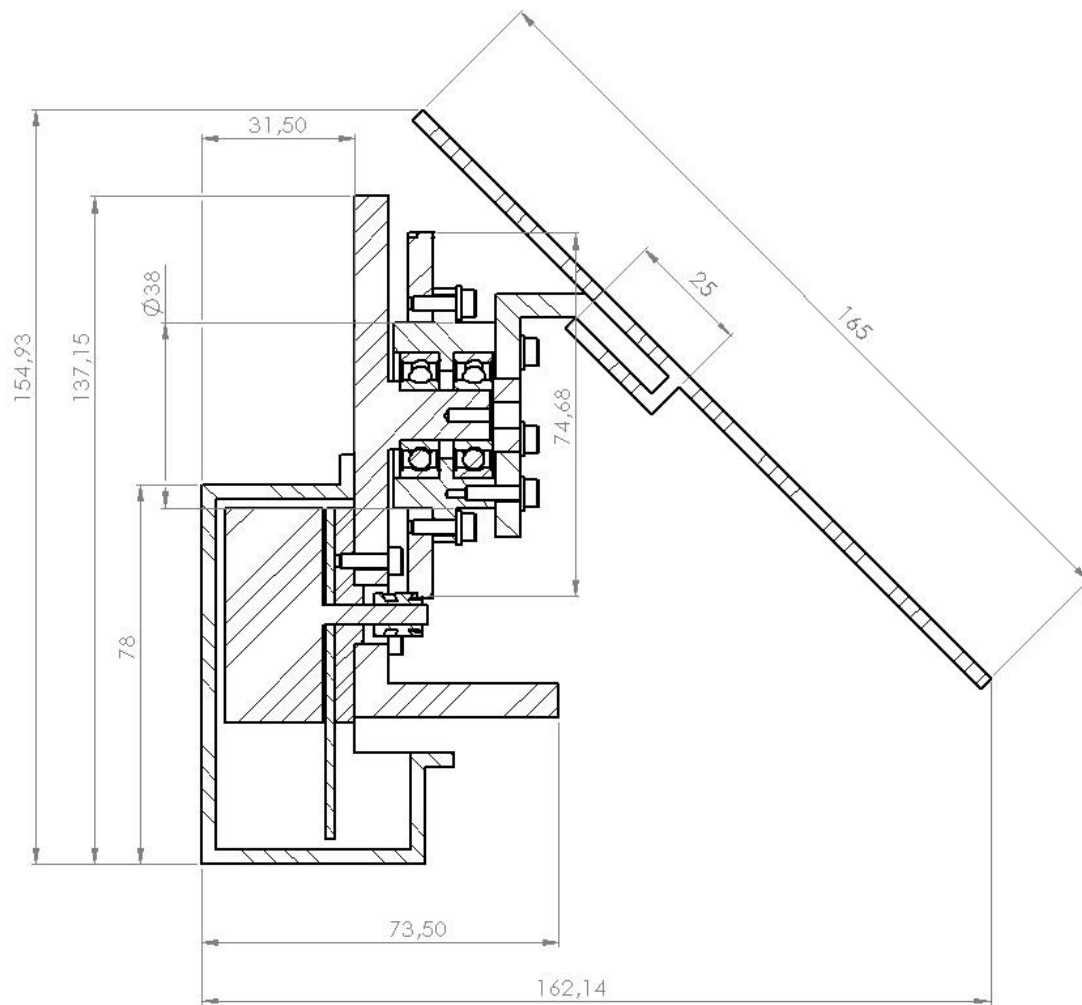
Figure 3. 11. 6: Dimension overview elevation

The azimuth and elevation stage is based on the same mechanism, only the dimensions are smaller. For example, the bearing house in the azimuth stage has a diameter of 60 mm versus the bearing house in the elevation stage which is 38 mm. The main difference from the azimuth stage is that the elevation has no need for a twist capsule. Another is that the mirror is attached directly to the mechanism, and a flange is used instead of a NUT to preload the bearings.

3.11.2.3. *Parabola*

Figure 3. 11. 7 shows a schematic overview of the parabola assembly. The assembly consists of:

- Sub reflector
- 3x struts
- Parabola
- Azimuth bracket
- Holder parabola
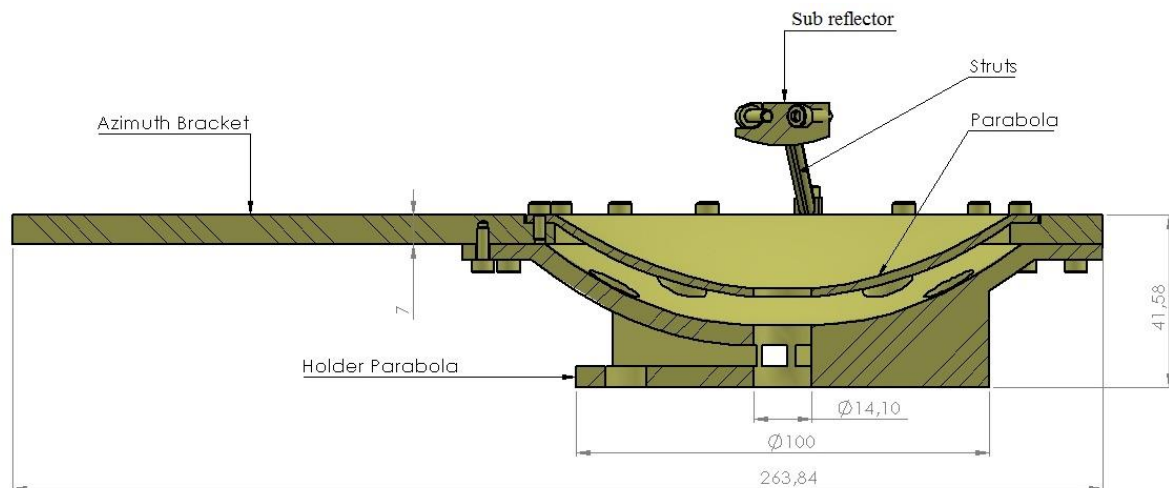
Figure 3. 11. 7: Parabola stage

In this concept the parabola is placed inside the azimuth bracket, above the parabola holder. The sub-reflector is held up by three struts, which are separated by an angle of 120 degrees.
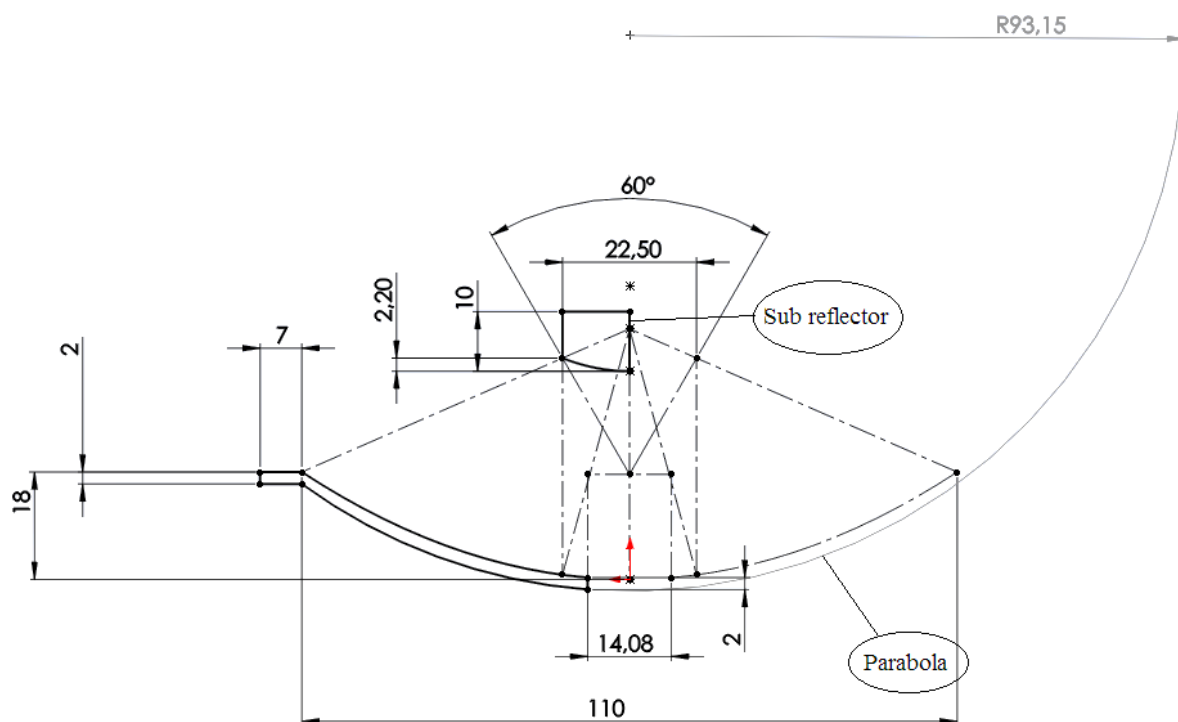
Figure 3. 11. 8: Cassegrain sub reflector and parabola

The parabola and the cassegrain sub reflector design is based on the "SSM-Antenna trade-off" (chapter 3.8), [4]. As shown in Figure 3. 11. 8, this was set to 18 mm, due to weight reduction and to achieve as small a parabola as possible. The thickness of the parabola is set to 2 mm [4].

3.11.2.4. *Mirror over azimuth*
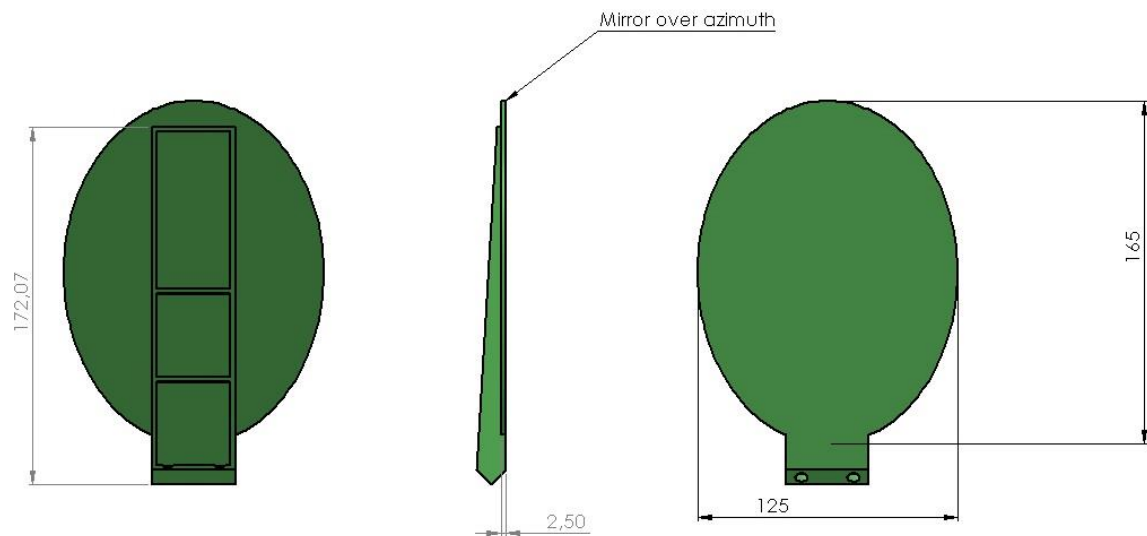
Figure 3. 11. 9: Mirror over azimuth

The size of the mirror is set to a width of 125 mm and a height of 165 mm. This is to make sure that the whole mirror is covering the parabola.

3.11.2.5. *Cable tray*
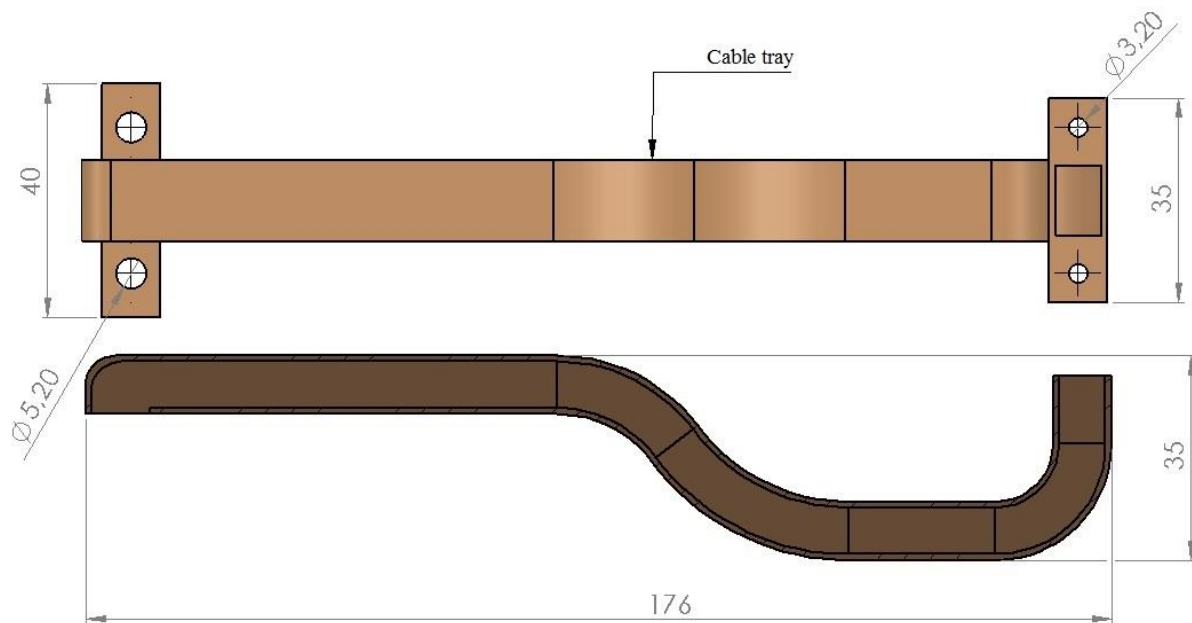
Figure 3. 11. 10: Cable tray

The cable tray is designed as a connection between the azimuth stage and elevation stage. The inside diameters are designed with respect to the number of cables which will go through the tray.

3.11.3. Azimuth and Elevation rotation

By review of design, the elevation and azimuth stage of the APM may at this point rotate from -180 degrees to +180 degrees in azimuth, and -90 degrees to +90 degrees in elevation as shown in Figure 3. 11. 11. This satisfies one of our primary requirements in this project.
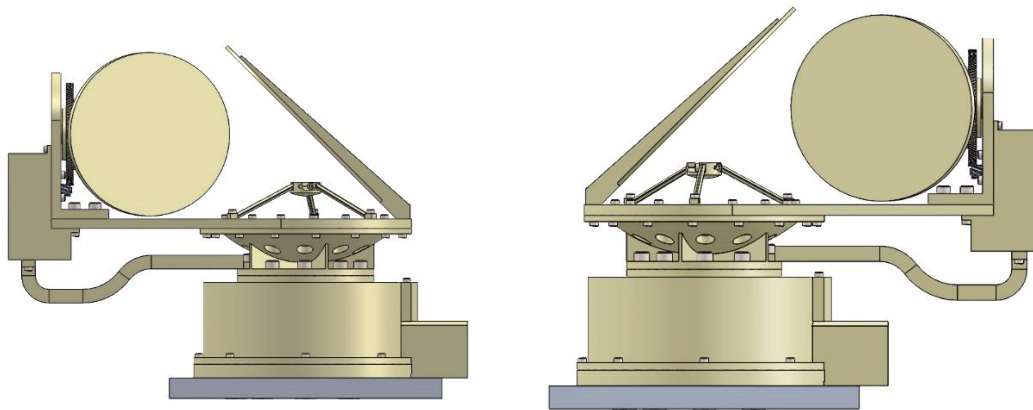
Figure 3. 11. 11: Azimuth and elevation rotation

3.11.4. Requirements verified by design

The following requirements are verified by the mechanical design of the APM (chapter 2.2), [2]:

- REQ 2.4.2 – The elevation stage shall be able to move minimum ± 90 deg.
  - o   By design the system can move ± 90 degrees in the elevation stage.

- REQ 2.4.3 – The azimuth stage shall be able to move minimum ± 180 deg.
  - o   By design the system can move ± 180 degrees in the azimuth stage

One of our primary requirements is that the mass of the mechanism shall be maximum 3kg (REQ-2.2.1.1). By this point, the mass of the APM is 4.017 kg, [3]. This does not satisfy the requirement. There are several factors leading to the mass being over exceeded. One of them is the gear ratio. A smaller gear ratio could be used, but this will be at the expense of other problems.

3.11.5. References

[1]   V. Orre Aarud et al, "Concept analysis", SSM-0900, Rev 1.0, 12.02.16

[2]   G. H. Stenseth and M. Dybendal, "Requirement Specification", SSM-2000, Rev 1.1, 24.02.16

[3]   E. Løken, et al, "Technical budgets", SSM-5901, Rev 0.2, 29.02.16

[4]   V.Orre Aarud and M.Dybendal, "Technical Report Bearing", SSM-5423, Rev 0.3, 21.04.2016

[5]   G.H. Stenseth and E. Løken, "Antenna Trade-Off", SSM-5211, Rev 1.1, 15.04.16

3.11.6. Appendices

The appendices in this section contains detailed 2D-drawings of the APM.

All the 2D drawings are from the parts which have been in focus in the two last phases of this project, the azimuth stage.

3.11.6.1. *2D Drawings Azimuth*

Figure 3. 11. 12: Bearing House Azimuth 2D Drawing
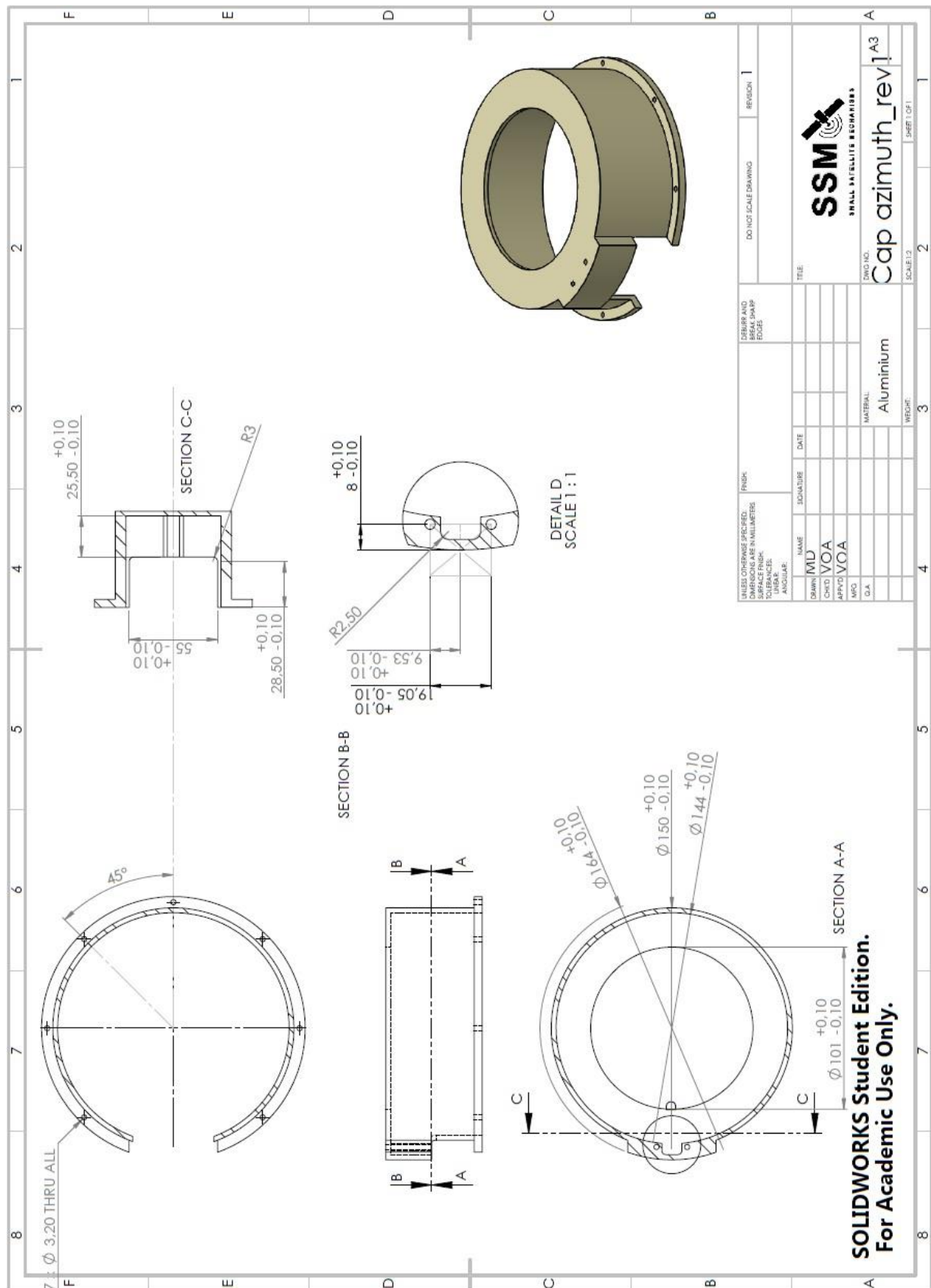
Figure 3. 11. 13: Cap azimuth 2D drawing
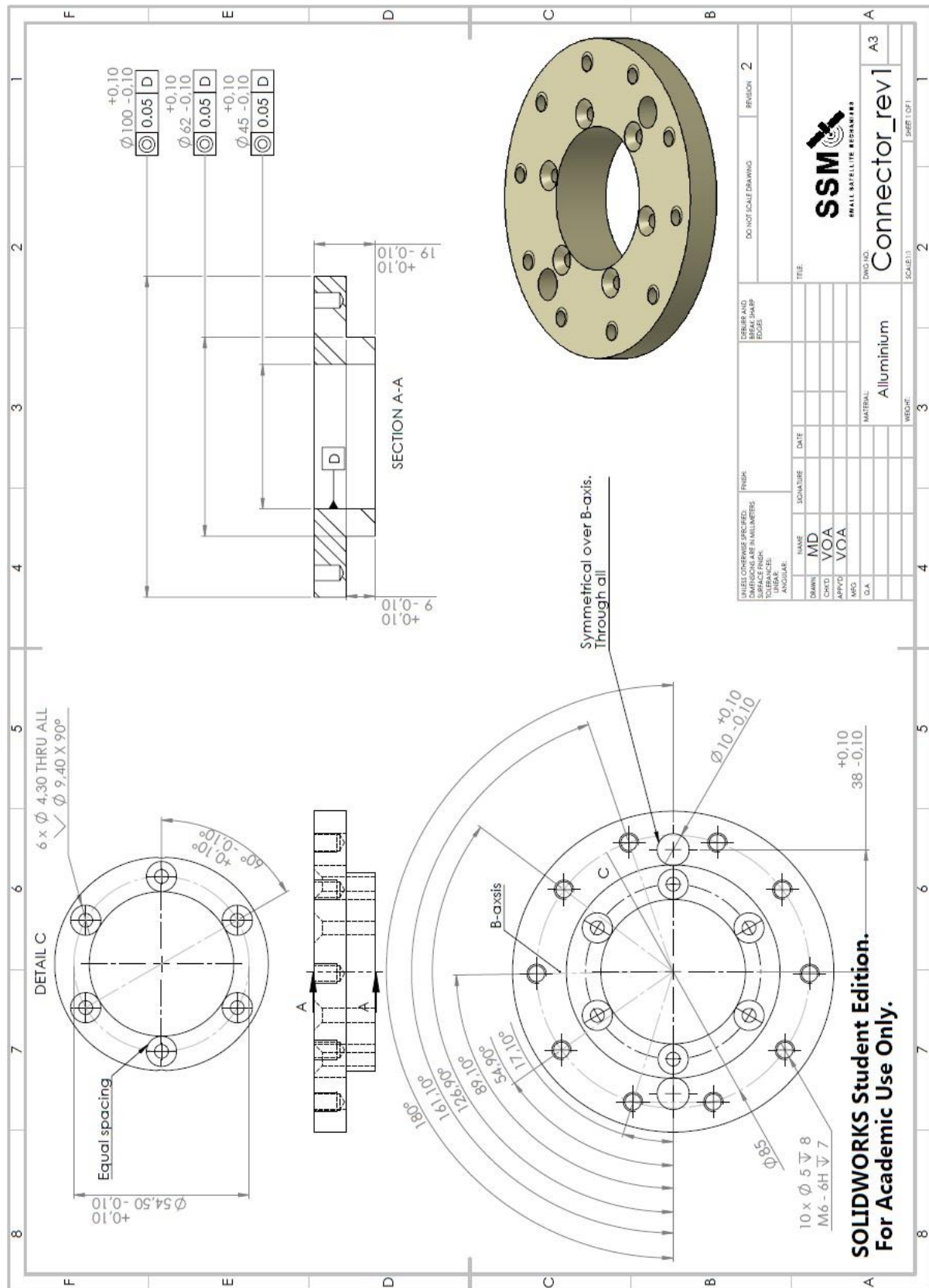
Figure 3. 11. 14: Connector 2D drawing
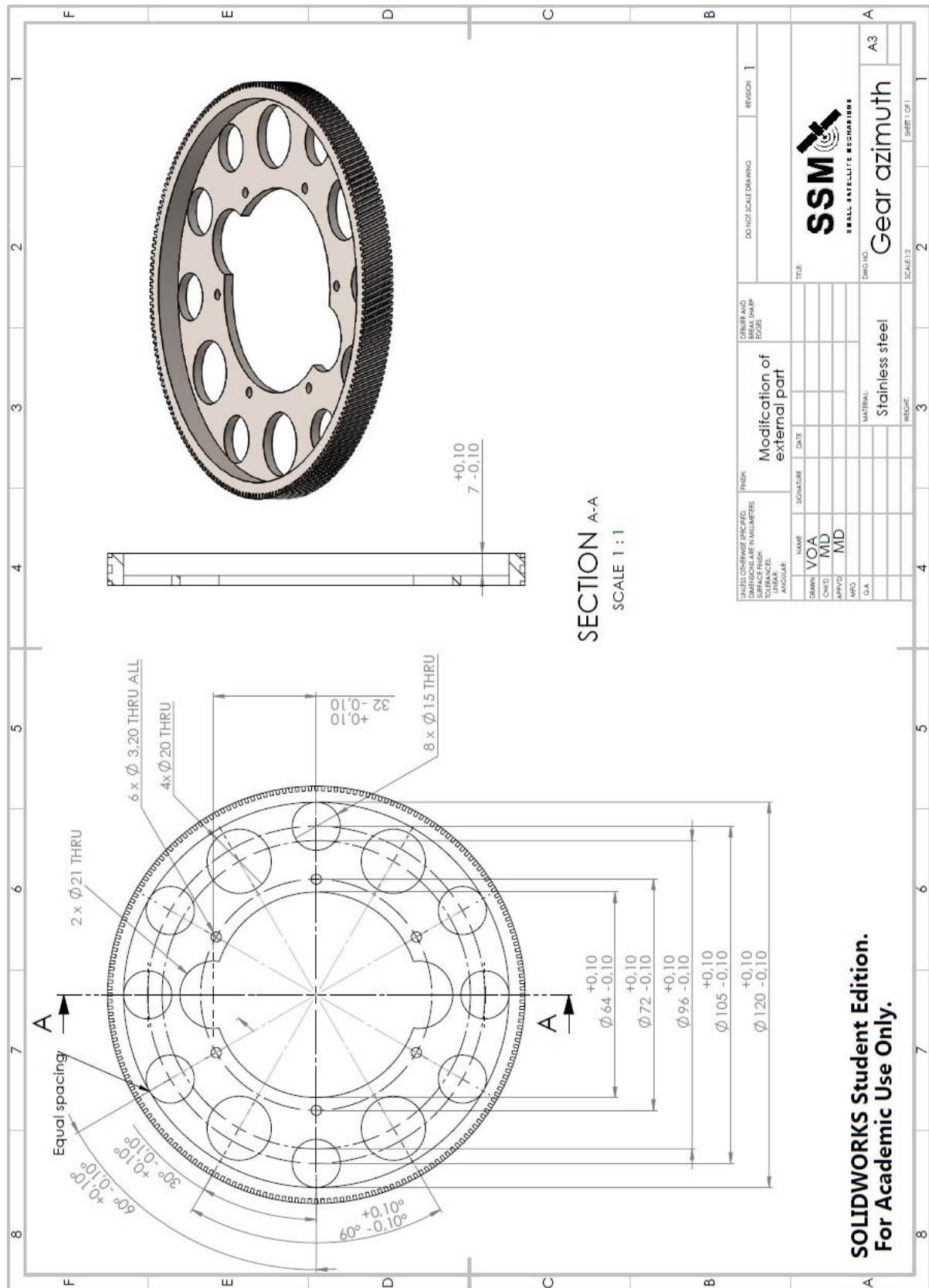
Figure 3. 11. 15: Gear azimuth 2D drawing
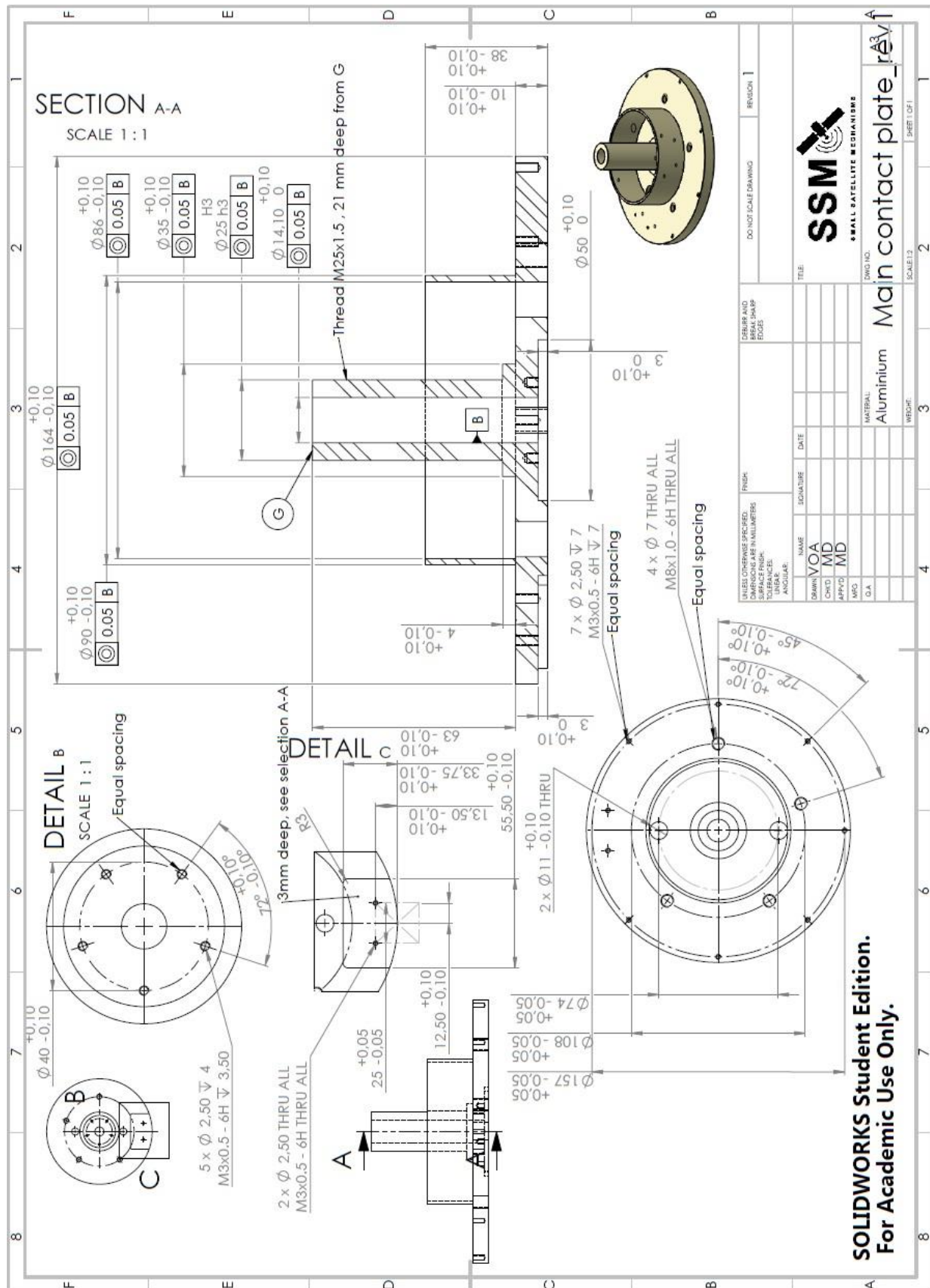
Figure 3. 11. 16: Main contact plate 2D drawing
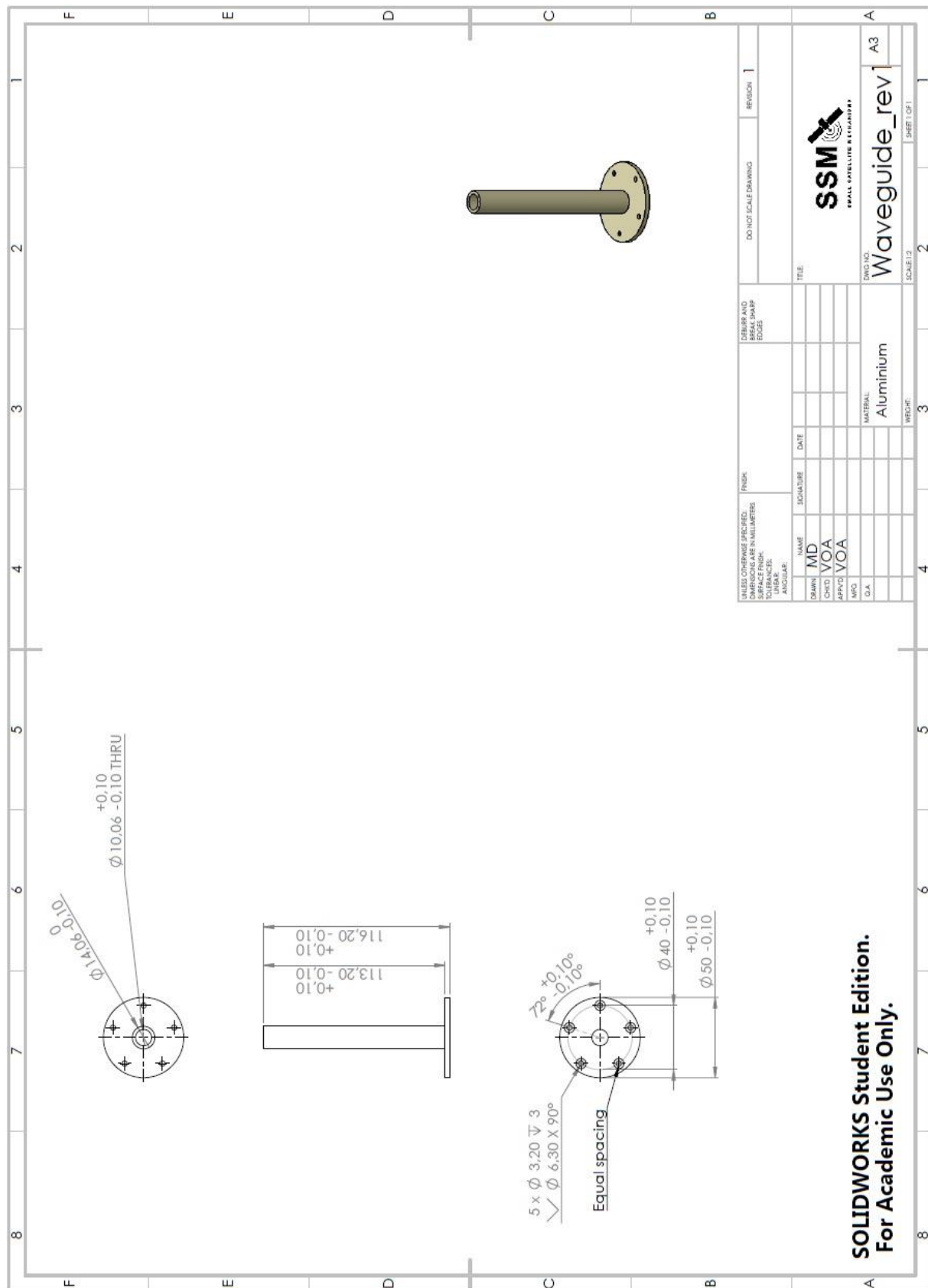
Figure 3. 11. 17: Waveguide 2D drawing

3.11.6.2.   *2D Drawings Parabola*
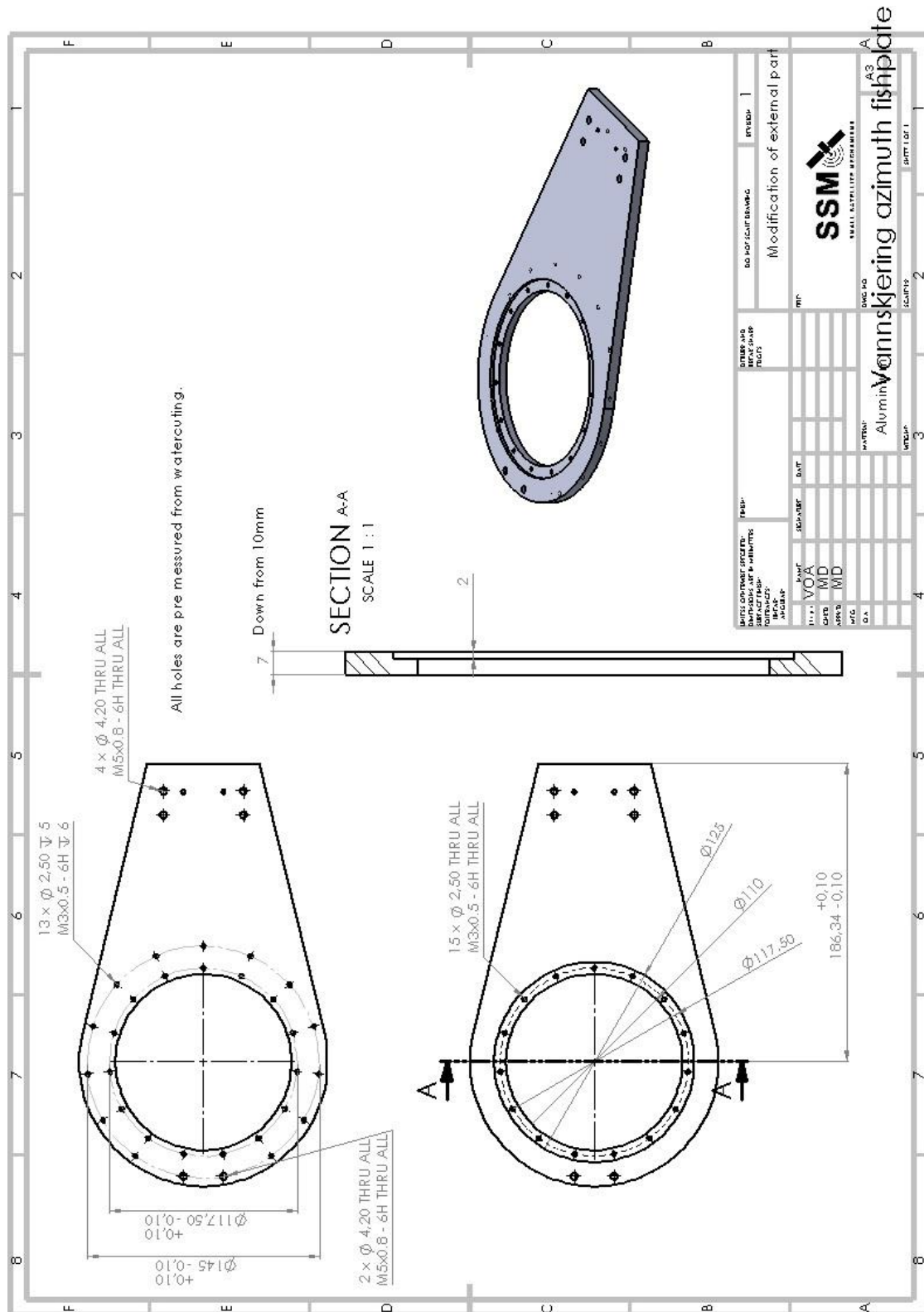
Figure 3. 11. 18: Water cut azimuth fishplate 2D drawing
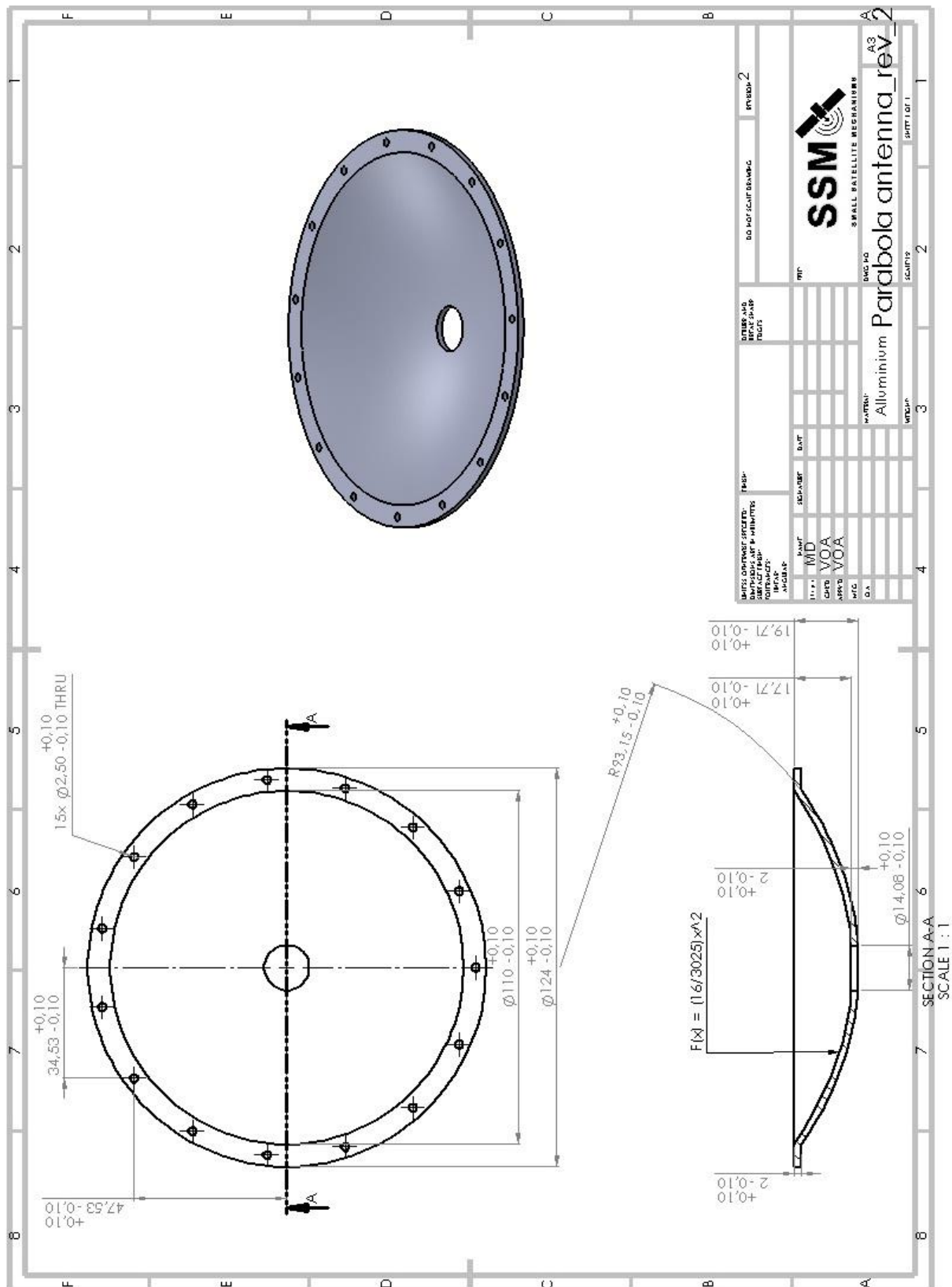
Figure 3. 11. 19: Parabola 2D drawing

Figure 3. 11. 20: Sub-reflector 2D drawing
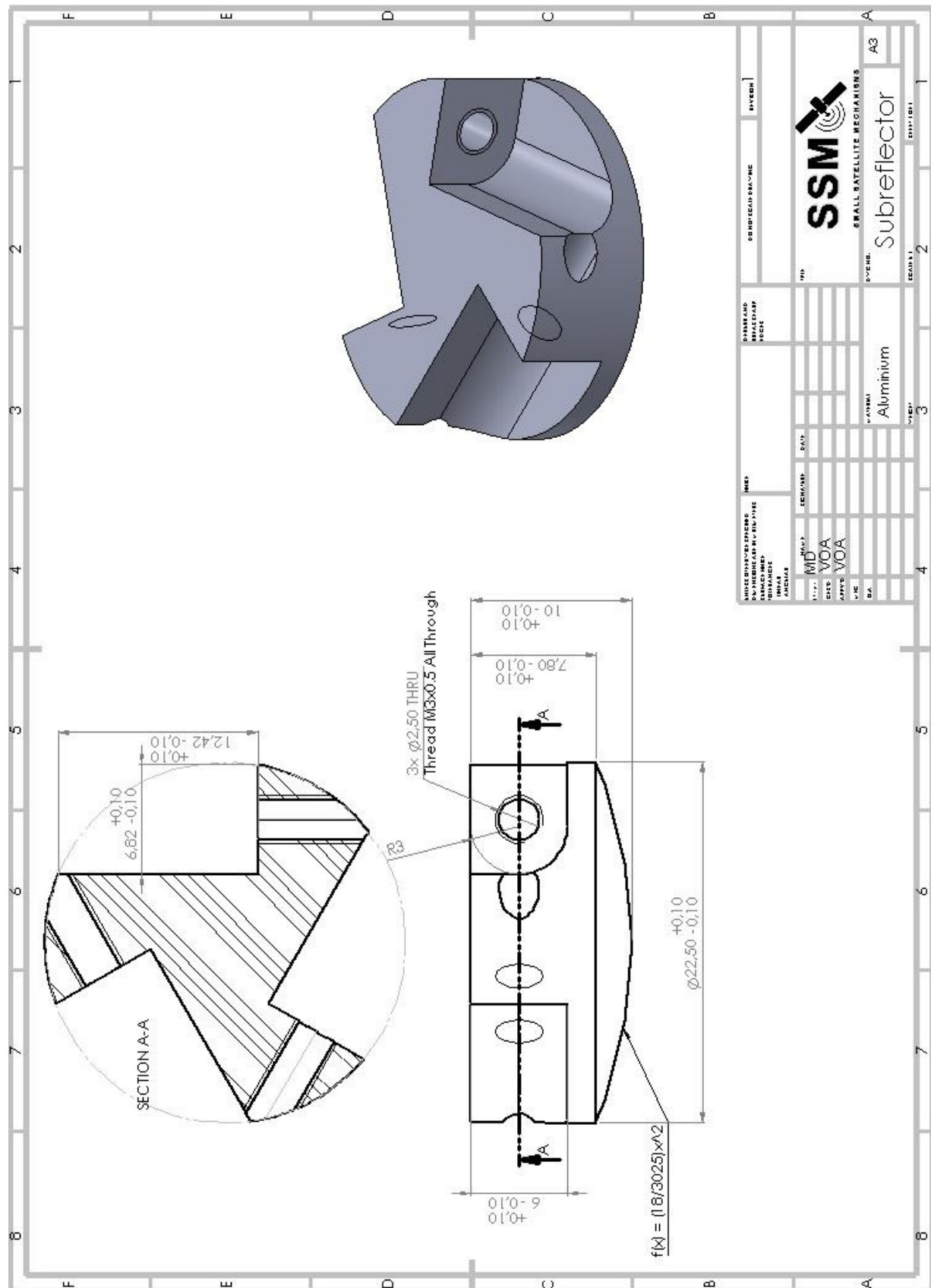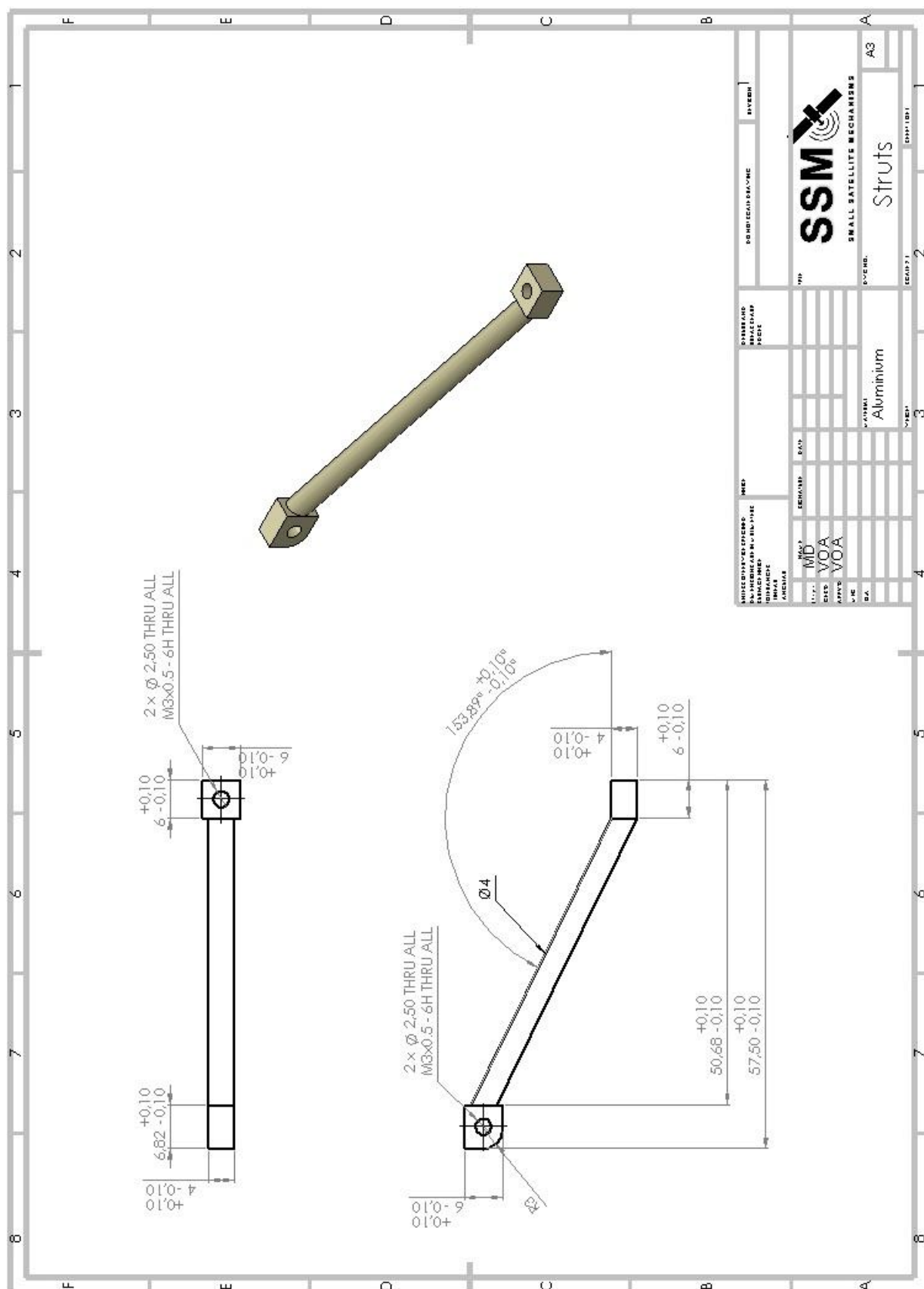
Figure 3. 11. 21: Struts 2D drawing

3.11.6.3. *2D Drawings Elevation*
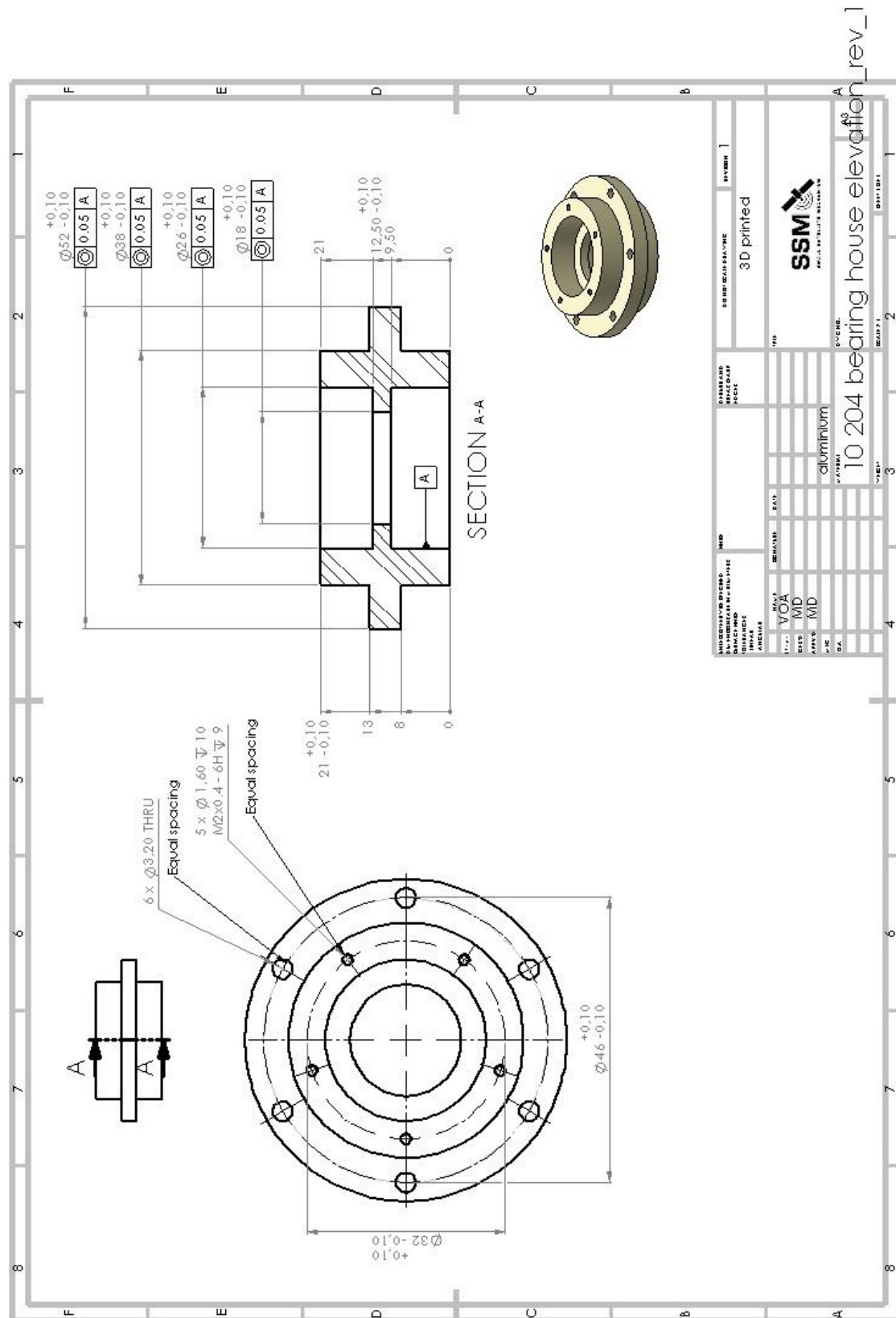
Figure 3. 11. 22: Bearing house elevation 2D drawing
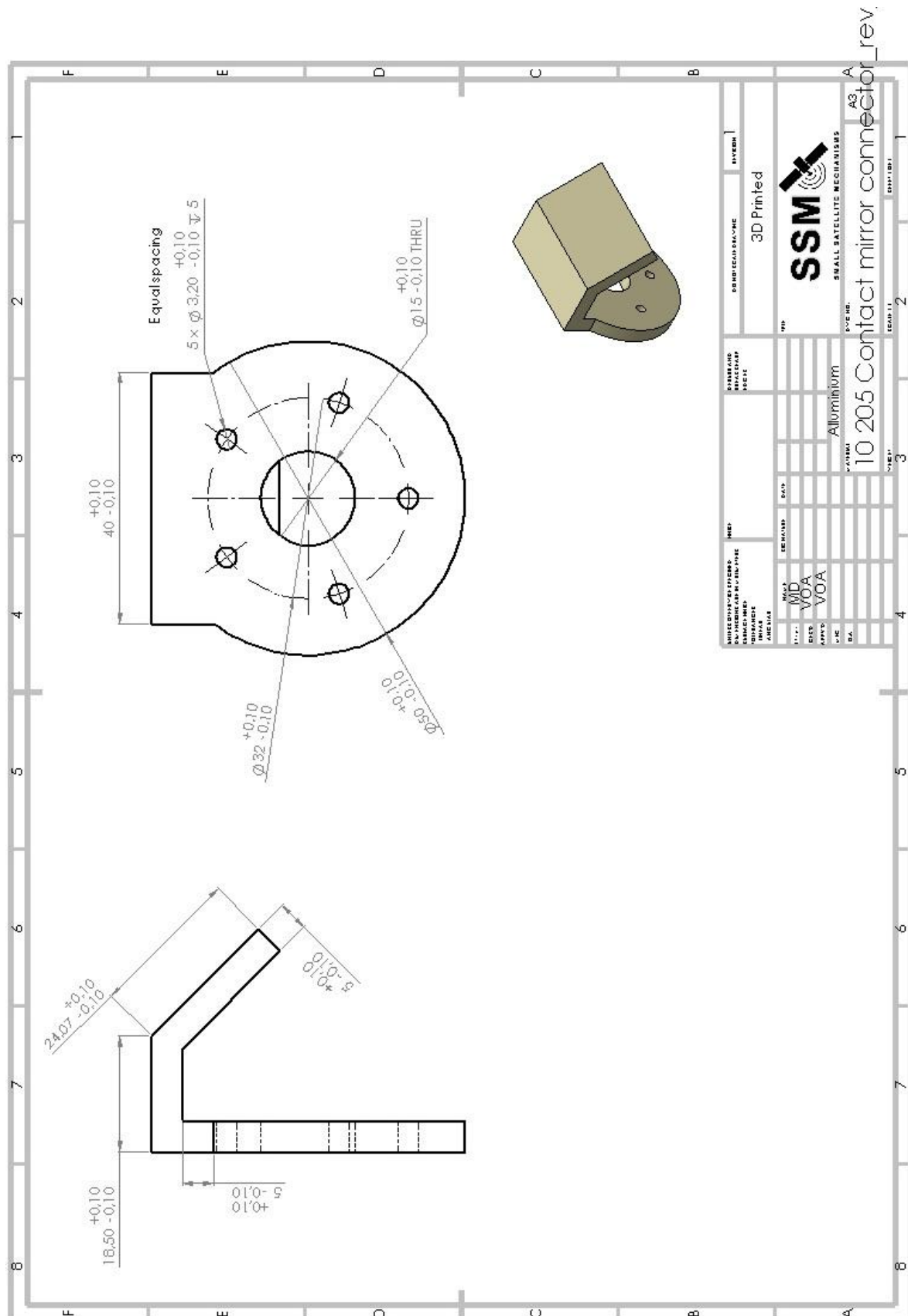
Figure 3. 11. 23: Contact mirror connector 2D drawing
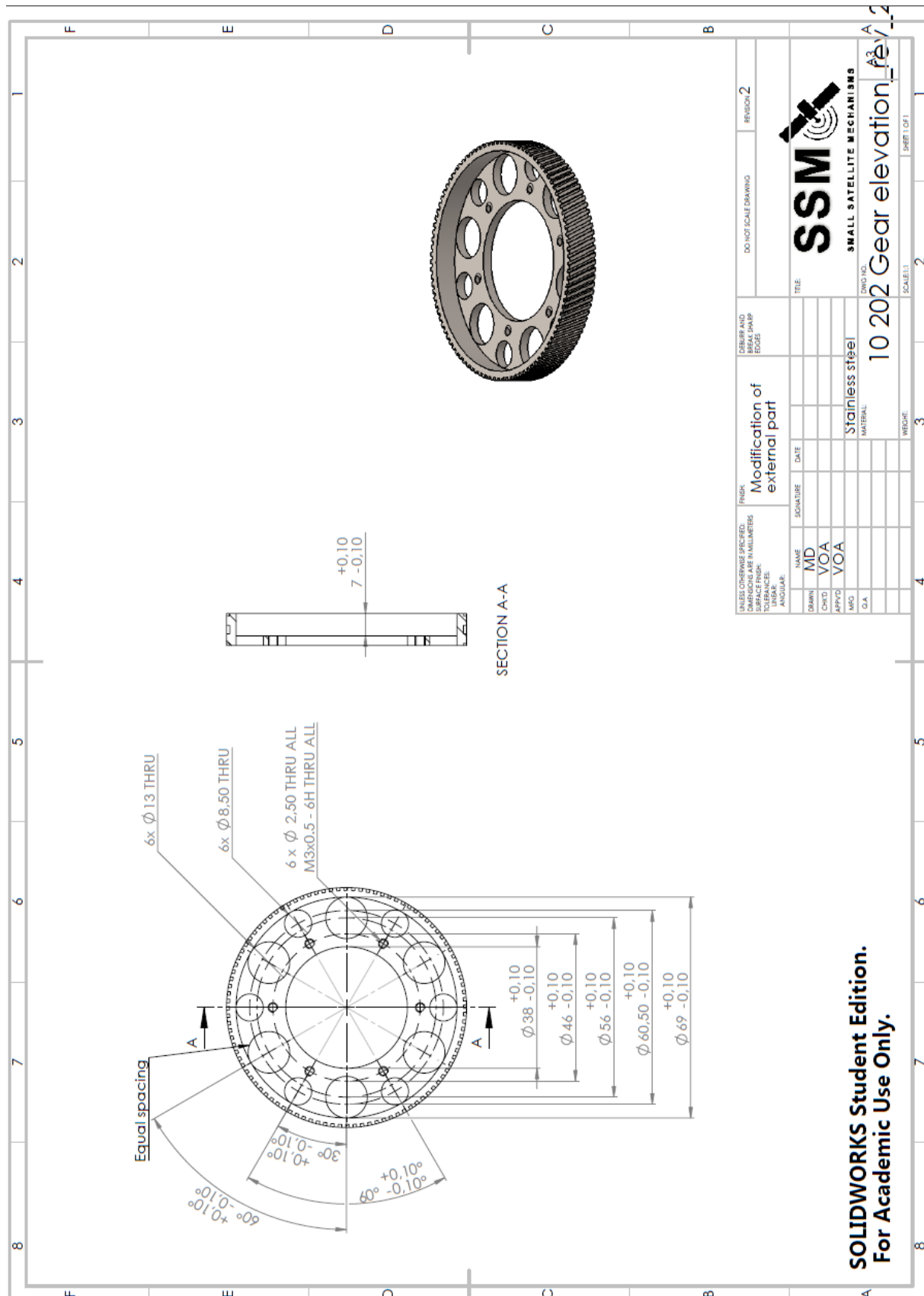
Figure 3. 11. 24; 2D drawing gear elevation

3.11.6.4. 2D Drawing Cable Tray

Figure 3. 11. 25: Cable tray 2D drawing

3.12. As built

i. Abstract

This chapter describes the APM's setup and design issues during assembly. The chapter serves as a step-by-step overview of the structure of the mechanism.

ii. Contents

iii. List of figures

iv. List of tables

v. Document history

Table 3. 12. 1: Document history

Rev.	Date	Author	Approved	Description
0.1	02.05.16	MD	EL	Created document
1.0	13.05.16	MD	TS	Reviewed and published

3.12.1. Introduction

Under the construction of a product, there will always exist errors. These errors may occur under manufacturing or they can be design issues. This chapter will describe how the APM is installed, in assemblies and sub-assemblies.

3.12.1.1.   *APM*

Figure 3.12.1 shows the azimuth and parabola sub-assembly mounted together.

Figure 3. 12. 1: APM

3.12.2. Assembly

3.12.2.1.　　*Azimuth*

The azimuth stage consists of 11 parts.
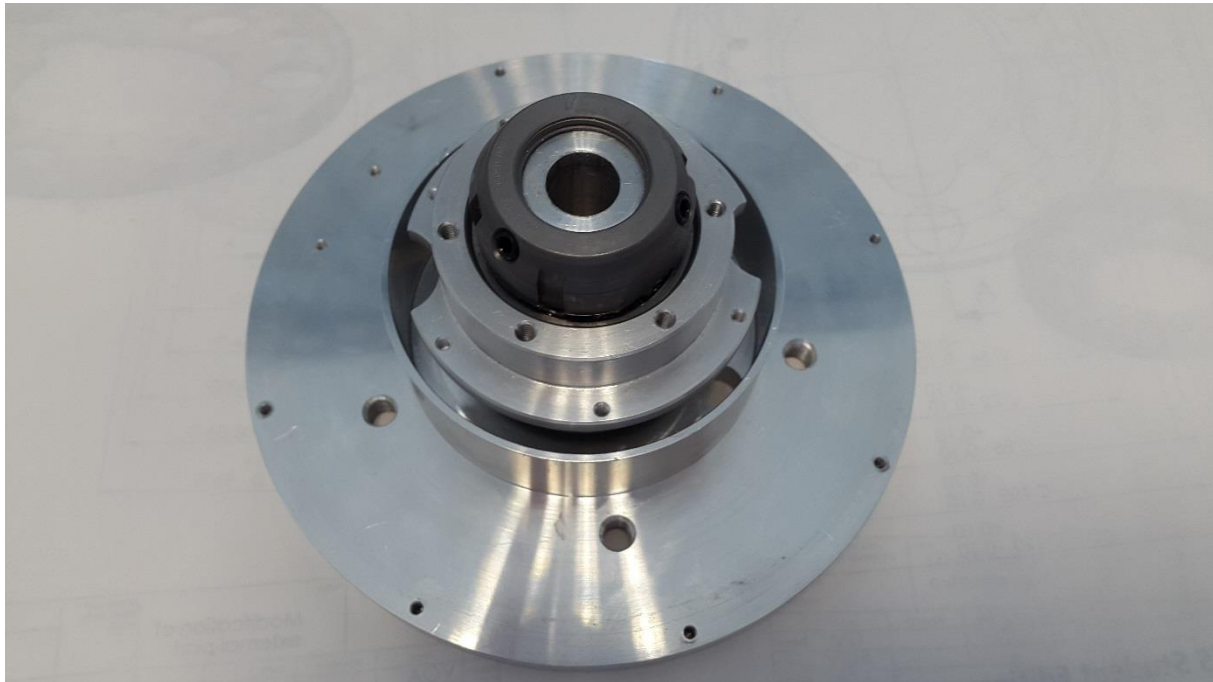
Figure 3. 12. 2: Bearings and housing

Figure 3.12.2 shows how the bearings and the bearing house is mounted on the main contact plate. We preheated the bearings and the bearing house to 80ºC, cooled down the main contact plate to 10ºC, and then pressed it on the rod. The nut was screwed on the rod, and given a calculated moment, which represents the preload [1].
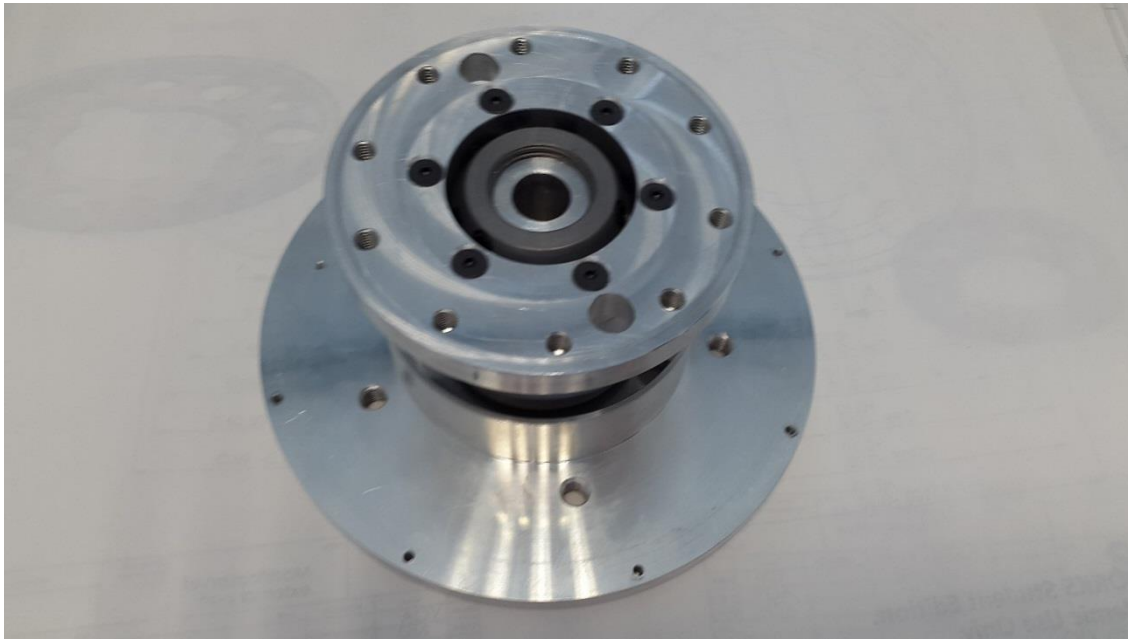
Figure 3. 12. 3: Connector

Figure 3.12.3 shows the connector mounted to the bearing house with 6x M4x0.7x25 mm socket countersunk head cap screws.
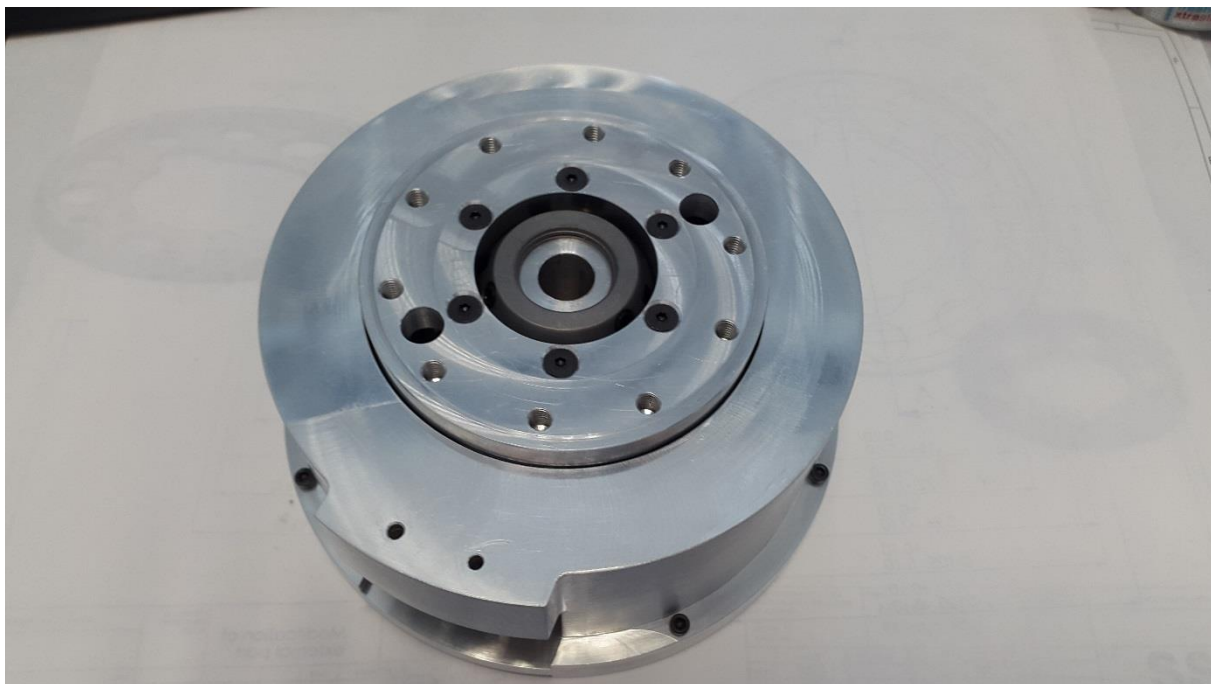
Figure 3. 12. 4: Dust cap

The last part mounted in the azimuth assembly is the dust cap. It contains 7x M3x0.5x10 socket head cap screws and 2x M3x0.5x35 socket head cap screws for the motor.

3.12.2.1.1.　　　Design errors

Under assembly, some issues arose. The first was when trying to press fit the bearings and the housing. The first bearing was stuck on the rod, so a cylinder was made at the same size as the inner ring of the bearing and placed above as shown in figure 3.12.5.
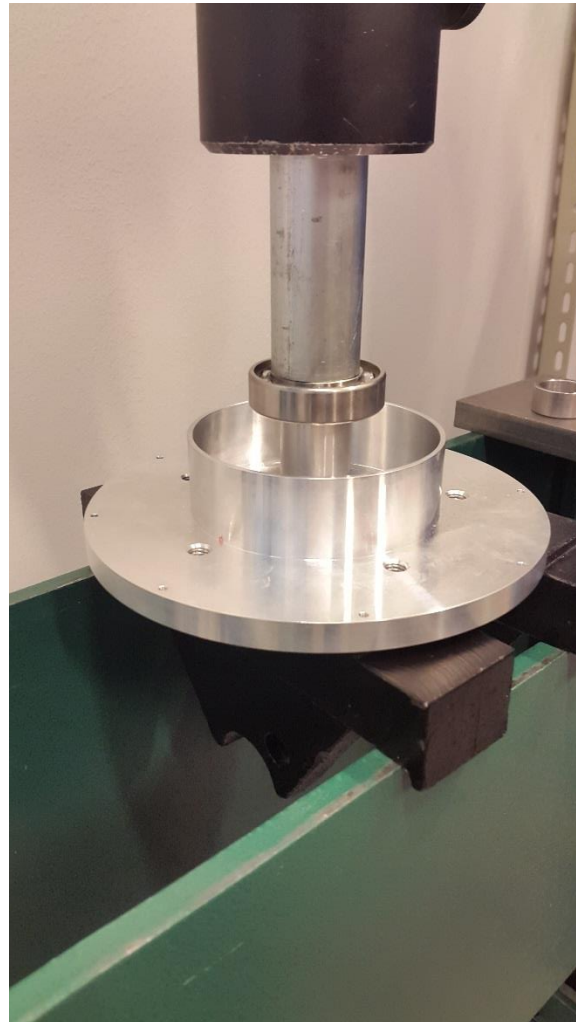
Figure 3. 12. 5: Cylinder above bearing 1

To press fit the bearing in the right position, hydraulic pressure was used. Gradually, the bearing came into the right position on the rod. After this, we inserted the bearing house and the upper bearing, using the same cylinder. The same procedure was used to press the bearing house in the right position, as shown in figure 3.12.6.
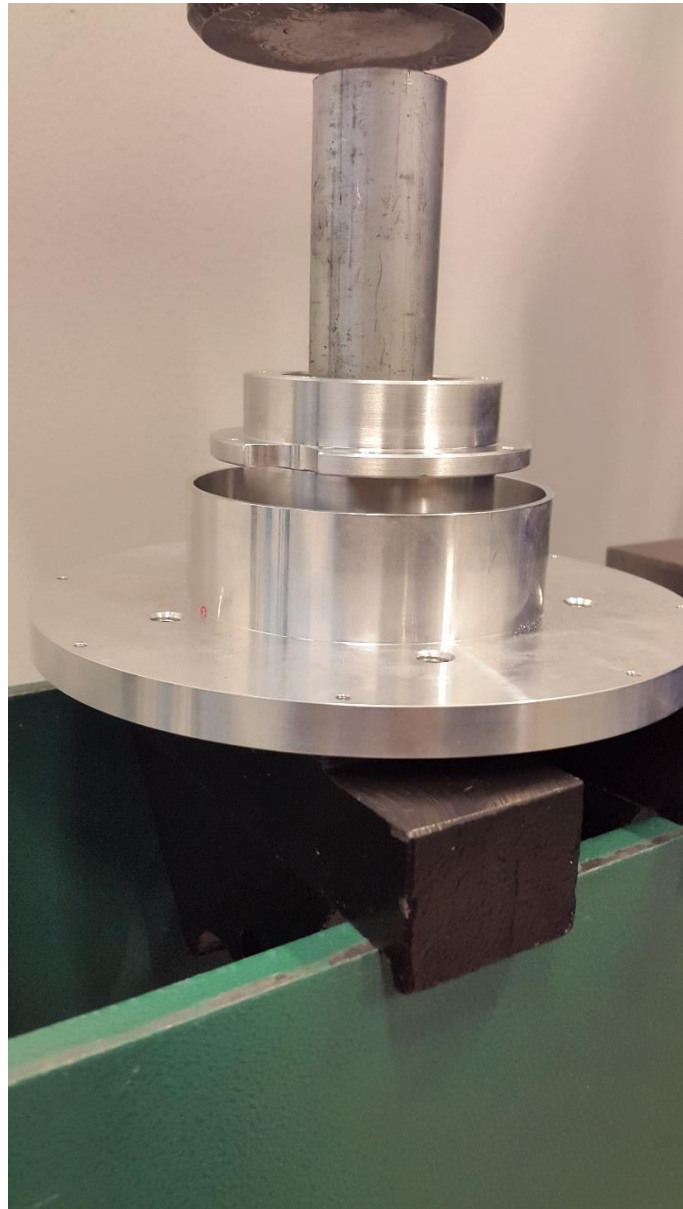
Figure 3. 12. 6: Bearing house and cylinder

Figure 3. 12. 7: Waveguide

After some hours, the azimuth stage stopped rotating, and we could not figure out the problem. After disassembling azimuth, we saw scratching marks on the waveguide as seen in figure 3.12.7. This was a design error, as the diameter was 0.2 mm larger than it should be. To solve this problem we used a milling machine to reduce the diameter from 14.06 mm to 13.86 mm.

3.12.2.2. *Parabola*

The parabola holder is mounted on the azimuth fishplate bracket with 13x M3x0.5x6 socket head cap screws as shown in figure 3.12.8.
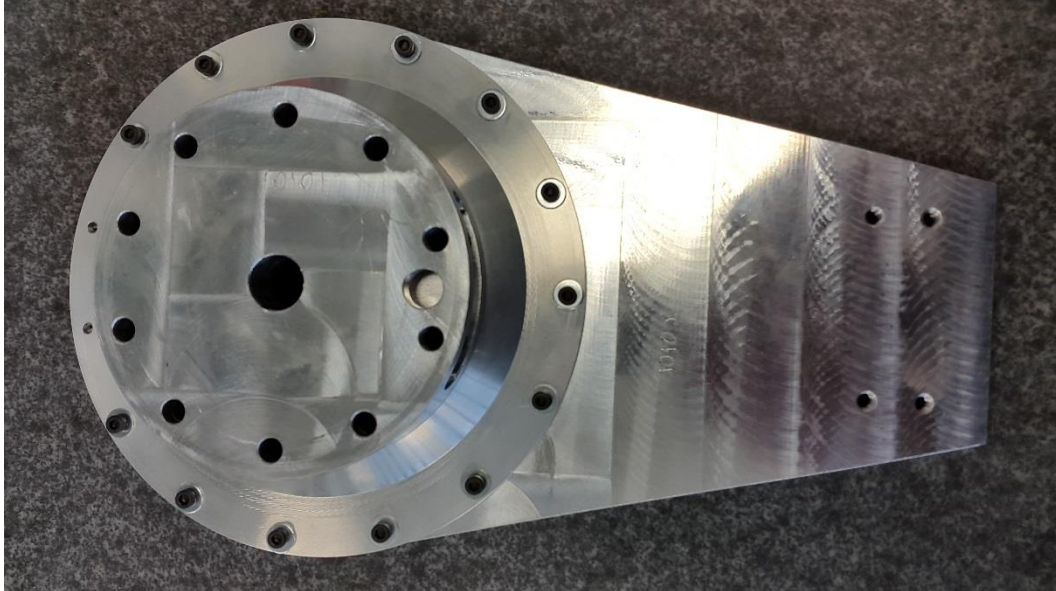
Figure 3. 12. 8: Parabola holder and azimuth fishplate bracket

Before we could put the sub reflector and the struts on the azimuth fishplate bracket we needed to place the parabola holder upon the azimuth assembly. Here we used 8x M6x1x15 mm socket head cap screws, but skipped the two holes where the cable tray will sit. For the two cable tray holes, we used 2x M6x1x20 mm socket head cap screws as shown in figure 3.12.9.
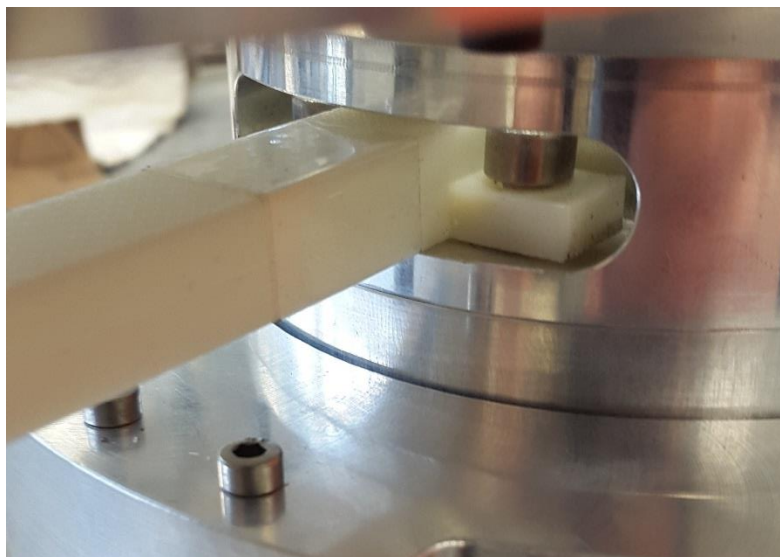
Figure 3. 12. 9: Cable tray attached to the parabola holder

Then we could mount the parabola, struts, and the sub reflector to the azimuth fishplate bracket with 12x M3x0.5x8 mm socket head cap screws for the parabola, 3x M3x0.5x10 mm for the struts. To

assemble the sub reflector to the struts we used 3x M3x0.5x10 mm socket head cap screws as shown in figure 3.12.10.
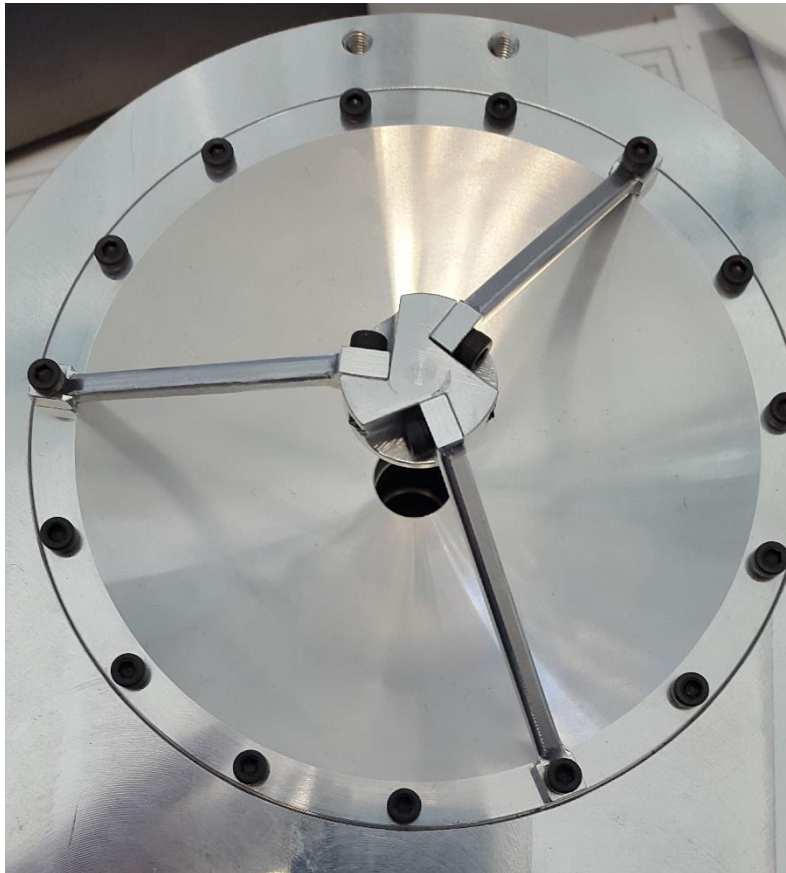
Figure 3. 12. 10: Parabola, sub reflector and struts

3.12.2.2.1. Design issues

One design issue we found was that the holes in the parabola were too small. We needed to drill them larger. We used a drill with a 3.2 mm bore size.
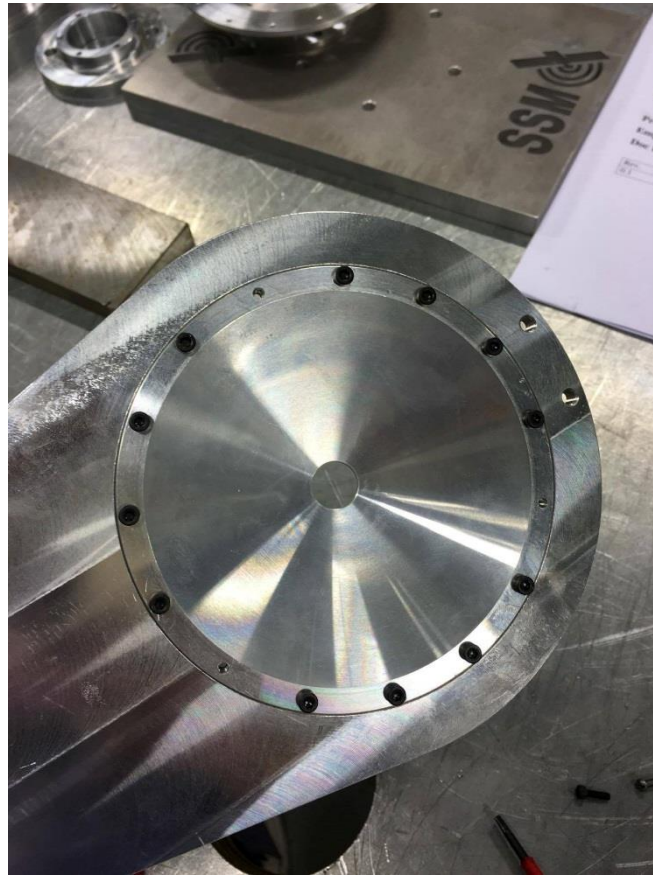
Figure 3. 12. 11: Parabola mounted to the fishplate.

3.12.2.3. *Elevation (3D printed)*

All the parts in the elevation stage are made from plastic, except the bearings and the gears, which are made of stainless steel. The whole mechanism is based on the same principle as the azimuth stage. The main difference is that there is no need for a twist capsule, and we used a bolt instead of a NUT to preload the bearings. Figure 3.12.12 shows the elevation stage as built.
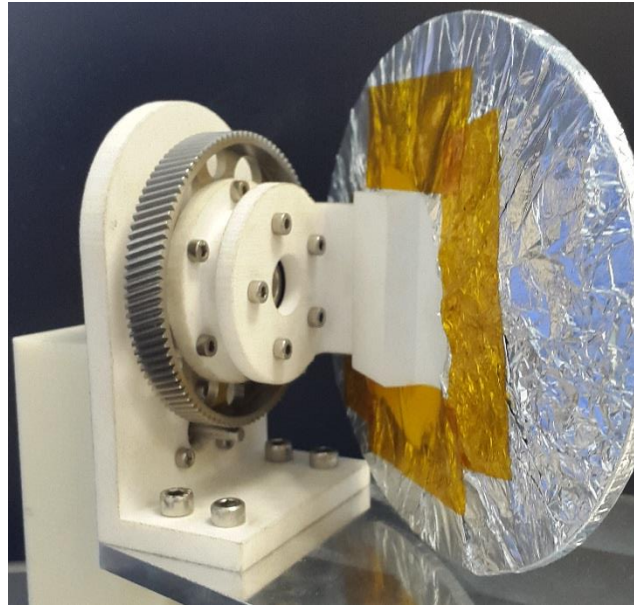
Figure 3. 12. 12: Elevation stage assembled

As in azimuth, we used hydraulic pressure to press fit the bearings. Before we could press the bearings and the bearing house on the rod on the elevation bracket, we needed to mount the gear. To mount the gear, we used 6x M3x0.5x8 socket head cap screws as shown in figure 3.12.13.

Figure 3. 12. 13: Gear mounted to bearing house elevation

When this was done, we could use hydraulic pressure to press the housing and the bearings on the rod of the bracket, then preload it with a M5x0.8 mm socket head cap screws. The preload shall be the

same as in the azimuth stage, 564 N. We used a torque wrench to get the exact amount of newton meters. The calculations for preloading is available in the "Bearing Setup" [1]. The next step was mounting the connector between the bearing house and the mirror with 5x M3x0.5x8 mm socket head cap screws. The mirror was then attached to the connector as shown in figure 3.12.14.
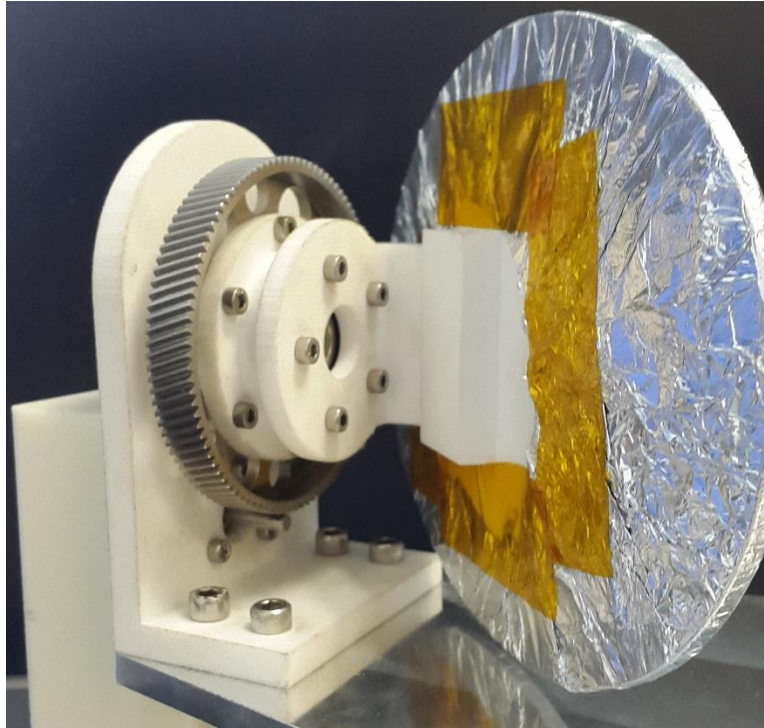
Figure 3. 12. 14: Mirror attached to the connector

When the elevation stage was assembled, it could now be mounted on the azimuth fishplate bracket. It was fastened with 4x M4x0.8x15 mm socket head cap screws.

When the elevation stage was finished, we put the motor on the bracket with 3x M3x0.5x6 mm socket head cap screws, then mounted the motor house on the mechanism, where the motor is connected to the mechanism, as shown in figure 15. Here we used 2x M3x0.5x10 mm socket head cap screws on the top of the motor house, and 2x M30.5x10 mm screws in the bottom. The cable tray was also mounted in the motor house.

Figure 3. 12. 15: Motor house mounted to the bracket

3.12.3. Conclusion

The assembly process of the APM was not without complications, as expected. There were two manufacturing errors (the size of the waveguide and the holes in the parabola), and some assembly errors (when press fitting the first bearing). The errors that occurred were fortunately small errors and could easily be fixed, thanks to access to the necessary equipment.

3.12.4. References

[1] Vebjørn Orre Aarud, SSM, 5423 «Technical report bearing», rev .3, 10.05.16, Kongsberg

4. Test & verification

4.1. Functional test procedure

i. Abstract

The "functional test procedure" chapter explains each step of the tests related to functional requirements for the APMA. The procedure shall be used to ensure solid test results and to provide a safe test environment.

ii. Contents

iii. List of figures

iv. List of tables

v. Document history

Table 4. 1. 1: Document history

Rev.	Date	Author	Approved	Description
0.1	08.04.16	SL		Created Document
0.2	06.05.16	VOA, SL		Document updated Inserted fixture chapter Minor document modifications
0.3	13.05.16	GHS, SL		Corrected typos and figures
1.0	15.05.16	SL, VOA	EL	Reviewed and published

4.1.1. Introduction

4.1.1.1. APMA system architecture

The APMA consists of two rotating stages, azimuth and elevation. For communication, a RF network with an antenna is included in the assembly. Figure 4.1.1 shows the system architecture of the APMA.
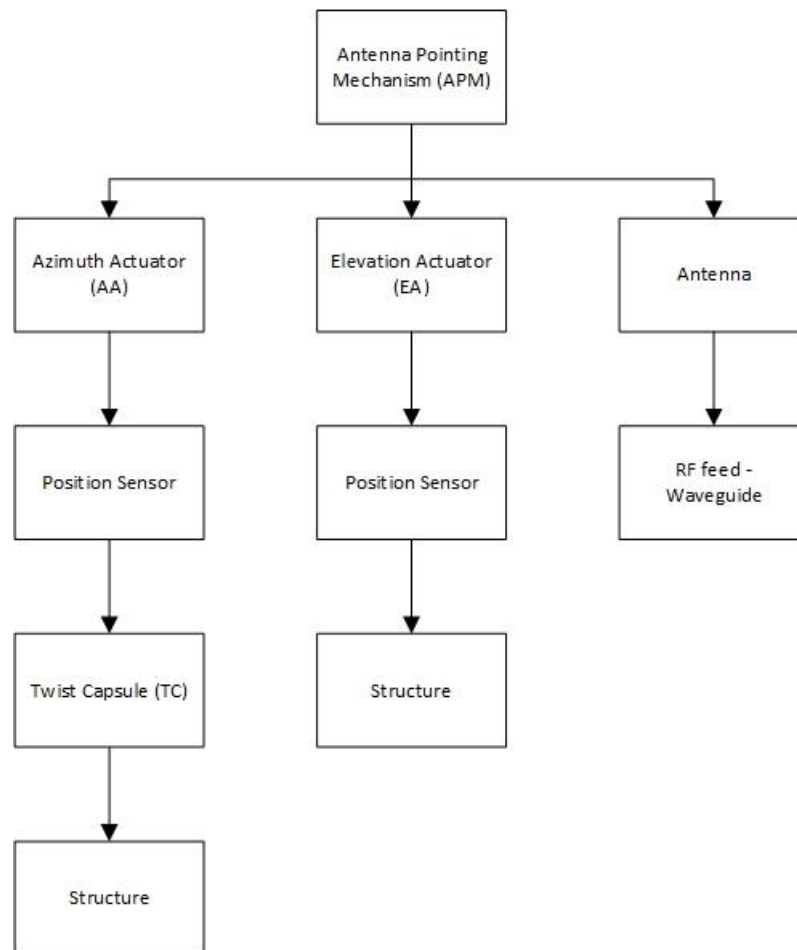
Figure 4. 1. 1: System architecture

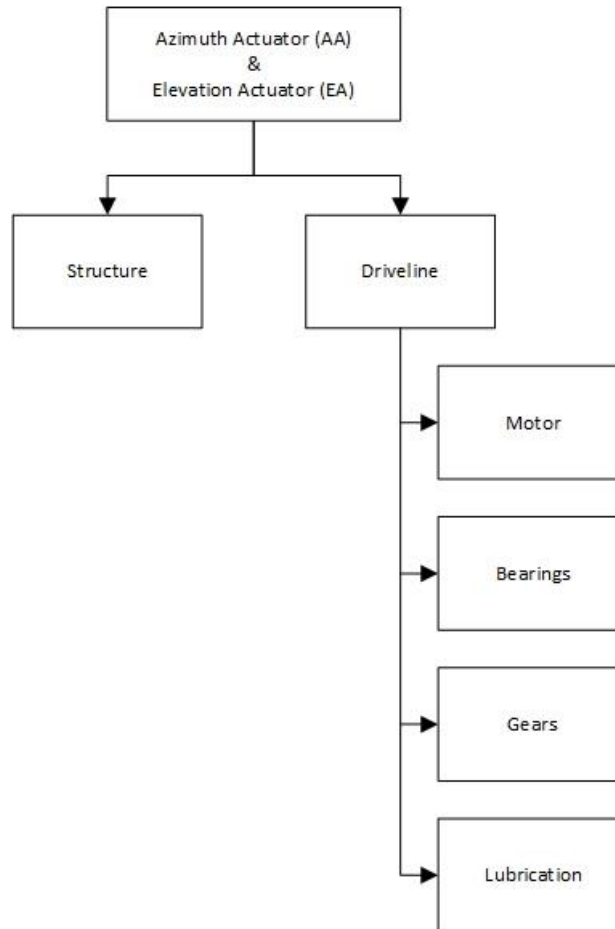The azimuth and elevation stage subsystem is presented in figure 4.1.2.

Figure 4. 1. 2: Actuator system architecture

4.1.1.2. Precautions

During assembly of the first real life prototype, some errors were observed. The errors are minor manufacturing and design errors and should be taken into account while performing the tests. In [1], manufacturing errors are to be determined. In this section the errors will be repaired or accepted. For major errors, parts will be remade. Design errors are errors made by the design engineer, such as wrong screws or distance between gears.

The purpose of precautions is to make sure that the tests are executed correctly so that the results are feasible.

Errors to be aware of in the first real life prototype:

- Wrong distance between gears, which results in increased backlash
- Wrong clamping of the bearings, which result in lower/higher rolling friction

The consequences of these errors are:

- Increased pointing errors
- Increased/decreased power consumption

4.1.1.3. Test fixtures

To perform the given tests, fixtures are made to be able to connect the prototype to sensors and other test equipment.

Figure 4.1.3 shows fixture 9000. This fixture connects the azimuth stage and the torque sensor.
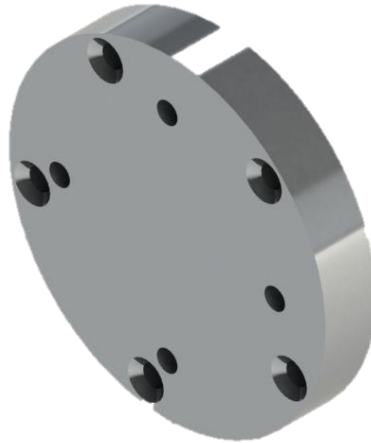

Figure 4. 1. 3: Fixture 9000

Figure 4.1.4 shows fixture 9100. This fixture holds the position sensor.

Figure 4. 1. 4: Fixture 9100

Figure 4.1.5 shows fixture 9200. This fixture makes a connection between the azimuth stage and the position sensor.
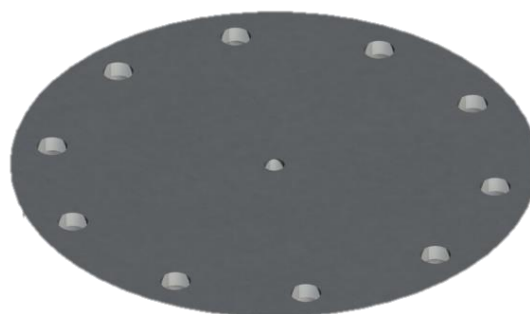

Figure 4. 1. 5: Fixture 9200

Figure 4.1.6. shows fixture 9300. This fixture makes a final stop of rotation in the azimuth stage, when the ends hit the external pylons at KDA.

Figure 4. 1. 6: Fixture 9300

Figure 4.1.7 shows a complete assembly of the accuracy and pointing test fixture. 9100 (green) and 9200 (yellow) represent the external fixtures. In addition to this, the position sensor (red) and azimuth stage (cream) components are shown.
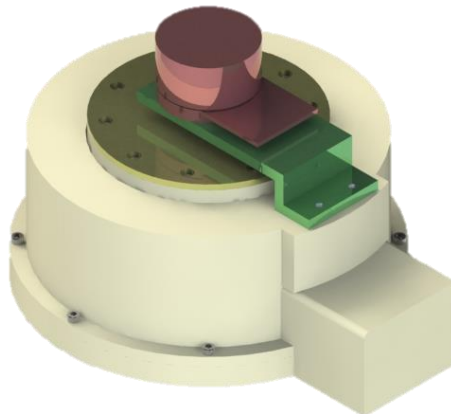

Figure 4. 1. 7: Fixture for accuracy and pointing test, mounted with motor.

Figure 4.1.8 shows a complete assembly of the torque test fixture. 9000 (red) and 9300 (green) represent the external fixtures, as well as the azimuth stage (cream), torque sensor (gray) and KDA baseplate (black) components.
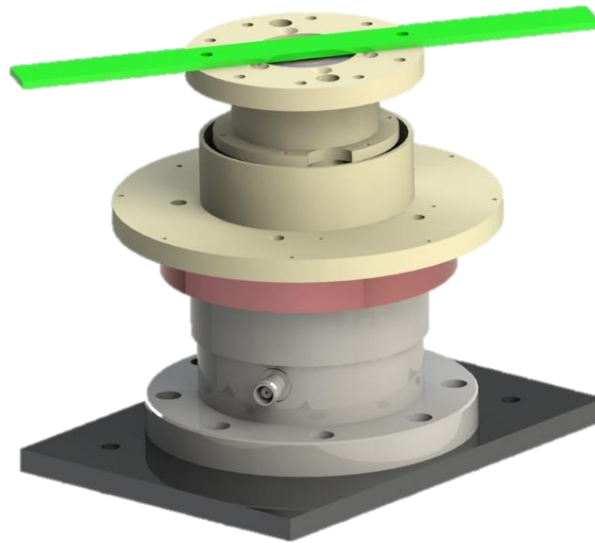
Figure 4. 1. 8: Fixture for torque test mounted

4.1.1.4. Tests to be performed

The tests to be performed can be found in [2].

TST-2.1.0	TR	Power consumption
TST-2.3.2	TAR	Torque
TST-2.4.0	TR	Pointing accuracy
TST-2.4.1	TR	Speed and acceleration
TST-2.5.1	T	Communication frequency
TST-2.9.0	T	Insulation
TST-2.9.1	TR	Supply voltage

4.1.1.5. Requirements to be verified

The requirements to be verified can be found in [3]:

REQ-2.1.1	Power
REQ-2.1.1.1	Power
REQ-2.1.1.2	Power
REQ-2.3.3	Torque
REQ-2.3.3.1	Torque
REQ-2.4.1	Pointing
REQ-2.4.3	Pointing
REQ-2.4.4	Pointing
REQ-2.4.5	Pointing
REQ-2.5.5	Communication
REQ-2.5.6	Communication
REQ-2.5.7	Communication
REQ-2.5.8	Communication
REQ-2.9.3	Electrical characteristics
REQ-2.9.5	Electrical characteristics

4.1.1.6. Test logic

The requirements specified in section 4.1.4.1.1.5 shall be verified through functional tests.

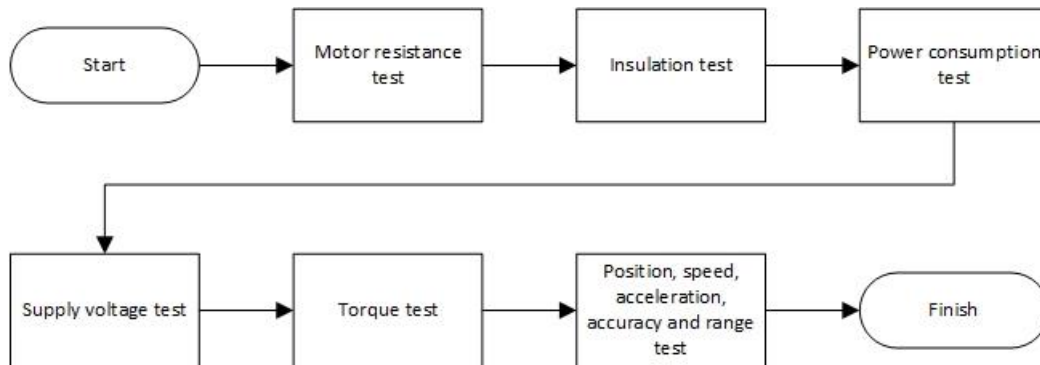Figure 4.1.9 presents the test flow this procedure is based on.

Figure 4. 1. 9: APMA test flow

4.1.1.7. Test organization

The persons responsible for the test are listed in table 4.1.2:

Table 4. 1. 2: Test responsibilities

Responsibility	Person in charge	Name
Overall responsibility	Project Manager	GHS
Test procedure	Test Engineer	SL/VOA
Test execution	Test Engineer	TS/GHS
Test report	Test Analyst	MD/GHS

4.1.1.7.1. Test responsible and documentation

The project manager is the overall responsible of making sure that the tests will be performed and are within the standards of SSM. The test engineer is responsible for carrying out the tests according to the current test procedure. All relevant data and incidents from the tests shall be documented in a test report.

Every step in the procedure requires the signature of the designated test engineer.

4.1.1.8. Test setup and test equipment

4.1.1.8.1. Test objects

Test objects are specified in table 4.1.3:

Table 4. 1. 3: Test objects

Name	Type of test
APMA - First real life prototype	Functional test

4.1.1.8.2. Test equipment

Desired test equipment is listed in table 4.1.4:

Table 4. 1. 4: Test equipment

Name	Function	Comments
Test fixture 9000	Connector	
Test fixture 9100	Bracket	
Test fixture 9200	Connector	
Test fixture 9300	Arm	
KDA baseplate	Represent the "satellite"	
Test station	Send position commands and data logging	
Power supplies	Power for the mechanism	
Digital multimeter	Electrical measurements	
Kistler Charge Meter 5015	Kistler Torque Transducer reader	
9275 Kistler Torque Sensor	Torque measurement	

4.1.1.8.2.1. Test station description

The test station, that sends position commands, is a computer connected to an Arduino which communicates with the system via UART protocol. For data logging KDA's Compact Rio 9082 will be used.

4.1.1.8.3. Environmental conditions

The functional test shall be performed at KDA and the working environment for test areas outside the thermal vacuum chamber is described in table 4.1.5:

Table 4. 1. 5: Test conditions

Condition	Requirement	Measured
Temperature	23 ºC ± 5 ºC	
Humidity	N/A	
Particle	N/A	

4.1.1.8.4. Pass/Fail criteria

Pass/Fail criteria is defined for each test in Test & Verification Specification [2]. The test results shall be documented in the step by step procedures and the test report.

4.1.2. Functional test procedure

4.1.2.1. Motor resistance test

Table 4. 1. 6: Motor resistance test

Test id:	N/A	Project state:	C:3
Requirement to be verified	Motor resistance of 6.89 Ω ± 10%.	Purpose:	Verify motor resistance.

Test equipment:

- Motor EC 45 flat 70 W or AA
- Digital Multimeter/Fluke
  8808A or similar

4.1.2.1.1.   Test logic and description

To verify motor resistance, one needs to measure the resistance between two windings. The motor datasheet defines the terminal resistance phase to phase. Figure 4.1.10 presents the test connection scheme with the representing pins from the motor datasheet.
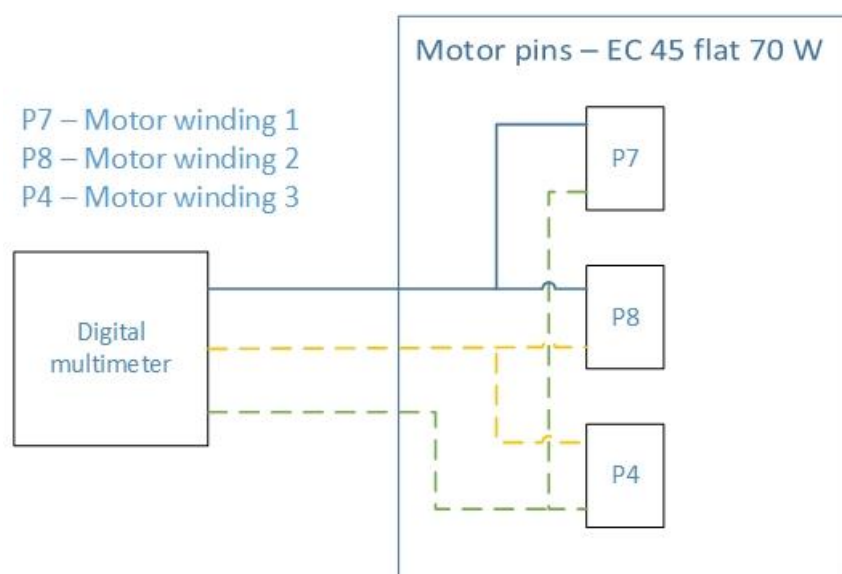
Figure 4. 1. 10: Motor resistance test setup scheme

4.1.2.1.2. Test procedure

4.1.2.1.2.1. Test Setup

Table 4. 1. 7: Test setup

Step	Description	Executed (sign)	Comment
1	Wire according to figure 4.1.10.		

Date: **Signature:**

4.1.2.1.2.2. Motor resistance verification

Table 4. 1. 8: Motor resistance measurement, step by step procedure

Step	Description	Requirement	Pass/Fail	Comments
1	Perform resistance measurement between winding 1-2.	Motor: $6.89\ \Omega \pm 10\%$		
3	Perform resistance measurement between winding 2-3.	Motor: $6.89\ \Omega \pm 10\%$		
5	Perform resistance measurement between winding 1-3.	Motor: $6.89\ \Omega \pm 10\%$		

Date: **Signature:**

Table 4. 1. 9: Insulation test

Test id:	TST-2.9.0	Project state:	C:3
Requirement to be verified:	REQ-2.9.3 Motor Windings: - 500 VDC - > 100 MΩ	Purpose:	To verify insulation between individual motor windings and electrical wires

Test equipment:

- Megaohm meter Hypot-III-3770
- Switch box

4.1.2.2.1. Precautions

The most interesting part of this test is to look at the insulation between the motor windings and the motor housing, and this is therefore the main part of this test. Due to unfinished cabling, the cable insulation part will not be prioritized.

WARNING:

Due to high voltages, do not touch the equipment while the test is being performed.

4.1.2.2.2. Test logic and description

The insulation test will be performed by using a megaohm meter, Hypot-III-3770 connected through a Switch Box that will ensure the connection between the motor windings and the megaohm meter. Figure 4.1.11 shows a simple connection scheme of the test.

Figure 4. 1. 11: Insulation test scheme

4.1.2.2.3.   Test procedure

4.1.2.2.3.1.   Instrument setup motor

Table 4. 1. 10: Instrument setup - motor, step by step procedure

Step	Description	Executed (sign)	Comment
1	Verify cable connection according to figure 11		
2	Configure instrument for DS: • 500 VAC RMS • 2 sec. ramp up • 1 min. dwell • 0 sec. ramp down • 1 mA limit • 50 Hz Configure instrument for IR: • 500 VDC • 2 sec. ramp up • 1 min. dwell • 0 sec. ramp down > 100 MΩ limit		During test, leakage current and insulation resistance shall be written down.
3	Stabilization criteria: • DS test is to be stable for 5 seconds. • IR test is to be stable for 5 seconds.		

Date: **Signature:**

4.1.2.2.3.2.   Motor insulation verification

Table 4. 1. 11: Motor insulation test, step by step procedure

Step	Description	Requirement	Pass/Fail	Comments/Results/report
1	Perform insulation measurement between winding 1 and the motor housing.	> 100 MΩ		
2	Perform insulation measurement between winding 2 and the motor housing.	> 100 MΩ		
3	Perform insulation measurement between winding 3 and the motor housing.	> 100 MΩ		

Date: **Signature:**

4.1.2.3. Power consumption, supply voltage and communication frequency test

Table 4. 1. 12: Power consumption, supply voltage and communication frequency test

Test id:	TST-2.1.0 TST-2.9.1 TST- 2.5.1	Project state:	C:3
Requirement to be verified:	REQ-2.1.1 REQ-2.1.1.1 REQ-2.1.1.2 REQ-2.9.5 REQ-2.5.5 REQ-2.5.6 REQ-2.5.7 REQ-2.5.8 - System power consumption ≤ 15 W - Motor power consumption ≤ 6 W - Control system power consumption ≤ 3 W. - Communication frequency of 100 Hz. - Position adjustments at any given time. - The system can send feedback at any given time.	**Purpose:**	- Verify system power consumption. - Verify that the system can handle the correct supply voltage. - Verify communication frequency. - Verify position adjustments. - Verify system feedback.

Test equipment:

- Fluke 8846A Multimeter or similar.
- PSU

4.1.2.3.1. Test logic and description

Figure 4.1.12 presents the power consumption test scheme.
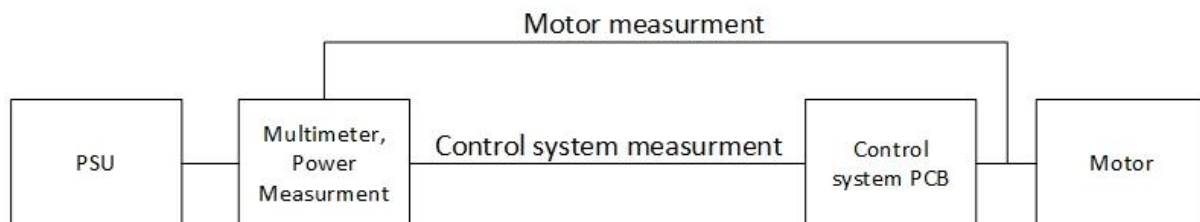
Figure 4. 1. 12: Power consumption test scheme

4.1.2.3.2.   Test procedure

4.1.2.3.2.1.   Power consumption and communication frequency test setup

Table 4. 1. 13: Power consumption and communication frequency test setup

Step	Description	Executed (sign)	Comment
1	Connect the system according to figure 12.		
2	Power up.		The system shall handle a supply voltage of 28 V.
3	Ensure that the system communicates correctly with the test station at 100 Hz.		

Date: **Signature:**

4.1.2.3.2.2.   Power consumption verification

Table 4. 1. 14: Power consumption, step by step procedure

Step	Description	Requirement	Pass/Fail	Comments/Results/report
1	Place the mechanism in - 180 °			
2	Speed: 60 °/s Acceleration: 40 °/s^2 Command the mechanism to rotate to +180 °.			
3	Measure the maximum power consumption of the control system.	Power consumption ≤ 3 W		
4	Measure the maximum power consumption of the AA motor.	Power consumption ≤ 6 W		
5	Measure the maximum power consumption of the EA motor.	Power consumption ≤ 6 W		
6	Total system power consumption equals to the sum of the results in step 3, 4, and 5.	Power consumption $\leq$ 15 W		

Date: **Signature:**

4.1.2.4. Torque test
Table 4. 1. 15: Torque test

Test id:	TST-2.3.2	Project state:	C:3
Requirement to be verified:	REQ-2.3.3 REQ-2.3.3.1 - Motorization according to ECSS-E-ST-33-01C - Azimuth motor torque > 0.114 Nm	Purpose:	- Validate compliance with torque motorization margins from ESA. - Verify motor torque.

Test equipment:

- Kistler 9275
- Test fixture SSM-9000
- Test plate (KDA)
- Test fixture SSM-9300
- Test station
- PSU

4.1.2.4.1. Test logic and description

The torque test shall be connected as presented in figure 4.1.13:
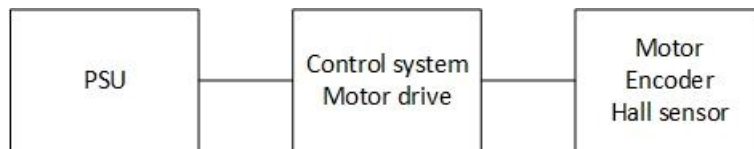
Figure 4. 1. 13: Torque verification connection scheme

4.1.2.4.2. Test procedure

The test verifies the minimum torque required to drive the mechanism, but also the torque the motor must produce to rotate at maximum acceleration and speed in a worst case scenario.

Table 4. 1. 16: Torque test setup

Step	Description	Executed (sign)	Comment
1	Connect the azimuth stage to connector plate as shown in figure 4.1.8.		
2	Connect the azimuth stage with connector to the torque sensor.		
3	Place the azimuth stage with connector plate on test table as shown in figure 4.1.8.		
4	Adjust end stops to proper function.		
5	Connect the system as shown in figure 4.1.13.		

4.1.2.4.2.1.   Torque verification

Table 4. 1. 17: Torque verification, step by step procedure

Step	Description	Requirement	Pass/Fail	Comments/Results
1	Speed: 60 °/s Acceleration: 40 °/s^2 Command the mechanism to rotate CW.			
2	Physically stop the mechanism.			
3	Log torque data.	Torque > 0.114 Nm		
4	Repeat the previous steps, but CCW.			

Date: **Signature:**

4.1.2.5. Position, speed, acceleration, accuracy and range

Table 4. 1. 18: Position, speed acceleration, accuracy and range test

Test id:	TST-2.4.0 TST-2.4.1	Project state:	C:3

Requirement to be verified:	REQ-2.4.1
	REQ-2.4.3
	REQ-2.4.4
	REQ-2.4.5
	  - Speed $\geq$ 60 °/s
	  - Acceleration $\geq$ 40 °/s^2
	  - Accuracy < 0.5 °, half cone, 3 sigma
	  - Range: $\pm$ 180 ° azimuth
		Purpose:	Verification of:
			  - Velocity
			  - Acceleration
			  - Accuracy
			  - Range

Test equipment:

  -   Motor
  -   Test plate (KDA)
  -   Test fixture 9100
  -   Test fixture 9200
  -   Test station
  -   PSU

4.1.2.5.1.   Test logic and description

The system shall be operating under normal conditions while performance is being evaluated. Figure 4.1.14 shows a simple connection scheme of the major electrical parts of the system.
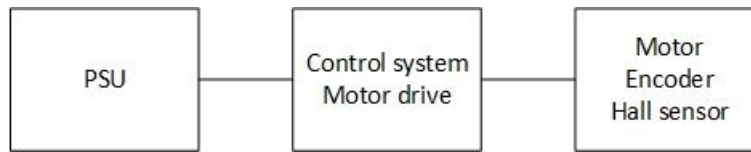
Figure 4. 1. 14: Performance test scheme

4.1.2.5.1.1.   Range of motion

By running the mechanism into two end-stops, the range of motion is verified through encoder readings.

4.1.2.5.1.2.   Positioning accuracy

The accuracy is verified by commanding the mechanism to move a certain amount of degrees. The actual movement is found by subtracting the final position from the starting position. The accuracy is found by calculating the difference between the commanded value and the measured value.

Table 4. 1. 19: Positioning accuracy cases

	Unit	Case 1	Case 2	Case 3
Speed	[°/s]	5	20	60
Acceleration	[°/s^2]	2	15	40
Position command	[°]	20	45	90
Repetition		2	2	2

4.1.2.5.1.3.   Speed and acceleration

The mechanism shall be running at a velocity of 60 °/s and an acceleration of 40 °/s^2. To be able to verify the speed and the acceleration, the position will be logged. Based on the results, the actual speed and acceleration can be calculated.

4.1.2.5.2.   Test procedure

Table 4. 1. 20: Position, speed acceleration, accuracy and range setup

Step	Description	Executed (sign)	Comment
1	Connect the azimuth stage to connector plate as shown in figure 4.1.8.		
2	Connect the azimuth stage with connector to the torque sensor.		
3	Place the azimuth stage with connector plate on test table as shown in figure 4.1.8.		
4	Connect the system as shown in figure 4.1.14.		

Date: **Signature:**

4.1.2.5.2.1.   Azimuth range verification

Table 4. 1. 21: Azimuth range verification, step by step procedure

Step	Description	Requirement	Pass/Fail	Comments/Results
1	Speed: 10 °/s Acceleration: 5 °/s^2			
2	Command mechanism to rotate to 0 ° position.			
3	Wait for 2 seconds.			
4	Command mechanism to rotate 190 ° CW.			
5	Manually stop the motor when end-stop occurs.			
6	Calculate the range based on encoder readings.	Range: 180 ° CW		
7	Repeat step 1 – 6.			
8	Command mechanism to rotate 190 ° CCW.			
9	Manually stop the motor when end-stop occurs.			
10	Calculate the range based on encoder readings.	Range: 180 ° CCW		
11	Repeat step 1-3 and 8-10.			

Date: **Signature:**

4.1.2.5.2.2.   Position accuracy verification

Table 4. 1. 22: Positioning accuracy, step by step procedure

Step	Description	Requirement	Pass/Fail	Comments/Results
1	Use the parameters from table 21 (case 1, case 2, case 3).			
2	Subtract starting position from final position.			
3	Calculate the difference between the position command and the result from step 3.	Accuracy: < 0.5 °, half cone, 3 sigma		Case 1.1: Case 1.2: Case 2.1: Case 2.2 Case 3.1: Case 3.2:
4	Repeat step 1 - 3 until all the cases in table 21 have been performed.			

Date: **Signature:**

SSM
SMALL SATELLITE MECHANISMS

4.1.2.5.2.3. Speed and acceleration verification

Table 4. 1. 23: Speed and acceleration, step by step procedure

Step	Description	Requirement	Pass/Fail	Comments/Results
1	Speed: 60 °/s Acceleration: 40 °/s^2			
2	Start encoder data logging.			
3	Command the mechanism to move ± 180 °.			
4	Calculate speed and acceleration based on encoder readings.	Speed ≥ 60 °/s Acceleration ≥ 40 °/s^2		Speed: Acceleration:
5	Repeat step 1 – 4.			Speed: Acceleration:

Date: **Signature:**

4.1.3. References

[1] V. O. AArud, "SSM-10000, Part Verification-Prototype 5421," Kongsberg, 2016.

[2] S. Laugerud and V. O. Aarud, "SSM-3000, Test & Verification Specification," Kongsberg, 2016.

[3] G. H. Stenseth and M. Dybendal, "SSM-2000, Requirement Specification," Kongsberg, 2016.

[4] M. M. Gorski, "KARMA 7, GSTP MSDDA, SRA EM functional test procedure (TN20.02)," KDA, Kongsberg, 2014.

[5] Microchip, "Space Vector Modulation," Microchip, [Online]. Available: http://microchip.wikidot.com/mct5001:space-vector-modulation. [Accessed 18 April 2016].

4.2. Test report

i. Abstract

This report is the documentation of the functional test performed at KDA, 10.05.16. It explains how the different requirements for the SSM project have been verified. Table 4.2.14 contains an overview of where the requirements are discussed in this chapter.

ii. Contents

SSM

SMALL SATELLITE MECHANISMS

v. Document history

Table 4. 2. 1: Document history

Rev.	Date	Author	Approved	Description
0.1	09.05.16	MD		Document created
0.2	11.05.16	GHS	VOA	Wrote the report
1.0	15.05.16	GHS	TS	Reviewed and published

4.2.1. Introduction

This chapter describes the tests performed. The tests were, to an extent, performed as described in [1], but modifications were made. Additional test were performed when needed or when seen as quick ways to verify more requirements.

Table 4. 2. 2: Tests

TST-2.1.0	TR	Power consumption
TST-2.3.2	TAR	Torque
TST-2.4.0	TR	Pointing accuracy
TST-2.4.0	TR	Speed and acceleration
TST-2.5.1	T	Communication frequency
TST-2.9.0	T	Insulation
TST-2.9.1	TR	Supply voltage

4.2.1.1. Precautions

During setup of the tests, modifications were made to the test fixtures. The height of bracket 9100 [1] had to be adjusted to account for the height of the screws holding fixture 9200 [1]. The bore of the 9200 fixture was too small for the shaft of the motor used in position measurement, and had to be bored to a diameter of 4 mm. This could cause the motor shaft to not be 100 % centered, causing small deviations in the measured position.

The data logger only logs the encoder position and the torque measured by the Kistler torque sensor [2]. It records data at a rate of approximately 750 Hz, and marks each sample with a 64 bit timestamp which is the time in microseconds since the data logger started. Due to the low sample rate and the low resolution of the encoder, the velocity and acceleration calculations are noisy. This is filtered in Matlab using a moving average filter. However, the acceleration calculations can only be seen as a coarse indicator as to whether the mechanism is accelerating or not. Figure 4.2.18 shows an example of the velocity and acceleration graphs.

The motor driving the mechanism was not properly installed, causing the gears to not be properly aligned. This caused higher backlash than expected. See 4.2.4.2.2.6.

The bearings were not preloaded with the right force due to tools not being available, which may have decreased or increased friction.

The electronics used in the breadboard model of the control system are not representative for the planned final system. High-ohm shunt resistors could have caused additional power consumption and lower torque.

4.2.1.2. Test personnel

The tests were performed by:

- Torstein Sundnes
- Magnus Dybendal
- Gisle Hovland Stenseth

The overall responsible engineers were:

- Vebjørn Orre Aarud
- Stian Laugerud

4.2.2. Functional tests

4.2.2.1. *Motor resistance test*

Table 4. 2. 3: Motor resistance test

		Project state:	C:3
Requirement to be verified	Motor resistance of 6.89 Ω ± 10%	**Purpose**	Verify motor resistance

Test equipment:

- Motor EC 45 flat 70 w
- Digital Multimeter/Fluke 8808A or similar

4.2.2.1.1. Description

The motor resistance is measured phase-to-phase in all windings in order to verify the motor resistance specified in the datasheet [3].

4.2.2.1.2. Results of motor resistance test

Table 4. 2. 4: Results of motor resistance test

Step	Description	Requirement	Comments	Pass/Fail
1	Measure resistance between winding 1-2	Motor: 6.89 Ω ± 10 %	With wires: 9.17 Direct: 8.84	Not a valid test
3	Measure resistance between winding 2-3	Motor: 6.89 Ω ± 10 %	With wires: 9.13 Direct: 8.87	Not a valid test
5	Measure resistance between winding 1-3	Motor: 6.89 Ω ± 10 %	With wires: 9.11 Direct: 7.28	Not a valid test

4.2.2.1.2.1. Comments to motor resistance test

The resistance was first measured at the end of the leads going from the control system to the motor. Secondly, the resistance was measured directly on the motor connector. Due to the Fluke 8808A output voltage, the coils in the motor were charged, causing the measured resistance to change. The values presented in table 4.2.4 are incorrect as a result of this. Due to these inaccuracies, the test is not valid. However, earlier measurements using a different digital multimeter have shown that the motor windings have the correct resistance.

4.2.2.2. *Insulation test*

Table 4. 2. 5: Insulation test

Test id:	TST-2.9.0	**Project state:**	C:3
Requirement to be verified:	REQ-2.9.1 REQ-2.9.2 REQ-2.9.3 REQ-2.9.4 Insulation Resistance:	**Purpose:**	To verify insulation between individual motor windings and electrical wires

	Motor Windings: - 500 VDC - > 100 MΩ Electrical wires: - 500 VDC - > 50 MΩ		

Test equipment:

- Mega ohm meter Hypot-III-3770 or
  similar
- Switch box

4.2.2.2.1.   Description

The insulation test was performed using a mega ohm meter, Chauvin Arnoux C.A 6525 instead of the mega ohm meter described above due to the unavailability of the Hypot-III-3770. The switch box was not used as it is not needed for such a small test. Switch boxes are mainly used to test the electrical insulation between wires in the system. At the time of the test, the system was a breadboard model with incomplete wiring. The test was done by measuring the resistance between each of the windings and the motor casing using 500 V.

4.2.2.2.2.   Results of insulation test

Table 4. 2. 6: Results of insulation test

Step	Description	Requirement	Comments	Pass/Fail
1	Measure resistance between winding 1- motor casing	>100 MΩ	>2 GΩ	Pass
3	Measure resistance between winding 2- motor casing	>100 MΩ	>2 GΩ	Pass
5	Measure resistance between winding 3- motor casing	>100 MΩ	>2 GΩ	Pass

4.2.2.2.2.1.   Comments to results of insulation test

The motor windings are isolated from the motor casing by >2 GΩ which is well above the required resistance. The test is passed.

4.2.2.3. *Power consumption, supply voltage and communication frequency test*

Table 4. 2. 7: Power consumption, supply voltage and communication frequency test

Test id:	TST-2.1.0 TST-2.9.1 TST- 2.5.1	Project state:	C:3
Requirement to be verified:	REQ-2.1.1 REQ-2.1.1.1 REQ-2.1.1.2 REQ-2.9.5 REQ-2.5.5 REQ-2.5.6 REQ-2.5.7 REQ-2.5.8 - System power consumption ≤ 15 W - Motor power consumption ≤ 6 W - Control system power consumption ≤ 3 W - Communication frequency of 100 Hz - Position adjustments at any given time - The system can send feedback at any given time	Purpose:	- Verify system power consumption. - Verify that the system can handle the correct supply voltage. - Verify communication frequency. - Verify position adjustments. - Verify system feedback. - Verify compatibility with 28 V power supply

Test equipment:

- Fluke 8846A Multimeter or similar
- PSU
- Compact Rio 9082 as data logger
- Motor with MILE, 1024 CPT
  encoder for position measurement

4.2.2.3.1. Description

The current was measured between the PSU and the motor driver instead of between the motor driver and the motor, due to the complexity of measuring the three phase switching signal between the motor driver and the motor. The measurement performed in the test therefore includes the power lost in the motor driver. In addition to measuring the current, the PSU was capped at 6W. The PSU never reached this power output.
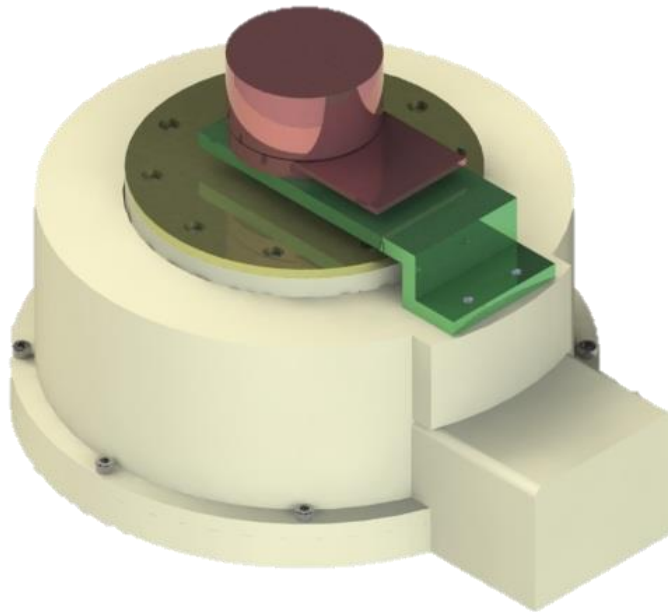
Figure 4. 2. 1: Mechanical setup for power consumption test

Figure 4.2.1 shows the mechanical setup for this test. A second motor is mounted on the mechanism with the encoder working as a position sensor.

4.2.2.3.2. Results of power consumption, supply voltage and communication frequency tests

Table 4. 2. 8: Results of power consumption, supply voltage and communication frequency tests

To be measured	Requirement	Measured value
Control system power consumption	≤ 3 W	< 2.5 W
Azimuth motor power consumption	≤ 6 W	No dummy mass: 19.6 mA, 550 mW With dummy mass: 20.4 mA, 566 mW
Total system power	≤ 15 W	< 3.066 W, 9.066 W assuming worst case in the elevation stage

The current going through the microcontroller and hall sensor part of the system was not measured, but was connected to an USB 2.0 port with a maximum current output of 500 mA at 5 V. This means that the power used by this part of the system was less than 2.5 W. Of course, this is a coarse estimate. The actual power should be lower.

The power used in the elevation stage is expected to be less than the power used in the azimuth stage as the mass and calculated torque is lower.

The test was done with and without the fishplate (part number 10102) and elevation stage (dummy mass).

The PSU for the motors was set to 28 V.

4.2.2.3.2.1. Comments of the tests

As seen in table 4.2.8, the APMA passed all power consumption tests. The motor and motor driver passed by a factor of >10. The reason for this is that the system is dimensioned according to the ECSS mechanisms standard [4] as per REQ-2.3.3 in [5].

In addition to the data in table 4.2.8, the current in off-mode (Control system on, but not switching the motor driver) and the current when locked in a position were tested:

- 5 mA in off-mode
- 13.8 mA when locked in a position

The low current in off-mode shows that the system does not power the motors while not receiving any commands, verifying REQ-2.7.8 in [5]. The low current of 13.8 mA when locked in a position is one of the main advantages of using a feedback system. If the motor was used as a stepper, this current would be the same as when rotating the mechanism.

In order to receive commands from the microcontroller emulating the spacecraft, the control system had to send a position update stating its current position. When the position update was received, the command microcontroller sent position commands at 100 Hz. The control system received the commands at 100 Hz, and sent position feedback continuously while driving the mechanism. This verifies REQ-2.5.1, REQ-2.5.2, REQ-2.5.5, REQ-2.5.7 and REQ-2.5.8.

The control loop implemented in the control system directly outputs the command from the spacecraft, verifying REQ-2.5.6.
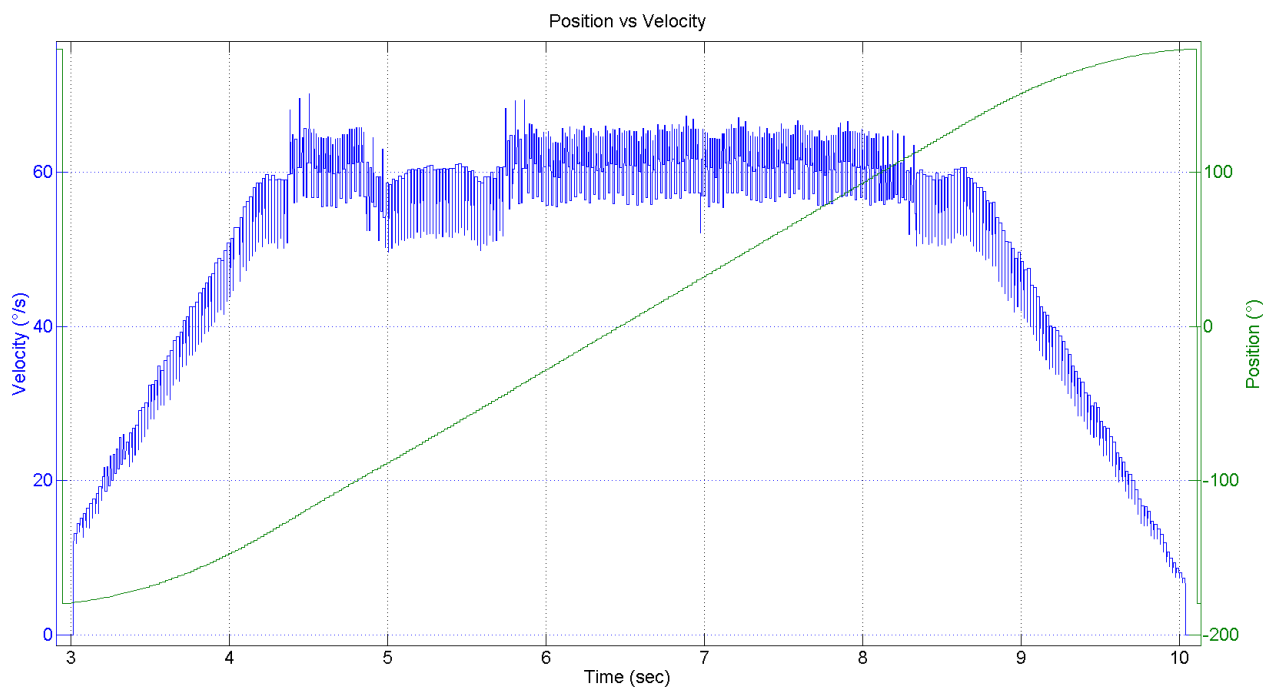

Figure 4. 2. 2: Position/velocity run

Figure 4.2.2 shows the measured position and velocity of the run used in this test. A velocity of 60 °/s is reached within 1.5 s, which gives an acceleration of 40 $°/s^2$.

All requirements in table 4.2.7 were confirmed. In addition, REQ-2.7.8 was verified and REQ-2.3.3 partly verified.

4.2.2.4. *Torque test*

Table 4. 2. 9: Torque test

Test id:	TST-2.3.2	Project state:	C:3
Requirement to be verified:	REQ-2.3.3.1 - Motor torque > 0.114 Nm	Purpose:	- Verify motor torque - Validate compliance with torque motorization margins from ESA

Test equipment:

- Kistler 9275
- Test fixture SSM-9000
- Test plate (KDA)
- Test fixture SSM-9300
- Test station
- Compact Rio 9082 as data logger

4.2.2.4.1.   Description

The torque test was not done according to the test procedure. Instead of the fixture 9300 shown in figure 4.2.3, the mechanism was tested by running the fishplate into the end-stop.
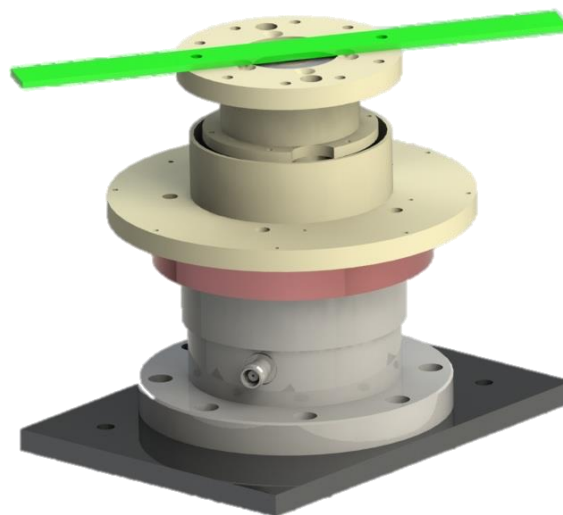
Figure 4. 2. 3: Torque test fixture

Running this test without fixture 9300 [1], means the mechanism runs into only one end stop, possibly altering the end result. Due to the low torque, this error is small and can be ignored.

![SSM Small Satellite Mechanisms logo]

The command procedure was changed, as the main goal of the test is to run into the end stops. A full 360° is not needed. The run was started from a position closer to the end-stops.

The test is supposed to verify REQ-2.3.3.1, relating to the motor's torque capabilities at 6 W. The torque produced by the motor can be calculated by taking the torque measured divided by the gear ratio (17.5). This does not account for potential losses in the mechanism. Losses in the mechanism can be found by calculating the average torque produced by the mechanism when running in constant speed:

$$T_{motor} = \frac{T_{mechanism}}{17.5} - L_{mechanism}. \tag{4.2.1}$$
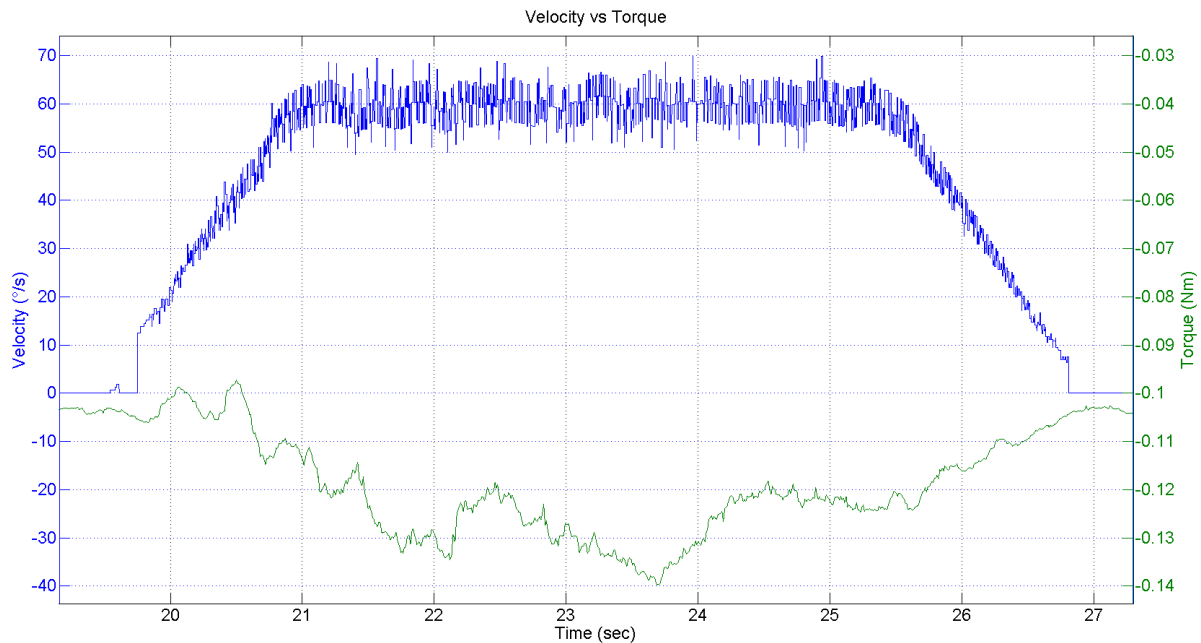
Figure 4. 2. 4: Torque at zero acceleration

The average torque at constant speed was found using the dataset in figure 4.2.4. The torque-measurement was not set to zero at the start of the run, and was biased at 0.103 Nm. The average torque measured was calculated to 0.126 Nm, making the average torque and the losses in the mechanism 23 mNm.

As the current could not be logged by the data logger, the PSU was limited to 6 W (28 V, 214.3 mA). This was a mistake, as the PSU limits the output voltage to account for the increasing current, thereby lowering the magnetic forces in the motor causing the torque to drop. The current should have been logged alongside the torque measurement, allowing higher currents without dropping the supply voltage.

4.2.2.4.2.   Results of torque test
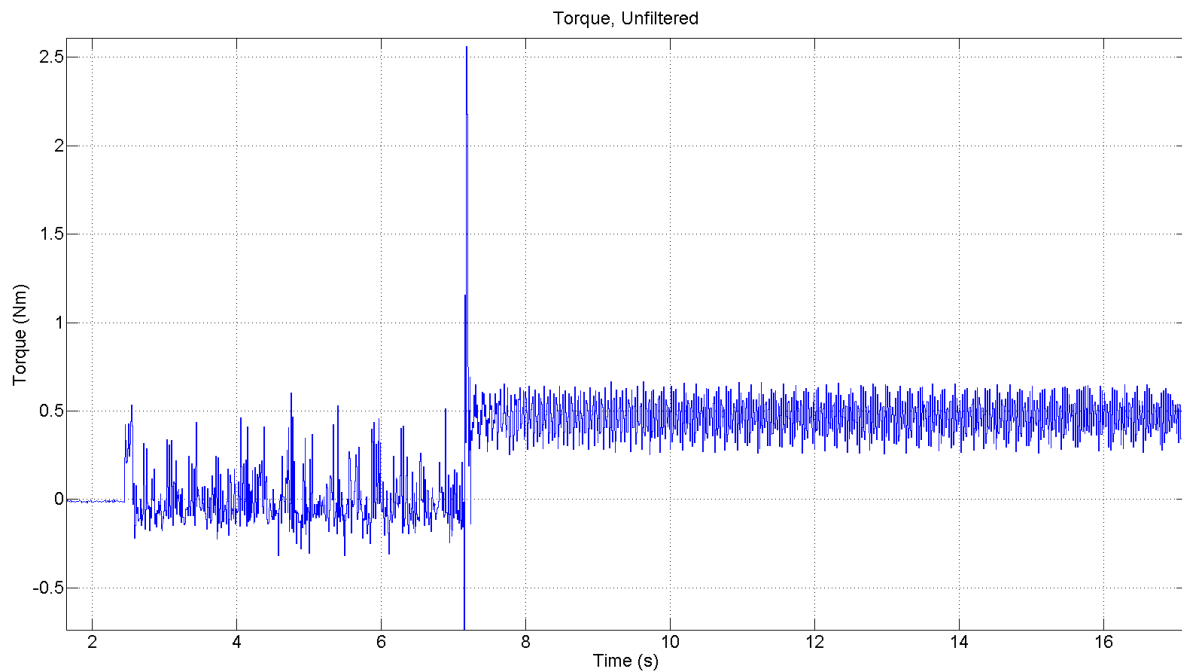### 4.2.2.4.2.1.   Clockwise

Figure 4. 2. 5: Stall torque running into end stop at 60 °/s CW

Figure 4.2.5 shows the torque when running the mechanism into the end-stop in clockwise rotation at 60 °/s. Where the mechanism hits the end-stop, a peak in torque appears. This is due to the momentum of the mechanism. In this test, the PSU runs directly into current limitation and the torque drops to approximately 0.45 Nm.
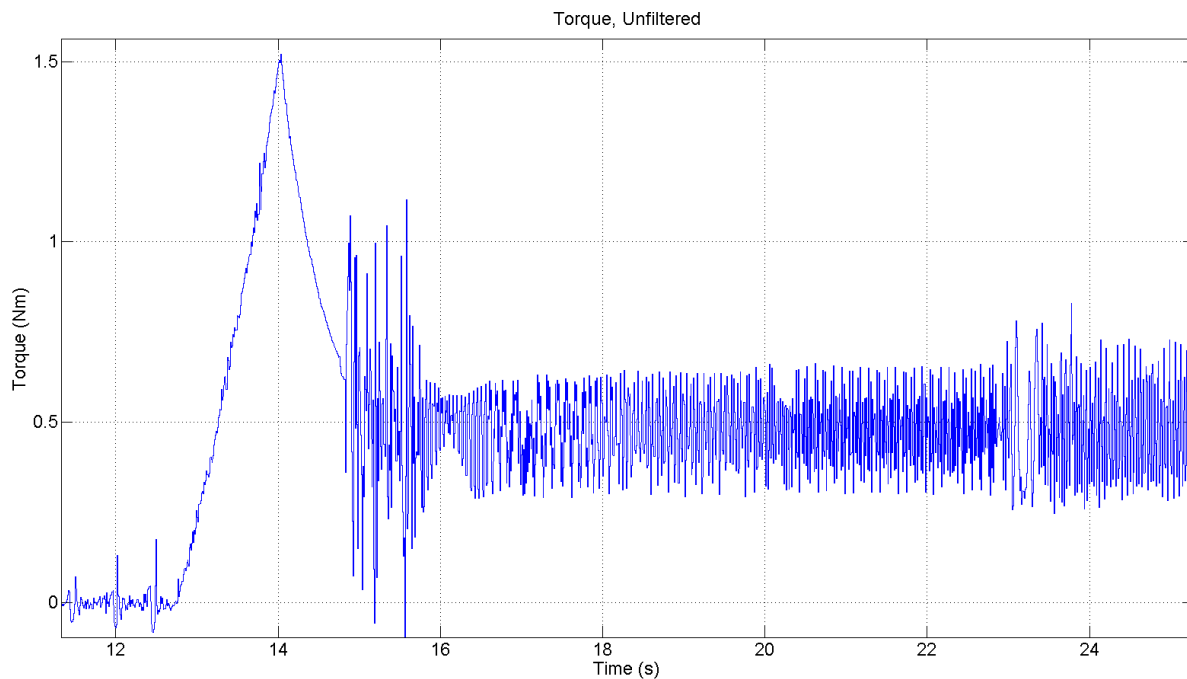

Figure 4. 2. 6: Stall torque running into end stop at 1 °/s CW

Figure 4.2.6 shows the torque when running the mechanism into the end-stop at 1 °/s in the clockwise direction. The peak seen at 14 s is the maximum torque of 1.521 Nm produced by the mechanism

before the current demand gets too high for the PSU and it starts limiting the output voltage. This gives a motor torque of 0.11 Nm, 0.04 Nm short of the requirement.
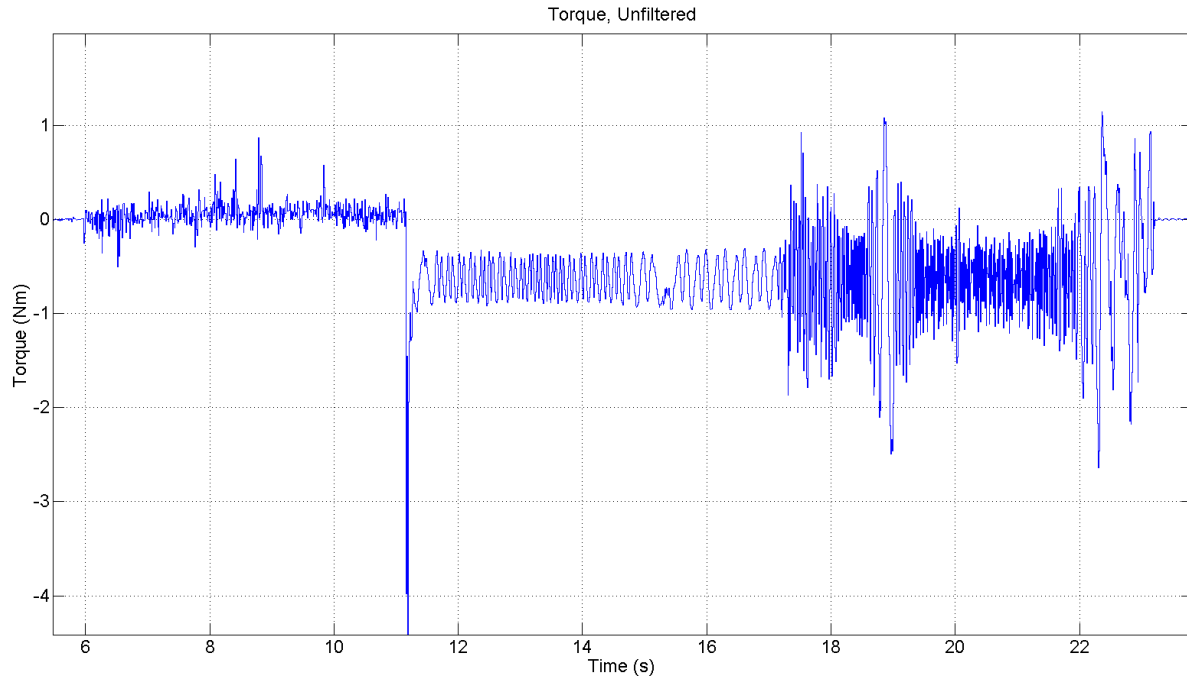
4.2.2.4.2.2.   Counter Clockwise

Figure 4. 2. 7: Stall torque running into end-stop at 60 °/s CCW

Figure 4.2.7 shows the torque test at 60 °/s CCW. As with the CW case, the PSU limits the current immediately after impact. Here the torque is stable around 0.6 Nm while the PSU limits the current. This is 0.15 Nm more than with the CW case.
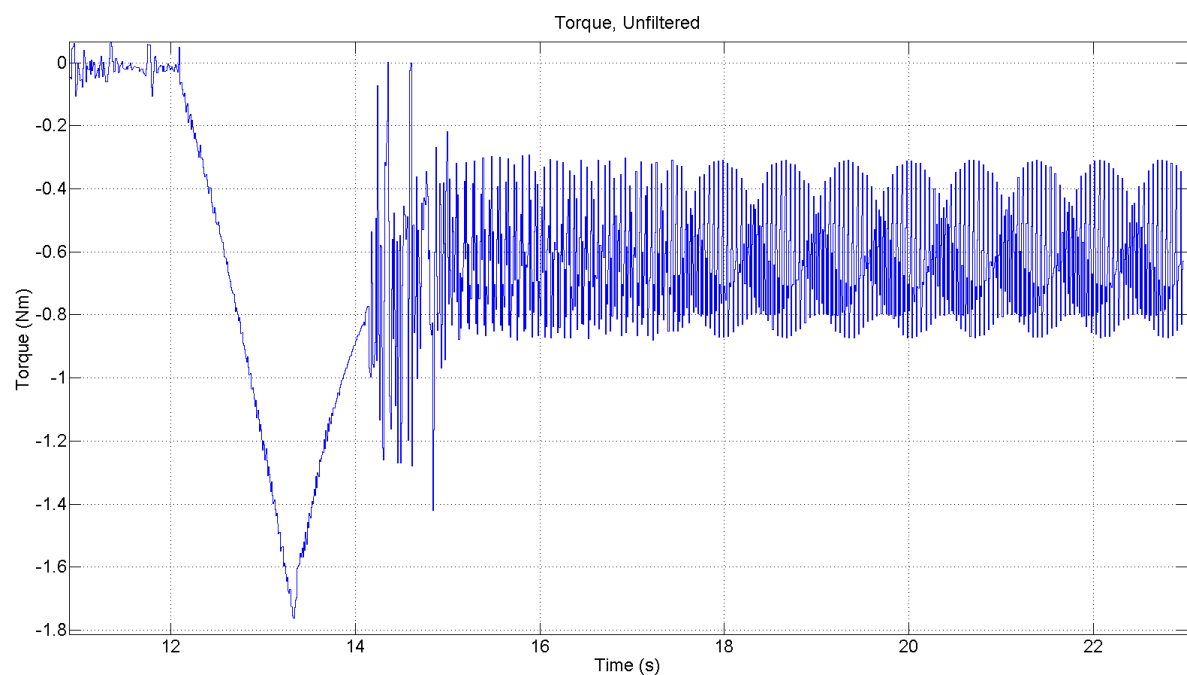

Figure 4. 2. 8: Stall torque running into end-stop at 1 °/s CCW

As seen in the slow case for CW rotation, the slow case for CCW rotation gives a better view of the actual torque produced. The peak torque before the PSU limits the voltage is 1.762 Nm which gives a motor torque of 0.1237 Nm. This is 9.69 mNm above the requirement.

4.2.2.4.2.3.   Comments

The torque in CCW direction is shown to be higher than the torque in the CW direction. A possible explanation for this is that the virtual motor pole position of the control system might not have been completely in line with the actual position of the motor poles at the start of the test, causing the magnetic field to be stronger in one direction. If this is the case, the difference in the magnetic fields should be close to linear, making the actual torque with the right pole position the average of the measurement in either direction. This average would be 0.1168 Nm, which is 2.8 mNm above the requirement, verifying REQ-2.3.3.1. In addition, the losses in the motor driver have not been measured, and although low, removing these losses would increase the performance. Some power is also lost in the shunt resistors used in the current measurement circuit. These resistors are 0.47 Ω, and will not be used in the final design. For this test, the gears were not lubricated, which can cause increased friction.

The requirement (REQ-2.3.3.1) is considered verified.

REQ-2.3.3.1 is based on requirement REQ-2.3.3. This requirement is also verified.

The torque produced by the motor is directly related to the stator current. By verifying that the control system controls the torque of the motor, the current control requirement REQ-2.7.5 is verified.

Table 4. 2. 10: Position, speed, acceleration, accuracy and range test

Test id:	TST-2.4.0 TST-2.4.1	**Project state:**	C:3
Requirement to be verified:	REQ-2.4.1 REQ-2.4.2 REQ-2.4.3 REQ-2.4.4 　- Speed ≥ 60 °/s 　- Acceleration ≥ 40 °/s^2 　- Accuracy < 0.5 ° 　- Range: ± 180 ° azimuth, ± 90 ° elevation	**Purpose:**	- Velocity - Acceleration - Accuracy - Range

Test equipment:

- Motor with MILE, 1024 CPT encoder for position measurement
- Test plate (KDA)
- Test fixture 9100
- Test fixture 9200
- Compact Rio 9082 as data logger

4.2.2.5.1.　　Description

This test is done to verify the range, accuracy, velocity and acceleration of the mechanism. The test used the same setup as seen in 4.2.2.3.

4.2.2.5.2.　　Azimuth range results

The positions for the range test was changed from (0°,-190°,0°,190°) , as described in [1], to (0°,-180°,180°) due to the nature of the calibration software and that the software in the command controller is made only for -180 to 180 rotation. There was no end stop mounted on the mechanism at the time of this test, meaning it could rotate freely for any amount of degrees in any direction without being stopped.
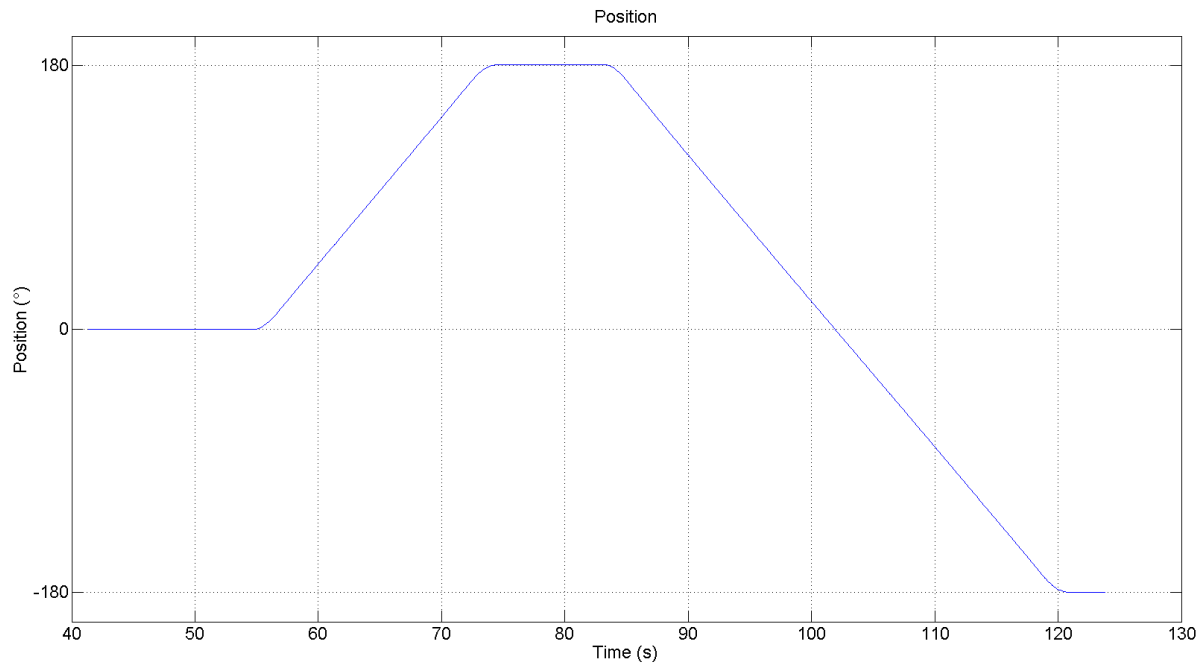
Figure 4. 2. 9: Full test run

Figure 4.2.9 shows the full test run. The graph shows that the mechanism moved a full 360°, thereby verifying REQ-2.4.3. It also shows that the control system has calibrated to zero-position, verifying REQ-2.7.7.

4.2.2.5.3.   Position accuracy results

The position accuracy was tested using the cases shown in table 4.2.11. By subtracting the final position from the commanded position, the pointing error was found. The accuracy requirement is <0.5° half cone, 3 σ. This value is the total pointing error for both axes. For one axis only, the pointing accuracy is 0.357°, 3 σ [6].

The resolution of the encoder used for this test is: $\frac{360°}{4096} = 0.08789°$. Values within plus/minus this value are uncertain.

Table 4. 2. 11: Position accuracy test run cases

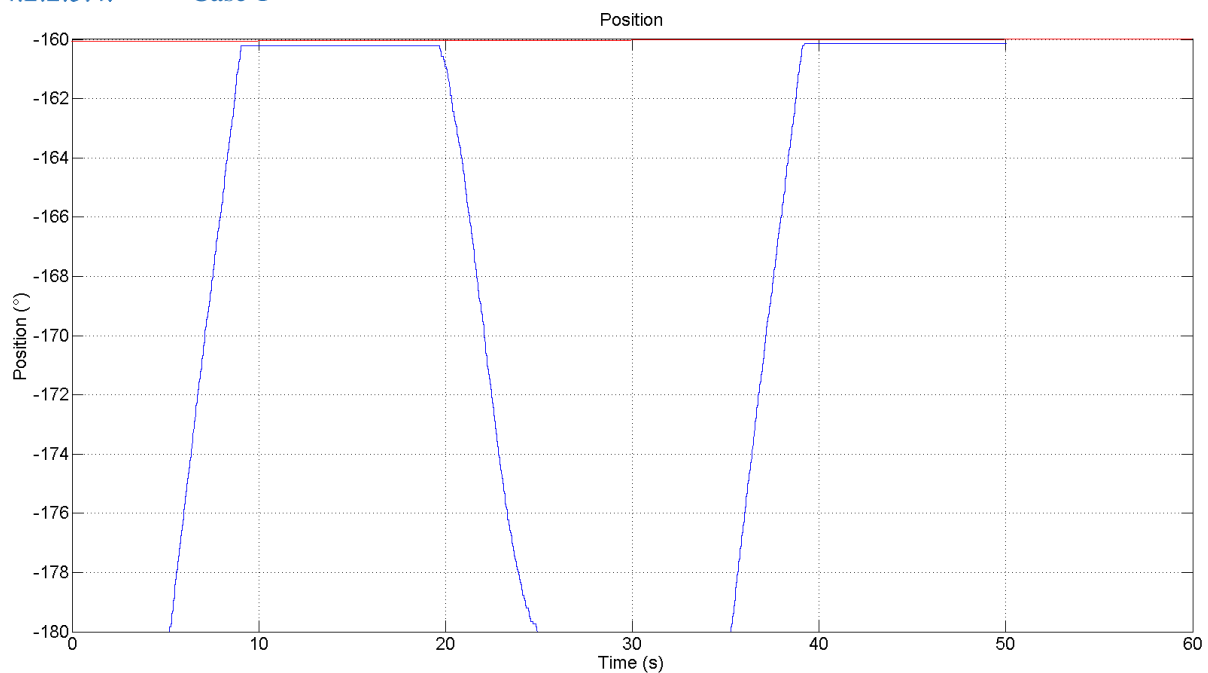|	Unit	Case 1	Case 2	Case 3
Speed	[°/s]	5	20	60
Acceleration	[°/s²]	2	15	40
Position command	[°]	20	45	90
Repetitions		2	2	2

Figure 4. 2. 10: Position accuracy case 1 zoomed out

Figure 4.2.10 shows the overall run of the case 1 test. The mechanism was commanded to move 20° from -180° to -160°.
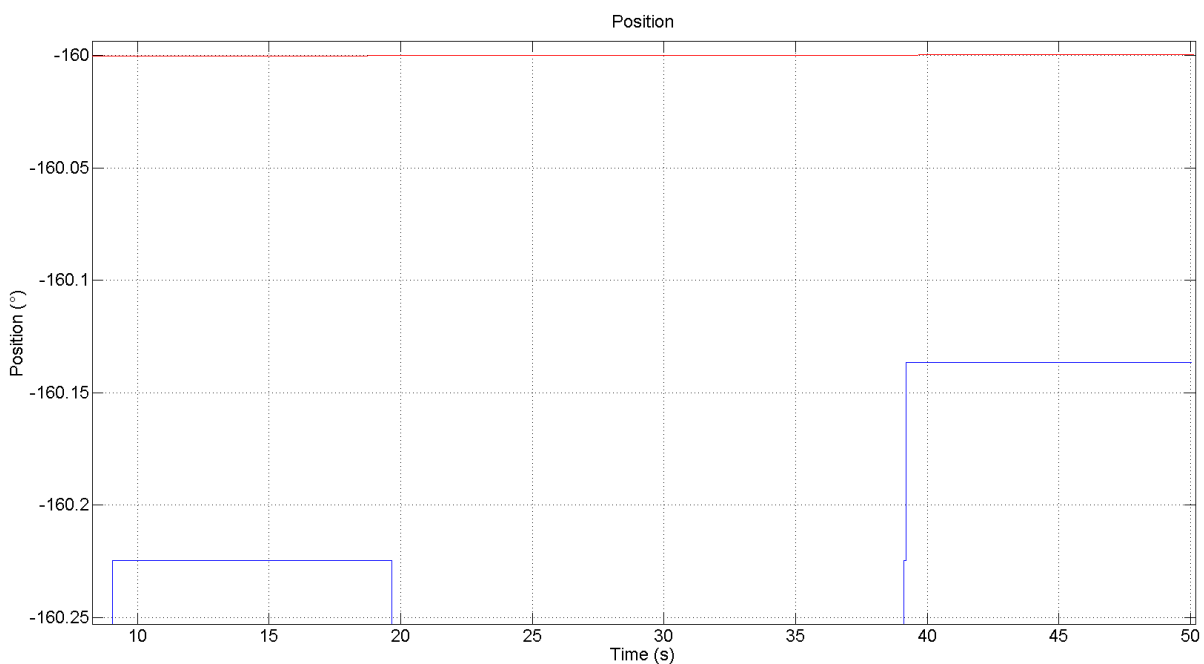

Figure 4. 2. 11: Position accuracy case 1 zoomed in

Figure 4.2.11 shows the same data as figure 4.2.10, but is zoomed in on the peaks of the position. The measured position for the first run is -160.225°, giving an error of 0.225° ± 0.08789°. The second run is closer, with an error of 0.137° ± 0.08789°. This case was repeated three times, and the results were the same every time. The motor encoder on the mechanism was 0.05° off its final position due to the control system not being able to reach its reference position.

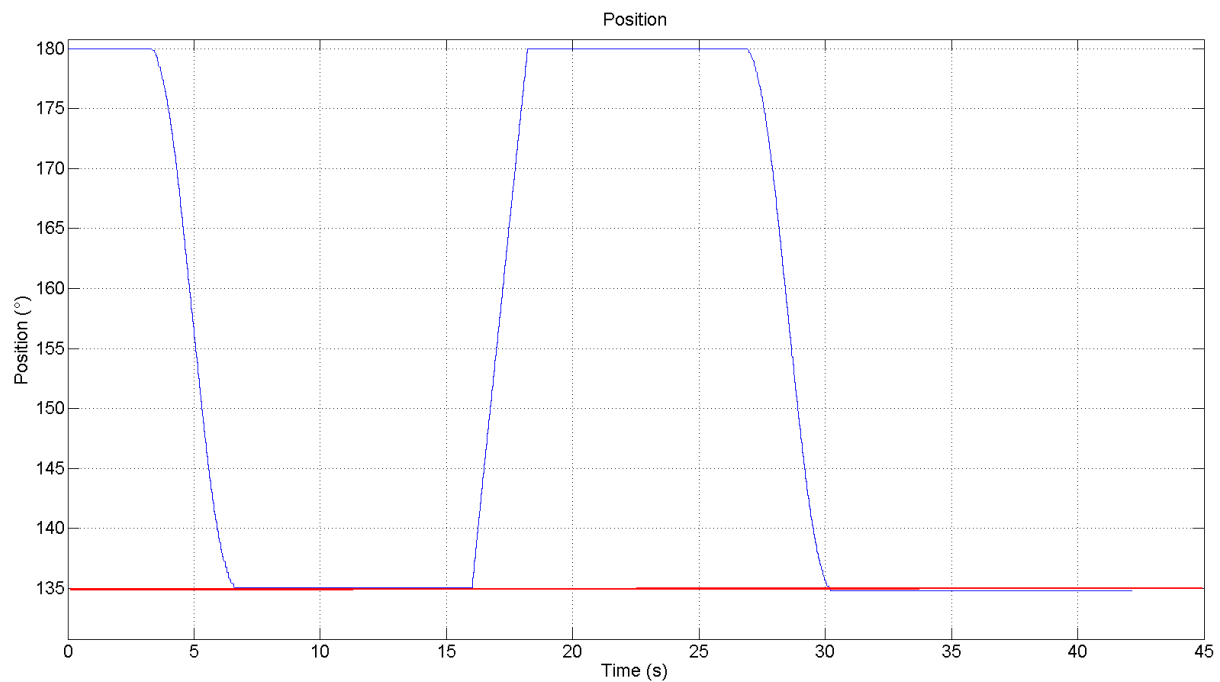The worst case error for case 1 is 0.31289°.

Figure 4. 2. 12: Position accuracy case 2

Figure 4.2.12 shows the full run of case 2. In this case, the mechanism was commanded 45°, from 180° to 135°.
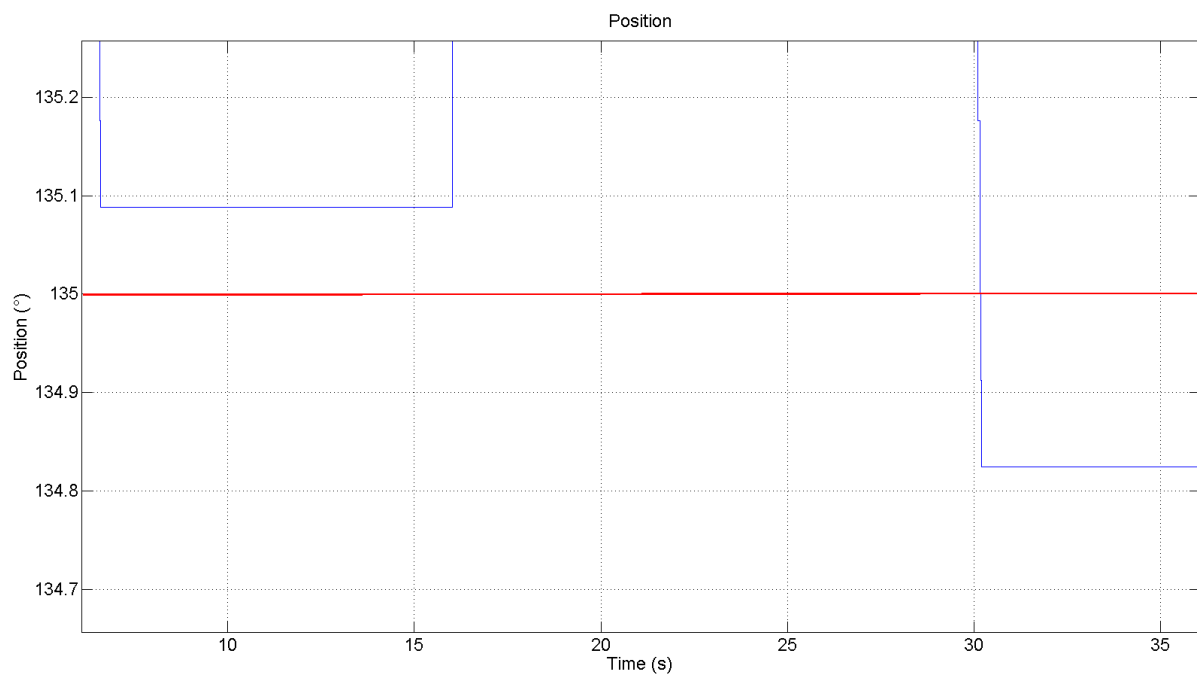

Figure 4. 2. 13: Position accuracy case 2, zoomed in

Figure 4.2.13 shows case 2 zoomed in. In the first run, the mechanism reached 135.9121°, making the pointing error 0.0879° ± 0.08789°. Exactly the same as one encoder pulse. In the second run, the

mechanism reached a position of 134.8242°, making the pointing error 0.1758° ± 0.08789°, exactly two encoder pulses away from the reference position.

The worst case error for case 2 is 0.26369°.

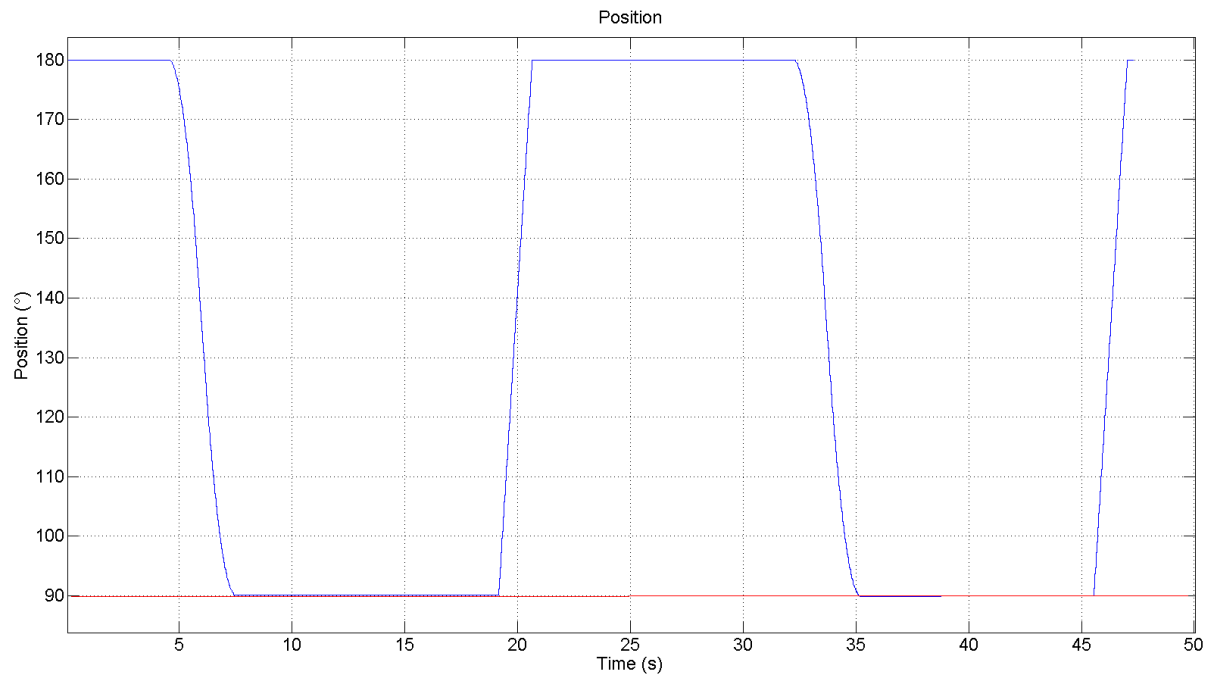### 4.2.2.5.6.   Case 3

Figure 4. 2. 14: Position accuracy case 3

Figure 4.2.14 shows the full run of case 3. In this case, the mechanism was commanded 90°, from 180° to 90°.
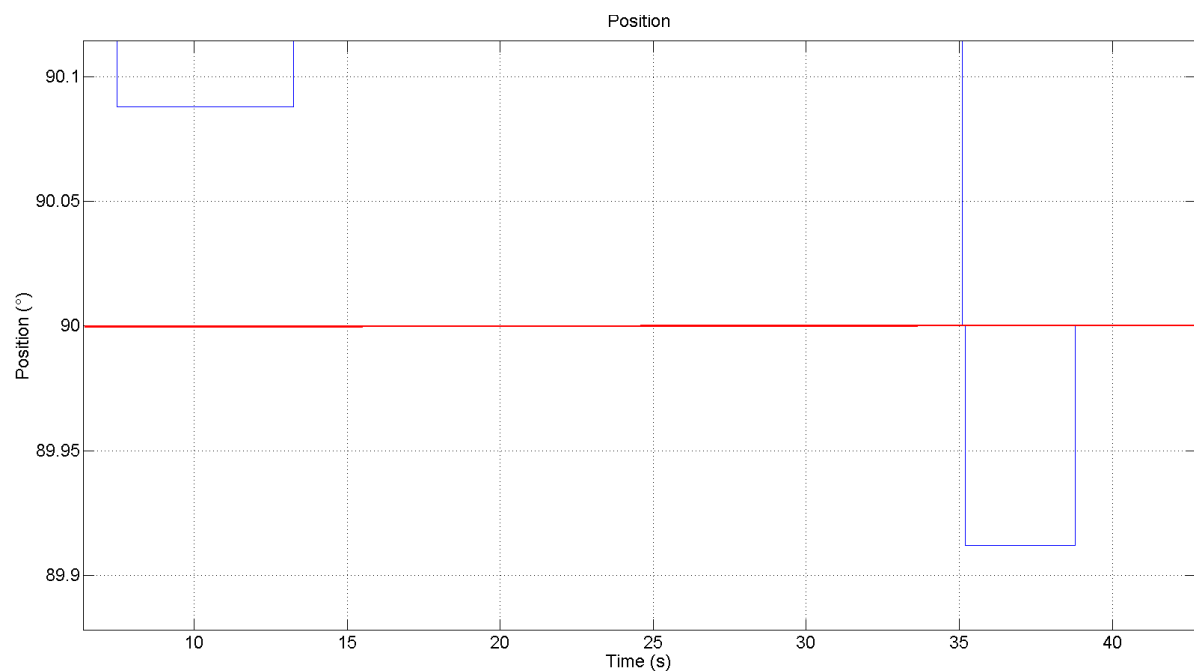

Figure 4. 2. 15: Position accuracy case 3, zoomed in

In the first run shown in figure 4.2.15, the mechanism reached a position of 90.0879° ± 0.08789°. In the second run, it first overshot the final position by 0.0879° before regulating back to 90° with 0° ± 0.08789° error. This case was also run a second time. That time, one of the positions had an error of 0.3516° ± 0.08789°, barely making the requirement.

The worst case error for case 3 is 0.43949°.

Table 4. 2. 12: Worst case error for all cases

Case	Worst case error
1	0.31289°
2	0.26369°
3	0.43949°
Average error:	0.33869°

4.2.2.5.6.1. Comments to position accuracy results

All the cases run were inside the requirements. The results are however more consistent when running clockwise. A possible explanation for this, is that the mechanism is calibrated running clockwise, meaning the backlash is removed if the test is run in the same direction.

In case 1.2, the mechanism was moved until the encoder on the output shaft showed the right position. Doing this did not change the motor encoder position. This means the backlash of the mechanism is ≥0.137 °. This is confirmed in 4.2.2.6, where the total backlash is found to be 0.3516° ± 0.08789°. Considering the motor was not in the right position at the time of the test, this is a good result.

Requirement REQ-2.4.1 is not verified for the azimuth stage. This is expected, as the gears were not properly aligned for the test. With the gears aligned, the total backlash is expected to drop to 0.139° [6]. This would make the worst case error ~0.22689°.

4.2.2.5.7. Speed and acceleration results

This test is done to verify the speed and acceleration of the mechanism .The requirements according to [5] are: A velocity of ≥60°/s and an acceleration of $40°/s^2$. The test is done by commanding the mechanism to do a full 360° run with the desired velocity and acceleration in both directions.
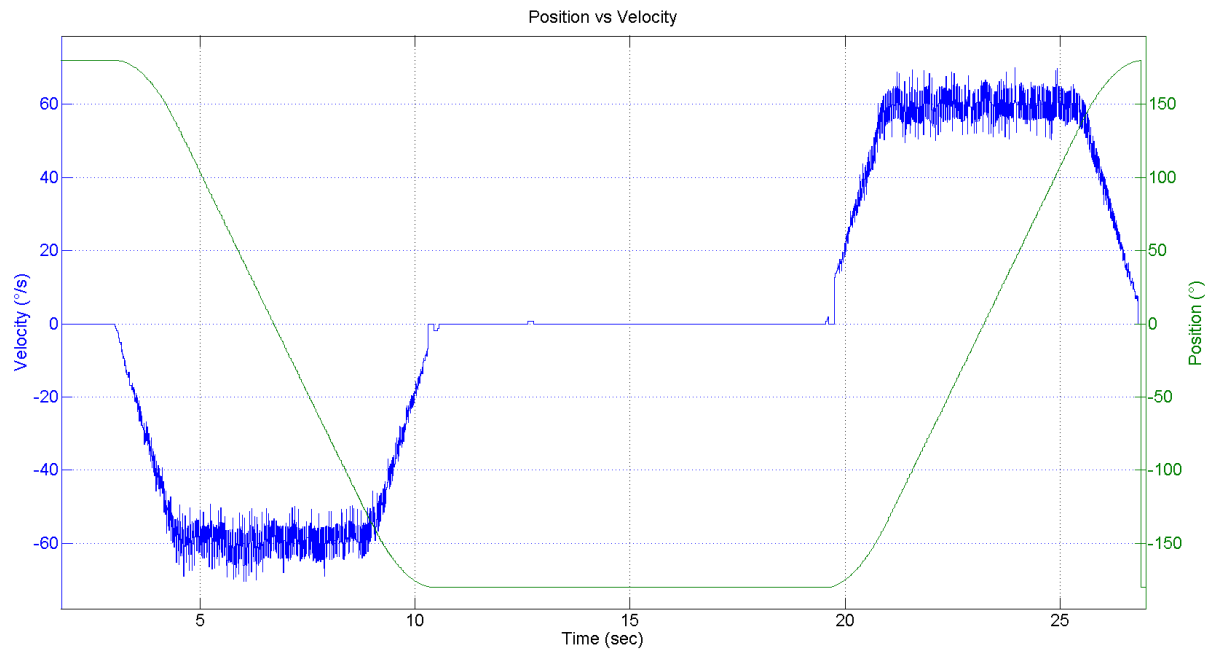
Figure 4. 2. 16: Velocity and position

Figure 4.2.16 shows the full run for the test. Although the data is noisy, the velocity is seen reaching 60°/s.

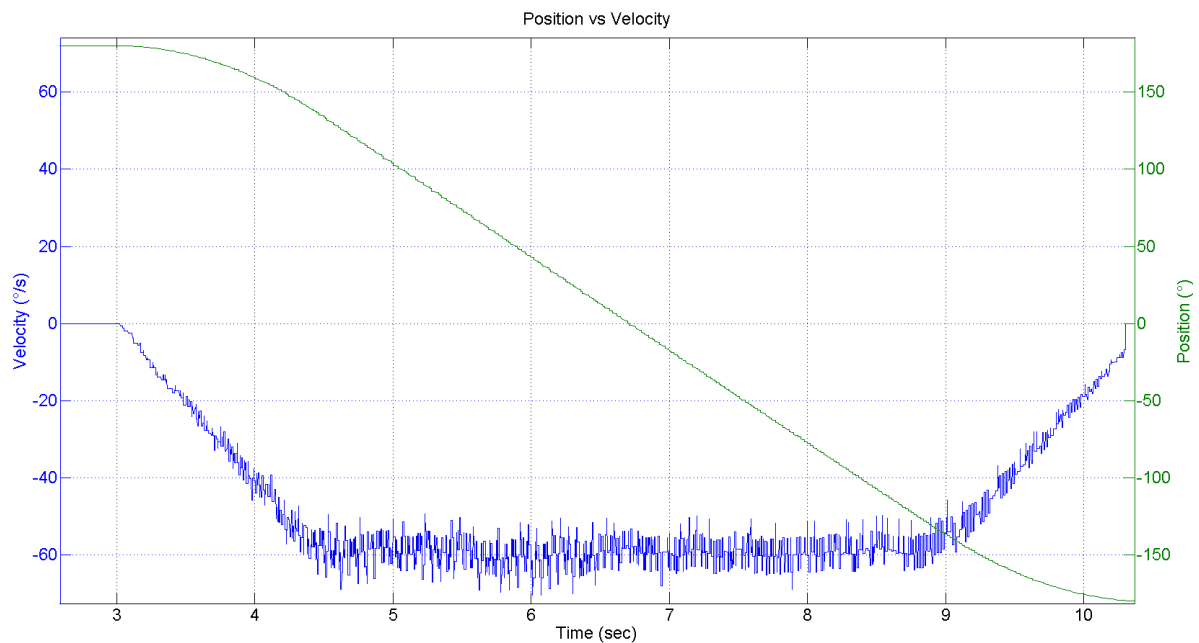*Figure 4. 2. 17: Velocity and position zoomed*

Figure 4.2.17 shows a zoomed-in view of the run from 180° to -180°. A velocity of 60°/s was reached within 1.5 seconds, confirming the 40°/s acceleration.
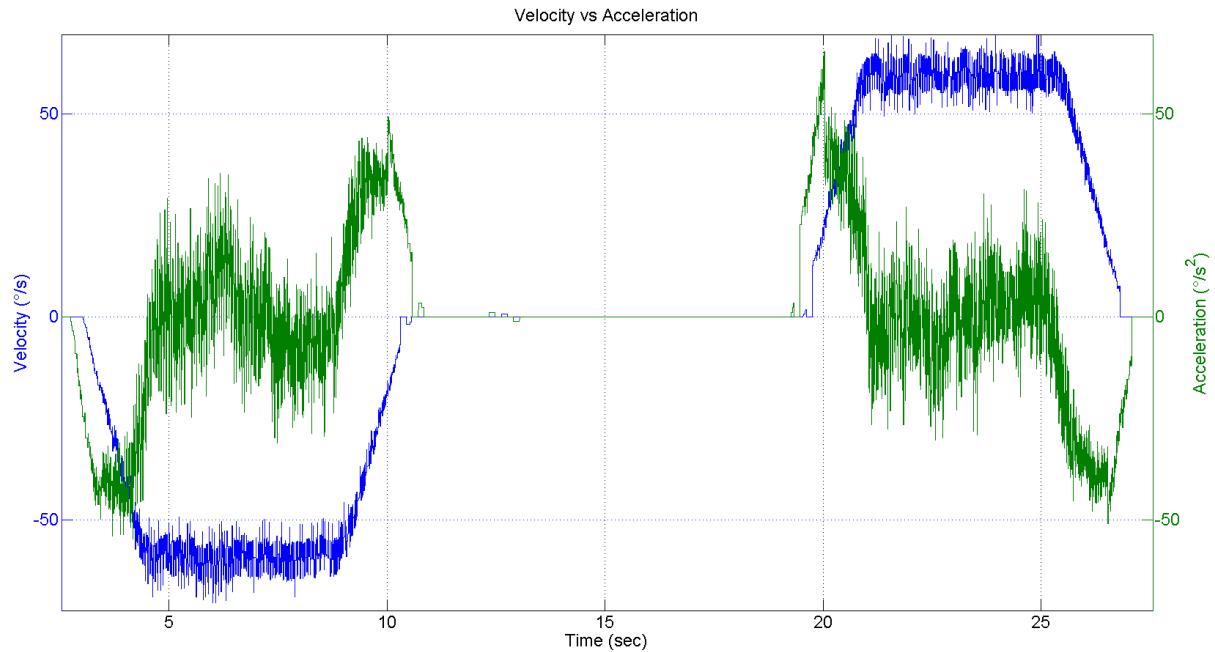
Figure 4. 2. 18: Velocity and acceleration

Figure 4.2.18 shows the acceleration and velocity of the mechanism for the full run. Even though it has been filtered through a large moving average filter, the acceleration data is too noisy to be used as a verification of the requirement, but it does show that the acceleration reaches $40°/s^2$.

4.2.2.5.7.1. Comments to speed and acceleration results

The test shows that the system can reach the desired speed and acceleration. The extreme acceleration seen, for instance, in figure 4.2.14 is due to a mistake in the software for the microcontroller emulating the spacecraft. This however, shows that the mechanism is capable of accelerating at a rate above the requirement.

Requirements REQ-2.4.4 and REQ-2.4.5 are verified.

4.2.2.6. Backlash test

A backlash test was added due to the measurements in 4.2.2.5.3. The backlash test is done by setting the mechanism in a zero-position, and commanding a series of positions as shown in figure 4.2.19.

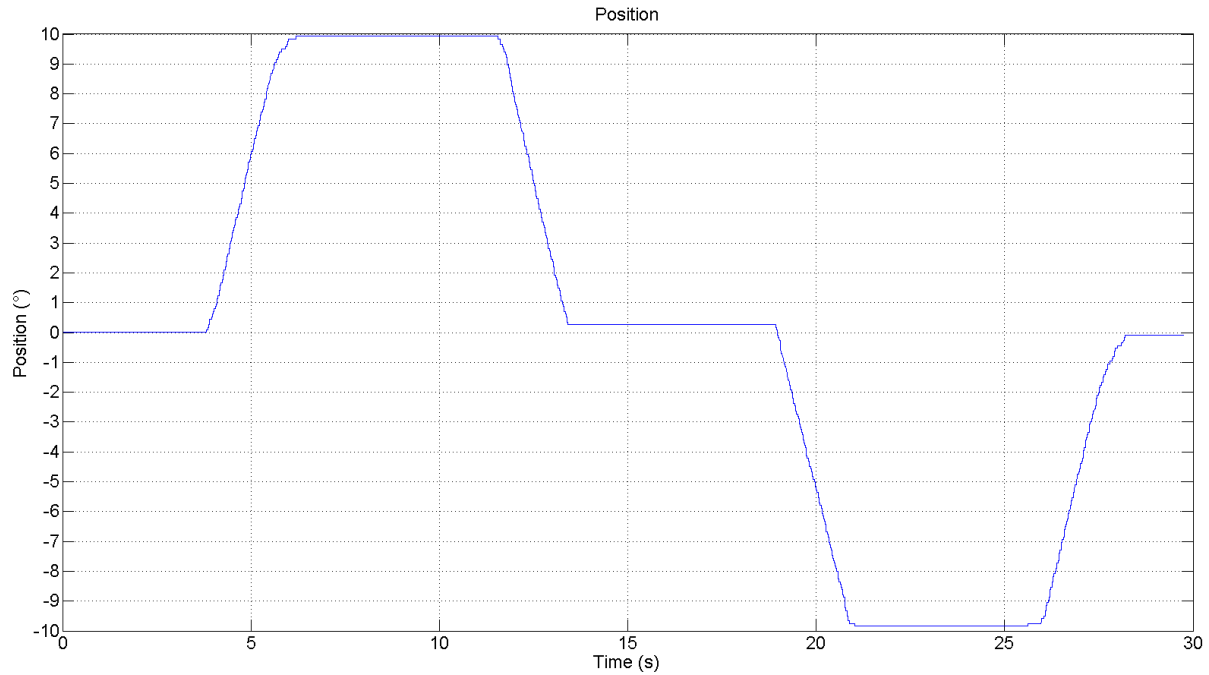The test was done with the setup described in 4.2.2.3.

Figure 4. 2. 19: Backlash run.

After doing this run, the backlash can be found by subtracting the final position from the third position. This test was done three times.

Table 4. 2. 13: Backlash test results

Start position	Position after first command	Position after second command	Position after third command	Position after fourth command	Backlash absolute value
0 °	4.834 °	0.1758 °	-4.834 °	-0.1758 °	0.3516 °
0 °	9.932 °	0.2637 °	-9.844 °	-0.08789 °	0.3516 °
0.5273 °	10.11 °	0.5273 °	-9.404 °	0.3516 °	0.1757 °

The backlash is found to be within 0.3516 ° ± 0.08789 °. The backlash is expected to drop to 0.139 ° once the gears are aligned [6].

4.2.3. Conclusion

The test shows that the mechanism and control system is functioning as predicted.

The power consumption and communication test was successful. All communications are operational, and the power consumption was less than one tenth of the requirement. Of course, the test was run without the added friction that would appear due to temperature variations in space. A margin factor of 10 is good. All power and communication requirements are verified.

The torque is lower in one direction due to a mismatch between the theoretical motor pole placement and the actual placement. The friction in the mechanism is lower than expected. The calculated friction force in the mechanism is 94.6 mNm [6] while the measured friction force is 23 mNm. The reason for this may be that the calculated friction is calculated at -20 °C, while the mechanism was tested at room temperature. In addition to this, the bearings are preloaded without measuring the actual forces. As

explained in 4.2.2.4.2.3, additional factors not included in the final design also reduce the torque. Accounting for all these factors, the minimum motor torque is considered to be verified.

The range was tested even though no end stop was installed. The range without an end stop was confirmed. However, the range needs to be verified with an end stop installed.

The position accuracy test failed. This is mainly due to the motor not being properly installed. This caused extra backlash. The control algorithm regulates to within 0.005 ° [6]. When the motor is installed in its casing, the backlash is expected to drop by 0.2126 °. This will allow the mechanism to pass the requirement.

All the speed and acceleration requirements were met. Errors in the position commands caused the acceleration to reach levels higher than the requirement at times.

4.2.3.1. *Requirements verified by functional tests*

Table 4.2.14 shows an overview of the requirements tested in this test. Not all of the requirements are explicitly mentioned in the test procedure, but have been verified through other tests.

Table 4. 2. 14: Requirement compliance matrix

Requirement [5]	Requirement text [5]	Test number [7]	Test Procedure paragraph [1]	Paragraph in this document	Compliance (C/NC)
REQ-2.1.1	The system shall have a power consumption of ≤ 15 W, including electronics and actuators.	TST-2.1.0	2.3.2.2	4.2.2.3.2	C
REQ-2.1.1.1	The motors shall have a maximum power consumption of 12 W.	TST-2.1.0	2.3.2.2	4.2.2.3.2	C
REQ-2.1.1.2	The control system shall have a maximum power consumption of 3 W.	TST-2.1.0	2.3.2.2	4.2.2.3.2	C
REQ-2.3.3	Motorization according to ECSS-E-ST-33-01C shall be satisfied.	TST-2.3.2	2.4.2	4.2.2.3.2 4.2.2.4.2	C
REQ-2.3.3.1	The motor for the azimuth stage shall produce a torque of minimum 0.114 Nm.	TST-2.3.2	2.4.2	4.2.2.4.2	C
REQ-2.4.1	The system shall have a pointing error of < 0.5 deg, half cone, 3 sigma.	TST-2.4.0	2.5.1.2	4.2.2.5.6.1	NC
REQ-2.4.3	The azimuth stage shall be able to move minimum ± 180 deg.	TST-2.4.0	2.5.1.1	4.2.2.5.2	C

REQ-2.4.4	The system shall be able to move with a velocity of ≥ 60 deg/s.	TST-2.4.1	2.5.1.3	4.2.2.5.7	C
REQ-2.4.5	The system shall be able to accelerate at a rate of ≥ 40 deg/s^2.	TST-2.4.1	2.5.1.3	4.2.2.5.7	C
REQ-2.5.1	The system shall receive absolute position commands from the spacecraft.	TST-2.5.0	2.3.2.1	4.2.2.3.2	C
REQ-2.5.2	The system shall send position updates to the spacecraft.	TST-2.5.0	2.3.2.1	4.2.2.3.2	C
REQ-2.5.5	The system shall be able to receive commands from the spacecraft at a frequency of 100 hertz.	TST-2.5.1	2.3.2.1	4.2.2.3.2	C
REQ-2.5.6	The system shall allow the spacecraft to adjust the antenna position at any given time.	TST-2.5.1	2.3.2.1	4.2.2.3.2	C
REQ-2.5.7	The system shall send feedback when it is moving.	TST-2.5.1	2.3.2.1	4.2.2.3.2	C
REQ-2.5.8	The system shall send feedback when it is not moving.	TST-2.5.1	2.3.2.1	4.2.2.3.2	C
REQ-2.7.3	The control system shall be able to control the velocity of the system	TST-2.7.1	2.5.1.3	4.2.2.5.7	C
REQ-2.7.4	The control system shall be able to control the acceleration of the system	TST-2.7.1	2.5.1.3	4.2.2.5.7	C
REQ-2.7.5	The control system shall be able to control the motor current.	TST-2.7.1	2.4 2.3.2.2	4.2.2.4.2.3	C
REQ-2.7.6	All pointing variables shall be set for each configuration call.	TST-2.7.2	-	4.2.2.3	C
REQ-2.7.7	The control system shall be able to calibrate the zero position.	TST-2.7.2	-	4.2.2.5.2	C
REQ-2.7.8	The system shall not move until a position	TST-2.7.2	-	4.2.2.3.2.1	C

	command is received.				
REQ-2.7.9	The control system shall be able to control the position of the system	TST-2.7.1	2.5.1.2	4.2.2.5.3	C
REQ-2.9.3	Electric motor windings shall be insulated from the structure by > 100 MΩ with a DC voltage of 500 V applied [4].	TST-2.9.0	2.2.3.2	4.2.2.2.2	C
REQ-2.9.5	They system shall tolerate a supply voltage of 28V	TST-2.9.1	2.3.2.1	4.2.2.3.2.1	C

4.2.4. References

[1] S. Laugerud and V. O. Aarud, "SSM-3002, Functional Test Procedure," Kongsberg, 2016.

[2] Kistler Instrument Corp, "Quartz Torque Dynamometer 9275," [Online]. Available: http://www.helmar.com.pl/helmar/plik/9275_nn3827.pdf. [Accessed 15 05 2016].

[3] Maxon Motor, "EC 45 fl at Ø42.8 mm, brushless, 70 Watt," April 2015. [Online]. Available: http://www.maxonmotor.com/medias/sys_master/root/8816806920222/15-263-EN.pdf.

[4] ECSS Secretariat, "Space engineering, Mechanisms," Noordwijk, 2009.

[5] G. H. Stenseth and M. Dybendal, "SSM-2000, Requirement Specification," Kongsberg, 2016.

[6] E. Løken, V. O. Aarud and M. Dybendal, "SSM-5901, Technical budgets," Kongsberg, 2016.

[7] V. O. Aarud and S. Laugerud, "SSM-3000, Test & Verification Specification," Kongsberg, 2016.

5. User manuals

5.1. Assembly user manual

i. Abstract

This chapter explains how to assemble the APM, step by step.

ii.　Contents

v.　Document history

Table 5. 1. 1: Document history

Rev.	Date	Author	Approved	Description
0.1	03.05.16	MD	EL	Document created
1.0	19.05.16	MD	TS	Reviewed and published

5.1.1. Introduction

The APM is assembled in three different main sub-assemblies, azimuth, elevation and parabola assembly. Throughout this chapter, a detailed description will guide you through the assembly, part by part. Figure 5.1.1 shows the APM as built.
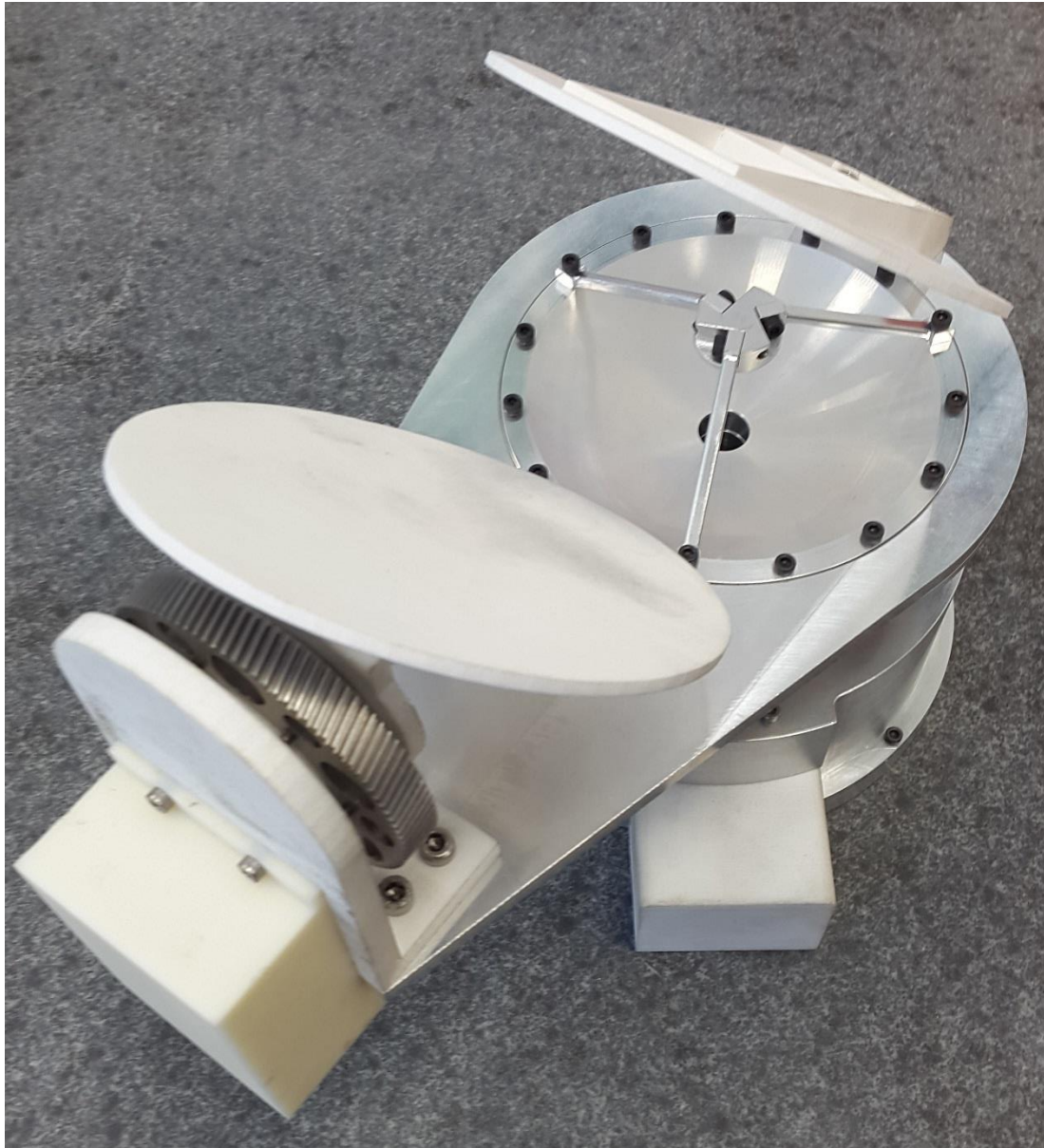
Figure 5. 1. 1: APM as built.

5.1.2. Assembly description

5.1.2.1. *Part list*

Table 5.1.2 gives an overview of the different parts of the APM, with the corresponding part numbers.

Table 5. 1. 2: Part list

Part name	Part number
Main contact plate	10 001
Waveguide	10 002
Motor	10 003
Motor housing azimuth	10 004
Cap azimuth	10 005
Bearing house azimuth	10 006
2 x W6005	10 007
Gear azimuth	10 008
Connector	10 009
KMT 5 NUT	10 010
Parabola holder	10 101
Azimuth fishplate	10 102
Parabola	10 103
Sub reflector	10 104
3 x Struts	10 105
Elevation bracket	10 201
Gear elevation	10 202
Motor	10 203
Connector elevation	10 204
Contact mirror connector	10 205
Mirror elevation	10 206
Motor house elevation	10 207
2 x W6000	10 208
Mirror over azimuth	10 301
Cable tray	10 302

5.1.2.2. Screw specification

Table 5. 1. 3: Screw specification

Kind	Material	Size (mm)		Length (mm)	PAX	Usage
		Diameter	Pitch			10 001 Main contact plate
Socket Head Cap	Stainless steel / steel (8.8)	M3	0.5	8	5	10 002 Waveguide
Socket Head Cap	Stainless steel / steel (8.8)	M3	0.5	35	2	10 003 Motor azimuth
						10 004 Motor housing azimuth
Socket Head Cap	Stainless steel / steel (8.8)	M3	0.5	10	7	10005 Cap azimuth
						10006 Bearing house azimuth
Socket Head Cap	Stainless steel / steel (8.8)	M3	0.5	8	6	10008 Gear azimuth
Socket countersunk head cap	Stainless steel / steel (8.8)	M4	0.7	25	6	10009 Connector
SKF KMT NUT	Stainless steel / steel (8.8)	M25	1.5	N/A	1	10010 KMT 5 NUT/ preload
Socket Head Cap	Stainless steel / steel (8.8)	M6	1	12	8	10101 Parabola holder
						10102 Azimuth fishplate
Socket Head Cap	Stainless steel / steel (8.8)	M3	0.5	6	12	10103 Parabola
Socket Head Cap	Stainless steel / steel (8.8)	M3	0.5	10	3	10104 Sub reflector
Socket Head Cap	Stainless steel / steel (8.8)	M3	0.5	10	3	10105 3 x struts
Socket Head Cap	Stainless steel / steel (8.8)	M5	0.8	12	4	10 201 Elevation bracket
						10 202 Gear elevation
Socket Head Cap	Stainless steel / steel (8.8)	M3	0.5	10	3	10 203 Motor elevation
						10 204 Bearing house elevation
Socket Head Cap	Stainless steel / steel (8.8)	M3	0.5	8	5	10 205 Contact mirror connector
Socket Head Cap	Stainless steel / steel (8.8)	M3	0.5	12	5	10 206 Mirror elevation
Socket Head Cap	Stainless steel / steel (8.8)	M3	0.5	8	6	10 207 Motor house elevation
Socket Head Cap	Stainless steel / steel (8.8)	M5	0.8	12	2	10 301 Mirror over azimuth

Socket Head Cap	Stainless steel / steel (8.8)	M6	1	16	2	10 302 Cable tray
Socket countersunk head cap	Stainless steel / steel (8.8)	M8	1	30	6	10 303 Mounting plate

5.1.2.3. *Azimuth assembly*

1. Put the lower bearing inside the bearing house, and put the cylindrical flange upon the first bearing. Then, put the second bearing inside the bearing house. Make sure the bearings are in contact with all contact surfaces.

2. Preheat the bearings and the bearing house to a temperature above 50° Celsius, and cool down the main contact plate to 10° Celsius.

3. When the parts reach the given temperature, press fit the bearings and the bearing house on the rod in the middle of the main contact plate.

4. Take the KMT 5 NUT and screw it on the rod on the main contact plate as shown in figure 5.1.2. Use a torque wrench and tighten the bolt with 27.4 Nm.[1]

Figure 5. 1. 2: KMT 5 NUT and bearing house.

5. Fasten the gear on the bearing house with 6 x M3x0.5x8 socket head cap screws. Make sure that the two cuts on the inner bore ring are placed in the same position as the cuts on the bearing house as shown in figure 5.1.3.

Figure 5. 1. 3: Gear mounted on bearing house.
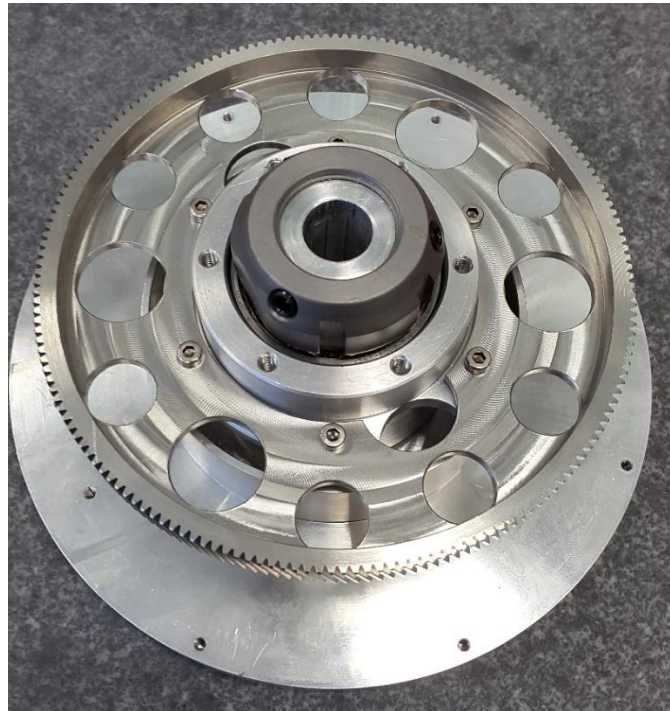
6. Put the connector above the bearing house and use 6x M4x0.7x25 socket countersunk head screws, as shown in figure 5.1.4. As in point number 3, make sure that the two holes are placed in the same position as the cuts on the bearing house.
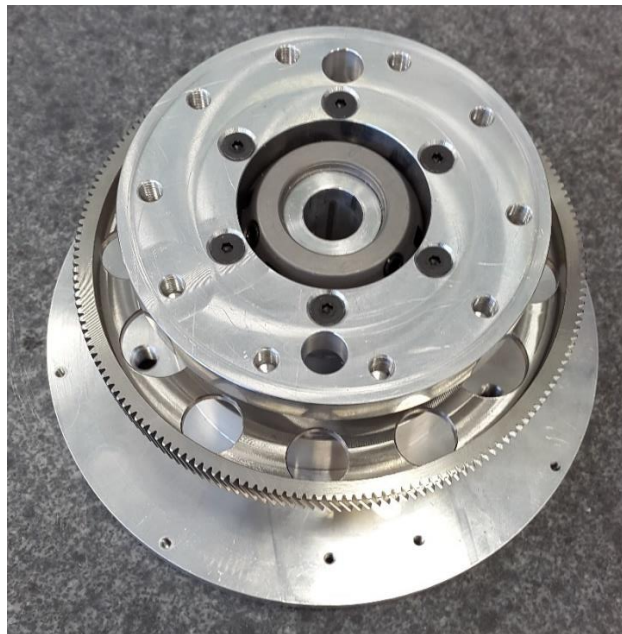

Figure 5. 1. 4: Connector mounted on bearing house.

7. Motor assembly
   a) Insert the gear with 4 mm bore size on the motor shaft.

b) Put the motor inside the motor house, with the encoder inside the housing so that the gear sticks up in front as shown in figure 5.1.5. Make sure that the gear on the shaft and the gear on the bearing house fits together.

Figure 5. 1. 5: Motor assembly azimuth.

c) Place the longest side of the housing in the trail beneath the main contact plate, and use 2x M3x0.5x8 mm socket countersunk head screws to fasten the motor house.

8. Take the dust cap and place it so the cut fits with the motor house.

9. Then use 2x M3x0.5x35 mm socket head cap screws to fasten the top side of the motor.

10. Fasten the dust cap with 7x M3x0.5x10 mm socket head cap screws as shown in figure 5.1.6.

Figure 5. 1. 6: Azimuth assembly

11. Finally, take the waveguide and insert it inside the rod on the main contact plate. Make sure it fits with the trail beneath it, and then fasten it with 6x M3x0.5x6 mm socket countersunk head screws.

5.1.2.4. *Parabola assembly*

1. Place the azimuth fishplate above the parabola holder. Make sure that the front side of the fishplate is placed where there are three holes between the two ribs. Fasten it with 13 x M3x0.5x8 socket head cap screws. Skip the two holes on the back of the fishplate as shown in figure 5.1.7.
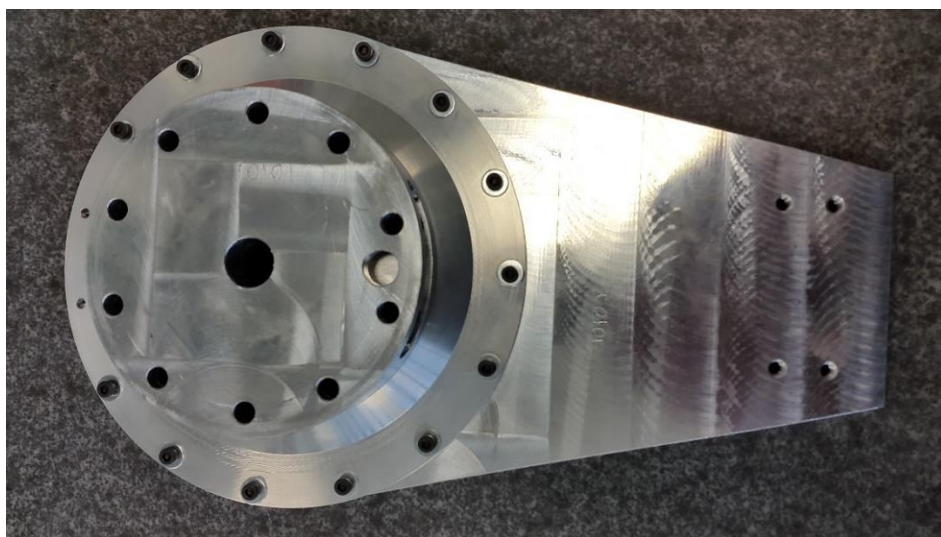

Figure 5. 1. 7: Parabola holder on the azimuth fishplate.

2. Parabola, sub reflector and struts
    a) Take the sub reflector and the three struts. Fasten the struts in the trails so the fillet of the struts and the fillet on the sub reflector fits together as shown in figure 5.1.8. Use 3x M3x0.5x10.

Figure 5. 1. 8: Sub-reflector and struts.

3. Mount the parabola holder and the fishplate above the azimuth assembly as shown in figure 5.1.9. Place the hole between the ribs in the same position as the cuts on the bearing house. Take the cable tray and place it in the same position as the hole between the ribs as shown in figure 5.1.10. Use 2x M5x1x16 mm socket head cap screws to fasten it, then use 8x M6x1x12 socket head cap screws to fasten the rest of the parabola holder.

Figure 5. 1. 9: Parabola holder and fishplate mounted on the azimuth stage.
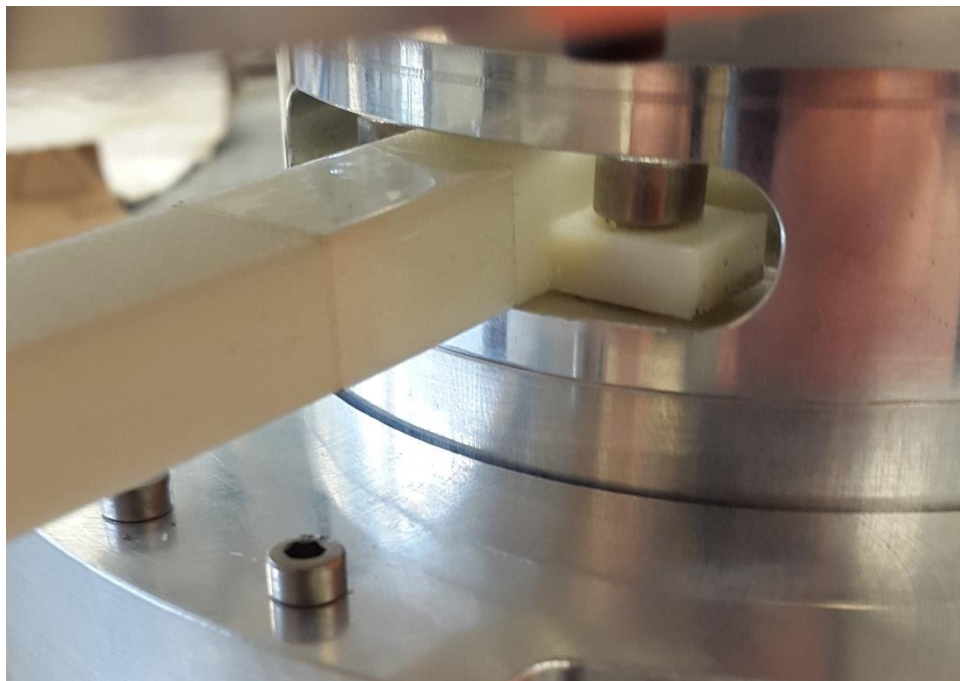
Figure 5. 1. 10: Cable tray mounted in the parabola holder.

4. Finally, take the parabola, sub reflector and the struts and fasten it inside the parabola holder. Use 3x M3x0.5x10 to fasten the struts, and 12x M3x0.5x6 to fasten the parabola as shown in figure 5.1.11.

Figure 5. 1. 11: Sub-reflector and struts mounted on the parabola.

5.1.2.5. *Mirror over azimuth*

1. Place the mirror over azimuth on the two holes in the back of the fishplate. Make sure that the mirror is placed over the parabola. Use 2x M5x0.8x10 socket head cap screws to fasten it as shown in figure 5.1.12.
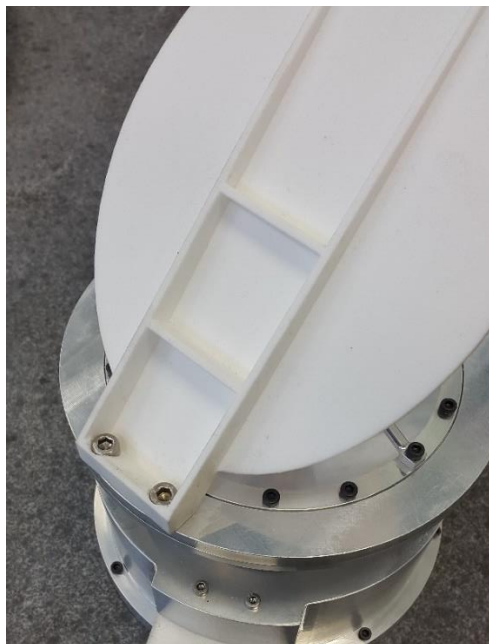
Figure 5. 1. 12: Mirror over azimuth.

5.1.2.6. *Elevation assembly*

1. Place the gear on the bearing house as shown in figure 5.1.13. Use 6x M3x0.5x10 socket head cap screws as shown.

Figure 5. 1. 13: Bearing on the rod.

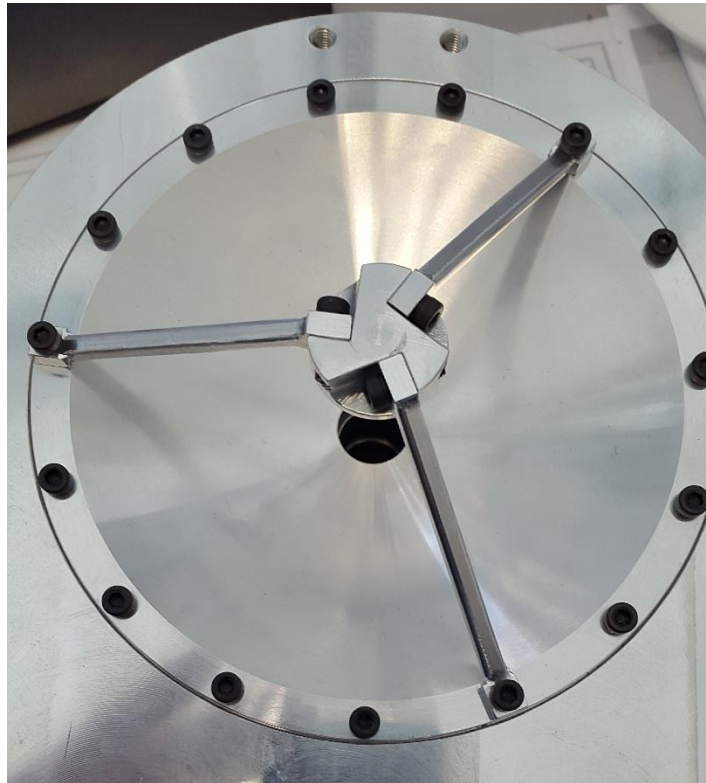2. For the bearings and the bearing house (with the gear), follow the same procedure as the three first steps in the azimuth assembly. The difference is that the elevation bracket should be cooled down. Mount the bearings and housing on the rod as shown in figure 5.1.14.

Figure 5. 1. 14: Gear on the elevation bearing house.

3. Place the contact mirror connector to the bearing house. Use 5x M3x0.5x12 socket head cap screws to fasten it. Then take a M5x0.8x12 socket head cap screw, place it inside the rod, and

preload the bearing with a torque wrench with a force equals to 564N.

4. Insert mirror elevation so it fits the trail on the contact mirror connector. Make sure it is connected at all surfaces. Fasten it with Loctite.

5. Elevation motor house and motor
   a) Place the 4mm bore size gear on the motor shaft.
   b) Put the motor inside the housing.

6. Mount the elevation bracket to the fishplate, the holes are located in the front of the plate as shown in figure 5.1.15. Make sure that the elevation mirror is placed parallel to the mirror over azimuth. Use 4x M5x0.8x12 mm socket head cap screws to fasten the elevation bracket.
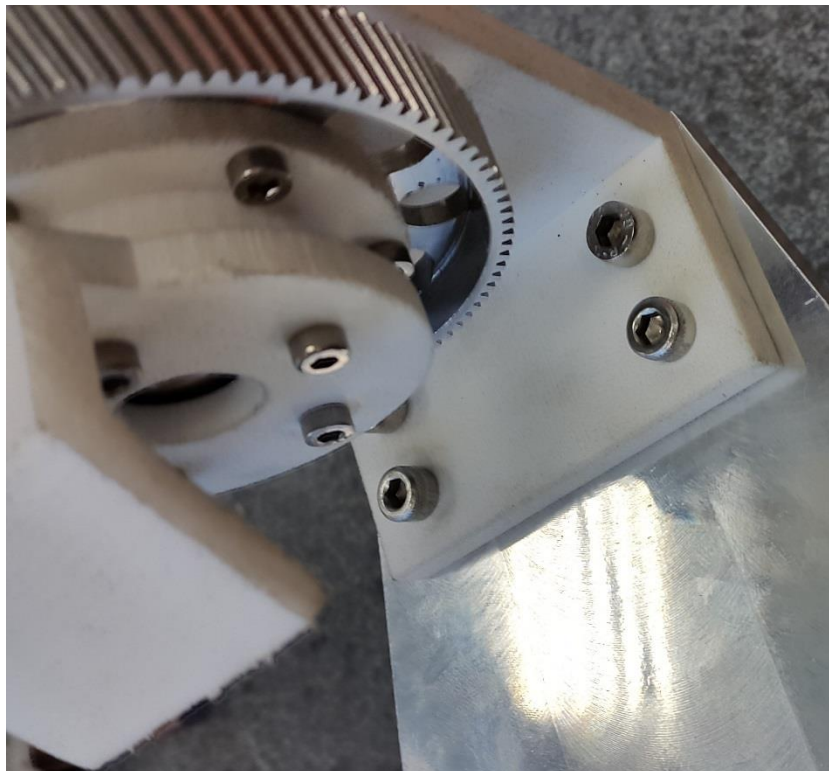
Figure 5. 1. 15: Elevation stage on the fishplate.

7. Place the motor and the housing as shown in figure 5.1.16 on the bracket. Fasten the motor with 3x M3x0.5x10 mm socket head cap screws.

Figure 5. 1. 16: Motor house on the elevation bracket.

8. Fasten the motor house in the holes located beneath the fishplate with 2x M3x0.5x8 mm socket head cap screws, and with 2x M3x0.5x10 socket head cap screws to the holes located on the elevation bracket.

9. Finally, fasten the cable tray beneath the motor house with 2x M3x0.5x8 socket head cap screws.

5.1.3. Conclusion

Figure 5.1.17 shows the APM as built. When following the steps explained in this user manual, the result shall equals this.
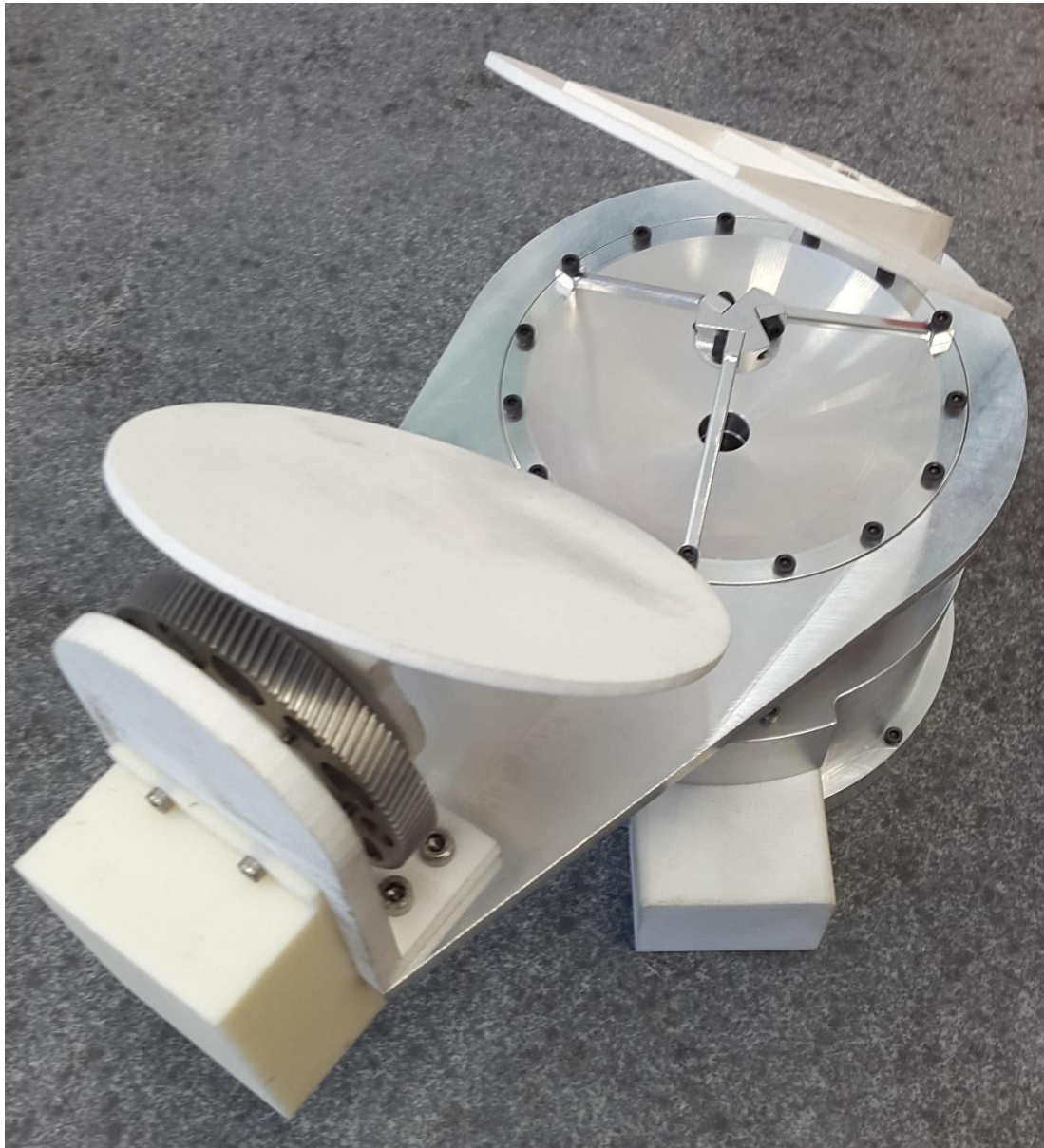
Figure 5. 1. 17: The APM as built by using the steps in the user manual.

5.1.4. References

[1]　V. O. Aarud, "Technical report bearing", SSM-5423,USN,　Kongsberg, rev. 0.3, 10.05.16

5.1.5. Appendices

Table 5. 1. 4: Azimuth assembly
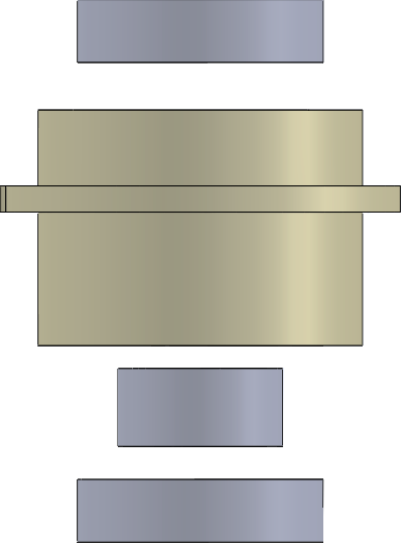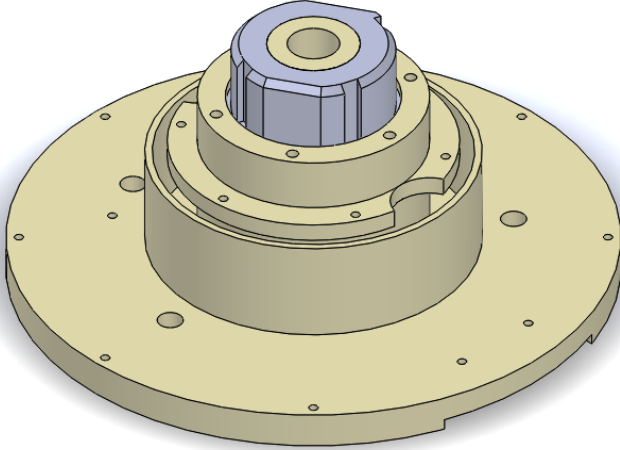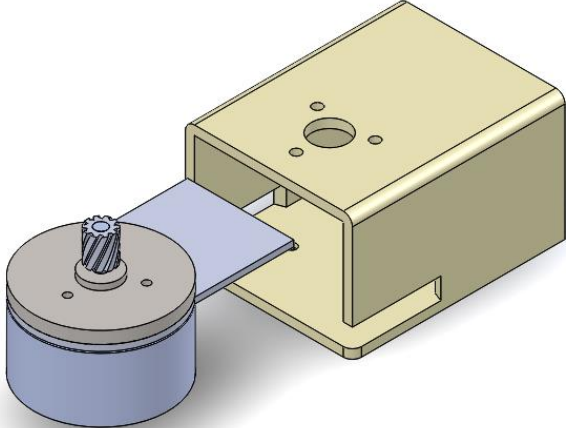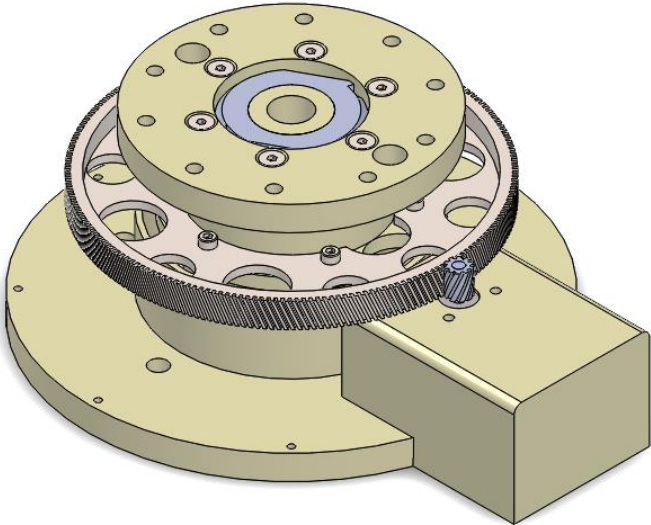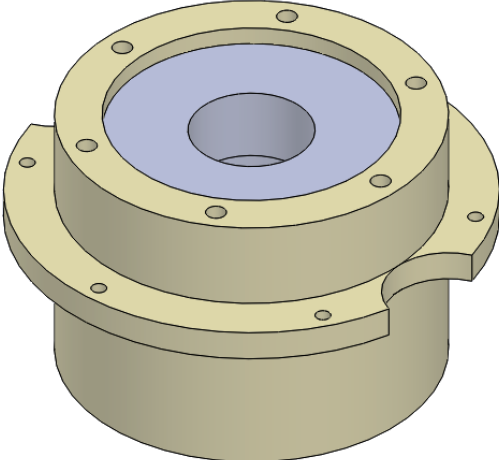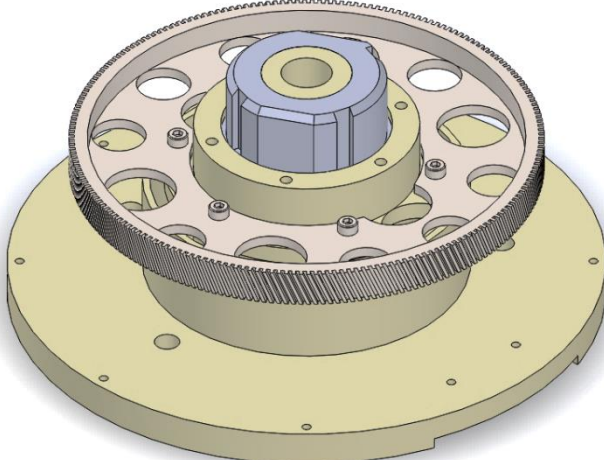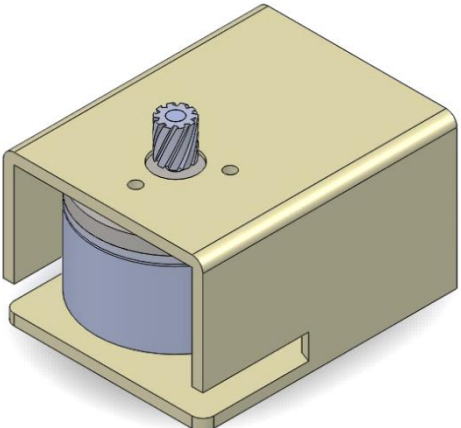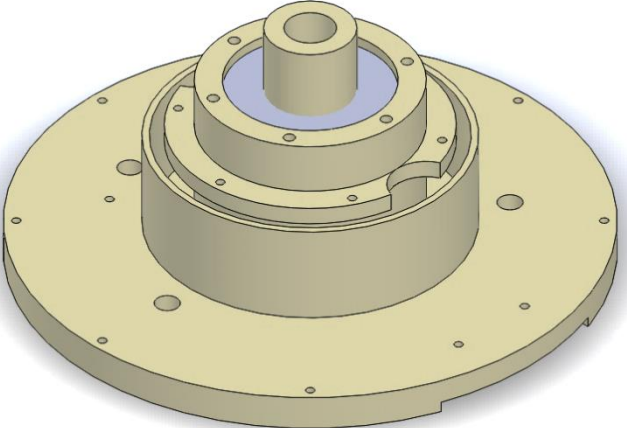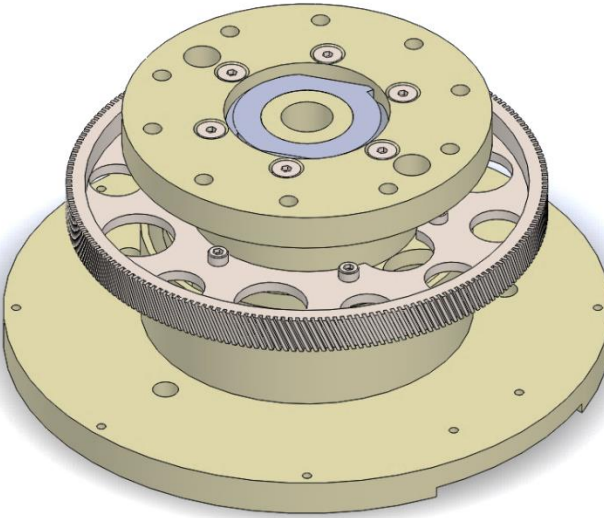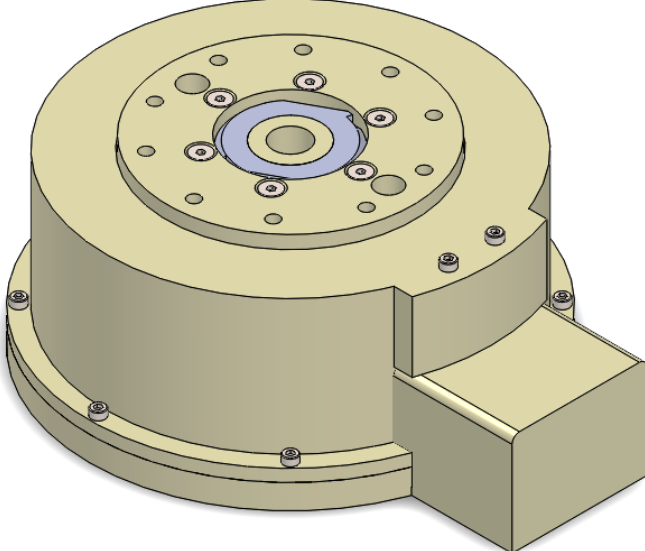
1.	4.	7.a	9.
2.	5.	7.b	
3.	6.	Final	

Table 5. 1. 5: Parabola assembly
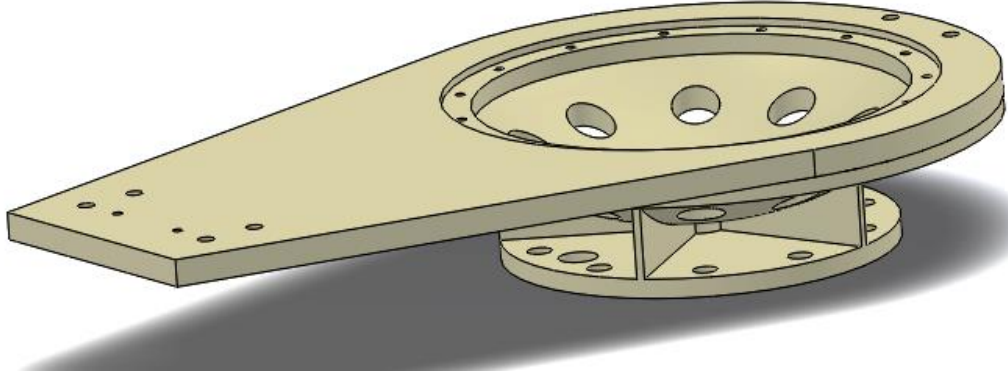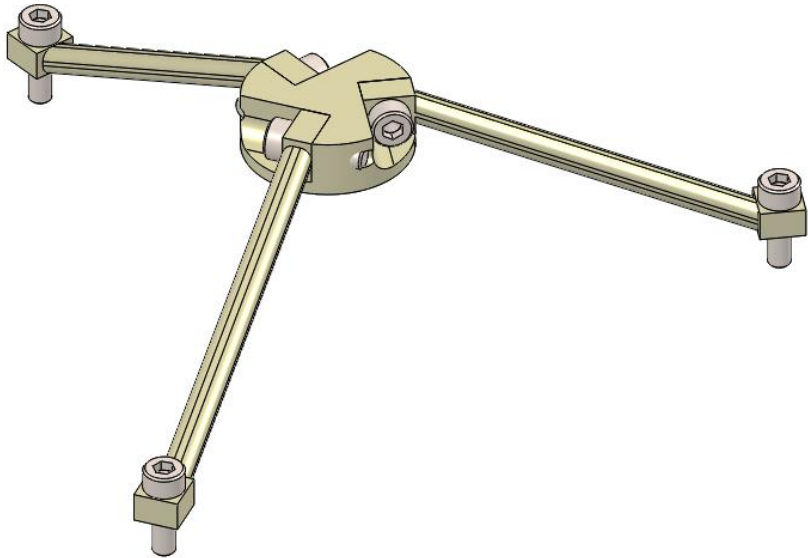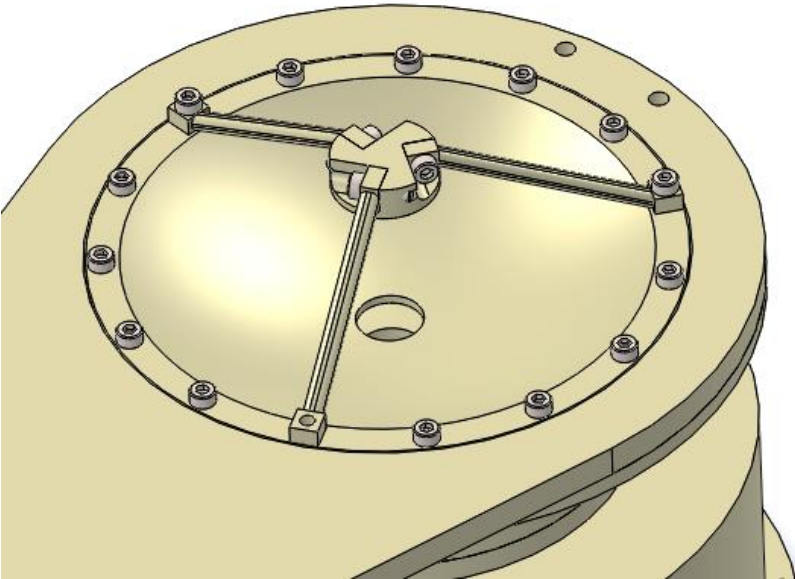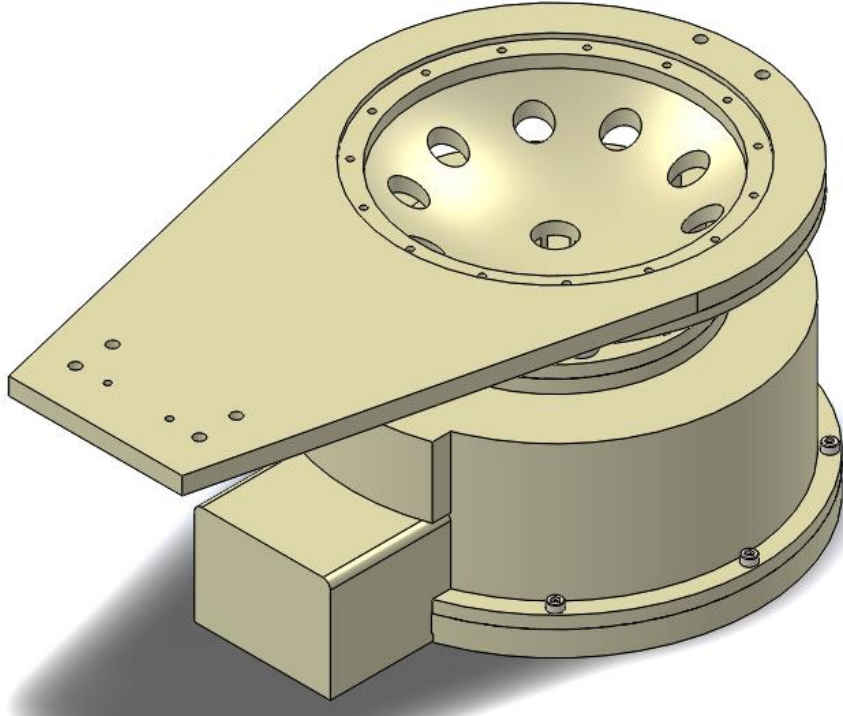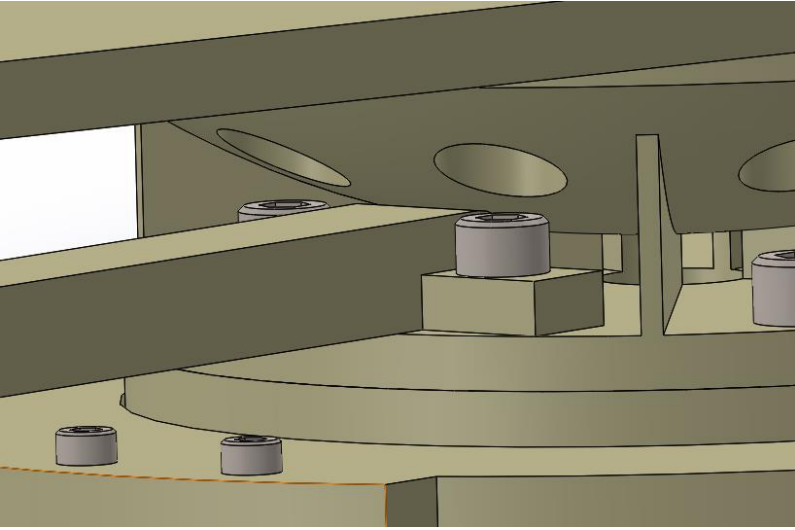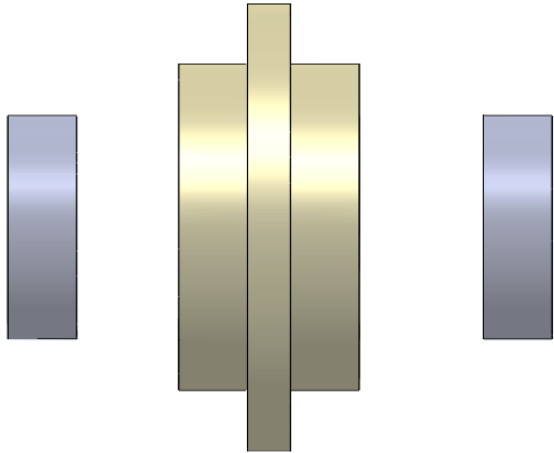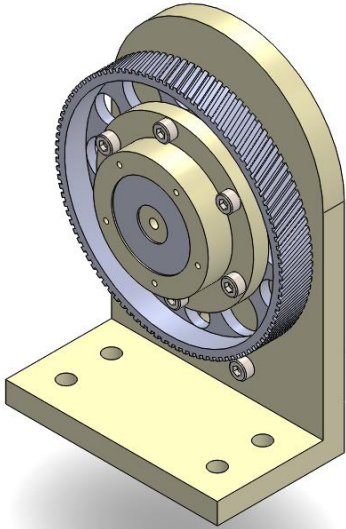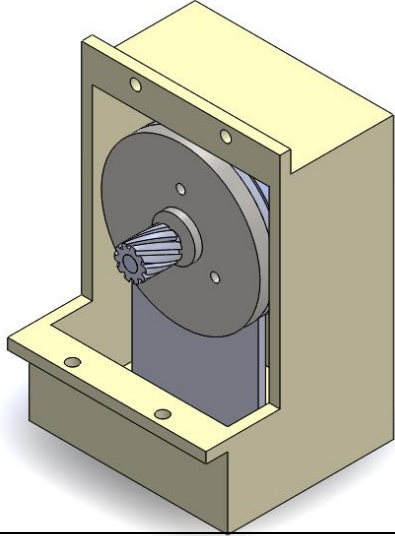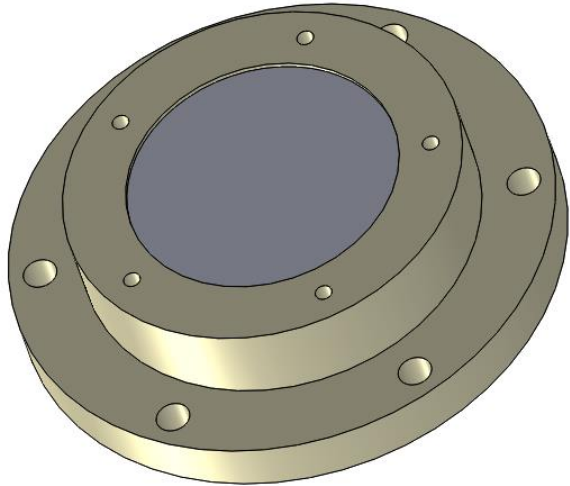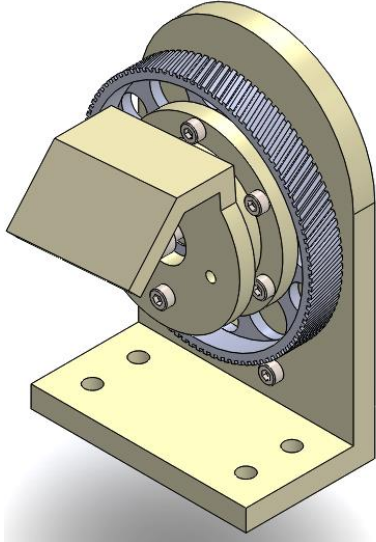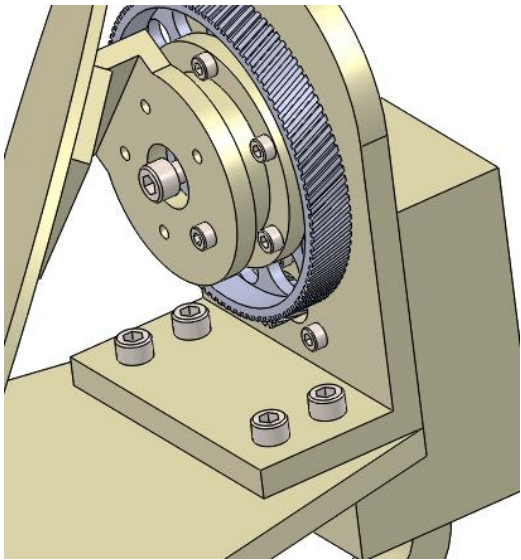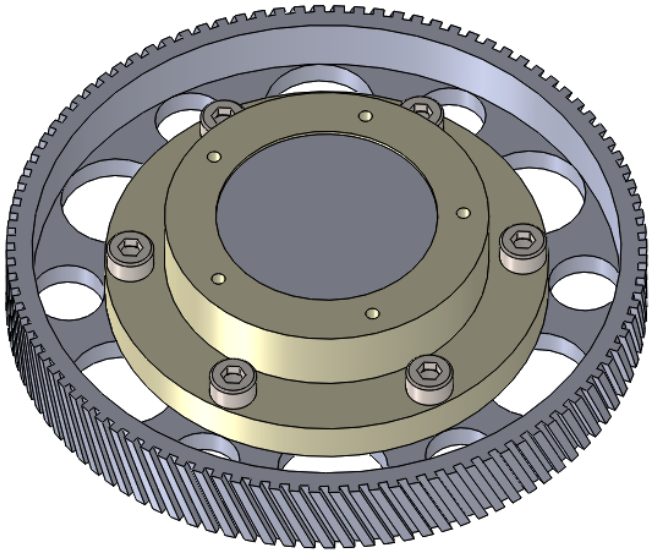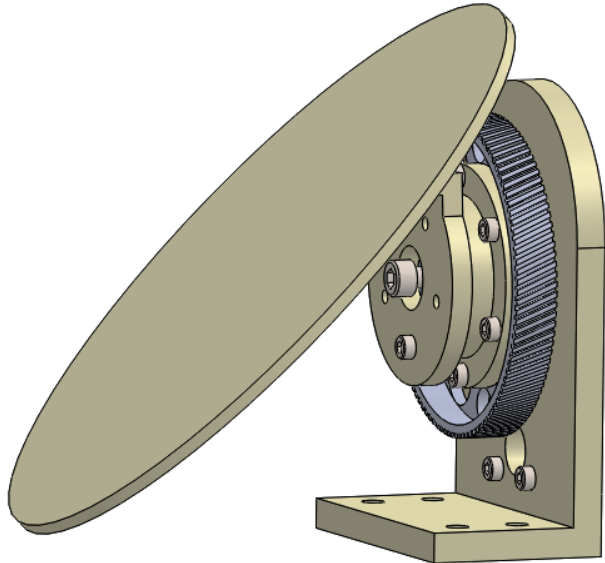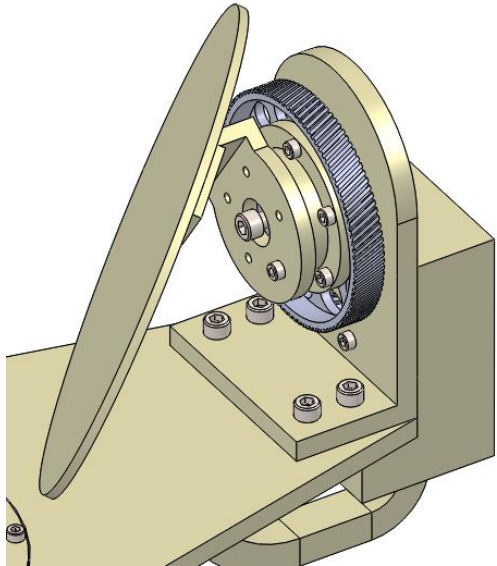
1.	2.a	Final
3.	3.a	

Table 5. 1. 6: Elevation assembly

5.2. Control system user manual

i. Abstract

This chapter serves as a manual for using the control system of the APMA and sending commands from a commanding microcontroller emulating the spacecraft.

ii. Contents

iii. List of figures

iv. List of tables

v. Document history

Table 5. 2. 1: Document history

Rev.	Date	Author	Approved	Description
0.1	13.05.16	TS, GHS		Document created
1.0	16.05.16	TS, GHS	EL	Reviewed and published

5.2.1. Introduction

The system should be connected as shown in [1]. The user can choose between the breadboard model and the final version for the different parts of the system. These parts are interchangeable. E.g. a breadboard model current sensing circuit can be used with the final controller design.

5.2.1.1. *UART setup:*

5.2.1.1.1. Protocol setup:

- Baud rate: 64 kbps
- 1 start bit
- 8 bytes of data
- 1 stop bit
- No parity

Neither the start bit nor the stop bit is inverted.
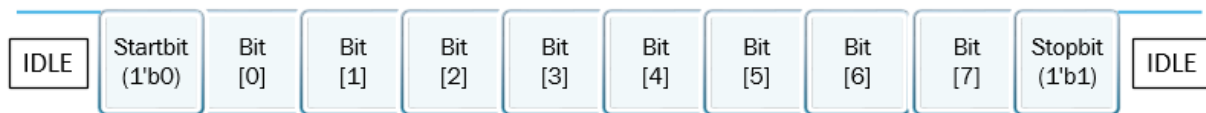
Figure 5. 2. 1: UART protocol setup

5.2.1.1.2. Connections on the microcontroller:

- UART RX pin: PA1. Connect to TX pin on commanding microcontroller
- UART TX pin: PA0. Connect to RX pin on commanding microcontroller.

5.2.1.1.3. Data pack setup

The data pack to be sent via UART is composed of 8 bytes.
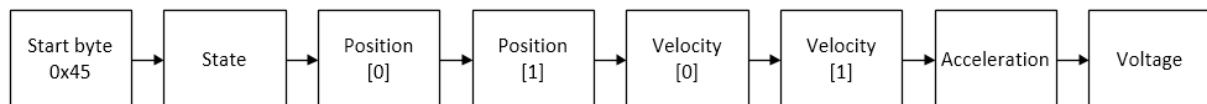
Figure 5. 2. 2: Data pack

The first byte is a start byte with the hex value 0x45. The state, acceleration and voltage bytes are values between 0x0 and 0xFF. To allow for decimal values, the velocity and position variables are sent as double bytes. See [2] for information on how to do this.

5.2.2. Calibration

Before the mechanism can receive position commands, it needs calibrating. The calibration command consists of:

- Start byte (0x45).
- Digit specifying the calibration mode (0x1).

The next 6 bytes should be set to zero.

When the APMA is powered up, it will wait for a calibration command before it will accept movement commands. When a calibration signal is received, the mechanism immediately commands the motor to a specific position, aligning the encoder's zero-position with the motor. 0.5 seconds later, the mechanism will rotate clockwise until stopped. When the mechanism stops, the control system will assume the current position to be -180 degrees. The mechanism is now ready for position commands.

5.2.3. Manual position commands

The manual position mode lets the commanding microcontroller (CM) send position commands, which the control system outputs to the mechanism as soon as they are received. This means the speed and acceleration is set by how often the CM sends the commands. Thus, sending velocity and acceleration is not needed. The commands can be sent up to 800 times per second.

- Start byte (0x45).
- Digit specifying the manual position mode (0x2).
- Position: Two bytes containing a 16 bit integer (-18000 to + 18000). This allows for two decimal places.
- Velocity and acceleration bytes are set to 0.
- Voltage: one byte containing maximum voltage for the space vector modulation (0 to 28).

5.2.4. Automatic S-curve positioning

The automatic S-curve request is sent once, and the APMA calculates the pointing values based on the position, velocity, acceleration and voltage input. The S-curve positioning command consists of:

- Start byte (0x45).
- Digit specifying the S-curve mode (0x3).
- Position: Two bytes containing a 16 bit integer (-1800 to +1800).
- Velocity: Two bytes containing a 16 bit integer (0 to +32767). Multiply desired velocity by 100.
- Acceleration: one byte containing an 8 bit integer (0 to +127).
- Voltage: one byte containing maximum voltage for the space vector modulation (0 to 28).

5.2.5. References

[1] Gisle Hovland Stenseth and Stian Laugerud, "SSM-5415, Electrical Design Document," KIFI, University College of Southeast Norway, Kongsberg, 2016.

[2] Elise Løken and Torstein Sundnes, "SSM-5131 Control System Design Rev. 2.0," KIFI, University College of South East Norway, Kongsberg, Technical Report 2016.

6. Post Analysis

i. Abstract

This chapter contains the post analysis of the SSM project. This includes administrative, technical, risk, further work and individual evaluations from each group member.

ii. Contents

iii. List of figures

iv. List of tables

v. Document history

Table 6. 1: Document history

Rev.	Date	Author	Approved	Description
0.1	18.05.2016	SSM		Document created
1.0	19.05.2016	SSM	TS	Reviewed and published

6.1. Introduction

The assignment given by Kongsberg Space was to design an APMA for radio communication between small satellites.

The goals for the project were to conceptually develop a low-cost APMA and prototype some parts of the mechanism and make it rotate. The result of the project is a new concept for the APMA, a double mirror reflector antenna without rotary joints. A real-life prototype of the whole mechanism is assembled in aluminium, and some of the parts are 3D-printed in plastic.

The azimuth stage of the mechanism was prioritized, and the control system is implemented in this stage. The control system rotates the mechanism along the horizontal axis and sends it to the commanded positions. This confirms that the goals for the SSM project were reached.

6.2. Administrative conclusion

6.2.1. Planning

The "Iterative development model" is the project model used in the SSM project. It has turned out to be a significant part of the planning process, and it has during the whole project ensured that the project was on schedule according to the plan. The project was divided into seven iterations. At the end of each iteration, an iteration report was written. The status and the progressivity of the project were discussed, and the next iteration was planned in detail. These situation reports were definitely helpful, and in addition to a hard working project group, resulted in the reaching of the project's goals.

In this project, a long-term project plan was used. This plan specified the time duration of the iterations and important deadlines throughout the whole project period. In addition to the long-term plan, the iterations were planned in detail, and the planned activities were divided between the group members.

The weekly follow-up documents have also been written throughout the project. These were even more detailed than the iteration plans, and ensured that all the activities planned in an iteration would be completed.

6.2.2. Meetings

The group has had weekly meetings with the internal supervisor. These meetings have generally consisted of feedback regarding the projects progress and documentation.

The group has had regular meetings with the external supervisor. These meetings have mainly consisted of discussions regarding technical solutions and some administrative issues. Without these meetings, and the technical discussions with Kongsberg Space, the accomplishments in this project would not have been possible.

6.3. Technical conclusion

6.3.1. Requirements

Of the 57 requirements set for this project, 30 are verified, 25 are not evaluated or only partly verified, and 2 requirements are not met [1].
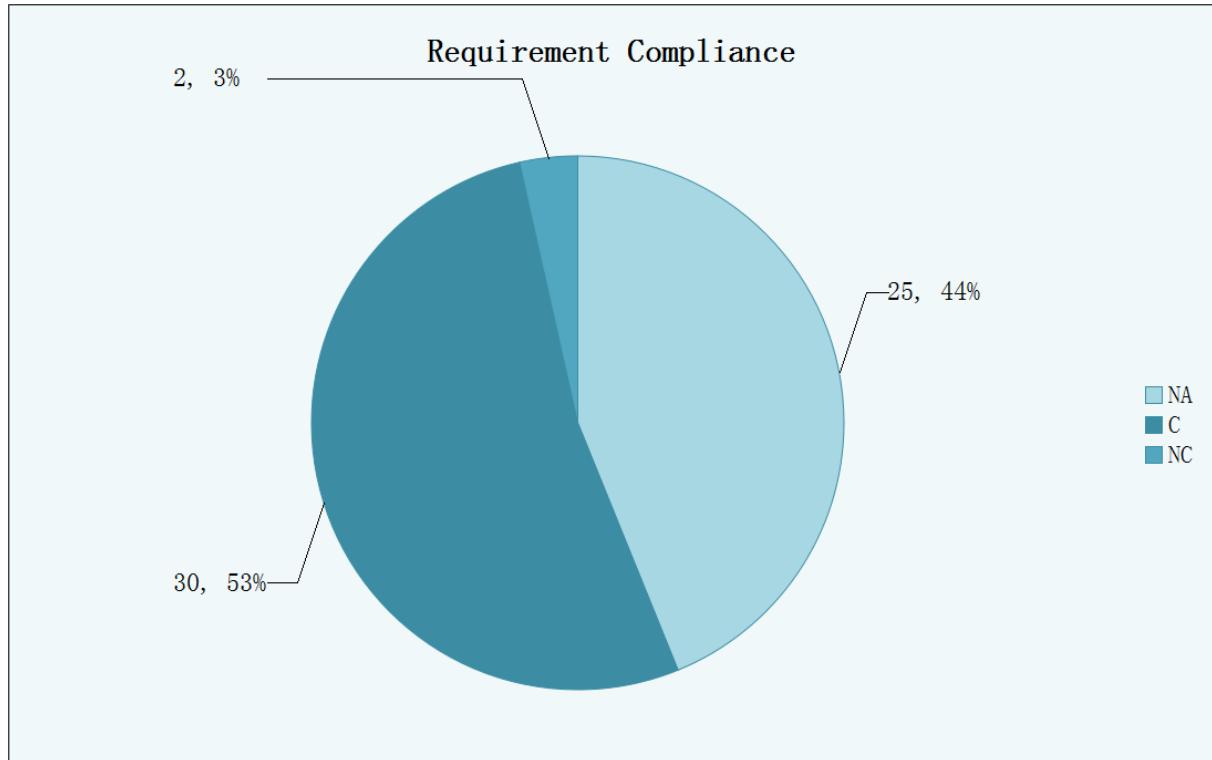
Figure 6. 1: Requirement compliance chart

Of the 25 requirements marked "NA", 10 are verified through review of design, but have not been tested. The main reason for the large amount of "NA" requirements is that the RF, thermal vacuum and vibration tests could not be performed.

The two requirements not met in this project are mass and pointing accuracy. The system failed the pointing accuracy test due to the motor being mounted in a slightly wrong position due to missing parts, causing increased backlash [2]. The backlash should be greatly reduced when the motor is mounted properly. The mass requirement was deprioritized in order to design a functional early prototype so that the system could be put through functional testing. Gears and bearings have been overdimensioned. Choosing lighter components in further designs will reduce the mass.

6.3.2. Tests

Of the 30 tests specified in the [45], 10 were performed, 8 partly performed and 12 were not performed.
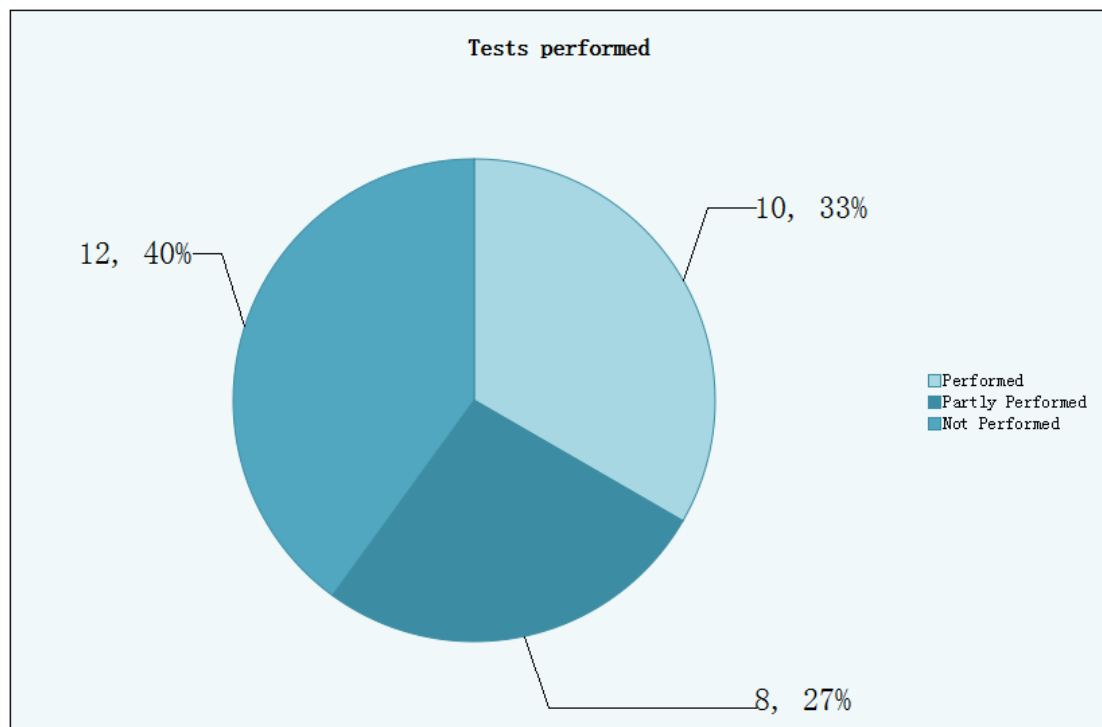
Figure 6. 2: Tests performed

Of the tests actually performed, only the pointing accuracy failed. The reason for the high number of unperformed tests is the same as explained in 6.3.1, time limitations. Some of the tests were made for the complete system, and could not be completely performed with the early prototype. An example of this could be the position accuracy test, which was only performed on the azimuth stage.

6.3.3. Mechanical

Using commercial parts in space is seen as controversial, and is not a main focus area of the large space agencies. Based on the materials study and the selected materials, the selected materials are not new to the space industry; however, bearings are selected from commercial suppliers. This was a main goal for the mechanical part of the project, and the bearing report shows that it is possible to use commercial bearings with small changes such as lubrication and preload.

The mass of the APM exceeds the requirement due to bearing setup and the size of the gears. The gears and bearings were overdimensioned because of the ECSS standard. A strength versus-mass analysis was not done, which may have led to the skeleton being oversized.

As a part conclusion, the commercial dynamical parts selected for this APM are seen as suited for space usage.

The system is only seen as plausible due to one of the main factors, thermal, being excluded. Adding this factor can result in major geometrical changes in the structure and change the dynamics of the bearings. However, this is an interesting point and there are no signs at this point showing that it would not work.

6.3.4. Electrical

The electrical system in this project is designed as simple as possible. Keeping the design simple gives the advantage that errors are less likely to appear, and can be fixed more easily. It also helps by keeping the costs down.

The electrical components were selected based on their operating temperature and performance. Most of the components chosen are automotive/industrial grade. This is because military grade components are too expensive for this project, and automotive grade components are well within the required operating temperature. A microcontroller was chosen over an FPGA due to the simplicity of programming microcontrollers compared to FPGAs. In retrospect, a SoC containing both an FPGA and a microcontroller would have made the sampling of signals, and the PWM generation easier.

The most notable challenges for the electrical system have been the availability of parts and the delivery times. This has been overcome by creating makeshift designs based on available parts [4]. These designs have been more complex than the final design, but they have had the right functionality. The elevation and azimuth electronics are the same, but only one system has been made at this time. The chosen components have shown good functionality and efficiency. Only the designs for the breadboard model have been made.

6.3.5. Software

The control system software is designed in relevance to the electrical components and simulations. The overall programming is performed in a straightforward way, keeping the Simulink block structure. This has ensured increased efficiency when applying changes from the Simulink model to the software.

Using an encoder for position reading is effective and provides a high pointing accuracy as long as the system is powered on, but does require a calibration to be performed on each start-up of the system. The microcontroller used is effective and performs the necessary calculations with desired speed, although certain aspects of the system would perform better with the use of an FPGA, with the FPGA's parallel processing and the CPU's effective calculations.

The limited amount of components and the need to wait for the electrical simulations have been the most challenging part of the implementation. As with the electrical system, there have been makeshift designs to compensate for certain setbacks, and the implementation of the elevation stage has been delayed until the electrical components are available.

6.3.6. Radio communication system

For the antenna, a Cassegrain design was chosen. The antenna feed is a simple cut-off waveguide. The calculations show that the antenna design is feasible. At the start of the project, a link analysis was performed to see if the project was feasible considering the antenna gain and distances between satellites. The transfer rate was found to be approximately 13 Mbps, quite acceptable for small satellites.

Unfortunately, the test equipment for the antenna system could not be made, and the antenna hasn't been tested.

6.3.7. Risk reduction

In the start-up phase of the project the most notable risks associated with the project were defined, [5]. The risks were divided into different categories and levels. Three mitigations for reducing the risks are carried out during the project, and the group members were responsible for the different mitigations. Through the mitigations, the total risk is significantly reduced. Table 6.2 shows the risk evaluation before mitigation 1 and after mitigation 3.

Table 6. 2: Total risk reduction after third mitigation

#	Risk	Before mitigation			After mitigation 3		
		Likelihood	Impact	Total Risk	Likelihood	Impact	Total Risk
1	Space Environment	3,5	4,1	**14,4**	3	2,8	**8,4**
2	Operational Risks	2,7	4,5	**12,0**	1,6	3,8	**6,1**
3	Cost risks	2,8	3,0	**8,4**	1,2	2,3	2,8
4	Schedule risks	2,8	4,0	**11,0**	1,2	4	**4,8**
5	Safety Risks	1,3	3,8	**5,1**	1,3	3,7	**4,8**
6	Development risk	3,4	3,1	**10,3**	1,7	2,9	**4,9**
7	Human resources risk	2,0	3,2	6,4	1,7	2,2	3,7

Figure 6.3 shows graphically how the main risks were reduced after the different mitigations, and give a view of the total reduction during the whole project.
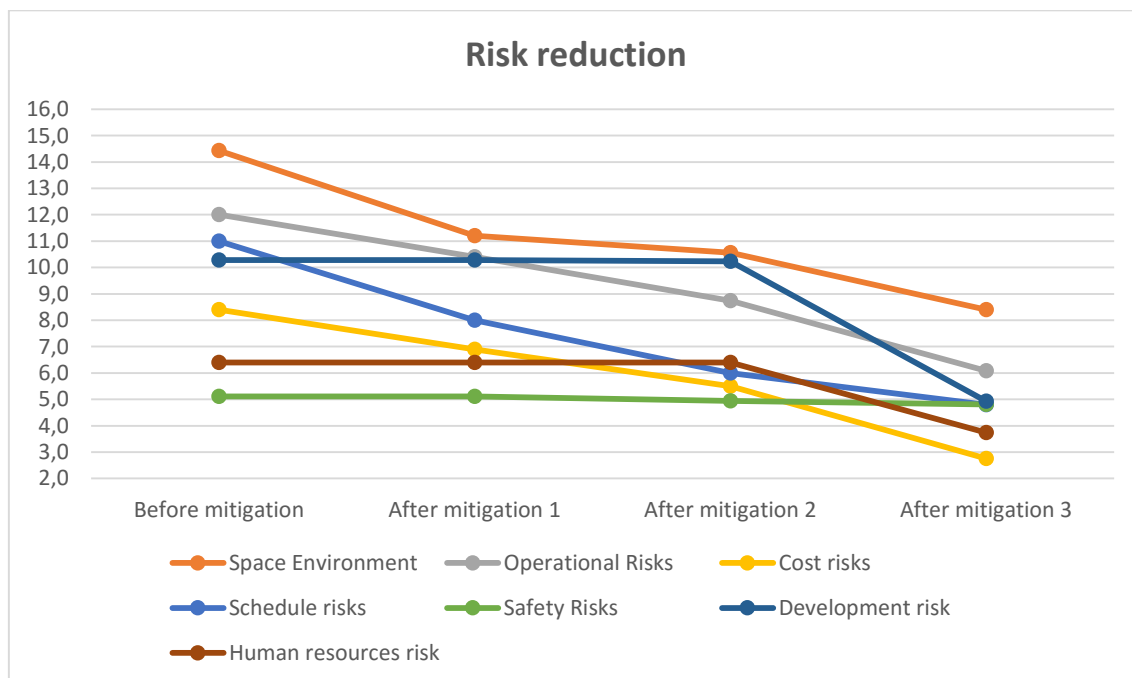
Figure 6. 3: Total risk reduction

6.4. Further work

6.4.1. Mechanical

The first round of development is complete, and possible improvements are easily seen. Overall, the first prototype provides good test results and performance. The main focus for the next prototype is to include a thermal factor to the calculations without making major changes to the design, and to reduce the mass.

Known improvements for the current APM:

- The APMs mass is too large and parts of the mechanism are overdimensioned. Static analysis must be executed on the APMs skeleton to optimize size versus strength according to ESA standards.
- Bearings need to be re-arranged and calculated from scratch to improve dynamic stress distribution. When this is done, the bearings have to be re-estimated to account for thermal factors and the new bearing setup.
- The elevation stage needs a full redesign with respect to mass.

6.4.2. Electrical

For further development of the electrical system, the final design should be made and tested. The differences in the breadboard model and the final design are too great for the system to be considered verified. The system also has to be tested in a space environment to verify the choice of components.

6.4.3. Software

The next step in software is to implement the elevation stage. This will be the main focus for the next prototype. The CAN protocol also needs to be implemented, to perfect the communication between the APMA and satellite. The automatically generated S-curve should also be improved, especially with respect to storing the array in flash memory, for higher resolution. Lastly, better voltage and current limitations should be implemented.

6.4.4. Radio communication system

In order to continue development of the radio communication system, the antenna and waveguide have to be tested. When the current design has been verified, the system can be improved. Preferably, the system should also be simulated in worst-case environments to ensure that it will have the intended functionality.

6.5. Reflection documents

6.5.1. Vebjørn Orre Aarud

My main role in the bachelor project was head of test and verification in collaboration with Stian Laugerud. I think it was natural to select this role due to my 1.5 year experience in test and testing gained at Kongsberg Automotive, Test laboratory.

During the first 6-8 weeks of the project, the role as head of test and verification was small and my focus changed more to technical development and resources for the mechanical part. For the first milestone I selected materials and lubrication e.g, for the second milestone I calculated torque for our system and as a final milestone I selected the bearings for our system. During the last 2-3 weeks my role came to life during real life testing.

Since I have experience with practical testing and test reports before I let our designer and constructor Magnus Dybendal preform the practical testing and report instead to gain valuable experience.

In collaboration with Stian Laugerud we verified the end result and did make sure that the report, test procedure and test related documents were up to project standard before and after testing.

Working with a space related project was interesting. Everything I have learned from before has changed. Tolerances, forces, material selection and more have so many more factors to deal with to gain a proper end result. I did find the first 4 weeks difficult due to the lack of space knowledge and I had a lot of questions about following ESA standards and how to adjust calculations for space. One of the most difficult parts was to estimate the right bearings for our system, the factors are endless and the segment all new, but in the end I think I ended up with a feasible results.

Late in 2015 I spoke with Gisle H. Stenseth about making a bachelor group, and I ended up with a group almost premade by Gisle. This group contained every aspect of engineering which I find very useful. The reason for this is that every challenge was discussed across disciplines, making the end result very good. This means that I have gained help and experience from every group member during my challenges and vice versa. I feel that such a group environment makes us great and every member has some knowledge about every aspect of the project. A non-technical part of our group environment was "healthy" discussions. This brought us closer together and made us more effective to handle group issues.

Our project stakeholders Kongsberg Space and Surveillance have been excellent. They have provided us with extended help during challenges and also founded our prototype and more. This helps to keep motivation up and keep a good group flow. I do also find that our stakeholder is truly passionate for our project.

As a recap of our project I do find it good, I have not met any motivation issues or big project issues. I have been working at Kongsberg Automotive approximately 10 hours a week during the project but gained back the lost time in the weekends. Some extra effort have been made such as making test fixtures overnight or bake a cake for our presentations. We ended our project with our first real life prototype and I would like to start a new round improving the next one, however our time has run out and the project is over. I am curious if Kongsberg Space and Surveillance will continue developing this project.

I am happy with the experience I have gained.

6.5.2. Magnus Dybendal

I've been the design and construction responsible in this project, in addition to mechanical engineer. My learning and outcome as a result of this project has been extraordinary. To work in a multidisciplinary environment with 5 other people has been both challenging and rewarding, but overall a huge pleasure.

The group was established early after the summer vacation in 2015. I was contacted by Vebjørn Orre Aarud who had spoken to Gisle Hovland Stenseth about finding a group to the bachelor project.

During the first weeks of the project, we developed an early concept. Therefore, since the beginning I always felt a responsibility for my given role to this project. I have also worked in collaboration with Vebjørn Orre Aarud with the different technical documents regarding the mechanical engineering during the phases of the project. During the project I had the responsibility of communication with distributor concerning the mechanical aspects, and make sure all the mechanical parts were manufactured. In collaboration with Vebjørn Orre Aarud, we made all the 2D drawings, and the distributors did not have any questions regarding manufacturing. Since I have been the responsible for the design and construction, I also made the whole 3D model of the APM in SolidWorks.

A big challenge has been related to the multi-discipline nature of the project. During the development of the prototype, for example, I had to wait for Vebjørn Orre Aarud to find the right torque needed to drive the system, and then wait for Stian Laugerud to find the right motor. After this was done I could finally implement the motor in the design.

I would strongly recommend other students to work in a multidisciplinary team in a bachelor project. This has given me an insight to what the different parts both electrical and software engineers are doing. To work in an interdisciplinary group has given me an intimation of how the real work life is, and what is required for a project to achieve its goals. To be a part of this team and worked with this people has been a pleasure. The group has been motivated since day one. Individually, to follow the unified process model has been a motivation for me, due to always having a goal for each iteration, and always having something to work for.

To write this bachelor project for KDA has been a pleasure. They have granted us guidance where needed throughout the whole project and been a huge resource. We also had several meetings both externally at KDA and in our office. Most of the meetings have been with the external supervisor, but several employees have also been joining us during the project. Lastly, I will mention SKF, they have been a huge resource for the bearing selection me and Vebjørn Orre Aarud worked on.

6.5.3. Stian Laugerud

My role during this project has been the test and verification responsible together with Vebjørn Orre Aarud. In addition to this, I have worked with electronic related tasks like the control system and the electrical design. I also took charge of ordering parts for the project. I am a structured person who gain knowledge rapidly and enjoy practical assignments. Because of this, it felt natural to be responsible of the test and verification part of the project.

This project has been extremely fun and interesting to me because of the great group members and the employers at KDA, but also because of the interdisciplinary aspect of the project and the fact that we produced a physical prototype. I am also very interested in mechanics and I have had the chance to learn a lot of this throughout the project. I could not have asked for a better bachelor project and the learning outcome has been amazing. The atmosphere in the group has been great throughout the project and the group members have worked very hard to reach the final result. We have been challenged to gain knowledge about the space environment, requirements and standards, which were new to all of us.

At the beginning of the project we worked together to decide the project group's goals and thoughts of the project. We also started planning how the project would evolve and what we wanted to achieve. The outcome of this made us choose the iterative project model of unified process. As the test and verification responsible, the early phases of the project were based on establishing the frame of the project. When the requirements were in place, we looked at methods to test and verify them. We then started to look at main components like motors, motor drives and microcontrollers. I wrote plenty of mails with a very helpful employee at Maxon motors in order to end up with a motor that would satisfy our requirements.

As the project continued, I started looking at the control system. Since we have only learned the basics on how to control a simple DC motor, I had to gain a lot of new knowledge about BLDC motors and control of a three-phase motor. I worked a lot with the Simulink model of the control system and the simulations and got the system up and running with the other electrical engineering students. This was a very interesting experience and it was fun to see Torstein Sundnes implement the system in software and make it work. I have also been working on the functional test procedure, which explains how all the tests should be performed. In addition to this, I have been working on the electrical design with Gisle Hovland Stenseth. This includes establishing circuits for testing, but also designing the final design, which would have been implemented if we had the time to continue the project. The final design includes microcontroller, motor drive, current measurements and circuits to handle the encoder output. I found this part of the project very interesting and I have learned a lot of working with electrical designs.

The project has been completed similarly to how it is done in the industry and I think that it has given me a good foundation of meeting the job marked. After working with this project for roughly six months, it has now become natural to document and explain every choice that is being made throughout a project. I can see the benefits of doing it and how much it simplifies others understanding of the given subject.

Kongsberg Space and Karl Patrik Mandelin has been extraordinary through the whole project and should have a lot of credit for the result we have presented. It made all the group members very motivated. I never expected an employer to show such interest in a bachelor project and therefore I am very grateful to have been a part of it.

6.5.4. Torstein Sundnes

I have been responsible for documentation in this project, together with Elise Løken. I am fluent in English grammar and writing, making this role a fitting one. Elise has been writing most of the iteration reports, follow-up documents and internal minutes of meetings. My main responsibility in this project however, is software. Being the only software engineering student has been challenging, but also very educational.

In the beginning of the project, the project plan and other key documents were created. The first weeks consisted of creating the base foundation of the project, and to plan the next phases to come. Elise and I researched the different models suitable for our project, and in collaboration with group members, external supervisors and sensors, we decided to implement the unified process. Later in the project, we divided the document work a little, and I focused more on correcting and approving all documents, along with writing minutes of meetings.

The software part of the project started slowly. Since a lot of work from mechanical engineering and electrical engineering had to be done before implementing software, a lot of research had to be done, to ensure efficiency when the implementation first started. A big part of the research was done on the space vector pulse width modulation, SVPWM, which was an integral part of the project and a main requirement. As most of the documentation on SVPWM was related to electrical engineering, this posed as a challenge, but also an interesting way to learn about the study. It is worth noting that I have learned so much about electrical engineering subjects the last months. It has been really interesting, especially when I am able to discuss technical solutions with the electrical engineering group members.

Towards the end of the project, I worked mostly in collaboration with Gisle H Stenseth and Elise Løken when implementing their Simulink model into software. The microcontroller we used was something none of us had been working with before, which proved a moderate challenge, but with enough work and a lot of reading, I was able to implement the control system. Due to the size and complexity of the control system in this project, much of my time has gone to programming and research instead of documentation. This can be seen in the weekly summary documents.

A big challenge has been related to the multi-discipline nature of the project. Since the software was dependent on the electrical parts, and the electrical parts were dependent on the mechanical parts, certain parts of the control system had to be improvised and performed with alternative solutions. For example, filtering the current measurement in software, and delays related to ordering electrical components like the microcontroller. However, thanks to these limitations I feel I have learned a lot; implementing creative solutions, the importance of planning ahead, and using the contacts and resources available to succeed.

Both the project group and all the people who have been invested in this project have been amazing. The group has been motivated since day one, much thanks to our external supervisor at Kongsberg Space, who seems just as interested in our project as we do. I think this really motivated us as a group, to the point that we looked forward to every day working with the project. Additionally, the group members are a pleasure to work with. Every member has some insight in all parts of the system. Not just because it is necessary due to the nature of the project, but also since the project is so interesting, we even talk about it during lunch hours.

Lastly, I want to point out how lucky we have been to have this project. People have been coming up to us from all disciplines, interested in what we are doing. Every presentation has been filled with audience, and it has been a pleasure working with these group members.

6.5.5. Gisle Hovland Stenseth

My responsibilities in this project have been as project leader and interface responsible. I was chosen as project leader partly due to my connections with Kongsberg Space, and my limited experience in space technology. As project leader I have delegated work and been the final voice in certain arguments. With a group as productive as SSM, it's easy to be a group leader.

As interface responsible, I have mainly been involved in the electrical-to software interfacing. I.e. discretization of continuous systems, current measurement circuits, communication protocols, etc. On the electrical-to mechanical side, I've been involved in the motor selection and the gearing of the system.

The problem presented by Kongsberg Space was challenging. Of the group members, only I had some previous experience in designing systems for space. In the space industry, the requirements, especially relating to mass, power consumption and environment are tough. Our goal was to cut the costs of antenna pointing mechanisms by building it using cheap, commercial parts while still keeping the same functionality as existing mechanisms. The system the group has designed has shown that the functionality is achievable. To know for sure if it can be done, it has to be tested in thermal vacuum and vibrated.

Theoretically, the project has been really challenging. For my part, I found that high frequency radio communication is a field in which few people had the knowledge to help us. Although I have some experience in the field from high school, the physics and mathematics of it are for the most part at master levels and hard to pick up in such a short time. Although this was a great challenge, I believe we have managed to make a good design.

The control system also posed a challenge. The school only teaches simple DC-motor designs, while we had to design a controller for a three-phase system. In addition, the system had to be discretizised in order for it to be programmed on a microcontroller. Here, the group really pulled it together, and designed a good system.

The low frequency electrical design is where my education has been the most useful, and the part of the design that has caused the least headaches. The circuits are pretty straight forward.

Putting the theory we've learned at school into practice has been a great learning point for me, and something I wish we would have done throughout our entire education. Project planning is something the industry calls for. To have been a part of a project such as this, where project planning plays such a big role is important for our future careers.

The group dynamic has been great throughout the entire project. Everyone has pulled their weight. To be part of such a motivated and productive group is something I've very rarely experienced in my academic career. When the theoretical foundation has been weak, all the group members have worked hard to gain a high enough level of knowledge to solve the challenges. It has been a privilege to work with this group.

The communication with the external supervisor and Kongsberg Space has been excellent. We have had regular meetings, and have received a lot of help from all the people we have asked at Kongsberg Space. The space industry in Norway is small, and not a lot of people have knowledge in this field. Therefore, the communication with Kongsberg Space has been crucial.

6.5.6. Elise Løken

My responsibility in the SSM project was documentation, together with Torstein Sundnes. As a person, I am structured and organized, and I am good at writing clearly and easily understandable documentation. Torstein has a more fluent English language than I have, and working together with him, using each other strengths in the work with the documentation, was a fitting responsibility for us.

Additionally, I am an electrical engineering student, together with Gisle Hovland Stenseth and Stian Laugerud, and this has been our main responsibility in this project.

In the start-up phase of the project, the whole group worked together defining the frames, limitations and goals for the project. Then, Torstein and I started working a lot with the project plan and the choice of the project model. The Unified Process inspired "Iterative Development Model" was chosen, and this model has turned out to be significant for the progressivity in the project. The time-boxed iterations and the clearly defined deadlines have been helpful in the planning of the project. It was also helpful in ensuring that the project at all times was on schedule according to the project plan. At the end of the project, we reached our goals. I think that the project model together with continuously hard work from the whole project group throughout the project, are some of the crucial reasons for this.

The main technical issues I have been working with in this project are the design of the antenna system and the design of the control system for the APMA. Gisle and I did a trade-off where different antenna concepts were evaluated. In this trade-off I did the calculations and dimensioning of the Cassegrain antenna, which became the final design of the system. I also worked a lot with the design of the control system, the model of the system in Simulink and the simulations, with inputs from the other electrical engineering students. A control system of a 3-phase system is much more complex than what we have been working with at school, so it was a lot of new things I had to study and learn(including the reference frame transformations and the space vector pulse width modulation converter). I found this both challenging and interesting, and it was really fun when the control system was implemented in the real-life prototype and worked as desired. Additionally, I have written the internal minutes of meetings and agendas, almost all of the follow-up documents and iteration reports and I had the main responsibility for the final document collection.

Even though the group members have been working with different technical issues and disciplines, important solutions have been discussed and decisions have been taken together as a group. Due to this, I have a quite good overview of the whole design process of the system, and I have insight in most aspects of the project. During the project, I have also learned a lot from the other disciplines.

The space environment and the requirements to our mechanism due to this were completely new to me. I have learned a lot from this, especially organizing an interdisciplinary project, where interfaces between mechanical-, software- and electrical engineering had to be taken into account. The education at the University of Southeast Norway is theoretical, and this practical, interdisciplinary bachelor project in cooperation with a professional employer was quite interesting to me.

As a group, we are satisfied with the results of the project. All the group members have been working hard and have been motivated throughout the whole project period. The communication within the group has been excellent, and I have learned a lot from the other group members.

Additionally, I want to thank our external supervisors at Kongsberg Space. It has been a pleasure working together with them, and they have shown a great interest in our project. I am convinced that this has been a great motivational factor for all the group members, and that it has motivated us to work hard to deliver a project that satisfies them.

6.5.7. References

[1] Gisle Hovland Stenseth and Magnus Dybendal, "SSM-2000, Requirement Specification," University college of South East Norway, Kongsberg, 2016.

[2] Gisle Hovland Stenseth, "SSM-3003, Functional Test Report Rev.1.0," KIFI, University College of Southeast Norway, Kongsberg, 2016.

[3] Stian Laugerud and Vebjørn Orre Aarud, "SSM-3000, Test & Verification Specification," University college of South East Norway, Kongsberg, 2016.

[4] Gisle Hovland Stenseth and Stian Laugerud, "SSM-5415, Electrical Design Document," KIFI, University College of Southeast Norway, Kongsberg, 2016.

[5] Gisle Hovland Stenseth, Magnus Dybendal, and Vebjørn Orre Aarud, *"SSM-1200, Risk Management, rev.1.1"*. Kongsberg: Small Satellite Mechanisms, 18.02.2016.

[6] Stian Laugerud and Vebjørn Orre Aarud, "SSM-3002, Functional Test Procedure," KIFI, University College of Southeast Norway, Kongsberg, 2016.

[7] Elise Løken, Vebjørn Orre Aarud, and Magnus Dybendal, "SSM-5901, Technical budgets," KIFI, University College of Southeast Norway, Kongsberg, 2016.

7. Appendices

ii. List of tables

7.1. Electrical design schematics

Figure 7. 1. 1: System overview 1
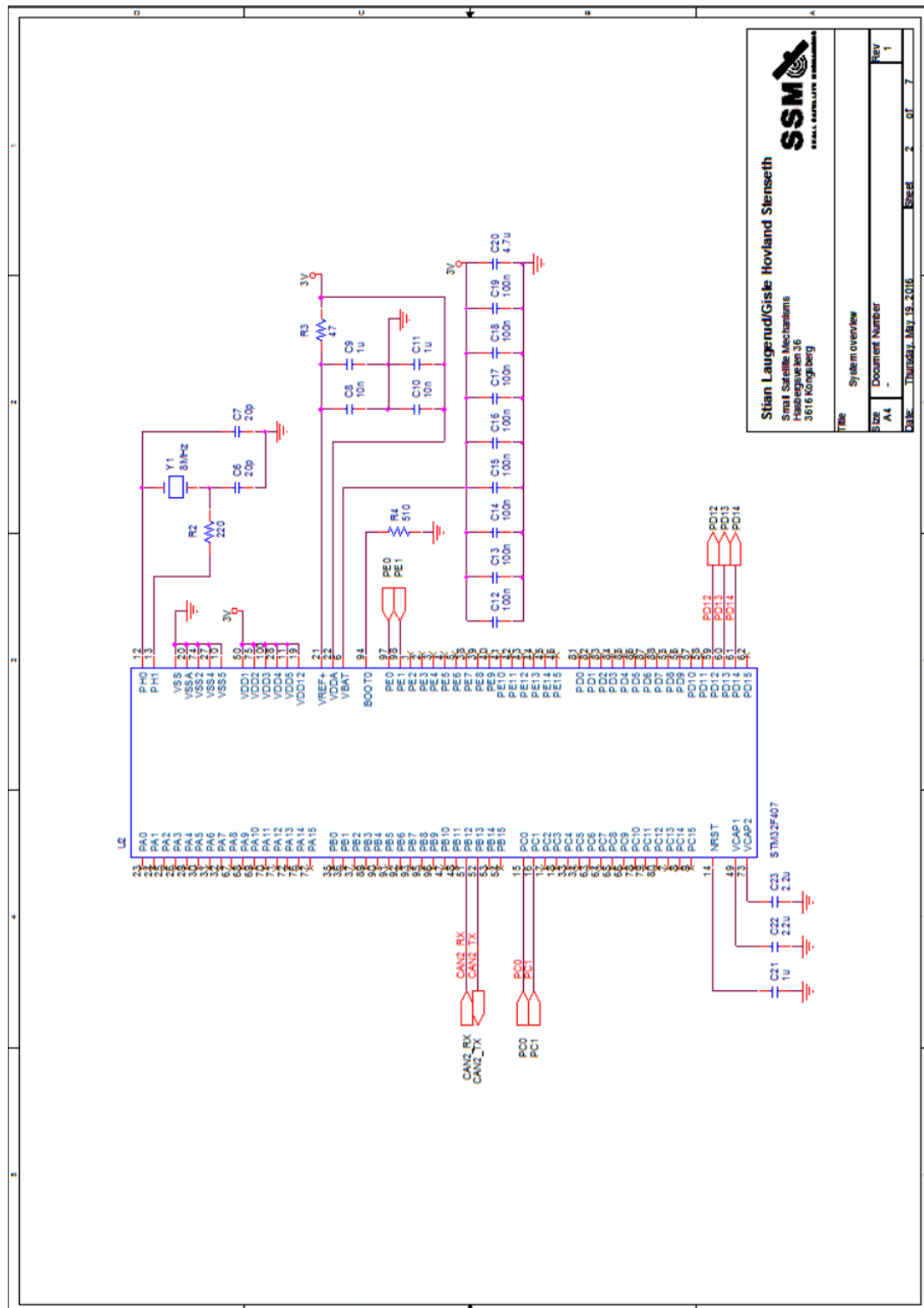
Figure 7. 1. 2: System overview 2
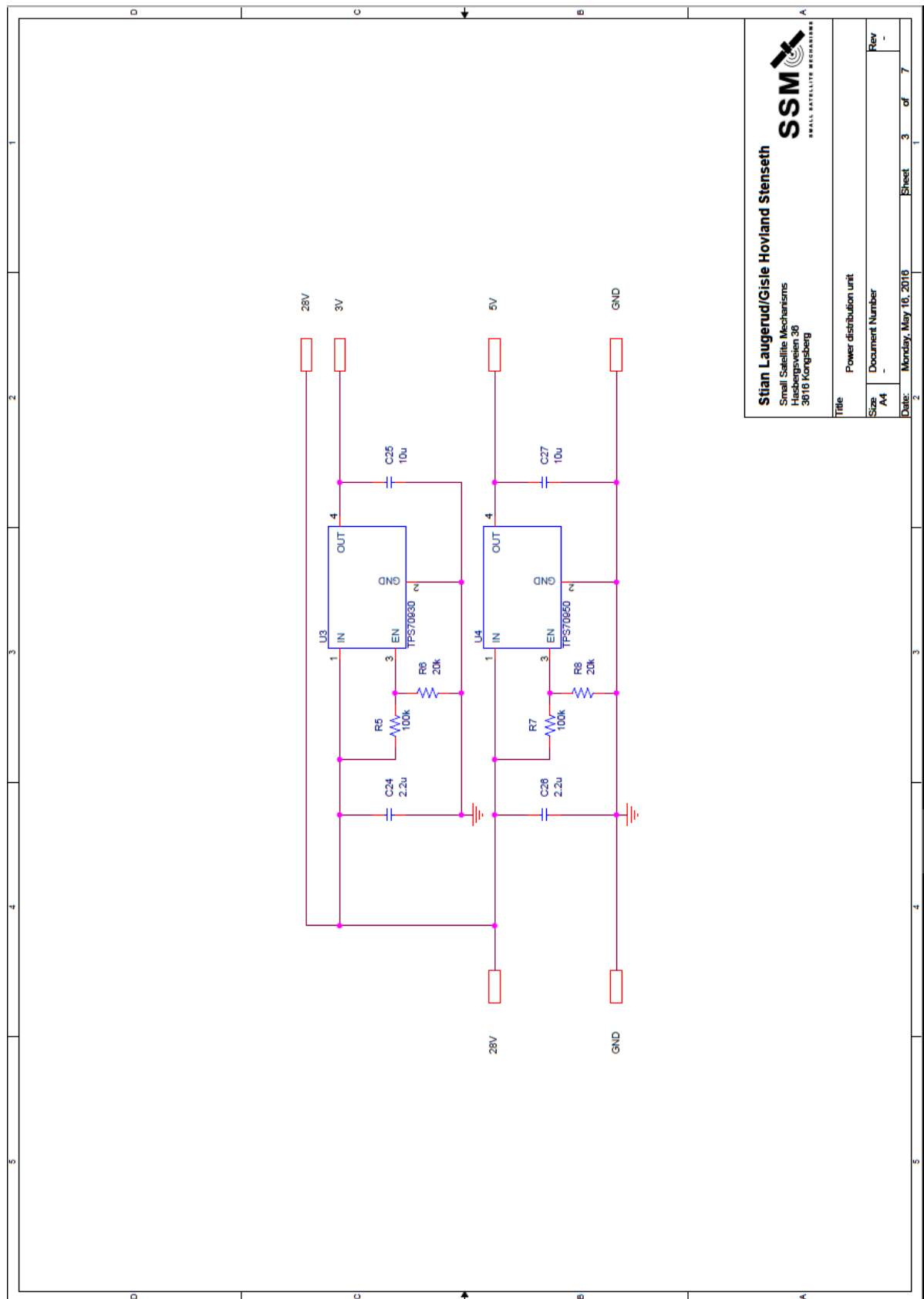
Figure 7. 1. 3: Power distribution
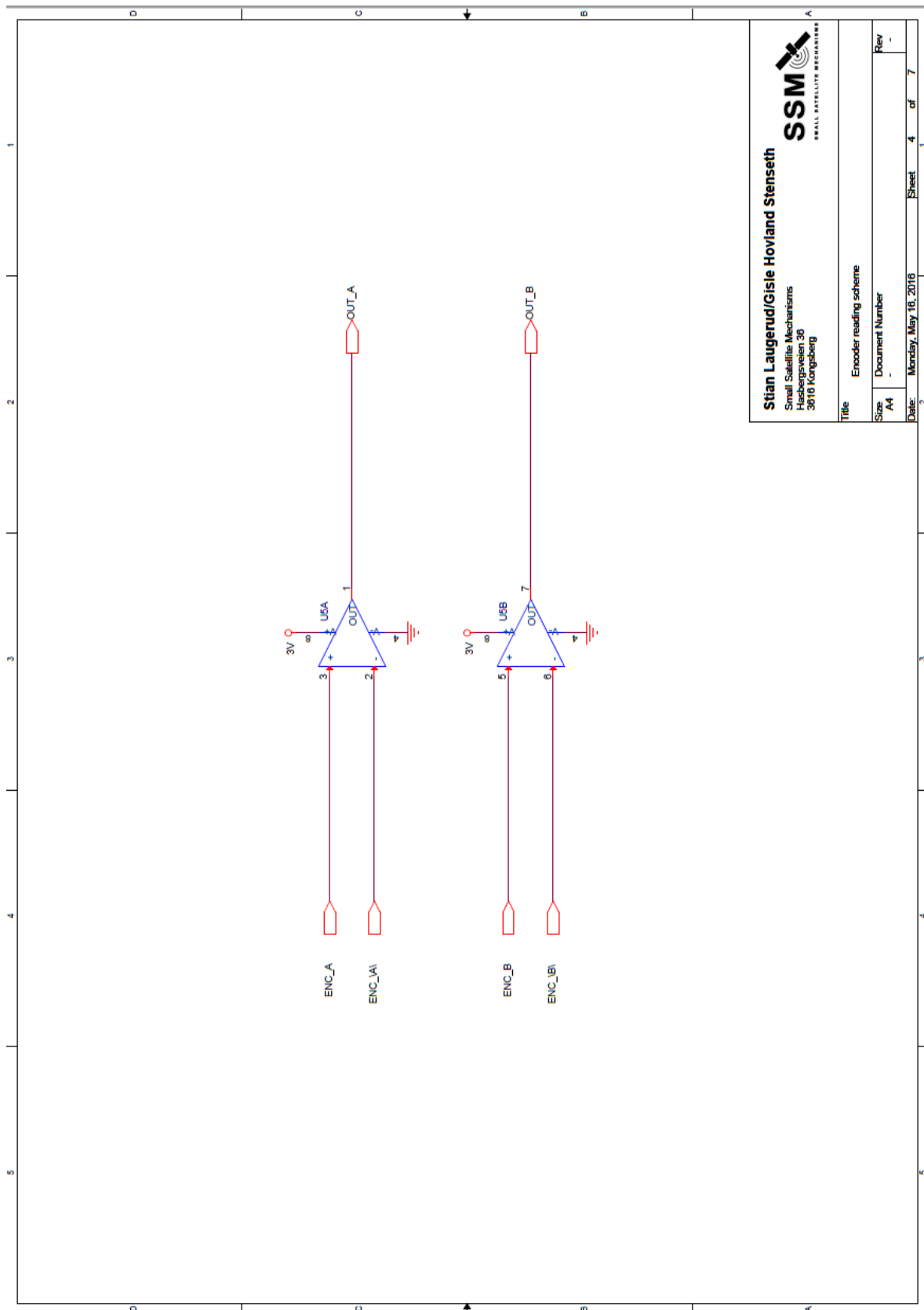
Figure 7. 1. 4: Line receiver

Figure 7. 1. 5: Current measurement overview
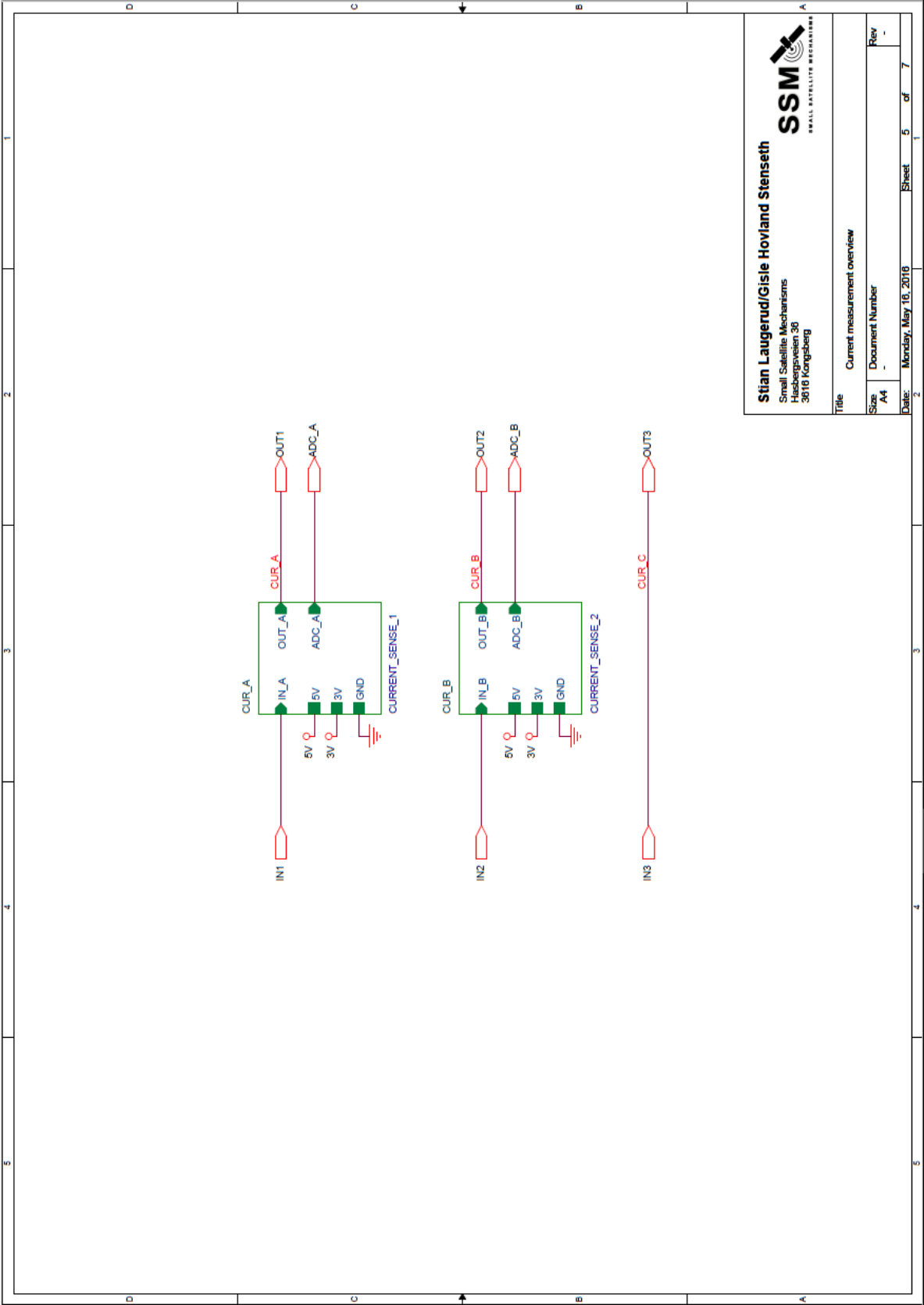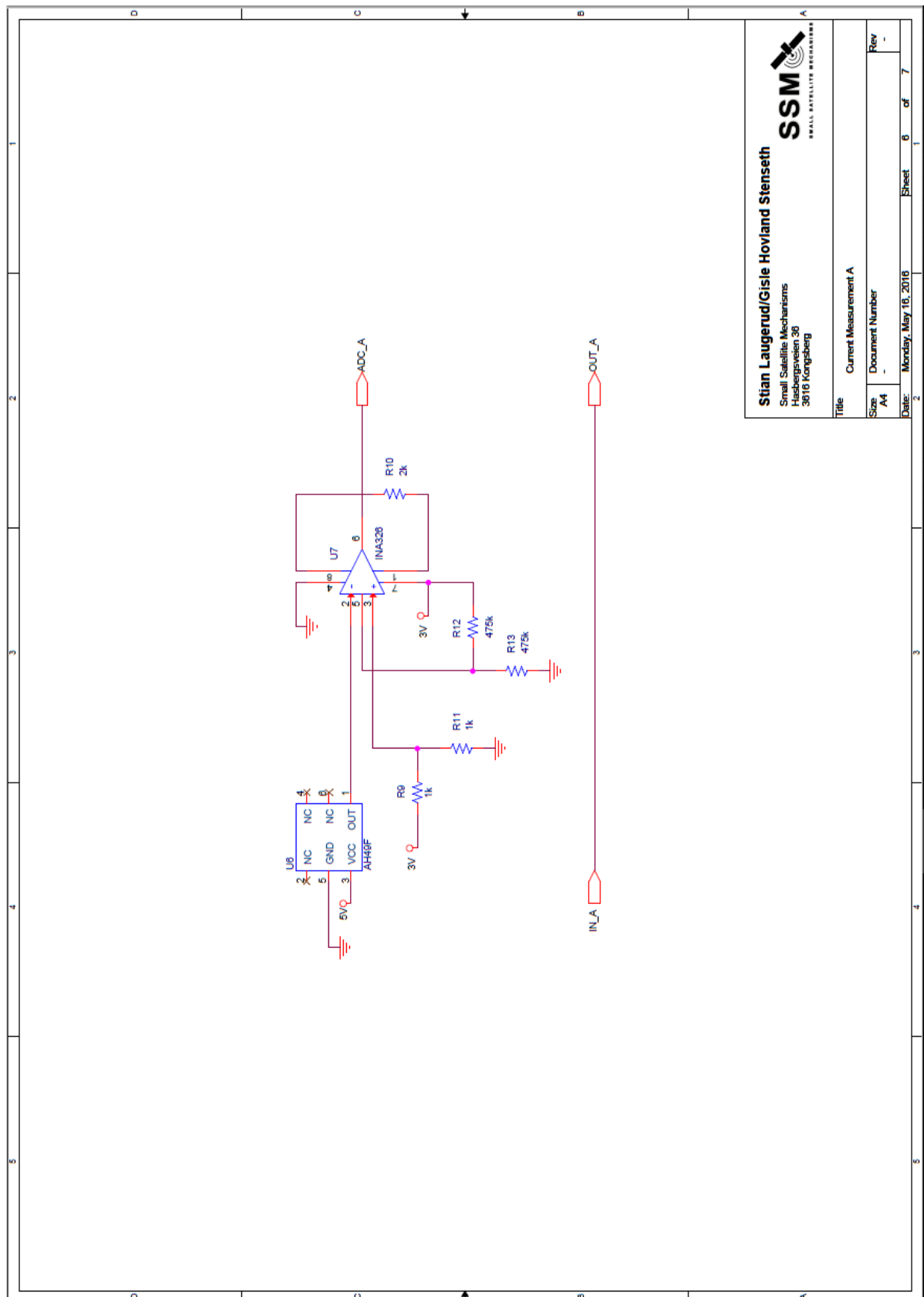
Figure 7. 1. 6: Current measurement 1
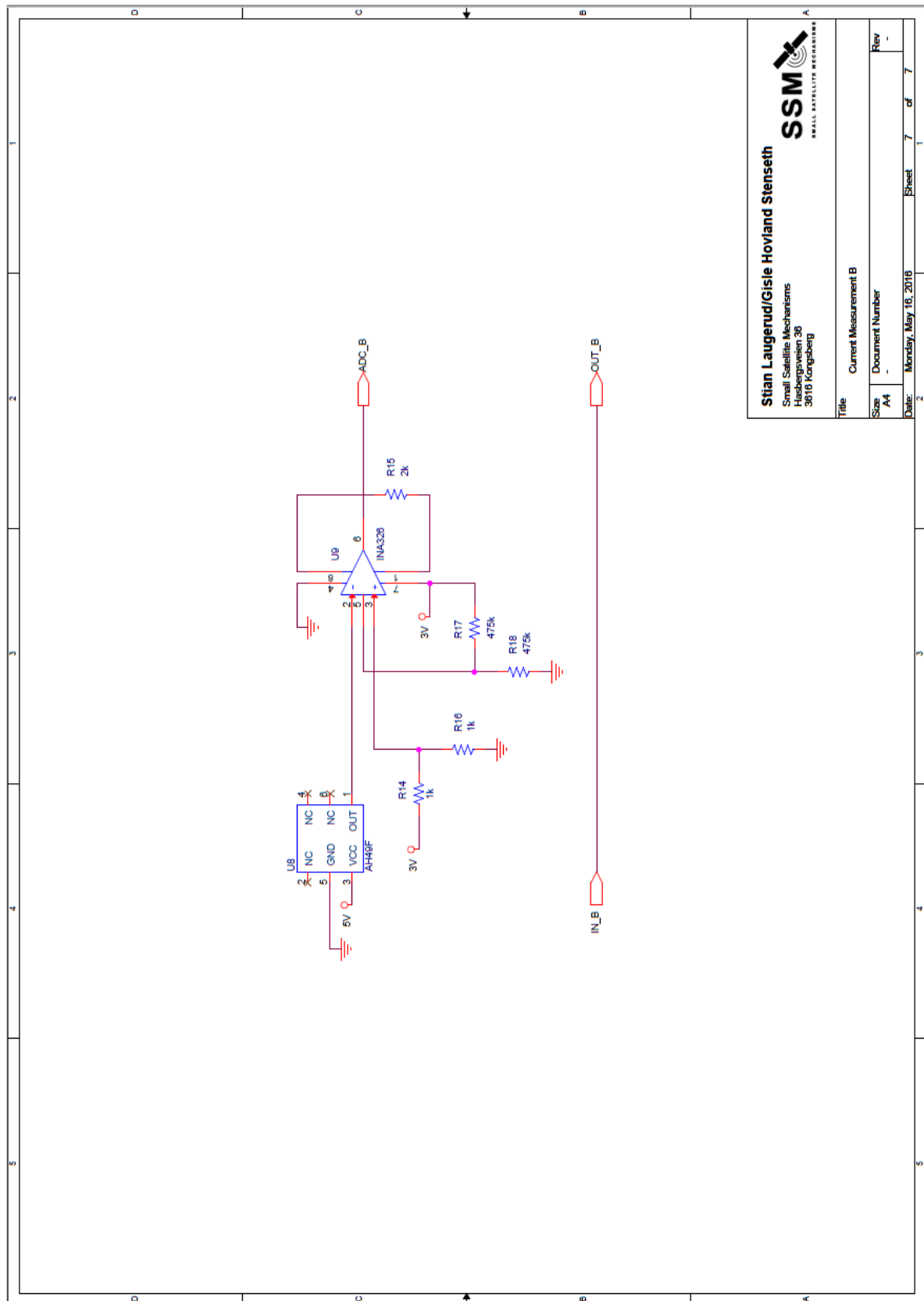
Figure 7. 1. 7: Current measurement 2

7.2. Ordered parts

Parts								
Description		Part number	Manufacture	Supplier	Amount	Price (NOK eks. mva.)	Total Price (NOK eks. mva.)	
Combination consisting the following elements:						2673	10692	
EC 45 flat Ø42,8 mm, brushless, 70 Watt, 48V with hall sensor		469303	Maxon	Stork Drives AB	4			
Encoder MILE, 1024 CPT, 2 Channels, with Line Driver		402687	Maxon	Stork Drives AB	4			
Må bestilles via arve.stensrud@storkdrives.no		462004	Maxon	Stork Drives AB	4			
Ref. tilbud ARST_16317-111458_Rev0 fra DJ Stork Drives AB								
ST microelectronics STEVAL-IHM039V1 with a STM32F415ZGT6 ARM Cortex-4M processor		511-STEVAL-IHM039V1	STMicroelectronics	Mouser	2	2144,72	4289,44	
Motor drive L6230PD		511-L6230PD	STMicroelectronics	Mouser	6	69,64	417,84	
39-01-2080 PLUG & SOCKET HOUSING, RECEPTACLE, 8 POSITION 2ROW, 4.2MM		2128431	Molex	Farnell	10	3,47	34,7	
90635-1102 SOCKET, IDC, 10WAY		9733175	Molex	Farnell	10	7,91	79,1	
Gears		SH0.7-10-RK04	HPC	HPC	2	497,675	995,35	
Gears		SH0.7-175-LK15	HPC	HPC	1	1918.90	1918.90	
Gears		SH0.7-100-LK08	HPC	HPC	1	986,9	986,9	
Bearings W6005		10007	SKF	TESS	4			
Bearings w6000		10208	SKF	TESS	4			
Lock nut KMT5 (M25x1,5)		10010	SKF	TESS	2			
STMicroelectronics STM32F407G-DISC1		511-STM32F407G-DISC1	STMicroelectronics	Mouser	2	176,89	353,78	
STMicroelectronics X-NUCLEO-IHM07M1		511-X-NUCLEO-IHM07M1	STMicroelectronics	Mouser	4	88,92	355,68	
Waterjet cutting								
Mounting bracket		-	Vannskjæresenteret	Vannskjæresenteret	1	2000	2000	
Azimuth bracket		10102	Vannskjæresenteret	Vannskjæresenteret	1	470	470	
3D printed :								
Holder big reflector		10101	KDA	KDA	1	N/A	N/A	
Mirror		10301	KDA	KDA	1	N/A	N/A	
Motor housing		10004	KDA	KDA	1	N/A	N/A	
Contact mirror bracket		10205	KDA	KDA	1	N/A	N/A	
Contact upper lower		10204	KDA	KDA	1	N/A	N/A	
Elevation bracket		10201	KDA	KDA	1	N/A	N/A	
Mirror elevation		10206	KDA	KDA	1	N/A	N/A	
Metal manurfacturing:								
Bearing house Azimuth		10006	Koberg	Koberg	1		7850	
Cap azimuth		10005	DEVOTEK	DEVOTEK	1			
Connector		10009	DEVOTEK	DEVOTEK	1			
Main contact place		10001	DEVOTEK	DEVOTEK	1		20000	
Parabol antenna		10103	DEVOTEK	DEVOTEK	1			
Struts		10105	DEVOTEK	DEVOTEK	3			
Subrefelctor		10104	DEVOTEK	DEVOTEK	1			
waveguide		10002	DEVOTEK	DEVOTEK	1			
Azimuth fishplate		10102	DEVOTEK	DEVOTEK	1			

Ordered	
Recieved	
To be ordered	
Missed	

Prices does not include delivery

Table 7. 2. 1: Ordered parts

7.3. Control system

7.3.1. Simulink model of the control system
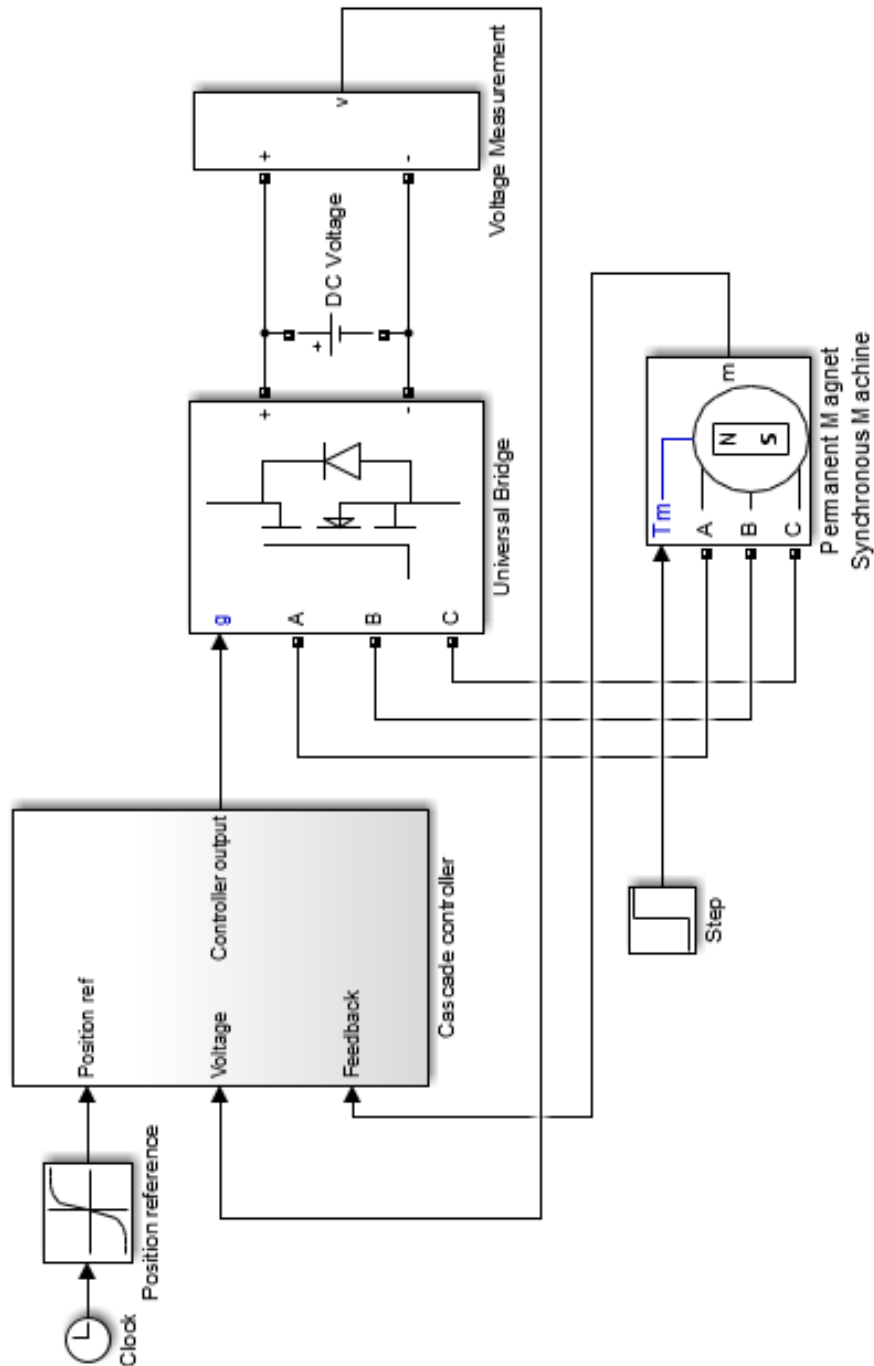
Figure 7. 3. 1. 1: Top-level model view
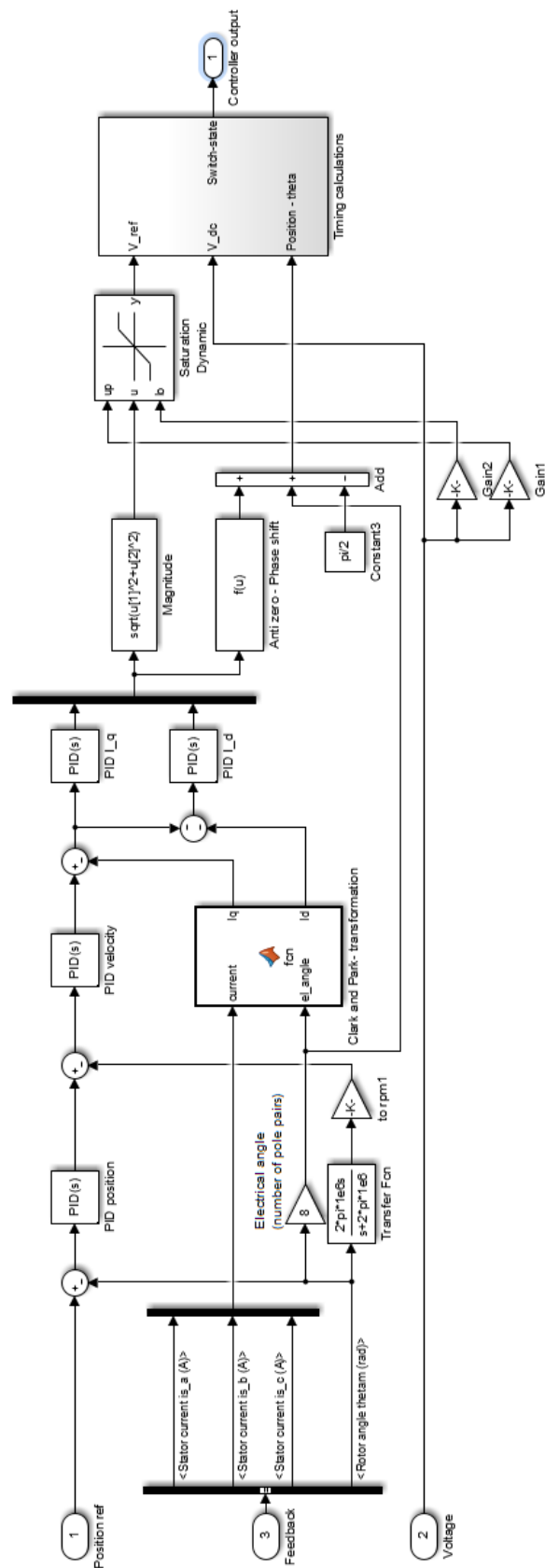
Figure 7. 3. 1. 2: Cascade controller
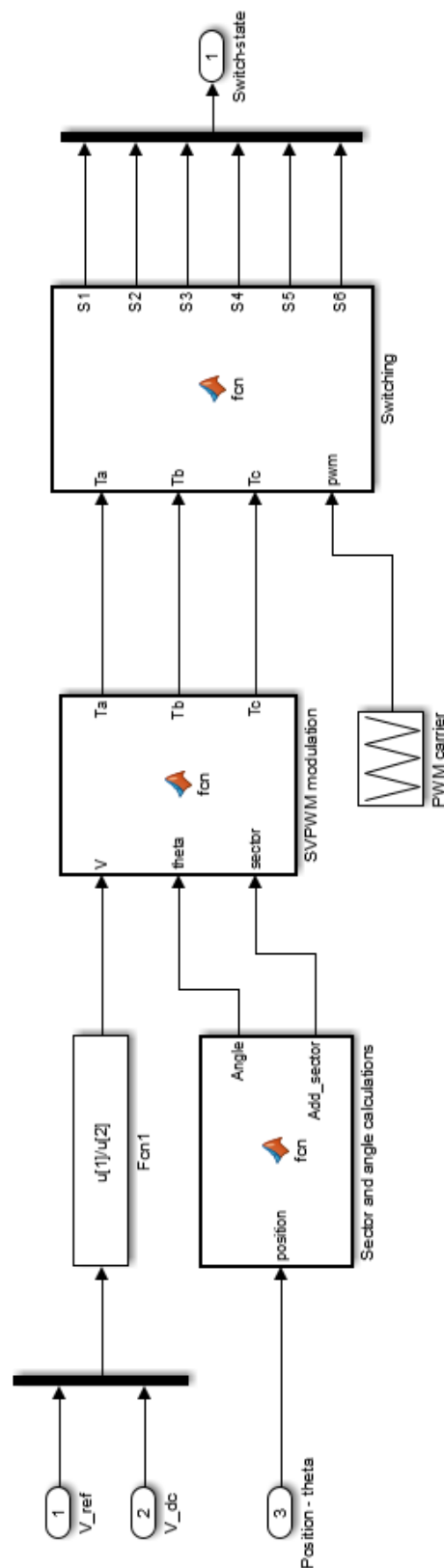
Figure 7. 3. 1. 3: Timing calculations

Table 7. 3. 1. 1: Matlab script for the Simulink model

```matlab
clc;
close all;
clear all;


Tz = 1/30e3;


x = linspace(0,1,100);%t, time
v = 25;% omega, velocity
a = 13; % alfa, acceleration
y = zeros(1,100); % theta, position array
i=1;
g = zeros(1,100);
q = zeros(1,100);
acc = zeros(1,100);

%%
while 0.5*a*x(i)^2 < v*(x(2)-x(1)) % 0.5a*(dt*count)^2 < v*dt*count
    y(i+1)=y(i)+0.5*a*x(i+1)^2; % Neste posisjon = posisjon no +
0.5*a*(dt*(count+1))^2
    i=i+1;
    if i >= 50
        break
    end
end
k=i;

%%
while i<(100-k)
    y(i+1) = y(i)+v*(x(2)-x(1));
    i=i+1;
end


d=k;

%%
while d>0
    y(i+1)= y(i) + 0.5*a*x(d+1)^2;
    d=d-1;
    i=i+1;
end
figure
plot(x,y)
grid on
title('S-curve, position reference', 'FontSize', 20);
xlabel('Time(s)', 'FontSize', 16)
ylabel('Position(rad)','FontSize', 16)

%%
for i = 1:99
    q(i)= (0.955*q(i)+y(i+1)-y(i))/0.001;
    g(i)= (y(i+1)-y(i))/0.001;
end

figure
plot(x,g);
grid on
title('Velocity reference(rpm)', 'FontSize', 20);
```

```matlab
xlabel('Time(s)', 'FontSize', 16)
ylabel('Velocity, rpm)','FontSize', 16)
figure
plot(x,q,'r');

for i=1:99
    acc(i)=(g(i+1)-g(i));
end
figure
plot(x,acc);
```

7.3.2. Control system software

7. 3. 2. 1: Control system software

```c
/**
  ******************************************************************************
  * File Name          : main.c
  * Description        : Main program body
  ******************************************************************************
  *
  * COPYRIGHT(c) 2016 STMicroelectronics
  *
  * Redistribution and use in source and binary forms, with or without modification,
  * are permitted provided that the following conditions are met:
  *   1. Redistributions of source code must retain the above copyright notice,
  *      this list of conditions and the following disclaimer.
  *   2. Redistributions in binary form must reproduce the above copyright notice,
  *      this list of conditions and the following disclaimer in the documentation
  *      and/or other materials provided with the distribution.
  *   3. Neither the name of STMicroelectronics nor the names of its contributors
  *      may be used to endorse or promote products derived from this software
  *      without specific prior written permission.
  *
  * THIS SOFTWARE IS PROVIDED BY THE COPYRIGHT HOLDERS AND CONTRIBUTORS "AS IS"
  * AND ANY EXPRESS OR IMPLIED WARRANTIES, INCLUDING, BUT NOT LIMITED TO, THE
  * IMPLIED WARRANTIES OF MERCHANTABILITY AND FITNESS FOR A PARTICULAR PURPOSE ARE
  * DISCLAIMED. IN NO EVENT SHALL THE COPYRIGHT HOLDER OR CONTRIBUTORS BE LIABLE
  * FOR ANY DIRECT, INDIRECT, INCIDENTAL, SPECIAL, EXEMPLARY, OR CONSEQUENTIAL
  * DAMAGES (INCLUDING, BUT NOT LIMITED TO, PROCUREMENT OF SUBSTITUTE GOODS OR
  * SERVICES; LOSS OF USE, DATA, OR PROFITS; OR BUSINESS INTERRUPTION) HOWEVER
  * CAUSED AND ON ANY THEORY OF LIABILITY, WHETHER IN CONTRACT, STRICT LIABILITY,
  * OR TORT (INCLUDING NEGLIGENCE OR OTHERWISE) ARISING IN ANY WAY OUT OF THE USE
  * OF THIS SOFTWARE, EVEN IF ADVISED OF THE POSSIBILITY OF SUCH DAMAGE.
  *
  ******************************************************************************
  */
/* Includes ------------------------------------------------------------------*/
#include "stm32f4xx_hal.h"

/* USER CODE BEGIN Includes */
#include "math.h"
#include <stdlib.h>
#define PI 3.141592654f
#define GearRatio 17.5f
#define PolePairs 8
#define millis 61.4
#define Clock_Time 0.00001628665f
#define Input_Current 1.5f

/* USER CODE END Includes */

/* Private variables ---------------------------------------------------------*/
ADC_HandleTypeDef hadc1;
ADC_HandleTypeDef hadc2;
ADC_HandleTypeDef hadc3;
DMA_HandleTypeDef hdma_adc1;
DMA_HandleTypeDef hdma_adc2;
DMA_HandleTypeDef hdma_adc3;
TIM_HandleTypeDef htim4;
UART_HandleTypeDef huart4;

/* USER CODE BEGIN PV */
/* Private variables ---------------------------------------------------------*/

/* Variables for transmit command. */
int32_t txPos;
int32_t txVel;
uint8_t transmit_Buffer[8];

/* Variables for receive command. */
```

```c
uint8_t buffer[50];
uint8_t Voltage = 28;

/* Encoder control. */
int32_t Encoder_Pos = 0;
int32_t Virtual_Encoder_Pos;
float Encoder_Rads;
float To_Radians = (36000/(4096*GearRatio)) * 2 * PI / 36000;
float el_Angle = 0;

/* S-curve Position control. */
float array[3500];
float *Reference_Pos = array;
int16_t Array_Values = 0;

/* General position control. */
int32_t Ref = 0;
int32_t INC_Position = 0;
int32_t INC_PosTimeStep = 6000;

/* ADC variables. */
float current_A[20];
float current_B[20];
int8_t A_inc = 0;
int8_t B_inc = 0;

/* PID variables. */
float PID_Iq_u = 0;
float PID_Id_u = 0;
float PID_Pos_u = 0;
float PID_Vel_u = 0;

/* Error variables. */
float Iq_Error_1 = 0;
float Id_Error_1 = 0;
float Pos_Error_1 = 0;
float Vel_Error_1 = 0;

/* Global control loop variable.*/
float Theta_Position;

/* Structures. */
typedef struct
    {
        float Iq;
        float Id;
    } current_struct;

current_struct I;

typedef struct
    {
        float Ta;
        float Tb;
        float Tc;
    } spaceVector_struct;

    spaceVector_struct Space_Vector;

typedef struct
{
    int8_t state;
    int16_t Pos;
    int16_t Vel;
    int16_t Acc;
    int8_t Vref;
} Request_Vars;
```

```c
/* USER CODE END PV */

/* Private function prototypes -----------------------------------------------*/
void SystemClock_Config(void);
static void MX_GPIO_Init(void);
static void MX_DMA_Init(void);
static void MX_ADC1_Init(void);
static void MX_ADC2_Init(void);
static void MX_ADC3_Init(void);
static void MX_TIM4_Init(void);
static void MX_UART4_Init(void);
void HAL_TIM_MspPostInit(TIM_HandleTypeDef *htim);

/* USER CODE BEGIN PFP */
/* Private function prototypes -----------------------------------------------*/
void NVIC_Init(void);
void EXTI0_IRQHandler(void);
void EXTI1_IRQHandler(void);
uint8_t CALIBRATION(void);
uint8_t RECEIVE_SIGNAL(void);
void POSITION_INIT(Request_Vars);
float ADC_Poll_PhaseA(void);
float ADC_Average_PhaseA(void);
float ADC_Poll_PhaseB(void);
float ADC_Average_PhaseB(void);
float ADC_Poll_PhaseC(void);
float Calc_Error(float, float);
float PID_Pos(float, float, float);
float PID_Vel(float, float, float);
current_struct Clarke_Park_Trans(float, float, float, float);
float PID_IQ(float, float, float);
float PID_ID(float, float, float);
float MAGNITUDE(current_struct);
float ANTI_ZERO_PHASE(current_struct);
float ADD(float, float, float);
spaceVector_struct TIMING_CALC(float, float, float);
/* USER CODE END PFP */

/* USER CODE BEGIN 0 */
    /* Current measurement. */
    float ADC1_Val;
    float ADC2_Val;
    float ADC3_Val;

    /* Velocity. */
    float Velocity = 0.0f;
/* USER CODE END 0 */

int main(void)
{

  /* USER CODE BEGIN 1 */
/* Local variables -----------------------------------------------------------*/
    float Encoder_Rads_1 = 0;
    float PID_Position = 0;
    float PID_Velocity = 0;

    /* control loop variables. */
    float Voltage_Ref;
    float U_AntiZero;


    int INC_Velocity = 0;

    /* Counter for transmitting status. */
```

```c
      int TXCount = 0;
  /* USER CODE END 1 */

 /* MCU Configuration--------------------------------------------------------*/

 /* Reset of all peripherals, Initializes the Flash interface and the Systick. */
  HAL_Init();

  /* Configure the system clock */
  SystemClock_Config();

  /* Initialize all configured peripherals */
  MX_GPIO_Init();
  MX_DMA_Init();
  MX_ADC1_Init();
  MX_ADC2_Init();
  MX_ADC3_Init();
  MX_TIM4_Init();
  MX_UART4_Init();

  /* USER CODE BEGIN 2 */
    NVIC_Init();
    HAL_TIM_PWM_Start(&htim4, TIM_CHANNEL_1);
    HAL_TIM_PWM_Start(&htim4, TIM_CHANNEL_2);
    HAL_TIM_PWM_Start(&htim4, TIM_CHANNEL_3);
    HAL_ADC_Start(&hadc1);
    HAL_ADC_Start(&hadc2);

  /* USER CODE END 2 */

  /* Infinite loops */
  /* USER CODE BEGIN WHILE */

/*---------------------Main section for execution of code--------------------*/
    while(RECEIVE_SIGNAL())
    {

    }
  while (1)
  {
  /* USER CODE END WHILE */

  /* USER CODE BEGIN 3 */

/*---------------------------Listening for signal----------------------------*/
    RECEIVE_SIGNAL();

/*----------------S-curve position update and status transmit----------------*/
    INC_PosTimeStep++;
    /* Each 10th millisecond. */
    if(INC_PosTimeStep >= millis * 10)
    {
    /* Each second. */
    if(TXCount >= 100)
    {
        /* Prepare position and velocity for transfer. */
        txPos = Virtual_Encoder_Pos >= 0 ? (Virtual_Encoder_Pos*To_Radians*18000/PI):0;
        txVel = Velocity  >= 0 ? Velocity * 180/PI : abs(Velocity);

        /* Assign to buffer. */
        transmit_Buffer[0] = 0x45;
        transmit_Buffer[1] = 0x2;
        transmit_Buffer[2] = txPos>>8;
        transmit_Buffer[3] = txPos - (transmit_Buffer[2]<<8);
        transmit_Buffer[4] = txVel>>8;
        transmit_Buffer[5] = txVel - (transmit_Buffer[4]<<8);
        transmit_Buffer[6] = 0x0;
```

```c
    transmit_Buffer[7] = 0x0;

    /* If the system is not moving, assign idle state. */
    if(txVel <= 0)
        transmit_Buffer[1] = 0x0;

    /* If the system runs on the auto-generated S-curve, assign state. */
    if(INC_Position < Array_Values)
    {
        INC_Position++;
        Ref = Reference_Pos[INC_Position] * 10;
        transmit_Buffer[1] = 0x3;
    }
    /* Transmit. */
    HAL_UART_Transmit_IT(&huart4, transmit_Buffer, 8);
    TXCount = 0;
    }
    INC_PosTimeStep = 0;
    TXCount++;
    }

/*------------------Updating velocity every 10th millisecond------------------*/
    INC_Velocity++;
    if(INC_Velocity >= millis * 10)
    {
        Velocity =  (Encoder_Rads - Encoder_Rads_1) * 100;
        INC_Velocity = 0;
        Encoder_Rads_1 = Encoder_Rads;
    }

/*----------------------------Current feedback----------------------------*/
    ADC1_Val = ADC_Average_PhaseA();
    ADC2_Val = ADC_Average_PhaseB();
    ADC3_Val = -ADC1_Val - ADC2_Val;

/*----------------------------Encoder feedback----------------------------*/
    Encoder_Rads = (Encoder_Pos * To_Radians);
    el_Angle = Encoder_Rads * PolePairs * GearRatio;

/*----------------------------Perform calculations----------------------------*/


/*--------------------------PID_Pos(error, Kp, Ki)--------------------------*/
    PID_Position = PID_Pos(Calc_Error(Ref*PI/18000,Virtual_Encoder_Pos * To_Radians),150,0);

/*--------------------------PID_Vel(error, Kp, Ki)--------------------------*/
    PID_Velocity = PID_Vel(Calc_Error(PID_Position, Velocity),1, 0);

/*--------------Clarke_Park_Trans(Phase A, Phase B, Phase C, angle)----------*/
    I = Clarke_Park_Trans(ADC1_Val, ADC2_Val, ADC3_Val, el_Angle);

/*----------------------PID_ID(error(-error), Kp, Ki)----------------------*/
    I.Id = PID_ID(Calc_Error(-Calc_Error(PID_Velocity, I.Iq), I.Id), 1, 0.8f);

/*--------------------------PID_IQ(error, Kp, Ki)--------------------------*/
    I.Iq = PID_IQ(Calc_Error(PID_Velocity, I.Iq), 1, 0.8f);

/*----------------------Magnitude(Current ID and IQ)----------------------*/
    Voltage_Ref = MAGNITUDE(I);

/*--------------------Anti_Zero_Phase(Current ID and IQ)-------------------*/
    U_AntiZero = ANTI_ZERO_PHASE(I);

/*------------------------ADD(Anti zero, angle, PI)------------------------*/
    Theta_Position = ADD(U_AntiZero, el_Angle, PI);

/*------------------------Timing_Calc(Vref, V, angle)------------------------*/
```

```
        Space_Vector = TIMING_CALC(Voltage_Ref, Voltage, Theta_Position);

/*-------------------------------PWM output--------------------------------*/
        TIM4->CCR1 = (Space_Vector.Ta + 0.37f)*1137.8f;
        TIM4->CCR2 = (Space_Vector.Tb + 0.37f)*1137.8f;
        TIM4->CCR3 = (Space_Vector.Tc + 0.37f)*1137.8f;
    }
    /* USER CODE END 3 */
}

/* System Clock Configuration */
void SystemClock_Config(void)
{

  RCC_OscInitTypeDef RCC_OscInitStruct;
  RCC_ClkInitTypeDef RCC_ClkInitStruct;

    __HAL_RCC_PWR_CLK_ENABLE();

    __HAL_PWR_VOLTAGESCALING_CONFIG(PWR_REGULATOR_VOLTAGE_SCALE1);

  RCC_OscInitStruct.OscillatorType = RCC_OSCILLATORTYPE_HSE;
  RCC_OscInitStruct.HSEState = RCC_HSE_ON;
  RCC_OscInitStruct.PLL.PLLState = RCC_PLL_ON;
  RCC_OscInitStruct.PLL.PLLSource = RCC_PLLSOURCE_HSE;
  RCC_OscInitStruct.PLL.PLLM = 4;
  RCC_OscInitStruct.PLL.PLLN = 168;
  RCC_OscInitStruct.PLL.PLLP = RCC_PLLP_DIV2;
  RCC_OscInitStruct.PLL.PLLQ = 4;
  HAL_RCC_OscConfig(&RCC_OscInitStruct);

  RCC_ClkInitStruct.ClockType = RCC_CLOCKTYPE_HCLK|RCC_CLOCKTYPE_SYSCLK
                              |RCC_CLOCKTYPE_PCLK1|RCC_CLOCKTYPE_PCLK2;
  RCC_ClkInitStruct.SYSCLKSource = RCC_SYSCLKSOURCE_PLLCLK;
  RCC_ClkInitStruct.AHBCLKDivider = RCC_SYSCLK_DIV1;
  RCC_ClkInitStruct.APB1CLKDivider = RCC_HCLK_DIV4;
  RCC_ClkInitStruct.APB2CLKDivider = RCC_HCLK_DIV2;
  HAL_RCC_ClockConfig(&RCC_ClkInitStruct, FLASH_LATENCY_5);

  HAL_SYSTICK_Config(HAL_RCC_GetHCLKFreq()/1000);

  HAL_SYSTICK_CLKSourceConfig(SYSTICK_CLKSOURCE_HCLK);

  /* SysTick_IRQn interrupt configuration */
  HAL_NVIC_SetPriority(SysTick_IRQn, 0, 0);
}

/* ADC1 init function */
void MX_ADC1_Init(void)
{

  ADC_ChannelConfTypeDef sConfig;


  hadc1.Instance = ADC1;
  hadc1.Init.ClockPrescaler = ADC_CLOCK_SYNC_PCLK_DIV2;
  hadc1.Init.Resolution = ADC_RESOLUTION_12B;
  hadc1.Init.ScanConvMode = ENABLE;
  hadc1.Init.ContinuousConvMode = ENABLE;
  hadc1.Init.DiscontinuousConvMode = DISABLE;
  hadc1.Init.ExternalTrigConvEdge = ADC_EXTERNALTRIGCONVEDGE_NONE;
  hadc1.Init.DataAlign = ADC_DATAALIGN_RIGHT;
  hadc1.Init.NbrOfConversion = 1;
  hadc1.Init.DMAContinuousRequests = ENABLE;
  hadc1.Init.EOCSelection = ADC_EOC_SEQ_CONV;
  HAL_ADC_Init(&hadc1);
```

```c
  sConfig.Channel = ADC_CHANNEL_10;
  sConfig.Rank = 1;
  sConfig.SamplingTime = ADC_SAMPLETIME_3CYCLES;
  HAL_ADC_ConfigChannel(&hadc1, &sConfig);

}

/* ADC2 init function */
void MX_ADC2_Init(void)
{

  ADC_ChannelConfTypeDef sConfig;


  hadc2.Instance = ADC2;
  hadc2.Init.ClockPrescaler = ADC_CLOCK_SYNC_PCLK_DIV2;
  hadc2.Init.Resolution = ADC_RESOLUTION_12B;
  hadc2.Init.ScanConvMode = ENABLE;
  hadc2.Init.ContinuousConvMode = ENABLE;
  hadc2.Init.DiscontinuousConvMode = DISABLE;
  hadc2.Init.ExternalTrigConvEdge = ADC_EXTERNALTRIGCONVEDGE_NONE;
  hadc2.Init.DataAlign = ADC_DATAALIGN_RIGHT;
  hadc2.Init.NbrOfConversion = 1;
  hadc2.Init.DMAContinuousRequests = ENABLE;
  hadc2.Init.EOCSelection = ADC_EOC_SEQ_CONV;
  HAL_ADC_Init(&hadc2);


  sConfig.Channel = ADC_CHANNEL_11;
  sConfig.Rank = 1;
  sConfig.SamplingTime = ADC_SAMPLETIME_3CYCLES;
  HAL_ADC_ConfigChannel(&hadc2, &sConfig);

}

/* ADC3 init function */
void MX_ADC3_Init(void)
{

  ADC_ChannelConfTypeDef sConfig;


  hadc3.Instance = ADC3;
  hadc3.Init.ClockPrescaler = ADC_CLOCK_SYNC_PCLK_DIV2;
  hadc3.Init.Resolution = ADC_RESOLUTION_12B;
  hadc3.Init.ScanConvMode = ENABLE;
  hadc3.Init.ContinuousConvMode = ENABLE;
  hadc3.Init.DiscontinuousConvMode = DISABLE;
  hadc3.Init.ExternalTrigConvEdge = ADC_EXTERNALTRIGCONVEDGE_NONE;
  hadc3.Init.DataAlign = ADC_DATAALIGN_RIGHT;
  hadc3.Init.NbrOfConversion = 1;
  hadc3.Init.DMAContinuousRequests = ENABLE;
  hadc3.Init.EOCSelection = ADC_EOC_SEQ_CONV;
  HAL_ADC_Init(&hadc3);


  sConfig.Channel = ADC_CHANNEL_12;
  sConfig.Rank = 1;
  sConfig.SamplingTime = ADC_SAMPLETIME_3CYCLES;
  HAL_ADC_ConfigChannel(&hadc3, &sConfig);

}

/* TIM4 init function */
void MX_TIM4_Init(void)
{
```

```c
  TIM_MasterConfigTypeDef sMasterConfig;
  TIM_OC_InitTypeDef sConfigOC;

  htim4.Instance = TIM4;
  htim4.Init.Prescaler = 1;
  htim4.Init.CounterMode = TIM_COUNTERMODE_UP;
  htim4.Init.Period = 2048;
  htim4.Init.ClockDivision = TIM_CLOCKDIVISION_DIV1;
  HAL_TIM_PWM_Init(&htim4);

  sMasterConfig.MasterOutputTrigger = TIM_TRGO_RESET;
  sMasterConfig.MasterSlaveMode = TIM_MASTERSLAVEMODE_DISABLE;
  HAL_TIMEx_MasterConfigSynchronization(&htim4, &sMasterConfig);

  sConfigOC.OCMode = TIM_OCMODE_PWM1;
  sConfigOC.Pulse = 0;
  sConfigOC.OCPolarity = TIM_OCPOLARITY_HIGH;
  sConfigOC.OCFastMode = TIM_OCFAST_DISABLE;
  HAL_TIM_PWM_ConfigChannel(&htim4, &sConfigOC, TIM_CHANNEL_1);

  HAL_TIM_PWM_ConfigChannel(&htim4, &sConfigOC, TIM_CHANNEL_2);

  HAL_TIM_PWM_ConfigChannel(&htim4, &sConfigOC, TIM_CHANNEL_3);

  HAL_TIM_MspPostInit(&htim4);

}

/* UART4 init function */
void MX_UART4_Init(void)
{

  huart4.Instance = UART4;
  huart4.Init.BaudRate = 64000;
  huart4.Init.WordLength = UART_WORDLENGTH_8B;
  huart4.Init.StopBits = UART_STOPBITS_1;
  huart4.Init.Parity = UART_PARITY_NONE;
  huart4.Init.Mode = UART_MODE_TX_RX;
  huart4.Init.HwFlowCtl = UART_HWCONTROL_NONE;
  huart4.Init.OverSampling = UART_OVERSAMPLING_16;
  HAL_UART_Init(&huart4);

}

/* Enable DMA controller clock */
void MX_DMA_Init(void)
{
  /* DMA controller clock enable */
  __HAL_RCC_DMA2_CLK_ENABLE();

  /* DMA interrupt init */
  /* DMA2_Stream0_IRQn interrupt configuration */
  HAL_NVIC_SetPriority(DMA2_Stream0_IRQn, 0, 0);
  HAL_NVIC_EnableIRQ(DMA2_Stream0_IRQn);
  /* DMA2_Stream1_IRQn interrupt configuration */
  HAL_NVIC_SetPriority(DMA2_Stream1_IRQn, 0, 0);
  HAL_NVIC_EnableIRQ(DMA2_Stream1_IRQn);
  /* DMA2_Stream2_IRQn interrupt configuration */
  HAL_NVIC_SetPriority(DMA2_Stream2_IRQn, 0, 0);
  HAL_NVIC_EnableIRQ(DMA2_Stream2_IRQn);

}

/** Configure pins as
        * Analog
        * Input
```

```
        * Output
        * EVENT_OUT
        * EXTI
*/
void MX_GPIO_Init(void)
{

  GPIO_InitTypeDef GPIO_InitStruct;

  /* GPIO Ports Clock Enable */
  __HAL_RCC_GPIOH_CLK_ENABLE();
  __HAL_RCC_GPIOC_CLK_ENABLE();
  __HAL_RCC_GPIOA_CLK_ENABLE();
  __HAL_RCC_GPIOD_CLK_ENABLE();
  __HAL_RCC_GPIOB_CLK_ENABLE();
  __HAL_RCC_GPIOE_CLK_ENABLE();

  /* Configure GPIO pins : PB3 PB4 PB5 PB6 */
  GPIO_InitStruct.Pin = GPIO_PIN_3|GPIO_PIN_4|GPIO_PIN_5|GPIO_PIN_6;
  GPIO_InitStruct.Mode = GPIO_MODE_INPUT;
  GPIO_InitStruct.Pull = GPIO_NOPULL;
  HAL_GPIO_Init(GPIOB, &GPIO_InitStruct);

  /* Configure GPIO pins : PE0 PE1 */
  GPIO_InitStruct.Pin = GPIO_PIN_0|GPIO_PIN_1;
  GPIO_InitStruct.Mode = GPIO_MODE_IT_RISING_FALLING;
  GPIO_InitStruct.Pull = GPIO_PULLDOWN;
  HAL_GPIO_Init(GPIOE, &GPIO_InitStruct);

}

/* USER CODE BEGIN 4 */
/*----------------------------Custom functions-----------------------------*/

/*-------------------------------Calibration-------------------------------*/
uint8_t CALIBRATION(void)
{
    /* Force a zero-position. */
    TIM4->CCR1 = 1816;
    TIM4->CCR2 = 280;
    TIM4->CCR3 = 280;

    /* Clear position array. */
    for(int i = 0; i<3500; i++)
    {
        Reference_Pos[i] = 0;
    }

    /* Reset transmit buffer. */
    for(int i = 0; i<8; i++)
    {
        transmit_Buffer[i] = 0x0;
    }

    Ref = 0;
    HAL_Delay(500);
    Encoder_Pos = 60;

    /* Initializing calibration variables. */
    int Cal_Count = 0;
    int Encoder_Pos_2;
    int Calibrated = 0;
    int txCount = 0;

    while(!Calibrated)
    {
        Encoder_Rads = (Encoder_Pos * To_Radians);
```

```c
        el_Angle = Encoder_Rads * PolePairs * GearRatio;

        Theta_Position = ADD(-0.6f, el_Angle, PI);

        Space_Vector = TIMING_CALC(6, Voltage, Theta_Position);

        TIM4->CCR1 = (Space_Vector.Ta+0.4f)*1137.8f;
        TIM4->CCR2 = (Space_Vector.Tb+0.4f)*1137.8f;
        TIM4->CCR3 = (Space_Vector.Tc+0.4f)*1137.8f;

        /* Transmit status and check if the mechanism has stopped. */
        Cal_Count++;
        if(Cal_Count >= millis * 100)//100 ms
        {
            /* Transmit. */
            if(txCount >= 10)// 1000 ms
            {
                txPos = Encoder_Pos >= 0 ? (Encoder_Pos*To_Radians*36000/(2*PI)):0;
                transmit_Buffer[0] = 0x45;
                transmit_Buffer[1] = 0x1;
                transmit_Buffer[2] = txPos>>8;
                transmit_Buffer[3] = txPos - (transmit_Buffer[2]<<8);
                transmit_Buffer[4] = 0x0;
                transmit_Buffer[5] = 0x0;
                transmit_Buffer[6] = 0x0;
                transmit_Buffer[7] = 0x0;
                HAL_UART_Transmit_IT(&huart4, transmit_Buffer, 8);
            }
            /* Check if the mechanism has stopped. if so, set zero-position. */
            Cal_Count = 0;
            if(Encoder_Pos == Encoder_Pos_2)
                {
                    Calibrated = 1;
                    Virtual_Encoder_Pos = 0;
                }
                else
                    {
                        Encoder_Pos_2 = Encoder_Pos;
                    }
        }
        transmit_Buffer[1] = 0x0;
        HAL_UART_Transmit_IT(&huart4, transmit_Buffer, 8);
        return 0;
}

/*-----------------------------Receive signal-------------------------------*/
uint8_t RECEIVE_SIGNAL(void)
{
    Request_Vars R;
    int BYT_Start = 0x45;

    /* check if received a command from spacecraft. */
    if(HAL_UART_Receive_IT(&huart4, buffer, 8) == HAL_OK)
        {
        if(buffer[0] == BYT_Start)
        {
            R.state = buffer[1];
            R.Pos = (buffer[2]<<8) + buffer[3];
            R.Vel = (buffer[4]<<8) + buffer[5];
            R.Acc =  buffer[6];
            R.Vref = buffer[7];

            /* Calibrate. */
            if(R.state == 1)
            {
                    CALIBRATION();
```

```
                return 0;
            }
            /* Manual position. */
            if(R.state == 2)
            {
                Ref = R.Pos + 18000;
                Voltage = R.Vref;
            }
            /* S-Curve. */
            if(R.state == 3)
            {
                POSITION_INIT(R);
                Voltage = R.Vref;
            }
        }
    }
    return 1;

}

/*----------------------------Position S-Curve----------------------------*/
void POSITION_INIT(Request_Vars Request)
{
    float millis_Update = 0.1f;
    INC_Position = 0;
    INC_PosTimeStep = 0;

    /* Variables sent from spacecraft. */
    int32_t pos_Req = Request.Pos + 1800;
    float max_Vel = Request.Vel * millis_Update * 1;
    float acc = Request.Acc * millis_Update * 0.1f;

        /* Initialize some vars. */
    int32_t start_Pos = (Virtual_Encoder_Pos) / 10 * (36000/(4096*GearRatio));
    int32_t inc = 1;
    float T2;
    int16_t k;
    Reference_Pos[0] = start_Pos;
    Reference_Pos[1] = start_Pos;

    while
(fabsl(Reference_Pos[inc] - Reference_Pos[inc-1]) <= max_Vel * millis_Update &&
((pos_Req - start_Pos >= 0 && Reference_Pos[inc] <= (pos_Req - start_Pos)/2) ||
(pos_Req - start_Pos <  0 && Reference_Pos[inc] >= (start_Pos - (start_Pos - pos_Req)/2))))
    {
        Reference_Pos[inc+1] = pos_Req - start_Pos >= 0 ?
        Reference_Pos[inc]+0.5f*acc*((millis_Update*(inc+1))*(millis_Update *(inc+1))):
        Reference_Pos[inc]-0.5f*acc*((millis_Update*(inc+1))*(millis_Update *(inc+1)));
        inc++;
    }

    T2 = Reference_Pos[inc];
    k = inc;

    while
((pos_Req - start_Pos > 0 && Reference_Pos[inc] <= pos_Req - fabsl(T2) )||
(  pos_Req - start_Pos < 0 && Reference_Pos[inc] - pos_Req >= start_Pos - fabsl(T2)))
    {
        Reference_Pos[inc+1] = pos_Req - start_Pos >= 0 ?
        Reference_Pos[inc] + max_Vel * millis_Update:
        Reference_Pos[inc] - max_Vel * millis_Update;
        inc++;
    }

    while(k > 0)
    {
        Reference_Pos[inc+1] = pos_Req - start_Pos >= 0 ?
```

```c
            Reference_Pos[inc] + 0.5f * acc * ((millis_Update * (k-1) ) * (millis_Update * (k-1) )):
            Reference_Pos[inc] - 0.5f * acc * ((millis_Update * (k-1) ) * (millis_Update * (k-1) ));
        inc++;
        k--;
    }

    /* Secure correction algorithm. */
    float diff = pos_Req - Reference_Pos[inc];
    for(int i=0; i<10; i++)
    {
        Reference_Pos[inc+1] = Reference_Pos[inc] + 0.1f * diff;
        inc++;
    }
    /* Tells how many steps to count in the main loop. */
    Array_Values = inc-1;
}

/*--------------------Nested Vector Interrupt Controller--------------------*/
void NVIC_Init(void)
{
    HAL_NVIC_SetPriorityGrouping(NVIC_PRIORITYGROUP_1);
  HAL_NVIC_SetPriority(EXTI0_IRQn, 0, 0);
  HAL_NVIC_EnableIRQ(EXTI0_IRQn);

    HAL_NVIC_SetPriorityGrouping(NVIC_PRIORITYGROUP_2);
  HAL_NVIC_SetPriority(EXTI1_IRQn, 0, 0);
  HAL_NVIC_EnableIRQ(EXTI1_IRQn);
}

/*----------------------------Interrupt pin A----------------------------*/
void EXTI0_IRQHandler(void)//A
{
  HAL_NVIC_ClearPendingIRQ(EXTI0_IRQn);
    //disabled IRQHandler in the HAL_GPIO C file.
  {
  /*EXTI line interrupt detected */
  if(__HAL_GPIO_EXTI_GET_IT(GPIO_PIN_0) != RESET)
  {
        if(HAL_GPIO_ReadPin(GPIOE, GPIO_PIN_0))
            {
                if(!HAL_GPIO_ReadPin(GPIOE, GPIO_PIN_1)){Encoder_Pos++; Virtual_Encoder_Pos++;}
                if(HAL_GPIO_ReadPin(GPIOE, GPIO_PIN_1)){Encoder_Pos--; Virtual_Encoder_Pos--;}
            }
        if(!HAL_GPIO_ReadPin(GPIOE, GPIO_PIN_0))
            {
                if(HAL_GPIO_ReadPin(GPIOE, GPIO_PIN_1)){Encoder_Pos++; Virtual_Encoder_Pos++;}
                if(!HAL_GPIO_ReadPin(GPIOE, GPIO_PIN_1)){Encoder_Pos--; Virtual_Encoder_Pos--;}
            }
    __HAL_GPIO_EXTI_CLEAR_IT(GPIO_PIN_0);
    HAL_GPIO_EXTI_Callback(GPIO_PIN_0);
        }
    }
}
/*----------------------------Interrupt pin B----------------------------*/
void EXTI1_IRQHandler(void)//B
{
  HAL_NVIC_ClearPendingIRQ(EXTI1_IRQn);
    //disabled IRQHandler in the HAL_GPIO C file.
  {
    /*EXTI line interrupt detected */
    if(__HAL_GPIO_EXTI_GET_IT(GPIO_PIN_1) != RESET)
  {
        if(HAL_GPIO_ReadPin(GPIOE, GPIO_PIN_1))
            {
                if(HAL_GPIO_ReadPin(GPIOE, GPIO_PIN_0)){Encoder_Pos++; Virtual_Encoder_Pos++;}
                if(!HAL_GPIO_ReadPin(GPIOE, GPIO_PIN_0)){Encoder_Pos--; Virtual_Encoder_Pos--;}
            }
```

```c
        if(!HAL_GPIO_ReadPin(GPIOE, GPIO_PIN_1))
            {
                if(HAL_GPIO_ReadPin(GPIOE, GPIO_PIN_0)){Encoder_Pos--; Virtual_Encoder_Pos--;}
                if(!HAL_GPIO_ReadPin(GPIOE, GPIO_PIN_0)){Encoder_Pos++; Virtual_Encoder_Pos++;}
            }
    __HAL_GPIO_EXTI_CLEAR_IT(GPIO_PIN_1);
    HAL_GPIO_EXTI_Callback(GPIO_PIN_1);
        }
    }
}

/*----------------------------Error calculations----------------------------*/
float Calc_Error(float Reference, float Difference)
{
    return Reference - Difference;
}

/*------------------------PI regulator for position------------------------*/
float PID_Pos(float Error, float Kp, float Ki)
{
    PID_Pos_u = PID_Pos_u + Kp * Error + (Ki * Clock_Time - Kp) * Pos_Error_1;
    Pos_Error_1 = Error;
    return PID_Pos_u;
}

/*------------------------PI regulator for velocity------------------------*/
float PID_Vel(float Error, float Kp, float Ki)
{
    PID_Vel_u = PID_Vel_u + Kp * Error + (Ki * Clock_Time - Kp) * Vel_Error_1;
    Vel_Error_1 = Error;
    return PID_Vel_u;
}

/*------------------------Polling for phase A current------------------------*/
float ADC_Poll_PhaseA(void)
{
    if (HAL_ADC_PollForConversion(&hadc1, 1) == HAL_OK)
    {
      return ((Input_Current * 2 / 4096.0f) * HAL_ADC_GetValue(&hadc1)) - Input_Current;
    }return 0;
}
/*------------------------Average for phase A current------------------------*/
float ADC_Average_PhaseA(void)
{
    float final_Val = 0;
    int n = 20;
    float current = ADC_Poll_PhaseA();

    //fill up on first run
    if(current_A[n-1] == 0)
            for(int z = 0; z < n; z++)
                current_A[z] = current;

    //assign variable to a place in the array
    current_A[A_inc] = current;

    //add all values together
    for(int y = 0; y< n; y++)
    final_Val += current_A[y];

    A_inc++;

    if(A_inc>=n)
        A_inc=0;

    //return total value divided by amount
    return final_Val/n;
```

```c
}

/*------------------------Polling for phase B current-----------------------*/
float ADC_Poll_PhaseB(void)
{
    if (HAL_ADC_PollForConversion(&hadc2, 1) == HAL_OK)
    {
      return ((Input_Current * 2 / 4096.0f) * HAL_ADC_GetValue(&hadc2)) - Input_Current;
       }return 0;
}

/*------------------------Average for phase B current-----------------------*/
float ADC_Average_PhaseB(void)
{
    float final_Val = 0;
    int n = 20;
    float current = ADC_Poll_PhaseB();

    //fill up on first run
    if(current_B[n-1] == 0)
            for(int z = 0; z < n; z++)
                current_B[z] = current;
        //assign variable to a place in the array
    current_B[B_inc] = current;

    //add all values together
    for(int y = 0; y< n; y++)
    final_Val += current_B[y];

    B_inc++;
    if(B_inc>=n)B_inc=0;

    //return total value divided by amount
    return final_Val / n;
}

/*-----------------------Clarke & Park transformation-----------------------*/
 current_struct Clarke_Park_Trans(float Ia, float Ib, float Ic, float el_angle)
{
    current_struct output;

    float alpha = (2.0f/3.0f * (Ia - 0.5f * Ib - 0.5f * Ic));
    float beta = (2.0f/3.0f * sqrtf(3.0f)/2.0f * (Ib - Ic));

    output.Iq = cosf(el_Angle) * alpha + sinf(el_Angle) * beta;
    output.Id = sinf(el_angle) * alpha - cosf(el_angle) * beta;

    return output;

}

/*------------------------PI regulator for Current IQ-----------------------*/
float PID_IQ(float Error, float Kp, float Ki)
{

    PID_Iq_u = PID_Iq_u + Kp * Error + (Ki * Clock_Time - Kp) * Iq_Error_1;
    Iq_Error_1 = Error;
    return PID_Iq_u;
}

/*------------------------PI regulator for Current ID-----------------------*/
float PID_ID(float Error, float Kp, float Ki)
{
    PID_Id_u = PID_Id_u + Kp * Error + (Ki * Clock_Time - Kp) * Id_Error_1;
    Id_Error_1 = Error;
    return PID_Id_u;
}
```

```c
/*-----------------------Calculating current magnitude----------------------*/
float MAGNITUDE(current_struct current)
{
    if (sqrtf((current.Iq)*(current.Iq) + (current.Id)*(current.Id)) >= Voltage)
        return Voltage;
    else
        return sqrtf((current.Iq)*(current.Iq) + (current.Id)*(current.Id));
}

/*---------------------Calculating anti-zero phase shift--------------------*/
float ANTI_ZERO_PHASE(current_struct current)
{
    if(current.Id > 0) return atanf(current.Iq / current.Id);
    else if(current.Id <0)  return PI + atanf(current.Iq / current.Id);
    else return PI/2;
}

/*---------------Add anti zero-phase, electric angle and pi/2----------------*/
float ADD(float PhaseShift, float angle, float pi)
{
    return PhaseShift + angle - pi/2;
}

/*---------------------Calculate the Space Vector values--------------------*/
spaceVector_struct TIMING_CALC(float V_Ref, float V_DC, float Pos_Theta)
{
    /* Theta position. */
    float a = Pos_Theta / (2.0f*PI);
    float b = floorf(a);
    float c = Pos_Theta - 2.0f * PI * b;
    float d = c / (PI / 3.0f);
    float e = floorf(d);

    /* Output. */
    float Angle = c - e * PI / 3.0f;
    int Sector = e + 1.0f;

    /* Velocity. */
    float V = V_Ref / V_DC;

    /* calc. */
    float A = V * sqrtf(3.0f) * sinf((PI / 3.0f) - Angle);
    float B = V * sqrtf(3.0f) * sinf(Angle);
    float C = (1 - A - B) / 2.0f;

    /* Assign sector values. */
    spaceVector_struct SV;

    if(Sector == 1){SV.Ta = A+B+C;  SV.Tb = B+C;        SV.Tc = C;      }
    if(Sector == 2){SV.Ta = A+C;     SV.Tb = A+B+C;      SV.Tc = C;      }
    if(Sector == 3){SV.Ta = C;       SV.Tb = A+B+C;      SV.Tc = B+C;   }
    if(Sector == 4){SV.Ta = C;       SV.Tb = A+C;        SV.Tc = A+B+C;}
    if(Sector == 5){SV.Ta = B+C;     SV.Tb = C;          SV.Tc = A+B+C;}
    if(Sector == 6){SV.Ta = A+B+C;   SV.Tb = C;          SV.Tc = A+C;  }

    return SV;
}

/* USER CODE END 4 */

#ifdef USE_FULL_ASSERT

/**
  * @brief Reports the name of the source file and the source line number
  * where the assert_param error has occurred.
  * @param file: pointer to the source file name
```

```c
   * @param line: assert_param error line source number
   * @retval None
   */
void assert_failed(uint8_t* file, uint32_t line)
{

}

#endif

/**
  * @}
  */

/**
  * @}
*/

/*********************** (C) COPYRIGHT STMicroelectronics *****END OF FILE****/
```

7.4. Antenna Trade-off: Matlab-scripts

Table 7. 4. 1: Cassegrain antenna calculations

```matlab
%% Cassegrain antenna design
clc
clear all
close all

%% Input parameters

% Main-reflector parameters:
%Diameter(m)
Dm = 0.11;
%Depth(m)
dm = 0.018;
%Focal length(m)
Fm = Dm^2/(16*dm)
%Subtended angle
theta_m = 2*atand(0.25*Dm/Fm)

% Sub-reflector parameters:
%Diameter(m)
Ds = 0.02245
%Substended angle:
theta_s = 30;

% Waveguide parameters:
%Diameter:
Dw = 0.01006;

% Signal wavelength(m)
f = 23e9; %Hz
lambda = (3*10^8)/f;


%% Plot: Focal length equivalent vs theta_s
x=linspace(15,35);
F_e=zeros(1,100);

for n=1:100
    F_e(n)= Dm/(4*tand(0.5*x(n)));
end
figure(1);
plot(x,F_e)
grid on
ylabel('Focal length equivalent, m','FontSize',16) % left y-axis
xlabel('Theta_s, degrees','FontSize',16);
title('Focal length equivalent vs angle','FontSize',16)
set(gca,'fontsize',16)

% Distance between focal point(main-reflector) and real focal point:
fs = 0.5*(cotd(theta_m)+cotd(theta_s))*Ds

% Focal lengtt of the equivalent reflector
Fe = Dm/(4*tand(0.5*theta_s));
%% Plot: Subreflector diameter vs. Fc (difference between the focal point,
% Fr and Fe)
```

```matlab
X =
(tand(theta_m)*tand(theta_s))/(2*tand(0.5*theta_m)*(tand(theta_m)+tand(theta_s)))

%F_c = D_s*Fm/(Dm*X);

figure(2);
syms('D_s')
ezplot(D_s*Fm/(Dm*X), [0.01 0.05])
grid on
xlabel('Subreflector diameter, m','FontSize',16)
ylabel('Difference between focal points(F og Fe), m','FontSize',16)
title('Subreflector diameter vs fs','FontSize',16)
set(gca,'fontsize',16)

%% Antenna efficiency
% Approximation for the combination of blockage and diffraction losses

% Edge taper:
et = 20*log10((cosd(theta_m/2))^2) %edge taper, dB
E = 10^(et/10) %edge taper

% Efficiency constant,n:
Cb = (-log(sqrt(E)))/(1-sqrt(E))
n = (1-Cb*(1+4*sqrt(1-Ds/Dm))*(Ds/Dm)^2)^2
L = 10*log10(n);

% Plot:Antenna efficiency vs subreflector diameter
figure(3);
syms('D_s')
ezplot((1-Cb*(1+4*sqrt(1-D_s/Dm))*(D_s/Dm)^2)^2, [0.005 0.04])
grid on
xlabel('Sub-reflector diameter, m','FontSize',16)
ylabel('Efficiency, n','FontSize',16)
title('Sub-reflector diameter vs. efficiency','FontSize',16)
set(gca,'fontsize',16)

% Plot:Antenna efficiency(dB) vs subreflector diameter
figure(4);
syms('D_s')
ezplot(10*log10((1-Cb*(1+4*sqrt(1-D_s/Dm))*(D_s/Dm)^2)^2), [0.005 0.04])
grid on
xlabel('Sub-reflector diameter, m','FontSize',16)
ylabel('Loss, dB','FontSize',16)
title('Sub-reflector diameter vs. losses(dB)','FontSize',16)
set(gca,'fontsize',16)
%% Far field

% Far field definiton:
R = (2*Dw^2)/lambda

% Effective feed
ef = 1/(4*tand(0.5*theta_s))
% Magnetification factor
M = ef/(Fm/Dm)
% Eccentricity
e = (M+1)/(M-1)
```

```matlab
c = fs/2
a = c/e
0.
ds = (c-a)- (Ds/2)/(tand(theta_m));

% Sub-reflector position in the field
R2 = a+c


%% Optimum size of the sub-reflector
Dso = Dm*(((cosd(theta_s/2))^4)/(4*pi^2*sind(theta_m))*E*(lambda/Dm))^(1/5)

%%
Ls = 0.5*(1-(sind(0.5*(theta_m-theta_s)))/(sind(0.5*(theta_m+theta_s))))*fs
R3 = c-a

Lr = fs-Ls;
%% Ratio tests

% Test 1
r1 = (Ds/Dm)/(fs/Fm)
r2 =
(tand(theta_m)*tand(theta_s))/(2*tand(0.5*theta_m)*(tand(theta_m)+tand(theta_s)))

% Test 2
r3 = Fe/Fm;
r4 = Lr/Ls;
r5 = tand(0.5*theta_m)/tand(0.5*theta_s);

%% Gain
 n1 = 0.55; %Efficiency constant
G = 10*log10(((pi*Dm/lambda)^2)*n1)

syms x
figure;
ezplot(10*log10(((pi*x/(lambda))^2)*n1),[0,0.9])
grid on;
title('Antenna gain vs diameter','FontSize',20);
ylabel('Gain, dBi','FontSize',16);
xlabel('Diameter, m','FontSize',16);
set(gca,'fontsize',16)
```

Table 7. 4. 2: Optimum horn calculations

```matlab
%% Optimum conical horn calculations [1]
clc
clear all
close all

% Length
l = 0.22
%l = 0.004
% freq
```

```
f = 23e9
% speed of light
c = 3e8
% Wavelength
lambda = c/f
% Diameter (optimum horn)
d = sqrt(3*l*lambda)
% depth
depth = sqrt(l^2-(0.5*d)^2)
% Circumference
C = pi*d
% Maximum phase deviation
s = (d^2)/(8*lambda*l)
% loss
L = (0.8-1.71*s+26.25*s^2-17.79*s^3)

% Gain
G = 10*log10((C/lambda)^2) - L

%% Corrugated horn in [2], approximate
% Original diameter
d_o = 0.0947
% Original depth
depth_o = 0.1704

% diameter
%d_2 = 0.1
d_2 = 0.013
% Approximate depth based on the d/depth relationships in [2]
depth_2 = (d_o*depth_o)/d_2

% Approximate length
length_2 = sqrt(d_2^2 + depth_2^2)
% Gain based on aperture area for the corrugated horn in[2] using an efficiency
of
% 0.45
G_2 = 10*log10((0.45*4*pi^2*(d_2/2)^2)/(lambda^2))


%% plot
% Length
syms 'l';
% Diameter (optimum horn)
d_1 = sqrt(3*l*lambda);

figure
ezplot(d_1,[0.001,0.40])
title('Horn diameter vs horn length','FontSize',20)
grid on
ylabel('Diameter, m','FontSize',16);
xlabel('Length, m','FontSize',16);
set(gca,'fontsize',16)

% depth
depth_1 = sqrt(l^2-0.5*d_1^2);

figure

ezplot(depth_1,[0.001,0.40]);
```

```matlab
title('Horn depth vs horn length','FontSize',20)
grid on
ylabel('Depth, m','FontSize',16);
xlabel('Length, m','FontSize',16);
set(gca,'fontsize',16)
% Circumfence
C_1 = pi*d_1;
% Maximum phase deviation in wavelengths
s_1 = (d_1^2)/(8*lambda*l);
% loss
L_1 = (0.8-1.71*s_1+26.25*s_1^2-17.79*s_1^3);
% Gain
G_1 = 10*log10((C_1/lambda)^2) - L_1;


figure
ezplot(G_1,[0.001,0.40])
title('Gain vs horn length','FontSize',20)
grid on
ylabel('Gain, dBi','FontSize',16);
xlabel('Length, m','FontSize',16);
set(gca,'fontsize',16)


%[1]C. A. Balanis, Antenna Theory Analysis and Design, pp 785
%[2]J. Teniente and C. del-Rio, "Astra 3B Horn Antenna Design", Grupo de
Antenas, Universidad Pública de Navarra, Campus Arrosadía s/n, 31006 Spain,
Available: http://antenas.unavarra.es/Publicaciones/Images/Pub347.pdf.
```

7.5. Part verification – real-life prototype

Table 7.5.1 contains an overview of the parts of the APMA and the corresponding part numbers:

Table 7. 5. 1: Part list

Part name	Part number
Main contact plate	10 001
Waveguide	10 002
Motor	10 003
Motor housing azimuth	10 004
Cap azimuth	10 005
Bearing house azimuth	10 006
2 x W6005	10 007
Gear azimuth	10 008
Connector	10 009
KMT 5 NUT	10 010
Parabola holder	10 101
Azimuth fishplate	10 102
Parabola	10 103
Sub reflector	10 104
3 x Struts	10 105
Elevation bracket	10 201
Gear elevation	10 202
Motor	10 203
Connector elevation	10 204
Contact mirror connector	10 205
Mirror elevation	10 206
Motor house elevation	10 207
2 x W6000	10 208
Mirror over azimuth	10 301
Cable trey	10 302

Explanation of table 7.5.2:

Part nr:

Note the part number in the list and engrave the part number on the part.

Date received:

Note the date the part was received in the list, and sign.

Date checked:

Note the date that the part was checked in the list, and sign.

Manufacturing errors:

If the part has no errors, enter N. If the part has errors, enter Y. A report, which focuses on these errors and how to fix them, will be made.

Cleaned:

Is the part cleaned, Y or N.

Table 7. 5. 2: Part verification

Part nr:	Rev	Date received:	By:	Manufacture errors (Y/N):	Cleaned (Y/N):	Date checked:	By:
10 001	1	29/4-16	MD	N	Y	30/4-16	MD
10 002	1	29/4-16	MD	Y	Y	30/4-16	MD
10 003	-	28/4-16	SL	N	Y	28/4-16	SL
10 004	1	29/4-16	MD	Y	Y	29/4-16	MD
10 005	1	29/4-16	MD	N	Y	30/4-16	MD
10 006	1	27/4-16	MD	N	Y	30/4-16	MD
4 x 10 007	-	25/4-16	VOA	N	N	25/4-16	VOA
10 008	1	02/5-16	VOA	N	N	02/5-16	VOA

10 009	1	29/4-16	MD	N	Y	30/4-16	MD
10 010	1	25/4-16	VOA	N	N	25/4-16	VOA
10 101	1	29/4-16	MD	N	Y	30/4-16	MD
10 102	1	29/4-16	MD	N	Y	30/4-16	MD
10 103	1	29/4-16	MD	Y	Y	30/4-16	MD
10 104	1	29/4-16	MD	N	Y	30/4-16	MD
3 x 10 105	1	29/4-16	MD	N	Y	30/4-16	MD
10 201	1	03/5-16	VOA	N	N	03/5-16	VOA
10 202	1	02/5-16	VOA	N	N	02/5-16	VOA
10 203	-	28/4-16	SL	N	Y	28/4-16	SL
10 204	1	03/5-16	VOA	N	N	03/5-16	VOA
10 205	1	03/5-16	VOA	N	N	03/5-16	VOA
10 206	1	03/5-16	VOA	N	N	03/5-16	VOA
10 207	1	25/4-16	MD	N	N	25/4-16	MD
2 x 10 208	-	25/4-16	VOA	N	N	25/4-16	VOA
10 301	1	03/5-16	VOA	N	N	03/5-16	VOA
10 302	1	25/4-16	VOA	N	N	25/4-16	VOA

7.6. Test fixtures

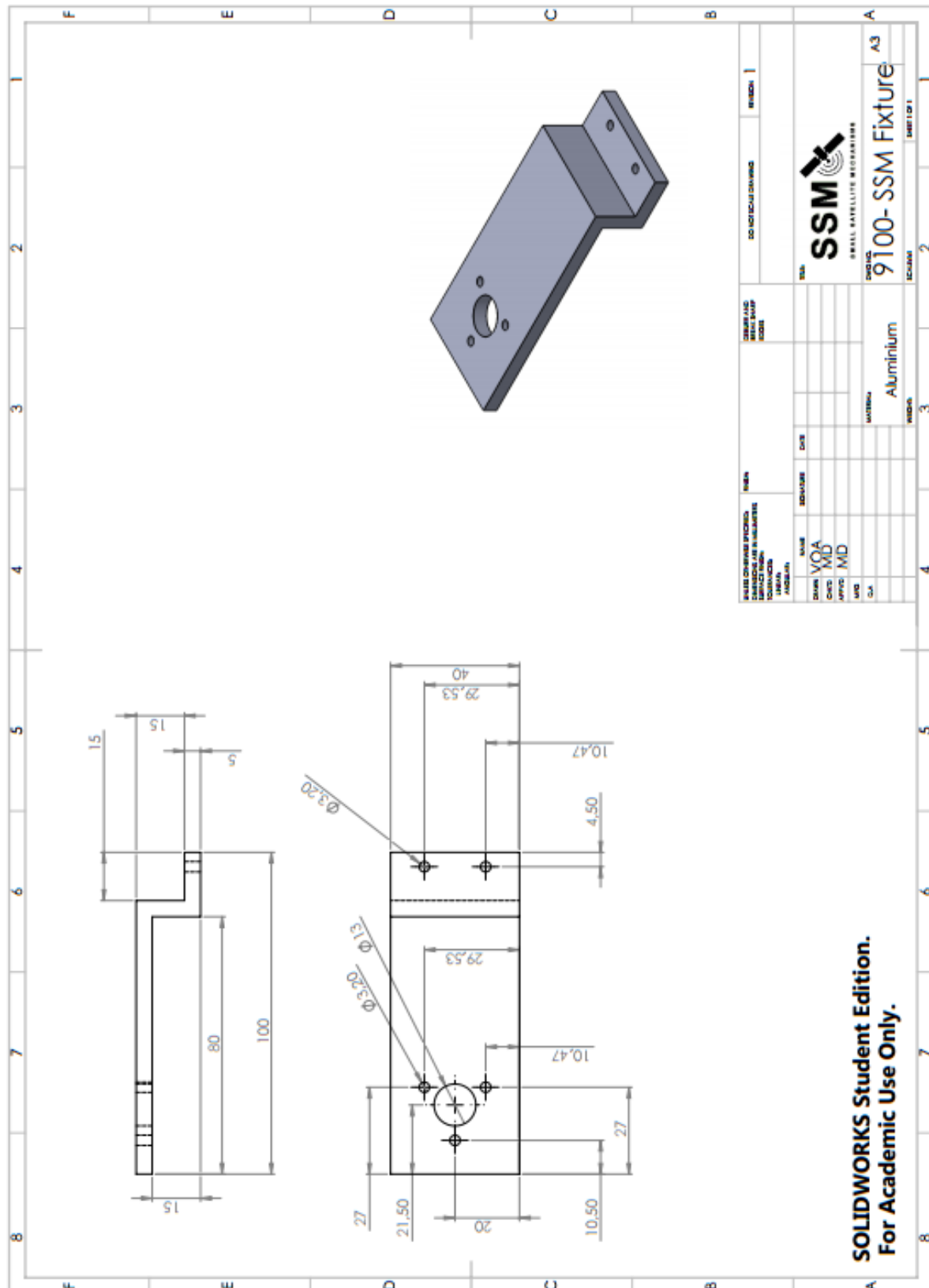*Figure 7. 6. 1: Test fixture 9000*
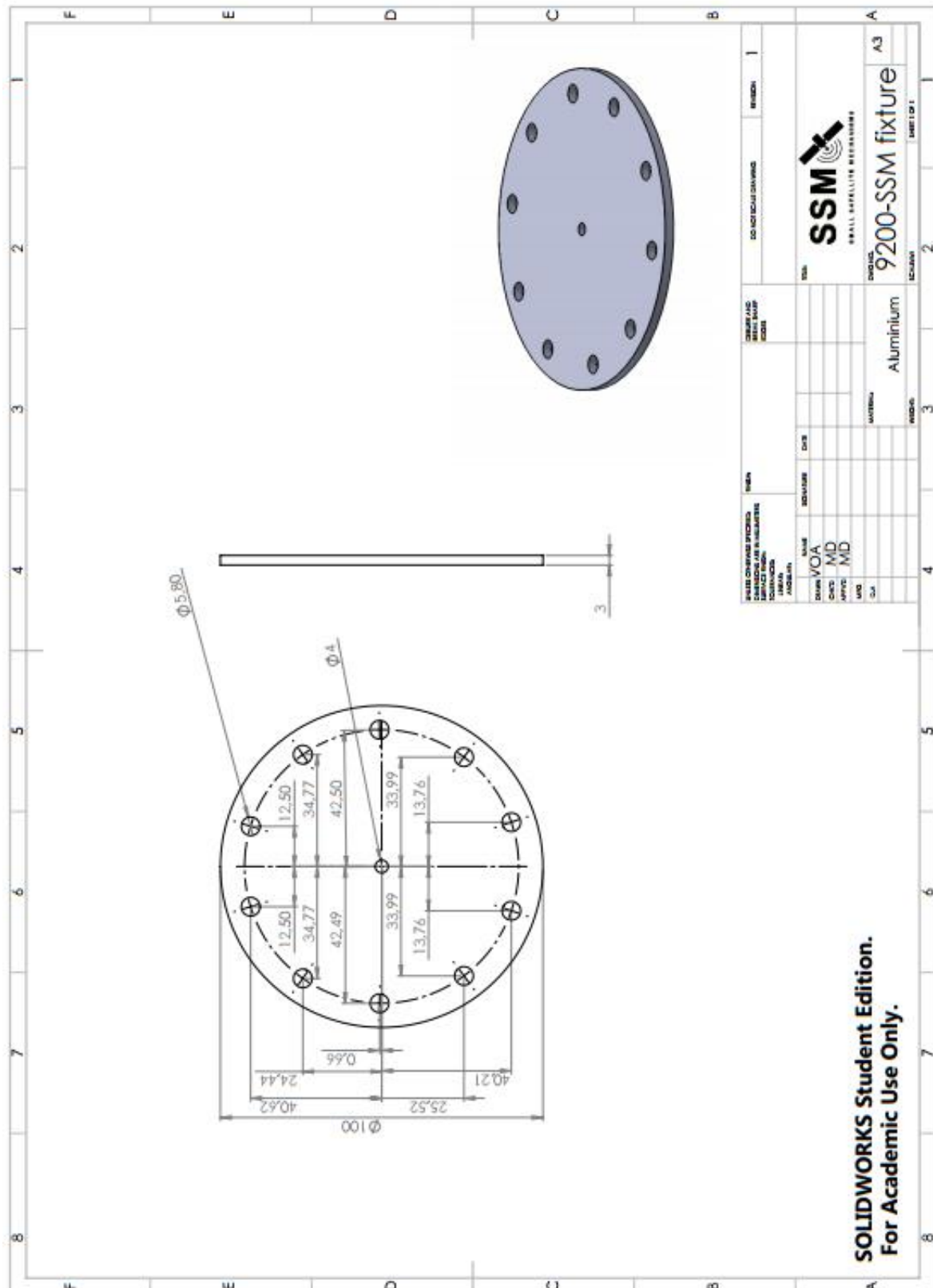
Figure 7. 6. 2: Test fixture 9100
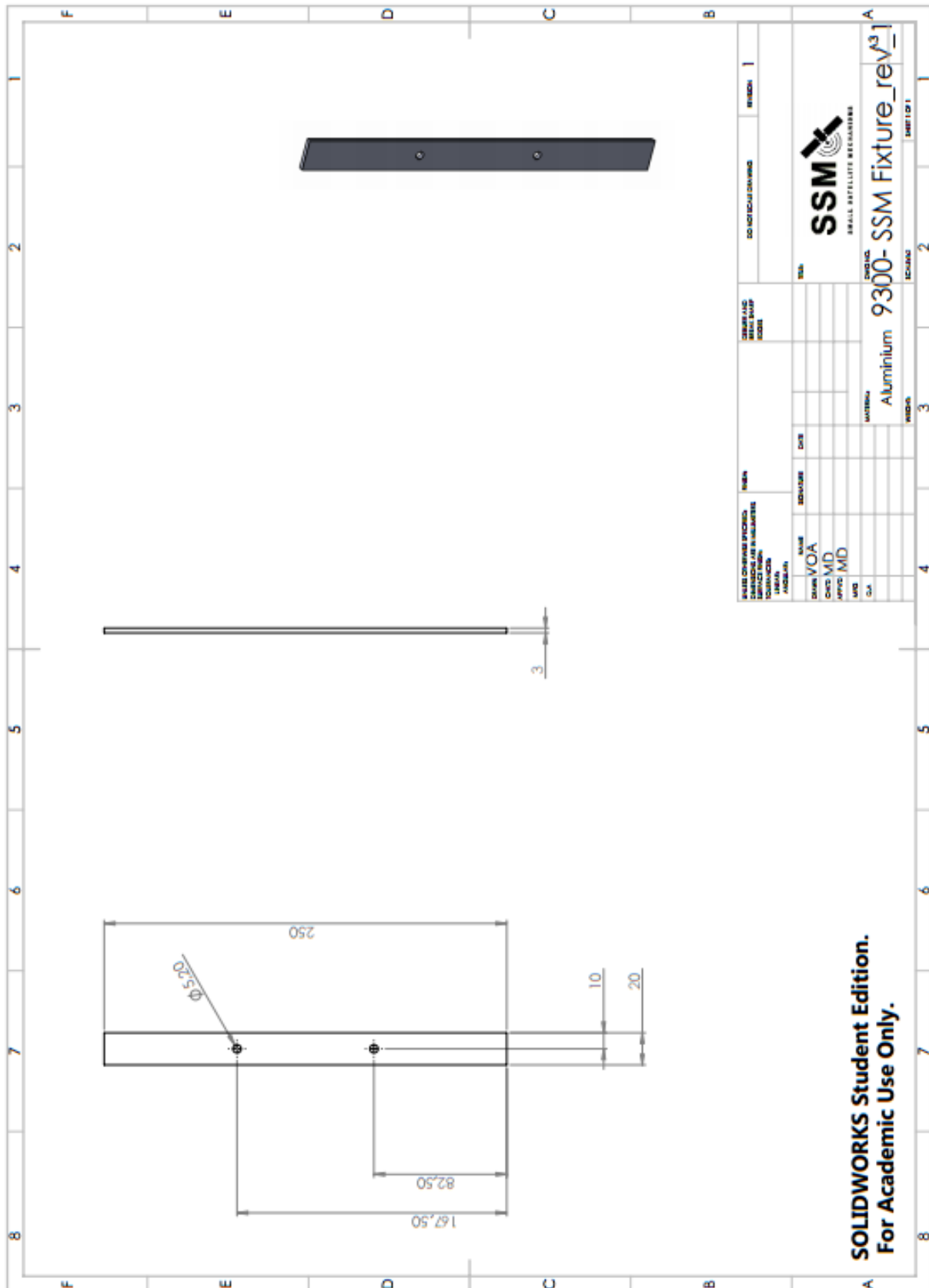
Figure 7. 6. 3: Test fixture 9200

Figure 7. 6. 4: Test fixture 9300

7.7. Microstrip calculations

Table 7. 7. 1: Microstrip calculations

```matlab
clc;
clear all;

%Er - dielectric constant
%Eeff - effective dielectric constant
%W - Microstrip width
%We - effective microstrip width
%h - board height
%Z0 - microstrip impedance
%t - conductor thickness
%up - phase velocity

t = 0.0347; %mm (1 oz)
Er = 3; %PTFE
h = 0.5; % mm
%Z0 = 50 ohm => W = 1.219 mm, 35 ohm => W = 2.045 mm
c = 3e8; % m/s (Speed of light)
W = 1.219; %mm
f = 23e9; %Hz


lambda = c/f;

l = (lambda/4)*1000*3; %Trace lenght (mm) 3/4lamda
s = 1/(2*pi);
i = W/h;


%%
%PS: The following formulas only apply if t <= h and if t < W/2

% Eeff1=((Er+1)/2)+((Er-1)/2)*(((1+12*h/W)^(-1/2))+(0.04*(1-W/h)^2)); %For i
<= 1

% Eeff_min = (1/2)*(Er+1);

% Eeff_max = Er;

% up1 = c/sqrt(Eeff1);

% Z01 = (60/sqrt(Eeff1))*log(8*(h/W)+(W/4*h));


We1_1 = W + (t/pi)*(1+log(2*h/t)); % For i >= s

%We1_2 = W + (t/pi)*(1+log(4*pi*W/t)); %For i <= s


%Z1 = Z01 * 0.707;

%%
%PS: The following formulas only apply if t <= h and if t < W/2

Eeff2=((Er+1)/2)+((Er-1)/2)*(((1+12*h/W)^(-1/2))); %For i >= 1

up2 = c/sqrt(Eeff2);
```

```matlab
Z02 = (120*pi)/((sqrt(Eeff2))*((W/h)+1.393+0.667*log((W/h)+1.444)));

Z2 = Z02 * 0.707; %Line impedance

%%
%Corrected equation

Eeff2_We1_1=((Er+1)/2)+((Er-1)/2)*(((1+12*h/We1_1)^(-1/2)));
%For i >= 1

Z02_We1_1 =
(120*pi)/((sqrt(Eeff2_We1_1))*((We1_1/h)+1.393+0.667*log((We1_1/h)+1.444)));
%Line impedance

lambda_eff = (c/f)/(sqrt(Eeff2_We1_1));
%Lamda used to calculate microstrip transmission line lenght

l_eff = (lambda_eff/4)*1000*5; %Trace lenght

%%
%Dispersion
k = sqrt (Er/Eeff2_We1_1);
F = ((4*h*sqrt(Er-1))/lambda)*(0.5+(1+2*log(1+i))^2);
Erf = Eeff2_We1_1*((1+0.25*k*F^1.5)/(1+0.25*F^1.5))^2;
```